ERDC/ITL TR-18-2

Information Technology Laboratory

US Army Corps
of Engineers®
Engineer Research and
Development Center

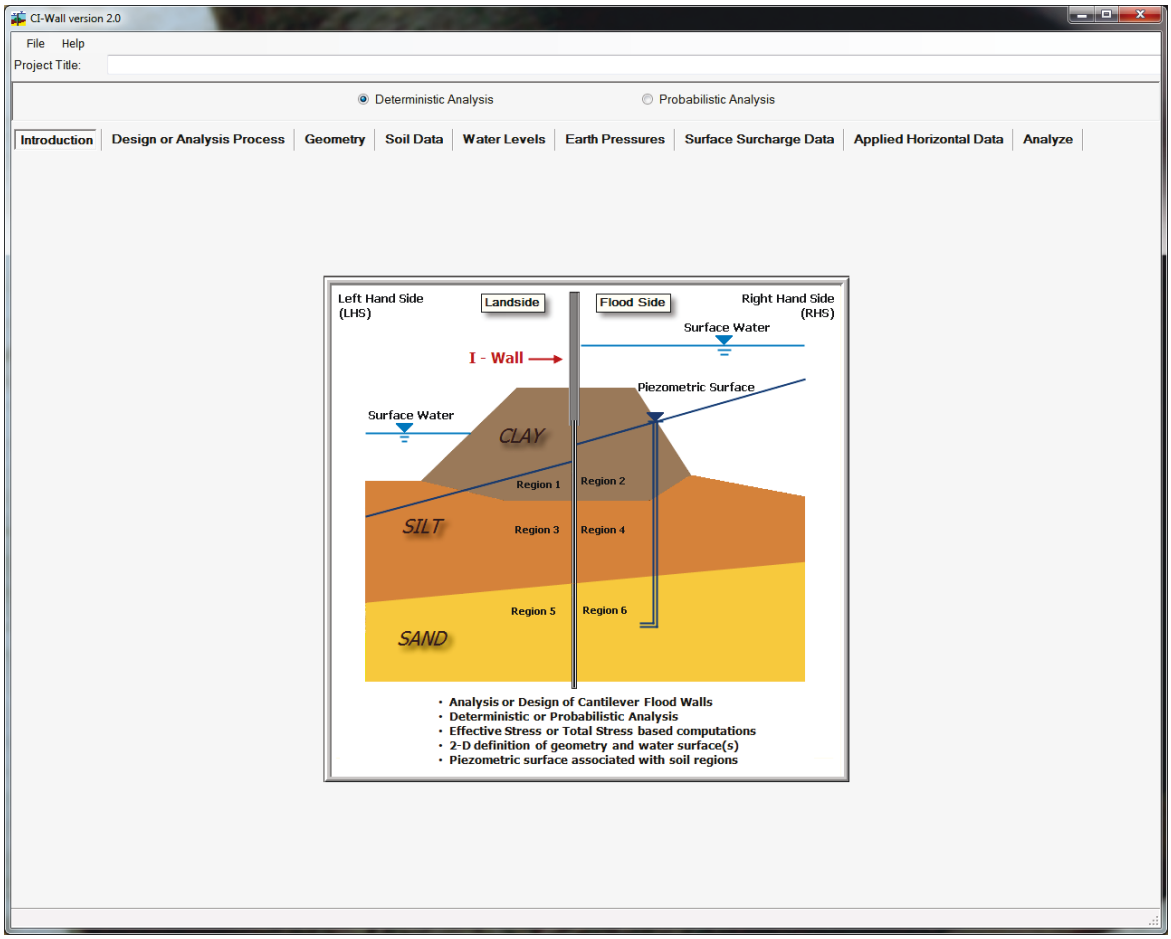
ERDC
ENGINEER RESEARCH & DEVELOPMENT CENTER

Flood and Coastal Storm Damage Reduction Program

Analysis of a River Bank, Levee, or Floodplain I-Wall Embedded in Stratified Soil Layers During Flood Events Using Corps_I-Wall (CI-Wall) Version 2.0

Robert M. Ebeling, Barry C. White, and Moira T. Fong

December 2018



Approved for public release; distribution is unlimited.

The U.S. Army Engineer Research and Development Center (ERDC) solves the nation's toughest engineering and environmental challenges. ERDC develops innovative solutions in civil and military engineering, geospatial sciences, water resources, and environmental sciences for the Army, the Department of Defense, civilian agencies, and our nation's public good. Find out more at www.erdc.usace.army.mil.

To search for other technical reports published by ERDC, visit the ERDC online library at http://acwc.sdp.sirsi.net/client/default.

Flood and Coastal Storm Damage
Reduction Program

ERDC/ITL TR-18-2
December 2018

Analysis of a River Bank, Levee, or Floodplain I-Wall Embedded in Stratified Soil Layers During Flood Events Using Corps_I-Wall (CI-Wall) Version 2.0

Robert M. Ebeling, Barry C. White, and Moira T. Fong

Information Technology Laboratory
U.S. Army Engineer Research and Development Center
3909 Halls Ferry Road
Vicksburg, MS 39180-6199

Final report

Approved for public release; distribution is unlimited.

Prepared for Headquarters, U.S. Army Corps of Engineers
441 G Street NW
Washington, DC 20314-1000

Under Work Unit CL618F

Abstract

The purpose of the I-Wall Analysis Research and Development (R&D) effort is to provide the U.S. Army Corps of Engineers (USACE) districts with essential tools in analyzing and evaluating I-Wall performance in riverine, fluvial, and coastal environments. This report summarizes an engineering method and its implementation in the software Corps_I-Wall Version 2.0. The executable program is referred to as CI-Wall. This version of Corps_I-Wall is used for the design of new I-Walls or the analysis of existing I-Walls in floodplains (i.e., level ground) or in riverbanks and levees (i.e., in non-level ground, with non-level soil layers and non-level piezometric surfaces) during flood loading.

Other Corps_I-Wall software capabilities for engineering analysis include total stress and/or effective stress earth pressure calculations by either 1) the Coefficient Method of analysis, or by 2) the Wedge Solution Method of analysis. The program accounts for gap initiation and propagation by invoking a hydraulic fracturing criteria. It also allows for pseudo-static modeling of wave loading of coastal structures. Probabilistic analysis is a primary component of Corps_I-Wall for new and existing I-Wall analysis.

Examples are provided to highlight each of these capabilities and a user's manual for using the Graphical User Interface (GUI) for CI-Wall is included.

DISCLAIMER: The contents of this report are not to be used for advertising, publication, or promotional purposes. Citation of trade names does not constitute an official endorsement or approval of the use of such commercial products. All product names and trademarks cited are the property of their respective owners. The findings of this report are not to be construed as an official Department of the Army position unless so designated by other authorized documents.

DESTROY THIS REPORT WHEN NO LONGER NEEDED. DO NOT RETURN IT TO THE ORIGINATOR.

Contents

Abstract ii

Figures and Tables vii

Preface xix

Unit Conversion Factors xx

Acronyms and Abbreviations xxi

1 Analysis of an I-Wall in Fluvial, Riverine, and Coastal Environments 1

1.1 Introduction 1
1.2 Background 2
1.3 Objective 5
1.4 Approach 5
1.5 Overview of Corps_I-Wall 5
1.6 Overview of the *Design* and *Analysis* modes 13
1.6.1 Design mode *14*
1.6.2 Analysis mode *16*

2 Engineering Formulation 17

2.1 Layered soils site model 17
2.2 Types of analysis used to define earth pressures 21
2.2.1 Total stress – mobilized active earth pressure *24*
2.2.2 Total stress – mobilized passive earth pressure *25*
2.2.3 Effective stress *26*
2.2.4 Effective stress – mobilized active earth pressure *27*
2.2.5 Effective stress – mobilized passive earth pressure *28*
2.3 Earth pressure Coefficient Methods used for computing earth pressures 29
2.3.1 Rankine's active earth pressure coefficients *30*
2.3.2 Rankine's passive earth pressure coefficients *31*
2.3.3 Coulomb's active earth pressure coefficients *31*
2.3.4 Coulomb's passive earth pressure coefficients *32*
2.3.5 Logarithmic-spiral method for the determination of a passive earth pressure coefficients *33*
2.4 Converting a trapezoidal pressure distribution acting on a discrete segment of the I-Wall face into equivalent end point forces 35
2.5 Clockwise or counterclockwise I-Wall rotation 36
2.6 Net active pressure and net passive pressure 37
2.7 Factors of safety applied to each soil region 37
2.8 Distributions of water pressures acting on the I-Wall and sheet-pile wall due to surface water and piezometric surfaces 38
2.9 Surcharge pressures, horizontal pressures and line loads 45
2.9.1 Externally applied horizontal pressure distribution and line loading *45*
2.9.2 Externally applied vertical pressure distribution and line loading *46*

2.10 Shear force and moment distribution internal to the I-Wall and sheet pile 48

3 Visual Modeler GUI User's Guide 51

3.1 Introduction 51
3.2 Example problem 51
3.3 *Introduction* tab 53
3.4 *Design or Analysis Process* tab 54
3.5 *Geometry* tab 58
3.6 *Soil Data* tab 70
3.7 *Water Levels* tab 75
3.8 *Earth Pressures* tab 86
3.9 *Surface Surcharge Data* tab 93
3.10 *Applied Horizontal Loads* tab 100
3.11 *Analyze* tab 102

4 Deterministic Example Problems 144

4.1 Example 4.1 sand site, effective stress strength definition with φ′ = 30, c′=0, with either hydrostatic pore water pressures or homogeneous seepage 144
4.1.1 Example 4.1.1 146
4.1.2 Example 4.1.2 150
4.1.3 Example 4.1.3 151
4.1.4 Example 4.1.4 153
4.1.5 Example 4.1.5 154
4.2 Example 4.1 sand site, effective stress strength definition with φ′ = 30 degrees and c′ = 125 psf, with either hydrostatic pore water pressures or homogeneous seepage 157
4.2.1 Example 4.2.1 159
4.2.2 Example 4.2.2 162
4.2.3 Example 4.2.3 166
4.3 Example 4.3 clay site, total stress strength definition with $\phi = 0$ 170
4.4 Example 4.4 mixed total and effective stress based shear strength definitions in layered soils site 175
4.5 Coastal site evaluation, designing for wave loads 181
4.5.1 Example 4.5.1: Coastal site, effective stress strength definition with φ ′ = 35° 182
4.5.2 Example 4.5.2 Coastal site with surge loading 187
4.5.3 Example 4.5.3 Coastal site including backfill 195
4.5.4 Example 4.5.4 coastal site including backfill with surge loading 201
4.5.5 Comparison and interpretation of backfill with surge loading 204
4.6 Example 4.6 comparison to Corps_I-Wall results contained within other technical publications (Das 2007; Bowles 1968; Pace et al. 2012) 211
4.6.1 Example 4.6.1 sheet-pile wall penetrating sand (Das 2007) 211
4.6.2 Example 4.6.2 sheet-pile wall penetrating saturated clay (Das 2007) 217
4.6.3 Sheet-pile wall penetrating sand (Bowles 1968) 223
4.6.4 Sheet-pile wall penetrating saturated clay (Bowles 1968) 230
4.6.5 Example 4.6.7 sheet-pile wall penetrating clay (Pace et al. 2012) 237
4.7 Example 4.7 *analysis* mode of operation for a clay site, an extension of Example 4.3 243

4.8 Model setup tips for calculating a depth of hydraulic fracturing 248
4.9 Comparison of Coefficient Method results with Wedge Method results 252
4.10 A nonlevel ground example showing the fexibility of Wedge Method results 257

5 Probability Analysis and Example Problems 262
5.1 Fragility curve (i.e., SRC) 262
5.2 Random variables for each soil layer (φ, c, δ, Ca) and correlation between variables 264
5.3 Finding the SRC for an analysis of an existing I-Wall 266
5.4 Accuracy and timing 267
5.5 Differences between the Coefficient Method and the Wedge Solution Method for computing earth pressures for probabilistic simulation 268
5.6 Example 5.1 sand site with hydraulic fracturing criteria and seepage, an extension of design problem 4.1.5 270
5.6.1 Evaluation of results from the deterministic solution with flood elevation pairs of 40 ft and 34 ft 272
5.6.2 Evaluation of results for 1,000 simulations with seepage 276
5.6.3 Comparisons of results for 100, 300, 600, and 1,000 simulations 280
5.6.4 Comparing the Coefficient Method solution to the Wedge Solution Method solution for Example 5.1 281
5.7 Example 5.2 SRC (clay site with hydraulic fracturing, an extension of Example 4.7) 289
5.8 Comparisons of results for 100, 300, 1,000, and 2,000 simulations 292
5.9 Comparisons of results Coefficient Method and Wedge Solution Method with 100 simulations 294
5.10 Example 5.3 SRC for a two-layer sand site with hydraulic fracturing criteria and seepage 296
5.11 Comparisons of results for 100, 300, 500, and 1,000 simulations 299
5.12 Comparisons of analysis results for the Coefficient Method and the Wedge Solution Method with 100 simulations 301
5.13 Comparisons of the Wedge Solution Method with 100 and 50 simulations 303

6 Summary, Conclusions, and Recommendations 306
6.1 Summary 306
6.2 Conclusions 307
6.2 Recommedations 307

References 308

Appendix A: Iterative Solution to Compute the Design Depth Using a Force and a Moment Imbalance Based Computational Procedure 312

Appendix B: Gap Initiation and Propagation Criteria and Formulation 320

Appendix C: Line of Seepage Formulation 331

Appendix D: Description of Corps_I-Wall Information Interchange (ASCII) Input Data File (*project*.in) 335

Appendix E: Description of Corps_I-Wall ASCII Output Data Files 347

Appendix F: Calculation of Coastal Surge Pressures Acting on an I-Wall for a Breaking Wave 352

Appendix G: Formulation for the Wedge Method of Analysis of Passive and Active Earth Pressure Forces Acting on the Sheet-Pile Wall 360

Appendix H: Benchmark Wedge Solution Method Analyses and Their Accuracy 388

Report Documentation Page

Figures and Tables

Figures

Figure 1.1. Idealization of I-Wall rotation about a point of rotation (PR) within proximity of the sheet-pile tip during flood loading. 3

Figure 1.2. Schematic idealization of the consideration of stresses imposed on a soil element for a gap originating and propagating in an overconsolidated clay layer and stopping within the normally consolidated clay below (according to the method implemented within Corps_I-Wall). 4

Figure 1.3. Idealization of a system response curve (SRC) for an I-Wall during variable flood elevation loading from 0–10 ft. 5

Figure 1.4. Corps_I-Wall Version 2.0 for level and non-level ground GUI. 6

Figure 1.5. Idealized example of a potential logarithmic spiral slip plane used to define an idealized eleven wedge soil mass for use in a passive earth force computation from the landside ground surface to a depth of Node i. 13

Figure 2.1. I-Wall site model configuration for Corps_I-Wall Version 1.0 absent any flood loading. 18

Figure 2.2. I-Wall flood load problem model setup for a Corps_I-Wall Coefficient Method of analysis, including wave loading. 19

Figure 2.3. Location of four select nodes identified along the RHS of the I-Wall for total vertical stress computations calculated during flood loading. 23

Figure 2.4. Distribution of stress acting normal to a discrete segment *k* of the wall face. (a) Trapezoidal pressure distribution. (b) Equivalent nodal point forces. 36

Figure 2.5. I-Wall rotation. (a) Counterclockwise rotation about a PR due to flood loading applied to the RHS of the I-Wall. (b) The net water and earth pressures acting on the I-Wall during its rotation. 38

Figure 2.6. Distributions of water pressures acting normal to the I-Wall and sheet-pile wall – hydrostatic water pressures. (a) Hydrostatic water and pore-water pressure distributions on the LHS and RHS. (b) The net water pressure distribution. 40

Figure 2.7. Distributions of hydrostatic water pressures acting normal to the I-Wall and sheet-pile wall – hydrostatic water pressures. (a) Hydrostatic water and pore water pressure distributions on the LHS and RHS. (b) The net water pressure distribution. 41

Figure 2.8. Distributions of water pressures acting normal to the I-Wall and sheet-pile wall – homogenous seepage. (a) Water and pore-water pressure distributions on the LHS and RHS. (b) The net water pressure distribution. 43

Figure 2.9. Distributions of water pressures acting normal to the I-Wall and sheet-pile wall – hetergenous seepage for two soil layers, (a) Water and pore-water pressure distributions on the LHS and RHS. (b) The net water pressure distribution. 44

Figure 2.10. External horizontal line load and pressures. (a) Line load. (b) Distributed pressures. 46

Figure 2.11. Vertical line load. 47

Figure 2.12. Vertical pressure distributions. (a) Strip pressure. (b) Ramp pressure. (c) Triangular pressure. (d) Trapezoidal pressure. 47

Figure 2.13. Internal shear and moment at node i+1 for wall segment *k*. (a) Trapezoidal pressure distribution. (b) Equivalent nodal point forces. 48

Figure 2.14. Internal shear and moment at node *i*+2 for wall segment *k*+1. (a) Trapezoidal pressure distributions. (b) Equivalent nodal point forces. 49
Figure 3.1. Example problem for an I-Wall section used to illustrate features of the GUI. 52
Figure 3.2. *Introduction* tab of Corps_I-Wall program. 54
Figure 3.3. *Design or Analysis Process - Design* mode. 55
Figure 3.4. *Design or Analysis process - Analysis* mode. 57
Figure 3.5. Creation of geometry is done with the *Geometry* tab. 58
Figure 3.6 The procedure to input a node into the I-Wall geometry. 60
Figure 3.7a-d. The procedure for creating a new edge in the I-Wall geometry. 62
Figure 3.8. The procedures for selecting a node, and for deleting the node (and its connected edges). 63
Figure 3.9. The procedure for selecting an edge. 63
Figure 3.10a-b. The procedure for zooming with the right mouse. 65
Figure 3.11. Using the *Zoom Extents* button. 66
Figure 3.12. Modifying the extents of the soil regions to the sides of the I-Wall. 67
Figure 3.13a-c. Usage of the *Undo* button. 68
Figure 3.14. Using the *Swap Landside* button to reverse the *Flood* and *Landsides* of the structure. 69
Figure 3.15 Generating regions adds new nodes and edges (to account for intersections with the I-Wall and other edges, and the full I-Wall area). Each area enclosed by edges is a region. 69
Figure 3.16 Choosing the method of gap creation. 70
Figure 3.17. Entering region attributes with the *Soil Data* tab. 71
Figure 3.18. Reference values for soil types. 72
Figure 3.19. Soil material probabilistic input. 73
Figure 3.20. Selecting/changing a distribution. 74
Figure 3.21. Water levels are defined either as level surface waters or piezometric surfaces described by piecewise linear elements. 76
Figure 3.22. Choosing the appropriate seepage method. 78
Figure 3.23. Entering a homogeneous seepage parameter (and the warnings associated with this method). 78
Figure 3.24 Creating a piezometric surface highlighting the selector and region creation buttons. 79
Figure 3.25. Assigning soil regions to a user-defined piezometric surface (whose point coordinates are in the piezometric area). 80
Figure 3.26. Assigning soil regions to the flood side surface water. 81
Figure 3.27. The piezometric surface immediately after the *Add Landside Piezometric Surface* button has been pushed. 82
Figure 3.28. The points of the piezometric are in the grid below the point definition area. 84
Figure 3.29. If an input point has an X value that is already on the curve, then that point is moved to the new Y location on confirmation. 85
Figure 3.30. After both ends of the piezometric surface have been moved. 85
Figure 3.31. Choosing the Coefficient Method of analysis using the *Earth Pressures* tab. 86

Figure 3.32. Choosing the Wedge Solution Method using the *Earth Pressures* tab. 87
Figure 3.33. The Distribution of Interslice Friction-Curves selector dialog. 88
Figure 3.34. Selecting the interslice friction curve for analysis. 89
Figure 3.35. Distributions describing the variation in interslice friction δ' normalized by the wall fiction δ'_{max} versus normalized distance along passive or active soil wedges. 91
Figure 3.36. Difference in percent between values of passive earth force by Wedge Method and standard solution as a function of δ' at the wall, expressed as a fraction of ϕ', and as a function of ϕ'. 92
Figure 3.37. Difference in percent between values of active earth force by Wedge Method and standard solution as a function of δ' at the wall, expressed as a fraction of ϕ', and as a function of ϕ'. 93
Figure 3.38. *Surface Surcharge Data* tab. 94
Figure 3.39. The input window for line loads. 95
Figure 3.40. The input window for uniform loads. 96
Figure 3.41. The input window for strip loads. 96
Figure 3.42. The input window for ramp loads. 97
Figure 3.43. The input window for triangular loads. 98
Figure 3.44. The input window for trapezoid/distributed loads. 99
Figure 3.45. *Surface Surcharge Data* tab with highlighted loads. 99
Figure 3.46. The *Applied Horizontal Loads* tab allows input of point loads (on the right) and linearly distributed loads (on the left). 100
Figure 3.47. The *Analyze* tab at the beginning of a deterministic analysis. 103
Figure 3.48. The *Analyze* tab for a probabilistic analysis without landside water levels. 104
Figure 3.49. The *Analyze* tab for a probabilistic analysis with constant landside water level. 105
Figure 3.50. (a) The *Analyze* tab. (b) Its procedure for a probabilistic analysis with interpolated landside water levels. 106
Figure 3.51. Plotting the input model for a deterministic analysis. 108
Figure 3.52. Plotting the input model for a probabilistic range of both flood and landside water levels. 109
Figure 3.53. View of the pile without horizontal and vertical loads. 110
Figure 3.54. Tolerance input dialog. 111
Figure 3.55. The Corps_I-Wall processor in action. 112
Figure 3.56. Adjusting rank correlation dialog. 112
Figure 3.57. If problems occur during adjustment of rank correlation, this dialog appears. 113
Figure 3.58. After the processor has finished, output options are made available. 114
Figure 3.59. The *Run Data* subsection allows the user to see processor input, results, and debugging information. 114
Figure 3.60. The display run window shows the output and debugging information from an analysis. 115
Figure 3.61. The display input data button allows the user to see the processor input file. 116
Figure 3.62. The output plot subsection allows the user to see data based on a flood elevation. 116

Figure 3.63. Pressure data for both the left and right sides of the I-Wall. 117
Figure 3.64. Left-side horizontal mobilized passive and active pressures. 118
Figure 3.65. Right-side horizontal mobilized active and passive pressures. 118
Figure 3.66. Left- and right-side water pressures. 119
Figure 3.67. Displaying the net pressure data. 120
Figure 3.68. Active and passive net pressures. 120
Figure 3.69. Displaying the net water pressures. 121
Figure 3.70. Shear, moment, and combined net pressures. 121
Figure 3.71. Combined net pressures with soil and water pressures. 122
Figure 3.72. Shear and moment diagrams for the I-Wall. 122
Figure 3.73. Display of seepage data for both the left and right sides of the I-Wall. 123
Figure 3.74. Seepage plot of total head loss in actual (untransformed) space. 125
Figure 3.75. Seepage plot items to display. 125
Figure 3.76. Seepage plots selector for untransformed or transformed space. 126
Figure 3.77. Seepage plot of total head loss in transformed space. 126
Figure 3.78. Seepage plot of seepage gradient due to soil region properties (untransformed). 127
Figure 3.79. Defining internal and external material correlations for probabilistic analysis for Example 5.2 input. 128
Figure 3.80. Probabilistic analysis options for the *Analysis* option run for Example 5.2 from Chapter 5. 129
Figure 3.81. Warning that the correlation matrix between variables may change. 130
Figure 3.82. Error dialog that occurs when the software altered correlations cannot match the user input correlations. 131
Figure 3.83. Active probabilistic output options in the *Analyze* tab after execution of a *Design* mode. 131
Figure 3.84. Displayed sheet-pile tip elevation histogram data after execution of a *Design* mode. 132
Figure 3.85. Plotted sheet-pile tip elevation histogram data after execution of a *Design* mode. 133
Figure 3.86. Plotting the sheet-pile tip elevation histogram data as a set of linear segments passing through the center of each bin after execution of a *Design* mode. 134
Figure 3.87. The combined plot of bins and linear interpolation of sheet-pile tip elevation histogram data after execution of a *Design* mode. 135
Figure 3.88. Displayed cumulative sheet-pile tip elevation distribution data after execution of a *Design* mode. 135
Figure 3.89. Plotted cumulative sheet-pile tip elevation distribution data after execution of a *Design* mode. 136
Figure 3.90. Displayed sheet-pile tip depth histogram data after execution of a *Design* mode. 137
Figure 3.91. Plotted sheet-pile tip depth histogram data after execution of a *Design* mode. 137
Figure 3.92. Displayed cumulative sheet-pile tip depth data after execution of a *Design* mode. 138

Figure 3.93. Plotted cumulative sheet-pile tip depth data after execution of a *Design* mode. 139
Figure 3.94. The selection of probabilistic output for an *Analysis* mode problem 139
Figure 3.95. Histogram data of passive Factor of Safety probabilities for flood elevation 4 ft after execution of an *Analysis* mode. 140
Figure 3.96. Histogram plot of passive Factor of Safety probabilities for flood elevation 4 ft after execution of an *Analysis* mode. 141
Figure 3.97. Cumulative distribution data of probabilities given a passive Factor of Safety for flood elevation 4 ft after execution of an *Analysis* mode. 141
Figure 3.98. Cumulative distribution plot of probabilities given a passive Factor of Safety for flood elevation 4 ft after execution of an *Analysis* mode. 142
Figure 3.99 Displayed SRC for 1,000 simulations per flood elevation with fifteen bins. 143
Figure 3.100. Plotted SRC for 1,000 simulations per flood elevation with fifteen bins. 143
Figure 4.1. Sheet-pile wall in sand site. 145
Figure 4.2. Corps_I-Wall schematic of sheet-pile wall in sand site. 145
Figure 4.3. Active and passive earth pressures. (a) LHS of wall. (b) RHS of wall. 147
Figure 4.4. (a) Pore water pressures for the LHS and RHS of the wall. (b) Net water pressures. 147
Figure 4.5. Net pressures. (a) Net active and net passive. (b) Net pressure diagram. 148
Figure 4.6. (a) Net pressure diagram. (b) Shear and moment. 148
Figure 4.7. Pore water pressures. (a) LHS and RHS of wall. (b) Net water pressures 155
Figure 4.8. Line of seepage. (a) Direction of flow. (b) Total head along distance of flow. 156
Figure 4.9. Corps_I-Wall schematic of sheet-pile wall in sand site. 158
Figure 4.10. Active and passive earth pressures. (a) LHS of wall. (b) RHS of wall. 160
Figure 4.11. Pore water pressures. (a) LHS and RHS of wall. (b) Net water pressures. 160
Figure 4.12. Net pressures. (a) Net active and net passive. (b) Net pressure diagram. 160
Figure 4.13. (a) Net pressure diagram. (b) Shear and moment. 161
Figure 4.14. Corps_I-Wall schematic of sheet-pile wall in sand site with two layers 163
Figure 4.15. Active and passive earth pressures. (a) LHS of wall. (b) RHS of wall. 164
Figure 4.16. Net pressures. (a) Net active and net passive. (b) Net pressure diagram. 165
Figure 4.17. (a) Net pressure diagram. (b) Shear and moment. 165
Figure 4.18. Active and passive earth pressures. (a) LHS of wall, (b) RHS of wall 167
Figure 4.19. Pore water pressures. (a) LHS and RHS of wall. (b) Net water pressures. 167
Figure 4.20. Net pressures. (a) Net active and net passive. (b) Net pressure diagram. 168
Figure 4.21. (a) Net pressure diagram. (b) Shear and moment. 168
Figure 4.22. Line of seepage. (a) Direction of flow. (b) Total head along distance of flow. 169
Figure 4.23. Corps_I-Wall schematic of sheet-pile wall in clay site. 171
Figure 4.24. Active and passive earth pressures for undrained shear strength. (a) LHS of wall. (b) RHS of wall. 173
Figure 4.25. Pore water pressures. (a) LHS and RHS of wall. (b) Net water pressures 173
Figure 4.26. Net pressures. (a) Net active and net passive. (b) Net pressure diagram. 174
Figure 4.27. (a) Net pressure diagram. (b) Shear and moment 175

Figure 4.28. Corps_I-Wall schematic of sheet-pile wall in clay site. 177
Figure 4.29. Active and passive earth pressures. (a) LHS of wall. (b) RHS of wall. 177
Figure 4.30. Pore water pressures. (a) LHS and RHS of wall. (b) Net water pressures. 178
Figure 4.31. Net pressures. (a) Net active and net passive. (b) Net pressure diagram. 179
Figure 4.32. (a) Net pressure diagram. (b) Shear and moment. 179
Figure 4.33. Corps_I-Wall schematic of sheet-pile wall in sand site. 183
Figure 4.34. Corps_I-Wall run file for the specified input. 184
Figure 4.35. Corps_I-Wall run file for the specified input. 184
Figure 4.36. Pore water pressures. (a) Left- and right- hand side of wall. (b) Net water pressures. 185
Figure 4.37. Net pressures. (a) Net active and net passive. (b) Net pressure diagram. 185
Figure 4.38. (a) Net pressure diagram, (b) Shear and moment. 186
Figure 4.39. Drop in total heads due to seepage diagram. 187
Figure 4.40. The components of Minikin wave pressure diagram. 189
Figure 4.41. Corps_I-Wall. (a) Schematic of sheet-pile wall in sand site. (b) Wave load applied to flood side (LHS) of sheet-pile wall. 191
Figure 4.42. Corps_I-Wall run file for the specified input. 192
Figure 4.43. Active and passive earth pressures for drained shear strength. (a) LHS of wall. (b) RHS of wall. 192
Figure 4.44. Pore water pressures. (a) LHS and RHS of wall. (b) Net water pressures. 193
Figure 4.45. Net pressures. (a) Net active and net passive. (b) Net pressure diagram. 193
Figure 4.46. (a) Net pressure diagram. (b) Shear and moment. 194
Figure 4.47. Drop in total heads due to seepage diagram. 195
Figure 4.48. Sheet-pile wall with berm on landside (RHS). (a) Schematic of sheet-pile wall in sand site. (b) Plot of external loads. 197
Figure 4.49. Corps_I-Wall run file for the specified input. 198
Figure 4.50. Active and passive earth pressures for drained shear strength. (a) LHS of wall. (b) RHS of wall. 199
Figure 4.51. Pore water pressures. (a) LHS and RHS of wall. (b) Net water pressures. 199
Figure 4.52. Net pressures. (a) Net active and net passive. (b) Net pressure diagram. 200
Figure 4.53. (a) Net pressure diagram. (b) Shear and moment. 200
Figure 4.54. Sheet-pile wall with berm on landside (RHS). (a) Schematic of sheet-pile wall in sand site. (b) Wave load applied to flood side (LHS) of sheet-pile wall. 202
Figure 4.55. Corps_I-Wall run file for the specified input (with seepage enabled). 203
Figure 4.56. Corps_I-Wall run file for the specified input (without seepage). 204
Figure 4.57. Representation (not to scale) of both the water and earth pressures acting on the I-Wall in Example 4.5.4. 205
Figure 4.58. Results of lateral berm extent calculations for a 15-ft-high berm and a Factor of Safety (passive) within the berm of 3.7581. 211
Figure 4.59. Sheet-pile wall penetrating sand. 213
Figure 4.60. Corps_I-Wall schematic of sheet-pile wall in sand site. 213
Figure 4.61. Corps_I-Wall output information. 214

Figure 4.62. Active and passive earth pressures for drained shear strength. (a) LHS. (b) RHS. 214
Figure 4.63. Hydrostatic water pressures. (a) LHS and RHS of wall. (b) Net water pressures. 214
Figure 4.64. (a) Net pressure diagram. (b) Shear and moment diagram. 216
Figure 4.65. (a) Net pressure diagram. (b) Shear and moment diagram. 217
Figure 4.66. Sheet-pile wall penetrating saturated clay. 218
Figure 4.67. Corps_I-Wall schematic of sheet-pile wall in sand and saturated clay site. 219
Figure 4.68. Corps_I-Wall output information. 220
Figure 4.69. Active and passive earth pressures. (a) LHS. (b) RHS. 221
Figure 4.70. Hydrostatic water pressures. (a) LHS and RHS of wall. (b) Net water pressures. 221
Figure 4.71. Net pressures. (a) Net active and net passive pressures. (b) Net pressure diagram. 221
Figure 4.72. (a) Net pressure diagram. (b) Shear and moment diagram. 222
Figure 4.73. Sheet-pile wall penetrating sand. 225
Figure 4.74. Corps_I-Wall schematic of sheet-pile wall in sand site. 225
Figure 4.75. Corps_I-Wall output information. 226
Figure 4.76. Active and passive earth pressures for drained shear strength. (a) LHS. (b) RHS. 227
Figure 4.77. Hydrostatic water pressures. (a) LHS and RHS of wall. (b) Net water pressures. 227
Figure 4.78. Net pressures. (a) Net active and net passive pressures. (b) Net pressure diagram. 228
Figure 4.79. (a) Net pressure diagram. (b) Shear and moment diagram. 228
Figure 4.80. Corps_I-Wall output information. 230
Figure 4.81. Sheet-pile wall penetrating saturated clay. 232
Figure 4.82. Corps_I-Wall schematic of sheet-pile wall in sand and saturated clay site. 232
Figure 4.83. Corps_I-Wall output information. 233
Figure 4.84. Active and passive earth pressures. (a) LHS. (b) RHS. 233
Figure 4.85. Hydrostatic water pressures. (a) LHS and RHS of wall. (b) Net water pressures. 233
Figure 4.86. Net pressures. (a) Net active and net passive pressures. (b) Net pressure diagram. 234
Figure 4.87. (a) Net pressure diagram. (b) Shear and moment diagram. 235
Figure 4.88. Corps_I-Wall output information. 236
Figure 4.89. Sheet-pile wall penetrating clay. 237
Figure 4.90. Corps_I-Wall schematic of sheet-pile wall in clay site. 238
Figure 4.91. Corps_I-Wall output information. 239
Figure 4.92. Active and passive earth pressures. (a) LHS. (b) RHS. 239
Figure 4.93. Hydrostatic water pressures. (a) LHS and RHS of wall.(b) Net water pressures. 240

Figure 4.94. Net pressures (a) Net active and net passive pressures. (b) Net pressure diagram. 240
Figure 4.95. (a) Net pressure diagram. (b) Shear and moment diagram. 241
Figure 4.96. Corps_I-Wall schematic of sheet-pile wall in clay site. 245
Figure 4.97. Active and passive earth pressures for undrained shear strength. (a) LHS of wall, (b) RHS of wall. 245
Figure 4.98. Pore water pressures. (a) LHS and RHS of wall. (b) Net water pressures. 246
Figure 4.99. Net pressures. (a) Net active and net passive. (b) Net pressure diagram. 247
Figure 4.100. (a) Net pressure diagram. (b) Shear and moment. 248
Figure 4.101. Sheet-pile wall penetrating clay with two soil layers. 249
Figure 4.102. Input geometry, material properties, and water levels used for Coefficient and Wedge Analysis of Example 4.3. 253
Figure 4.103 Results from analyzing the Example 4.3 input using the (a) Coefficient and (b) Wedge Method. 254
Figure 4.104 Resulting left and right hand side water pressures for the (a) Coefficient and (b) Wedge Methods. 255
Figure 4.105 Resulting net water pressures for the (a) Coefficient and (b) Wedge Methods. 255
Figure 4.106 Resulting LHS active and passive soil pressures for the (a) Coefficient and (b) Wedge Methods. 256
Figure 4.107 Resulting right hand side active and passive soil pressures for the (a) Coefficient and (b) Wedge Methods. 256
Figure 4.108 Resulting net active and passive pressures given the direction of rotation for the (a) Coefficient and (b) Wedge Methods 256
Figure 4.109 Resulting net pressures given wall tip depth and PR resulting in balanced forces and moments for the (a) Coefficient and (b) Wedge Methods. 257
Figure 4.110 Shear and moment diagrams for the pressures acting along the designed I-wall 257
Figure 4.111 Material properties and water levels for the Wedge Method model. 259
Figure 4.112 Non-level soil geometry for the Wedge Method model. 259
Figure 4.113 Effective soil geometry for the Coefficient Method model. 260
Figure 4.114 Changed soil geometry for hypothesis Wedge Solution Method model. 261
Figure 5.1. SRC for rotational limit state. 263
Figure 5.2. System response curve. (a) Underestimated flood elevations for SRC. (b) Overestimated flood elevations for SRC. (c) Located region of SRC curve. 267
Figure 5.3. Corps_I-Wall schematic of sheet-pile wall in sand site. 271
Figure 5.4. Statistical parameters of sandy soil. 272
Figure 5.5. Active and passive earth pressures. (a) LHS of wall, (b) RHS of wall. 273
Figure 5.6. Pore water pressures. (a) LHS and RHS of wall, (b) net water pressures. 273
Figure 5.7. Net pressures. (a) Net active and net passive. (b) Net pressure diagram. 275
Figure 5.8. (a) Net pressure diagram. (b) Shear and moment. 275
Figure 5.9. Line of seepage. (a) Direction of flow. (b) Head loss along distance of flow. 276
Figure 5.10. Output runtime file. 277

Figure 5.11. Design probabilistic analysis of sheet-pile tip with 1,000 simulations. (a) Histogram. (b) Cumulative distribution function.... 278
Figure 5.12. Design probabilistic analysis of depth of embedment with 1,000 simulations. (a) Histogram. (b) Cumulative distribution function.... 279
Figure 5.13. Cumulative distribution function for sheet-pile tip elevation for 100, 300, 600, and 1,000 simulations.... 280
Figure 5.14. Establishing design mode parameters for Example 5.1 in Corps_I-Wall Version 2.0. 282
Figure 5.15. Establishing geometry for Example 5.1 in Corps_I-Wall Version 2.0. 282
Figure 5.16. Establishing soil property parameters for Example 5.1 in Corps_I-Wall Version 2.0. 283
Figure 5.17. Establishing water and seepage parameters for Example 5.1 in Corps_I-Wall Version 2.0. 283
Figure 5.18. Establishing the Earth Pressure Solution Method for Example 5.1 in Corps_I-Wall Version 2.0.... 284
Figure 5.19. Establishing simulation parameters for Example 5.1 in Corps_I-Wall Version 2.0.... 284
Figure 5.20. Binned distributions of the dependent output parameter (wall tip elevation) in Example 5.1 with flood height 40.0 ft.... 285
Figure 5.21. Binned distributions (plotted) of the dependent output parameter (wall tip elevation) in Example 5.1 with flood heights ranging from 40.0 to 36.0 ft using the Wedge Solution Method. (continued).... 286
Figure 5.22. Binned distributions (plotted) of the dependent output parameter (wall tip elevation) in Example 5.1 with flood height 40.0 ft using the Coefficient Method.... 288
Figure 5.23. Wedge Solution Method results for Example 5.1 with a flood height 40.0 ft and 1,000 simulations.... 289
Figure 5.24. Schematic of sheet-pile wall in clay site for various water levels. 290
Figure 5.25. Statistical parameters for the clayey soil of material M01.... 291
Figure 5.26. SRC for 1,000 simulations at 0.25 ft and 1 ft flood increments.... 293
Figure 5.27. SRC for 100, 300, 1,000, and 2,000 simulations at 0.25 ft increments.... 294
Figure 5.28. SRC for Design, Coefficient Method vs Wedge Solution Method.... 296
Figure 5.29. Schematic of sheet-pile wall in sandy site for twelve flood levels.... 297
Figure 5.30. Statistical parameters for the sandy soils.... 299
Figure 5.31. SRC for 100, 300, 500, and 1,000 simulations. 300
Figure 5.32. SRC for Analysis: Coefficient Method vs Wedge Solution Method.... 302
Figure 5.33. SRC for Analysis: Coefficient Method vs Wedge Solution Method.... 304
Figure A1. Cantilever retaining wall. (a) Two layered soil site. (b) Counterclockwise rotation of the cantilever sheet-pile wall about its PR.... 312
Figure A2. Schematic of summation of horizontal forces versus trial points of rotation. 316
Figure A3. Schematic of summation of moments versus trial points of rotation.... 317
Figure B1. Schematic of gap propagation for a soil element above the PR with a mobilized total horizontal earth pressure definition. 322
Figure B2. Schematic of gap propagation for a soil element above the PR with a mobilized effective horizontal earth pressure definition. 324
Figure B3. Schematic of gap propagation for a soil element located at the PR with a mobilized total horizontal earth pressure definition. 325

Figure B4. Schematic of gap propagation for a soil element located above the PR with a mobilized effective horizontal earth pressure definition. 327

Figure C1. I-Wall. (a) Potential slip plane within soil regions with different saturated hydraulic conductivities (*K*) (lengths not to scale). (b) Constant slope in total head with distance along the transformed length of line of seepage. (c) Variation of slope in total head with distance along the three soil regions of the line of seepage. 332

Figure F1. Profile used in the initial I-Wall design calculations, including a soil buttress on the landside using an overly simplified and incomplete representation of wave load-induced, pseudo-static pressures. 354

Figure F2. Minikin breaking wave pressure diagram (after Figure 7-99; *Shore protection manual* 1984). 356

Figure F3. Dimensionless design breaker height versus relative depth at the wall (after Figure 7-4 *Shore Protection Manual* 1984 and Weggel 1972). 357

Figure F4. Dimensionless Minikin wave pressure and force (after Figure 7-100; *Shore protection manual* 1984). 359

Tables

Table 1.1. Appropriate method for computing the passive earth pressure coefficient, $K_{passive}$, as a function of the magnitude of the interface friction, δ, between the soil and the sheet pile and in comparison to the magnitude of the soil's angle of internal friction, φ. 12

Table 2.1. I-Wall flood loading problem soil layering, piezometric surface definitions, and material property specifications for a Corps_I-Wall Version 1.0 model setup. 20

Table 2.2. Passive earth pressure coefficient $K_{Passive}$ *(Kp)* values for −δ equal to φ and a solution based on assuming a failure surface composed of logarithmic spiral portion and a planar surface portion. 34

Table 2.3. Reduction factor, *R*, values for various ratios of $-\delta/\phi$. 35

Table 3.1. Input soil properties for the example problem. 53

Table 4.1. Examples of effective stress strength definitions (sands with c′=0). 149

Table 4.2. Comparison of earth coefficient results to Wedge Solution Method results for Example 4.1.1 150

Table 4.3. Comparison of Earth Coefficient results to Wedge Solution Method results - Example 4.1.2. 151

Table 4.4. Results from wall friction angles with K_p coefficients from logarithmic spiral procedure. 152

Table 4.5. Comparison of earth coefficient results to Wedge Solution Method results - Example Problems of 4.1.3. 153

Table 4.6. Comparison of Earth Coefficient results to Wedge Solution Method results - Example 4.1.2. 154

Table 4.7. Comparison of Earth Coefficient results to Wedge Solution Method results - Example 4.1.5. 157

Table 4.8. Examples of effective stress strength definitions (sands with c′ = 125). 161

Table 4.9. Comparison of Earth Coefficient results to Wedge Solution Method results - Example 4.2.1. 162

Table 4.10. Comparison of Earth Coefficient results to Wedge Solution Method results - Example 4.2.2. 166

Table 4.11. Comparison of Earth Coefficient results to Wedge Solution Method results - Example 4.2.3. 170
Table 4.12. Comparison of Earth Coefficient results to Wedge Solution Method results - Example 4.3. 175
Table 4.13. Multilayered soils with effective stress strength definitions (sands with c′ = 0) and total stress strength definitions (clays with φ = 0). 180
Table 4.14. Comparison of Earth Coefficient results to Wedge Solution Method results - Example 4.4. 181
Table 4.15. Comparison of Earth Coefficient results to Wedge Solution Method results - Example 4.5.1. 187
Table 4.16. Comparison of Earth Coefficient results to Wedge Solution Method results - Example 4.5.2. 195
Table 4.17. Comparison of Earth Coefficient results to Wedge Solution Method results - Example 4.5.3. 201
Table 4.18. Comparison of Earth Coefficient results to Wedge Solution Method results - Example 4.5.3. 204
Table 4.19. Hydrostatic pressures with elevations from the site. 206
Table 4.20. Combining the LHS and RHS hydrostatic pressures to get the net pressure. 206
Table 4.21. Dynamic water pressures with elevations calculated with the Minikin method. 206
Table 4.22. Forces and moments calculated from water pressure distributions at the datum elevation. 206
Table 4.23. Determining earth pressures on the RHS of the wall with Factor of Safety 1.5. 208
Table 4.24. Forces and moments acting on the RHS of the wall with Factor of Safety 1.5. 209
Table 4.25. Determining earth pressures on the RHS of the wall with Factor of Safety 3.7581. 209
Table 4.26. Forces and moments acting on the RHS of the wall with Factor of Safety 3.7581. 209
Table 4.27. Comparisons of I-Wall results contained within Das (2007). 215
Table 4.28. Comparison of Earth Coefficient results to Wedge Solution Method results - Example 4.6.1. 217
Table 4.29. Comparison of Earth Coefficient results to Wedge Solution Method results - Example 4.6.2. 223
Table 4.30. Comparisons of I-Wall results contained within Bowles (1968). 224
Table 4.31. Comparison of Earth Coefficient results to Wedge Solution Method results - Example 4.6.3. 229
Table 4.32. Comparison of Earth Coefficient results to Wedge Solution Method results - Example 4.6.4. 230
Table 4.33. Comparison of Earth Coefficient results to Wedge Solution Method results - Example 4.6.5. 235
Table 4.34. Comparison of Earth Coefficient results to Wedge Solution Method results - Example 4.6.6. 236
Table 4.35. Comparisons of I-Wall results contained within Pace (2012). 242
Table 4.36. Comparison of Earth Coefficient results to Wedge Solution Method results - Example problems of 4.6.7. 243

Table 4.37. Comparison of Earth Coefficient results to Wedge Solution Method results - Example 4.7. 248
Table 4.38. Geotechnical properties for the two soil layers contained in Example 4.6.7. 250
Table 4.39. Material property information for the four-region model of Example 4.6.7. 251
Table 4.40. Material property assignments to the four-region model of Example 4.6.7. 251
Table 5.1. Correlations used among variables in some example problems. 265
Table 5.2. Ranges of the most frequent values of COVs. 266
Table 5.3. Execution times for 100, 300, 600, and 1,000 simulations. 281
Table 5.4. Results of Example 5.1 using the Coefficient Method and the Wedge Solution Method. 288
Table 5.5. Results of Example 5.1 with a flood elevation of 40 ft using 1,000 and 100 simulation runs with the Wedge Solution Method. 289
Table 5.6. Probabilities of a rotational limit state for 100, 300, 1,000, and 2,000 number of simulations. 292
Table 5.7. Execution times for 100, 300, 1,000, and 2,000 number of simulations. 294
Table 5.8. Comparison of probability of limit state between the Coefficient Method and the Wedge Solution Method. 295
Table 5.9. Probabilities of a rotational stability for 100, 300, 500, and 1,000 simulations. 300
Table 5.10. Execution times for 100, 300, 500, and 1,000 simulations. 301
Table 5.11. Comparison of probability of limit state between Coefficient Method and Wedge Solution Method. 302
Table 5.12. Comparison of probability of limit state for the Wedge Solution Method with 100 and 50 simulations. 304
Table 5.13. Run times for Example 5.3 Wedge Solution Method with 100 and 50 simulations. 305
Table A1. Factors of Safety assigned to the sand and clay layers. 313
Table A2. PR elevations bounding the zero crossings for summation of forces. 316
Table A3. PR elevations bounding the zero crossings for summation of moments. 318
Table F1. Summary of 2008 preliminary I-Wall analysis results for varied heights of soil surface on the landside for an overly simplified and incomplete representation of wave load-induced pressures. 354

Preface

The engineering formulation and software programming reported herein was authorized by Headquarters, U.S. Army Corps of Engineers (HQUSACE), and was conducted from July 2014 through September 2017 under the Infrastructure Resiliency and Reliability Research Program (Work Unit CL618F). The Technical Director for the Infrastructure Resiliency and Reliability Research Program was Dr. Michael K. Sharp, U.S. Army Engineer Research and Development Center (ERDC), Geotechnical and Structures Laboratory (GSL). Dr. Maureen Corcoran, GSL Associate Technical Director, was the program manager for the Infrastructure Resiliency and Reliability Research Program. Funding was provided by the Infrastructure Resiliency and Reliability Research Program under the Flood and Coastal Storm Damage Reduction (FCSDR) Research and Development Program in the focus area title I-Wall Analysis. Dr. Julie D. Rosati was the Technical Director of the Coastal and Hydraulics Laboratory (CHL) for the FCSDR Program. The Program Manager for FCSDR was Dr. Julie D. Rosati, CHL.

The research discussed in this report was conducted by the Information Technology Laboratory (ITL), under the general supervision of Dr. Reed L. Mosher (retired) and Dr. David A. Horner (current) Director, ITL. Ms. Patti S. Duett was the Deputy Director, ITL. Additional general supervision was provided by Dr. Jerrell R. Ballard, Chief, Computational Science and Engineering Division (CSED), ITL, during software development.

Mr. Anjana Chudgar (HQ-retired), Mr. Kent D. Hokens, and Mr Neil T. Schwanz (retired), both of the USACE St. Paul District, were team members providing input and guidance on District needs during the course of this research.

COL Ivan P. Beckman was the Commander of ERDC, and Dr. David W. Pittman was the Director of ERDC.

Unit Conversion Factors

Multiply	By	To Obtain
cubic feet	0.02831685	cubic meters
cubic inches	1.6387064 E-05	cubic meters
degrees (angle)	0.01745329	radians
feet	0.3048	meters
inches	0.0254	meters
pounds (force)	4.448222	newtons
pounds (force) per square foot	47.88026	pascals
pounds (force) per square inch	6.894757	kilopascals
square feet	0.09290304	square meters
square inches	6.4516 E-04	square meters
square miles	2.589998 E+06	square meters

Acronyms and Abbreviations

1-D	One-Dimensional
2-D	Two-Dimensional
ASCII	American Standard Code for Information Interchange
CASE	Computer-Aided Structural Engineering
CCDF	Complementary Cumulative Distribution Function
CDF	Cumulative Distribution Function
CHL	Coastal and Hydraulics Laboratory
COV	Coefficient Of Variation
CSED	Computational Science and Engineering Division
CWALSHT	Computer Program for Design and Analysis of Sheet-Pile Walls by Classical Analysis
DoD	Department of Defense
el	Elevation
ERDC	Engineer Research Development Center
FCSDR	Flood and Coastal Storm Damage Reduction
FORTRAN	Formula Translating System
Ft	Foot/Feet
GSL	Geotechnical and Structures Laboratory
GUI	Graphical User Interface
HQUSACE	Headquarters, U.S. Army Corps of Engineers
ID	Identification
IPET	Interagency Performance Evaluation Task Force
ITL	Information Technology Laboratory
LHS	Left-Hand Side
.ohd	Output Header Designation
PLC	Piecewise Linear Curve
PR	Point of Rotation
PROSPECT	Proponent-Sponsored Engineering Corps Training

RHS	Right-Hand Side
R&D	Research and Development
SRC	System Response Curve
TR	Technical Report
SSI	Soil-Structure Interaction
SWL	Still-Water Level
USACE	U.S. Army Corps of Engineers

1 Analysis of an I-Wall in Fluvial, Riverine, and Coastal Environments

1.1 Introduction

Hurricane Katrina produced unparalleled wave and storm surge conditions for New Orleans, LA, and vicinities when it passed the area on the morning of 29 August 2005 (IPET 2007). To provide an understanding of the impact Hurricane Katrina had on the New Orleans Hurricane Protection System, the Interagency Performance Evaluation Task Force (IPET) was established by the Chief of Engineers. As a result of this study, a possible development of a zone of separation was identified, forming along the flood side of the soil-to-I-Wall interface as flood loading occurred (IPET 2007). In response to this discovery, Headquarters, U.S. Army Corps of Engineers (HQUSACE) recognized the lack of a method to fully evaluate I-Walls, and thereby, tasked the U.S. Army Engineer Research and Development Center (ERDC) with providing the USACE Districts the engineering capability to analyze and evaluate I-Wall performance in all geomorphic environments (fluvial, riverine, and coastal) where I-Walls exist. To meet this objective, the ERDC developed and designed the Corps_I-Wall software Version 2.0. Corps_I-Wall includes a PC-based Formula Translating System (FORTRAN) program, a graphical user interface (GUI), engineering processor, and visual post-processor. The Corps_I-Wall software is accessed using the CI-Wall executable program contained on ERDC's Knowledge Hub (https://knowledge.usace.army.mil) within the Computer-Aided Structural Engineering (CASE) community.

This version of Corps_I-Wall is used for the design of new I-Walls, or the analysis of existing I-Walls in fluvial, riverine, or coastal environments during flood loading. In coastal regions, the capability to analyze I-Wall performance to storm surge is of particular importance because of the potential destructive force of storm surge. Horizontally stratified soil layers are assumed for the Coefficient Method of analysis. The Wedge Solution Method of analysis allows for the specification of a non-level ground surface, non-level soil layers, and non-level piezometric surfaces. This Technical Report (TR) summarizes Corps_I-Wall, Version 2.0.

1.2 Background

Two previous numerical studies (IPET 2007; Pace et al. 2012) of complete soil-structure interaction (SSI) using nonlinear finite element analyses were conducted by ERDC that directly apply to developing Corps_I-Wall. The studies used different soils and cross sections. Dr. Robert Ebeling, of the ERDC-Information Technology Laboratory (ERDC-ITL), was the technical lead on both complete SSI studies and principal investigator on the second (Pace et al. 2012) study.

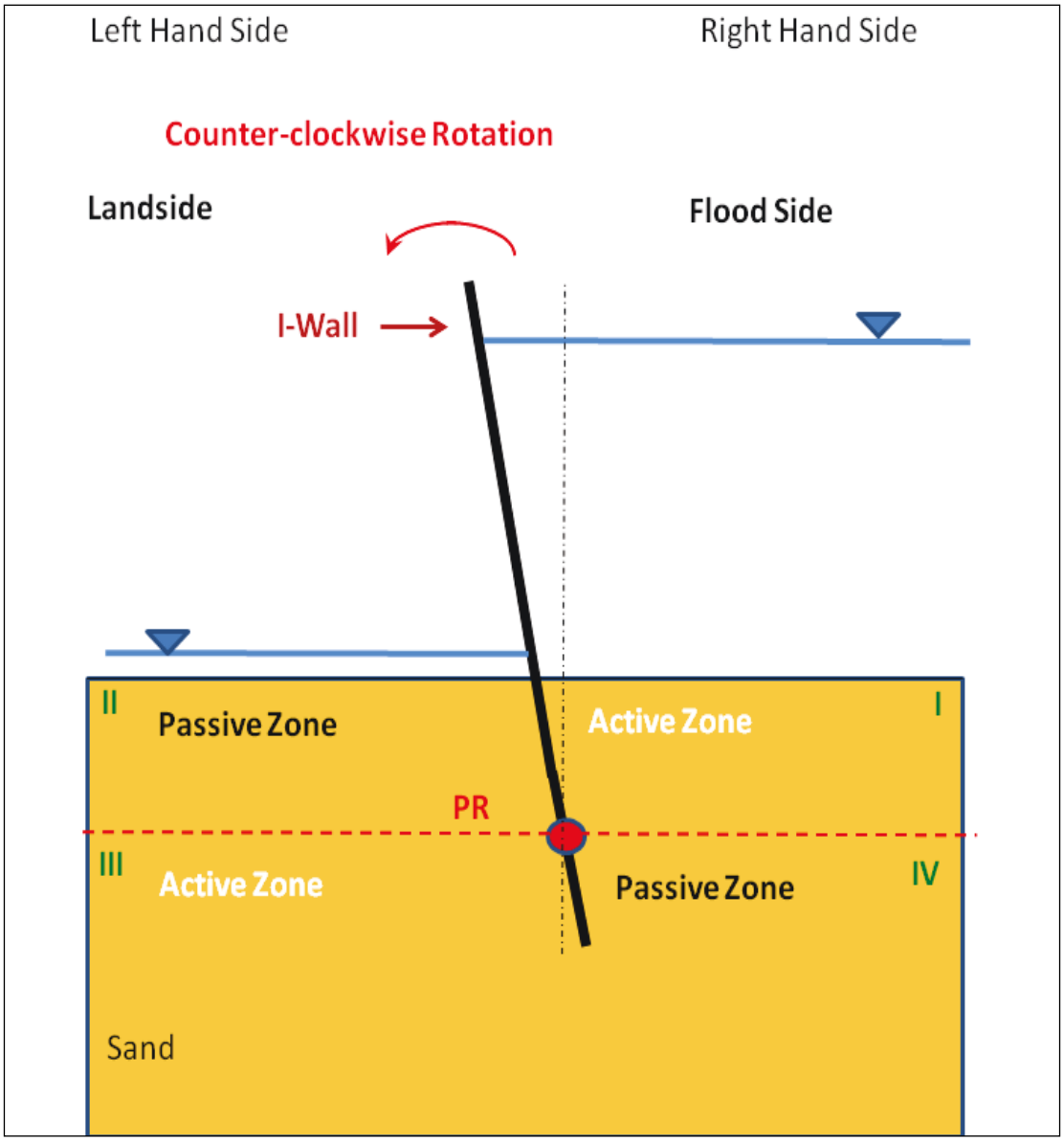
As part of the IPET (2007) evaluation, the first study devised a method to assess the implementation of a zone of separation in the complete SSI analyses of four different New Orleans I-Wall cross sections as floodwaters were raised (in 0.5 to 1 foot [ft] increments). The second study followed the same approach. The assessment included when, and to what depth, the zone of separation was expected to occur. Hydrostatic floodwater loading of the I-Wall due to floodwater penetration was then applied to understand the effect of loading on the zone of separation.

The second complete SSI numerical effort investigated I-Walls embedded in level ground consisting of four different soils that were stronger and stiffer than the fine-grained New Orleans soils (Pace et al. 2012). The different soils considered I-Walls founded in overconsolidated lean clay, stratified clays of high plasticity, homogenous clay, and silt of low plasticity.

Both the field observations of the New Orleans I-Walls made during the IPET (2007) study, and the results from the two complete SSI nonlinear finite element studies, demonstrated the need for the analysis to account for gap initiation and gap propagation on the flood side of an I-Wall as floodwaters rise. An important observation is revealed by these two complete SSI numerical studies of I-Walls designed according to USACE guidance, EM 1110-2-2504 (HQUSACE 1994): When an I-Wall possesses global stability and local stability of the I-Wall dominates the soil pressures acting on the I-Wall, there is a tendency for the I-Wall to rotate about a point (designated as point of rotation (PR) in Figure 1.1) that is often within the proximity of the sheet-pile tip. This deformation behavior results in the development of a passive soil zone on the flood side of the I-Wall, located between the point of I-Wall rotation and the sheet-pile tip (i.e., within Quadrant IV of Figure 1.1). In Figure 1.1, the quadrants are identified as zones of either (mobilized) active or (mobilized) passive earth pressures, and also include the side of the I-Wall where the soil zone exists. Quadrant I

is the soil zone labeled as the active zone on the flood side of the I-Wall. Quadrant II is the soil zone labeled as the passive zone on the landside of the I-Wall. Quadrant III is the soil zone labeled as the active zone on the landside of the I-Wall. Quadrant IV is the soil zone labeled as the passive zone on the flood side of the I-Wall.

Figure 1.1. Idealization of I-Wall rotation about a point of rotation (PR) within proximity of the sheet-pile tip during flood loading.

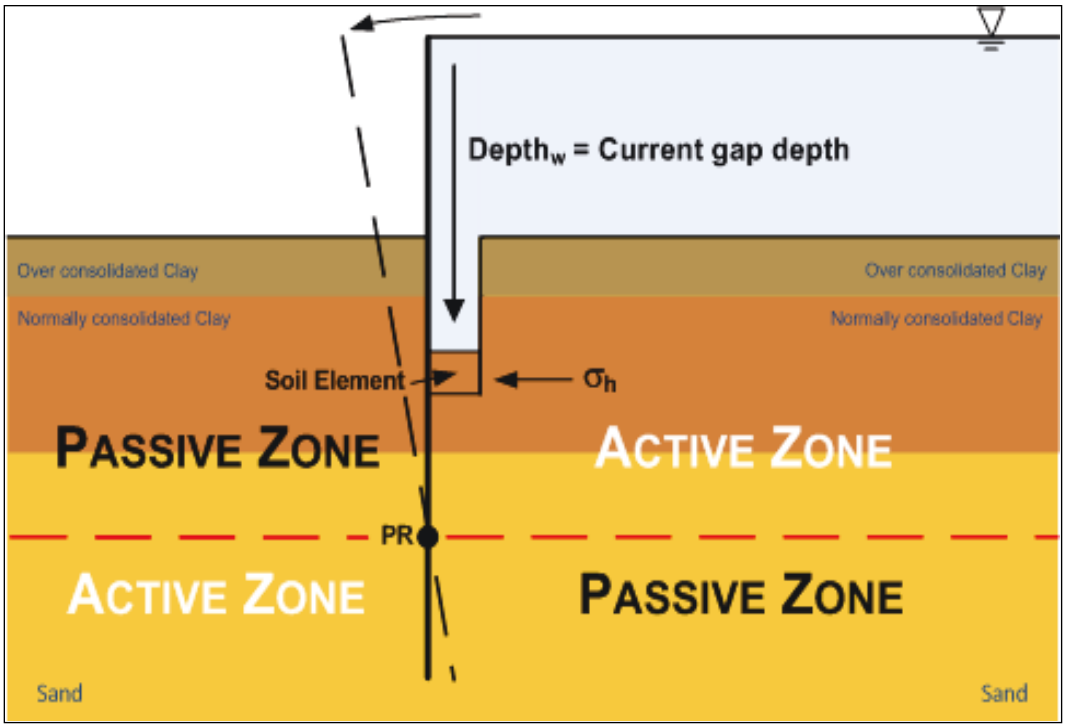


The completed SSI numerical studies also show a sufficiently large magnitude (mobilized) passive pressure within this zone (Quadrant IV, Figure 1.1) below the PR, this terminates the gap propagation of a cohesive

soil on the flood side of the I-Wall (if global instability and seepage along the sheet pile, or an underseepage-induced piping failure are not an issue).

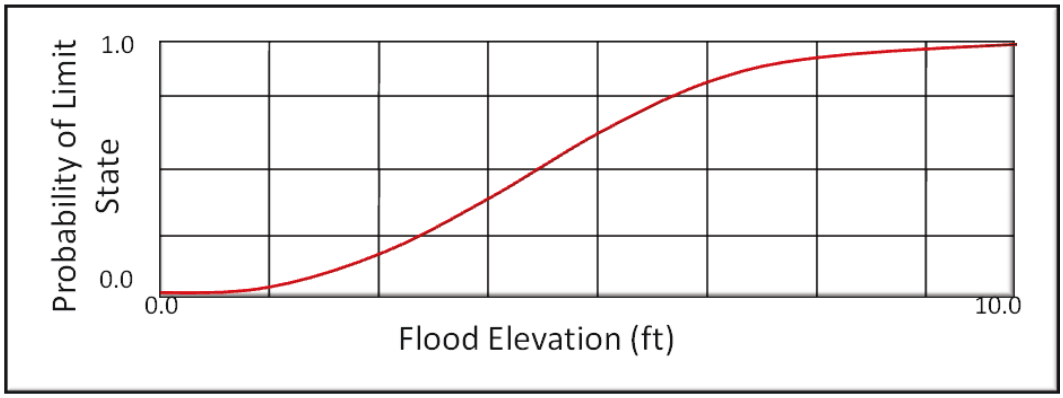
Thus, the ability to identify gap initiation and to propagate this gap on the flood side of an I-Wall is an important capability that has been implemented within the Corps_I-Wall engineering computational procedure of analysis (Figure 1.2).[1] This capability is especially needed for analyses where the flood elevation is increased for the different loading cases being considered, as is the case when constructing a system response curve (SRC) (sometimes referred to as a fragility curve) in a probabilistic fragility analysis (Figure 1.3). The SRC in (Figure 1.3) shows the probability of a rotational limit state range in magnitude between a value of 0 and 1.0, with a higher probability of failure occurring for higher flood elevations.

Figure 1.2. Schematic idealization of the consideration of stresses imposed on a soil element for a gap originating and propagating in an overconsolidated clay layer and stopping within the normally consolidated clay below (according to the method implemented within Corps_I-Wall).



[1] Appendix B describes the hydraulic fracture phenomenon applied in Corps-I-Wall to gap initiation/propagation.

Figure 1.3. Idealization of a system response curve (SRC) for an I-Wall during variable flood elevation loading from 0–10 ft.



1.3 Objective

The objective of this research is to devise engineering formulations and develop the corresponding software that provides a design depth of embedment for flood walls for a user specified Factor of Safety in a deterministic mode of analysis, including gap initiation and propagation on the flood side of the wall. In a probabilistic mode of analysis, distribution estimates for the depth of embedment of new flood walls are needed that consider variability in the Mohr-Coulomb shear strength parameters for the soils. For existing flood walls, probabilistic estimates for flood wall stability are needed to be expressed as a function of flood elevation, and to generate an SRC for the rotational stability limit state of a flood wall.

1.4 Approach

Recent development work at ERDC has produced a software product, (Corps_I-Wall) that performs deterministic or probabilistic designs for new or existing flood walls. Corps_I-Wall incorporates knowledge gained during the complete SSI studies of IPET (2007) and Pace et al. (2012) in devising gap initiation, and gap propagation criteria implemented in this software. The following section provides further details for this approach.

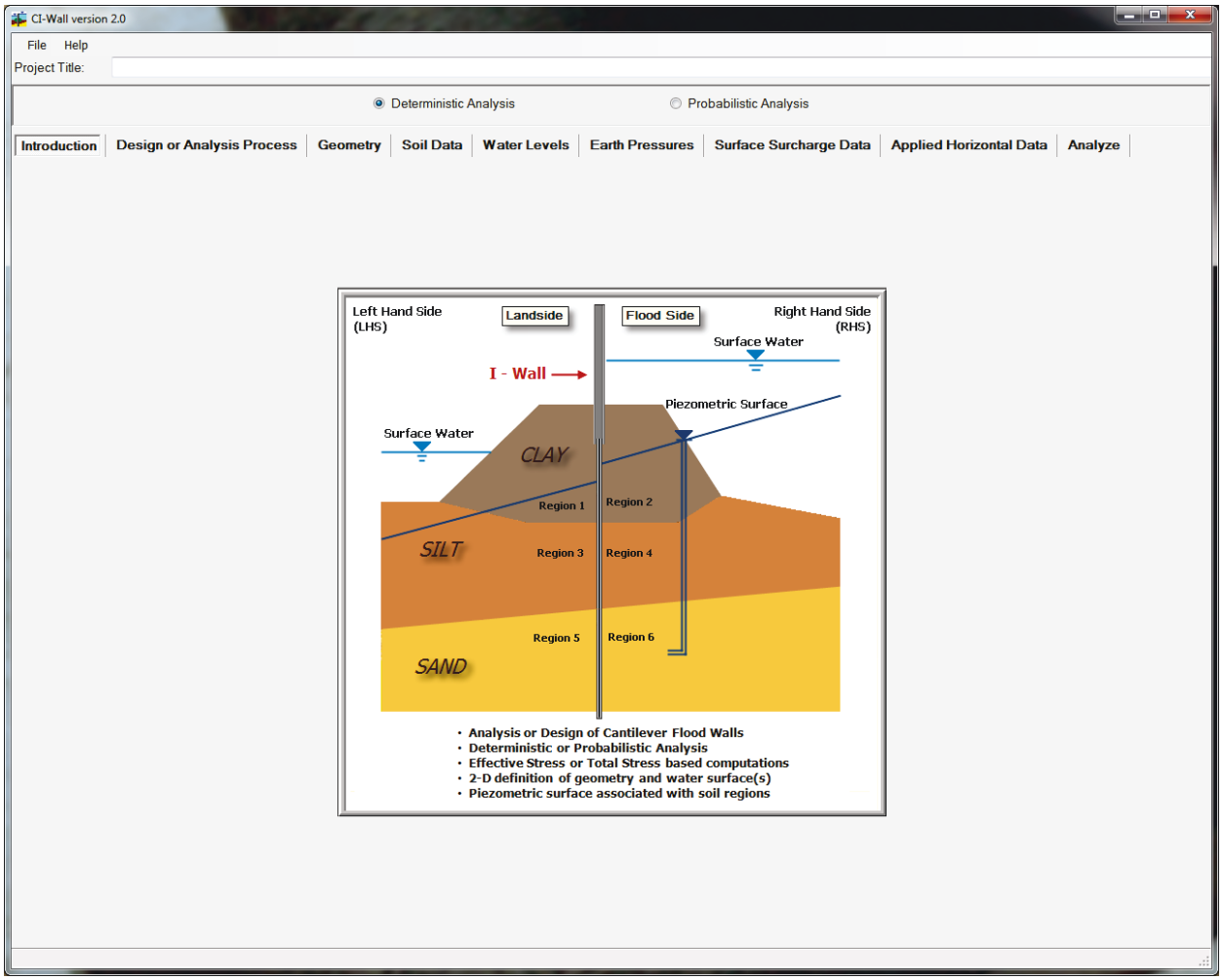
1.5 Overview of Corps_I-Wall

This section briefly describes selecting a method for analysis, *Deterministic* or *Probabilistic*, and includes the problem-solving capabilities within Corps_I-Wall. The purpose of this discussion is to provide the user with an understanding of the following engineering features involved in I-Wall analysis: layered soil strata, factors of safety, total or effective stress

analysis, piezometric surface or surface water, gap initiation/propagation, clockwise or counterclockwise, I-Wall rotation, boundary pressures, point loads, and methods for computing the earth pressure coefficient. Figure 1.4 depicts the engineering features relevant to an analysis within Corps_I-Wall. The capability of Corps_I-Wall to evaluate a coastal problem is also described.

The visual modeler for Corps_I-Wall is tab-based (Figure 1.4). Nine tabs define the I-Wall problem configuration and the input of the soil properties: *Introduction*, *Design or Analysis Process*, *Geometry*, *Soil Data*, *Water Levels*, *Earth Pressures*, *Surface Surcharge Data*, *Applied Horizontal Data*, and *Analyze*. For a detailed discussion of these tabs, refer to Chapter 3.

Figure 1.4. Corps_I-Wall Version 2.0 for level and non-level ground GUI.



Deterministic or Probabilistic - When selecting a method for analysis, either Deterministic or Probabilistic[1], the user must consider the inherent aleatoric uncertainty of soil properties. In Corps_I-Wall, the floodwall loading conditions on I-Walls can be analyzed for a deterministic problem and for a probabilistic method of analysis based on consideration of the inherent aleatoric uncertainty of soil properties. In a deterministic I-Wall design or analysis, all user-specified input for the shear strength parameters of the soils is made with absolute certainty in their assigned values. In a probabilistic analysis, the user has the ability to account for uncertainty in the soil's shear strength parameters by specifying for each variable in each soil region, a mean value, its standard deviation, and its distribution type (e.g., truncated normal, logarithmic normal, or uniform). When the user **conducts** an *Analysis* of an existing I-Wall for a user-specified sheet-pile tip elevation while the *Probabilistic* feature is **selected**, a Fragility Analysis is performed. The computations result in construction of a SRC (Figure 1.3). This SRC depicts the probability of a rotation about a point along the embedded portion of the sheet-pile wall as a function of flood elevation. In a safety or risk assessment of I-Walls, the rotational limit state or probability of rotational failure of the I-Wall about a point along the embedded portion of the sheet-pile wall serves as a *yardstick* of floodwall system performance. As stated previously, the SRC is used to predict the probability of failure, given the flood hazard (Figure 1.3).

When the user **conducts** a *Design* of a new I-Wall for a user-specified sheet-pile tip elevation while the *Probabilistic* feature is **selected**, a Fragility Analysis is performed. With appropriate consideration of uncertainty in the shear strength parameters for the soils, both the force and moment equilibrium computations result in a statistical distribution for sheet-pile tip elevation. This distribution provides the mean and variance of sheet-pile tip depths for interpretation by the design engineer. The engineer can see this distribution in a histogram plot (Figure 3.85) (mentioned here for reference but included in Chapter 3 for detailed discussion).

Layered Soil Strata - Corps_I-Wall has the ability to analyze level ground soil sites (e.g., floodplains) and non-level ground soil sites (i.e., riverbanks, levees, etc.) with layered soil strata. The boundary between each of the user-specified soil layers is user specified. The soil strata are referred to as soil regions within the Corps_I-Wall formulation. Although

[1] Refer to the user's selection option for selection of either probabilistic or deterministic analysis located above the labels for the nine tabs shown in Figure 1.4

the I-Wall may be embedded within a single soil stratum, the following two different soil regions are specified: 1) on the flood side of the I-Wall, and a 2) on the landside of the I-Wall. For multiple soil strata, the number of soil regions is generally twice the number of soil strata.

Factors of Safety - In the *Design* mode, Corps_I-Wall allows the user to specify a value for the Factor of Safety to be used in active earth pressure computations (FS_{active}), and a value for the Factor of Safety to be used in passive earth pressure computations ($FS_{passive}$). The value for FS_{active} is typically set equal to 1.0 in a Corps I-Wall Design according to EM 1110-2-2504 (HQUSACE 1994). In an *Analysis*, the user **specifies** the elevation of the sheet-pile tip, then the corresponding value of Factor of Safety for the two passive earth pressure zones ($FS_{passive}$) (Figure 1.1) is computed. The user is allowed to specify the value for the active earth pressure computations (FS_{active}), but the value is typically set to 1.0 according to EM 1110-2-2504.

These Factors of Safety are applied to the Mohr-Coulomb total stress-based shear strength parameters c and φ (or c' and φ' in an effective stress based strength definition), and interface friction angle δ (or δ') which define the mobilized shear strength parameters c_{mob}, φ_{mob} and δ_{mob} (or c'_{mob}, φ'_{mob} and δ'_{mob}) used to compute the mobilized active and passive earth pressures action on the I-Wall/sheet-pile wall. For each soil region type, the mobilized active and passive earth pressure coefficients, $(K_{active})_{mob}$ and $(K_{passive})_{mob}$ are defined by the values of φ_{mob} and δ_{mob} for a total stress material type assigned to the soil region (or by φ'_{mob} and δ'_{mob} for an effective stress material type).

Total or Effective Stress Analysis - Total stress, or effective stress-based soil strength properties used for computing earth pressure coefficients are specified for each material type. Moist and saturated soil unit weights are specified by the user for each soil material type. A specific material type number is assigned to each soil region. Different soil regions may be assigned the same material type number designation. The total, and/or effective stress-based soil regions can be intermixed in the I-Wall/ sheet-pile wall model.

Within an *Effective Stress*-designated material type that is assigned to a particular soil region, the total vertical overburden pressures are combined with pore water pressures, a cohesion value (if any), a sheet-pile-to-soil interface friction value (if any), and a horizontal earth pressure coefficient

to obtain the distribution of horizontal earth pressures acting normal to the face of the sheet-pile wall within each soil region. Within a soil region containing a *Total Stress* designated material type, pore-water pressures are excluded from these computations.

Piezometric Surface or Surface Water - Either a *Piezometric Surface* or a *Surface Water* elevation may be assigned to each region. During the vertical earth pressure computations, saturated unit weights are assigned to soil elevations that lie below the *Piezometric Surface* (or *Surface Water*) in the computations for each soil region. If the *Piezometric Surface* (or *Surface Water*) lies within the soil region, then moist soil unit weights are used in the vertical total overburden stress computation for soil elevations above the *Piezometric Surface* (or *Surface Water*) elevation, with saturated soil unit weights assigned below this elevation and down to the bottom of this region. If no *Piezometric Surface* (or *Surface Water*) is assigned to a soil region, then the moist unit weight of the soil is used in the vertical total overburden stress computations made within this region.

Pore-water Pressures - Corps_I-Wall contains a feature to compute pore-water pressures acting on the landside and flood side faces of the I-Wall, assuming either 1) the hydrostatic water pressures of a "no flow" condition within various soil regions, or 2) the water pressures computed by means of steady-state seepage analysis within a homogenous, or a heterogeneous, multilayered soil regions system exist.

- *Hydrostatic*: In the case of hydrostatic water pressure, a *Piezometric Surface* is assigned to the soil region, and the pore-water pressures at any point within the region are computed as equal to the unit weight of water, γ_w, times the depth from the *Piezometric Surface* to that point in the soil at which the computation is being made. A *Surface Water* elevation may be assigned in lieu of a *Piezometric Surface* elevation to the strata.
- *Seepage*: Assuming steady-state flow, pore-water pressures along the entire wetted perimeter of the I-Wall (i.e., on both faces), total heads are computed from the results of a simplified steady-state flow analysis using the line of seepage (a.k.a. line of creep) method of analysis. Use of Bernoulli's equation allows for the conversion of total heads into pore-water pressures. To conduct this analysis, values for hydraulic conductivity are assigned to every soil strata, including any stratum defined as a *Total Stress* material zone.[1] The user specified value for

[1] For those stratum designated as a *Total Stress* material zone, pore-water pressures are computed during a steady-state line of seepage analysis, but they are not assigned during the earth pressure computations

hydraulic conductivity is not required to be the same for the material types assigned to the different soil regions. In the line of seepage analysis, no more than one *Surface Water* elevation (or *Piezometric Surface* elevation) is assigned to the right-hand side (RHS) of the I-Wall and no more than one is assigned to the left-hand side (LHS). The procedure of steady-state, line of seepage analysis implemented in Corps_I-Wall is described in Appendix C. Note that the steady-state seepage analysis is restricted to level ground sites and use of the Coefficient Method of analysis. Seepage analysis is not performed under the Wedge Solution Method of analysis.

Gap Initiation/Propagation - Corps_I-Wall accommodates gap initiation/propagation emanating at the ground surface on the flood side of the I-Wall. A surface water elevation at, or above the ground surface on the flood side of the I-Wall is required for a gaping to initiate. Cohesive soil properties (either effective or total stress based) are required on the flood side of the wall to allow for the potential of gap development. It is a top down method of analysis, therefore, the gap starts at the ground surface and proceeds downward. A gap moves progressively deeper from the upper-most stratum down to the next (e.g., intermediate) stratum down, and so forth. It does not skip by this intermediate strata on to the lower strata. A gap can be engaged in either a hydrostatic or line of seepage type of analysis.

Clockwise or Counterclockwise I-Wall Rotation - Corps_I-Wall has the ability to accommodate either a clockwise or a counterclockwise I-Wall rotation. The direction of I-Wall rotation is dictated by the direction of net loading and its corresponding moment applied to the I-Wall.[1] Logic was developed to ascertain the direction of I-Wall rotation based upon the flood and earth loading specified for the problem. This capability was specifically developed to accommodate the coastal problem when the magnitude of user-specified surge water pressure (i.e., height of design storm surge wave) can alter the direction of I-Wall rotation relative to the calm water design case. The direction of rotation is determined internally by Corps_I-Wall, and reported in the output information contained within the *Analysis* tab.

within the *Total Stress* zone(s). For a mixed soil layers of *Total Stress* and *Effective Stress* zones, computed pore-water pressures are only assigned to the soil regions designated as an *Effective Stress* zone.

[1] To determine the direction of I-Wall rotation, the moment for the net loading is computed about the lower of the RHS or LHS ground surfaces.

Boundary Pressures - Horizontal and/or vertical boundary pressure distributions may be specified. For coastal problems, a horizontal boundary pressure distribution is used to represent the storm surge in a Corps_I-Wall analysis. Vertical boundary pressures are typically used to represent surcharge(s).

Point Loads - Horizontal and/or vertical point loads per ft run of wall (often referred to as line loads in this type of two-dimensional [2-D] analysis) may be specified.

Methods for Computing the Distribution of Active and Passive Earth Pressures - Corps_I-Wall Version 2.0 contains a feature to compute active and passive earth pressure distributions acting on the embedded landside and flood side faces of the sheet-pile wall using either 1) the earth pressure Coefficient Method of analysis, or 2) by using the Wedge Sloution Method of analysis.

- *Coefficient Method of Analysis:* Within each soil region, the horizontal earth pressure acting normal to the sheet-pile wall is computed using 1) the vertical overburden pressure, 2) the earth pressure coefficient for the soil, 3) the soil's cohesion value, 4) the sheet-pile-to-soil interface friction value, and when conducting an *Effective Stress* analysis, the 5) the pore-water pressure.[1] The Corps_I-Wall Coefficient Method of analysis allows the user to request that the passive earth pressure coefficient ($K_{passive}$), this is used in the horizontal earth pressure computations for the two mobilized passive zones identified in Figure 1.1. These are computed by the 1) Rankine theory, 2) Coulomb theory, or 3) a logarithmic spiral procedure. The appropriateness for selecting the computational method to use depends upon the value of interface friction between the soil and the sheet-pile (δ) relative to the value for the angle of internal friction, φ. Table 1.1 provides general guidance using information from Dr. Ebeling's lecture on *Earth Pressure Theory* that is taught annually in the Proponent-Sponsored Engineering Corps Training (PROSPECT) SSI course provided at ERDC in Vicksburg, MS.

[1] The complete equations used to compute the horizontal earth pressure acting normal to the sheet-pile-to-soil interface in a *Total Stress* or an *Effective Stress* analysis are given in Chapter 2 for the Coefficient Method of analysis.

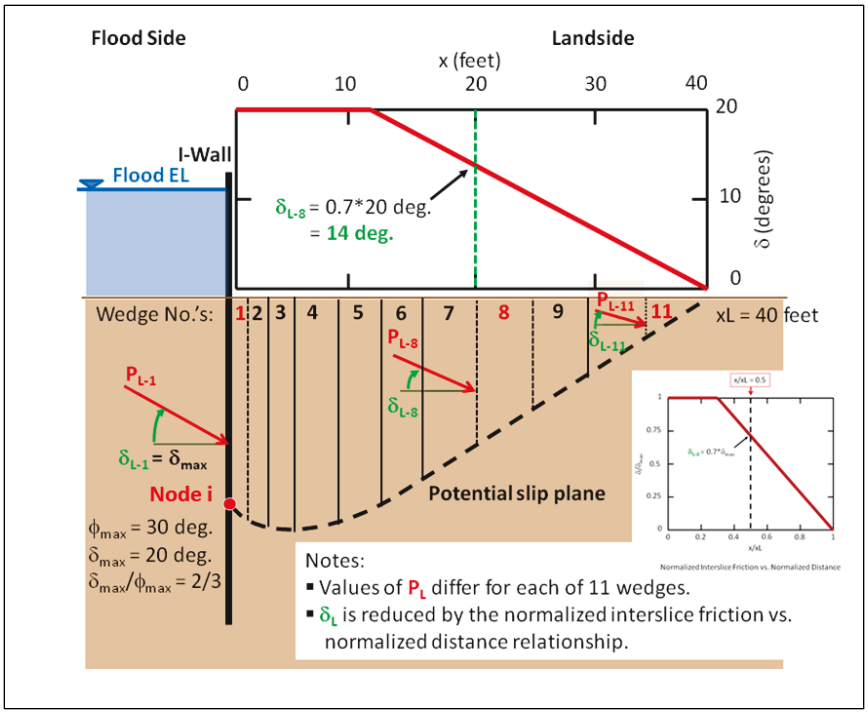
Table 1.1. Appropriate method for computing the passive earth pressure coefficient, $K_{passive}$, as a function of the magnitude of the interface friction, δ, between the soil and the sheet pile and in comparison to the magnitude of the soil's angle of internal friction, φ.

δ greater than φ/2	Use coefficients from logarithmic spiral procedure.
δ less than or equal to φ /2	Use coefficients from logarithmic spiral procedure, or Coulomb theory, or trial wedge procedure.
δ equal to 0	Use coefficients from logarithmic spiral procedure, or Coulomb theory, or trial wedge procedure, or Rankine theory.

It is important that the Table 1.1 guidelines are adhered to so that an unconservative, overestimate of the mobilized passive earth pressures is not made within the two passive zones identified in Figure 1.1. An overestimate for the $K_{passive}$ value(s) would result in a calculated depth of sheet-pile embedment shallower than is actually required.

- *Wedge Solution Method of analysis:* The *method of slices* (Duncan et al. 2014; Abramson et al. 1996) is the specified procedure used to determine the active and passive earth forces acting on the sheet-pile wall, with each slice corresponding to the earthen wedges used in the analysis (e.g., for Figure 1.5, passive earth force corresponding to a depth of Node i). These passive (and similarly, active) wedge computations are made at several nodes spaced down the embedded portion of the sheet-pile wall, and along the front and back sheet-pile faces. In companion active earth force analyses, a planer potential slip surface is assumed (not shown). Once the distribution (with depth) of passive and active forces with depth are determined, these two force distributions are numerically differentiated in order to obtain distributions of active and passive earth pressures with depth along the wall. Details regarding the Wedge Method procedure of analysis implemented in Corps_I-Wall is described in Appendix G.

Figure 1.5. Idealized example of a potential logarithmic spiral slip plane used to define an idealized eleven wedge soil mass for use in a passive earth force computation from the landside ground surface to a depth of Node i.



Coastal Problem - The PC-based Corps_I-Wall Visual Modeler package includes the capability to analyze coastal problems. The capability to model storm surge on I-Wall performance is of particular importance because of the destructive force of storm surge. The calculation of coastal surge pressures acting on an I-Wall is discussed in Appendix F for a breaking wave example. Breaking waves or nonbreaking waves may be specified in the I-Wall rotational stability analysis. Wave loading is specified as a pseudo-static water pressure force along the vertical exposed face of the I-Wall being analyzed. This software program allows the engineer to rapidly make an accurate assessment of the effects of storm surge on I-Walls and to add a protective berm when deemed necessary.

1.6 Overview of the *Design* and *Analysis* modes

This section provides background on the *Design* or *Analysis* mode. For information on the other tabs, refer to Chapter 3.

Corps_I-Wall can be used to either design a new I-Wall or analyze an existing I-Wall. The functionality of Corps_I-Wall includes a *Design* or *Analysis* mode of stability analysis. The *Design* mode is used to design

new I-Walls. This mode computes the required depth of embedment, and the shear and moment demands internal to the I-Wall/sheet-pile structural system. These computed results are then used to size the sheet-pile for the user-prescribed flood loading. The *Analysis* mode is used to evaluate existing I-Walls with a known depth of embedment. The primary unknown is the Factor of Safety contained within the two mobilized passive zones (identified in Figure 1.1).

This subsection provides an overview of the iterative procedures used in both the *Design* mode and the *Analysis* mode solution formulations of Corps_I-Wall.

1.6.1 *Design* mode

Corps_I-Wall can be used to design a new I-Wall. The primary series of computations are used to determine the required depth of sheet-pile embedment for the user-prescribed flood loading. An iterative procedure computes the required depth of penetration in a *Design* mode. This calculation procedure proceeds as follows:

1. A trial depth of penetration is established by Corps_I-Wall. For this trial depth of penetration the following occur:
    a. Distributions of surface water pressures, gap water pressures, and pore-water pressures (for the effective stress designated soil regions) are established along both the LHS and the RHS of the I-Wall (Figure 1.1).
    b. The net water pressure distribution is calculated by taking the difference between the water pressures acting along the two sides of the I-Wall.
    c. Active and mobilized passive earth pressures distributions are established along both sides of the I-Wall.
    d. A calculation is made (internal to Corps_I-Wall) using the applied water and (active and factored passive) earth pressure distributions, to determine if the I-Wall will rotate clockwise or counterclockwise.
2. An initial trial PR is assigned (for the first computation) to a point just below the ground surface.[1] For this trial PR the following occur:
    a. The net active pressure distribution is formed within the soil region(s) on the side the I-Wall rotates away from. In Figure 1.1 this is labeled

[1] Note that the PR cannot be at or below the trial sheet-pile tip elevation in a Corps_I-Wall rotational

the flood side (i.e., the right-hand side). It consists of the active pressure on the side that the I-Wall rotates away from (Quadrant I labeled Active Zone in Figure 1.1 on the flood side) minus the mobilized passive pressure on the side the I-Wall rotates into (Quadrant II labeled Passive Zone in Figure 1.1 on the landside). The net water pressure distribution, along with any external horizontal net pressures and/or overburden induced horizontal pressures, if present, are added on this diagram.

b. The net passive pressure distribution is also formed deep on the side that the I-Wall rotates away from. In Figure 1.1, this is labeled the flood side (i.e., the right-hand side). It consists of the mobilized passive pressure (Quadrant IV labeled Passive Zone in Figure 1.1 on the flood side) below the PR minus the active pressure (Quadrant III labeled Active Zone in Figure 1.1 on the landside) below the PR. The net water pressure distribution, along with any external horizontal net pressures and/or overburden induced horizontal pressures, if present, is added on this diagram.
c. The net active pressure distribution becomes the net pressure distribution, down to the trial PR. At the sheet-pile tip, the value for the net passive pressure diagram at this elevation becomes the value for net pressure.
d. Between the trial PR elevation and the sheet-pile tip, the net pressure diagram is assumed linear.
e. The net pressure diagram is then converted into equivalent nodal point forces. Horizontal equilibrium and moment equilibrium (about the trial PR) is checked.
f. If there is a force imbalance and/or a moment imbalance, the trial PR is moved down the sheet-pile wall by a small increment, and Step two is repeated.

3. Should this trial PR reach the elevation for the trial sheet-pile tip in this iterative process, then the program returns to Step one. The trial sheet-pile tip elevation is moved downward by a small increment, and Step two is started again with a trial PR established just below the ground surface.
4. Convergence of the trial sheet-pile tip and trial PR on their final values is achieved when the force and moment imbalances are within tolerances.

stability analysis. Corps_I-Wall Version 2.0 does not perform a global stability assessment.

1.6.2 *Analysis* mode

The *Analysis* mode is used to evaluate existing I-Walls. Existing I-Walls possess a known depth of embedment. Therefore, the primary unknown is the Factor of Safety contained within the two mobilized passive zones ($FS_{passive}$) identified in Figure 1.1. An iterative procedure is used to calculate the value for $FS_{passive}$. This procedure is as follows:

1. Assume a trial value for $FS_{passive}$. The procedure usually starts with $FS_{passive} = 1.5$.
2. Use the *Design* mode to compute an imaginary sheet-pile tip elevation.
3. If the imaginary sheet-pile tip elevation computed via the *Design* mode is above the actual sheet-pile tip elevation of the existing I-Wall, reduce the trial $FS_{passive}$ value. If the imaginary sheet-pile tip elevation computed via the *Design* mode is below the actual sheet-pile tip elevation of the existing I-Wall, increase the trial $FS_{passive}$ value.
4. Repeat Step two until the imaginary sheet-pile tip elevation is within a small tolerance of the actual sheet-pile tip elevation.

2 Engineering Formulation

The engineering formulation used in Corps_I-Wall Version 2.0 software's Coefficient Method of analysis for a floodplain I-Wall embedded in horizontally stratified soil layers during flood events is discussed in this chapter. This discussion includes the relationships used to compute the horizontal water and earth pressures acting normal to the freestanding and embedded regions of the I-Wall. The earth pressure coefficient relationships used in computing earth pressures and how water pressures are included in the calculations are also included in the discussion. Key details regarding the procedure of rotational stability analysis are also described. Relationships for converting the different types of surcharge pressures and line loadings into horizontal loads acting on the I-Wall are summarized. Last, the procedure used to compute the shears and moments internal to the I-Wall/sheet-pile wall is provided.

The engineering formulation used in the Wedge Method of analysis is summarized in Appendix G. The Wedge Method computes results for non-level ground surfaces, non-level soil layers, and non-level piezometric surfaces.

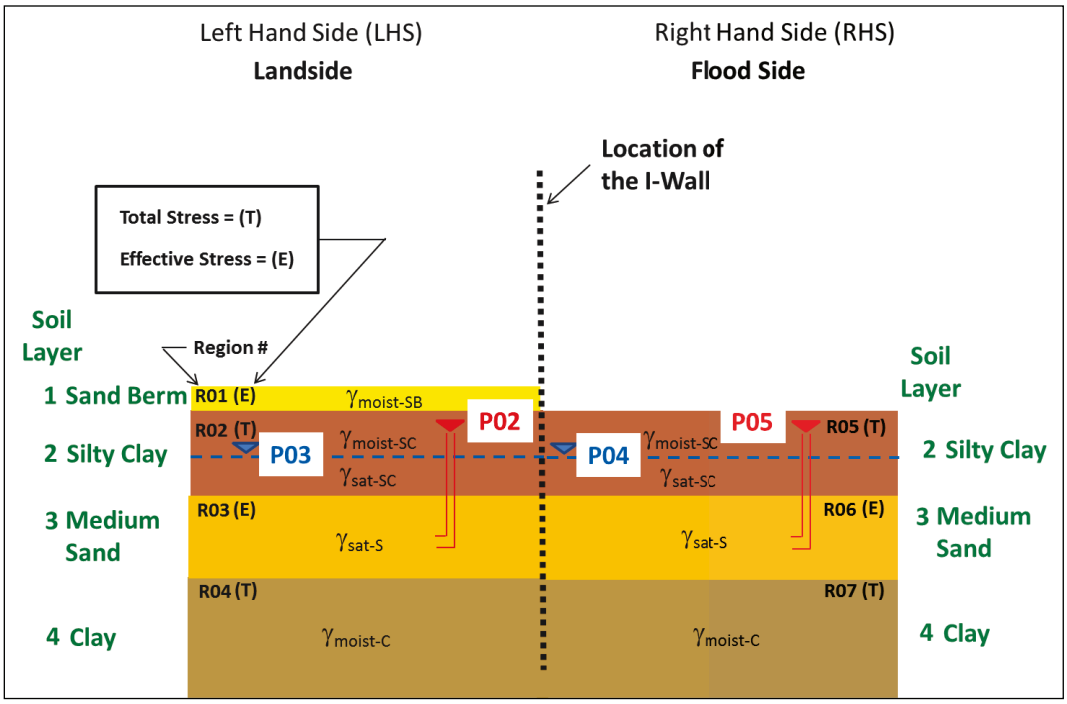
2.1 Layered soils site model

Using the Coefficient Method of analysis, Corps_I-Wall Version 2.0 is able to model and design I-Walls to be embedded within a horizontally-stratified soil site. Figure 2.1 depicts a typical site configuration for which the Coefficient Method of analysis would be used to design the I-Wall for rotational stability and compute the minimum depth of sheet-pile embedment. The soil stratum where the I-Wall is to be embedded consists of the following three different types: 1) silty clay, 2) medium sand, and 3) clay. The I-Wall is to be buttressed on the landside (i.e., left-hand side) by a shallow sand berm. The ground surface interfaces between soil layering, surface water (when present), and piezometric surfaces, all are modeled as horizontal interfaces in the Coefficient Method of analysis.

The upper soil layer at the site shown in Figure 2.1 consists of silty clay. The left-hand side of Figure 2.1 is depicted as Region R02, and the RHS is Region R05 for the silty clay. A piezometric surface exists about mid-elevation within this layer, this separates the moist and saturated zones with unit weights of $\gamma_{moist\text{-}SC}$ and $\gamma_{sat\text{-}SC}$, respectively. Even though the soil

layer is the same for both regions, the software requires separate LHS and RHS region numbers, and separate piezometric surface numbers (i.e., P03 and P04). The Corps_I-Wall GUI will automatically generate each of the pair of region and piezometric surface numbers. The horizontal earth pressures are computed using total stress analysis (to be discussed in the next subsection).

Figure 2.1. I-Wall site model configuration for Corps_I-Wall Version 1.0 absent any flood loading.



The middle soil layer (soil layer 3) consists of medium sand. On the LHS of Figure 2.1, it is depicted as Region R03 and on the RHS as Region R06. Due to access by this soil layer to a water source beyond the extent of this section, the piezometric surface within this soil layer rises to a head that is above the top of this layer. The LHS and RHS piezometric surface numbers are P02 and P04, respectively, and are at the same elevation. The saturated sand soil unit weight of $\gamma_{sat\text{-}S}$ is input as a material property by the user and assigned to the two respective soil regions. The horizontal earth pressures are computed using effective stress analysis (to be discussed in subsection 2.2).

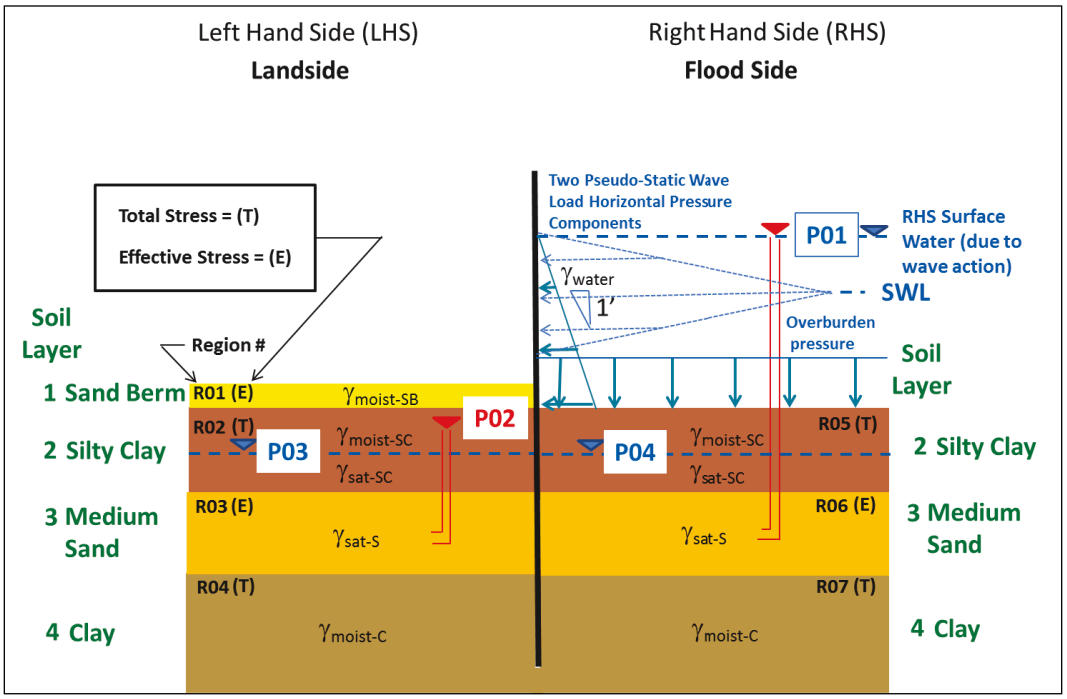
The lowest soil layer (soil layer 4) consists of clay. On the LHS of Figure 2.1, the layer is depicted as Region R04 and on the RHS, as Region R07. No piezometric surface is assigned to this soil layer. The moist clay soil unit weight of $\gamma_{moist\text{-}C}$ is input as a material property by the

user and assigned to the two respective soil regions. The horizontal earth pressures are computed using total stress analysis.

A sand berm is to be added landside during construction of the I-Wall. On the LHS of Figure 2.1, it is depicted as Region R01. No piezometric surface is assigned to this soil layer. The moist sand unit weight of $\gamma_{moist\text{-}SB}$ is input as a material property by the user and assigned to the single berm soil region. The horizontal earth pressures are computed using effective stress analysis.

Figure 2.2 shows the I-Wall site from Figure 2.1 configured with temporary flood loading (i.e., short-term loading), including the wave action on the RHS of the I-Wall. The rotational stability analysis scenario will be evaluated using the Corps_I-Wall Coefficient Method of analysis. The minimum depth of sheet-pile embedment will be computed during the design process by the software at this layered soil site.

Figure 2.2. I-Wall flood load problem model setup for a Corps_I-Wall Coefficient Method of analysis, including wave loading.



The Figure 2.2 site configuration expands on the Figure 2.1 site details to accommodate a flood of short duration (i.e., several days) to the RHS of the I-Wall. The following changes from Figure 2.1 include:

The addition of a rise in still-water level (SWL) on the RHS of the I-Wall.

The application of two pseudo-static wave load horizontal pressure components to account for the effects of wave loading on the I-Wall. A pseudo-static procedure in Corps_I-Wall is used in a design to represent a dynamic event, such as either breaking or nonbreaking waves. This procedure is discussed in Appendix F. These two components of horizontal pressure distributions act normal to the RHS of the I-Wall, as shown in Figure 2.2.

Because the middle soil layer of medium sand responds to the water heads of the surface water and flood conditions, Region R06, on the RHS, is now subjected to a piezometric head corresponding to the surface water elevation. This piezometric surface is designated as number P01 by the Corps_I-Wall GUI.[1]

Table 2.1 summarizes the soil layers, piezometric surface definitions, and material property specifications for a Corps_I-Wall Version 1.0 model setup for the Figure 2.2 I-Wall flood loading problem.

Table 2.1. I-Wall flood loading problem soil layering, piezometric surface definitions, and material property specifications for a Corps_I-Wall Version 1.0 model setup.

I-Wall Side	Region No.	Piezometric Surface No.	Soil		Soil Unit Weight		(T) or (E)[a]
			Layer No.	Type	Above the Piezometric Surface	Below the Piezometric Surface	
LHS	R01	None	1	Sand Berm	$\gamma_{moist\text{-}SB}$	-	(E)
	R02	P03	2	Silty Clay	$\gamma_{moist\text{-}SC}$	$\gamma_{sat\text{-}SC}$	(T)
	R03	P02	3	Medium Sand	-	$\gamma_{sat\text{-}S}$	(E)
	R04	None	4	Clay	$\gamma_{moist\text{-}C}$	-	(T)
RHS	R05	P04	2	Silty Clay	$\gamma_{moist\text{-}SC}$	-	(T)
	R06	P01[b]	3	Medium Sand	-	$\gamma_{sat\text{-}S}$	(E)
	R07	None	4	Clay	$\gamma_{moist\text{-}C}$	-	(T)

[a] Total Stress (T) or Effective Stress (E) region.

[b] The elevation of P01 on the RHS of the I-Wall is set equal to the surface water elevation in this example. The piezometric surface is obtained from the water surface and is, therefore, labeled in blue. The RHS medium sand, Region R06, is in contact with the floodwater (not shown). Consequently, the pore-water pressures within this region are controlled by the floodwater.

[1] Whenever surface water is specified, the Corps_I-Wall GUI always designates it with the label P01. P01 has values for the surface water levels on both the LHS and RHS of the I-Wall. Piezometric surfaces other than the surface water level only have values for the LHS or RHS, but not both.

2.2 Types of analysis used to define earth pressures

Total stress, or effective stress based soil strength properties that are used for computing earth pressure coefficients are specified for each material type. Thus, two different methods are used to compute the magnitude of the earth pressures acting on the embedded sheet-pile portion of the I-Wall based on which is specified, total or effective stress.

Each of the seven soil regions in Figure 2.2 is assigned a soil material type. Each material type is identified by a material type number that is assigned using the Corps_I-Wall GUI (discussed in Chapter 3). At the discretion of the user, horizontal earth pressures acting normal to the embedded sheet-pile wall portion of the I-Wall are based on either total stress, or effective stress. Total stress - or effective stress-based soil strength properties are used for computing earth pressure coefficients and are specified for each material type.

Points along the center line of the vertical Figure 2.2 I-Wall/sheet-pile wall are discretized in two phases. The first phase is to define an initial set of nodal points at elevations corresponding to top and bottom region elevations, surface water and/or piezometric surface elevations, points of horizontal traction pressures, and/or point/line loads. This occurs for both sides of the I-Wall. The second phase adds additional nodes below each of the initial node segments at approximately every foot,[1] and then sequentially connects all of the nodes by a series of vertical I-Wall/sheet-pile wall line elements. On each side of the I-Wall/sheet-pile wall, and at each nodal elevation, computations are made of the 1) net water pressures, and 2) net soil pressure distributions acting normal to the vertical I-Wall/sheet-pile wall line model, along with 3) the net external horizontal forces (or pressures), and 4) horizontal forces due to external overburden pressures acting on an elevation behind the sheet-pile wall. Each is then converted into equivalent nodal point forces using the one-third/one-sixth relationship.[2] Force and moment equilibrium are imposed on this I-Wall model in order to compute either (a) the minimum depth of sheet-pile penetration (in *Design* mode), or (b) the Factor of Safety applied to the mobilized shear strength(s) of the soil region(s) when computing passive earth pressures (in *Analysis* mode).

[1] The nodal point discretization may be revised in subsequent versions.

[2] The one-third/one-sixth force computation is discussed in Section 2.4.

Total stress - or effective stress-based soil strength properties are used for computing the earth pressure coefficients.[1] These earth pressure coefficients are then used by the software to compute the horizontal earth pressures acting normal to the I-Wall/sheet-pile wall. The details of these two series of calculations are different, depending upon if the soil region is defined as either total stress or effective stress material type. However, both computation processes start with the calculation of the total vertical stress acting within the soil adjacent to each node. This evaluation process is made for each node and for each side of the I-Wall/sheet-pile wall.

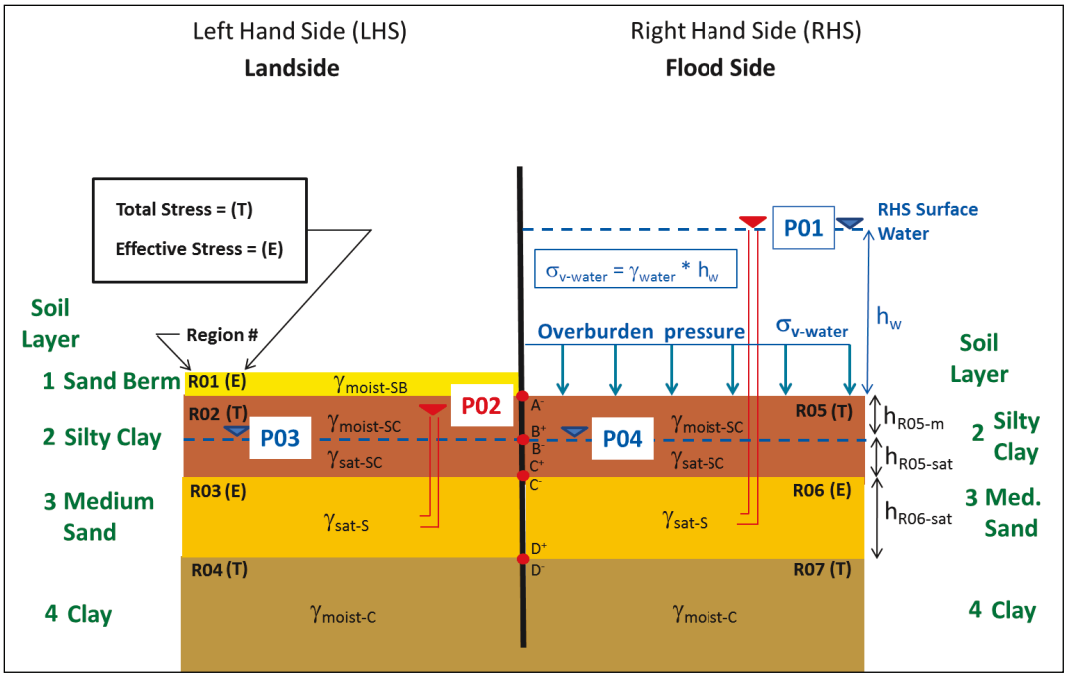
For either a total stress or effective stress analysis, the computation of the horizontal earth pressure acting normal to the sheet-pile wall starts with a calculation of total vertical stress. An example of this computation will be made within the three soil regimes labeled R05, R06, and R07 located along the RHS of the I-Wall/sheet-pile wall at the four nodes labeled A, B, C, and D (Figure 2.3). Because of the possibility of intermixed layers, each node (A, B, C, and D) is further designated with a plus and a minus (Figure 2.3). Considering Region R05 is a total stress layer, and Region R06 is an effective stress layer, the earth pressure computations will be different immediately above and below this region interface boundary. Two separate earth pressure computations are calculated by the software at each node to accommodate this possibility, they are designated as C^+ and C^- on the upper and lower side of this identified interface node, respectively. This computational approach is followed at all nodes.

On the RHS of Figure 2.3, the total vertical stress, σ_v, is computed incrementally from the surface water node, down from node-to-node by the software. This means that at the RHS ground surface, node A has a total vertical stress, $\sigma_{v\text{-}A}$, corresponding to the overburden pressure of water to a depth h_w,

$$\sigma_{v-A} = \gamma_{water} \cdot h_w \tag{2.1}$$

[1] The computation of earth pressure coefficients using Mohr-Coulomb soil shear strength parameters is discussed in Section 2.3.

Figure 2.3. Location of four select nodes identified along the RHS of the I-Wall for total vertical stress computations calculated during flood loading.



Similarly, at nodes B, C and D, the total vertical stresses are equal to

$$\sigma_{v-B} = \sigma_{v-A} + \gamma_{moist-SC} \cdot h_{R05-m} \tag{2.2}$$

$$\sigma_{v-C} = \sigma_{v-B} + \gamma_{sat-SC} \cdot h_{R05-sat} \tag{2.3}$$

and

$$\sigma_{v-D} = \sigma_{v-C} + \gamma_{sat-SC} \cdot h_{R06-sat} \tag{2.4}$$

The computation of the total vertical stress within the soil regime for all RHS nodes by the software follows this incremental node-to-node computational approach downward along the embedded sheet-pile wall. The value for total vertical stress is the same at above and below the regions boundary, and on the plus and minus side of each Figure 2.3 node.

This same incremental top down, node-to-node computational approach is used for computing the total vertical stress within the soil regime for all LHS nodes, as is used for the RHS nodes by the software.

2.2.1 Total stress – mobilized active earth pressure

For each side, and within each soil region that is designated with a total stress material property (through its user provided material type input information), the mobilized active earth pressure is computed at each node in a Coefficient Method of analysis using the relationship

$$\sigma_{mob-Active} = K_{mob-Active} \cdot \sigma_v - 2 \cdot c_{mob-Active} \cdot \sqrt{K_{mob-Active}} \quad (2.5)$$

According to Jumikis (1984), consideration of stress condition in soil shows that cohesion of a cohesive-frictional {*c*, φ} soil does not affect the position of the rupture surface. Because of this, Jumikis (1984 [page 380]) concludes that the earth pressure of a cohesive-frictional {*c*, φ} soil can be approximately determined by the method used for cohesionless (i.e., noncohesive) soil. Jumikis (1984) extended this procedure to {*c*, φ} soils for Coulomb active and passive earth pressure-based calculations. By this Jumikis (1984) approximation, and by a similar procedure presented in EM-1110-2-2502 (HQUSACE 1989) of Coulomb wedge results, Coulomb active and passive earth pressure coefficients of a {*c*, φ} soil (computed using the relationships given in Sections 2.3.3 and 2.3.4) may be used in Equations 2.5 and 2.9 to compute the active and passive soil pressure distributions. This same logic holds true for the effective stress-based earth pressure relationships given by Equations 2.19 and 2.23 for mobilized active and passive earth pressures, respectively.

The mobilized active earth pressure (given by Equation 2.5) acts at an angle of $\delta_{mob\text{-}Active}$ from horizontal.[1] The horizontal component of $\sigma_{mob\text{-}Active}$ given by

$$\sigma_{mob-Active-horizontal} = \sigma_{mob-Active} \cdot \cos(\delta_{mob-Active}) \quad (2.6)$$

The value of the active earth pressure coefficient $K_{mob\text{-}Active}$ is computed using one of two relationships given in subsection 2.3. The computation of the total vertical stress, σ_v, is made at each node down the I-Wall and follows the procedure outlined in the Section 2.2. The mobilized cohesion $c_{mob\text{-}Active}$ and mobilized interface friction $\delta_{mob\text{-}Active}$ are given by

[1] When the user selects $K_{mob\text{-}Active}$ to be calculated by Rankine earth pressure theory in the software the mobilized interface friction $\delta_{mob\text{-}Active}$ is set equal to zero, as will be discussed in Section 2.3.1.

$$c_{mob-Active} = \frac{c}{FS_{Active}} \quad (2.7)$$

$$\tan(\delta_{mob-Active}) = \frac{\tan(\delta)}{FS_{Active}} \quad (2.8)$$

with c and δ being the user-specified values for cohesion and interface friction, respectively, assigned to the soil region. Because each soil region may be assigned different strength parameters, there can be a discontinuity in the active earth pressure at each interface between adjoining soil regions. Thus, the need for maintaining an upper and a lower earth pressure computation per node to accommodate this possibility (e.g., for node C, designating it as C^+ and C^- as shown in Figure 2.3). FS_{Active} is the user-specified Factor of Safety to be used in the active earth pressure computations and is usually assigned a value of 1.0 in a Corps_I-Wall design effort.

2.2.2 Total stress – mobilized passive earth pressure

For each side, and within each soil region that is designated with a total stress material property (through its user provided material type input information), the mobilized passive earth pressure is computed at each node in a Coefficient Method of analysis using the relationship

$$\sigma_{mob-Passive} = K_{mob-Passive} \cdot \sigma_v + 2 \cdot c_{mob-Passive} \cdot \sqrt{K_{mob-Passive}} \quad (2.9)$$

This mobilized passive earth pressure acts at an angle of $\delta_{mob\text{-}Passive}$ from horizontal.[1] The horizontal component of $\sigma_{mob\text{-}Passive}$ given by

$$\sigma_{mob-Passive-horizonal} = \sigma_{mob-Passive} \cdot \cos(\delta_{mob-Passive}) \quad (2.10)$$

The value of the passive earth pressure coefficient $K_{mob\text{-}Passive}$ is computed using one of three relationships given in a subsequent subsection. The computation of the total vertical stress σ_v is made at each node down the I-Wall and follows the procedure outlined in the Section 2.2. The mobilized cohesion $c_{mob\text{-}Passive}$ and mobilized interface friction $\delta_{mob\text{-}Passive}$ are given by

$$c_{mob-passive} = \frac{c}{FS_{Passive}} \quad (2.11)$$

[1] When the user selects $K_{mob\text{-}Passive}$ to be calculated by Rankine earth pressure theory in the software the mobilized interface friction $\delta_{mob\text{-}Passive}$ is set equal to zero, as will be discussed in Section 2.3.2.

$$\tan(\delta_{mob-Passive}) = \frac{\tan(\delta)}{FS_{Passive}} \quad (2.12)$$

with *c* and δ being the user-specified values for cohesion and interface friction, respectively, assigned to each soil region. Because each soil region may be assigned different strength parameters, there can be a discontinuity in the earth pressure at each interface between adjoining soil regions. Thus, the need for maintaining an upper and a lower earth pressure computation per node to accommodate this possibility (e.g., for node C, designating it as C^+ and C^- in Figure 2.3). $FS_{Passive}$ is the user-specified Factor of Safety for the passive earth pressure computations and is assigned a value greater than 1.0 in a Corps_I-Wall design effort.

2.2.3 Effective stress

Within an effective stress designated material type assigned to a particular soil region, the total vertical stress σ_v acting in the soil adjacent to each node is combined with the soil regions pore water pressure u (if any) to compute the vertical effective stress σ'_v. Terzaghi's principle of effective stress is expressed as

$$\sigma_v = \sigma'_v + u \quad (2.13)$$

Rearranging terms,

$$\sigma'_v = \sigma_v - u \quad (2.14)$$

Recall that σ_v is computed using the procedure outlined in Section 2.2. The effective vertical stress is then used to compute the mobilized active earth pressure acting on the node of the embedded sheet pile in a Coefficient Method of analysis.

Example: The Figure 2.3 medium sand Region R06 is designated an effective stress material type. At the top of this medium sand region, and at a point designated in Figure 2.3 as node C^-, the vertical effective stress $\sigma'_{v\text{-}C^-}$ is computed at to be

$$\sigma'_{v-C^-} = \sigma_{v-C} - u_{C^-} \quad (2.15)$$

where, the pore water pressure u at the top of this effective stress region and, at node C^- is computed as

$$u_{C^-} = \gamma_{water} \cdot (h_w + h_{R05-m} + h_{R05-sat}) \quad (2.16)$$

and $\sigma_{v\text{-}C}$ is computed using Equation 2.3. Referring to Figure 2.3, the piezometric surface number P01 for this soil Region R06 has an elevation that corresponds to the RHS surface water.

At the bottom of this medium sand region, and at a point designated in Figure 2.3 as node D^+, the vertical effective stress $\sigma'_{v\text{-}D^+}$ is computed at to be

$$\sigma'_{v-D^+} = \sigma_{v-D} - u_{D^+} \quad (2.17)$$

where, the pore-water pressure u at the bottom of this effective stress region, and at node D^+ is computed as

$$u_{D^+} = \gamma_{water} \cdot (h_w + h_{R05-m} + h_{R05-sat} + h_{R06-sat}) \quad (2.18)$$

and $\sigma_{v\text{-}D}$ is computed using Equation 2.4.

Since soil Region R05 in Figure 2.3 is a total stress material, and Region R06 is an effective stress material, there will be a discontinuity in the active earth pressures at node C. The same is true for node D, the interface of the effective stress, medium sand Region R06 with the total stress, and clay Region R07. The same is true for passive earth pressures.

2.2.4 Effective stress – mobilized active earth pressure

For each side, and within each soil region that is designated with an effective stress material property, the mobilized effective active earth pressure is computed at each node in a Coefficient Method of analysis using the relationship

$$\sigma'_{mob-Active} = K_{mob-Active} \cdot \sigma'_v - 2 \cdot c'_{mob-Active} \cdot \sqrt{K_{mob-Active}} \quad (2.19)$$

This mobilized effective active earth pressure acts at an angle of $\delta'_{mob\text{-}Active}$ from horizontal.[1] The computation of the effective vertical stress σ'_v is made at each node down the I-Wall and follows the procedure outlined in the Section 2.2.3.The horizontal component of $\sigma'_{mob\text{-}Active}$ given by

[1] When the user selects $K_{mob\text{-}Active}$ to be calculated by Rankine earth pressure theory in the software the mobilized interface friction $\delta'_{mob\text{-}Active}$ is set equal to zero, as will be discussed in Section 2.3.1.

$$\sigma'_{mob-Active-horizontal} = \sigma'_{mob-Active} \cdot \cos(\delta'_{mob-Active}) \quad (2.20)$$

The value of the active earth pressure coefficient $K_{mob\text{-}Active}$ is computed using one of two relationships given in a subsequent subsection. The mobilized effective cohesion $c'_{mob\text{-}Active}$ and mobilized effective interface friction $\delta'_{mob\text{-}Active}$ are given by

$$c'_{mob-Active} = \frac{c'}{FS_{Active}} \quad (2.21)$$

$$\tan(\delta'_{mob-Active}) = \frac{\tan(\delta')}{FS_{Active}} \quad (2.22)$$

with c' and δ' being the user-specified values for effective cohesion and effective interface friction, respectively, assigned to the soil region. FS_{Active} is the user-specified Factor of Safety to be used in the active earth pressure computations and is usually assigned a value of 1.0 in a Corps_I-Wall design.

In an effective stress-based analysis, in addition to the mobilized active earth pressure, the pore-water pressure also acts normal to the node on the sheet-pile wall.

Last, there can be a discontinuity in the active earth pressure at each soil region because each soil region may be assigned different strength parameters.

2.2.5 Effective stress – mobilized passive earth pressure

For each side, and within each soil region that is designated with an effective stress material property, the mobilized effective passive earth pressure is computed at each node in a Coefficient Method of analysis using the relationship

$$\sigma'_{mob-Passive} = K_{mob-Passive} \cdot \sigma'_v + 2 \cdot c'_{mob-Passive} \cdot \sqrt{K_{mob-Passive}} \quad (2.23)$$

This mobilized effective passive earth pressure acts at an angle of $\delta'_{mob\text{-}Passive}$ from horizontal.[1] The computation of the effective vertical stress σ'_v is made at each node down the I-Wall and follows the procedure

[1] When the user selects $K_{mob\text{-}Passive}$ to be calculated by Rankine earth pressure theory in the software the mobilized interface friction $\delta'_{mob\text{-}Passive}$ is set equal to zero, as will be discussed in Section 2.3.2.

outlined in the Section 2.2.3. The horizontal component of $\sigma'_{mob\text{-}Passive}$ given by

$$\sigma'_{mob-Passive-horizontal} = \sigma'_{mob-Passive} \cdot \cos(\delta'_{mob-Passive}) \quad (2.24)$$

The value of the passive earth pressure coefficient $K_{mob\text{-}Passive}$ is computed using one of three relationships given in a subsequent subsection. The mobilized effective cohesion $c'_{mob\text{-}Passive}$ and mobilized effective interface friction $\delta'_{mob\text{-}Passive}$ are given by

$$c'_{mob-Passive} = \frac{c'}{FS_{Passive}} \quad (2.25)$$

$$\tan(\delta'_{mob-Passive}) = \frac{\tan(\delta')}{FS_{Passive}} \quad (2.26)$$

with c' and δ' being the user-specified values for effective cohesion and effective interface friction, respectively, assigned to the soil region. $FS_{Passive}$ is the user-specified Factor of Safety in the passive earth pressure computations and is usually assigned a value greater than 1.0 in a Corps_I-Wall design effort.

In an effective stress based analysis, in addition to the mobilized passive earth pressure, the pore water pressure also acts normal to the node on the sheet-pile wall.

Last, there can be a discontinuity in the passive earth pressure at each soil region because each soil region may be assigned different strength parameters.

2.3 Earth pressure Coefficient Methods used for computing earth pressures

Earth pressure Coefficient Methods of analysis is one of two options that are used in Corps_I-Wall Version 2.0 to compute the mobilized active and passive horizontal pressures acting along the sheet-pile wall to soil interface (as described in Section 2). The user may select one of two methods to compute a value for the active earth pressure coefficient, Rankine or Coulomb. To compute a value for the passive earth pressure coefficient, the following three options available: Rankine, Coulomb or a passive earth pressure coefficient computed using a logarithmic spiral based method.

Rankine earth pressures always act normal to the (sheet-pile) wall. Consequently, δ in a total stress soil or δ′ in an effective stress soil is set equal to zero degrees for the active earth pressure relationships of Equations 2.6, 2.10, 2.20 and 2.24.

2.3.1 Rankine's active earth pressure coefficients

For total stress of a horizontal ground surface, Rankine's active earth pressure coefficient of a total stress designated soil region, $K_{mob\text{-}Active}$ is

$$K_{mob-Active} = tan^2\left(45° - \frac{\varphi_{mob-Active}}{2}\right) \tag{2.27}$$

where φ_{mob} is the mobilized angle of internal friction of the soil. The value for φ_{mob} is given by

$$\tan(\varphi_{mob-Active}) = \frac{\tan(\varphi)}{FS_{Active}} \tag{2.28}$$

Rankine's earth pressure theory for a $\{c, \varphi\}$ soil assumes the earth pressure acts normal to the sheet-pile wall. When the user selects $K_{mob\text{-}Active}$ to be calculated by Rankine earth pressure theory, the interface friction δ is set equal to zero in Equation 2.8 and thus, Equation 2.5 describes the earth pressure normal to the sheet-pile wall.

For effective stress of an effective stress soil region below a horizontal ground surface, Rankine's mobilized effective active earth pressure coefficient $K_{mob\text{-}Active}$ is

$$K_{mob-Active} = tan^2\left(45° - \frac{\varphi'_{mob-Active}}{2}\right) \tag{2.29}$$

where, φ'_{mob} is the mobilized effective angle of internal friction of the soil. The value for δ'_{mob} is given by

$$\tan(\varphi'_{mob-Active}) = \frac{\tan(\varphi')}{FS_{Active}} \tag{2.30}$$

Rankine's earth pressure theory for a $\{c', \varphi'\}$ soil assumes the earth pressure acts normal to the sheet-pile wall. So when the user selects $K_{mob\text{-}Active}$ to be calculated by Rankine's earth pressure theory, the interface friction δ′ is set equal to zero in Equation 2.22 and thus, Equation 2.19 describes the earth pressure normal to the sheet-pile wall.

2.3.2 Rankine's passive earth pressure coefficients

For a horizontal ground surface, Rankine's passive earth pressure coefficient of a total stress designated soil region, $K_{mob\text{-}Passive}$ is

$$K_{mob-Passive} = tan^2\left(45° - \frac{\varphi_{mob-Passive}}{2}\right) \tag{2.31}$$

where, φ_{mob} is the mobilized angle of internal friction of the soil. The value for φ_{mob} is given by

$$\tan(\varphi_{mob-Passive}) = \frac{\tan(\varphi)}{FS_{Passive}} \tag{2.32}$$

Rankine's earth pressure theory for a $\{c, \varphi\}$ soil assumes the earth pressure acts normal to the sheet-pile wall. When the user selects $K_{mob\text{-}Passive}$ to be calculated by Rankine's earth pressure theory, the interface friction δ is set equal to zero in Equation 2.12 and thus, Equation 2.9 describes the earth pressure normal to the sheet-pile wall.

Effective stress: For an effective stress soil region, Rankine's mobilized effective passive earth pressure coefficient $K_{mob\text{-}Active}$ is

$$K_{mob-Passive} = tan^2\left(45° - \frac{\varphi'_{mob-Passive}}{2}\right) \tag{2.33}$$

where, φ'_{mob} is the mobilized effective angle of internal friction of the soil. The value for φ'_{mob} is given by

$$\tan(\varphi'_{mob-Passive}) = \frac{\tan(\varphi')}{FS_{Passive}} \tag{2.34}$$

Rankine's earth pressure theory for a $\{c', \varphi'\}$ soil assumes the earth pressure acts normal to the sheet-pile wall. When the user selects $K_{mob\text{-}Passive}$ to be calculated by Rankine's earth pressure theory, the interface friction δ' is set equal to zero in Equation 2.26 and thus, Equation 2.23 describes the earth pressure normal to the sheet-pile wall.

2.3.3 Coulomb's active earth pressure coefficients

Total stress for a horizontal ground surface, Coulomb's active earth pressure coefficient (Ebeling and Morrison 1992) of a total stress designated soil region, $K_{mob\text{-}Active}$ is

$$K_{mob-Active} = \frac{\cos^2 \varphi_{mob-Active}}{\cos(\delta_{mob-Active})\left[1+\sqrt{\frac{\sin(\varphi_{mob-Active}+\delta_{mob-Active})\sin(\varphi_{mob-Active})}{\cos(\delta_{mob-Active})}}\right]^2} \quad (2.35)$$

where, $\varphi_{mob\text{-}Active}$ is the mobilized angle of internal friction of the soil, and $\delta_{mob\text{-}Active}$ is the mobilized soil to sheet-pile interface angle of friction. The values for $\varphi_{mob\text{-}Active}$ and $\delta_{mob\text{-}Active}$ are given by Equations 2.28 and 2.8, respectively.

Effective stress: For an effective stress soil region below a horizontal ground surface, Coulomb's mobilized effective active earth pressure coefficient $K_{mob\text{-}Active}$ is

$$K_{mob-Active} = \frac{cos^2 \varphi'_{mob-Active}}{\cos(\delta'_{mob-Active})\left[1+\sqrt{\frac{\sin(\varphi'_{mob-Active}+\delta'_{mob-Active})\sin(\varphi'_{mob-Active})}{\cos(\delta'_{mob-Active})}}\right]^2} \quad (2.36)$$

where, $\varphi'_{mob\text{-}Active}$ is the mobilized effective angle of internal friction of the soil, and $\delta'_{mob\text{-}Active}$ is the mobilized soil to sheet-pile interface angle of friction. The values for $\varphi'_{mob\text{-}Active}$ and $\delta'_{mob\text{-}Active}$ are given by Equations 2.30 and 2.22, respectively.

2.3.4 Coulomb's passive earth pressure coefficients

Total stress: For a horizontal ground surface, Coulomb's passive earth pressure coefficient (Ebeling and Morrison 1992) of a total stress designated soil region, $K_{mob\text{-}Passive}$ is

$$K_{mob-Passive} = \frac{\cos^2 \varphi_{mob-Passive}}{\cos(\delta_{mob-Passive})\left[1-\sqrt{\frac{\sin(\varphi_{mob-Passive}+\delta_{mob-Passive})\sin(\varphi_{mob-Passive})}{\cos(\delta_{mob-Passive})}}\right]^2} \quad (2.37)$$

where, $\varphi_{mob\text{-}Passive}$ is the mobilized angle of internal friction of the soil, and $\delta_{mob\text{-}Passive}$ is the mobilized soil to sheet-pile interface angle of friction. The values for $\varphi_{mob\text{-}Passive}$ and $\delta_{mob\text{-}Passive}$ are given by Equations 2.32 and 2.12, respectively.

The application of this Coulomb $K_{mob\text{-}Passive}$ relationship is to soils with $\delta_{mob\text{-}Passive}$ less than or equal to $\varphi_{mob\text{-}Passive}/2$, as discussed in Section 3.3.4.1 of Ebeling and Morrison (1992) or Section 4.6 of Chen and Liu (1990). This is due to the inappropriateness of a planar slip surface assumption

used in defining the resultant passive earth pressure force relationship from which the Coulomb passive earth coefficient is derived. A curved slip surface is more appropriate when $\delta_{mob\text{-}Passive}$ is greater than $\varphi_{mob\text{-}Passive}/2$.

Effective stress: For an effective stress soil region below a horizontal ground surface, Coulomb's mobilized effective passive earth pressure coefficient $K_{mob\text{-}Passive}$ is

$$K_{mob-Passive} = \frac{cos^2\varphi'_{mob-Passive}}{\cos(\delta'_{mob-Passive})\left[1-\sqrt{\frac{\sin(\varphi'_{mob-Passive}+\delta'_{mob-Passive})\sin(\varphi'_{mob-Passive})}{\cos(\delta'_{mob-Passive})}}\right]^2} \quad (2.38)$$

where, $\varphi'_{mob\text{-}Passive}$ is the mobilized effective angle of internal friction of the soil, and $\delta'_{mob\text{-}Passive}$ is the mobilized soil to sheet-pile interface angle of friction. The values for $\varphi'_{mob\text{-}Passive}$ and $\delta'_{mob\text{-}Passive}$ are given by Equations 2.34 and 2.26, respectively.

The application of this Coulomb $K_{mob\text{-}Passive}$ relationship is to soils with $\delta'_{mob\text{-}Passive}$ less than or equal to $\varphi'_{mob\text{-}Passive}/2$, as discussed in Section 3.3.4.1 of Ebeling and Morrison (1992) or Section 4.6 of Chen and Liu (1990). This is due to the inappropriateness of a planar slip surface assumption used in defining the resultant passive earth pressure force relationship from which the Coulomb passive earth coefficient is derived. A curved slip surface is more appropriate when $\delta'_{mob\text{-}Passive}$ is greater than $\varphi'_{mob\text{-}Passive}/2$.

2.3.5 Logarithmic-spiral method for the determination of a passive earth pressure coefficients

The logarithmic spiral earth pressure theory (sometimes referred to as the logarithmic spiral method) is described by Terzaghi (1943), Chen and Liu (1990), and others. A significant portion of the slip surface in a retained soil regime is approximated by a logarithmic spiral. Under this condition, and using different sets of engineering formulations, values for passive earth coefficients were produced as a function of internal friction values for cohesionless soils (e.g., tabulations given in Caquot 1948; Kerisel and Absi 1990; Chen and Liu 1990; Sokolovskii 1965; and in the Figure 5 chart in Chapter 3 of NAVFAC DM 7.2 [Department of the Navy 1982]). The Figure 5 chart given in Chapter 3 in NAVFAC DM 7.2 (1982) provides values for $K_{Passive}$ for δ equal to φ as a nonlinear curve that is a function of φ. Using this information, a tabulation of $K_{Passive}$ values was assembled (Table 2.2). In order to determine an appropriate value for $K_{Passive}$ in those

cases when δ is less then φ, a reduction factor, *R*, is applied to the Table 2.3 $K_{Passive}$ value.

$$K_{Passive}(\delta) = K_{Passive} \cdot R(\delta, \phi) \quad (2.39)$$

Values for *R* are provided in Table 2.3 as a function of the value of φ and the value of the ratio δ/φ. For intermediate values, interpolation of the Tables 2.2 and 2.3 are appropriate.

Table 2.2. Passive earth pressure coefficient $K_{Passive}$ *(Kp)* values for –δ equal to φ and a solution based on assuming a failure surface composed of logarithmic spiral portion and a planar surface portion.

φ	Kp(-δ=φ)
0	1
5	1.28
10	1.64
15	2.19
20	3.01
25	4.29
30	6.42
35	10.2
40	17.5
45	33.5
50	74.3
51	90
52	110
53	130
54	160
55	204
60	782

To use the Tables 2.2 and 2.3 data in total stress designated materials, the value for mobilized interface friction, $\delta_{mob\text{-}Passive}$ is substituted for δ and the value for mobilized angle of internal friction $\varphi_{mob\text{-}Passive}$ is substituted for φ. A similar substitution is made for effective stress designated materials. These tables of values may be used for soils designated as either total or effective stress materials. Last, due to the sign convention used to describe the passive earth pressure force based on the data contained in the Figure 5 chart in Chapter 3 of NAVFAC DM 7.2 (Department of the Navy 1982), δ is expressed as a negative value when using Tables 2.2 and 2.3.

Within the software, the $K_{Passive}$ and *R* value data contained in Tables 2.2 and 2.3 are stored in separate arrays. When the user requests via the GUI

that the value for $K_{mob\text{-}Passive}$ be calculated using the logarithmic-spiral method, the values of both $K_{mob\text{-}Passive}$ and R are obtained by linear interpolation for the region specific $\delta_{mob\text{-}Passive}$ and $\varphi_{mob\text{-}Passive}$ values.

Table 2.3. Reduction factor, *R*, values for various ratios of $-\delta/\phi$.

ϕ (deg)	δ/ϕ										
	-1	-0.9	-0.8	-0.7	-0.6	-0.5	-0.4	-0.3	-0.2	-0.1	0
0	1	1	1	1	1	1	1	1	1	1	1
5	1	0.996	0.995	0.989	0.981	0.973	0.9645	0.956	0.949	0.9405	0.932
10	1	0.991	0.989	0.978	0.962	0.946	0.929	0.912	0.898	0.881	0.864
15	1	0.986	0.979	0.961	0.934	0.907	0.881	0.854	0.83	0.803	0.775
20	1	0.983	0.968	0.939	0.901	0.862	0.824	0.787	0.752	0.716	0.678
25	1	0.980	0.954	0.912	0.86	0.808	0.759	0.711	0.666	0.62	0.574
30	1	0.980	0.937	0.878	0.811	0.746	0.686	0.627	0.574	0.52	0.467
35	1	0.980	0.916	0.836	0.752	0.674	0.603	0.536	0.475	0.417	0.362
40	1	0.980	0.886	0.783	0.682	0.592	0.512	0.439	0.375	0.316	0.262
45	1	0.979	0.848	0.718	0.6	0.5	0.414	0.339	0.276	0.221	0.174
50	1	0.975	0.797	0.638	0.506	0.399	0.313	0.242	0.185	0.138	0.102
55	1	0.966	0.731	0.543	0.401	0.295	0.215	0.153	0.108	0.0737	0.0492
60	1	0.948	0.647	0.434	0.29	0.193	0.127	0.0809	0.0505	0.0301	0.0178

2.4 Converting a trapezoidal pressure distribution acting on a discrete segment of the I-Wall face into equivalent end point forces

Both the earth and water pressure distributions acting on the I-Wall are converted into equivalent forces. The Corps_I-Wall software uses the one-third/one-sixth force computational procedure to convert a trapezoidal distribution of a segment of stress between the closest nodes into equivalent nodal forces. This computational procedure is summarized using the generalized trapezoidal stress distribution between node i and node i+1 acting normal to the I-Wall and/or sheet-pile wall segment k, designated as $length_k$ in Figure 2.4. The equivalent nodal point forces at node i and node i+1 are computed to be

$$F_i^- = length_k * \left[\frac{\sigma_i^-}{3} + \frac{\sigma_{i+1}^+}{6}\right] \tag{2.40}$$

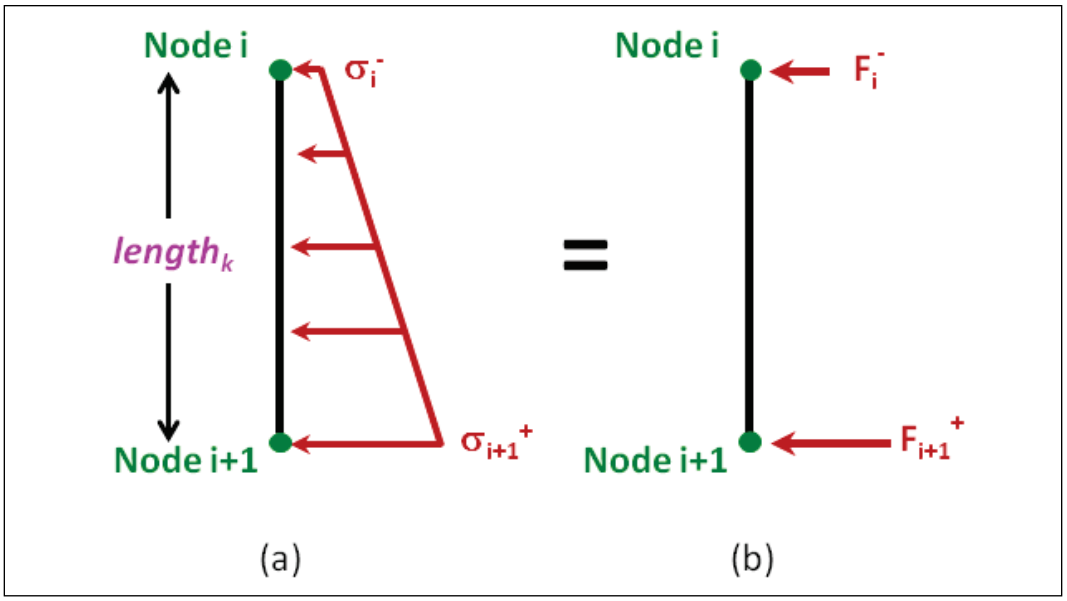
and

$$F_{i+1}^+ = length_k * \left[\frac{\sigma_i^-}{6} + \frac{\sigma_{i+1}^+}{3}\right] \tag{2.41}$$

where, $length_k$ is the distance from node i to node i+1, σ_i^- is the stress normal to node i on wall segment k, and σ^+_{i+1} is the stress normal to node i+1 on wall segment k. These two relationships for equivalent end forces

F_i^- and F_{i+1}^+ will exactly reflect the trapezoidal pressure diagram along its nodal pair wall segment k. The sum of these two forces equals the area under the trapezodial pressure diagram. Moment equlibrium for the wall segment k is statisfied for the applied trapezoidal pressure distribution and these two equivalent end normal forces.

Figure 2.4. Distribution of stress acting normal to a discrete segment k of the wall face. (a) Trapezoidal pressure distribution. (b) Equivalent nodal point forces.



2.5 Clockwise or counterclockwise I-Wall rotation

Corps_I-Wall has the ability to accommodate either a clockwise or a counterclockwise I-Wall rotation. The direction of I-Wall rotation is dictated by the direction of net loading and its corresponding moment applied to the I-Wall. Logic was developed to ascertain the direction of I-Wall rotation based upon flood and earth loading specified for the problem. This capability was specifically developed to accommodate the coastal problem for which the magnitude of user-specified wave or surge water pressure (i.e., height of design storm surge wave) can alter the direction of I-Wall rotation, relative to the calm water design case, especially when a soil berm exists on the landside of the I-Wall. The direction of rotation is determined internally by Corps_I-Wall and reported in the output information contain within the *Analysis* tab.

To determine the direction of I-Wall rotation for a retaining wall design with differential ground surfaces and for differential water surfaces, the moment for the net loading is computed about the lower of the RHS or LHS

ground surfaces for the ground level at the wall. A resultant positive moment will produce a counterclockwise rotation, which should agree with mobilized active pressures on the RHS of the I-Wall. If this initial assumption is incorrect, mobilized active pressures on the LHS and mobilized passive pressures on the RHS of the I-Wall will be used to determine if a clockwise rotation will occur from a resultant negative moment. If this next calculation does not agree, the sheet-pile I-Wall is deemed stable and no further rotational stability analysis is necessary.

2.6 Net active pressure and net passive pressure

In the design of a sheet-pile I-Wall, all applicable pressures are used to compute the net active and net passive pressures along the I-Wall for the final design. The Figure 2.5 schematic shows the I-Wall rotating in the counterclockwise direction with the net active and net passive pressure distributions. The net active pressure distribution with elevation is shown in red solid and dashed line segments while the net passive pressure distribution is shown by a green-dashed line segment. Above the RHS ground surface, the net passive and net active pressure distributions coincide. These two net pressures are determined by the following pressures:

- Net active pressure = RHS soil active pressure – LHS soil passive pressure + net water pressure + surcharge pressure + distributed external horizontal pressure.
- Net passive pressure = RHS soil passive pressure – LHS soil active pressure + net water pressure + surcharge pressure + external horizontal pressure.

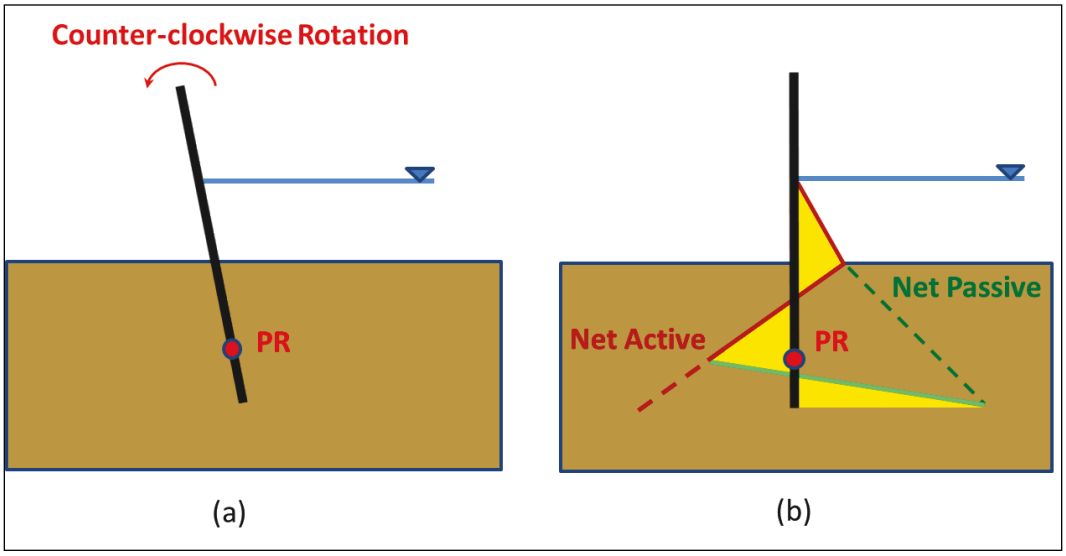
Figure 2.5b shows the net active pressures are calculated along the I-Wall from the surface water on the RHS until the elevation at the PR is reached (a solid red line segment). A linear interpolation is made between the net active pressure at elevation PR and the net passive pressure at the sheet-pile tip elevation to calculate subsequent net pressures along the sheet-pile wall. This segment of net pressure is shown as a solid green line segment in Figure 2.5b.

2.7 Factors of safety applied to each soil region

Corps_I-Wall Version 1.0 allows the user to specify a value for the factors of safety used in both active and passive earth pressure calculations per

soil region. The GUI allows the user to define default values for FS_{Active} and $FS_{Passive}$ that will pre-populate the factors of safety per soil region (this is discussed further in Chapter 3).

Figure 2.5. I-Wall rotation. (a) Counterclockwise rotation about a PR due to flood loading applied to the RHS of the I-Wall. (b) The net water and earth pressures acting on the I-Wall during its rotation.



In *Design* mode, the user specifies values for FS_{Active} and $FS_{Passive}$. The value assigned to FS_{Active} is usualy 1.0. Guidance on the value to be assigned to $FS_{Passive}$ is given in EM 1110-2-2504 (HQUSACE 1994) and ETL 1110-2-575 (HQUSACE 2011b).

In *Analysis* mode, the value assigned to FS_{Active} is usually 1.0. The software will compute the value for $FS_{Passive}$ assuming the same value is applied to all soil regions developing mobilized passive earth pressures. This engineering evaluation mode is typically used to evaluate the rotational stability of an existing I-Wall.

2.8 Distributions of water pressures acting on the I-Wall and sheet-pile wall due to surface water and piezometric surfaces

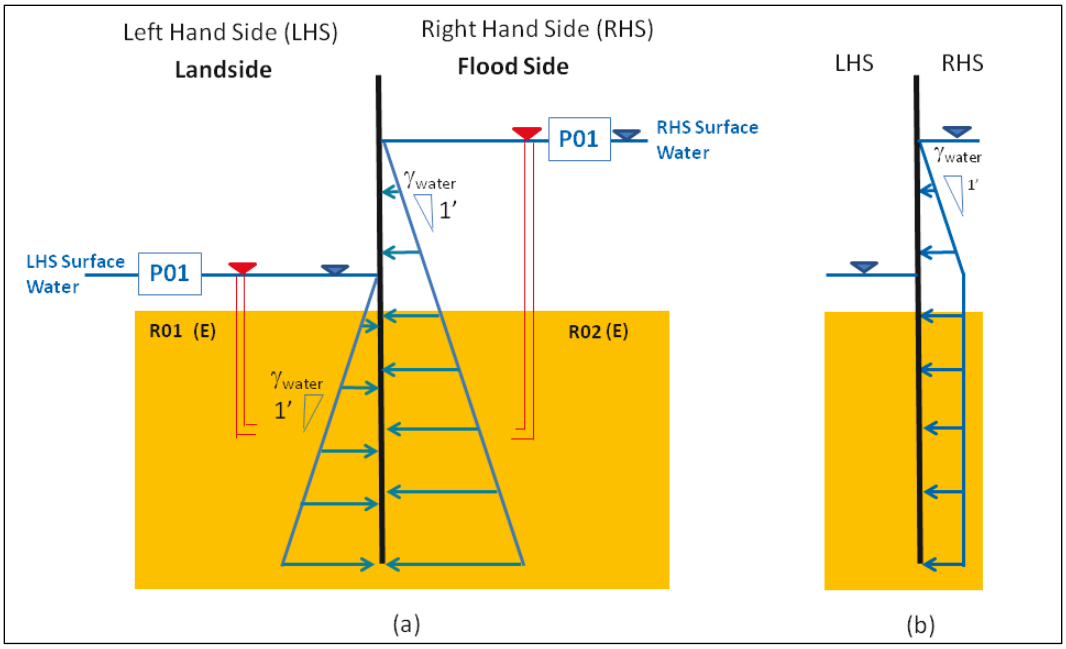
When surface water is specified by the user along the side of an I-Wall, hydrostatic water pressures are specified normal to the I-Wall from the water surface down to the ground surface. One surface water may be specified for the flood side and a second, independent, surface water may be specifed for the landside, as discussed in Chapter 3.

When specifing water pressures to be used in computing pore water pressures internal to the soil regime, the user has the following two options: 1) hydrostatic water pressures and 2) water pressures computed assuming homogenous seepage or heterogeneous seepage. The seepage option is only available when used in conjunction with the Coefficient Method of analysis. Figure 3.22 in Chapter 3 shows these three user options within the GUI. Water pressures internal to the soil are applied normal to the embedded sheet-pile wall when the soil region is specified as an effective stress material. No water pressures internal to the soil are applied normal to the sheet-pile wall when the soil region is specified as a total stress material. When a gap opens between the soil and the sheet-pile wall, hydrostatic water pressures (with the calculations starting at the elevation of the surface water) are applied normal to the sheet-pile wall irrespective of the soil region material specification (Appendix B).

Example 1: Figure 2.6 shows an example of the hydrostatic water pressure distributions acting normal to the sheet-pile wall for a user-selected hydrostatic water pressures option. Both soil regions (R01 and R02) represent a single, homogenous soil layer and are specified to be an effective stress material (E). The LHS soil region's piezometric surface is associated with the LHS surface water (designated as the LHS surface water number P01) and the RHS soil region's piezometric surface is associated with the RHS surface water (designated as the RHS surface water number P01). The water pressures above the LHS and RHS ground sufaces, and the pore water pressures below these two ground surfaces, increase in value at a rate of the unit weight of water (i.e., γ_{water} = 62.4 pcf) per unit of depth (i.e., 1 ft in this case). Observe at the sheet-pile tip in Figure 2.6,° that there is a discontinuity in the LHS and RHS hydrostatic pore water pressure values.

Figure 2.6b shows the distribution of net water pressures acting normal to the I-Wall and sheet-pile wall. The distribution of net water pressures is equal to the difference between the RHS and LHS Figure 2.6a water pressures. For the discontinuity shown in Figure 2.6a, pore-water pressures at the sheet-pile tip are reflected in the net water pressure diagram of Figure 2.6b with a non-zero net water pressure.

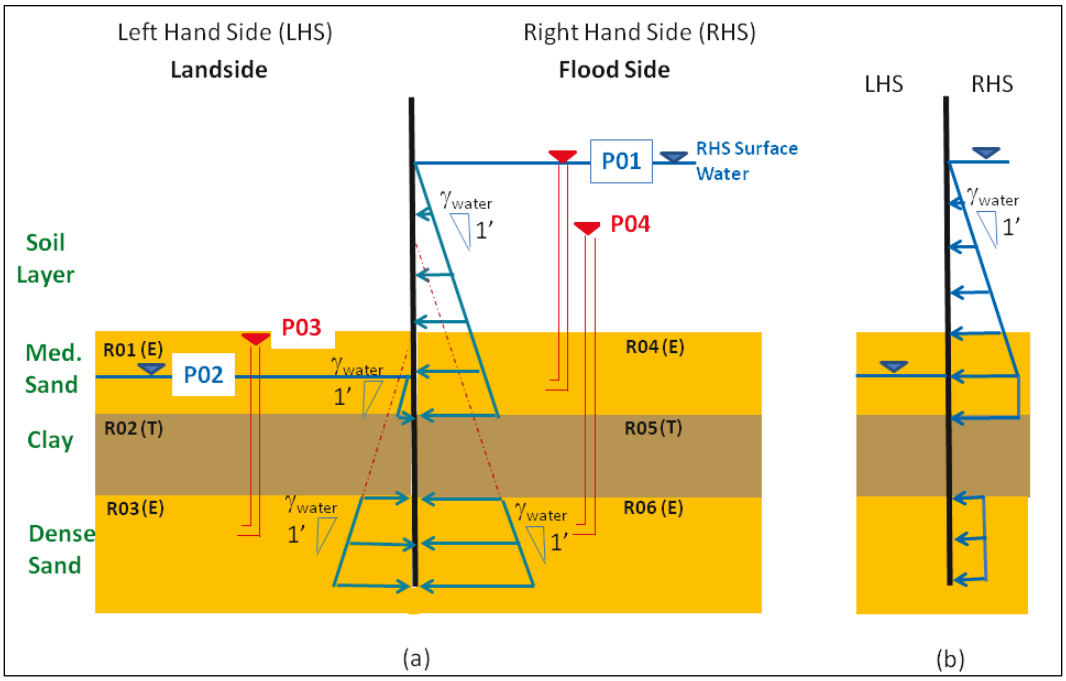
Figure 2.6. Distributions of water pressures acting normal to the I-Wall and sheet-pile wall – hydrostatic water pressures. (a) Hydrostatic water and pore-water pressure distributions on the LHS and RHS. (b) The net water pressure distribution.



Example 2: Under the *Hydrostatic Water Pressures* option (see Figure 3.22 in Chapter 3) and for sites with multiple soil regions, Corps_I-Wall Version 2.0 allows for the definition of more than one piezometric surface on each side. Consider the case shown in Figure 2.7 flood I-Wall. The foundation consists of the following three soil layers: upper medium sand, clay,and lower dense sand. Both sand layers are designated effective stress-based materials. The intermediate layer is clay and is designated as a total stress material. The software model requires a defintion of this site using six soil regions as shown in Figure 3.22. The LHS medium sand, Region 01, has a piezometric surface (designated P02) associated with it, and the dense sand, Region 03, has a piezometric surface (designated P03) associated with it. The RHS medium sand, Region 04, has a piezometric surface (designated P01) associated with it, and the dense sand, Region 06, has a piezometric surface (designated P04) associated with it. Observe that the RHS Region R04 piezometric surface (P01) corresponds to the RHS surface water of flood loading. The water pressures above the RHS ground surface and within Region 04 increase with decreasing elevation at a rate of γ_{water} (i.e., 62.4 pcf). This is consistent with the Figure 3.22 *Hydrostatic Water Pressures* option selected by the user. A distribution of hydrostatic water pressure is also computed within the RHS dense sand of Region R06, but uses the piezometric surface of P04 to compute the pore water pressures. The increase in water pressure with decreasing elevation in

Region R06 is hydrostatic at the rate of γ_{water}. Observe that the elevation of P04 is lower than P01, so the pore water pressures in Region R06 are lower than what would occur if the piezometric surface would have been designated to be P01 for this region.

Figure 2.7. Distributions of hydrostatic water pressures acting normal to the I-Wall and sheet-pile wall – hydrostatic water pressures. (a) Hydrostatic water and pore water pressure distributions on the LHS and RHS. (b) The net water pressure distribution.



The LHS medium sand, Region 01, has a piezometric surface (designated P02) associated with it, and the dense sand, Region 03, has a piezometric surface (designated P03) associated with it. The water pressures start within Region 01 at its piezometric surface (P02) elevation and increase with decreasing elevation at a rate of γ_{water}. A distribution of hydrostatic water pressure is also computed within the LHS dense sand of Region R03 but using the piezometric surface of P03 to compute the pore-water pressures. The increase in water pressure with decreasing elevation in Region R03 is hydrostatic at the rate of γ_{water}. Observe that the elevation of P03 is higher than P02, so the pore-water pressures in Region R03 are higher than what would occur if the piezometric surface would have been designated as P02 for this region.

For stratified soils regions with different piezometric sufaces assigned to adjacent regions, there will be a disjoint in pore-water pressure values at

the interface between the two regions under the (Figure 3.22) *Hydrostatic Water Pressures* option.

Figure 2.7b shows the distribution of net water pressures acting normal to the I-Wall and sheet-pile wall. The distribution of net water pressures is equal to the difference between the RHS and LHS Figure 2.7a water pressures. Observe that the discontinuity in the Figure 2.7a pore-water pressures at the sheet-pile tip is reflected in the net water pressure diagram of Figure 2.7b with non-zero net water pressure.

Example 3: Figure 2.8a shows an example of the water pressure distributions acting normal to the sheet-pile wall for a user-selected *Homogenous Seepage* option (and using the Coefficient Method of analysis). Both soil regions (R01 and R02) represent a single soil layer and are specified to be an effective stress material (E). The soil layer and both soil regions possess a single value for vertical hydraulic conductivity. The line of seepage (a.k.a. line of creep) is used to compute pore-water pressures for a steady-state seepage condition (Appendix C) within the soil, starting at the ground surface on the high head RHS of the sheet-pile, down to the tip of the sheet pile, and then back up to the ground surface on the low head LHS of the sheet pile.

The Figure 2.8a LHS soil region's piezometric surface is associated with the LHS surface water (designated as the LHS surface water number P01) and the RHS soil region's piezometric surface is associated with the RHS surface water (designated as the RHS surface water number P01).[1] Hydrostatic water presures act against the I-Wall above both the LHS and RHS ground surfaces. These two (surface) water pressure distributions increase with decreasing elevation at a rate equal to the unit weight of water (i.e., γ_{water} = 62.4 pcf) per unit of depth (i.e., 1 ft in this case). Because of head loss due to seepage, the pore-water pressures within the soil below the LHS and RHS ground increase in value with decreasing elevation at a rate equal to less than γ_{water} per unit of depth. Observe at the sheet-pile tip in Figure 2.8a that there is continuity in the LHS and RHS hydrostatic pore-water pressure values.

[1] By the theory of steady-state seepage, the seepage of water through the soil surrounding the sheet-pile wall occurs down the high head side, around the tip of the sheet-pile, and up the soil on the low head side. When a seepage analysis is specified, the software requires that only one piezometric surface (or surface water assigned as a piezometric surface) be assigned per side. This restriction is for either the *Homogeneous* or *Heterogeneous Seepage* option.

Figure 2.8. Distributions of water pressures acting normal to the I-Wall and sheet-pile wall – homogenous seepage. (a) Water and pore-water pressure distributions on the LHS and RHS. (b) The net water pressure distribution.

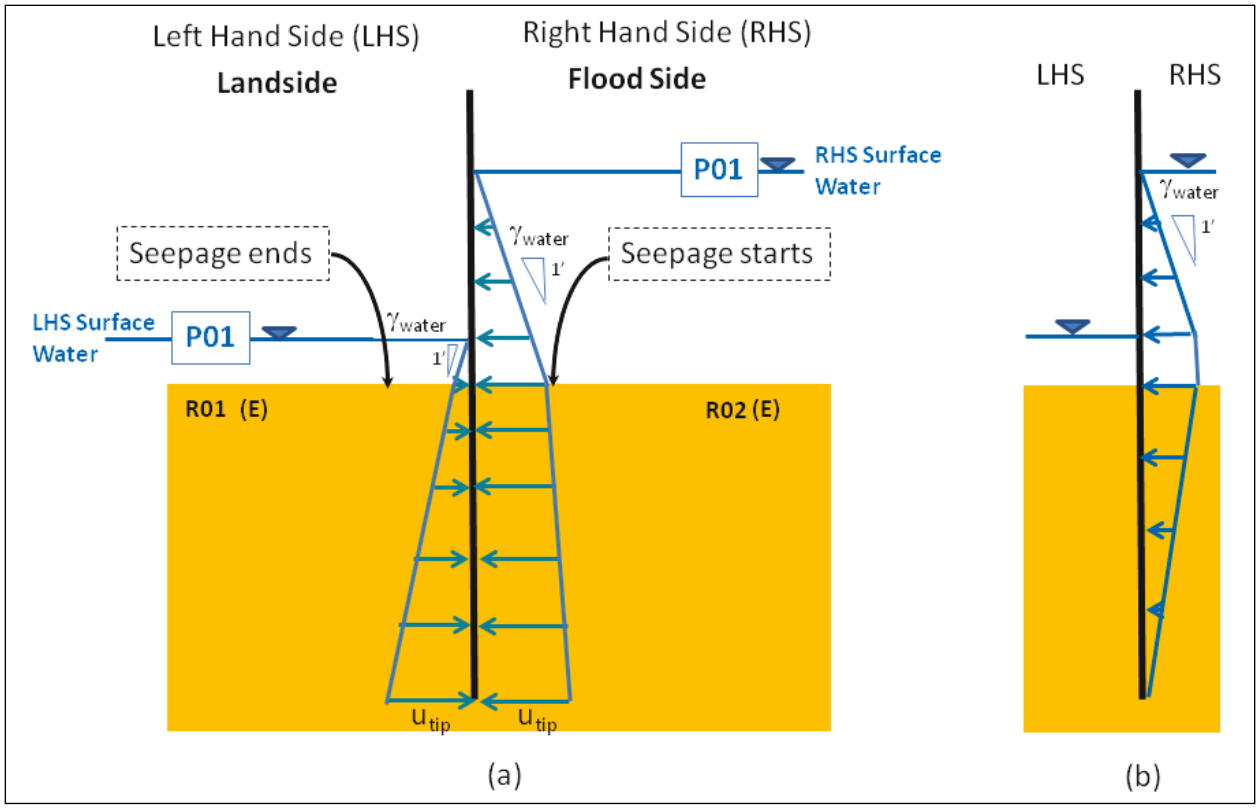
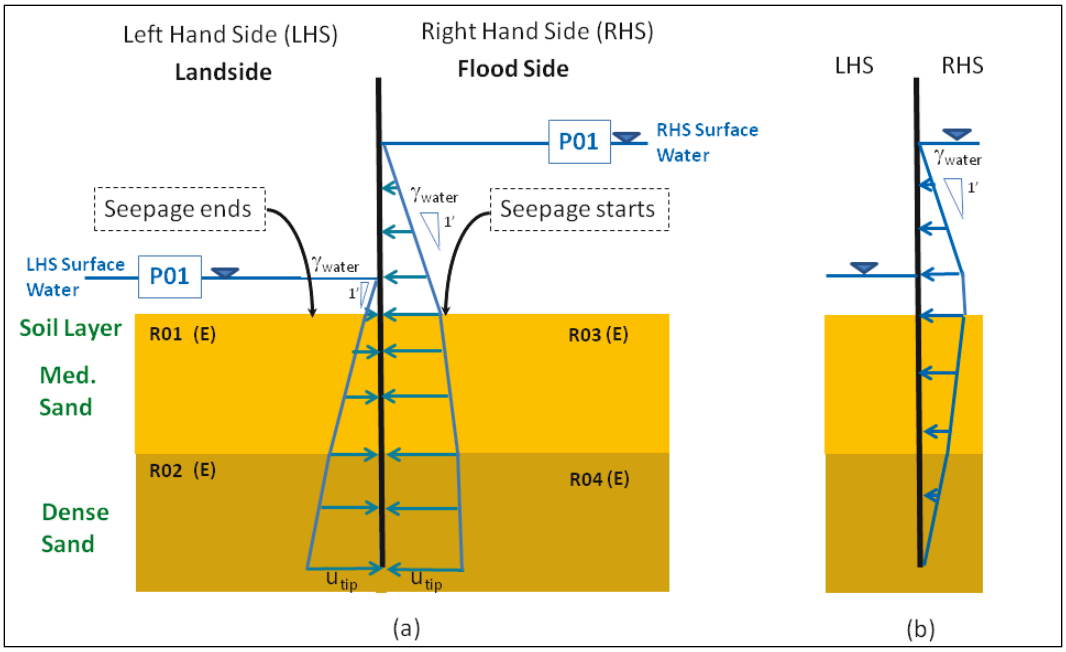


Figure 2.8b shows the distribution of net water pressures acting normal to the I-Wall and sheet-pile wall. The distribution of net water pressures is equal to the difference between the RHS and LHS Figure 2.8a water pressures. Observe that the continuity in the Figure 2.8a pore-water pressures at the sheet-pile tip is reflected in the net water pressure diagram of Figure 2.8b with a zero net water pressure.

Example 4: Figure 2.9a shows an example of the water pressure distributions acting normal to the sheet-pile wall for a user-selected *Heterogenous Seepage* option (and using the Coefficient Method of analysis). The site consists of the following two soil layers: a medium dense sand overlaying a dense sand. This software requires that the upper soil layer be modeled by two soil regions (R01 and R03), which are specified to be an effective stress material (E). This upper soil layer (and both soil regions), possess a single value for vertical hydraulic conductivity with a value of k_1 (in units of length/time [e.g., ft/sec]). The lower soil layer is also modeled by two soil regions (R02 and R04), these are specified to be an effective stress material (E). This lower soil layer (and both soil regions) possess a single value for vertical hydraulic conductivity with a value of k_2. The value for k_2 is one-half the value of k_1.

Figure 2.9. Distributions of water pressures acting normal to the I-Wall and sheet-pile wall – hetergenous seepage for two soil layers, (a) Water and pore-water pressure distributions on the LHS and RHS. (b) The net water pressure distribution.



The Appendix C line of seepage (a.k.a. line of creep) is used to compute pore-water pressures for a steady-state seepage condition within the soil starting at the ground surface on the high head RHS of the sheet pile, down to the tip of the sheet pile, and then back up to the ground surface on the low head LHS of the sheet pile.

The two Figure 2.9a LHS soil region's (R01 and R02) are associated with a single piezometric surface that corresponds to the LHS surface water (designated as the LHS surface water number P01). The two RHS soil region's (R03 and R04) are associated with a single piezometric surface that corresponds to the RHS surface water (designated as the RHS surface water number P01). Hydrostatic water pressures act against the I-Wall above the LHS and RHS ground surfaces. These two (surface) water pressure distributions increase with decreasing elevation at a rate equal to the unit weight of water (i.e., γ_{water} = 62.4 pcf) per unit of depth (i.e., 1 ft in this case). Because of head loss due to seepage, the pore-water pressures within the soil below the LHS and RHS ground increase in value with decreasing elevation at a rate equal to less than γ_{water} per unit of depth. Additionally, at the interface between the upper soil region and the lower soil region, there is a change in the rate of pore water pressure computed with depth by the Appendix C line of seepage procedure due to the contrast in hydraulic conductivity values for the two soil layers. Observe at the sheet-pile tip

(Figure 2.9a), that there is continuity in the LHS and RHS hydrostatic pore water pressure values.

Figure 2.9b shows the distribution of net water pressures acting normal to the I-Wall and sheet-pile wall. The distribution of net water pressures is equal to the difference between the RHS and LHS Figure 2.9a water pressures. Observe that the continuity in the Figure 2.9a pore-water pressures at the sheet-pile tip is reflected in the net water pressure diagram of Figure 2.9b with a zero net water pressure.

2.9 Surcharge pressures, horizontal pressures and line loads

Externally applied pressures and line loads are used in Corps_I-Wall Version 1.0 to compute equivalent horizontal pressures acting along the sheet-pile wall. These surcharges will increase the overall horizontal pressures. Horizontal distributed pressures and horizontal line loads always act normal to the sheet-pile wall and can be assigned by specifying line loads at particular elevations at the wall or by specifying one or a series of trapezoid pressures at elevations along the I-Wall. Vertical pressures and line loads always act normal to the ground surface[1]. There are six methods used to define externally applied pressures and line loads. These pressure distributions and line loads will compute a value of equivalent horizontal pressure at nodal points along the wall.

2.9.1 Externally applied horizontal pressure distribution and line loading

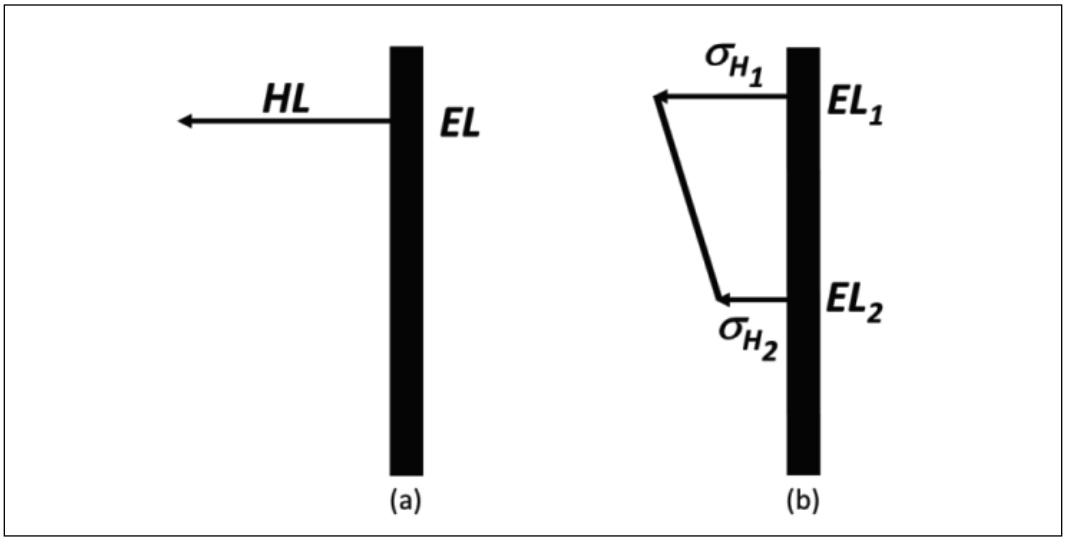
Horizontal pressures and line loads are usually introduced for an I-Wall rotational stability analysis when wave actions originating from storms with available wave loading information are being considered. The two types of user-defined horizontal pressure distribution and line loads are illustrated by Figure 2.10. Figure 2.10a represents a line load applied at elevation (el) with loading of HL force. Figure 2.10b represents a pressure distribution of two horizontal pressures. The first is applied at elevation el_1 with pressure of σ_{H1} and the second at elevation el_2 with pressure of σ_{H2}. Multiple line loads and combinations of distributed pressures can be assigned. A positive line load or pressure distribution acts toward the left[2]

[1] Analyses of I-Walls produced from Corps_I-Wall, Version 2.0 using the Coefficient Method of analysis, are on level ground. Therefore, all pressures and forces are vertical and act normal to the ground surface.

[2] Surcharge pressures or loads located (a) on the RHS of the I-Wall will act toward the I-Wall and (b) on the LHS of the I-Wall will act away from the I-Wall.

and a negative line load or pressure distribution will act toward the right[1]. Therefore, there can be positive or negative loads and pressure distributions on either side of the I-Wall.

Figure 2.10. External horizontal line load and pressures. (a) Line load. (b) Distributed pressures.



2.9.2 Externally applied vertical pressure distribution and line loading

Surface surcharge pressures and line loads are usually introduced for an I-Wall rotational stability analysis when external structures, such as buildings, construction equipment, vegetation, or stockpiles are considered. There is one definition for applying vertical line loads and four variations for describing possible applied vertical pressure distributions. Pressures due to line loads can be calculated using Figure 2.11. The two elastic half-space theory-based relationships given in Figure 2.11 include a factor of two, as per Clough and Duncan's (1991) concept figure (Figure 6.14) for a wall retaining non-yielding soil. A uniform surface surcharge pressure (Q) is added directly as overburden pressure at the ground surface. The vertical stress will increase by the amount of the surcharge. Horizontal pressures from strip, ramp, triangular, and trapezoidal distributions can be calculated using Figure 2.12. These relationships are for a wall retaining yielding backfill. For walls retaining non-yielding backfills, a factor of two would be applied to these relationships. Horizontal pressures due to the various surcharge distributions can be calculated by applying the principle of superposition to the solutions.

[1] Surcharge pressures or loads located (a) on the RHS of the I-Wall will act away from the I-Wall and (b) on the LHS of the I-Wall will act toward the I-Wall.

Figure 2.11. Vertical line load.

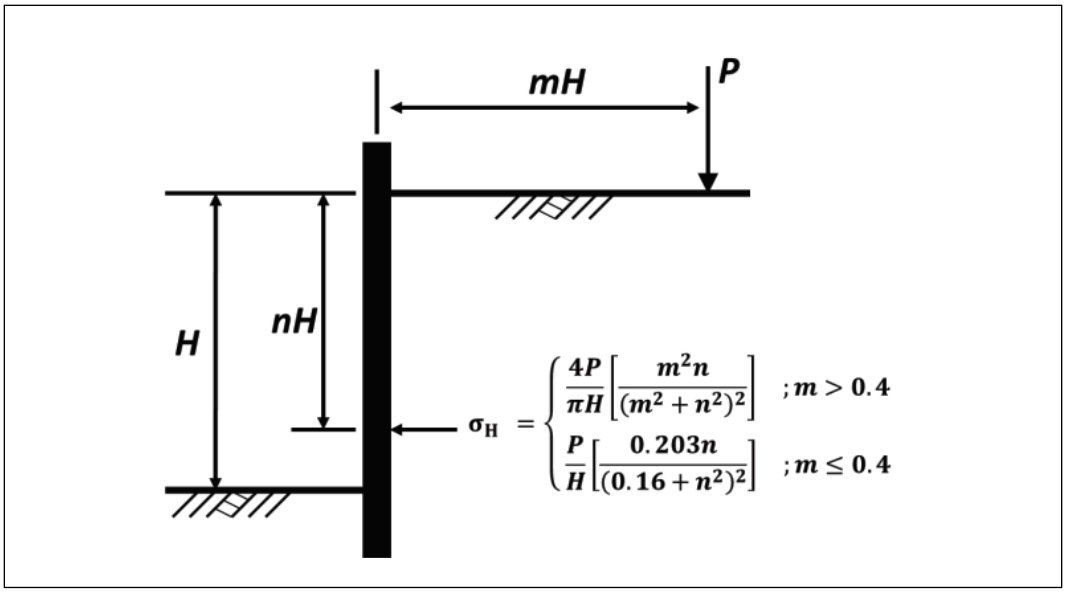
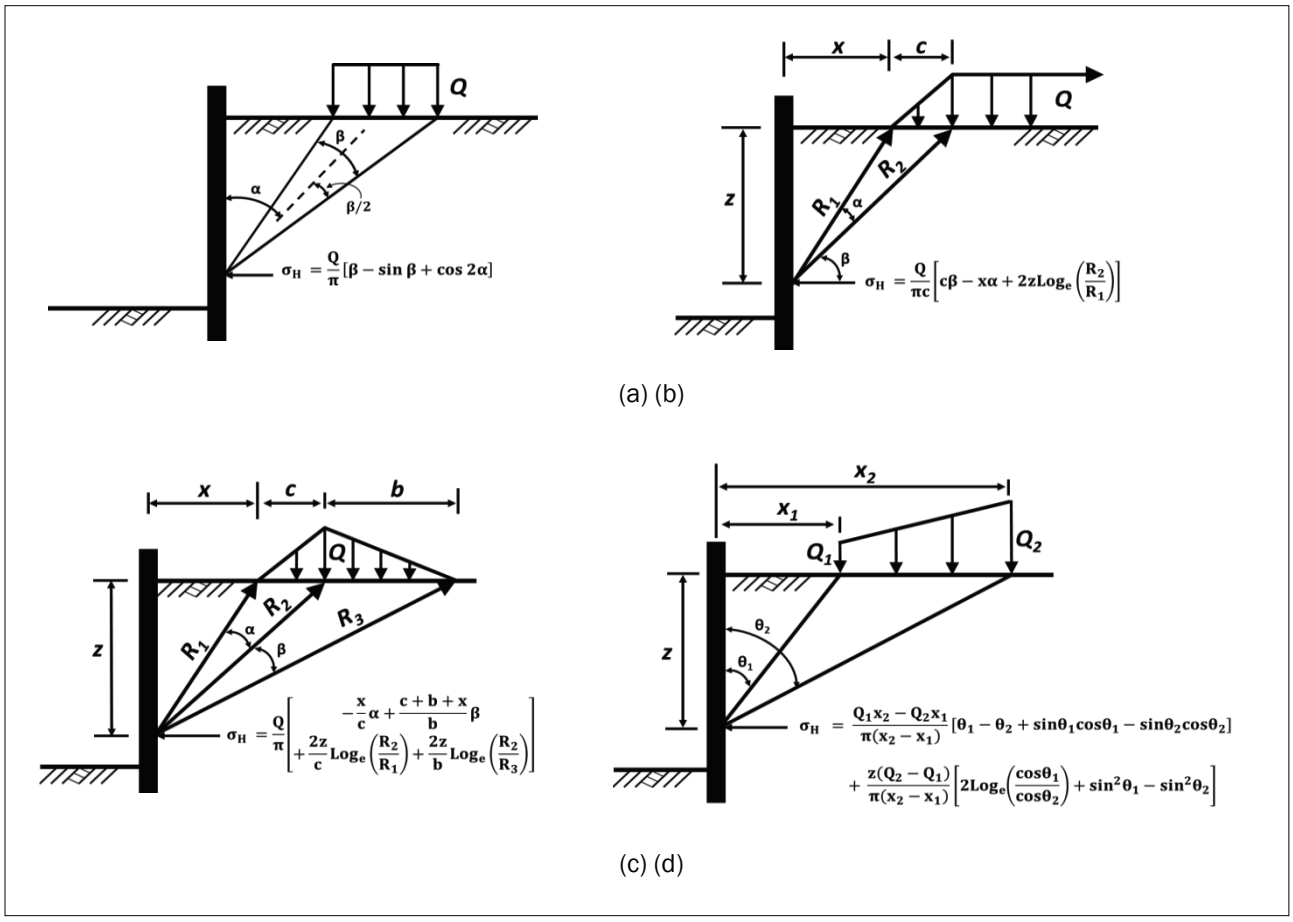


Figure 2.12. Vertical pressure distributions. (a) Strip pressure. (b) Ramp pressure. (c) Triangular pressure. (d) Trapezoidal pressure.



2.10 Shear force and moment distribution internal to the I-Wall and sheet pile

The shear force and moment internal to the I-Wall/sheet-pile wall are computed following the procedure outlined in Figures 2.13 and 2.14. From the top of the I-Wall down to the sheet-pile tip, wall segments are defined by each pair of adjacent nodes. Figure 2.13 depicts wall segment *k* between node *i* and node *i*+1. Similarly, Figure 2.14 depicts the Figure 2.13 wall segment *k* and wall segment *k*+1 between node *i*+1 and node *i*+2. Since there can be a discontinuity in normal pressure at each interface between adjoining soil regions (e.g., at node *i*+1 in Figure 2.14), there is a need to maintain an upper and a lower earth pressure computation per node to accommodate this possibility (e.g., for node *i*+1, designating it as σ_{i+1}^{+} and σ_{i+1}^{-} in Figure 2.14).

For each wall segment, the software converts the applied pressure distribution into equivalent nodal point forces (F_i^- and F_{i+1}^+) using the one-third/one-sixth force computational procedure described in Section 2.4. With the exception of the top node, and the node at the sheet-pile tip, a plus and minus designated equivalent nodal point force is computed. At the top of the I-Wall loaded wall segment, only a minus designated equivalent nodal point force is computed. Similarly, at the tip of the sheet-pile wall, only a plus designated equivalent nodal point force is computed.

Figure 2.13. Internal shear and moment at node *i*+1 for wall segment *k*. (a) Trapezoidal pressure distribution. (b) Equivalent nodal point forces.

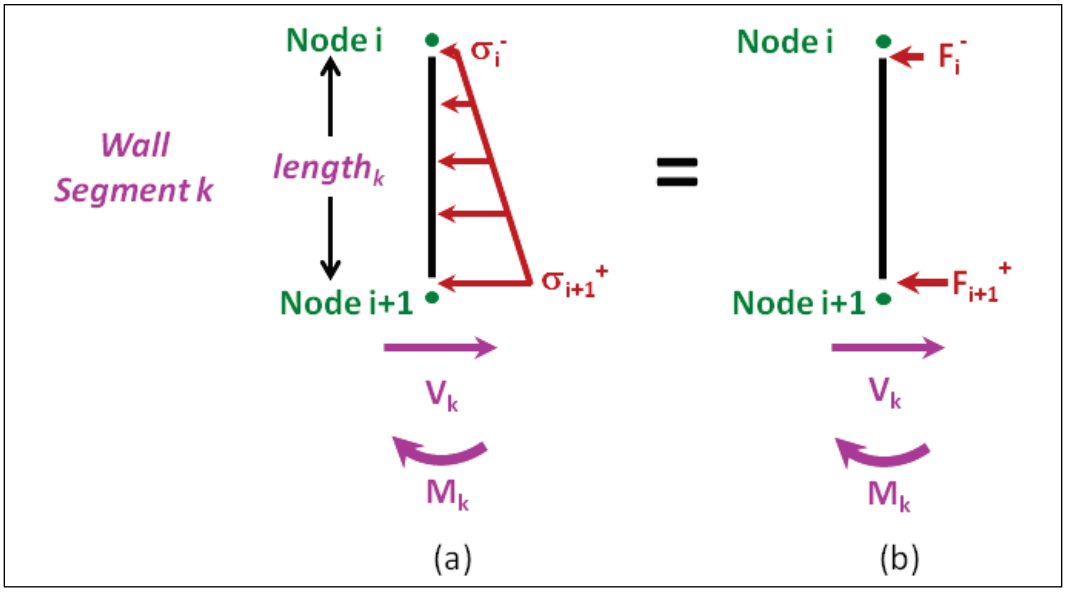
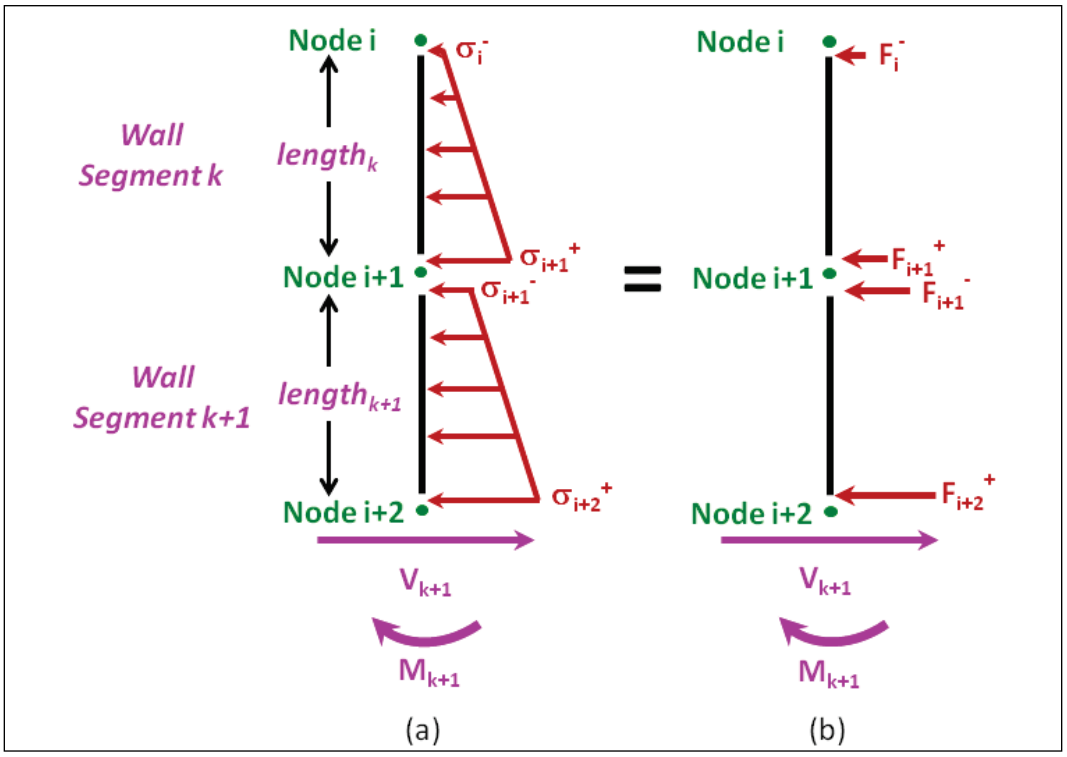


Figure 2.14. Internal shear and moment at node i+2 for wall segment k+1. (a) Trapezoidal pressure distributions. (b) Equivalent nodal point forces.



Internal shear force: The shear force V_k, located at the bottom of Figure 2.13 wall segment k, is equal to the sum of forces acting on wall segment k.

$$V_k = F_i^- + F_{i+1}^+ \tag{2.42}$$

This shear force V_k is assigned at the elevation of node i+1 within the software.

The shear force V_{k+1}, located at the bottom of Figure 2.14 wall segment k+1, is equal to the sum of forces acting on wall segments k and k+1.

$$V_{k+1} = F_i^- + F_{i+1}^+ + F_{i+1}^- + F_{i+2}^+ \tag{2.43}$$

This shear force V_{k+1} is assigned at the elevation of node i+2 within the software.

This calculation procedure is followed top down for all wall nodes to define the distribution of shear force internal to the wall.

Internal moment:

The moment M_k, located at the bottom of the Figure 2.13 wall segment k, is equal to the sum of forces acting on wall segment k.

$$M_k = F_i^- \cdot length_k \tag{2.44}$$

This moment, M_k, is assigned at the elevation of node i+1 within the software.

The moment M_{k+1}, located at the bottom of the Figure 2.14 wall segment k+1, is equal to the sum of forces acting on wall segments k and k+1 times their respective lever arm.

$$M_{k+1} = F_i^- \cdot (length_k + length_{k+1}) + \{F_{i+1}^+ + F_{i+1}^-\} * (length_{k+1}) \tag{2.45}$$

This moment, M_{k+1}, is assigned at the elevation of node i+2 within the software.

This calculation procedure is followed top down for all wall nodes to define the distribution of moment internal to the wall.

The resulting distributions of internal shear and moment are tabulated and presented in graphical form by the software, as shown in Figures 3.70 and 3.72 of Chapter 3.

3 Visual Modeler GUI User's Guide

3.1 Introduction

This chapter discusses the Visual Modeler for the Corps_I-Wall software. The Visual Modeler allows the user to create the input that will be processed, to process the input to gather results, and to visualize the results in a meaningful fashion. An example problem is used to demonstrate the features for input and output visualization.

3.2 Example problem

The input and screen captures are all built around an example problem that illustrate many of the more involved features in the GUI. This subsection defines the input parameters for the I-Wall section being analyzed.

The I-Wall section in the example problem (Figure 3.1) is 12 ft high, has a layer of loose sand beginning at el 0.0, and has another layer of dense sand beginning at el -10 ft. Because the sheet-pile section is being designed, the program will determine an appropriate depth of embedment for the I-Wall. Because the Wedge Method will extend the soil regions, the modeled soils will only extend a short way from the I-Wall (for input with the GUI).

On the flood side of the I-Wall, which is arbitrarily chosen to be on the LHS of the I-Wall, there is surface water, which begins at el 10 ft. On the landside of the I-Wall (RHS), there is a water table, which is modeled as a piezometric surface at an el -1.0 ft. γ_{water} is given as 62.4 pcf.

The soil properties for loose and dense sand use effective stress and are given in Table 3.1.

Gap propagation is enabled, and heterogeneous seepage is enabled to show the effects of different soil properties.

Figure 3.1. Example problem for an I-Wall section used to illustrate features of the GUI.

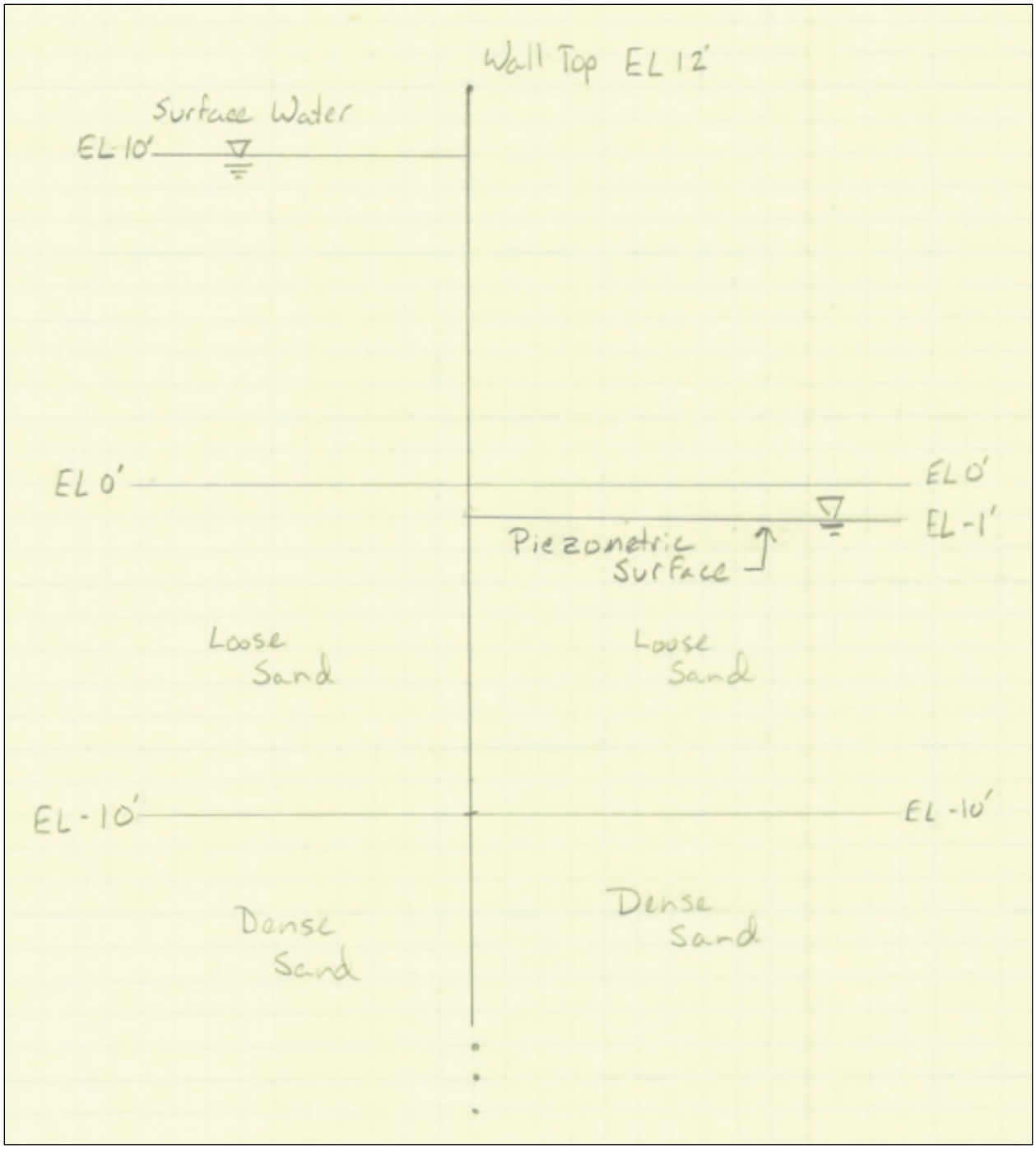


Table 3.1. Input soil properties for the example problem.

Soil Layer	Loose Sand	Dense Sand
γ_{moist} (pcf)	110	115
$\gamma_{saturated}$ (pcf)	122.4	126
FS_{active}	1.0	1.5
$FS_{passive}$	1.0	1.5
C′	5.0	0.0
φ′	30°	36°
δ′	15°	18°
C_A′ (psf)	0.0	0.0
K (cm/sec)	3×10^{-3}	1×10^{-3}
K (ft/sec)	0.000098425	0.000032808

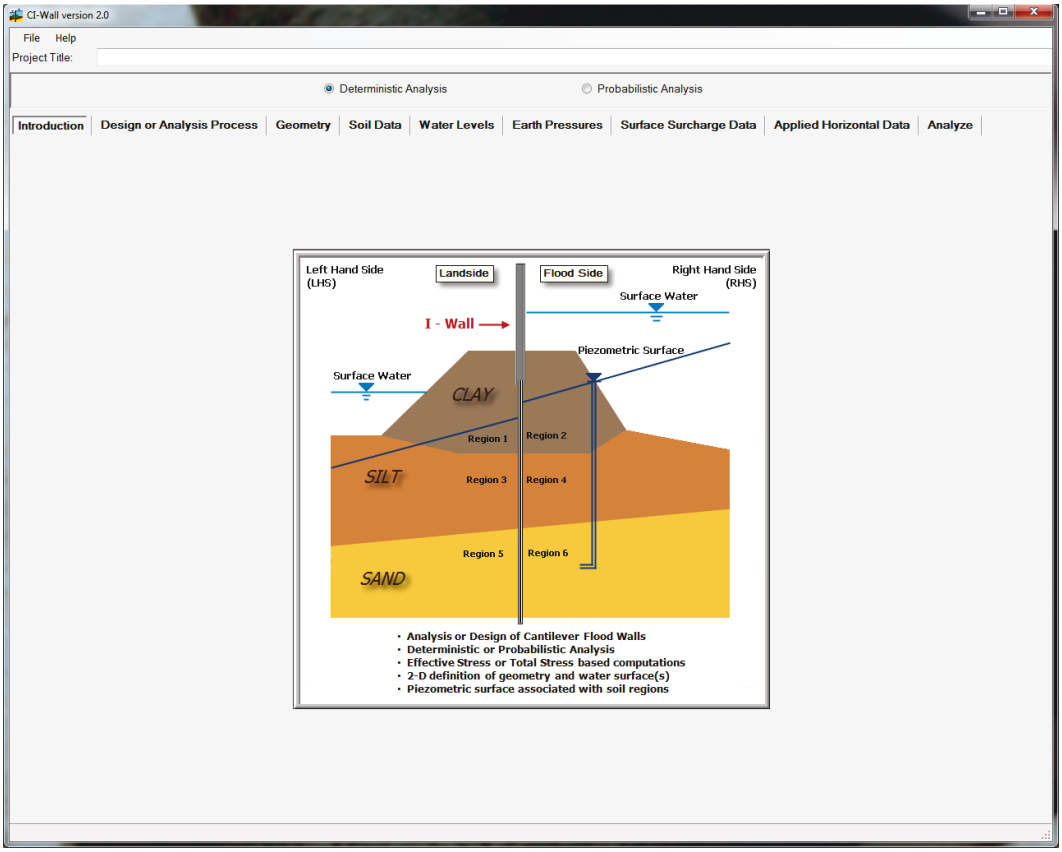
3.3 *Introduction* tab

When the Corps_I-Wall program opens, the first display is the *Introduction* tab (Figure 3.2) and problem-specific input fields at the top of the page. The *Introduction* tab contains an image that illustrates the kind of problems that Corps_I-Wall will be able to analyze.

The input data at the top of the window (which is available no matter which tab is selected) contains a project title text entry box and radio button selectors for whether the current analysis will be deterministic or probabilistic. Each project should be given a unique title, multiple projects and analyses can be saved in the same directory. Because filenames can become cryptic, a good description of the problem in the project title can provide a way to differentiate files.

The selector for whether a project will be deterministic or probabilistic will be discussed in more detail in the section dealing with soil properties.

Figure 3.2. *Introduction* tab of Corps_I-Wall program.



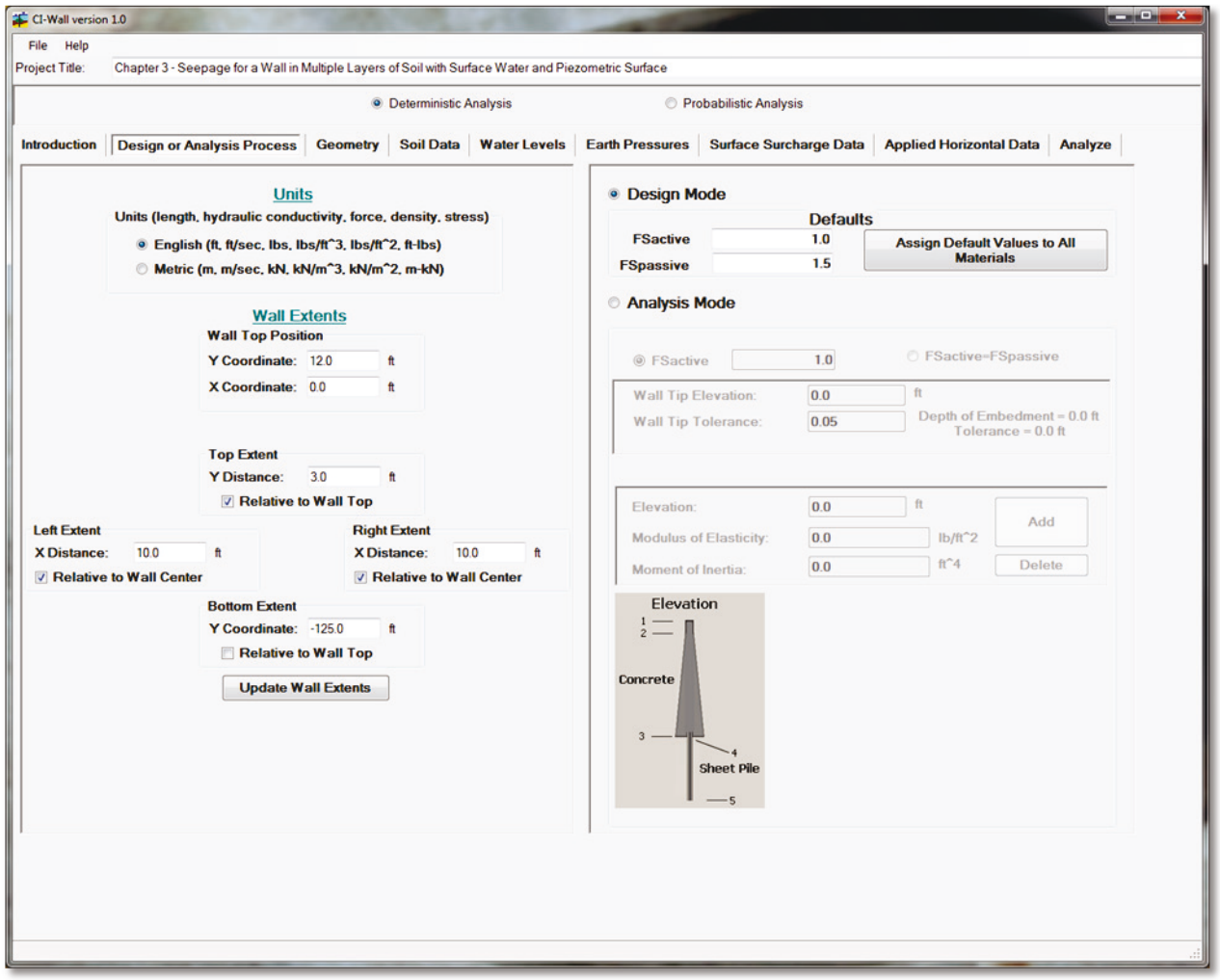
3.4 *Design or Analysis Process* tab

While named the *Design or Analysis Process* tab, this tab actually also has a geometric extent and unit information section. The geometric extents describe the area in which a problem will be solved. It is used for visualization purposes; the fully-defined model will be expected to reach the left and right extents and to be sitting on the bottom extent.

The area for unit selection and extent entry is to the left of the *Design or Analysis Process* tab (as shown in Figure 3.3). Radio buttons allow the user to choose the appropriate units of measure that will be used for the project. If the user selects metric units, all distance coordinates will be entered in with decimal meters. For English measurements, distance coordinate data entry will be in decimal feet.

The I-Wall extent entries are next. The first two entries for the I-Wall extents are the y- and x- axis coordinates of the I-Wall top. These are given in absolute coordinates and establish the right-handed coordinate system for the I-Wall system, with the I-Wall extending along the y-axis.

Figure 3.3. *Design or Analysis Process - Design* mode.



The next entry is the *y*-coordinate for the highest data point expected to be used for the model. Because some models may be built with water levels that exceed the height of the I-Wall, this elevation should be set to the higher of the two elevations. Notice that this entry does not create data points, but only affects the highest point that may be created and shown in the *Geometry* tab discussed later. This coordinate can be entered with either relative coordinates (given by a distance above the I-Wall top) or as an absolute coordinate, depending on the checkbox below the input. Changing the checkbox also adjusts the current value to show the absolute or relative value of the extent. This same process is used for the left, right, and bottom extents.

The left and right extents give the maximum distance that soil-based regions can extend to in the *x*-coordinate. The Corps_I-Wall program uses a right-hand coordinate system, so the extents to the left are in

the -*x* direction and the extents to the right are in the +*x* direction. These extents can be modified in the *Geometry* tab, however, as a good rule-of-thumb, extents should be used to describe how much soil on either side of I-Wall will be needed to solve the problem. It is expected that regions will extend to the extents on either side of the I-Wall. Using relative distances, the extents should be specified with positive numbers. Therefore, if the I-Wall top has a 0.0 *x*-coordinate, the relative left distance of 10.0 gives an absolute extent coordinate of -10.0.

The final entry for the extents of the model is the elevation at the bottom extent of the model. In the *Design* mode, where the program is attempting to determine the appropriate I-Wall tip depth of embedment, this extent should be set deeper than the deepest elevation expected for the I-Wall tip. In *Analysis* mode, this extent should be set to the I-Wall tip depth. In either circumstance, soil regions will be created extending from this elevation to the bottom of the lowest region drawn in the *Geometry* tab.

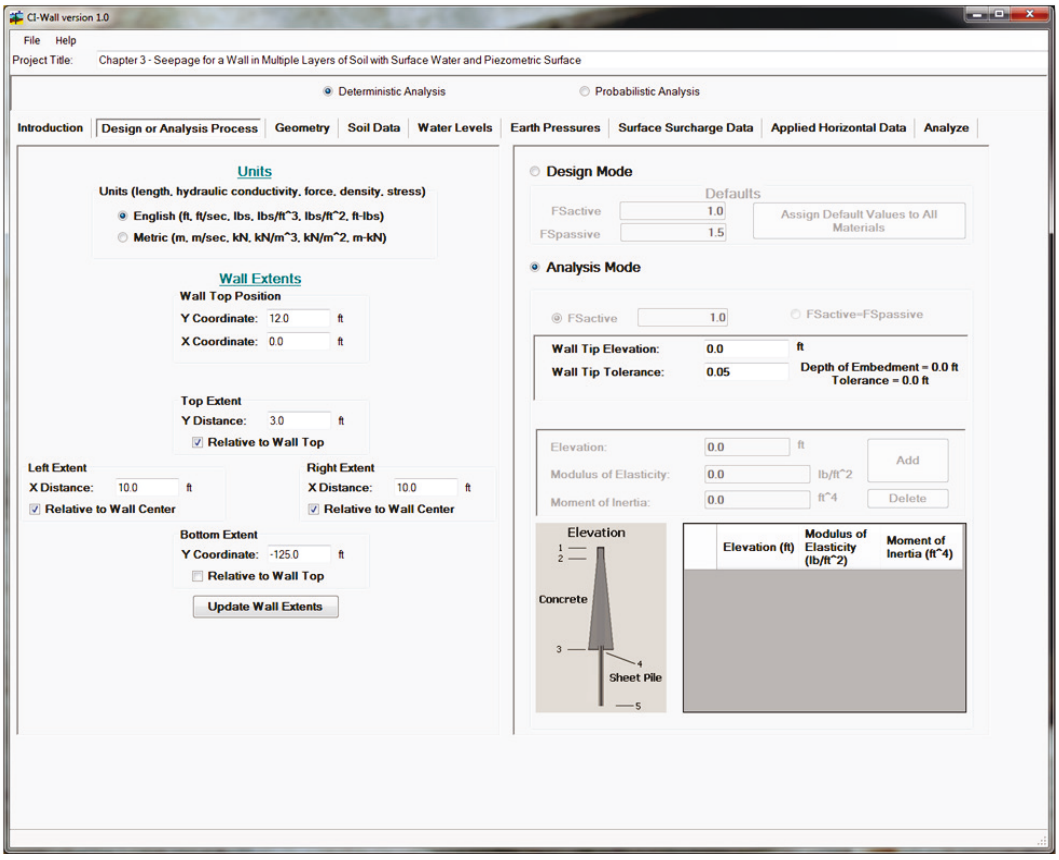
On the right side of the *Design or Analysis Process* tab is the entry for selecting either the *Design* or *Analysis* mode for the solver. Radio buttons allow the user to select the appropriate mode. Each mode has ancillary data that may be entered.

If the *Design* mode is selected, the user is able to set default values for the FS_{active} and $FS_{passive}$ soil data values. When these values have changed, any new soil materials that are created will have these values set to the defaults, and previously existing materials that have the previous default value will be changed to the new default value. A button with the caption *Assign Default Values to All Materials* is next to the text entries for these defaults. If the button is pressed, all previously created soil materials will be assigned the current value of the default entries.

In future versions of Corps_I-Wall for the *Analysis* mode, the user can specify how the FS_{active} is defined, either as a constant value, or equivalent to the each soil material's specified $FS_{passive}$ value. At the moment, this option is grayed out. In *Design* mode, the Corps_I-Wall program is attempting to find a near-optimal I-Wall depth of embedment. In *Analysis* mode, the Corps_I-Wall program is attempting to analyze a fully specified I-Wall, therefore an I-Wall tip elevation should be input, with a tolerance.

Finally, future versions of Corps_I-Wall in *Analysis* mode (shown in Figure 3.4) will allow the user to analyze I-Walls with different properties at different depths and elevations (as shown in the input image at the bottom left of the *Analysis* mode section of the *Design or Analysis Process* tab (Figure 3.4). Future versions will allow the user to specify the I-Wall properties at different elevations. This option is grayed out for the current version. To specify the properties at any point of the I-Wall, the user enters an elevation, modulus of elasticity, and moment of inertia into the text boxes provided. Clicking the *Add* button puts those properties in the list describing the I-Wall, sorted by elevation. The properties at the top of the I-Wall are linearly interpolated to the next data point. If an elevation is entered more than once, then the interpolation ends at the first entered data point and proceeds from the last entered data point at that elevation.

Figure 3.4. *Design or Analysis process - Analysis* mode.

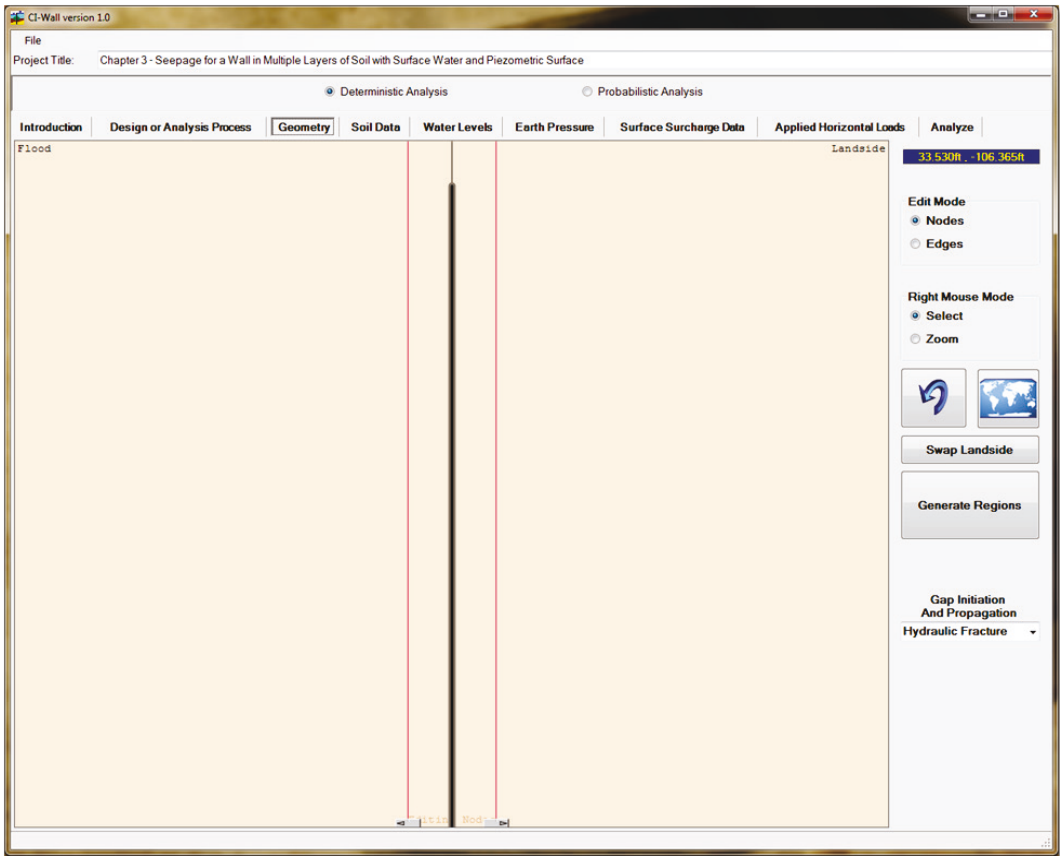


Clicking on the list allows the user to select a specific data point. The *Delete* button gives the user the option to remove points. This operation may be necessary if data points are specified in the wrong order, leading to errors in interpolation of I-Wall properties.

3.5 *Geometry* tab

The *Geometry* tab (Figure 3.5) is where the shapes of the soil regions that lie on either side of the I-Wall are defined. These regions are described using nodes, edges, the I-Wall itself, and the extents entered on the *Design or Analysis Process* tab. Also on this tab is information that will help the user orient the model, designating the sides as either **flood side** or **landside**. While these orientation distinctions do not come to bear in the solver (which works from the materials and properties of the soil and water), they provide the means for the user to establish directionality in the model.

Figure 3.5. Creation of geometry is done with the *Geometry* tab.



The most prominent feature of the tab is the area where the model is displayed. The I-Wall is displayed, as well as the left and right extents of the model, when a new model is created. When the mouse is moved across the model display area, its coordinates in model space are displayed in the upper right-hand corner of the *Geometry* tab in the units selected in the *Design or Analysis Process* tab.

Below the coordinate display are boxes that set the input mode (either nodes or edges) and the right mouse button mode (either *Zoom* or *Select*), and buttons that *Undo* the previous actions, zoom to the current extents of the model, and create the actual regions that will be used from the edges, nodes, and extents of the model.

When the input mode is set to *Nodes* (Figure 3.6a), the user can left-click in the model display area or on the extents of the model. A dialog for node creation then appears with the current coordinates of the mouse and snapped to a certain tolerance (Figure 3.6b). These coordinates can be edited or left as they are in the dialog. Selecting **Ok** creates the node at the selected location (Figure 3.6c), and **Cancel** does not create the node.

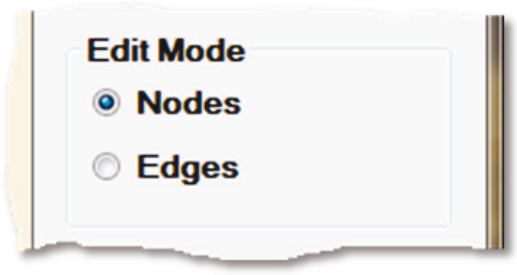
If the left mouse button is pressed when the mouse is over an existing node, then that node will be moved with the mouse until the left mouse button is released. Again, a dialog appears with the new node position, which can be edited. Clicking **Ok** moves the node to the new position and clicking **Cancel** returns the node to its original position.

When the mouse is within a certain distance from the extents, the node positions will snap to the extent.

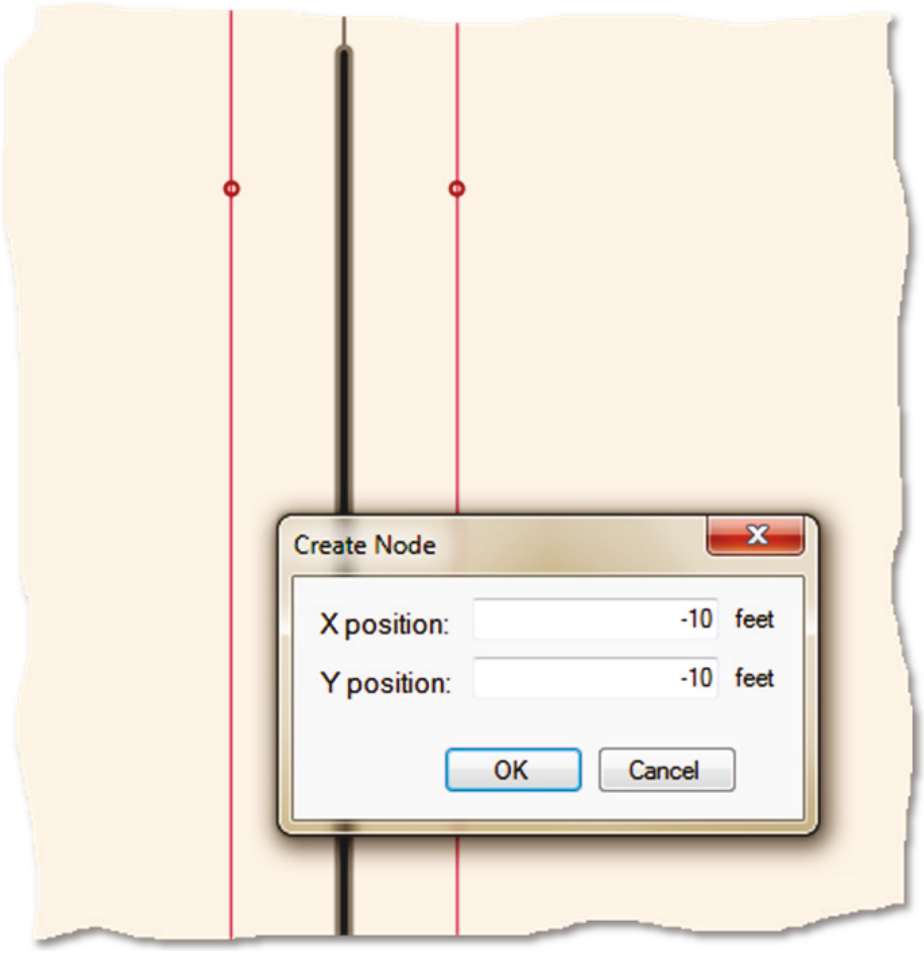
When the input mode is set to *Edges* (Figure 3.7a), the user can connect nodes via edges. To create an edge, the user must press the left mouse button when the mouse is on one node (Figure 3.7b), drag the mouse to another node (Figure 3.7c), and release the left mouse button over this other node (Figure 3.7d). Releasing the left mouse button when it is not over another node will not create an edge.

By default, the right mouse button is in the *Select* mode. By click-dragging the right mouse button, nodes or edges can be selected, depending on the input mode. Nodes are selected when the node is inside the box (or boxes) defined by the right mouse click-drag operation (Figure 3.8a and b). Edges are selected whenever any part of the edge is inside the box (or boxes) defined by the right mouse click-drag operation (Figure 3.9a and b). Multiple selection boxes can be created by holding the shift button while doing multiple right mouse button click-drag operations. To deselect all nodes or edges, the users can right-click anywhere away from any edges or nodes. When a node or edge is selected, it can be deleted by pressing the **Delete** key on the keyboard (Figure 3.8c).

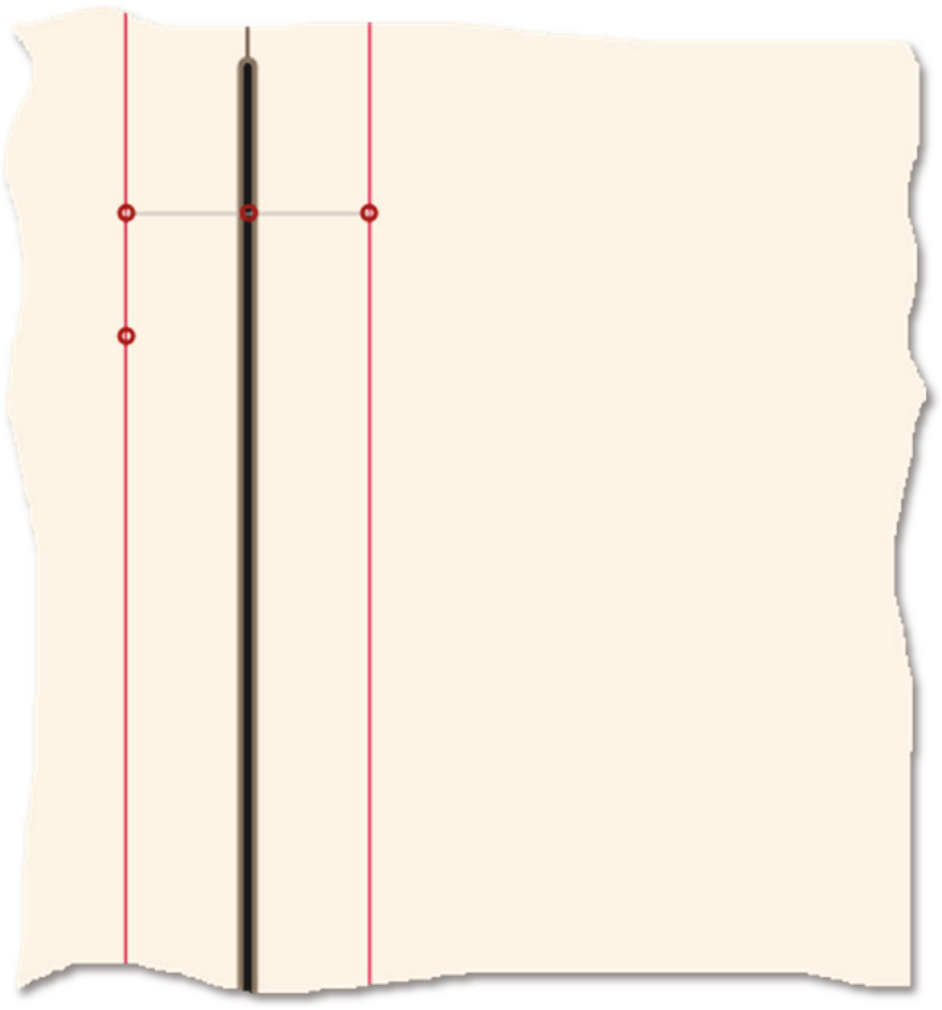
Figure 3.6 The procedure to input a node into the I-Wall geometry.



a. Select the editing mode as Nodes.

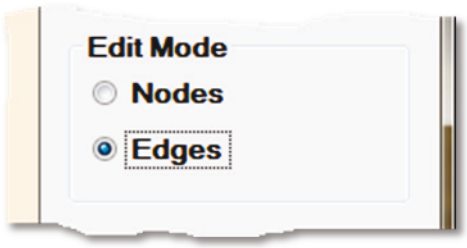


b. Clicking at a close point to where the node should be created brings up a dialog box for accurate input.

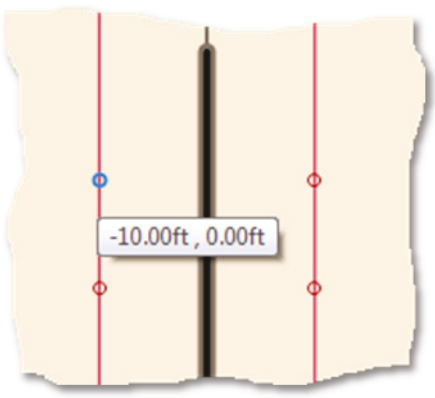


c. Clicking OK in the dialog box creates a node at the specified location.

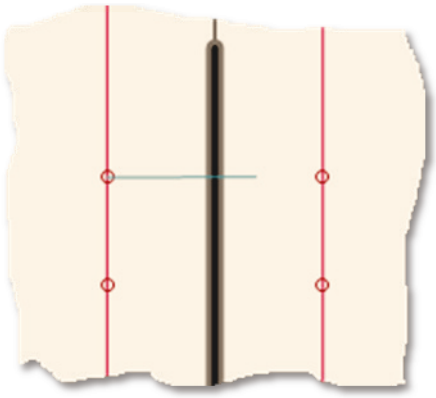
Figure 3.7a-d. The procedure for creating a new edge in the I-Wall geometry.



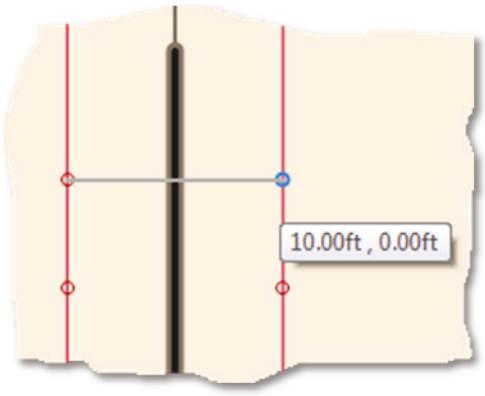
a. Select the editing mode as *Edges*.



b. Click (but don't release) on the beginning node.

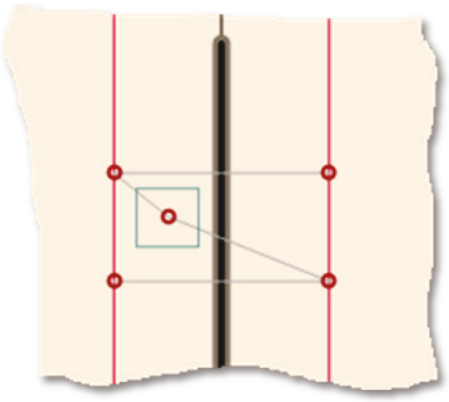


c. Drag the mouse.

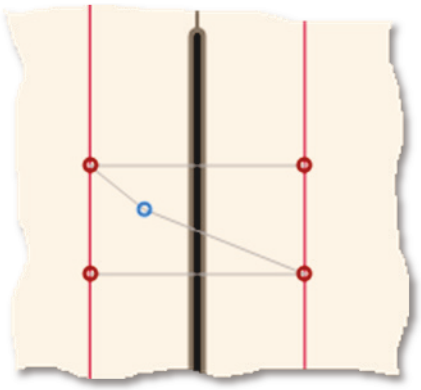


d. Release the mouse button over the ending node position.

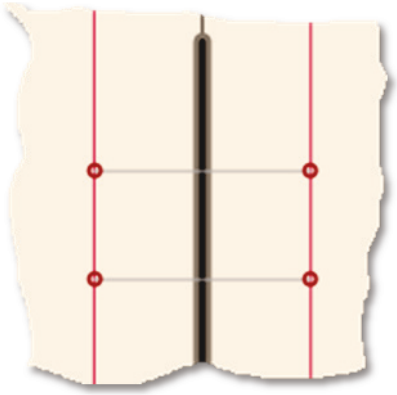
Figure 3.8. The procedures for selecting a node, and for deleting the node (and its connected edges).



a. Click-drag with the mouse.

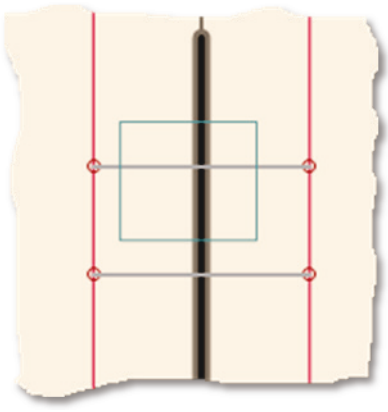


b. The selected node.

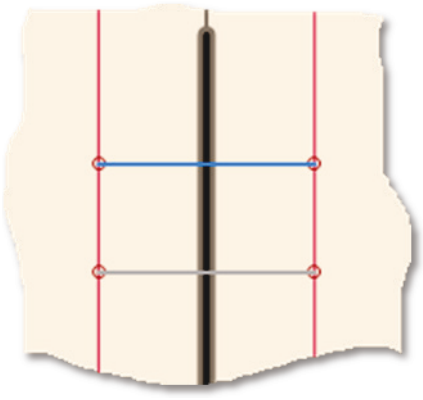


c. After the selected node (with connected edges) is deleted.

Figure 3.9. The procedure for selecting an edge.



a. Click-drag a box over an edge.



b. The selected edge.

When the right mouse button mode is set to **Zoom**, a zoom region can be created by doing a click-drag operation in the model display area (Figure 3.10a and b). The area selected is zoomed and displayed in the model display area. To return to a full extent view, click on the **Zoom Extents** button (Figure 3.11a and b).

At the bottom of each extent line in the model display area is a slider that allows the extents to be widened (Figure 3.12). Sliding the extent causes any nodes that are on the original extent to share an edge at the original extent. This will add a node at the same elevation at the new extent that is also connected with an edge to the node at the original extent. In effect, this creates all the information to describe a new rectangular region to the new extent.

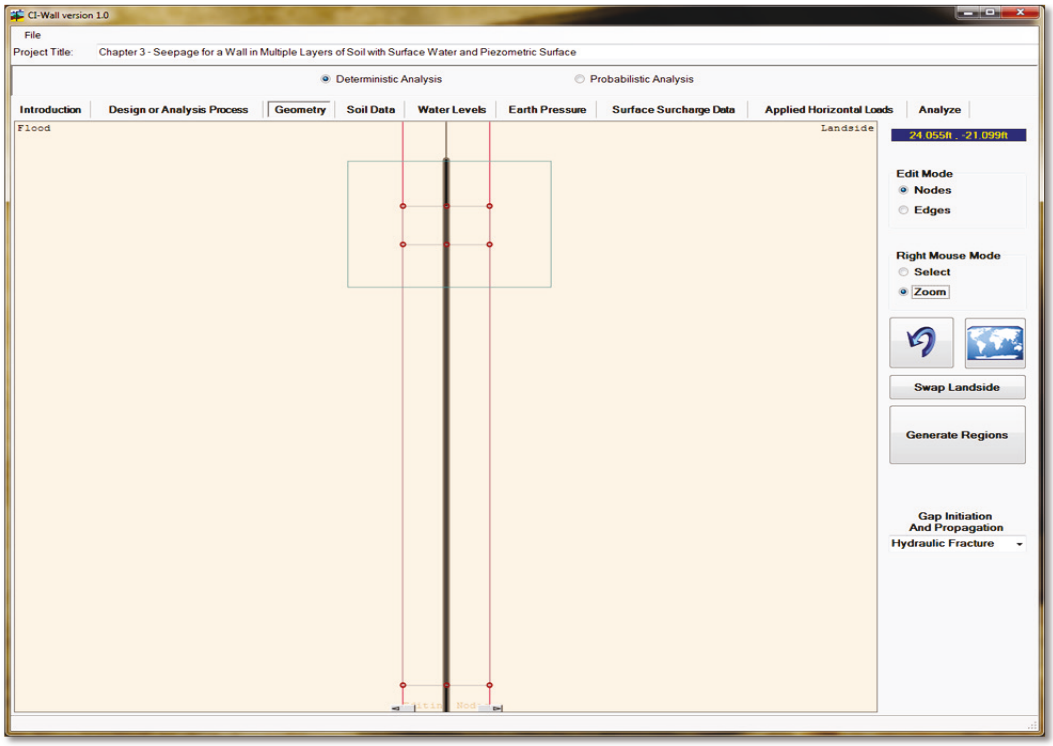
An *Undo* button exists with multiple undo capabilities in a last-in, first-out queue (Figure 3.13a). In this way, the last node or edge created or deleted, or the last movement of an extent can be undone (Figure 3.13b). If a change that involves more than one element is performed (i.e., a node is deleted and therefore deletes two edges that are dependent on the node), then all of the elements are affected by the *Undo* (e.g., the node is replaced with the two edges as in Figure 3.13c).

There is a button that can change the orientation of the model for the user. This button swaps the landside and flood side of the I-Wall (Figure 3.14). By default, the landside of the I-Wall is to the LHS of the I-Wall (in the -x direction). Swapping the sides will not affect the solver operation, but will affect the location of flood and landside water surfaces defined in the *Water Levels* tab.

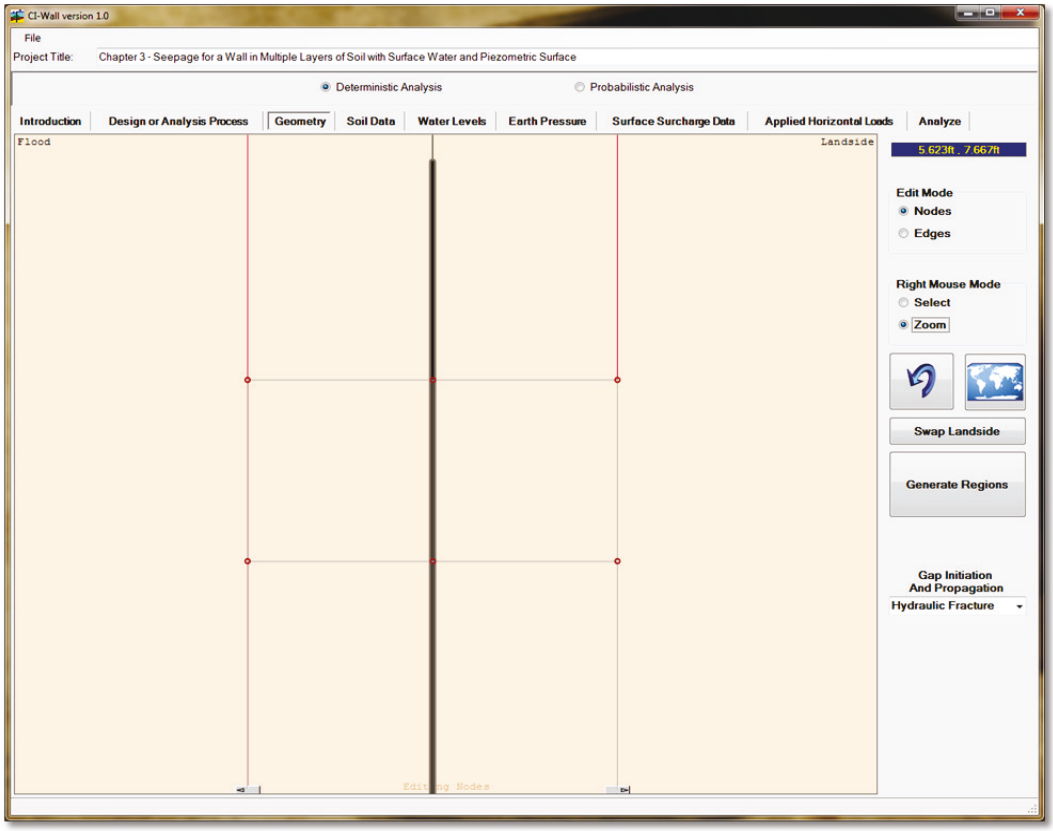
The last button on the *Geometry* tab is the *Region Creation* button (Figure 3.15). When this button is pressed, all of the edges, nodes, and extents are processed to generate a set of regions (where a region is defined as a polygon that encloses an area). These regions will be assigned soil properties on the *Soil Data* tab.

In the *Geometry* tab is a drop-down menu to determine how gap initiation and propagation are handled by Corps_I-Wall (Figure 3.16). The options available in this version of Corps_I-Wall are *No Propagation* and *Hydraulic Fracture*. Gap development occurs when the I-Wall moves away from the containing soil regions and affects the pressure and seepage of the model.

Figure 3.10a-b. The procedure for zooming with the right mouse.



a. Click-drag with the right mouse button to define the zoomed area.

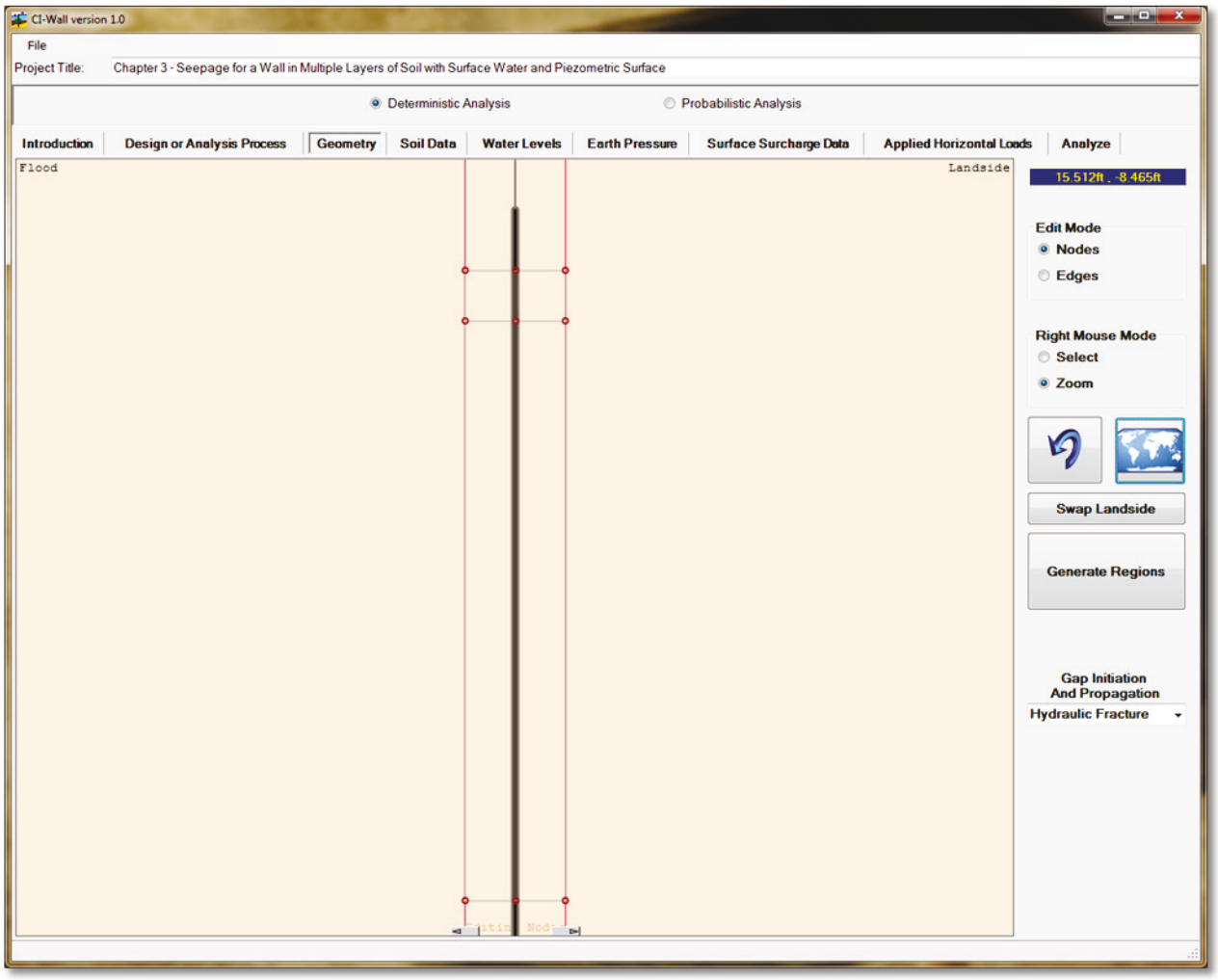


b. The drawing region is then zoomed to that area.

Figure 3.11. Using the *Zoom Extents* button.



a. Clicking the *Zoom Extents* button will restore the full view of the I-Wall.



b. After the *Zoom Extents* button has been pressed.

Figure 3.12. Modifying the extents of the soil regions to the sides of the I-Wall.

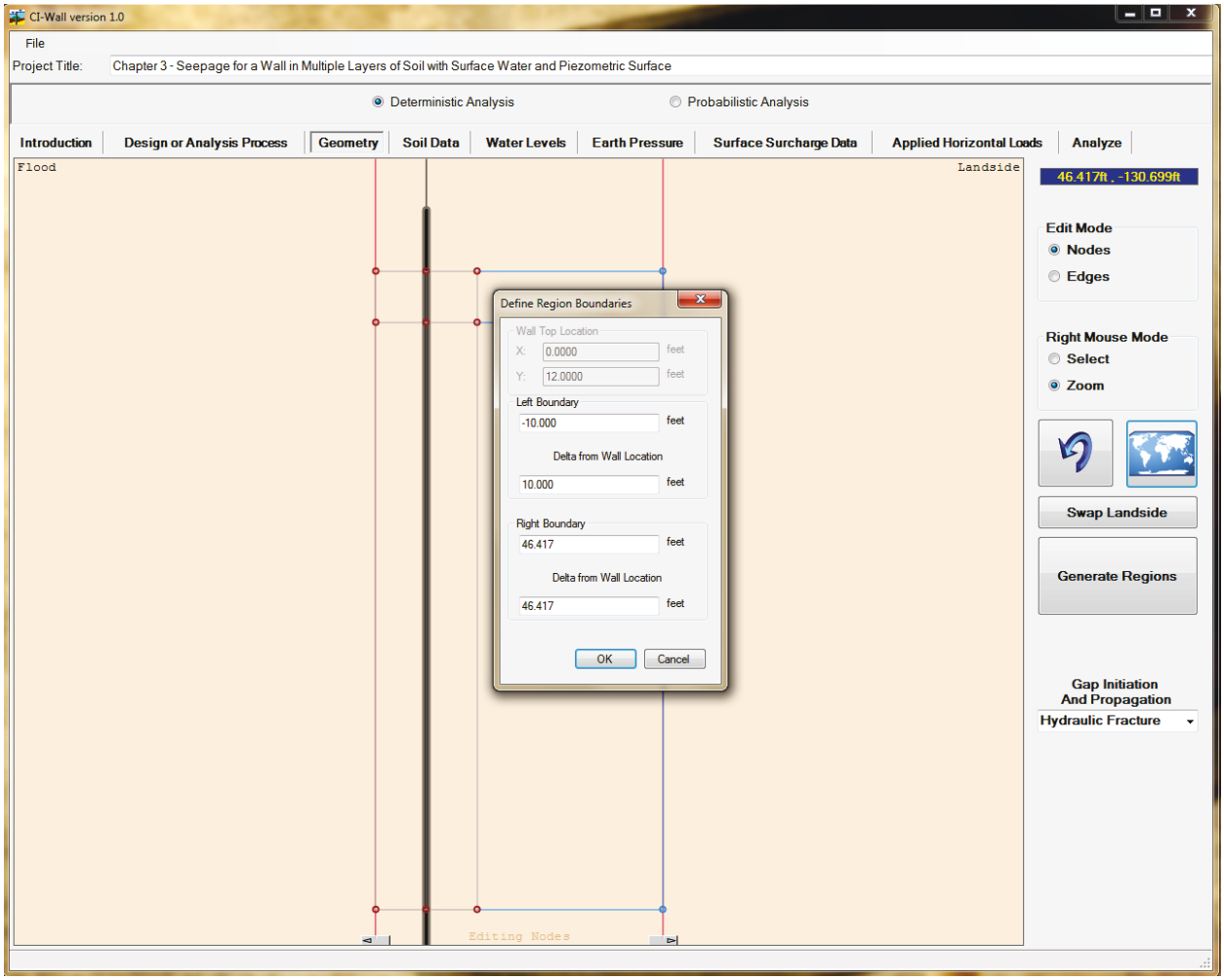
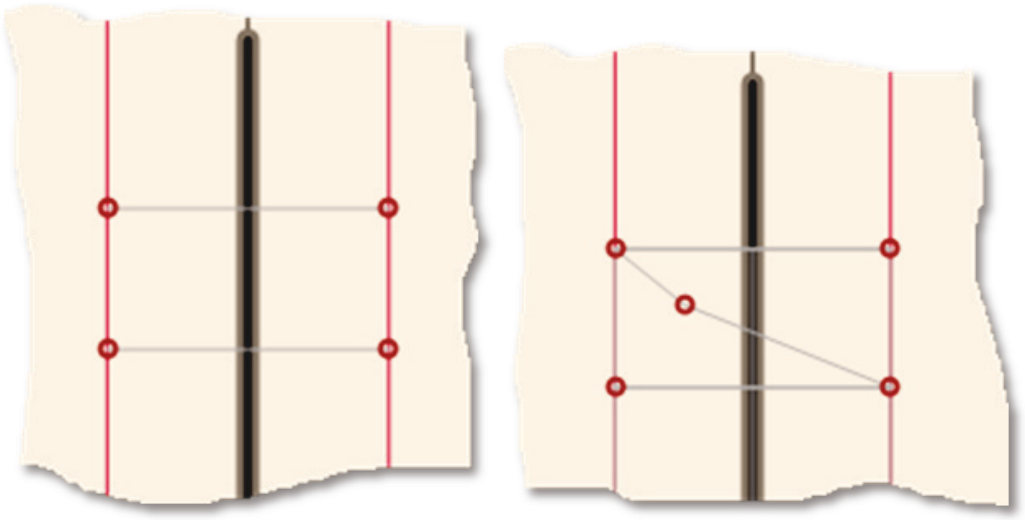


Figure 3.13a-c. Usage of the *Undo* button.



a. The *Undo* button.



b. Before the *Undo*.

c. After the *Undo*.

Figure 3.14. Using the *Swap Landside* button to reverse the *Flood* and *Landside*s of the structure.

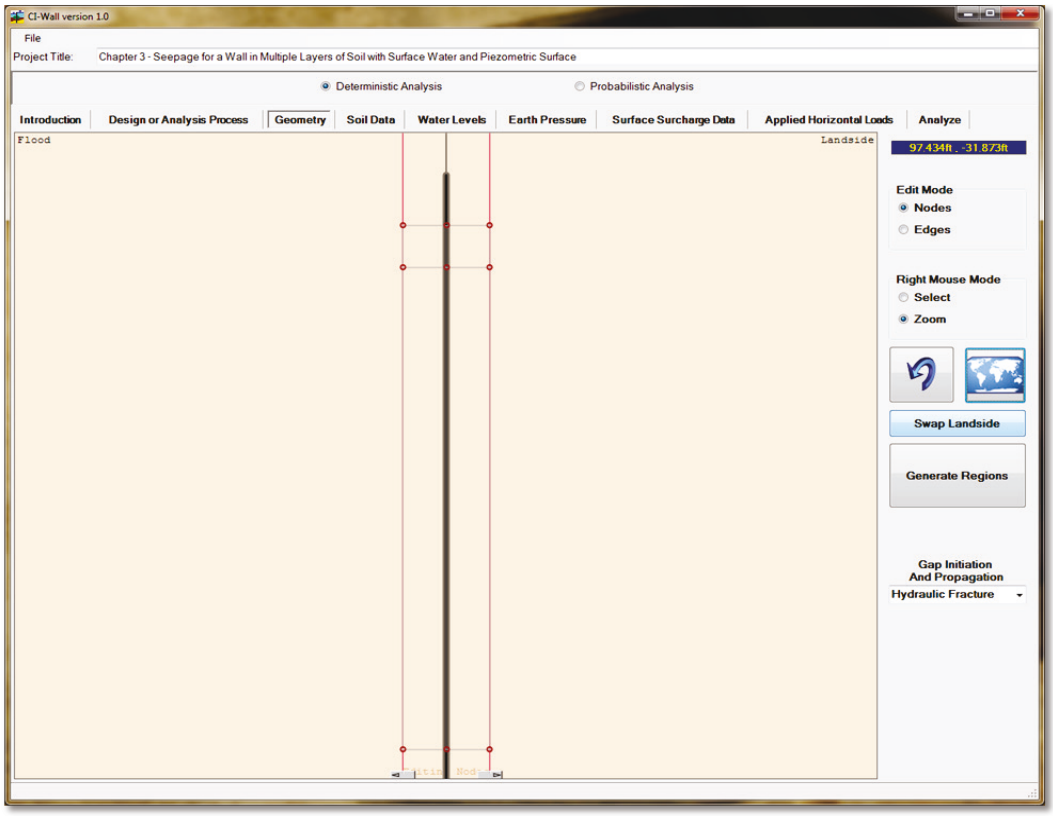


Figure 3.15 Generating regions adds new nodes and edges (to account for intersections with the I-Wall and other edges, and the full I-Wall area). Each area enclosed by edges is a region.

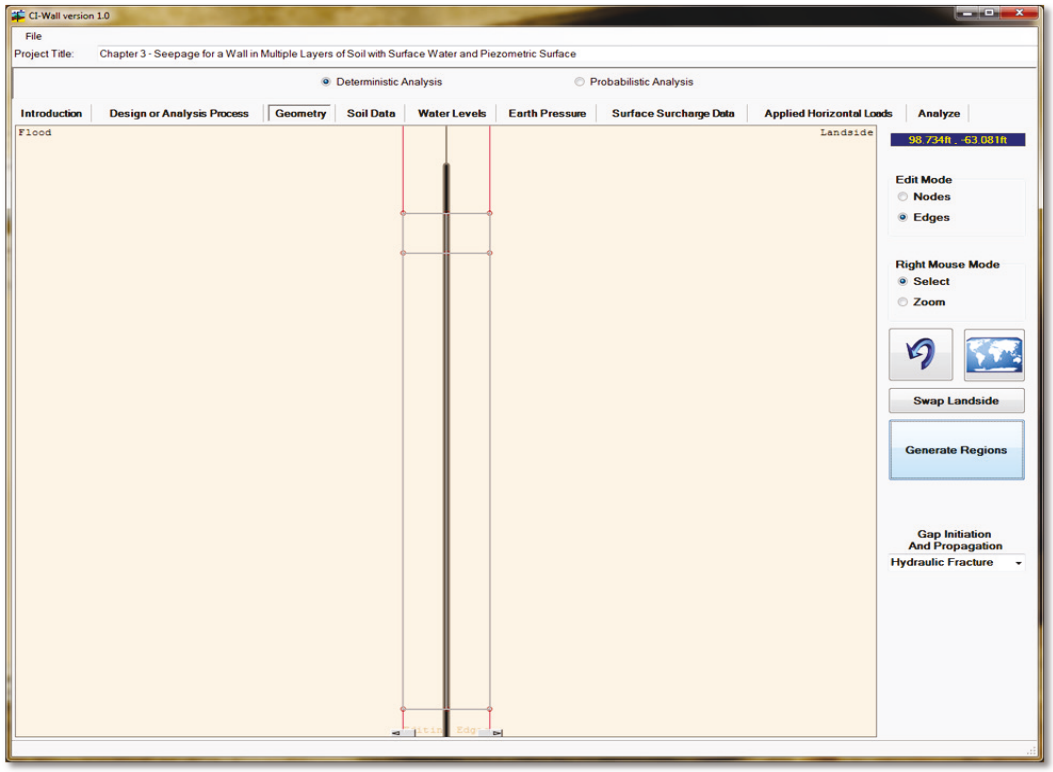
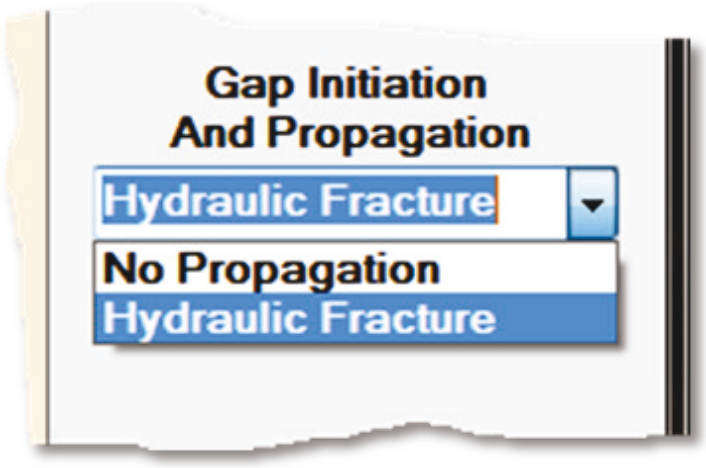


Figure 3.16 Choosing the method of gap creation.



3.6 *Soil Data* tab

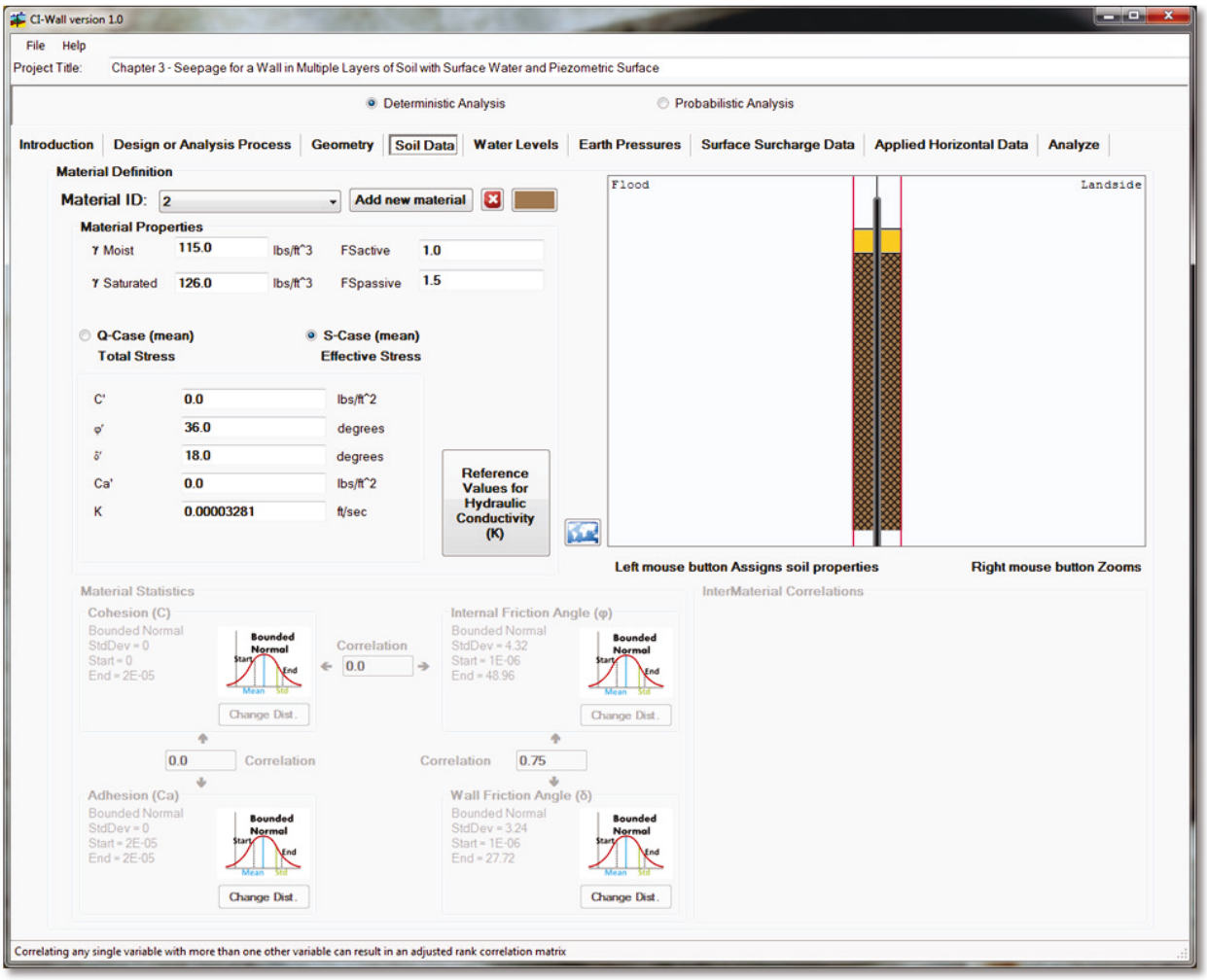
In the *Soil Data* tab, the user can create and edit soil materials deterministically and probabilistically, and assign those materials to the soil regions created in the *Geometry* tab (Figure 3.17). For a new model, there are initially no new materials. Material IDs are the means by which soil properties will be assigned to each region that was generated according to the Section 3.5 instructions.

At the upper left corner of the *Soil Data* tab is a drop-down list, this allows the user to select the current material that is being defined. Next to that drop-down list is a button that allows the user to create a new material. When a new material is created, it is added to the bottom of the list and is set to the current material.

The button next to the *Add New Material* button shows a color. This color is the color with which that material will be displayed (once it is assigned to the region). Pressing that button brings up a color dialog box from which a color may be selected/defined. Default values for high-contrast materials are provided for selection. In order to avoid confusion, each material should be assigned a unique color.

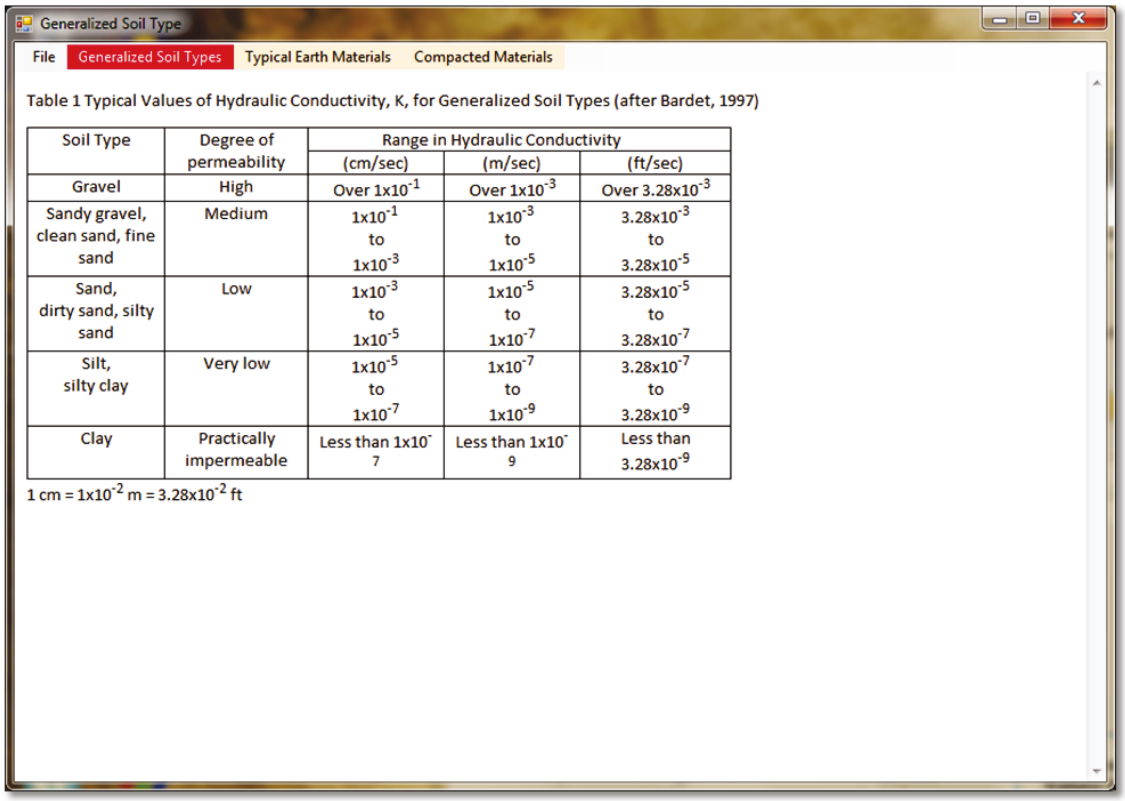
Underneath these controls are the areas where the material properties for the currently selected material are defined. The *Material Properties* box has the input boxes and selectors for deterministic material properties. The unit weights and FS_{active} and $FS_{passive}$ are absolute and are entered separately from the values that can be entered in due to relative stress. Recall that the FS_{active} and $FS_{passive}$ defaults are defined in the *Design or Analysis* tab and that these values can change outside of the *Soil Data* tab.

Figure 3.17. Entering region attributes with the *Soil Data* tab.



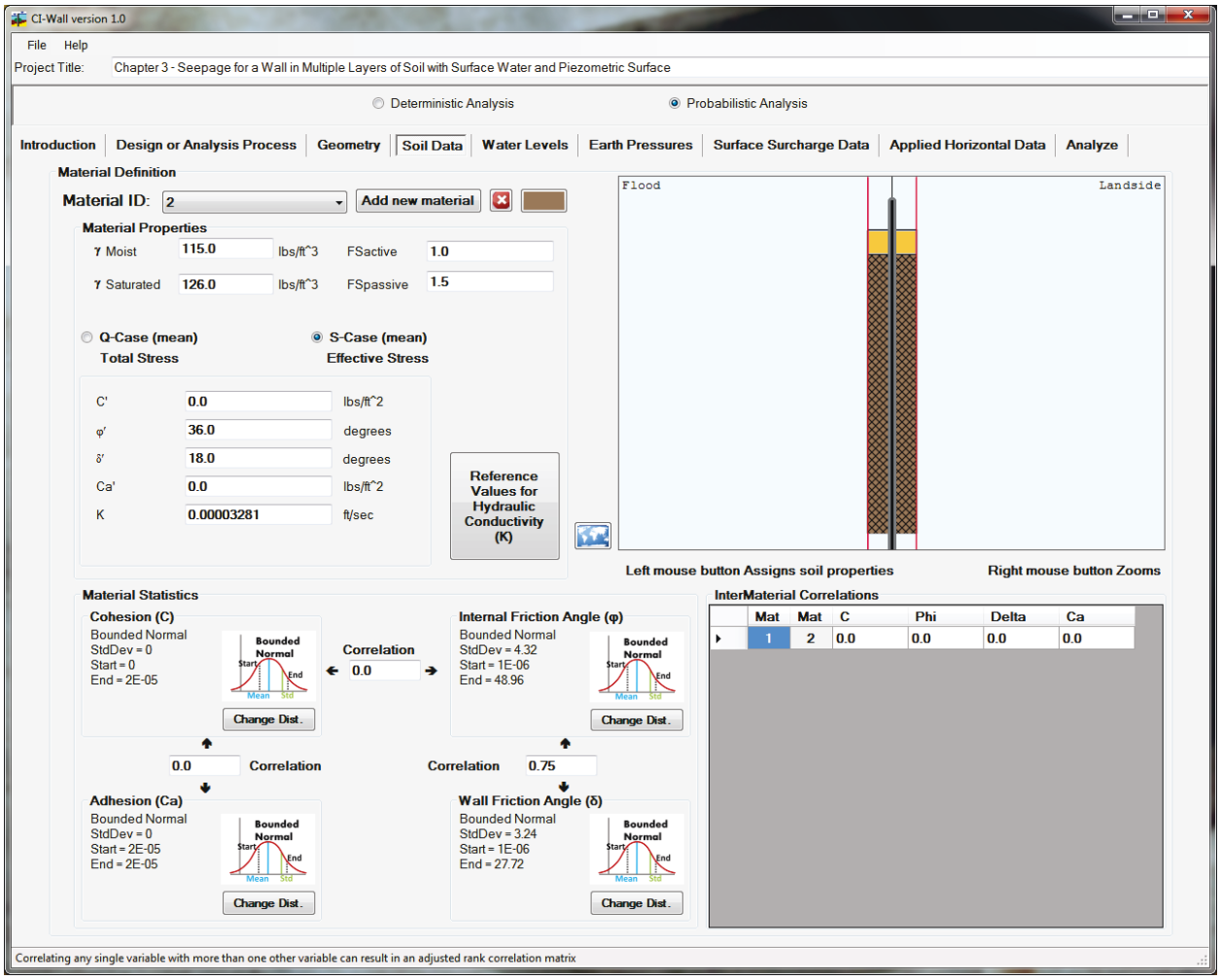
Clicking the button titled *Reference Values for Hydraulic Conductivity (K)* brings up a window with tables containing typical hydraulic conductivity for standard materials (Figure 3.18). This table gives ranges of values in different units for generalized soil types, typical earthen materials, and compacted materials.

Figure 3.18. Reference values for soil types.



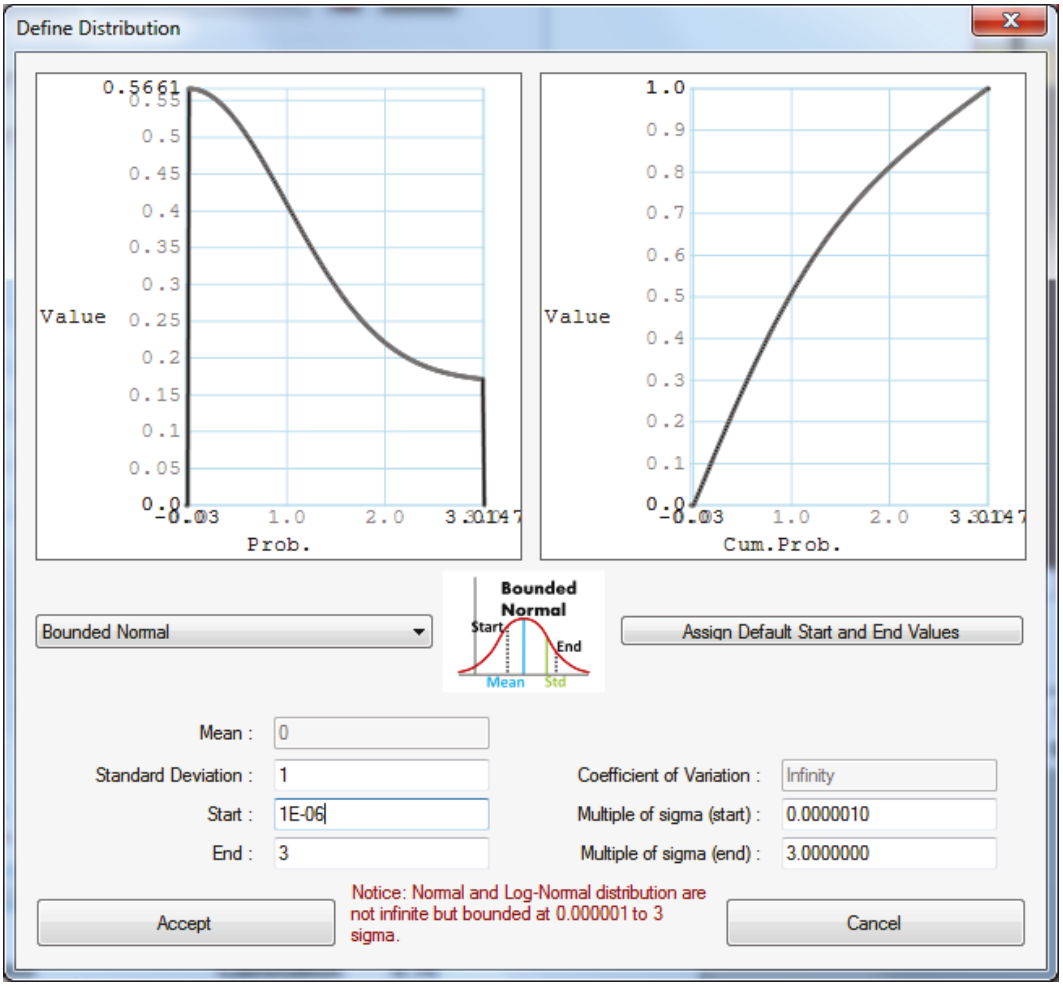
If the *Probabilistic Analysis* radio button is selected at the top of the screen, the *Material Statistics* data input section is enabled (Figure 3.19). This box allows the user to choose a statistical distribution as input for the currently selected material properties. For each property (cohesion *C*, adhesion *Ca*, internal friction angle φ, and soil-to-sheet-pile [wall] friction angle δ), the user is able to specify a distribution method by clicking the *Change Dist.* button. When this button has been clicked, a new input dialog is opened (Figure 3.20). This dialog allows the user to select from the following seven distribution methods: constant, normal, bounded normal, lognormal, bounded lognormal, uniform, and triangular. The probability density function of the currently specified distribution is plotted at the upper left of the dialog box, and the cumulative density function is plotted in the upper right. Below these plots are the *distribution selector* and a symbolic representation of the currently selected distribution and its input values. If the currently selected distribution is either one of the bounded distributions, then a button that fills the bounds with default values is displayed. Below this area is where the input values are input for each distribution.

Figure 3.19. Soil material probabilistic input.



For the constant, normal, bounded normal, lognormal, and bounded log normal distributions, the mean value is fixed at the original value of the currently selected material properties. The normal and lognormal distributions also require a standard deviation to be entered. If the Figure 3.19 (input) mean value of the distributed variable is not 0.0, then the coefficient of variation can be used to define a standard deviation value. For the bounded functions, the function will be defined by a certain region with a start and end point. Both the start and end points can be defined as actual values, or as multiples of the standard deviation. Both the start and end points must also be positive values, with the end value being greater than or equal to the start value. Clicking the **Assign Default Start and End** Values button populates the start value with 0.000001 and the end value with a value equal to 3.0 times the standard deviation plus the mean value, as shown in Figure 3.20, for one of the variables.

Figure 3.20. Selecting/changing a distribution.



For a uniform distribution of a variable, only the start and end values of the distribution need to be specified. Both the start and end values must be greater or equal to 0.0, and the end value must be greater than the start value.

For a triangular distribution of a variable, the start value, end value, and midpoint value of the distribution need to be entered. The start value must be greater than or equal to 0.0. The end value must be greater than the start value. The midpoint value has to be in the range from start to end.

Internal-soil material correlations can also be assigned between adhesion and cohesion, cohesion and internal friction angle, and internal friction angle and soil-to-sheet-pile (wall) friction angle (Figure 3.19).

When the *Probabilistic Analysis* radio button is selected, the box titled *InterMaterial Correlations* is also enabled. Each permutation of pairs of soils is shown in a list. For example, if there are three soil materials, the pairs would be material 1 and 2, material 1 and 3, and material 2 and 3. The user is allowed to input the correlation coefficient value (from -1.0 to 1.0) for similar material properties between two regions. For example, the C′ material property of material 1 can be correlated with the C′ material property of material 3 but the C′ material property of material 1 cannot be correlated with the φ′ property of material 3. Entering an appropriate value in the table for the appropriate pair of materials and the appropriate material property sets the correlation factor between the materials for the property. For example, putting 0.65 into the C′ property of material 2 and 3 correlates the material 2 and 3 C′ values by 65 percent. A correlation coefficient value of 0.0 implies that there is no correlation between material properties.[1]

After a material is defined, it can be assigned to a soil region. In the upper-right of the *Soil Data* tab is the soil assignment box. This box displays the I-Wall and the soil regions. By right-click-dragging a box, this image of the regions and the I-Walls can be zoomed to more effectively display small regions. The button at the bottom left of the soil assignment box (with a picture of the map of the world) is a *Zoom Extents* button to return a full view from the zoomed area.

To assign the currently selected material to any region, simply left-click the mouse button when the mouse button is inside the region. That enclosed region will then be displayed with the color of the currently selected region, affirming the selection. All of the regions with the currently selected material are shown with a pattern, so they can be easily recognized.

It is vital that each region be assigned a Material ID number, thus, assigning soil properties to that region(s). The same Material ID number may be assigned to multiple regions.

3.7 *Water Levels* tab

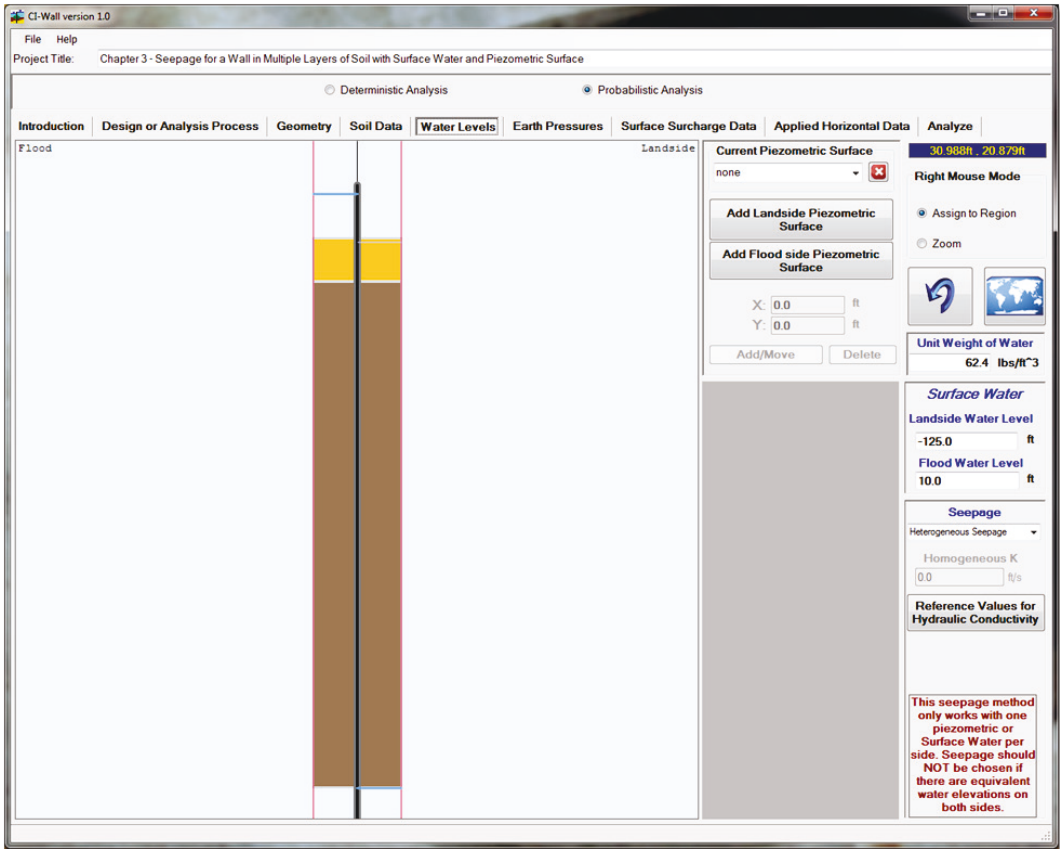
The *Water Levels* tab is one of the most complicated tabs in the Corps_I-Wall software (Figure 3.21). Surface water levels can be input for

[1] In statistics, a correlation coefficient of 0.0 does not mean that the variables are independent. But two independent variables will possess a correlation coefficient value of 0.0.

lateral pressure and overburden pressures on the soil. Piezometric surfaces can be entered to reflect changes of water pressures, including the determination whether soil is moist or saturated. Surface water may also serve to act as a piezometric surface (in an effective stress analysis) for port water pressure calculations. Finally, the effects of seepage can be defined on this tab.

At the left of the tab is the *Soil Assignment Area*. This area initially displays the regions with materials in muted colors. To the upper right of the tab is a *Coordinate Indicator* which shows the current position of the cursor in the *Soil Assignment Area*. Below the coordinate indicator is the right mouse mode selector box. The *Assign to region* option will be discussed later in this subsection. When the right mouse mode is set to *zoom*, then right-click-dragging in the soil assignment area will select a region to zoom to. To zoom back to the extents of the model, simply click the world map button under the right mouse mode selector box. Zooming will allow the user to more closely view piezometric surfaces and assign surfaces to small thin regions.

Figure 3.21. Water levels are defined either as level surface waters or piezometric surfaces described by piecewise linear elements.



At any time in the creation, deletion, or assignment of water level and piezometric surfaces to regions, the previous operation can be undone using the *Undo* button immediately to the left of the *Zoom Extents* button.

Beneath the *Undo* and *Zoom Extents* button is the input box for the unit weight of water, and inputs for the elevation of the surface water levels on the flood and landside of the structure (as defined by the user). Changing the values of the surface water levels adjusts the plot of data in the *Soil Assignment Area*. Water surfaces determine hydrostatic water pressures against the I-Wall and overburden pressures on the uppermost regions in the model, but they are not applied to the wall in a soil region until they are assigned to the soil region because user-defined piezometric pressures may apply. The process of assigning surface water to regions will be discussed later in this subsection.

At the bottom of the left-hand column of input on the *Water Levels* tab are the inputs to determine the seepage method to be used in computation (Figure 3.22). The selection box gives the three following methods for seepage: no seepage, homogeneous seepage, and heterogeneous seepage. If either homogeneous or heterogeneous seepage is selected, then there should only be two water surfaces assigned, one water surface, or user-defined piezometric surface to all of the regions on each side (flood or landside) of the I-Wall. A message indicating this restriction is included in the GUI (Figure 3.23).

For heterogeneous seepage, each soil material's permeability is used to determine the head loss along the I-Wall as per the line of seepage (a.k.a. the line of creep) method of analysis discussed in Appendix C. Homogeneous seepage assumes that the permeability is consistent across all of the soil materials. When the homogeneous seepage method is chosen, the user is prompted to enter this common permeability value. When the *.in* file is written for the solver, this permeability value is substituted as the permeability for each soil material. A message indicating this substitution is shown in the GUI in the *Water Levels* tab and a comment line is added to the *.in* file noting this fact.

Figure 3.22. Choosing the appropriate seepage method.

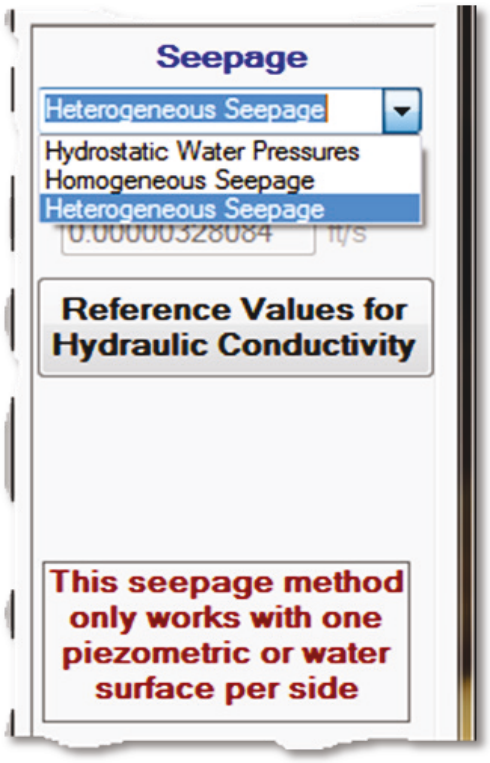
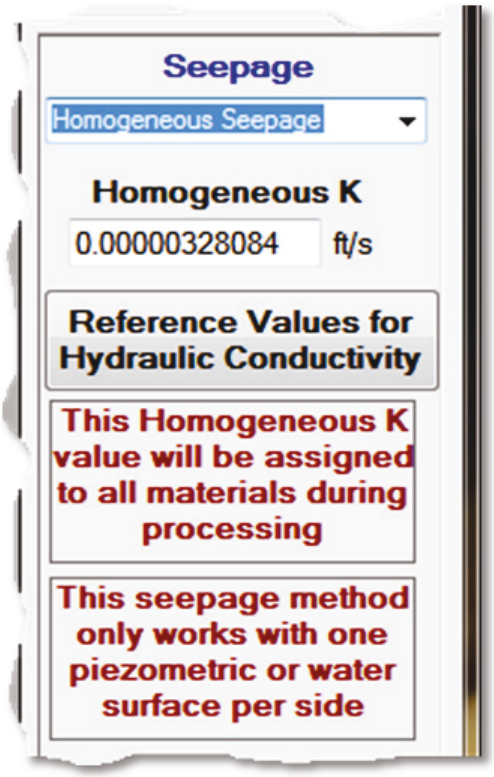
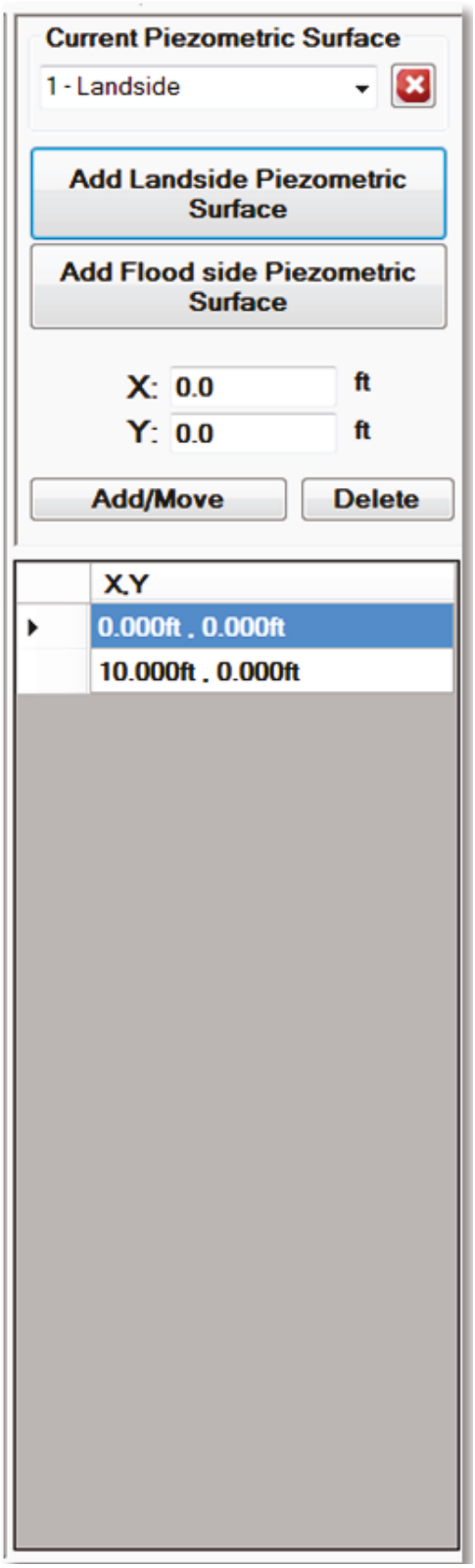


Figure 3.23. Entering a homogeneous seepage parameter (and the warnings associated with this method).



Near the middle of the *Water Levels* tab is the selectors and input for piezometric water levels (Figure 3.24), whether determined from water surfaces or user-defined. At the top of this input area is a selector for the current piezometric surface to assign to earth regions or edit for user-defined water levels for pore-water pressure calculations.

Figure 3.24 Creating a piezometric surface highlighting the selector and region creation buttons.



Assigning a water level to a soil region is performed by using the piezometric water surface selector to determine the current water surface to assign to a region (Figures 3.25 and 3.26). The currently assigned regions for that current water surface will be plotted with bold colors, and regions that are not assigned to that water surface will be shown with faded colors. For a new model, none of the soil regions has a piezometric water surface and so all of the regions are shown as bold with the selection of *none* in the piezometric water surface selector. To assign a region to the currently selected piezometric surface, the user only needs to left-click on the soil region to assign. Soil regions can only be assigned to the current piezometric surface if the current piezometric surface is on the same side of the I-Wall as the soil region. For instance, a soil region on the landside of the I-Wall cannot be assigned to a user-defined piezometric surface on the flood side of the structure.

Figure 3.25. Assigning soil regions to a user-defined piezometric surface (whose point coordinates are in the piezometric area).

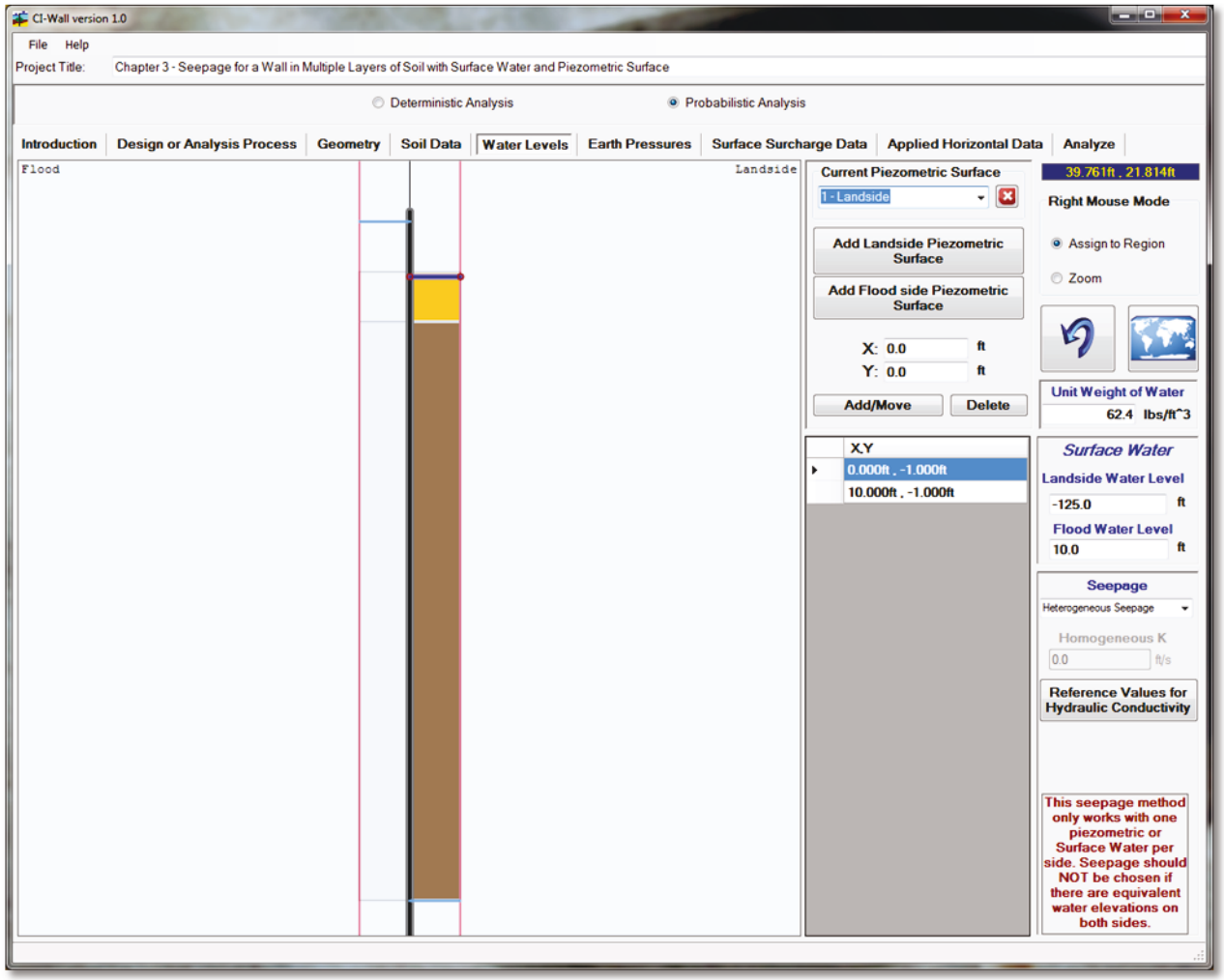
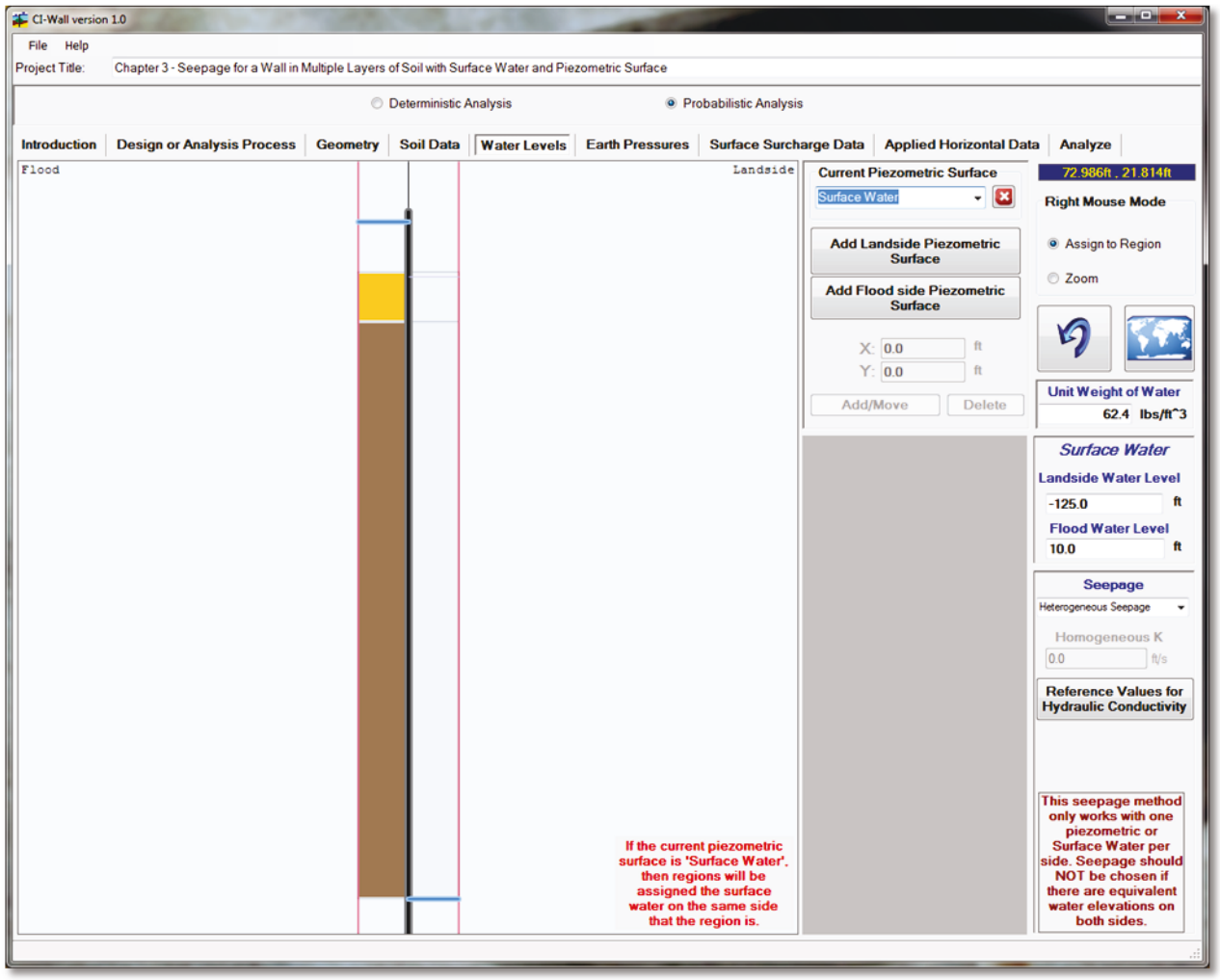


Figure 3.26. Assigning soil regions to the flood side surface water.



The *none* and *Water Surface* piezometric levels that can be chosen with the selector apply to both sides of the structure and can thus be assigned to any of the soil regions. It should be noted that the *Water Surface* option applies the surfaces defined by the *Water Level* inputs in the rightmost input section of the tab, and that the appropriate level piezometric surface is assigned to the region based on the side of the region with respect to the structure.

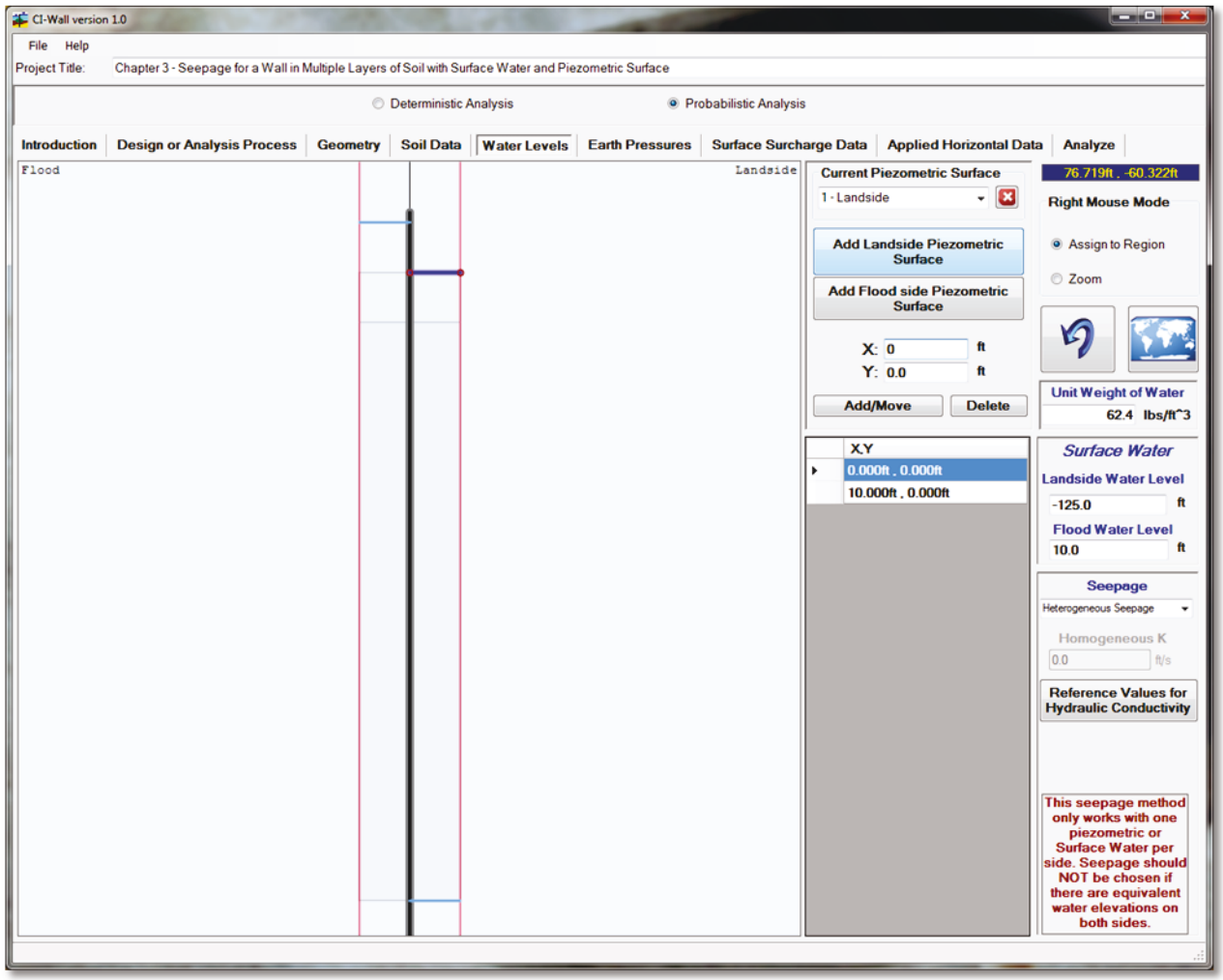
Notice: Applying *Water Surface* piezometric levels to a surface region means that the soil region can have a varying piezometric water table in a probabilistic analysis. This possibility will be discussed in the *Analyze* tab discussion.

The *X* image button (with a red background) next to the current piezometric surface selector allows the user to delete the currently selected surface (if

the currently selected surface is a user-defined surface). Clicking the button removes the currently selected surface (and its definition).

In order to create a new user-defined piezometric surface, the user can click either of the two buttons beneath the current piezometric surface selector. The buttons add a new user-defined piezometric surface to either the user-defined (in the *Geometry* tab) *Flood* or *Landside* of the structure, which are labeled in the *Soil Assignment Area*. The new surface is created with an appropriate water level of zero and proceeds from the I-Wall structure to the extent on the *Flood* or *Landside* (Figure 3.27). The coordinates of the two nodes (shown in red) used to define the landside piezometric surface are as listed in the data box (with the heading of *X,Y*).

Figure 3.27. The piezometric surface immediately after the *Add Landside Piezometric Surface* button has been pushed.



The piezometric water surface is assumed to have an elevation that is a function of distance from the I-Wall (i.e., Y=f(X)). In this vein, the piezometric surface is defined as a set of linear interpolations of Y for points with continually increasing X-values. These points are shown in the area below the *Add/Move* button, as shown in Figure 3.28.

To edit the currently selected piezometric surface, a (X,Y) location should be entered into the text boxes below the buttons to create piezometric surfaces. Clicking the ***Add/Move*** button either adds the input point values to the currently selected surface sorted by X, or replaces a point in the currently selected piezometric surface that shares the same X value (Figure 3.29 and 3.30). This input is shown by the changed surface shown in the *Soil Assignment Area* (the current piezometric surface is drawn with bold colors) and by the change of the data in the current piezometric surface list under the *Add/Move* button.

To remove a point from the currently selected piezometric surface, click on that point in the piezometric surface list (under the *Add/Move* button) and click the ***Delete*** button next to the *Add/Move* button.

Figure 3.28. The points of the piezometric are in the grid below the point definition area.

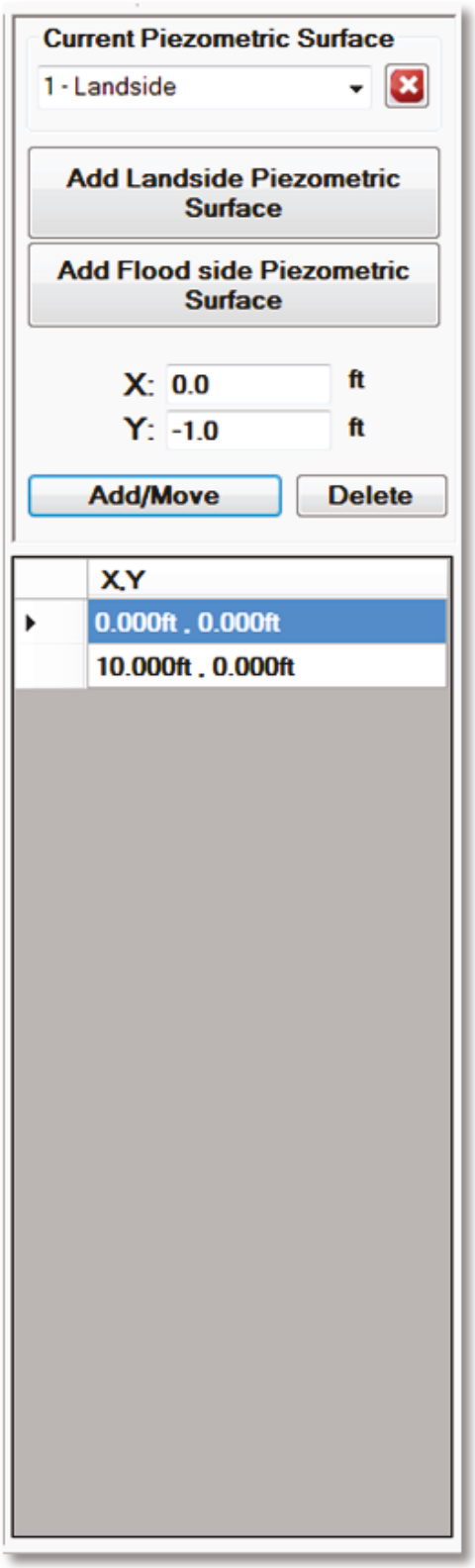


Figure 3.29. If an input point has an X value that is already on the curve, then that point is moved to the new Y location on confirmation.

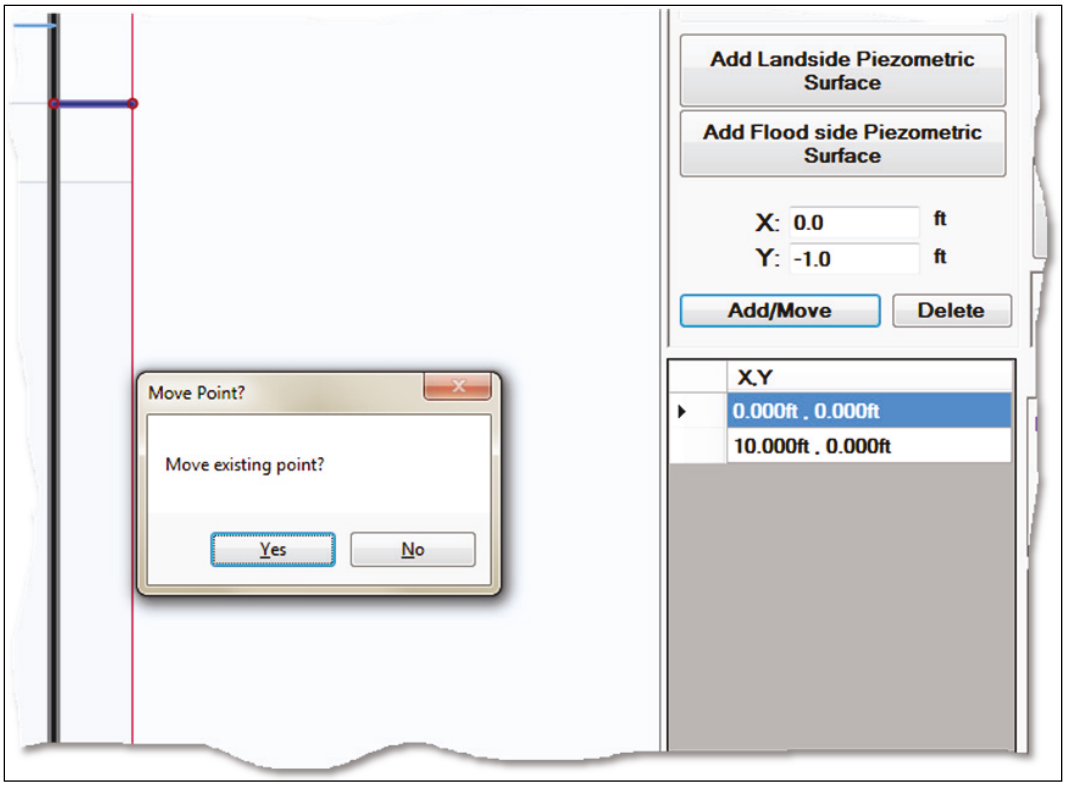
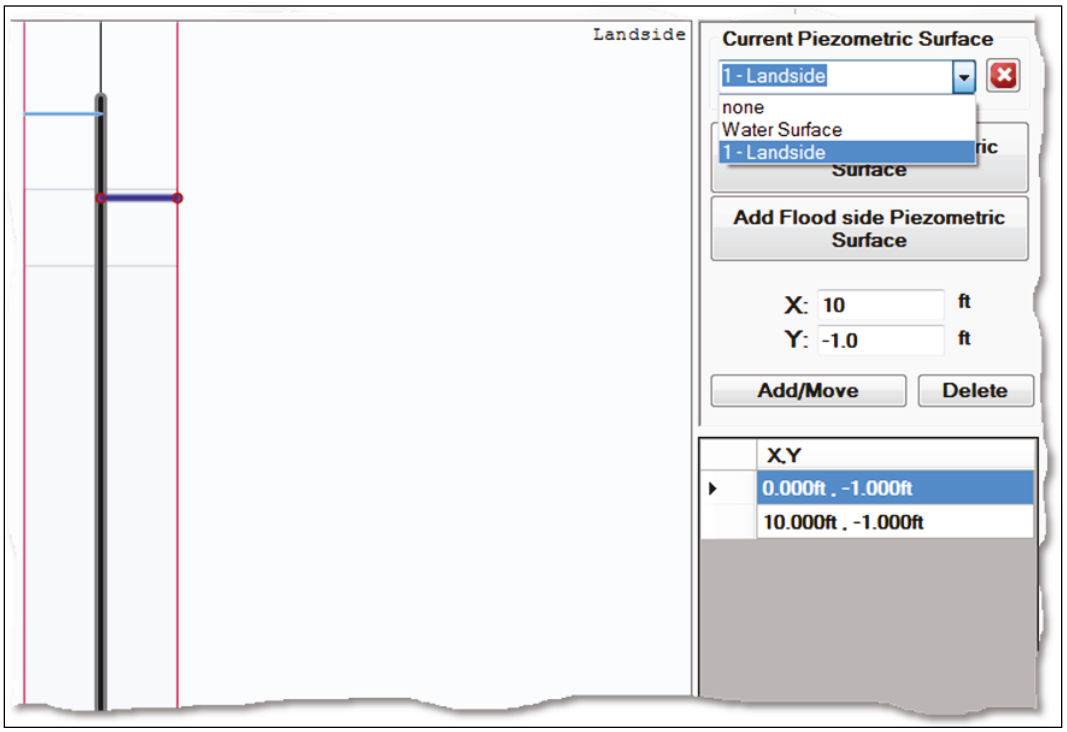


Figure 3.30. After both ends of the piezometric surface have been moved.

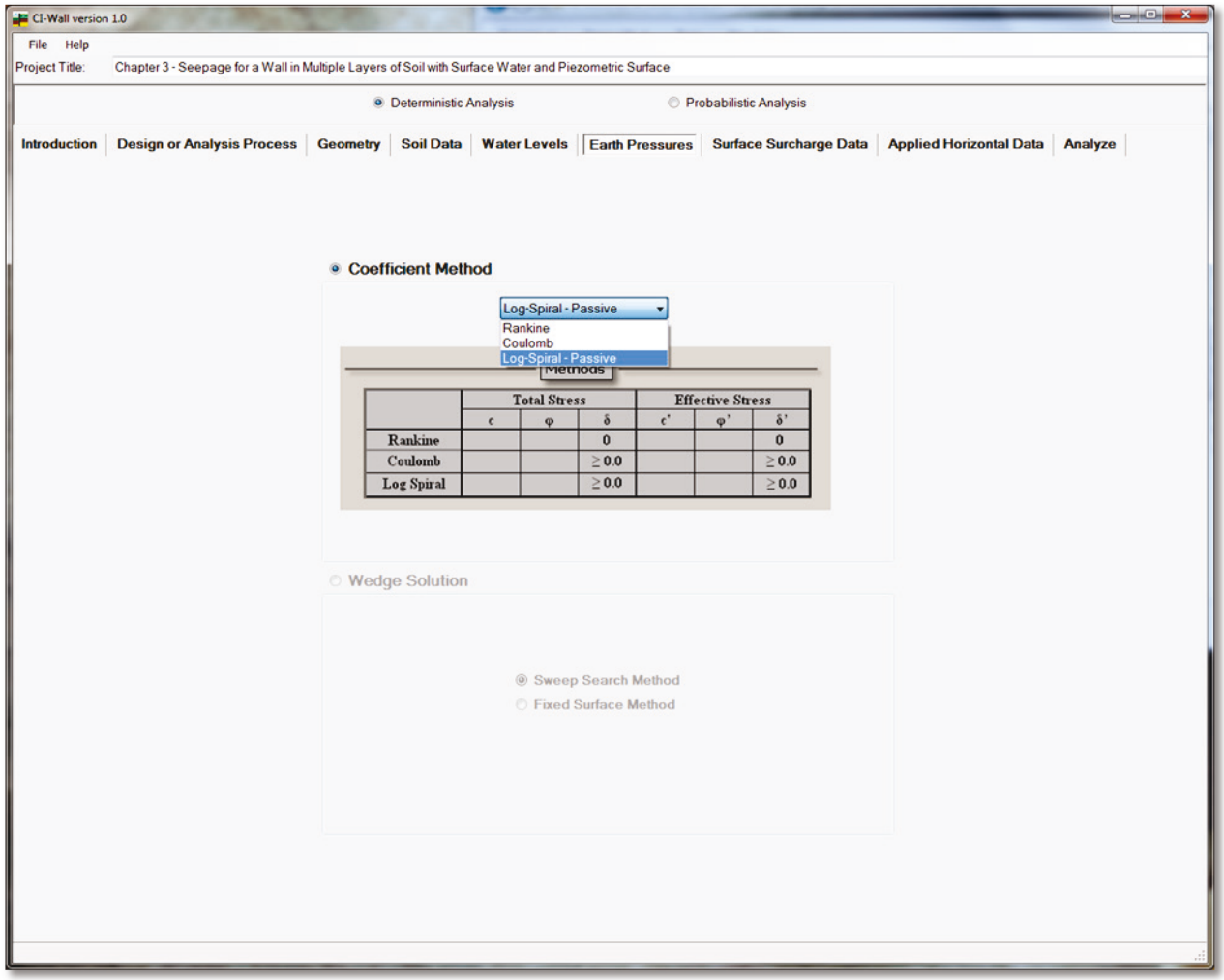


3.8 *Earth Pressures* tab

In the *Earth Pressures* tab, the user can decide whether the computation of earth pressures will be performed using the Coefficient Method of analysis, or the Wedge Method of analysis, by selecting the provided radio buttons. Selecting an option allows the user to specify information specific to that option.

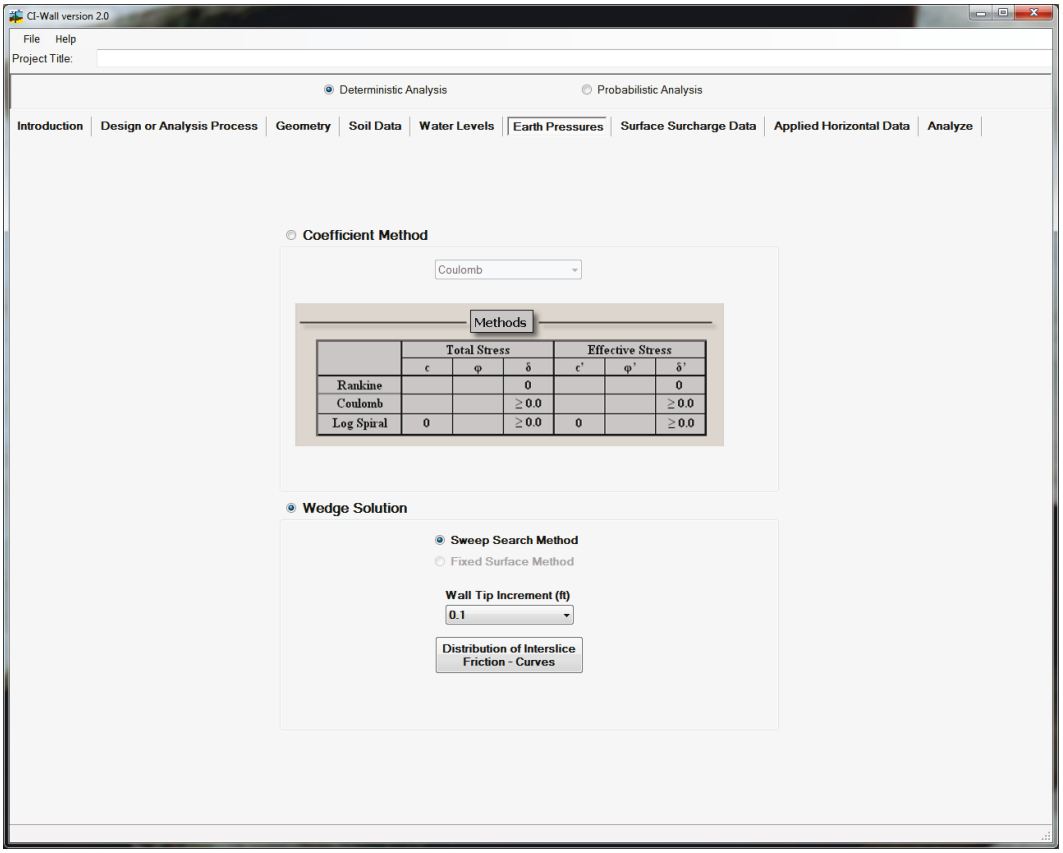
In the Coefficient Method of analysis data input area, the only input required is the selection of a method to use from a drop-down menu (Figure 3.31). The methods and the requirements for those methods are presented in an image beneath the dropdown combo-box. For instance, if the logarithmic spiral Coefficient Method is selected, all soil materials would be required to have a value for $\delta \geq 0.0$. The default Coefficient Method of analysis is the Coulomb method.

Figure 3.31. Choosing the Coefficient Method of analysis using the *Earth Pressures* tab.



In the *Wedge Solution* data input area (Figure 3.32), the user is shown two radio buttons for the choice of slip planes definition methods that will be used in the analysis. These two options are the sweep search method and the fixed surface method.

Figure 3.32. Choosing the Wedge Solution Method using the *Earth Pressures* tab.



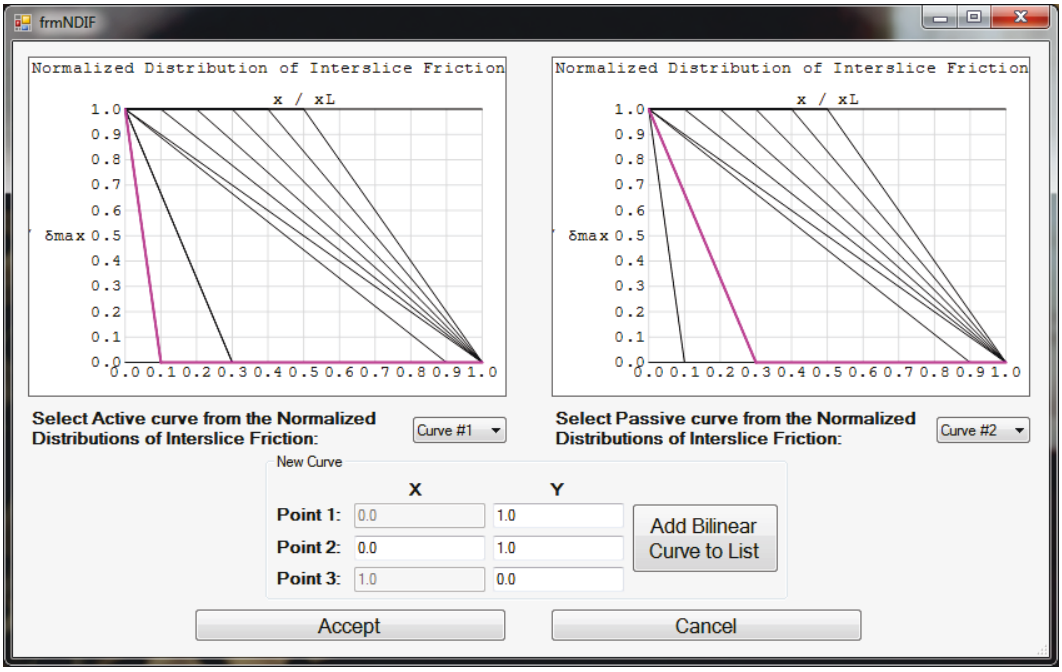
The sweep search method searches for the critical slip plane to determine the active and passive earth mass regions that have an effect on the wall. The active force search criterion is based on finding the maximum force generated by the slip plane earth mass at the wall. The passive force search criterion is based on finding the minimal resisting force generated by the slip plane earth mass at the wall. Selecting this method instructs the analysis program to do these searches. This option is the default method and the only one enabled in this version of the program.

The fixed surface method is intended to allow the user to define the slip plane manually. This option is not available in Version 2.0 of the Corps_I-Wall program.

The second control in the *Wedge Solution* area is a drop-down list labeled *Wall Tip Increment*. This control allows the user to specify the precision of the search along the wall in increments of either 0.1 or 0.01 feet or meters, determined by the selected units. For solving the design depths, the wall tip depth will increase by either increment until a balance of moments and forces are met for the wall. For most cases, the default of 0.1 will give satisfactory results.

Also in the *Wedge Solution* area is a button labeled *Distribution of Interslice Friction-Curves*. Selecting this button allows the user to select or define an interslice friction curve which will have an effect on the interactions between wedges in the Wedge Method as discussed later in this section. Selecting this button brings up the pop-up window shown in Figure 3.33.

Figure 3.33. The Distribution of Interslice Friction-Curves selector dialog.



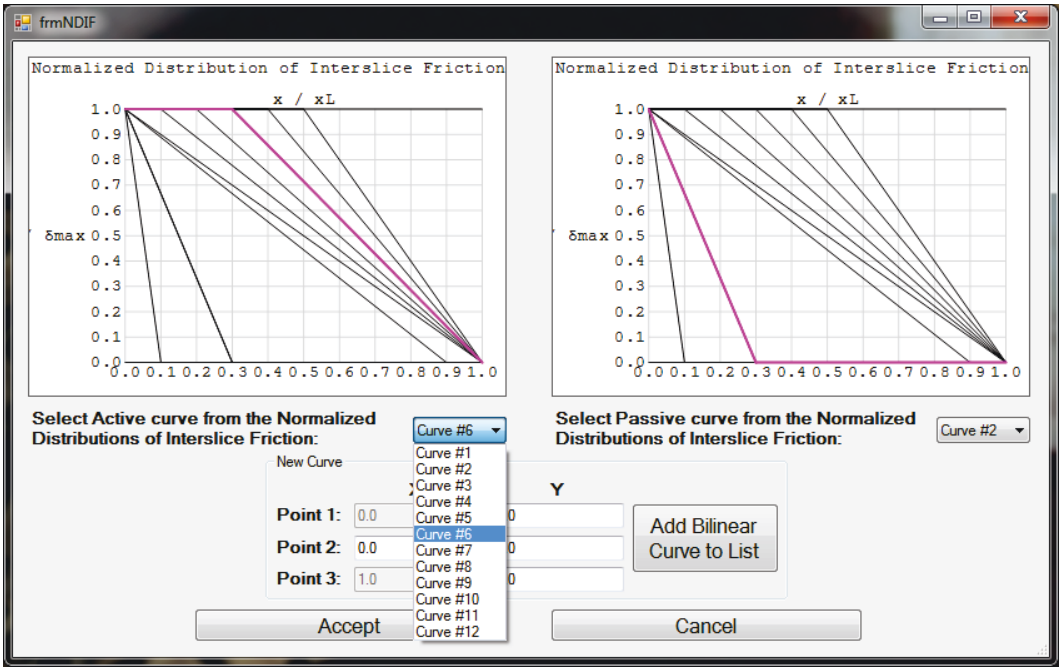
The interface of Figure 3.33 shows two normalized interslice friction curve diagrams, selectors for the curves, and the means to enter a new curve. These curves are normalized so that they can be scaled to slip planes of different widths and differing soil properties. Each curve is piecewise, consisting of two linear segments.

The two normalized friction curve diagrams are for the interslice friction curves for the determination of active and passive forces that act between

wedges. The diagrams are similar and show a plot of all of the normalized curves that can be selected, with the currently selected curve highlighted by being displayed in a purple color.

Below the diagram are selectors for the currently selected curve for the active and passive slip planes. The selector is a drop-down menu of the curves, labeled as "Curve #" (with the curve number) (Figure 3.34). There are thirteen program defined curves, but curves can be added by the user as described later in this section. Selecting an item from the drop-down list changes the currently selected curve.

Figure 3.34. Selecting the interslice friction curve for analysis.



The user can create a new curve for the selectors. This section is a box labeled *New Curve*. Because each curve is normalized by distance for the *X*-axis, the first and third *X*-points are fixed at 0.0 and 1.0, respectively. The user can enter the second *X*-point as a value in the range greater than or equal to 0.0 and less than or equal to 1.0. The *Y*-values describe the fraction of interslice friction that will have an effect on wedge interslice forces. This value must have a value in the range greater than or equal to 0.0 and less than or equal to 1.0. Entering the three values for *X* and *Y* describes the two part piecewise linear curve.

At this point, the piecewise linear curve needs to be added to the selectable list of curves. Pressing the button labeled *Add Bilinear Curve to List* will

add the curve to the end of the curve list so that it can be selected for either the active or passive curve. The curve will be displayed in the diagram windows and will be available through the selectors.

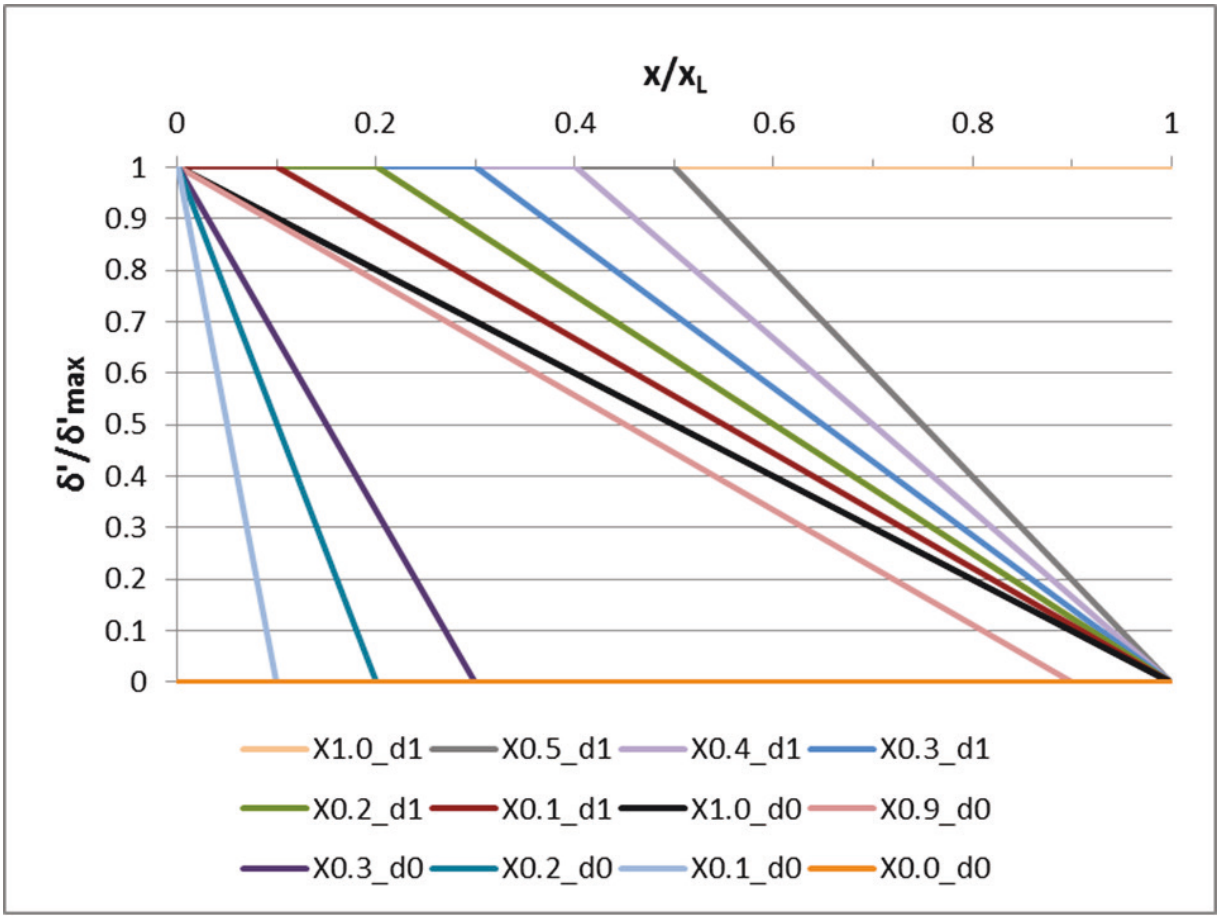
When the user is satisfied with the currently selected curves for active and passive regions, the user can Accept the changes. If the user does not want to change the currently selected curves then the user can select Cancel.

Using the Wedge Method of analysis, the interslice friction acting on the left and right face of each of the individual (Figure G.5) soil wedges comprising the soil mass must be specified. In a Corps_I-Wall Wedge Method of analysis, the soil mass is typically defined by more than ten soil wedges (Figure 1.5). The value for interslice friction δ' can be assigned any value between zero and ϕ' for each interslice. Corps_I-Wall Version 2.0 uses a normalized interslice friction variation with distance from the wall relationship, in conjunction with the value of interface friction at the wall, to define the values for interlice friction for all the soil wedge faces.

Normalized interslice friction variation with distance from the wall: Figure 3.35 shows some of the distributions of normalized interslice friction distribution available for use in a Wedge Analysis. In this figure, x is the distance to each interslice and x_L is the lateral extent of the soil wedge, as measured from the wall. The Figure 3.35 normalized plot is a convenient plot that scales to the interslice friction at the wall, and scales to the specific geometry of every logarithmically defined (Figure G.4) potential soil wedge being investigated in the Corps_I-Wall analyses. The transformation of the the selected normalized interslice friction distribution, to the logarithmic spiral defined slip plane being analyzed, to real space, follows the steps outlined in Appendix H.

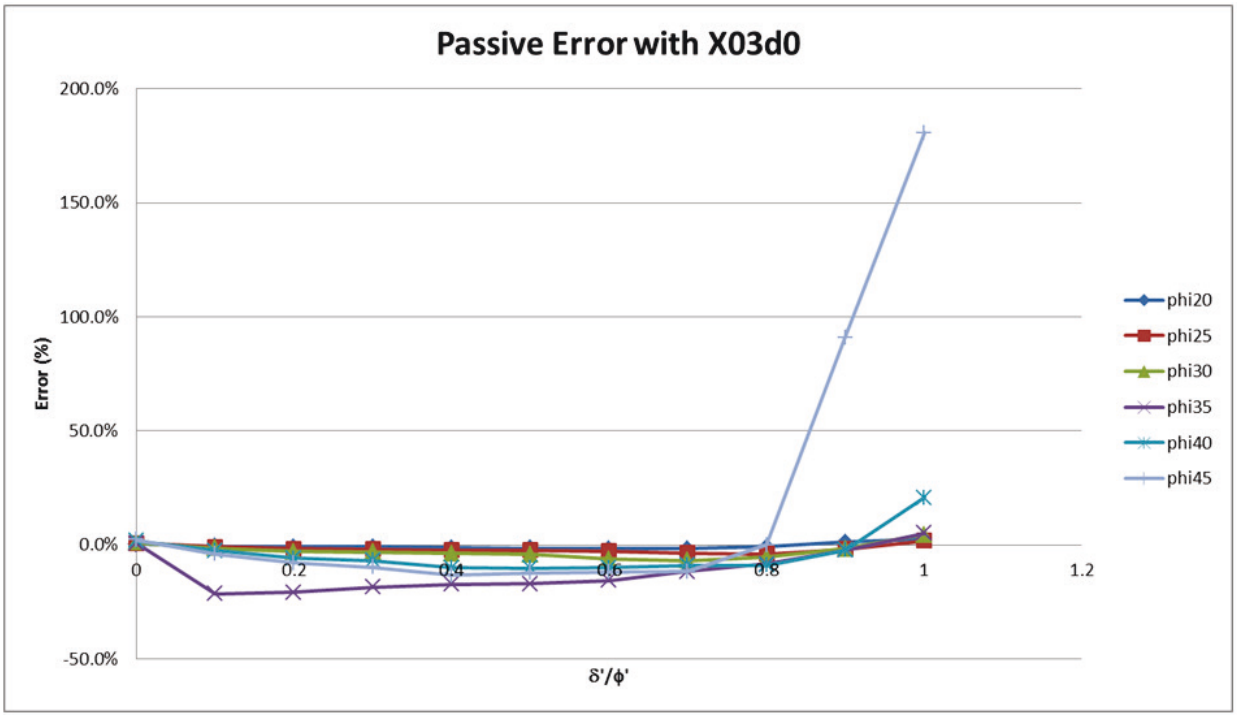
Appendix H summarizes an investigation with the objective of finding which of the Figure 3.35 distributions result in a computed passive earth force value at the wall that comes closest to the standard passive force value over the wide range in values of ϕ' and wall friction δ' at the wall.

Figure 3.35. Distributions describing the variation in interslice friction δ' normalized by the wall fiction δ'_{max} versus normalized distance along passive or active soil wedges.



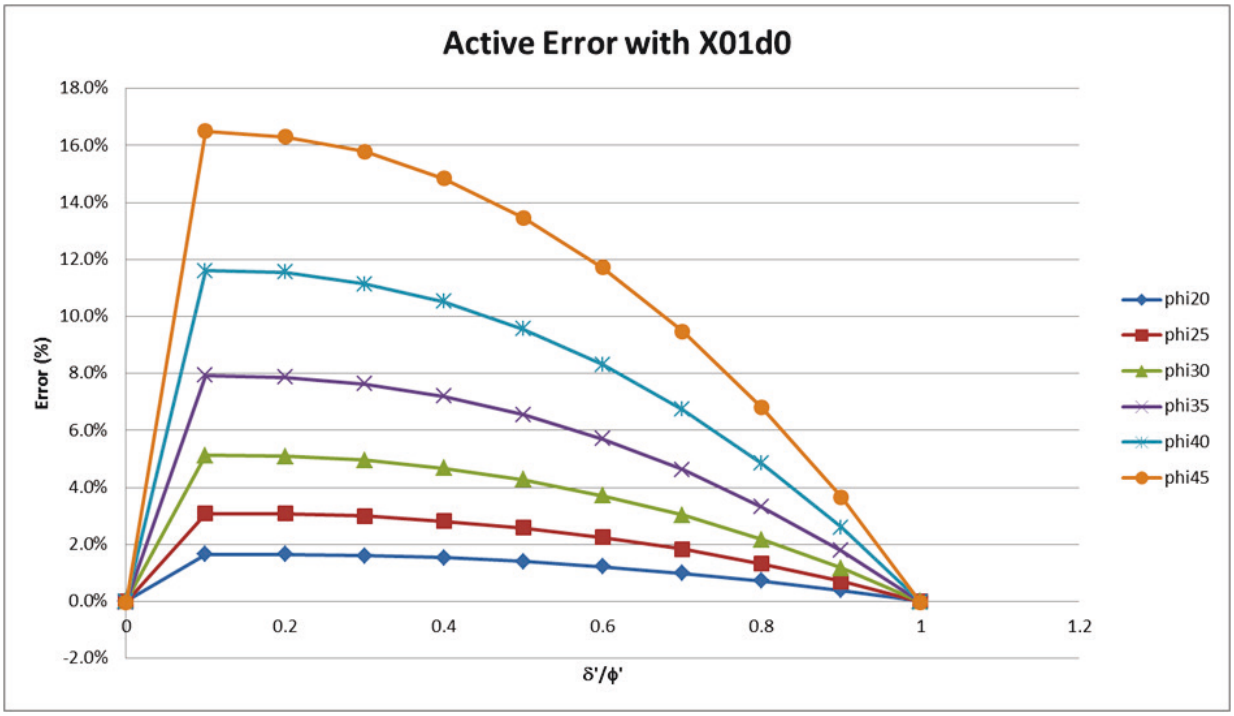
Passive force: Based on the result of the error analysis study summarized in Appendix H, the normalized interslice friction distribution (designated as X0.3_d0) provides for the minimum passive force error over the widest range in δ' and ϕ' values of all the Figure 3.35 distributions that were investigated. For this normalized distribution, the value of (δ'/δ'_{max}) is equal to 1.0 at (x/x_L) equal to zero. The distribution decreases linearly with distance to a value for (δ'/δ'_{max}) equal to zero at (x/x_L) equal to 0.3. The value of (δ'/δ'_{max}) is maintained at a value of zero from (x/x_L) equal to 0.3 to a value of 1.0. Figure 3.36 shows the error as a function of δ' at the wall in proportion to the ϕ' value of the retained soil and with ϕ' ranging from a low of 20 degrees to a high of 45 degrees. The X0.3_d0 distribution was therefore selected as the default distribution in the Corps_I-Wall Version 2.0 software for use by the Wedge Method for passive force computations. Note that for high ϕ' values (e.g., ϕ' on the order of 40 to 45 degrees) and with wall friction δ' at or above 0.8*ϕ' to 0.9*ϕ', the user may consider specifying the X02_d0 or X0.1_d0 distribution in the Corps_I-Wall analysis.

Figure 3.36. Difference in percent between values of passive earth force by Wedge Method and standard solution as a function of δ‘ at the wall, expressed as a fraction of ϕ’, and as a function of ϕ‘.



Active force: A similar type of study to the passive study discussed in Appendix H was also conducted using the Corps_I-Wall Wedge Method of analysis, but for the active earth force. The result of these studies are summarized in the error plot Figure 3.37. It was concluded that the normalized interslice friction distribution designated as X0.1_d0 in Figure 3.35 provides for the minimum active force error over the widest range in δ’ and ϕ’ values of all the Figure 3.35 distributions that were investigated. For this normalized distribution, the value of (δ'/δ'_{max}) is equal to 1.0 at (x/x_L) equal to zero. The distribution decreases linearly with distance to a value for (δ'/δ'_{max}) equal to zero at (x/x_L) equal to 0.1. The value of (δ'/δ'_{max}) is maintained at a value of zero from (x/x_L) equal to 0.1 to a value of 1.0. This distribution was therefore selected as the default distribution in the Corps_I-Wall software for use by the Wedge Method for active force computations.

Figure 3.37. Difference in percent between values of active earth force by Wedge Method and standard solution as a function of δ‘ at the wall, expressed as a fraction of ϕ’, and as a function of ϕ‘.



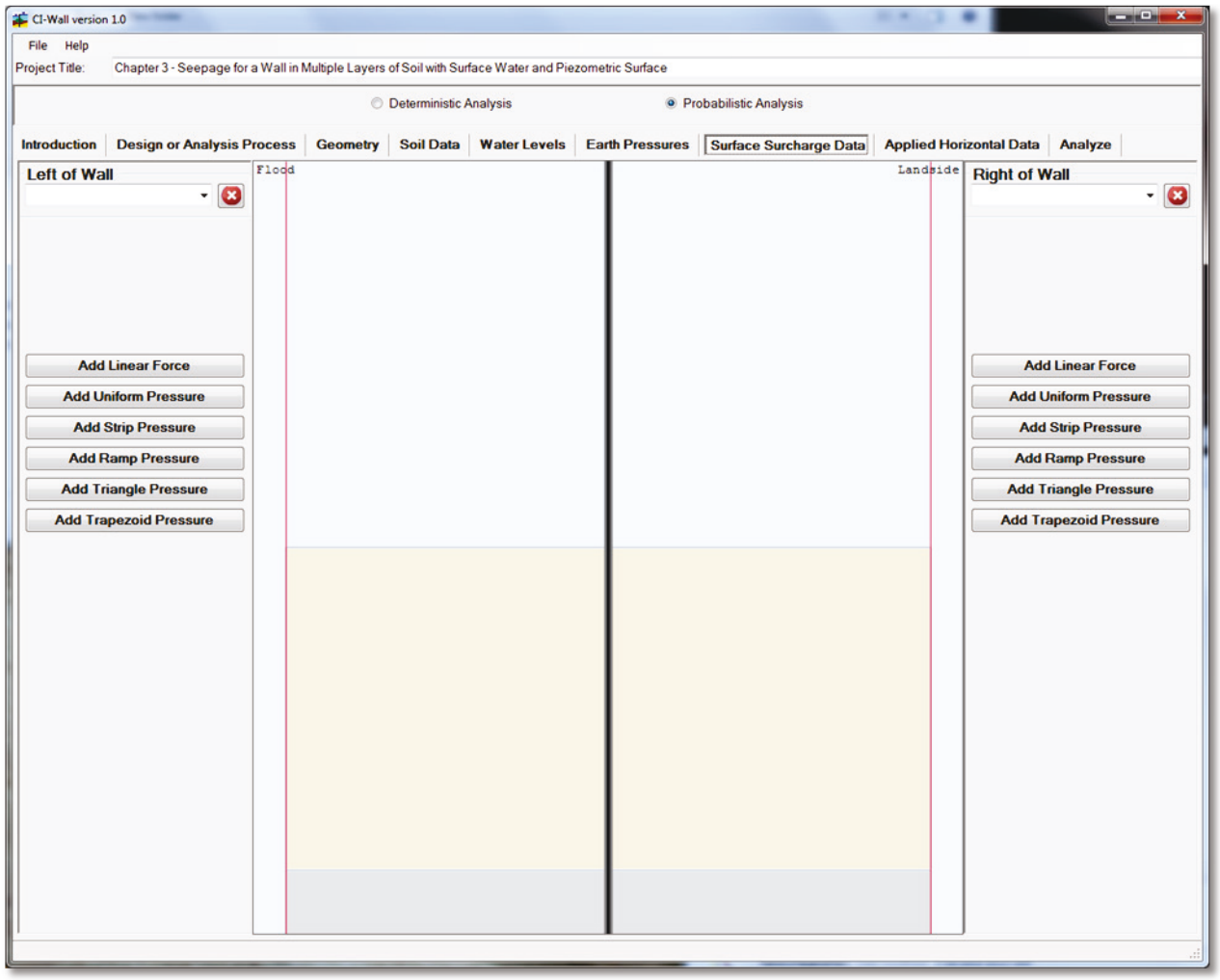
3.9 *Surface Surcharge Data* tab

The *Surface Surcharge Data* tab allows the user to add line loads or distributed pressures that are applied vertically to the ground surface. Surface loads can be applied to the ground surface, either to the left or right of the I-Wall, irrespective of which side is classified as the flood or landside (Figure 3.38).

At the center of the tab is a display showing the model, zoomed to show the ground surface explicitly. The different loads are displayed on this plot and they are scaled to each other for the display. To the left and right of the display are the controls for selecting and adding loads to the existing model. Both sides behave in a similar manner, so therefore, the following discussion applies to both sides.

At the top of the vertical loads section is a drop-down combo-box, this contains a list of the existing loads. When one of these loads is selected in the combo-box, that load becomes the current load. This load is displayed in an enhanced manner in the center screen for verification.

Figure 3.38. *Surface Surcharge Data* tab.



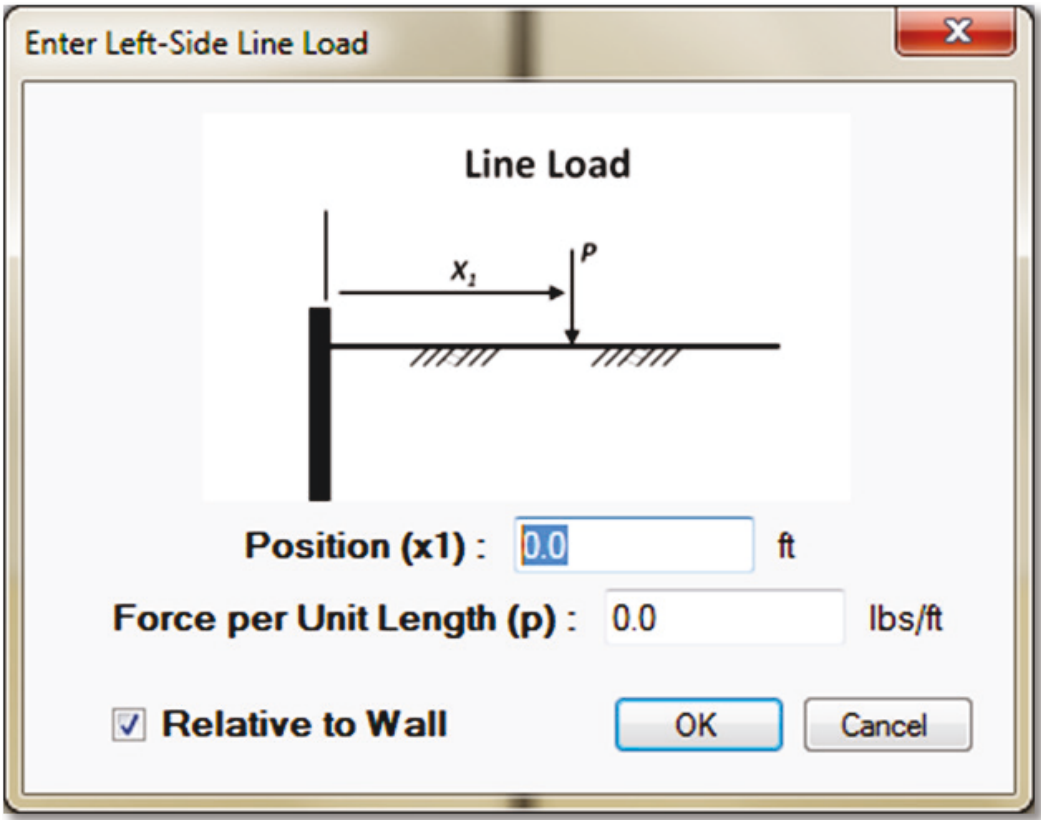
To the right of the combo-box is a button with an *X* icon in a red box. Clicking that button deletes the currently selected vertical load from its respective list.

Below the current load selector and delete buttons, are the buttons that allow a new vertical load to be added to the model. Clicking either of these buttons brings up a dialog to create a new vertical load and add it to the bottom of the selector list.

These buttons allow for the creation of one of six types of the following vertical area loads: line load, uniform load, strip load, ramp load, triangle load, and trapezoid load. These loads follow the slope of the ground surface (for Version 2.0 and above).

The line load is a point vertical load acting on the ground surface. It is defined by giving a distance from the I-Wall and a load magnitude in relative mode, and a specific position and magnitude (Figure 3.39).

Figure 3.39. The input window for line loads.



The uniform load is a vertical load acting on the ground surface from the I-Wall position to an infinite distance to the I-Wall. It is defined by inputting a pressure magnitude (Figure 3.40).

The strip load is a pressure that is uniform in magnitude but acts in a certain range across the surface (Figure 3.41). The range is defined by a distance from the I-Wall for the start and end of the range in relative coordinates, and in actual start and ending X-distance from the I-Wall for actual coordinates. The consistent magnitude of the strip load pressure must also be input.

Figure 3.40. The input window for uniform loads.

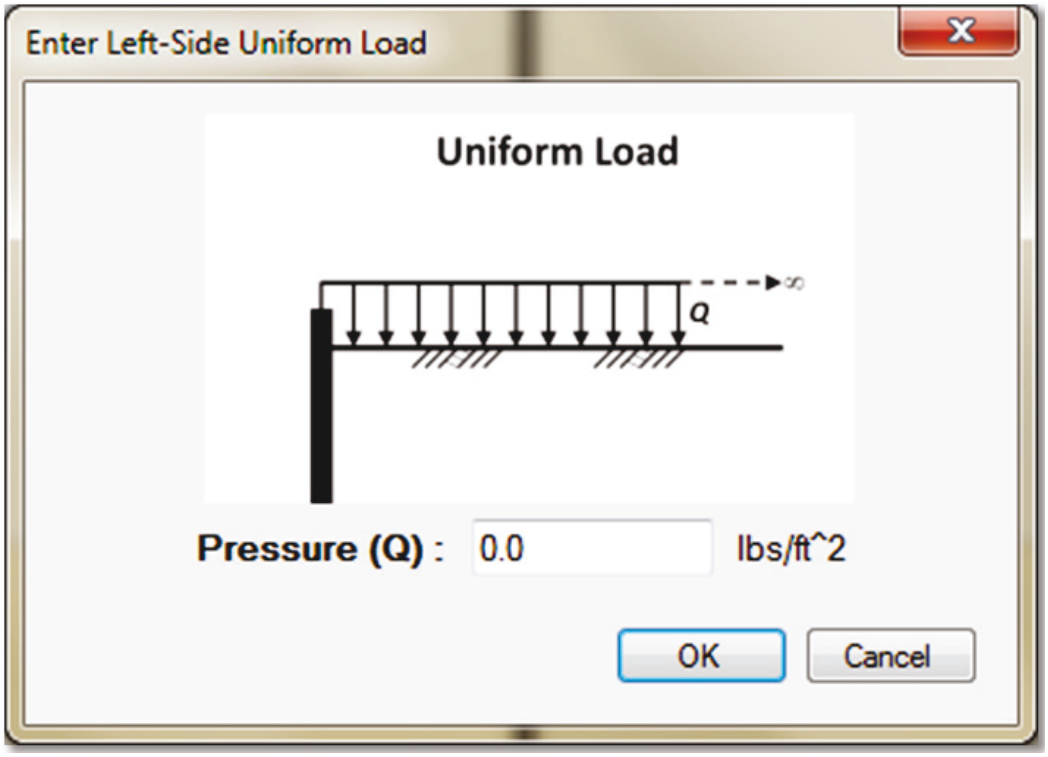
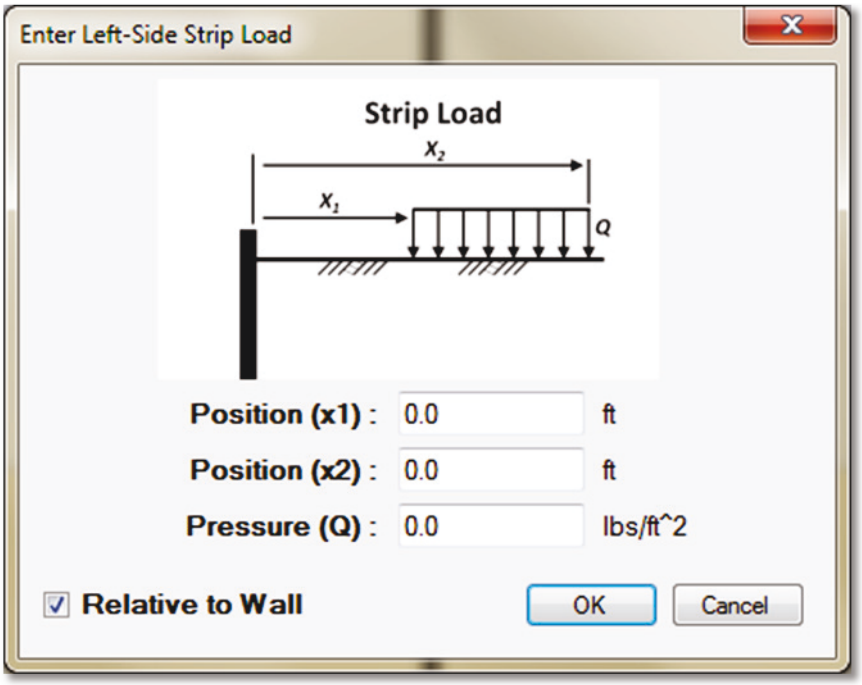


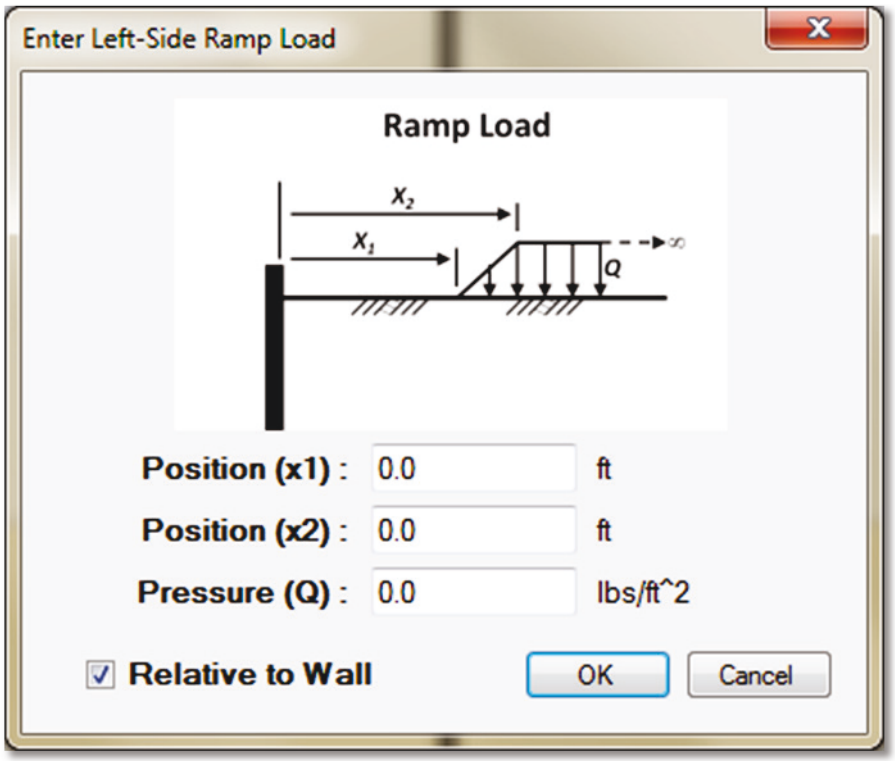
Figure 3.41. The input window for strip loads.



The ramp load is a vertical load. At the starting *X*-coordinate of the load, the magnitude of the pressure is zero, but it increases to an input value by the ending *X*-coordinate of the pressure. The magnitude of the pressure

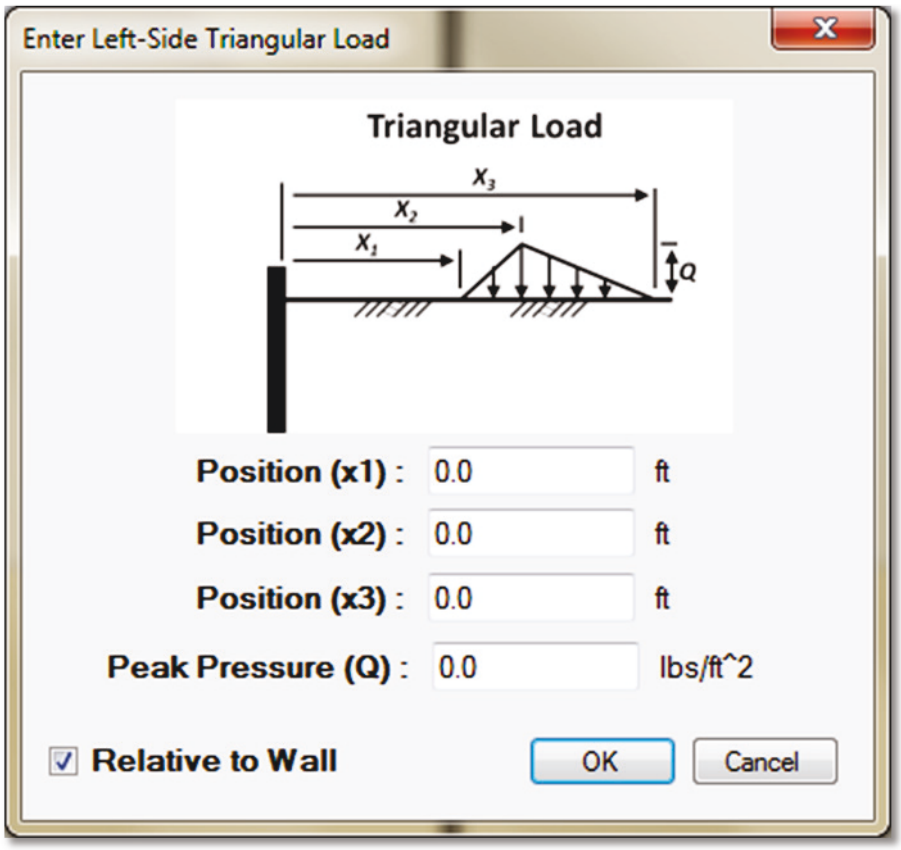
continues from that point to an infinite distance from the I-Wall, in the same manner as the uniform pressure. Both the start and ending points are entered in relative or absolute coordinates and the final pressure magnitude is also entered (Figure 3.42).

Figure 3.42. The input window for ramp loads.



The triangle load has three *X*-coordinates and a single pressure magnitude for entry (Figure 3.43). The first *X*-coordinate entered is the point at which the load begins. The magnitude of the pressure at its beginning point is zero. The second *X*-coordinate is the location at which the pressure has its peak magnitude, as input by the user. The last *X*-coordinate is the point at which the pressure ends (and has a magnitude of zero). The *X*-coordinates (as always) may be entered in relative or absolute coordinates. The peak magnitude must also be entered. The load is linearly interpolated from the start point to the peak point and from the peak point back down to the end point. In order to create a right triangular pressure distribution, the first or last *X*-coordinate can be the same as the peak *X*-coordinate.

Figure 3.43. The input window for triangular loads.



The last vertical load type is the trapezoid load (Figure 3.44). The trapezoid of pressure is defined by two points. Each point has an *X*-coordinate (specified in either relative or absolute coordinates) and a magnitude at that *X*-coordinate. The pressure is linearly interpolated between the start point and the end point.

It is assumed that these loads will fall within the extents of the defined regions where materials are defined. Loads can be applied up to 125 ft away from the I-Wall or the extents of the regions, whichever is greater.

Figure 3.45 shows the example problem with sample surcharge loads applied. The currently selected surcharge loads, on either side, are highlighted and the relevant information for that load is shown.

Figure 3.44. The input window for trapezoid/distributed loads.

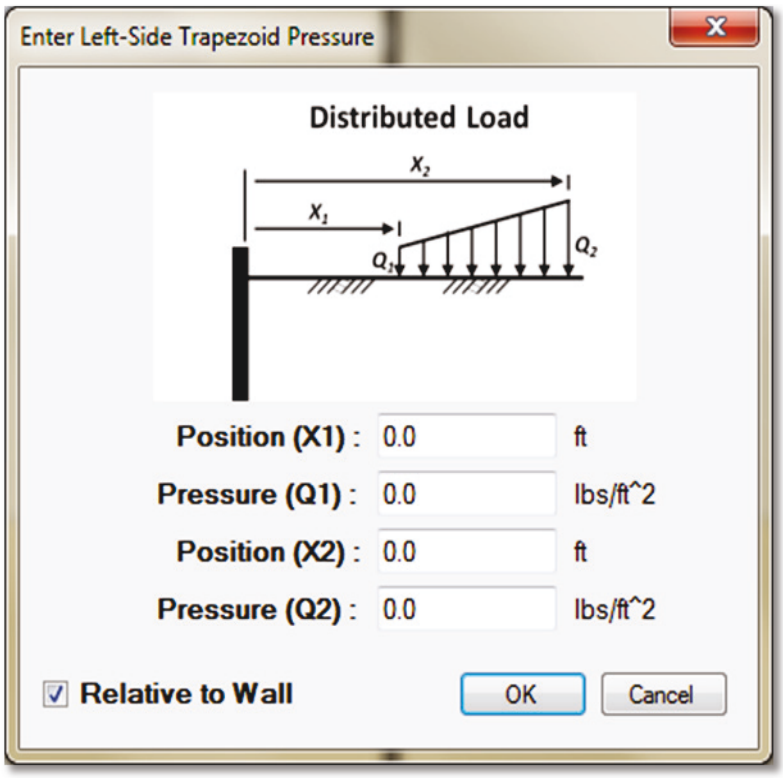
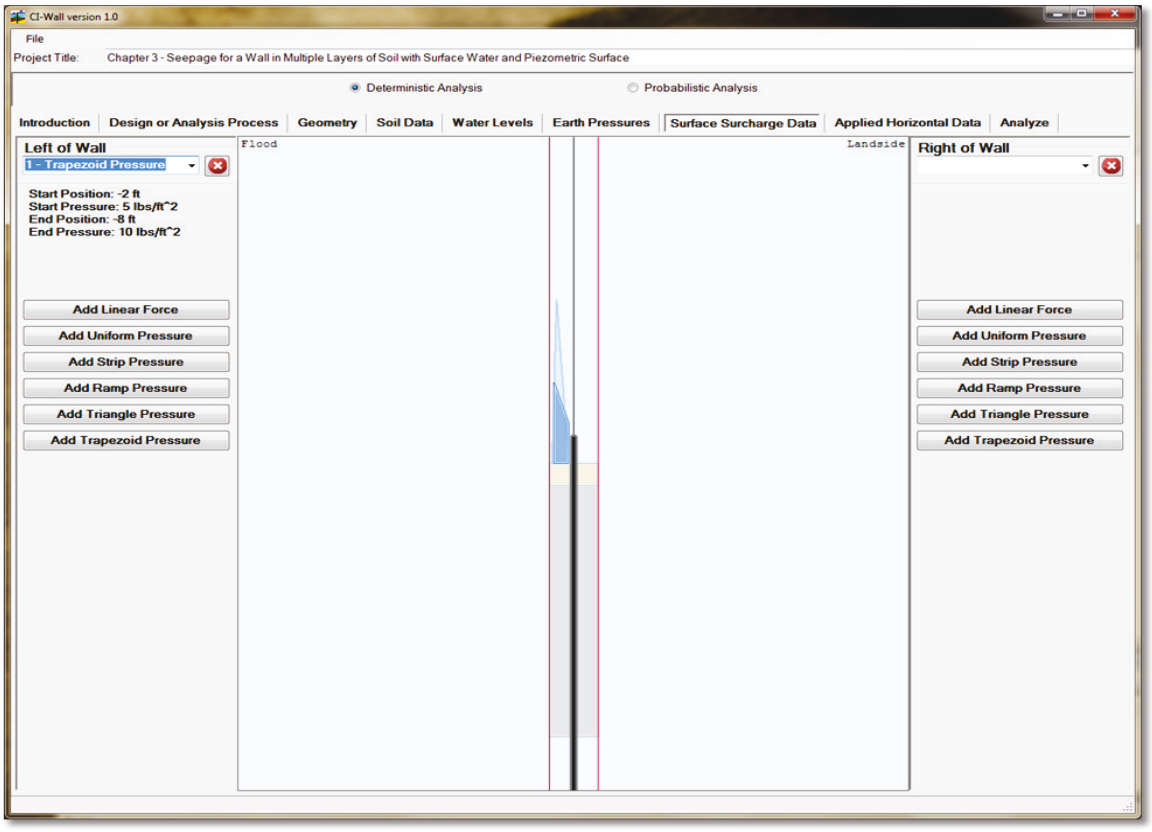


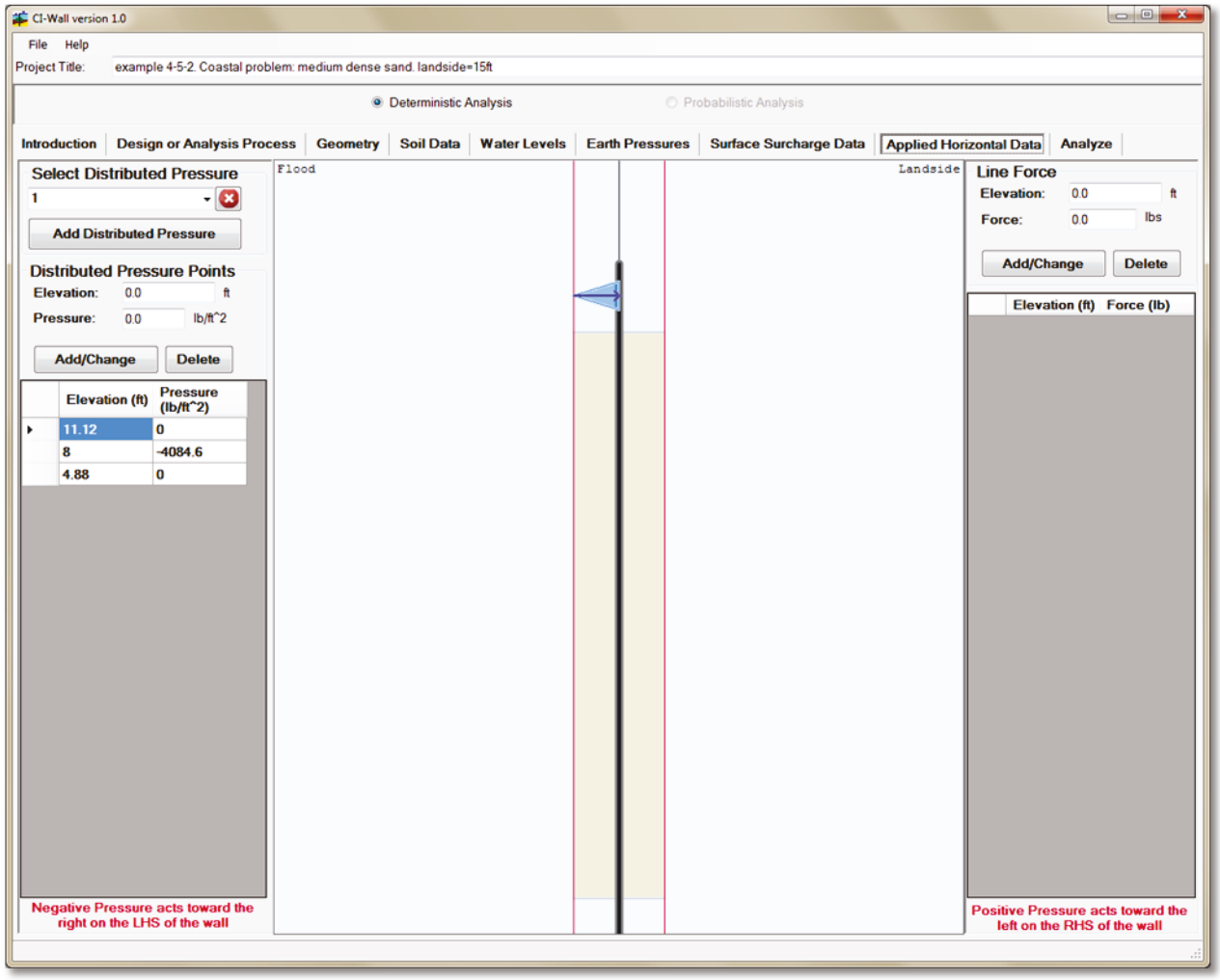
Figure 3.45. *Surface Surcharge Data* tab with highlighted loads.



3.10 *Applied Horizontal Loads* tab

The *Applied Horizontal Loads* tab allows the user to specify loads that act horizontally directly against the I-Wall (Figure 3.46). Line loads and distributed loads (which are interpolated between elevation and magnitude points) can be entered. Distributed loads are input to the left of the display window and line loads are input to the right of the display window. The display window shows all of the loads acting upon the I-Wall. The entire I-Wall is displayed. The visualized loads are scaled with respect to each other. The currently selected distributed load is highlighted in the display.

Figure 3.46. The *Applied Horizontal Loads* tab allows input of point loads (on the right) and linearly distributed loads (on the left).



Notice that pressures and loads that act toward the right are negative and that positive pressures and loads act toward the leftward direction (opposite of the global coordinate system *x*-axis). Because a right-handed coordinate system is being used, positive forces acting against a surface act to the right of the surface definition tangent. Because the I-Wall is defined from the I-Wall top down to the I-Wall tip, the positive direction is to the right of the I-Wall looking down the global *y*-axis and therefore in the negative global *x*-axis direction. The notes in red at the bottom of the tab serve as reminders of this unintuitive situation.

A list of distributed loads can be created in much the same way that surface surcharge loads can be created to either side of the structure. A selector exists that allows the user to select the currently active distributed load. This currently selected, active load case is shown enhanced in the display window. This currently active load can be deleted by clicking the *X* button (in the red box) next to the selection drop-down list for the currently active distributed load. The list of loads is renumbered sequentially when the currently active load is deleted from the list.

Distributed horizontal loads are created as a set of piecewise linear curves. In order to start the generation of a piecewise linear distributed horizontal load, click the *Add Distributed Load* button. This creates a new distributed load at the end of the currently active load selector and selects it. At the beginning of the process, the distributed load is empty.

To change the currently active distributed load, an elevation must be entered with the pressure at that elevation, under the *Distributed Load Point* label. When these numbers have been entered, clicking the *Add/ Change* button will place the horizontal pressure load at that elevation. This pressure will be displayed in the display window and in the list below the entry. As additional entries are added to the list, the list is sorted by elevation and the resulting surface shown. If an elevation is entered that is the same as an existing elevation, the existing elevation and its pressure data are overwritten with the new values.

If an elevation/pressure pair is in error and needs to be removed, the user can left mouse-click the pair anywhere on the list beneath the *Add/Change* button and click the *Delete* button, which is to the right of the *Add/Change* button.

Line loads are entered to the right of the display screen. These line loads are horizontal loads that act on the I-Wall with a prescribed force, and at a certain elevation. All of the existing line loads are shown in the list underneath the line load creation entry text boxes and buttons. Individual line loads can be created by entering an elevation and horizontal pressure acting at that elevation. Clicking the *Add/Change* button adds that line load to the line load list or overwrites existing loads at that elevation. To remove a line load, click anywhere on that load in the list and click the *Delete* button in the line load region. Line loads are displayed in a purple color in the display window.

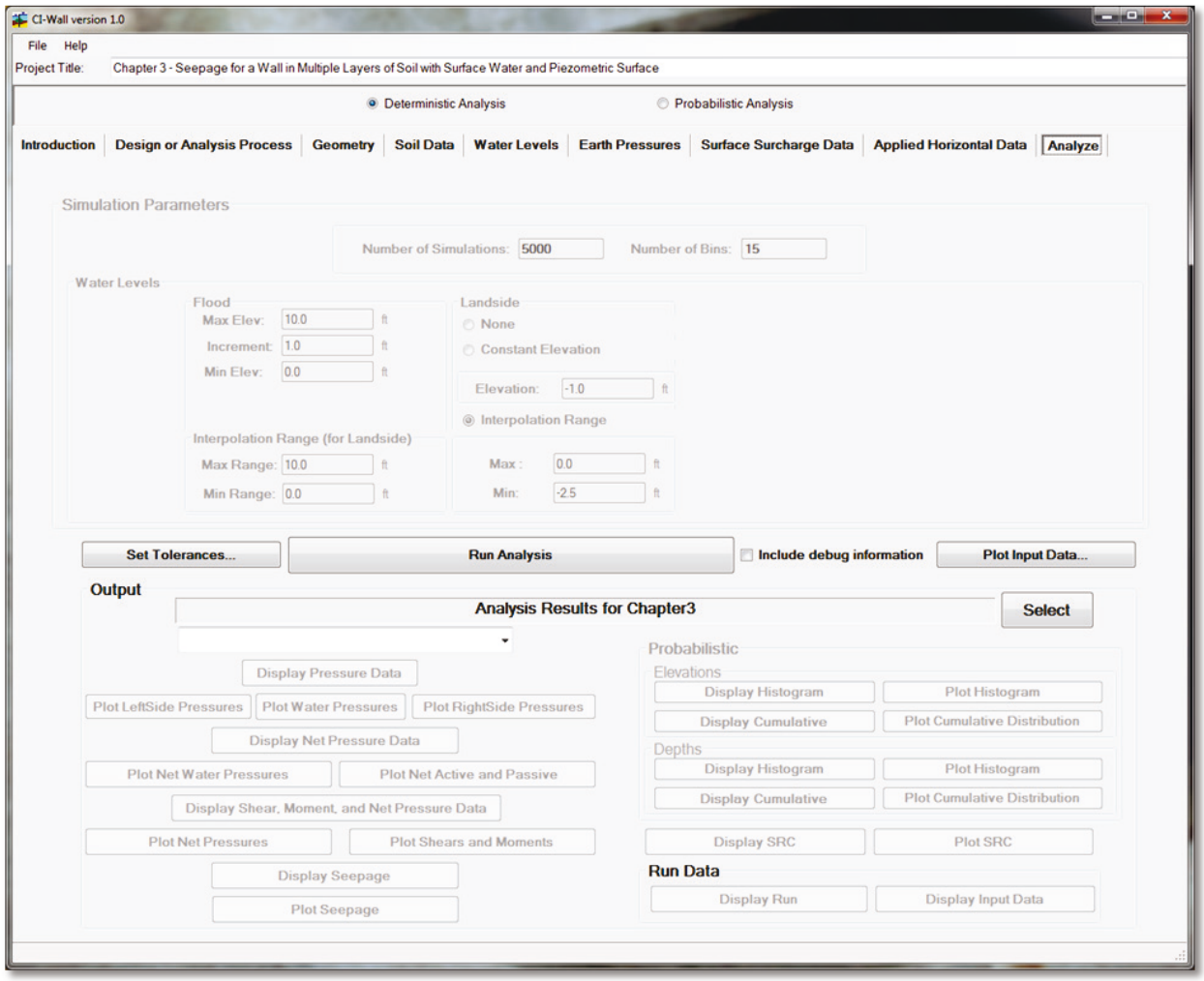
3.11 *Analyze* tab

The *Analyze* tab has the final input information for simulation runs necessary to perform a probabilistic run of Corps_I-Wall, as well as controls for running the FORTRAN processing code and viewing the results of a run. When the program is performing a deterministic calculation, the tab looks like Figure 3.47. The probabilistic input is shown in Figure 3.48.

The simulation parameters to be input for probabilistic analysis are at the top of the *Analyze* tab. The number of simulations that will run and the number of bins used in a Latin hypercube simulation are the first input boxes. Increasing the number of bins, increases the resolution and therefore, precision of the resulting simulations. Increasing the number of simulations used for each flood elevation increases the accuracy of the computations but also lengthens the time for execution.

The water levels can also be varied during the simulation runs, resulting in a system response curve, also referred to as a fragility curve. This presents the probability of performance rotational limit state as a function of load conditions (i.e., flood elevation).

Figure 3.47. The *Analyze* tab at the beginning of a deterministic analysis.

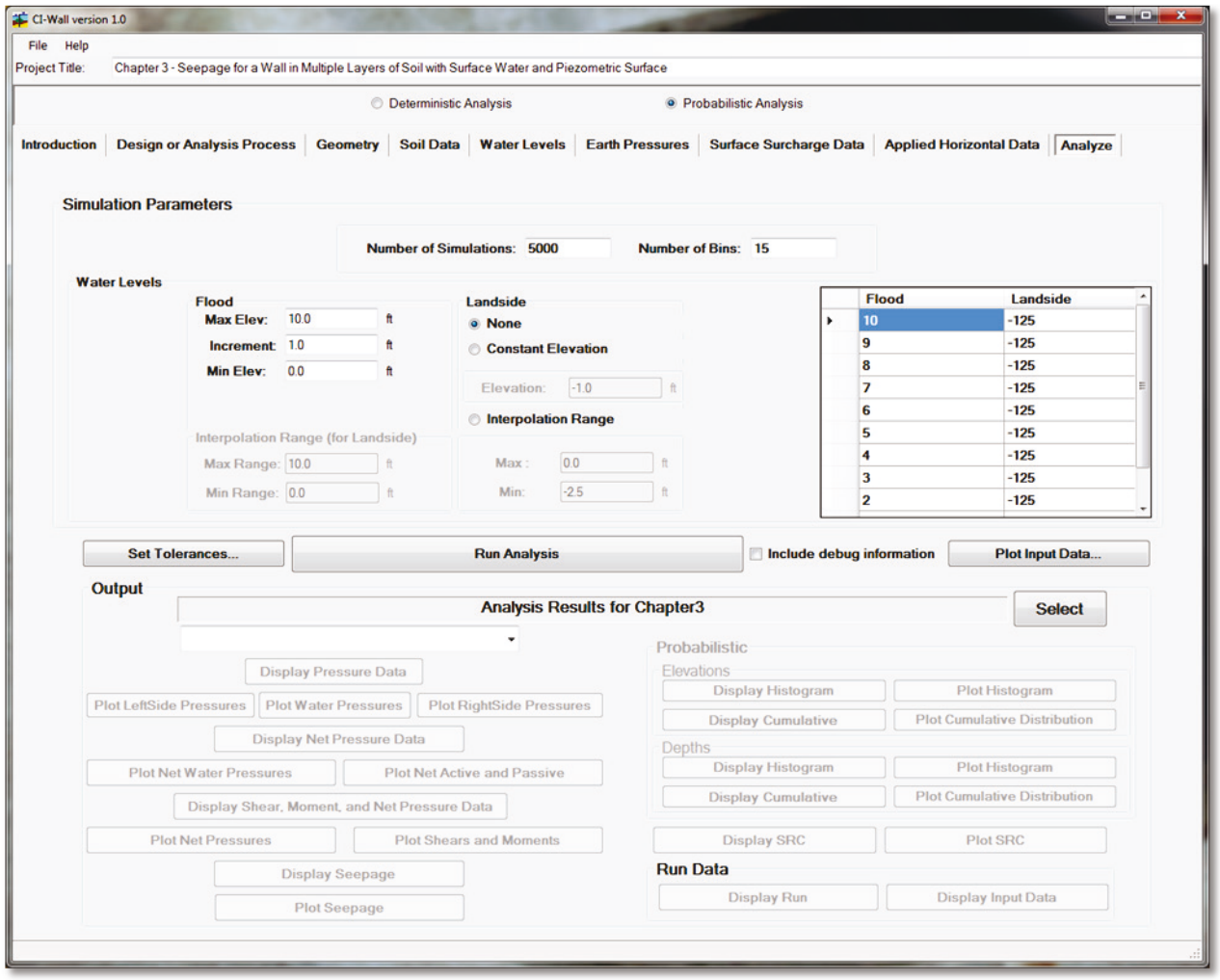


The levels are set differently for both the flood and landside of the I-Wall. The flood levels are set by giving a range of elevations, defined by the minimum and maximum elevations, and an increment of elevations from the minimum to the maximum. The set of elevations created is shown in a table to the right side of the tab.

Landside water elevations can be defined by either no water level, constant water level, or a range of interpolated levels that vary with the flood elevations. One of these methods is chosen using radio buttons.

Selecting the radio button labeled *None,* sets the landside water elevation to the base of the bottom soil region on the landside for every flood elevation (Figure 3.48). This means that the water levels on that side of the structure have no impact on the final solution.

Figure 3.48. The *Analyze* tab for a probabilistic analysis without landside water levels.



Selecting the radio button labeled *Constant Elevation* allows the user to enter a constant elevation that will be used for the landside water levels (Figure 3.49). This value is used for every flood level simulation.

Choosing the *Interpolation Range* radio button for assigning the landside causes a set of input windows to be opened. Data for the flood and landside are requested. This is because the values of the landside water levels can vary over a range of possible floodwater level elevations. The minimum and maximum water elevations for the landside are entered under the *Interpolation Range* radio button. The landside increment is determined by specifying the lower and upper limits of the flood elevations (Figure 3.50a).

Figure 3.49. The *Analyze* tab for a probabilistic analysis with constant landside water level.

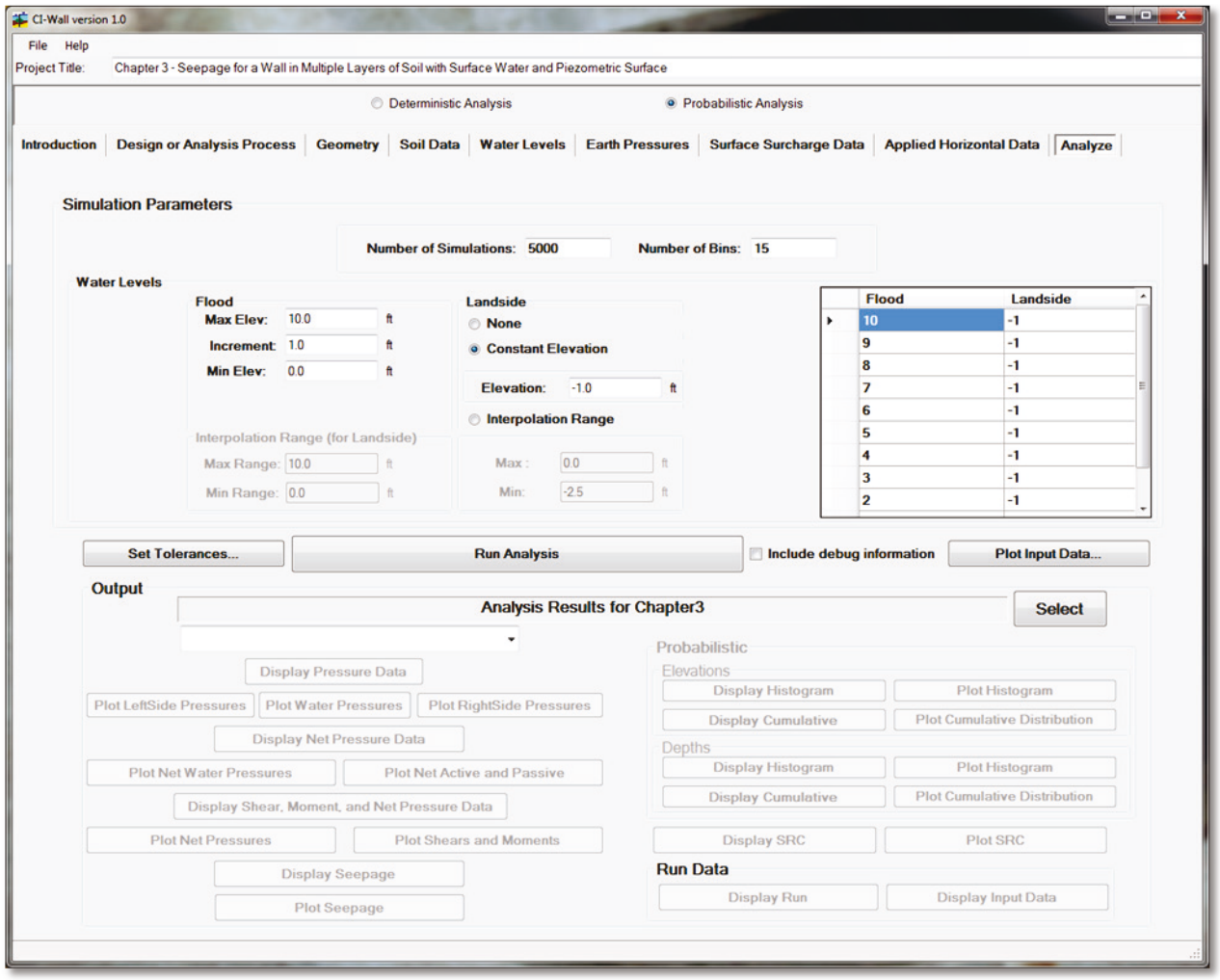
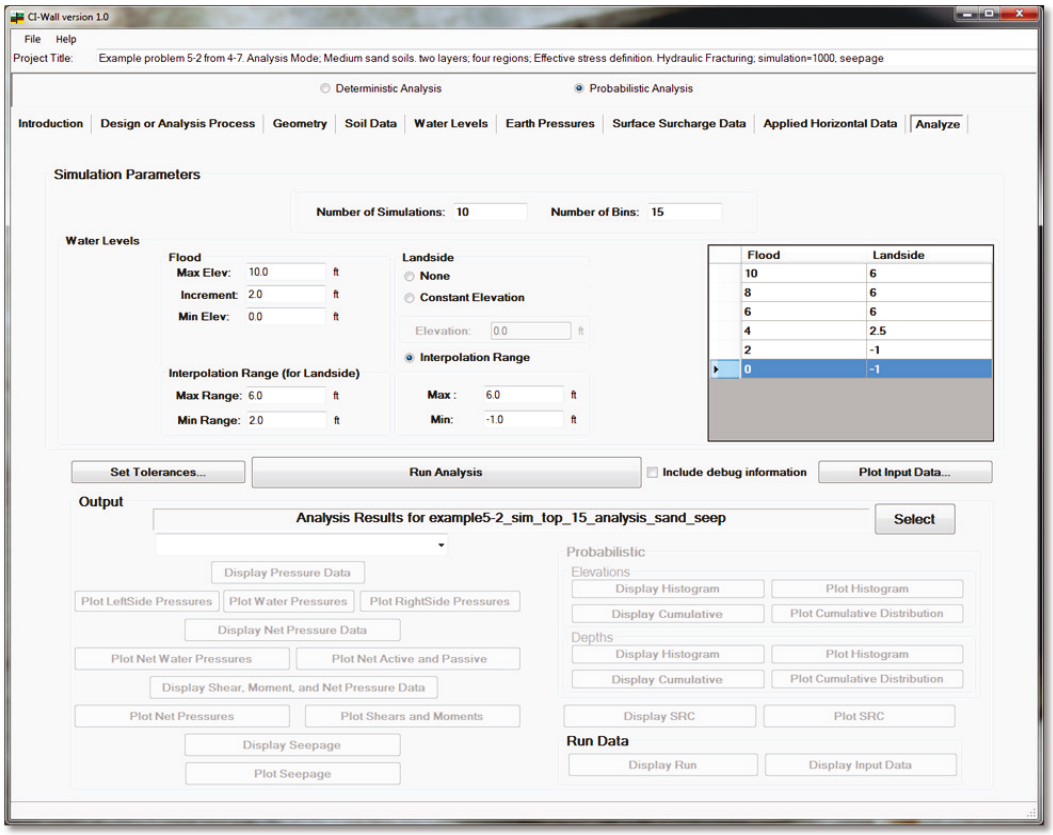
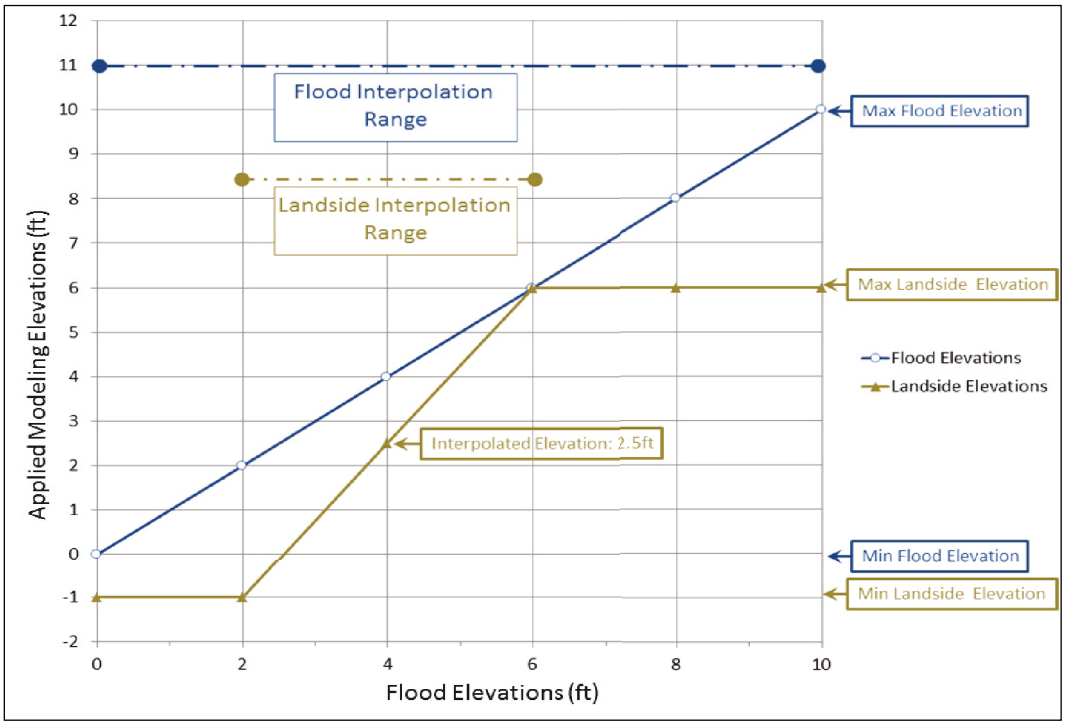


Figure 3.50a and b shows a probabilistic run that is generated using the *Interpolation Range* option. The flood levels are defined by a minimum elevation of 0.0 ft with increments of 2.0 ft, to the maximum elevation of 10 ft (input in the Flood section). This will result in the following six *x*-values of flood elevations: 0, 2, 4, 6, 8, 10 ft. Therefore, six *x*-values of landside water elevations are needed. The landside elevation range of values for water levels go from a minimum of -1 ft to a maximum of 6 ft (input in the *Interpolation Range* section at the lower right of the *Simulation Parameters* input section), however, these values are interpolated for only a subrange of the flood elevations. The lower left input of *Flood Side Interpolation Range* of a *Min Range* value of 2 ft and a *Max Range* value of 6 ft establishes the subrange of flood elevations over which the landside water elevations will be linearly interpolated.

Figure 3.50. (a) The *Analyze* tab. (b) Its procedure for a probabilistic analysis with interpolated landside water levels.



a.



b.

Figure 3.50b shows the water elevations for the flood and landside of the I-Wall as a function of the flood side water elevations. Because the flood side has a 1-to-1 correspondence to itself in this figure, the flood elevations plot at a 45 degree angle. The landside water elevation is a three part, piecewise linear function of flood side water elevations. The landside water elevations are linearly interpolated when the flood side elevations are in the range between 2 and 6 ft. For these two flood elevations, the corresponding landside water elevations are -1 and 6 ft, respectively. Outside of the flood side range of 2 to 6 ft, the values for the landside water elevations are horizontal with the landside values of -1 and 6 ft, respectively. Between these two flood elevations of 2 and 6 ft, a linear interpolation is required. In this case, the value for the landside water elevation has to be calculated for the corresponding flood side elevation of 4 ft. Between flood elevations of 2 and 6 ft, the landside water elevation relationship follows the linear equation

$$y = m * x + b \tag{3.1}$$

After substitutions, the relationship becomes

$$y = \{6 - -1\}\{6 - 2\} * 4 - 2 + -1 = 1.75 * 2 - 1 = 2.5 \tag{3.2}$$

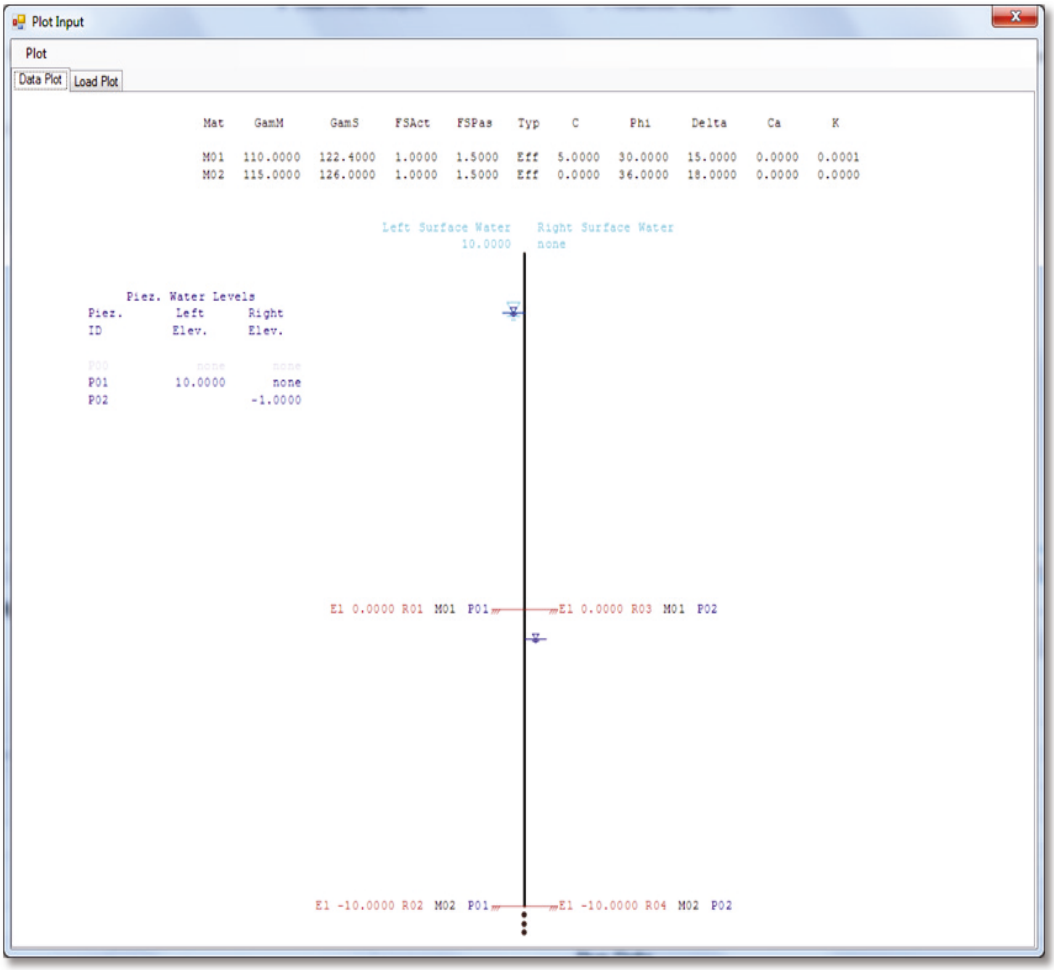
So for a flood elevation of 4 ft, the corresponding landside water elevation is 2.5 ft. This linear interpolation computation is made by the CI-Wall GUI software. If the range had included more flood elevations between the extremes, multiple landside water elevations would have been computed using the linear interpolation based on Equation 3.1. The table to the right in Figure 3.50a summarizes the results of this interpolation for the six pairs of flood side and landside water elevations.

It is possible to enter values for the interpolation range to extend outside of the range of flood values, but this will usually lead to unexpected results and is discouraged.

The buttons under the simulation parameter box allow the user to run the Corps_I-Wall FORTRAN processor. The *Plot Input* button provides the user a final chance to see the input geometry of the input data as a verification step. Figure 3.51 shows a resulting plot for a deterministic analysis. At the top of the plot is a list of the material descriptions. The first column has a material identification (ID) (e.g., M02) that is displayed

at the top of each surface region in the plot below. Used materials are shown in black, unused materials are those that may be used as input, but not assigned to a region, are in gray.

Figure 3.51. Plotting the input model for a deterministic analysis.

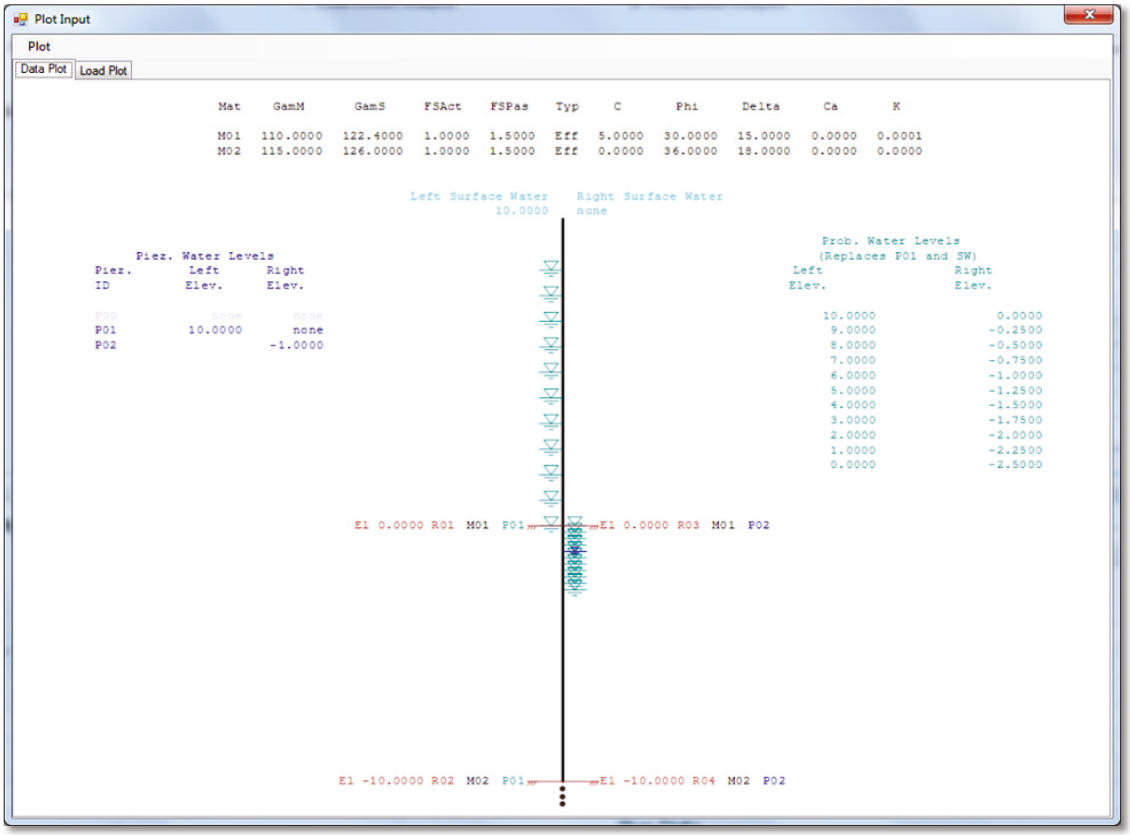


Immediately below the material definitions are the water surface elevations for the LHS and RHS of the I-Wall in cyan. A table of defined piezometric surfaces is given to the left of the plot in blue. Assigned piezometric surfaces are shown in dark blue, and unassigned piezometric surfaces are shown in light blue. The first two piezometric surfaces are special. The first piezometric surface is only applied if there is no water pressure acting on a material region. The second piezoemetric surface acts as if the surface water were acting on the side of the I-Wall as the material region, so both surface elevations are shown. The rest of the piezometric surfaces are user-defined surfaces and only apply to one side of the I-Wall, so they only have a value on that side of the I-Wall. The piezometric surface ID (e.g., P01) is given in the leftmost column.

The plot shows the I-Wall, at least to the top of the lowest soil material layer, or the lowest water elevation. The surface water elevations are displayed with a typical water symbol in cyan. Assigned piezometric surfaces are displayed in a like manner with a dark blue color. For each surface material region, a brown line extends from the I-Wall with an earth symbol. The elevation is marked, and the region ID (e.g., R01) is given. Also shown are the material properties assigned to the region (acting below the surface to the top of the next surface) and the piezometric surface exerting pore water pressure on this region.

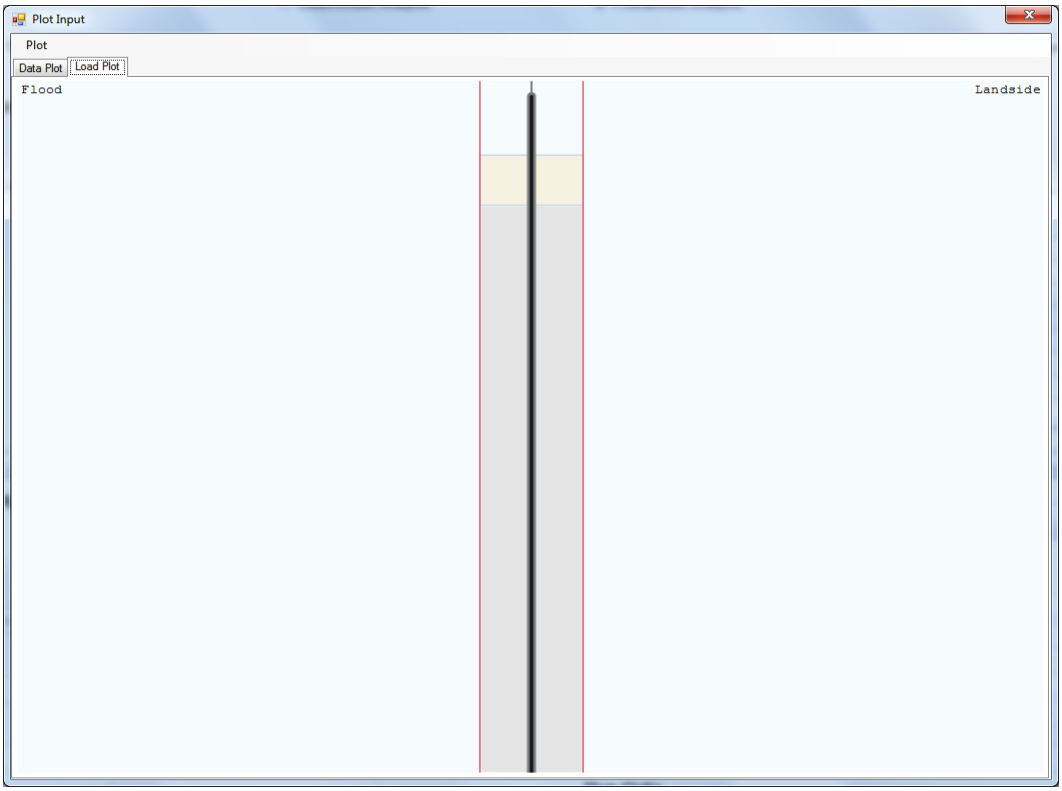
Figure 3.52 shows the results of plotting the input for a probabilistic run of the Corps_I-Wall program. The only additions to this plot are the table to the left of the various water surface elevations that will be tested for the simulation runs, and these elevations on the plot itself. These additions are in a green color. These water levels not only provide different overburdens, but also affect the material regions that are assigned the piezometric surface water (P01). This is represented in the region plots by displaying the piezometric surface water R01 in green.

Figure 3.52. Plotting the input model for a probabilistic range of both flood and landside water levels.



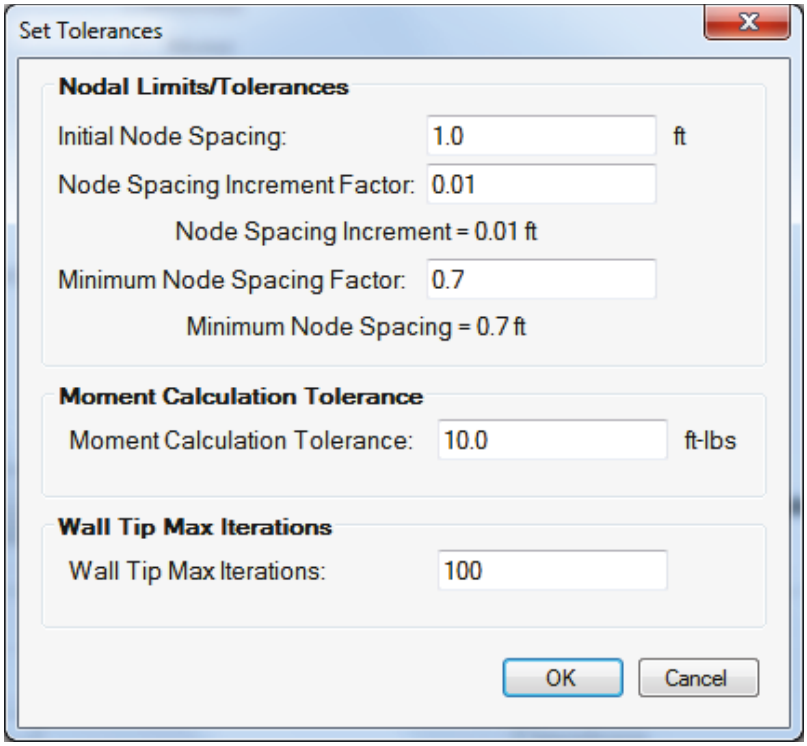
If surface surcharge or applied horizontal loads are specified, they can be viewed in the same fashion as they are displayed in the GUI by selecting the *Load Plot* tab (Figure 3.53).

Figure 3.53. View of the pile without horizontal and vertical loads.



The *Set Tolerances* button opens the *Set Tolerances* dialog box (Figure 3.54), allowing for the input of the initial node spacing along the I-Wall, the node spacing increment (so that Corps_I-Wall can meet convergence criteria), and the minimum space allowed between nodes. There is also input of moment calculation tolerance, this allows Corps_I-Wall to converge to a solution faster. The number of iterations allowed to calculate the I-Wall tip depth is also given. It is anticipated that these default values will be adequate for the majority of I-Wall analyses.

Figure 3.54. Tolerance input dialog.



The *Run Analysis* button performs the analysis as requested for *Analysis* or *Design* mode, and for deterministic or probabilistic mode. The *Include debug information* checkbox allows the user to specify the output to include debug information when the FORTRAN processor runs (Figure 3.55). When the processor has finished, a database of output files is created. It is not anticipated that a user will request execution in debug mode. This option was put in place for use by program developers.

There is a caveat to this procedure. In probabilistic mode, it is possible to specify correlations that are impossible to fulfill when cross-correlation occurs. Cross-correlation occurs when a variable (e.g., material property *Ca*) is correlated with more than one other material property variable or correlated across materials. When a cross-correlation is recognized by the GUI, a message dialog will pop up warning that this condition may occur (Figure 3.56).

Figure 3.55. The Corps_I-Wall processor in action.

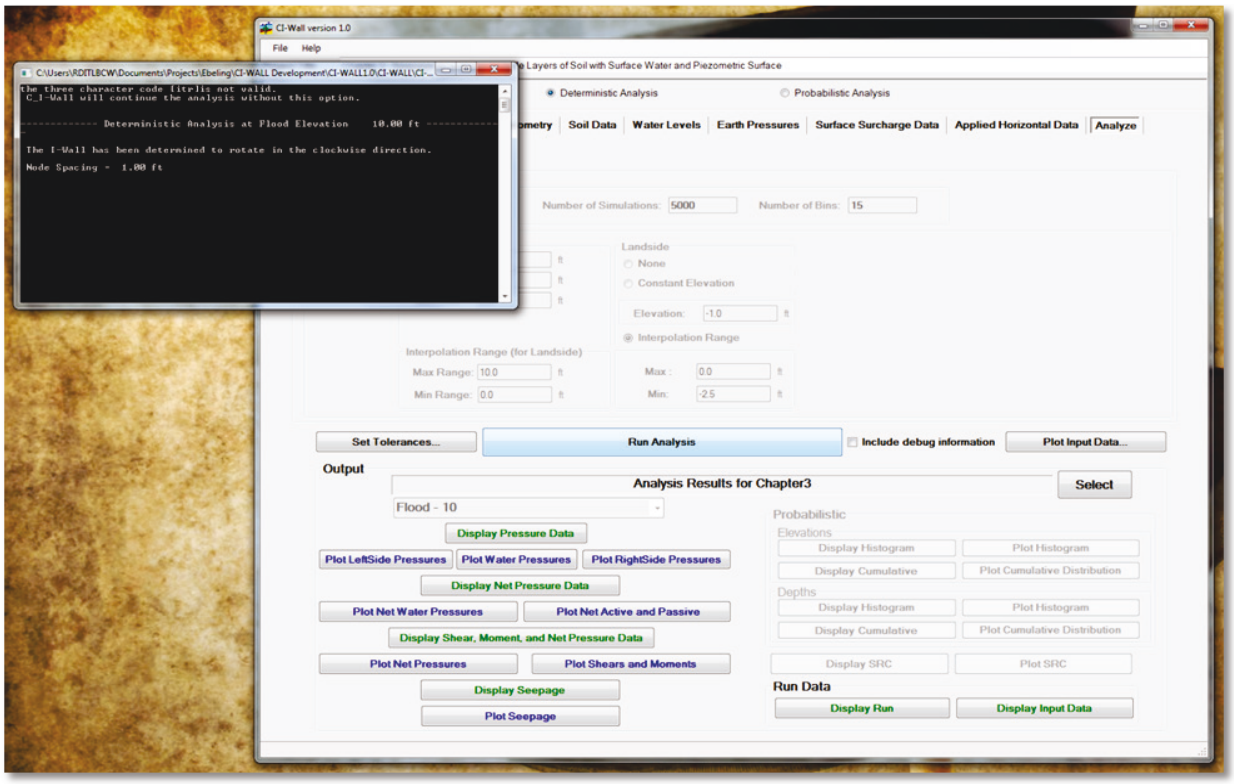
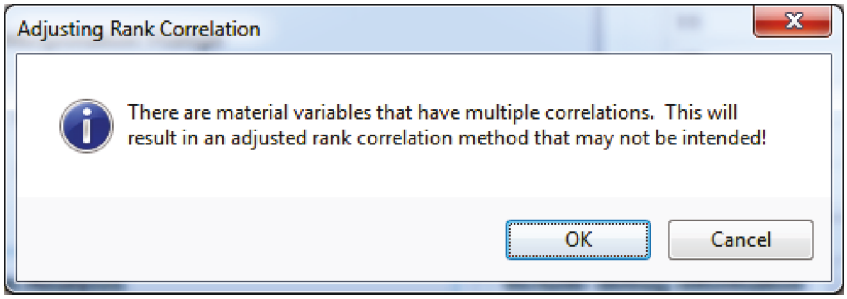
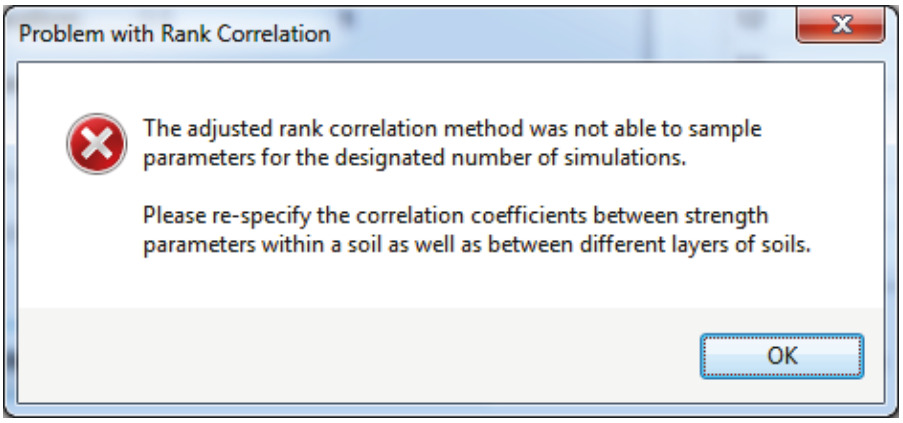


Figure 3.56. Adjusting rank correlation dialog.



At this point, the user can choose to abort the attempted run to check the correlations or continue to run. If the run is continued, the software will attempt to adjust the offending correlations so that there are no conflicts, and to remain as close to the specified correlations as possible. If this is successful, the run will complete with the adjusted correlations. If the values cannot be adjusted to achieve a meaningful set of correlations, a message dialog will appear informing the user that the correlations must be adjusted in the GUI (Figure 3.57), and the run will not be completed.

Figure 3.57. If problems occur during adjustment of rank correlation, this dialog appears.



The Output section of the *Analyze* tab allows the user to view outputs from any runs that have been performed (Figure 3.58). At the top of this form is a label showing the currently selected output data set. The *Select* button to the right of this label allows the user to search for existing output data sets that may exist on their computer. The file that designates the data set has an *.ohd* (Output Header Designation) extension. When an *.ohd* file has been selected, that data set is populated in the Output section, and the output options are enabled for each option that has a valid output file. For instance, if a deterministic analysis was performed, the probabilistic section options will remain disabled, but if a probabilistic analysis was performed, those options would be enabled.

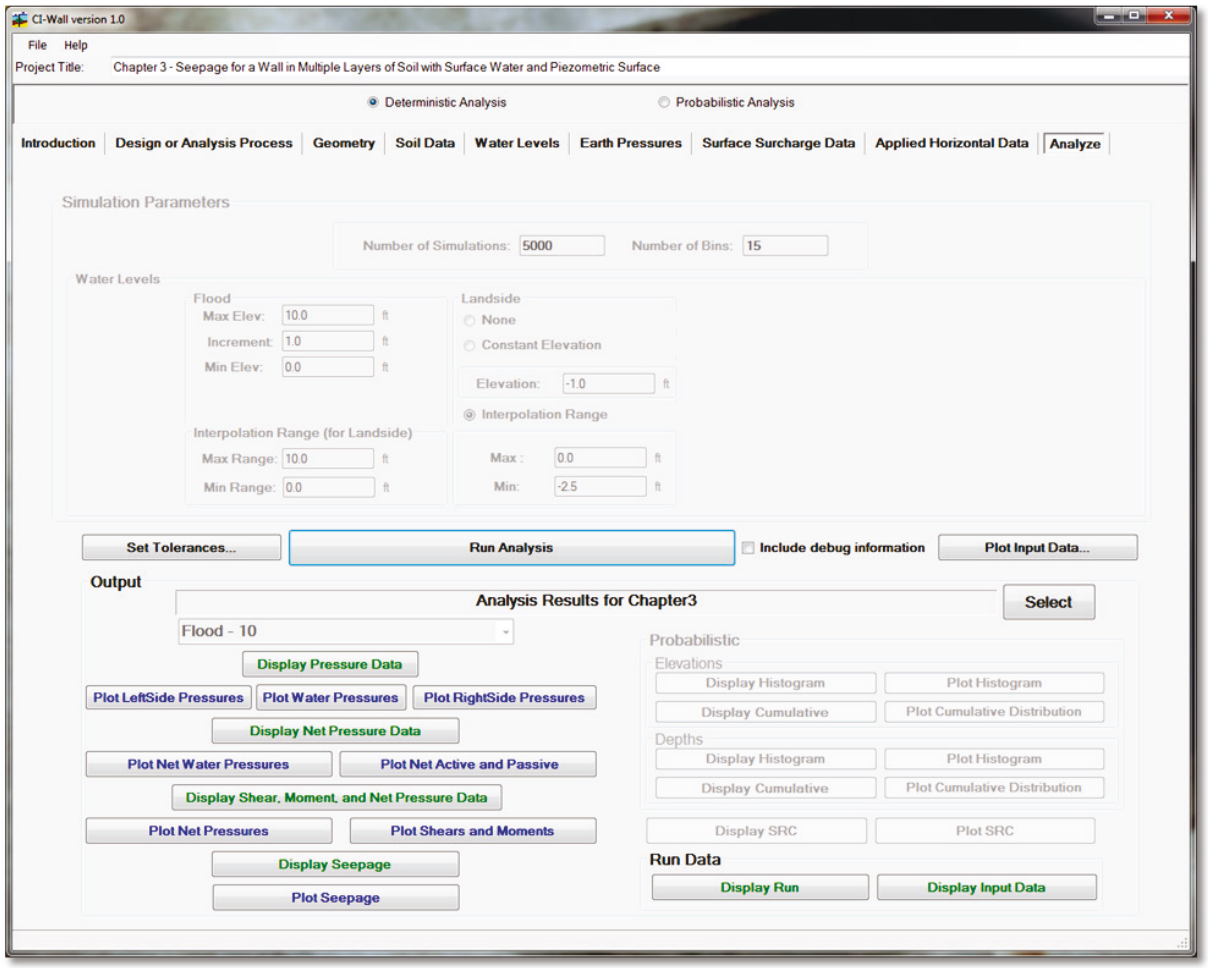
NOTICE: If an error occurred during an analysis, then only the *Run Data* subsection options will be enabled.

When the *Run Analysis* button has been performed, the *.ohd* for that run is automatically selected and the Output section is automatically populated with the values of that data set. This enables the user to proceed directly to analyzing the results from the existing input immediately.

Each output option begins with either the word *Display* or *Plot*. The *Display* options show the relevant data as a text file. The display window shows the data and allows the user to print the data or save it to another file.

The *Plot* options display the data in the files in some graphical manner. At this time, the drawn data cannot be sent to a printer or the clipboard, but these options will be added in later versions.

Figure 3.58. After the processor has finished, output options are made available.

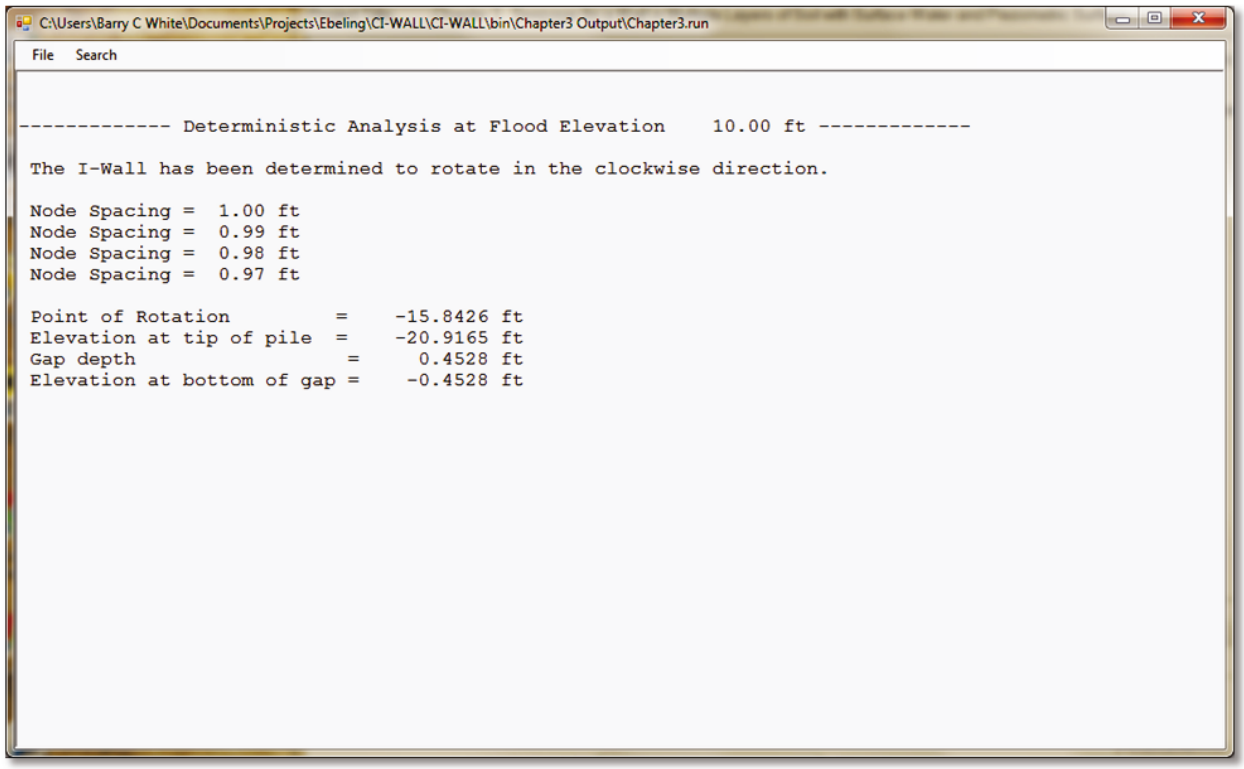


At the bottom left of the Output section of the *Analyze* tab, is the *Run Data* subsection (Figure 3.59). The *Display Run* button in this subsection brings up another window that has a permanent copy of the running output of the FORTRAN processor, as well as any debug information if it was requested (Figure 3.60). Pertinent information, such as the elevation of rotation, pile tip elevation, and gap depth are presented.

Figure 3.59. The *Run Data* subsection allows the user to see processor input, results, and debugging information.



Figure 3.60. The display run window shows the output and debugging information from an analysis.



The *Display Input Data* option of the *Run Data* subsection allows the user to review the input file for the FORTRAN processor that has been generated by the visual pre-processor (Figure 3.61). The file format for this input file is discussed in Appendix D.

To the left of the *Run Data* subsection are the buttons that display the output file data (Figure 3.62). Above these buttons is a selector that allows the user to select and view data for a flood level elevation. For a deterministic run, this selector will only have one value and the selector will be disabled. For a probabilistic run, multiple values will be available. The currently selected flood elevation output data will be the data displayed and plotted by the buttons shown.

The example problem is deterministic, and the following plots are for the fixed flood elevation of 10 ft.

Clicking the *Display Pressure Data* opens the output file related to water pressures on the LHS and RHS of the I-Wall (Figure 3.63). If gap propagation has been enabled, information about the gap is presented.

Figure 3.61. The display input data button allows the user to see the processor input file.

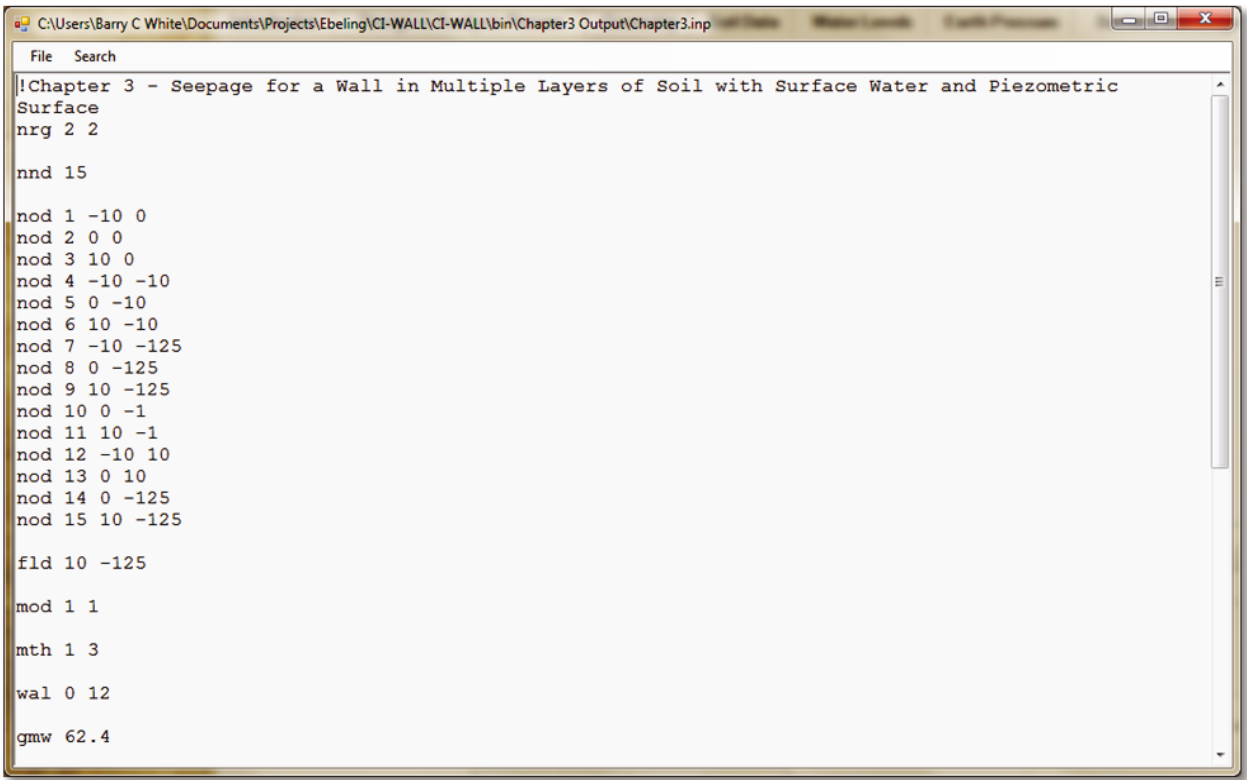


Figure 3.62. The output plot subsection allows the user to see data based on a flood elevation.

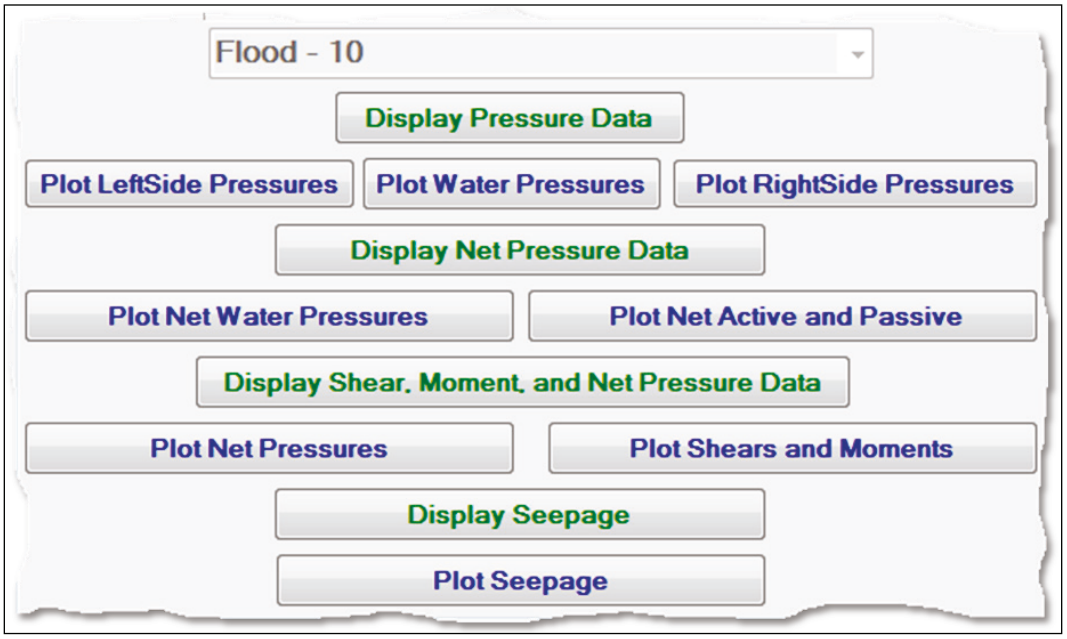
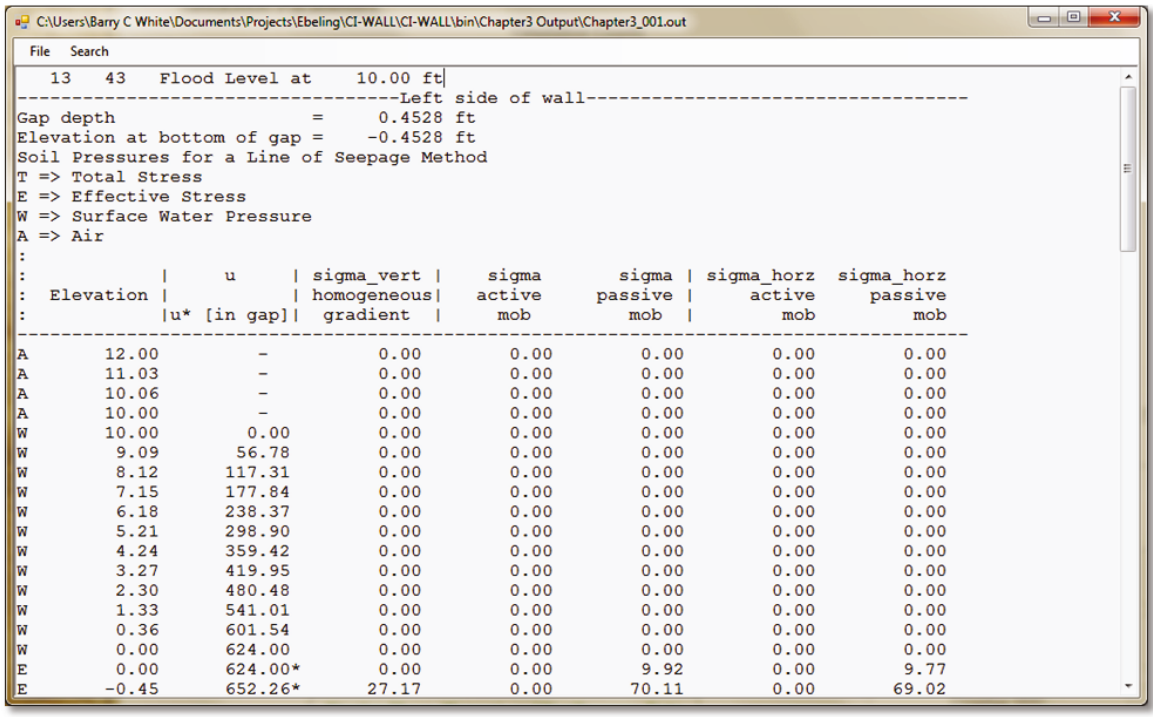


Figure 3.63. Pressure data for both the left and right sides of the I-Wall.



C:\Users\Barry C White\Documents\Projects\Ebeling\CI-WALL\CI-WALL\bin\Chapter3 Output\Chapter3_001.out

File Search

```
   13    43    Flood Level at     10.00 ft
---------------------------------Left side of wall-----------------------------------
Gap depth                    =      0.4528 ft
Elevation at bottom of gap =     -0.4528 ft
Soil Pressures for a Line of Seepage Method
T => Total Stress
E => Effective Stress
W => Surface Water Pressure
A => Air
:
:            |     u      | sigma_vert |    sigma       sigma | sigma_horz  sigma_horz
:  Elevation |            | homogeneous|   active     passive |     active     passive
:            |u* [in gap]|  gradient  |     mob         mob  |       mob         mob
-------------------------------------------------------------------------------------
A       12.00          -          0.00        0.00        0.00        0.00        0.00
A       11.03          -          0.00        0.00        0.00        0.00        0.00
A       10.06          -          0.00        0.00        0.00        0.00        0.00
A       10.00          -          0.00        0.00        0.00        0.00        0.00
W       10.00       0.00          0.00        0.00        0.00        0.00        0.00
W        9.09      56.78          0.00        0.00        0.00        0.00        0.00
W        8.12     117.31          0.00        0.00        0.00        0.00        0.00
W        7.15     177.84          0.00        0.00        0.00        0.00        0.00
W        6.18     238.37          0.00        0.00        0.00        0.00        0.00
W        5.21     298.90          0.00        0.00        0.00        0.00        0.00
W        4.24     359.42          0.00        0.00        0.00        0.00        0.00
W        3.27     419.95          0.00        0.00        0.00        0.00        0.00
W        2.30     480.48          0.00        0.00        0.00        0.00        0.00
W        1.33     541.01          0.00        0.00        0.00        0.00        0.00
W        0.36     601.54          0.00        0.00        0.00        0.00        0.00
W        0.00     624.00          0.00        0.00        0.00        0.00        0.00
E        0.00     624.00*         0.00        0.00        9.92        0.00        9.77
E       -0.45     652.26*        27.17        0.00       70.11        0.00       69.02
```

Each side of the I-Wall has a table presenting a series of elevations from the top of the I-Wall to the calculated tip of the I-Wall. A one letter tag (at the left of the table) tells how the I-Wall is loaded at each elevation. After the elevation data, data are presented for the pressure (u), the vertical homogeneous gradient, the active and passive mobilizing pressure, and the mobilized active and passive pressure acting in the horizontal direction (parallel to the ground surface).

Figures 3.64 through 3.66 show the plots of data from selecting the *Plot Leftside Data*, *Plot Rightside Data*, and *Plot Water Pressures*, respectively. The LHS (Figure 3.64) and RHS (Figure 3.65) data displayed are the horizontal active and passive pressures in red and green, respectively. The heights of the regions for each side are presented with brick-red lines and a region number with the *R#* format. These plots go from the top of the I-Wall to the tip. When the user moves the cursor over the plot, the y-coordinate of the point is determined, and the relevant pressure is interpolated from the piecewise linear curve representing the pressure. These data are presented in a tooltip at the cursor location.

Figure 3.66 shows the water pressures based on the head and region materials for each side of the I-Wall. The data for Figures 3.64 through 3.66 are presented with the *Display Pressure Data* button presented above the *Plot* buttons.

Figure 3.64. Left-side horizontal mobilized passive and active pressures.

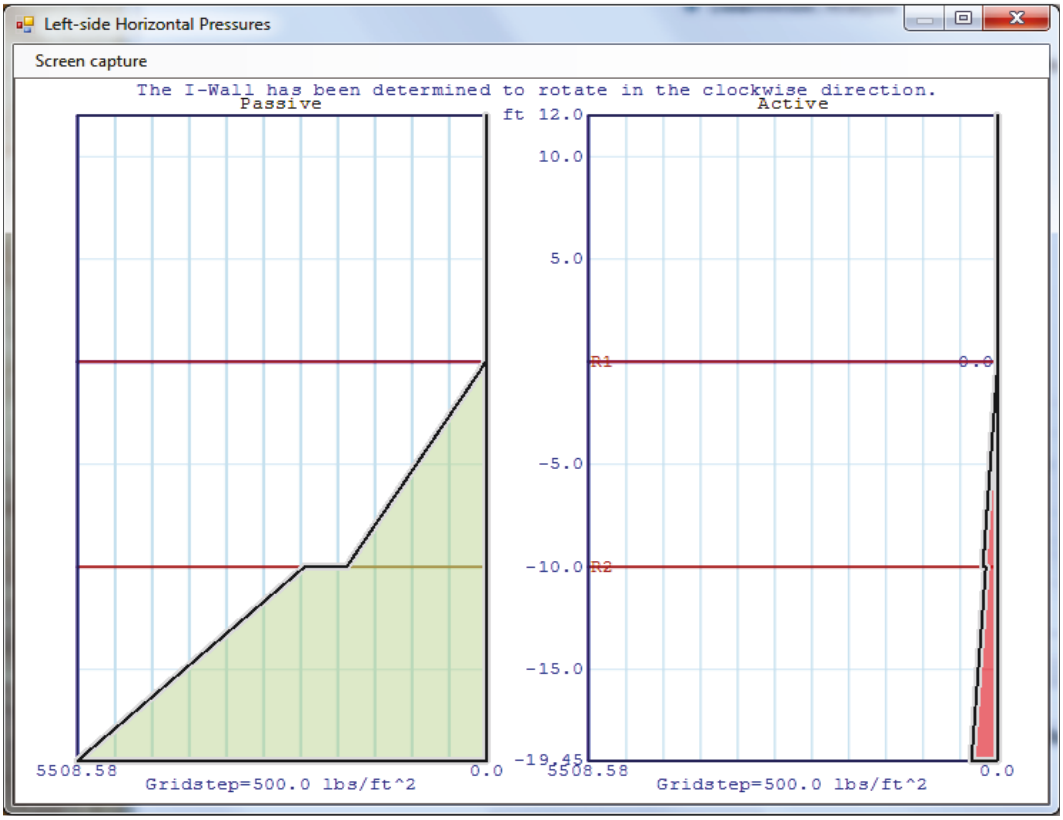


Figure 3.65. Right-side horizontal mobilized active and passive pressures.

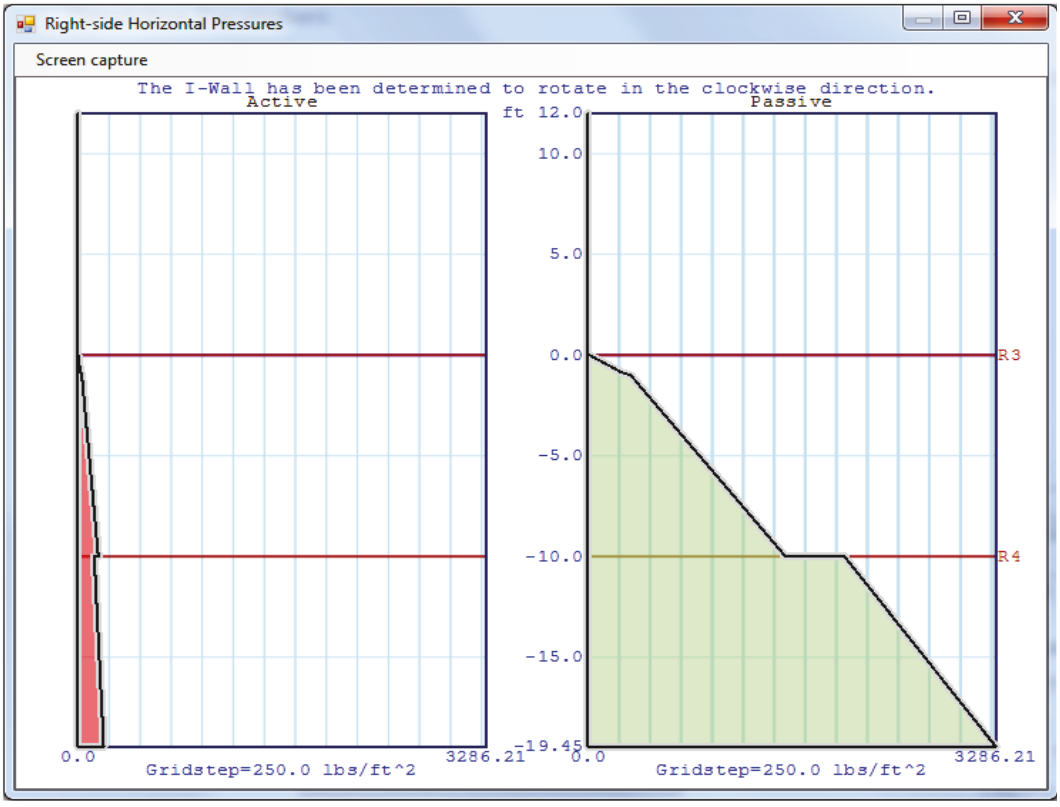
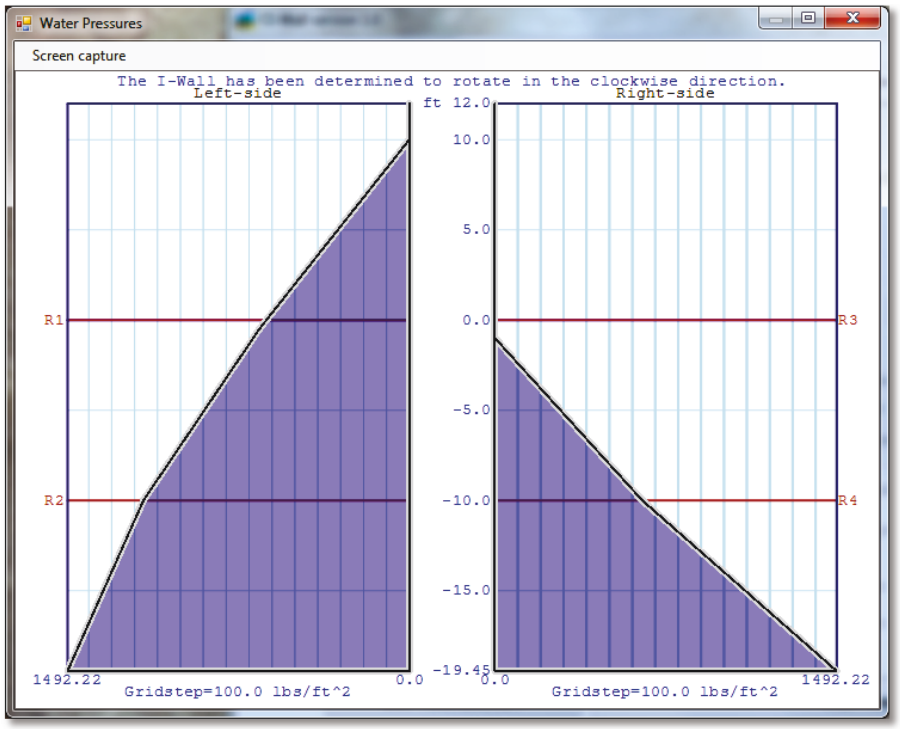


Figure 3.66. Left- and right-side water pressures.

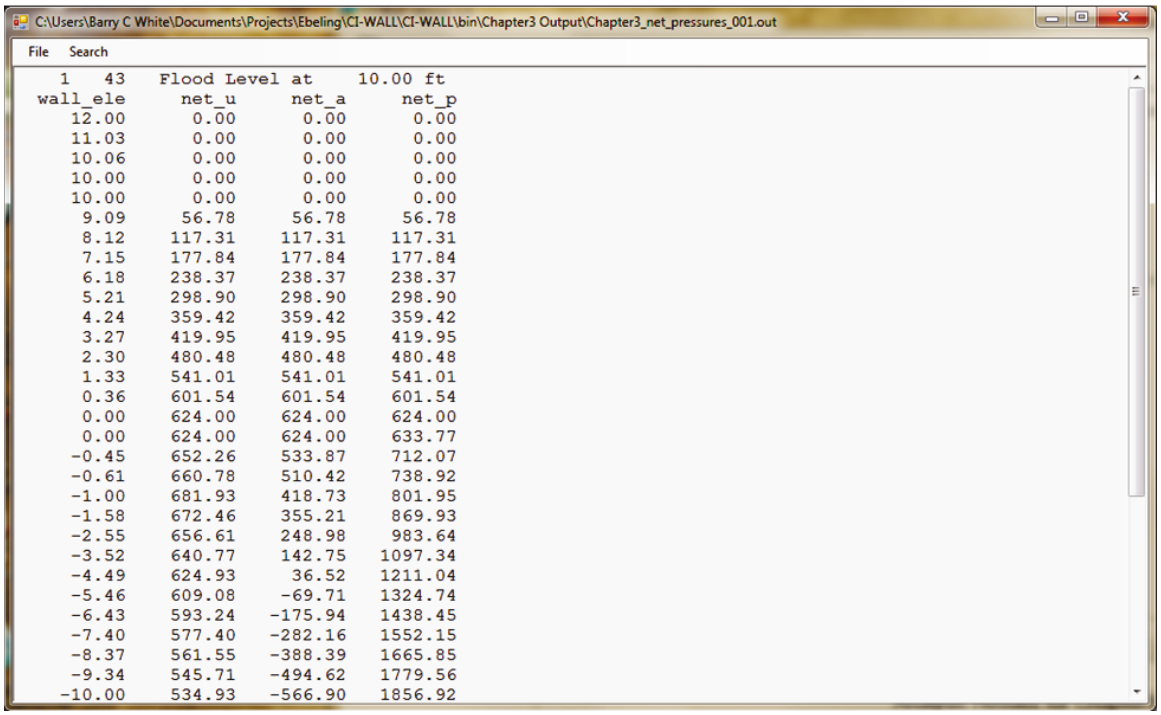


The *Net Pressure Data* combine the information from the water pressures plot with the display data. The data contain the I-Wall elevations and the summed water pressures and mobilized active and passive horizontal pressures. These net data are presented in summed form with the *Display Net Pressures* button (Figure 3.67), the *Display Side Net Water Pressures* (Figure 3.68), and plotted with the *Plot Net Water Pressures* button (Figure 3.69). Again, a tooltip tracks the location of the map and interpolates the piecewise linear net_u information.

Both the net active and passive pressures are listed in Figure 3.70 along with shear and moment values internal to the I-Wall.

Figures 3.71 and 3.72 show how the combined net pressure against the I-Wall from soil and water, shear, and moment along the I-Wall are presented to the user. The plots have the active tooltip interpolation for the piecewise linear curves.

Figure 3.67. Displaying the net pressure data.




```
   1    43   Flood Level at    10.00 ft
 wall_ele      net_u      net_a      net_p
    12.00       0.00       0.00       0.00
    11.03       0.00       0.00       0.00
    10.06       0.00       0.00       0.00
    10.00       0.00       0.00       0.00
    10.00       0.00       0.00       0.00
     9.09      56.78      56.78      56.78
     8.12     117.31     117.31     117.31
     7.15     177.84     177.84     177.84
     6.18     238.37     238.37     238.37
     5.21     298.90     298.90     298.90
     4.24     359.42     359.42     359.42
     3.27     419.95     419.95     419.95
     2.30     480.48     480.48     480.48
     1.33     541.01     541.01     541.01
     0.36     601.54     601.54     601.54
     0.00     624.00     624.00     624.00
     0.00     624.00     624.00     633.77
    -0.45     652.26     533.87     712.07
    -0.61     660.78     510.42     738.92
    -1.00     681.93     418.73     801.95
    -1.58     672.46     355.21     869.93
    -2.55     656.61     248.98     983.64
    -3.52     640.77     142.75    1097.34
    -4.49     624.93      36.52    1211.04
    -5.46     609.08     -69.71    1324.74
    -6.43     593.24    -175.94    1438.45
    -7.40     577.40    -282.16    1552.15
    -8.37     561.55    -388.39    1665.85
    -9.34     545.71    -494.62    1779.56
   -10.00     534.93    -566.90    1856.92
```

Figure 3.68. Active and passive net pressures.

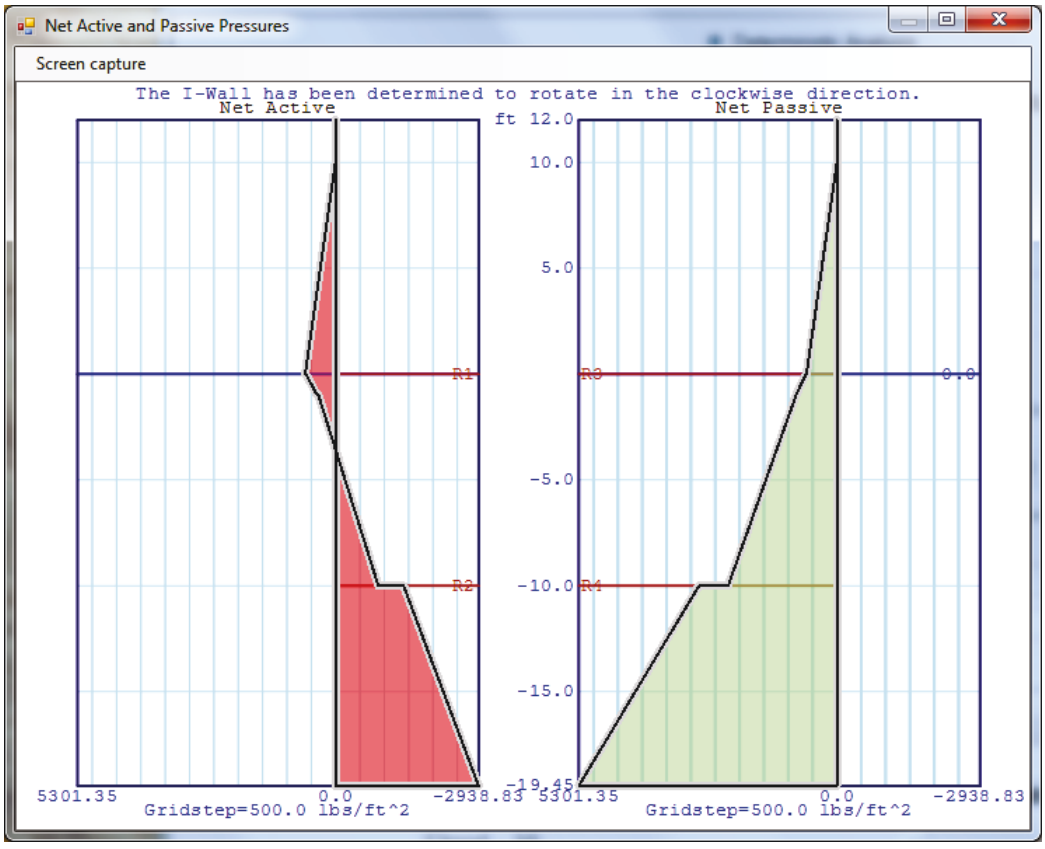


Figure 3.69. Displaying the net water pressures.

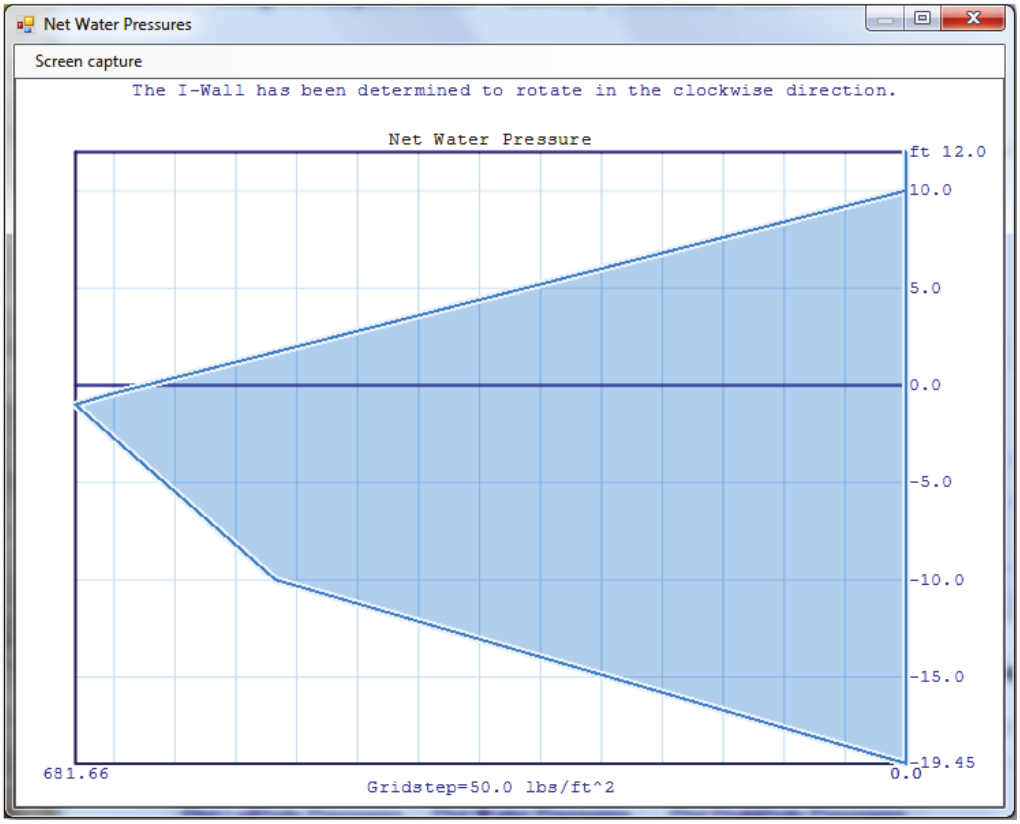


Figure 3.70. Shear, moment, and combined net pressures.

C:\Users\Barry C White\Documents\Projects\Ebeling\CI-WALL\CI-WALL\bin\Chapter3 Output\Chapter3_internal_shear_moment_001.out

File Search

1 44 Flood Level at 10.00 ft

Elevation	Shear	Moment	Net Pressure
12.00	0.000000	0.000000	0.000000
11.03	0.000000	0.000000	0.000000
10.06	0.000000	0.000000	0.000000
10.00	0.000000	0.000000	0.000000
9.09	25.836720	7.837138	56.784000
8.12	110.273280	69.104589	117.312000
7.15	253.422000	240.750900	177.840000
6.18	455.282880	579.726867	238.368000
5.21	715.855920	1142.983286	298.896000
4.24	1035.141120	1987.470950	359.424000
3.27	1413.138480	3170.140657	419.952000
2.30	1849.848000	4747.943200	480.480000
1.33	2345.269680	6777.829375	541.008000
0.36	2899.403520	9316.749978	601.536000
0.00	3120.000000	10400.000000	624.000000
-0.45	3382.164806	11873.760905	533.869055
-0.61	3464.225089	12411.797925	510.421708
-1.00	3645.408887	13799.338794	418.725973
-1.58	3869.849662	15980.544401	355.207735
-2.55	4162.880209	19884.747610	248.978959
-3.52	4352.868843	24023.215121	142.750183
-4.49	4439.815564	28295.996280	36.521407
-5.46	4423.720373	32603.140431	-69.707369
-5.46	4423.720373	32603.140431	-69.707369
-6.43	4304.583269	36844.696919	-175.936145
-7.40	4082.404252	40920.715087	-282.164921
-8.37	3757.183322	44731.244282	-388.393697
-9.34	3328.920480	48176.333848	-494.622473
-10.00	2978.617454	50260.445107	-566.901846
-10.00	2978.617454	50260.445107	-1410.162110

Figure 3.71. Combined net pressures with soil and water pressures.

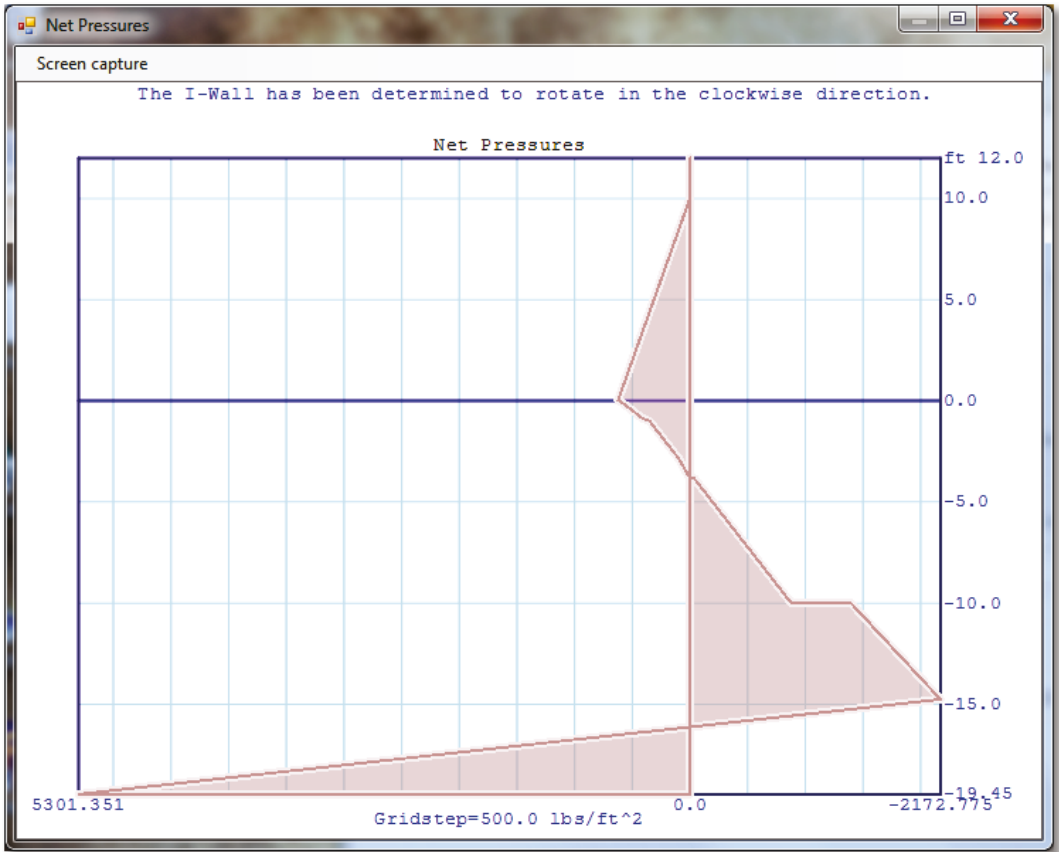
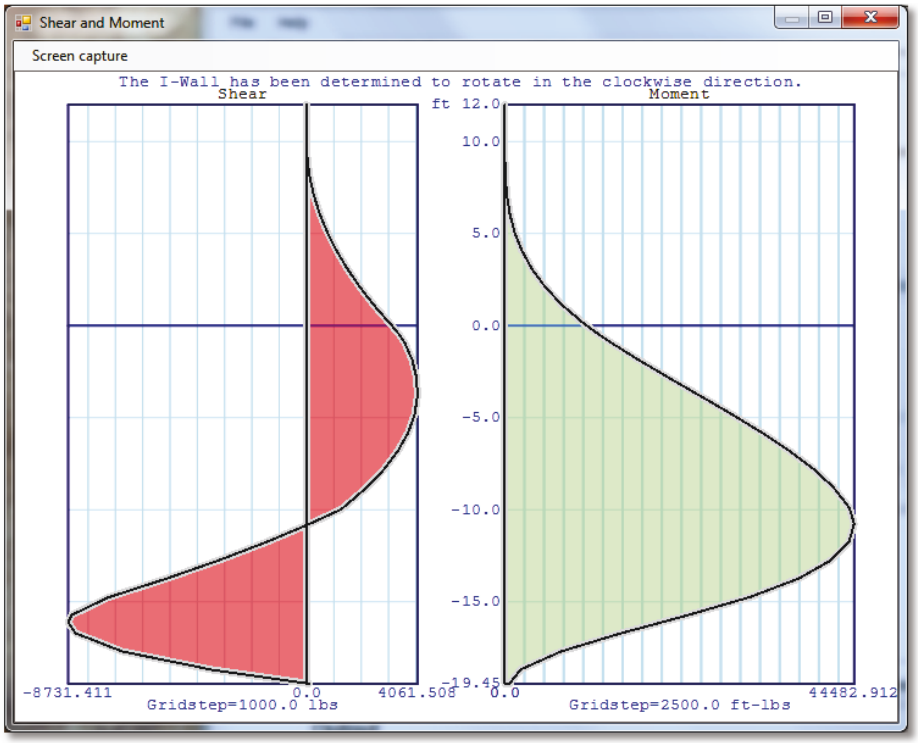
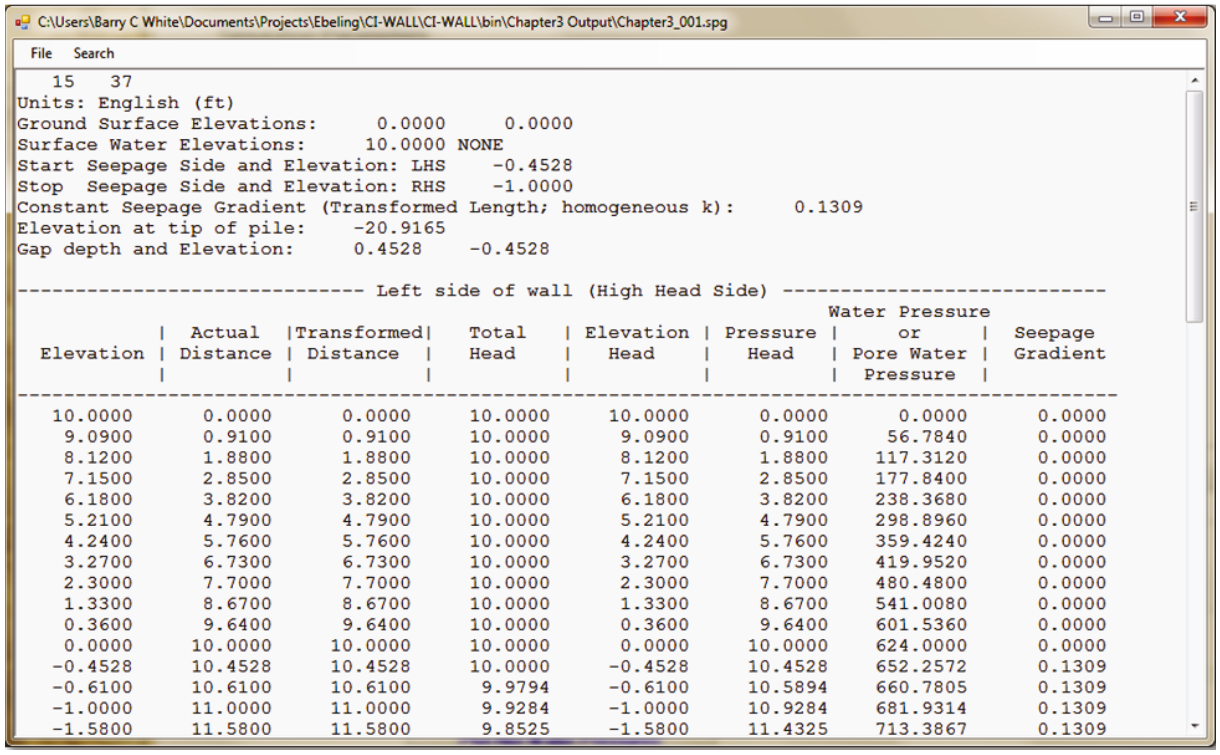


Figure 3.72. Shear and moment diagrams for the I-Wall.



The last two buttons in the Output section are the *Display Seepage* and *Plot Seepage* buttons. The Display Seepage button opens a window as shown in Figure 3.73. In the header of the file, after numbers that aid the reading of the data, is the information for the seepage analysis. This includes the following information: the units for elevation, the ground surface elevations for the LHS and RHS of the structure, the water surface elevations for the LHS and RHS of the structure, the side and elevation for the start of seepage, the side and elevation for the point where seepage stops, the constant seepage gradient (for transformed coordinates), the pile tip elevation, and the gap depth (on the side where seepage starts) and elevation.

Figure 3.73. Display of seepage data for both the left and right sides of the I-Wall.



C:\Users\Barry C White\Documents\Projects\Ebeling\CI-WALL\CI-WALL\bin\Chapter3 Output\Chapter3_001.spg

File Search

```
   15   37
Units: English (ft)
Ground Surface Elevations:     0.0000     0.0000
Surface Water Elevations:     10.0000 NONE
Start Seepage Side and Elevation: LHS    -0.4528
Stop  Seepage Side and Elevation: RHS    -1.0000
Constant Seepage Gradient (Transformed Length; homogeneous k):     0.1309
Elevation at tip of pile:    -20.9165
Gap depth and Elevation:     0.4528    -0.4528

------------------------------ Left side of wall (High Head Side) ----------------------------
                                                                          Water Pressure
            |  Actual   |Transformed|   Total    | Elevation | Pressure |     or     |  Seepage
  Elevation | Distance  | Distance  |   Head     |   Head    |   Head   | Pore Water |  Gradient
            |           |           |            |           |          |  Pressure  |
-------------------------------------------------------------------------------------------------
   10.0000      0.0000      0.0000     10.0000     10.0000      0.0000      0.0000      0.0000
    9.0900      0.9100      0.9100     10.0000      9.0900      0.9100     56.7840      0.0000
    8.1200      1.8800      1.8800     10.0000      8.1200      1.8800    117.3120      0.0000
    7.1500      2.8500      2.8500     10.0000      7.1500      2.8500    177.8400      0.0000
    6.1800      3.8200      3.8200     10.0000      6.1800      3.8200    238.3680      0.0000
    5.2100      4.7900      4.7900     10.0000      5.2100      4.7900    298.8960      0.0000
    4.2400      5.7600      5.7600     10.0000      4.2400      5.7600    359.4240      0.0000
    3.2700      6.7300      6.7300     10.0000      3.2700      6.7300    419.9520      0.0000
    2.3000      7.7000      7.7000     10.0000      2.3000      7.7000    480.4800      0.0000
    1.3300      8.6700      8.6700     10.0000      1.3300      8.6700    541.0080      0.0000
    0.3600      9.6400      9.6400     10.0000      0.3600      9.6400    601.5360      0.0000
    0.0000     10.0000     10.0000     10.0000      0.0000     10.0000    624.0000      0.0000
   -0.4528     10.4528     10.4528     10.0000     -0.4528     10.4528    652.2572      0.1309
   -0.6100     10.6100     10.6100      9.9794     -0.6100     10.5894    660.7805      0.1309
   -1.0000     11.0000     11.0000      9.9284     -1.0000     10.9284    681.9314      0.1309
   -1.5800     11.5800     11.5800      9.8525     -1.5800     11.4325    713.3867      0.1309
```

The constant seepage gradient is explained in Appendix C, but a brief description is as follows. For homogeneous soils, the head loss due to seepage is linear along the line of seepage (from the high head top of soil or gap depth to the pile tip, and then back up to the low head soil level or piezometric surface level). This line has a constant gradient. A set of heterogeneous soils will have different permeabilities, and therefore, the gradient will vary, although the head values at the start and end of seepage will remain the same. In order to model this behavior linearly, a transformed space with distances based on the permeabilities of the soil

regions is created. Thus, a single line will represent the change in head from the start-to-end seepage region, reducing the problem to a single constant gradient in the transformed space.

After the header information, tables are presented for each side of the I-Wall. This table contains data points at elevations from the top of the water surface on that side of the I-Wall, to the pile tip. The columns contain information about distance for the line of seepage (both actual distance and transformed distance according to soil region properties), the heads (total, elevation, and pressure) that are acting on the system, the pore water pressures acting on the structure, and the actual seepage gradient based on soil region properties.

Figure 3.74 is the initial plot as shown by the *Plot Seepage* button. This plot has the following five main areas: the line of seepage plot, the header information, the plot type indicator, the plot, and the axes for the plot. The line of seepage plot is in the white area to the left of the window. This plot provides a scaled overview of the I-Wall and how seepage occurs. On this plot are surface waters (if they exist), piezometric water surfaces, soil region information, the bottom of the gap, the pile tip, and the line of seepage with direction arrows.

The header information is a repeat of the header information from the file.

The plot type indicator reveals what information is being displayed (as discussed later) and whether the plot is in transformed space or not.

The plot is a simple linear function plot, showing either head information (*Total, Elevation, or Pressure*), pore water pressures, or the seepage gradient.

The axes at the bottom of the plot show 1) either the actual or transformed distances, and 2) the positions of points of interest along the structure (surface water, piezometric surface, region tops, gap location, and pile tip location).

Figures 3.75 and 3.76 show the menu options for selecting the data to display on the vertical axis and horizontal axis, respectively.

Figure 3.77 shows the result of plotting the total head in transformed coordinates for heterogeneous soil regions. As expected, the seepage occurs along a single line with a constant gradient.

Figure 3.74. Seepage plot of total head loss in actual (untransformed) space.

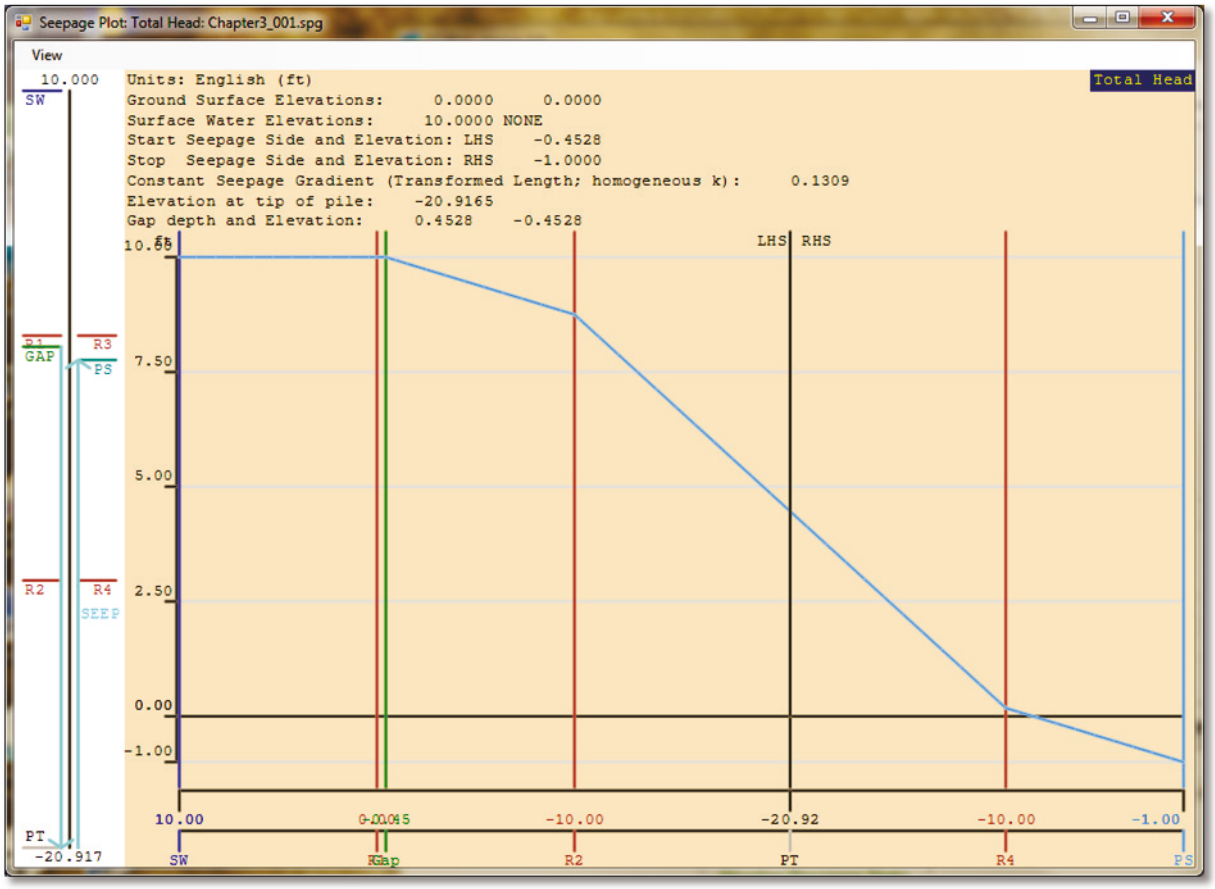


Figure 3.75. Seepage plot items to display.

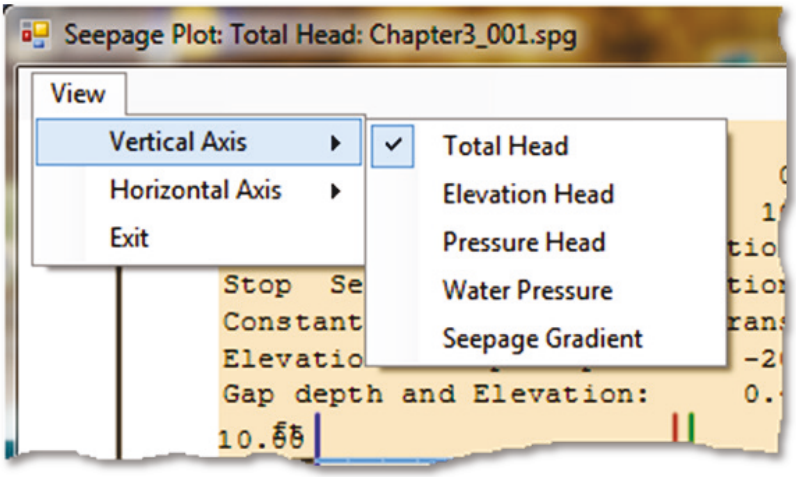


Figure 3.76. Seepage plots selector for untransformed or transformed space.

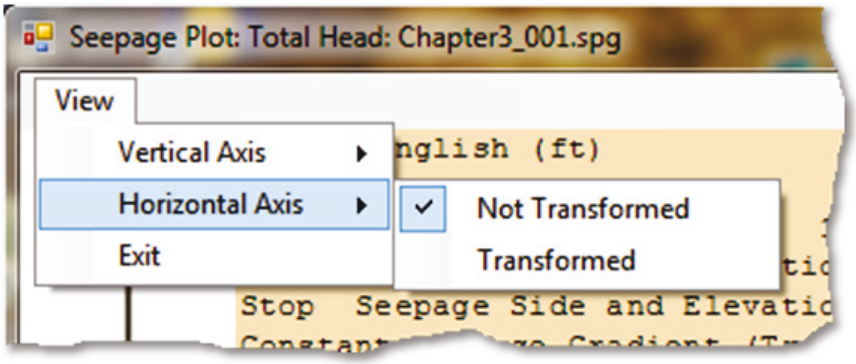


Figure 3.77. Seepage plot of total head loss in transformed space.

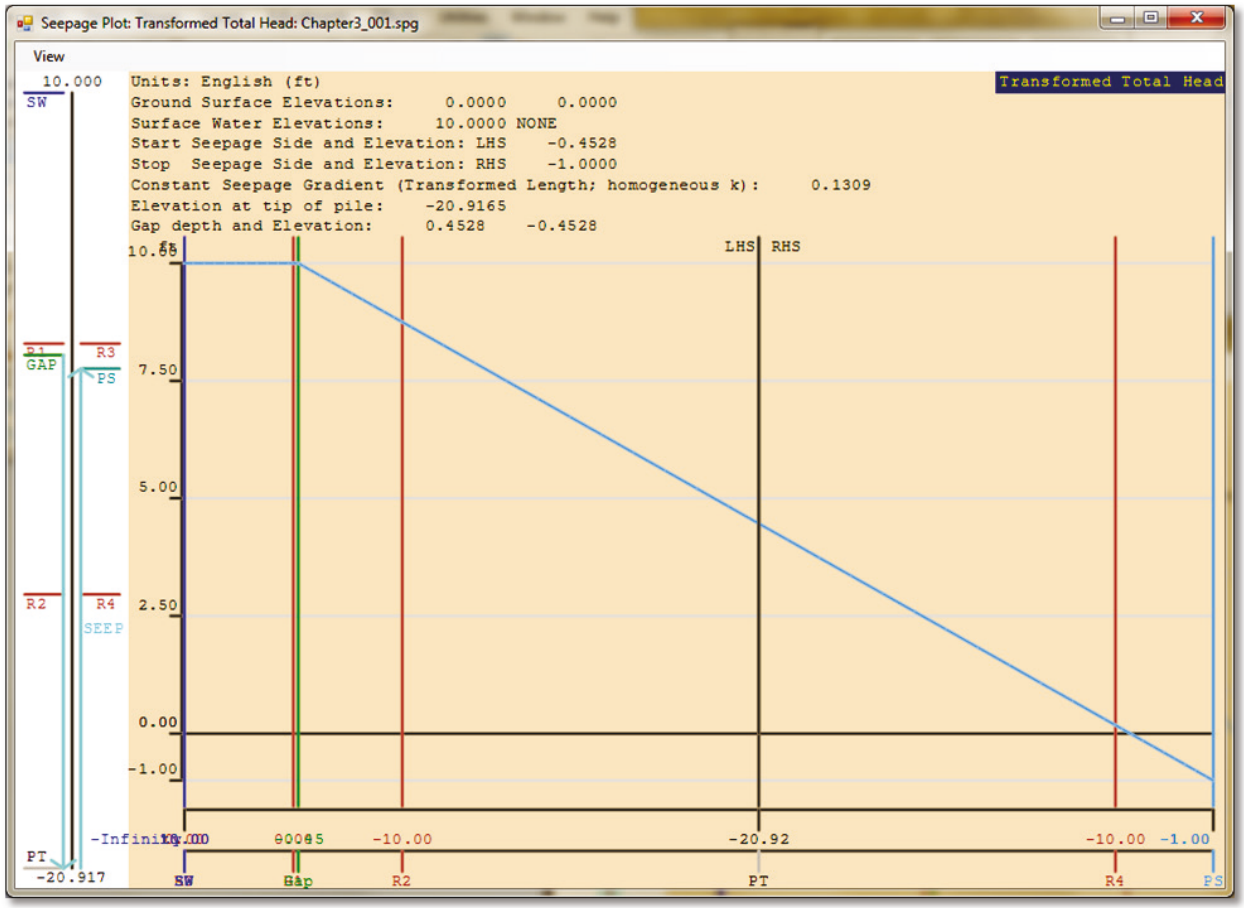
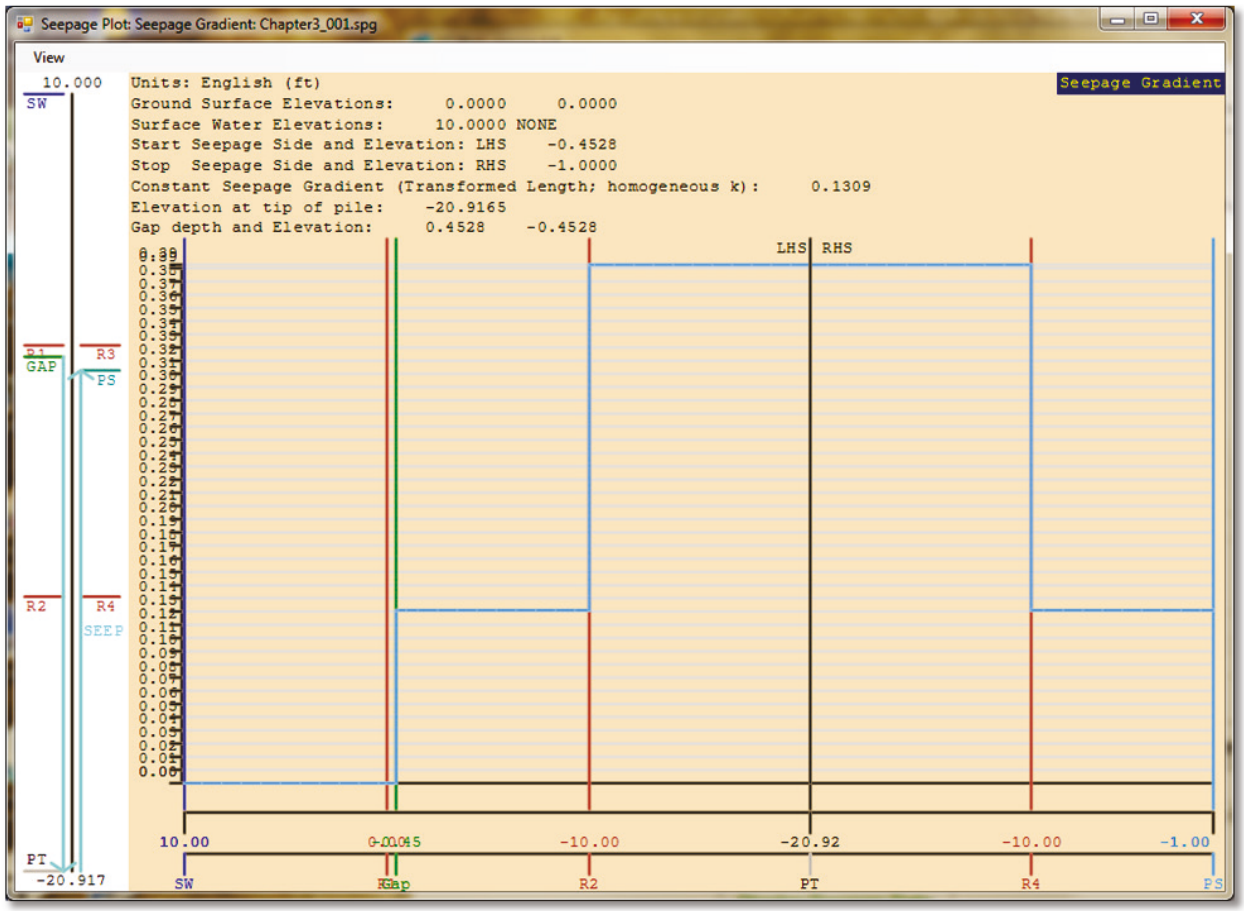


Figure 3.78 shows the result of displaying the seepage gradient data across the structure. The gradients are constant across a soil region. These are the actual gradients formed by taking the constant gradient from the transformed space back into the untransformed space.

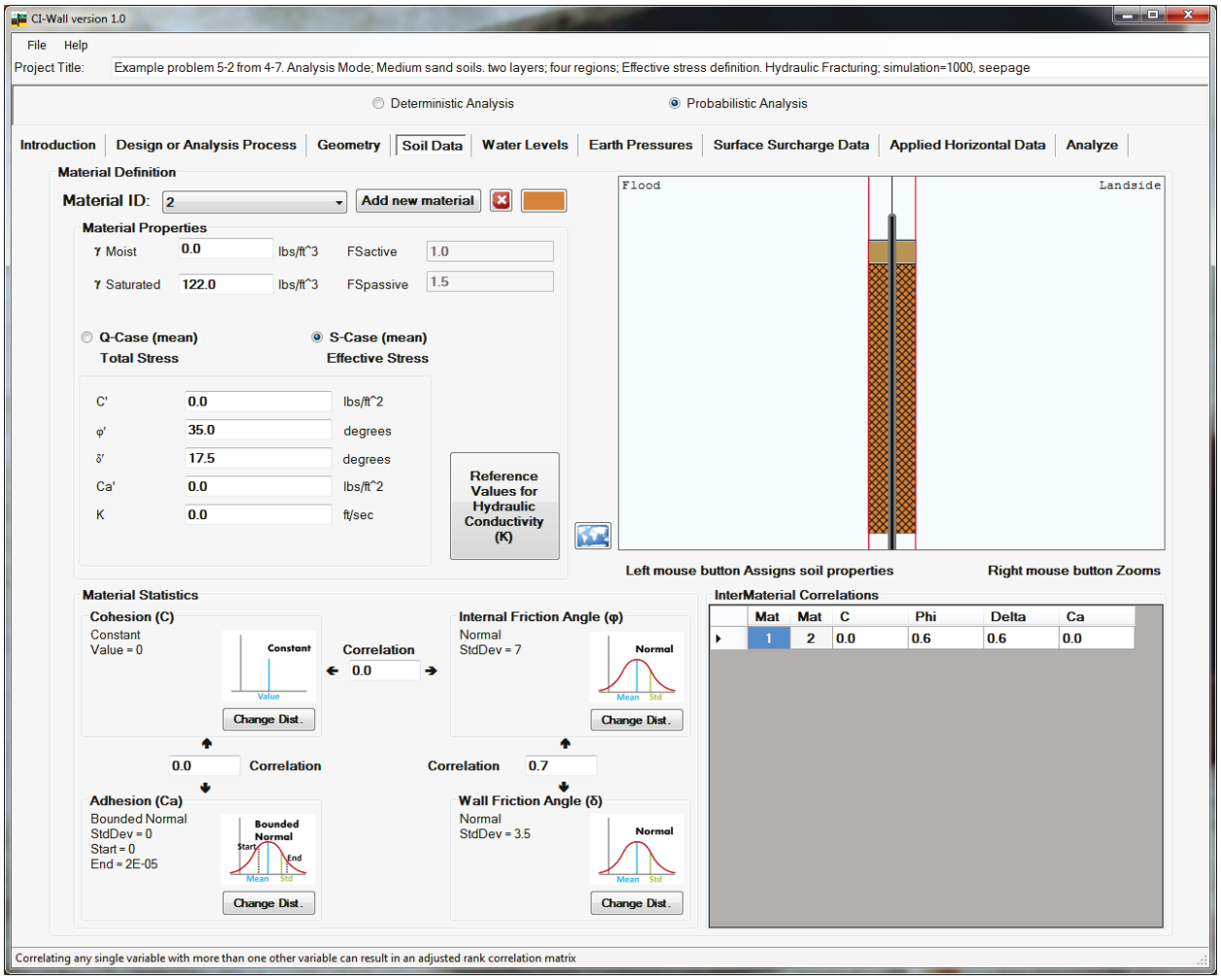
Figure 3.78. Seepage plot of seepage gradient due to soil region properties (untransformed).



Of interest are the correlations between variables. In this case, the internal friction angle and the soil-to-sheet-pile (wall) friction angles have a correlation coefficient of 0.7. This correlation is the same for both materials, although only one material is shown in Figure 3.79.

The intra-material correlations are also shown at the bottom right of Figure 3.79. The *Internal Friction Angle* between material 1 and material 2 has a correlation coefficient of 0.6, as does the soil-to-sheet-pile *Friction Angle* between material 1 and material 2.

Figure 3.79. Defining internal and external material correlations for probabilistic analysis for Example 5.2 input.

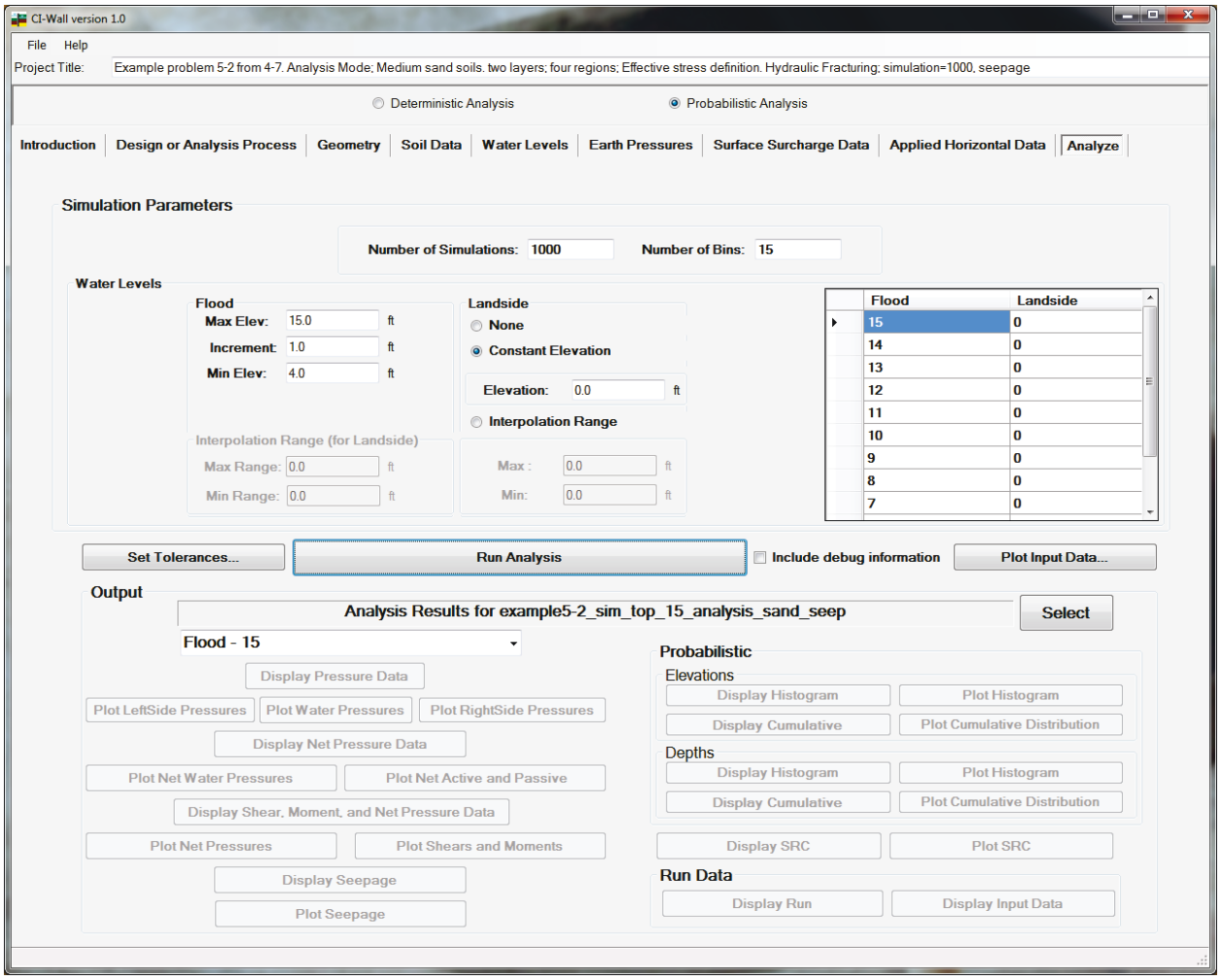


These inputs can lead to contradictory solutions when probabilistic inputs are created (because when a variable is correlated to more than one other variable, it may not be possible to maintain the correlation factors with both other variables). For this example, the material 1 *Internal Friction Angle* is correlated with the material 1 soil-to-sheet-pile (wall) *Friction Angle* using a correlation coefficient of 0.7. The material 1 *Internal Friction Angle* is also correlated with the material 2 *Internal Friction Angle* using a correlation coefficient of 0.6. These constraints may be contradictory, and lead to a reformulation of the correlation matrix to get the correlation factors as close as possible. The user is warned when this instance may occur.

Figure 3.80 shows the probabilistic input for variations of water levels for the *Analysis* option run. The varying water levels for Example 5.2 from Chapter 5, allow the analysis to determine a safe penetration depth for the I-Wall to withstand the changing I-Wall pressures due to changes of water

elevation. In this example, the water levels on the flood side range from an elevation of 15 ft to an elevation of 4 ft, while the water elevation on the landside is fixed at an elevation is 0 ft.

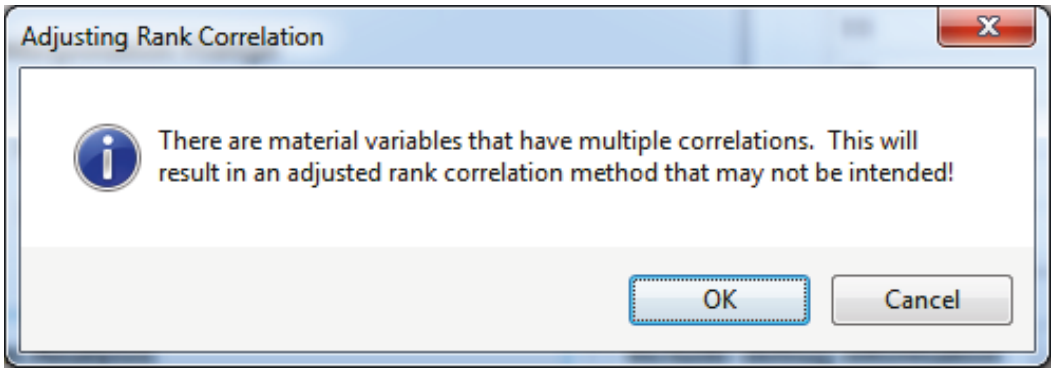
Figure 3.80. Probabilistic analysis options for the *Analysis* option run for Example 5.2 from Chapter 5.



The probabilistic analysis will consist of 1,000 simulations at each set of water elevations, and the output will be divided into fifteen bins. The greater the number of simulations, the more accurate the results will be, but the analysis will take longer to perform. Performance times are presented in Chapter 5 and range from minutes to hours. Chapter 5 also provides a strategy for performing simulations to reduce the amount of run-time involved. The greater the number of bins, the more precision can be gathered at each level of the output. If the number of bins is increased, the number of simulations should also be increased because each bin is susceptible to noise in the generated input.

If multiple correlations exist between variables (as is the case with the Example 5.2 problem of Chapter 5), clicking the *Run Analysis* button will cause the dialog box of Figure 3.81 to appear. This dialog is a warning that the correlations specified by the user may not be maintained as the program is run. If the user is content to let the software alter the correlation matrix between the variables, clicking the *OK* button will allow the probabilistic analysis to continue. By clicking the *Cancel* button, the user can go back to the input and vary the correlations to remove the likelihood of contradictions between correlations.

Figure 3.81. Warning that the correlation matrix between variables may change.



If the user continues to run the analysis after receiving the warning of Figure 3.81, then it is possible that the error dialog of Figure 3.82 will appear. When this error appears, then the Corps_I-Wall software was not able to adjust contradictory correlations in the correlation matrices to maintain a close set of correlations to what the user specified. In this case, the analysis is not performed, and the user will have to change one or more correlations in the soil material input window to reduce the contradictions between correlations.

The probabilistic analysis output is dependent on whether a *Design* or *Analysis* mode problem is run. Figure 3.83 show the probabilistic output area of the *Analyze* tab after a *Design* mode probabilistic run has been performed. For a *Design* mode probabilistic run, probabilistic data are returned for the range of tip depths that are required at each flood elevation. The flood elevations are selected using the *Flood selector* box directly to the left of the word *Probabilistic* on the frame in Figure 3.83.

Figure 3.82. Error dialog that occurs when the software altered correlations cannot match the user input correlations.

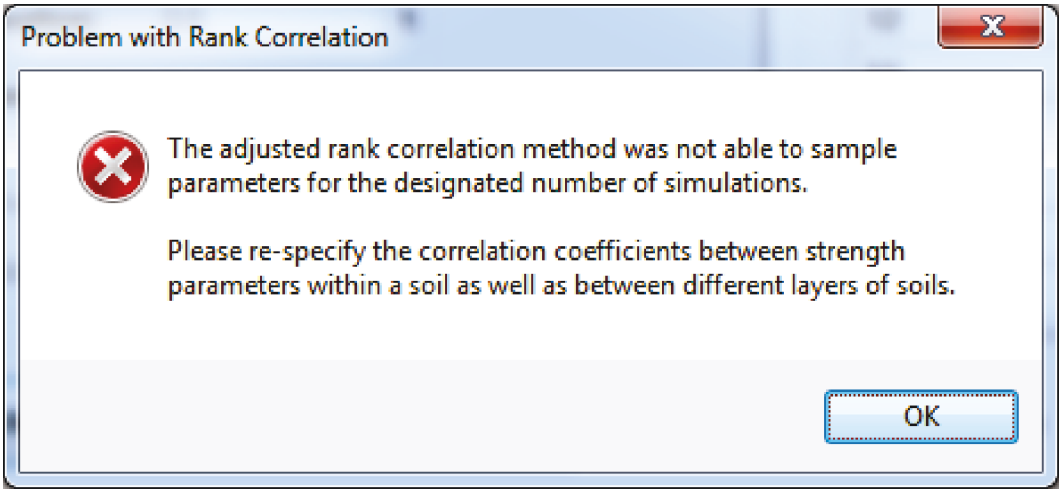
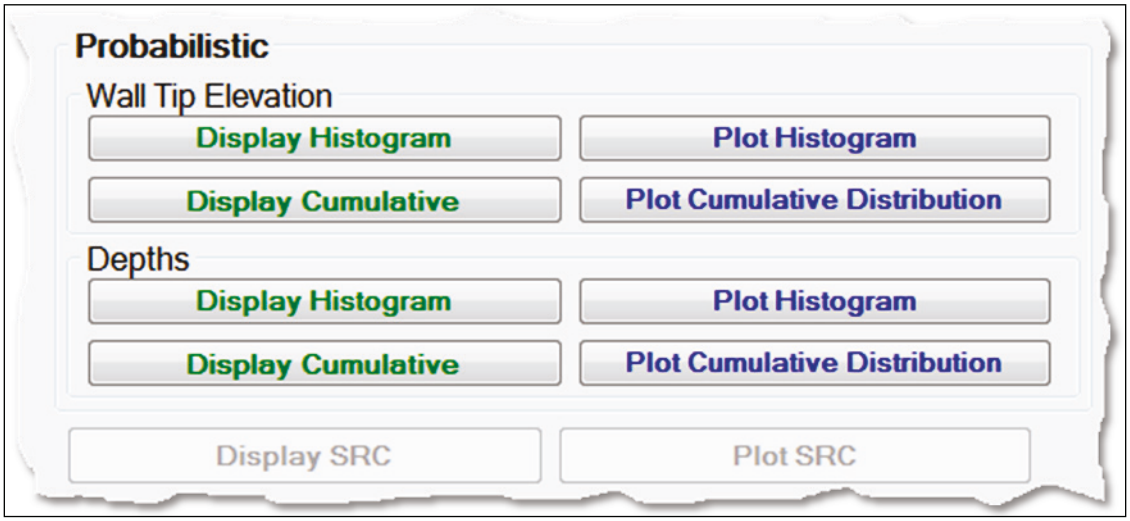


Figure 3.83. Active probabilistic output options in the *Analyze* tab after execution of a *Design* mode.



The output probabilistic data after the *Design* mode are reported using two datums, elevations of the I-Wall tip (based on user input), and depths below the lower ground surface of the I-Wall tip (on either the LHS or RHS of the I-Wall). Elevation data use the coordinate system established by the user, this may be based on a datum, such as mean sea level. These data are reported (histograms and cumulative distribution passive Factor of Safety data) for the number of bins specified over the range of simulations for the selected flood elevation.

The *Display* buttons for each of these options opens a dialog that displays the contents of the file containing the data to be viewed. This dialog has menu options that allow the user to save a copy of the file to a different

location, to print the file, and to exit the dialog. The *Plot* buttons behave in a different fashion, depending on whether a histogram is plotted, or cumulative distributions are plotted as discussed below.

Figures 3.84 and 3.85 provide the histogram data and a plot of the histogram data for I-Wall tip elevations, respectively. The histogram data have the following three columns: bin number, midpoint elevation of that bin, and probability that that I-Wall tip elevation will occur. Because the full range of possible I-Wall tip elevations is divided into the number of calculated sheet-pile design depths contained within each of the bins, the summation of these probabilities will always be unity (1.0).

The histogram data are presented with the flood level elevation, the number of simulations, the minimum, maximum, and mean elevations generated by the *Design* mode analysis, and the standard deviation and coefficient of variation of elevations.

Figure 3.84. Displayed sheet-pile tip elevation histogram data after execution of a *Design* mode.

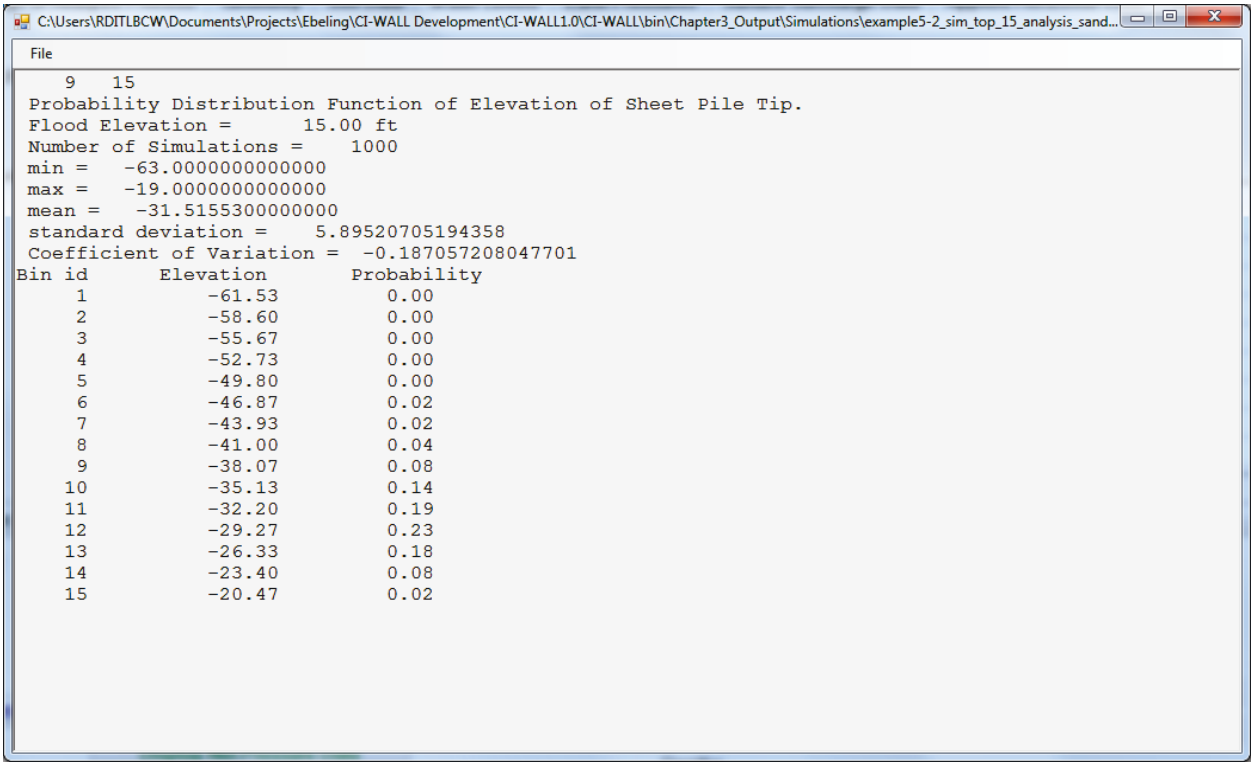
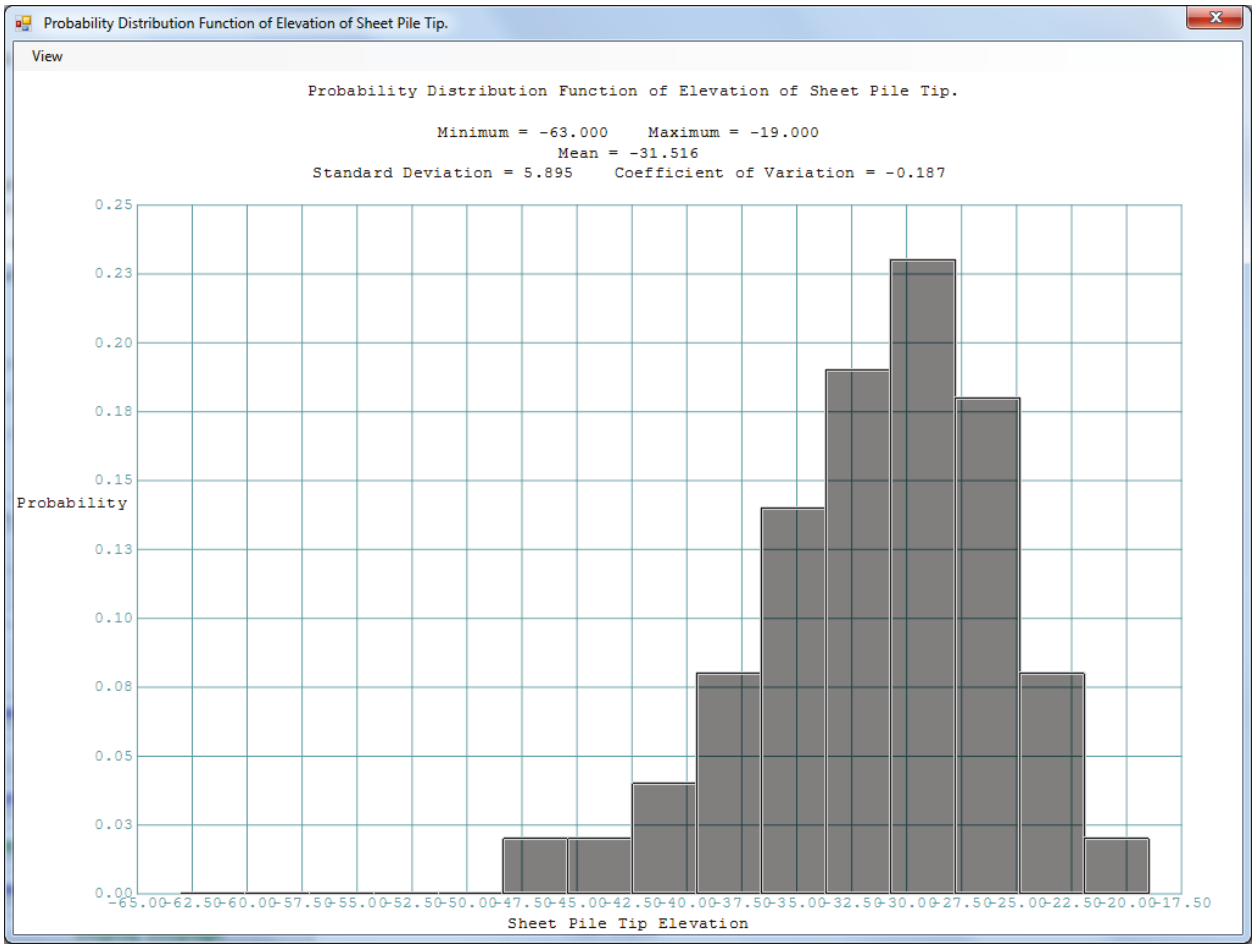


Figure 3.85. Plotted sheet-pile tip elevation histogram data after execution of a *Design* mode.

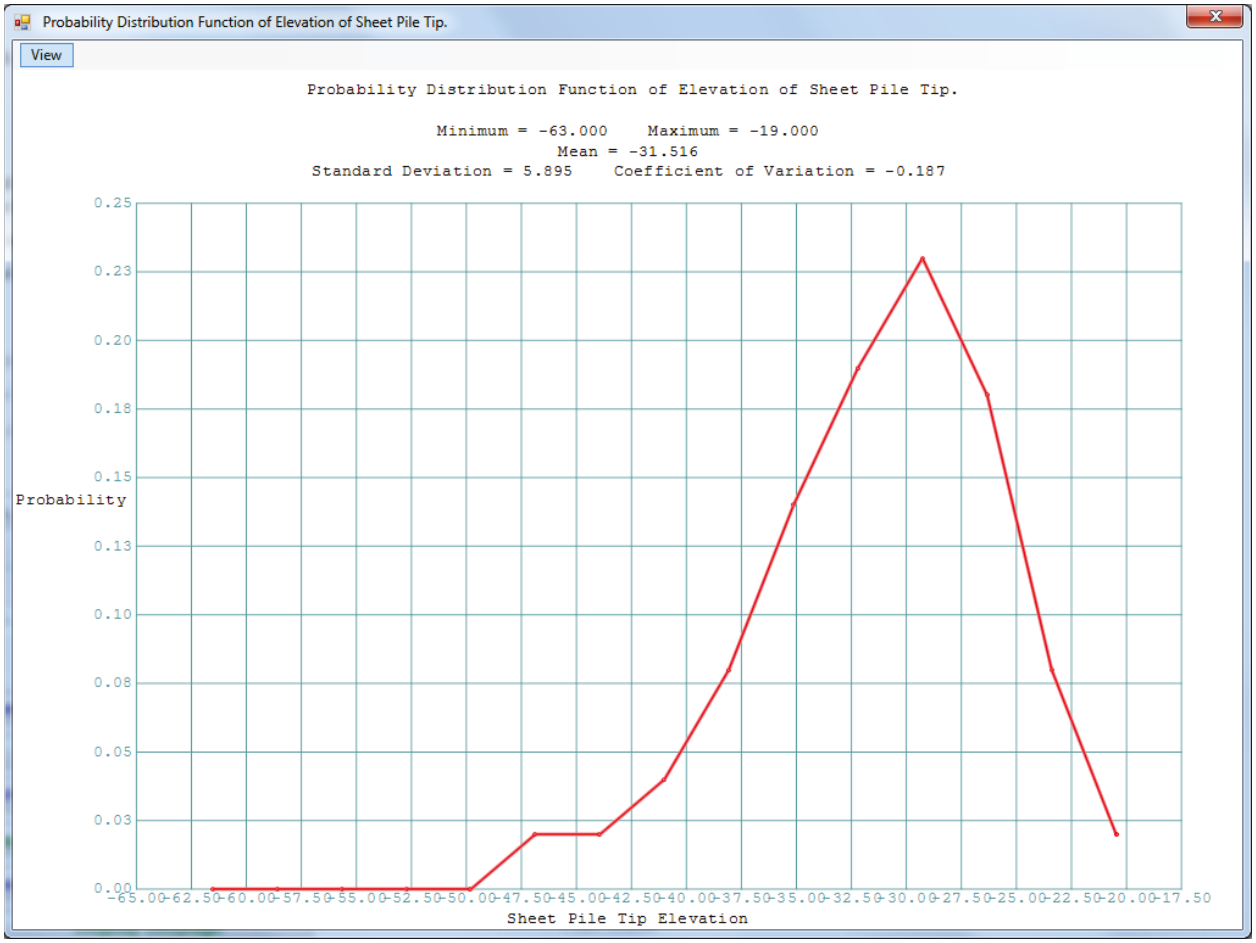


The bin with the greatest probability is bin number twelve, this is centered about the I-Wall tip elevation of -29.27 ft. The computed mean gives an elevation of -31.51 ft, and the standard deviation is 5.9 ft.

Histogram data can either be shown as filled bins centered about a data point (elevation, in this case), or as a linear interpolation of the data through the midpoints of the bins. The *Histogram* plot dialog provides the user the means to choose either or both. Figure 3.85 shows the data as filled bins, Figure 3.86 reveals the data as a linear interpolation, and Figure 3.87 shows the data with both options. These options, and the option to exit the dialog, are available through the menu.

Figures 3.88 and 3.89 provide the cumulative distribution of elevation of sheet-pile tip data and a plot of the cumulative distribution data, respectively. In these figures, 1,000 simulation results for calculated tip elevation are gathered in fifteen bins for a flood elevation of 15 ft, which is 15 ft above the ground surface for this example.

Figure 3.86. Plotting the sheet-pile tip elevation histogram data as a set of linear segments passing through the center of each bin after execution of a *Design* mode.



The computed mean and standard deviation stay the same, as these data are a cumulative summation of the histogram probabilities.

Because the cumulative distribution data are based on a summation of the bin probabilities, the data are best plotted as a linear interpolation of the data. Therefore, the dialog box has no options for other methods of plotting the data and must be closed by using the Windows *close dialog* button at the upper right of the dialog.

Figure 3.87. The combined plot of bins and linear interpolation of sheet-pile tip elevation histogram data after execution of a *Design* mode.

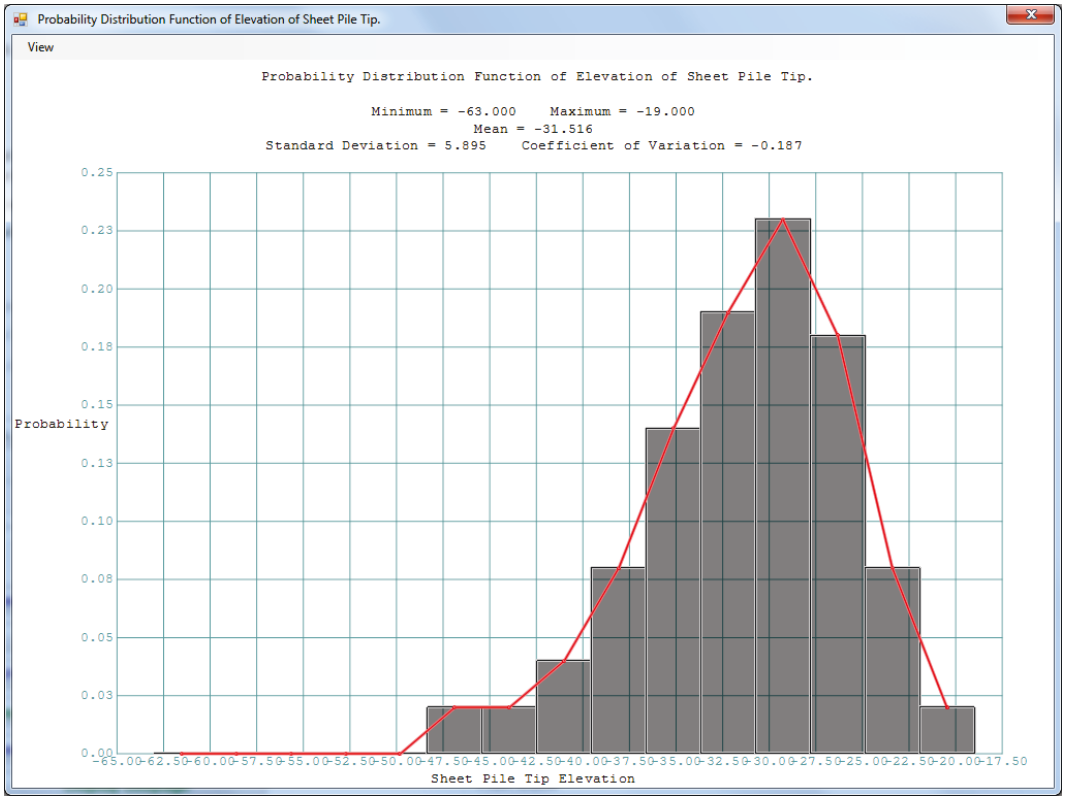


Figure 3.88. Displayed cumulative sheet-pile tip elevation distribution data after execution of a *Design* mode.

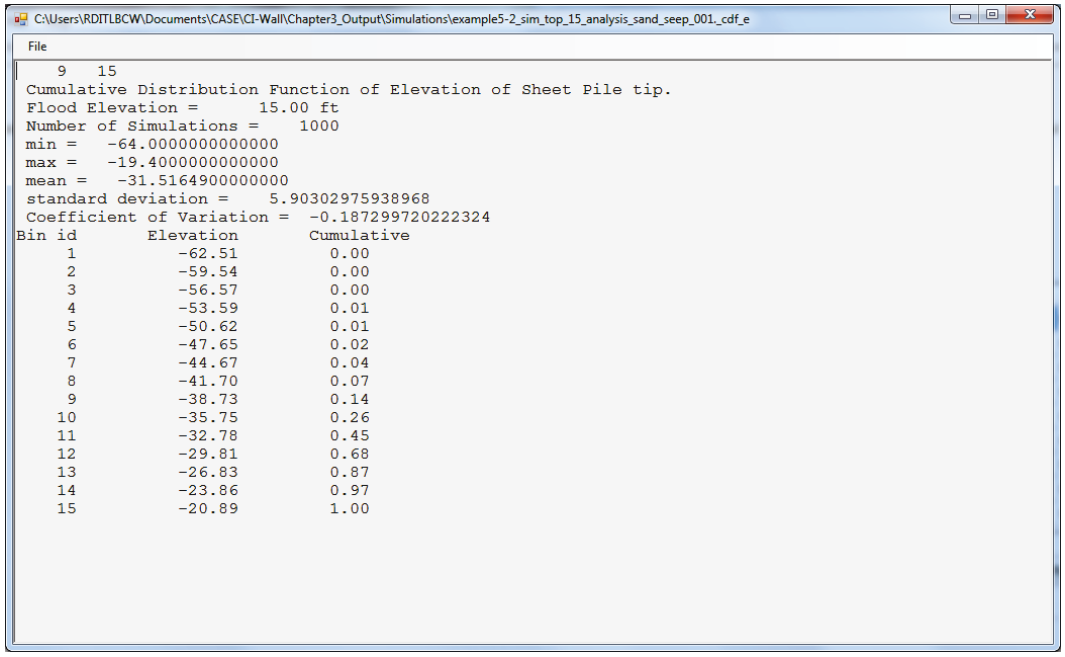
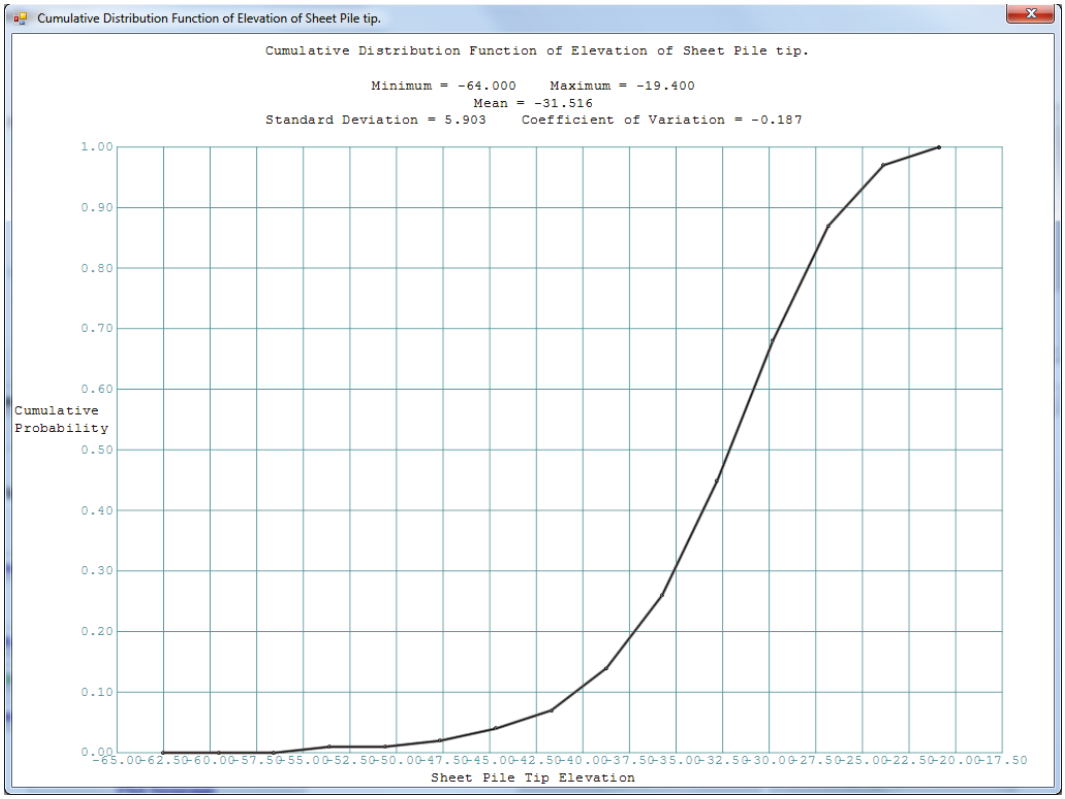


Figure 3.89. Plotted cumulative sheet-pile tip elevation distribution data after execution of a *Design* mode.



Figures 3.90 and 3.91 provide the histogram data and a plot of the histogram data for I-Wall tip depths, respectively. The histogram data have the following three columns: bin number, midpoint depth of that bin, and probability that the I-Wall tip depth will occur. Because the full summation of possible I-Wall tip depths is divided into the number of calculated sheet-pile design depths contained within each of the bins, the summation of these probabilities will always be unity (1.0). Note that these data are essentially the same as the elevation data, but the elevation information has been transformed to depth, resulting in a different base and an inverse scale factor. Therefore, the values in the bins are in the reverse order.

The histogram data are presented with the flood level elevation, the number of simulations that do not exceed the rotational limit state of the I-Wall, the minimum, maximum, and mean passive Factor of Safety, and the standard deviation and coefficient of variation of the passive Factor of Safety.

Figure 3.90. Displayed sheet-pile tip depth histogram data after execution of a *Design* mode.

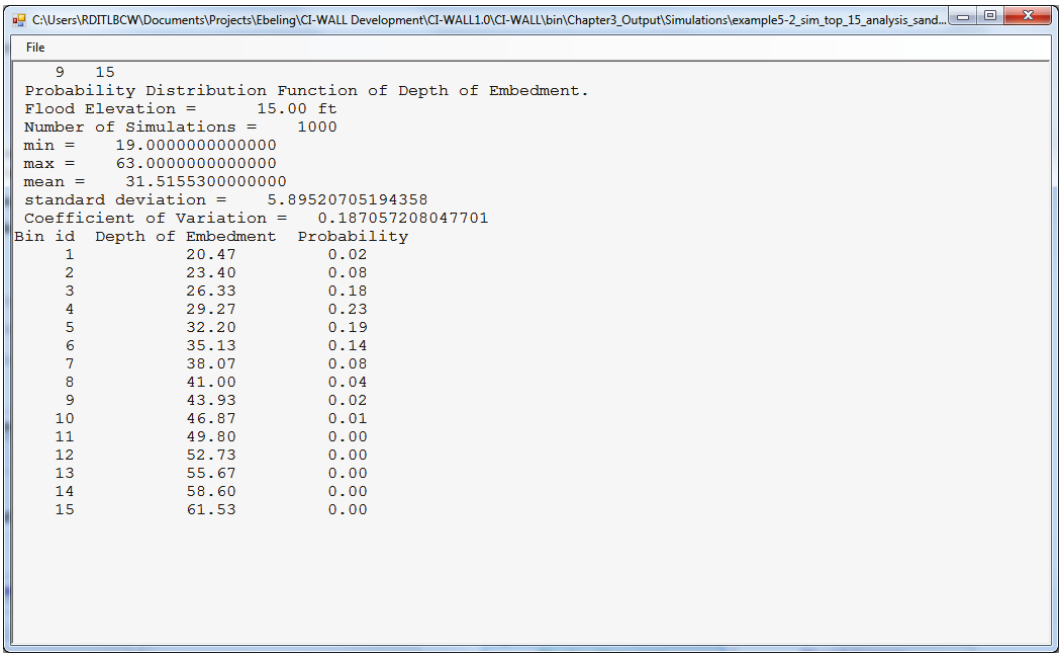
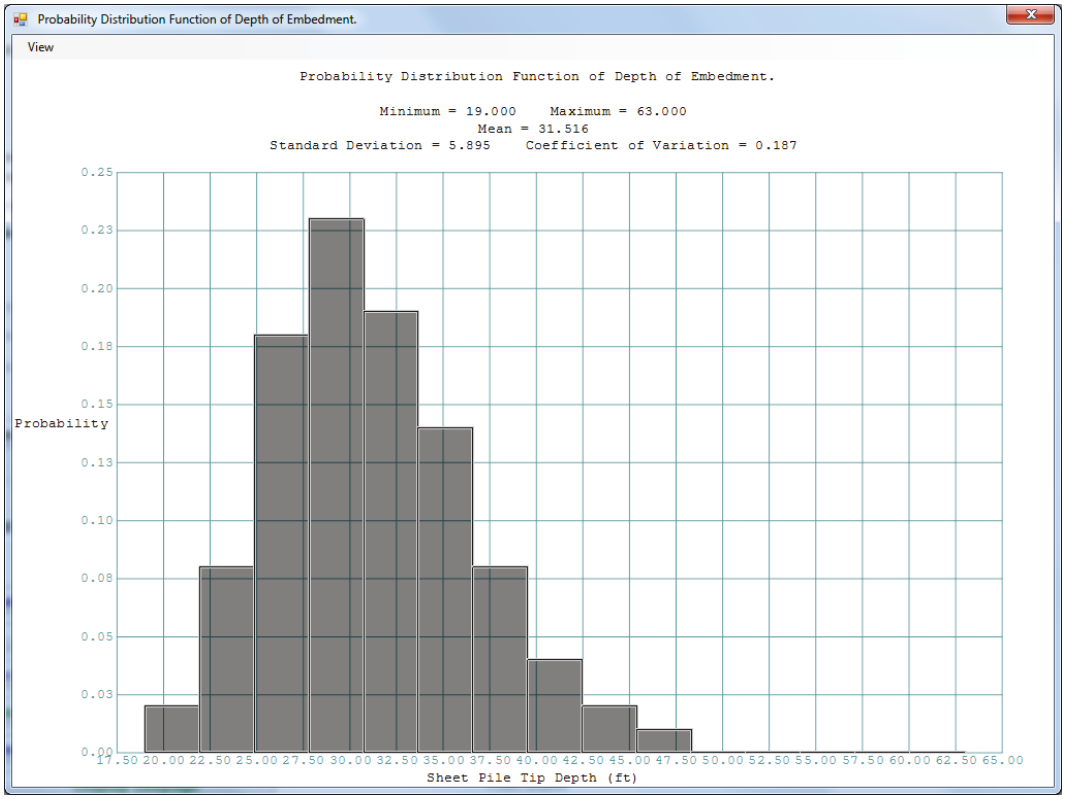


Figure 3.91. Plotted sheet-pile tip depth histogram data after execution of a *Design* mode.



The histogram data are presented with the flood level elevation, the number of simulations that do not exceed the rotational limit state of the I-Wall, the minimum, maximum, and mean passive Factor of Safety, and the standard deviation and coefficient of variation of the passive Factor of Safety.

Figures 3.92 and 3.93 provide the cumulative distribution data and a plot of the cumulative distribution data for the depth based coordinates, respectively. In these figures, results from 994 simulations are gathered in fifteen bins for a flood elevation of 15 ft, this is 15 ft above the ground surface in this example.

The computed mean and standard deviation stay the same, as these data are just a cumulative summation of the histogram probabilities.

For an *Analysis* mode solution, the probabilistic output area of the *Analyze* tab looks like Figure 3.94. The Passive Factor of Safety section has the output that is specific to the *Flood Level* selector on the left side of the *Analyze* tab (immediately left of the word *Probabilistic*). Once an elevation is chosen, the user can select one of the *Passive Factor of Safety* options for information about the passive Factor of Safety for that flood elevation.

Figure 3.92. Displayed cumulative sheet-pile tip depth data after execution of a *Design* mode.

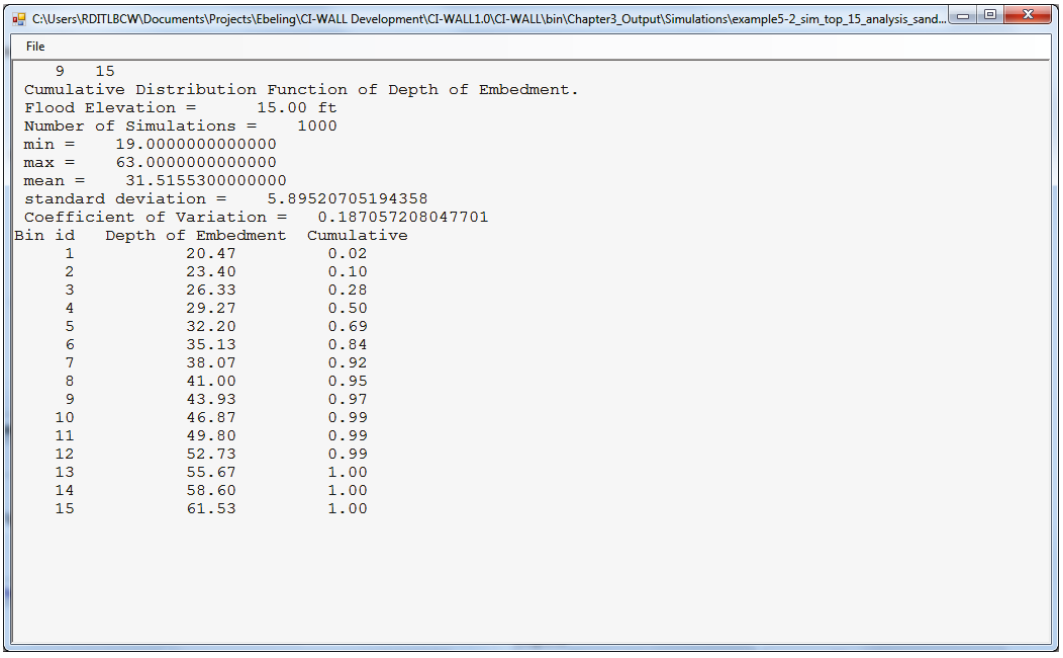


Figure 3.93. Plotted cumulative sheet-pile tip depth data after execution of a *Design* mode.

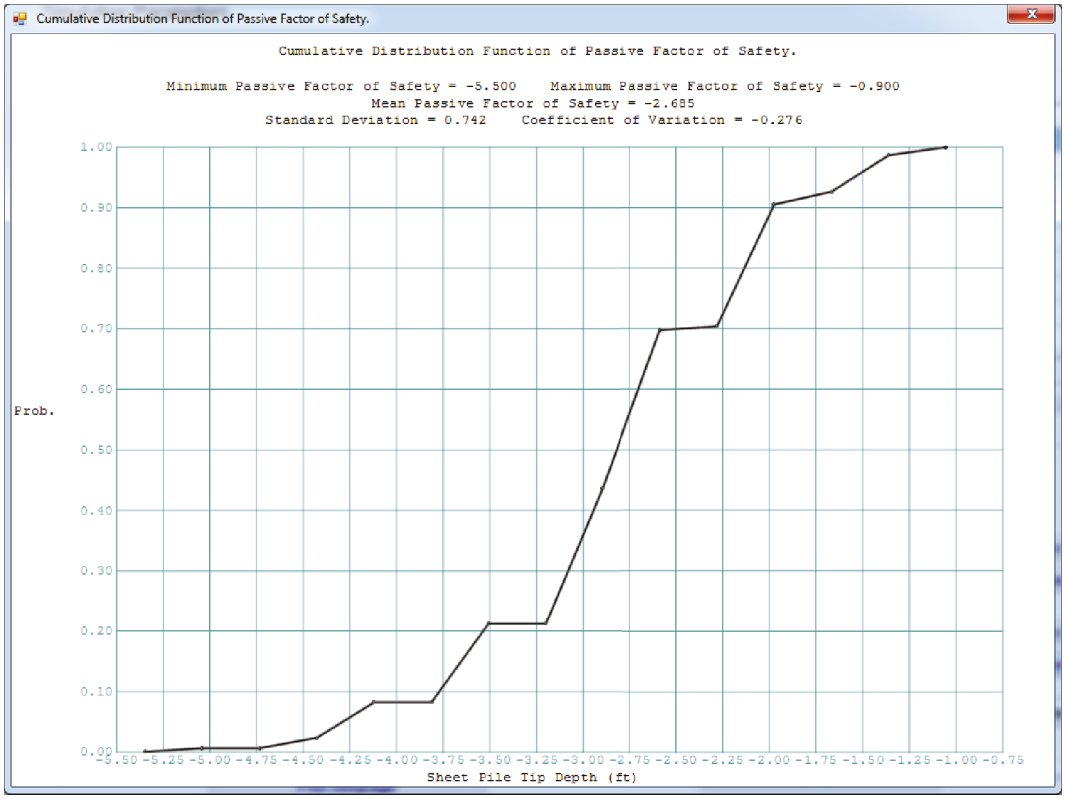
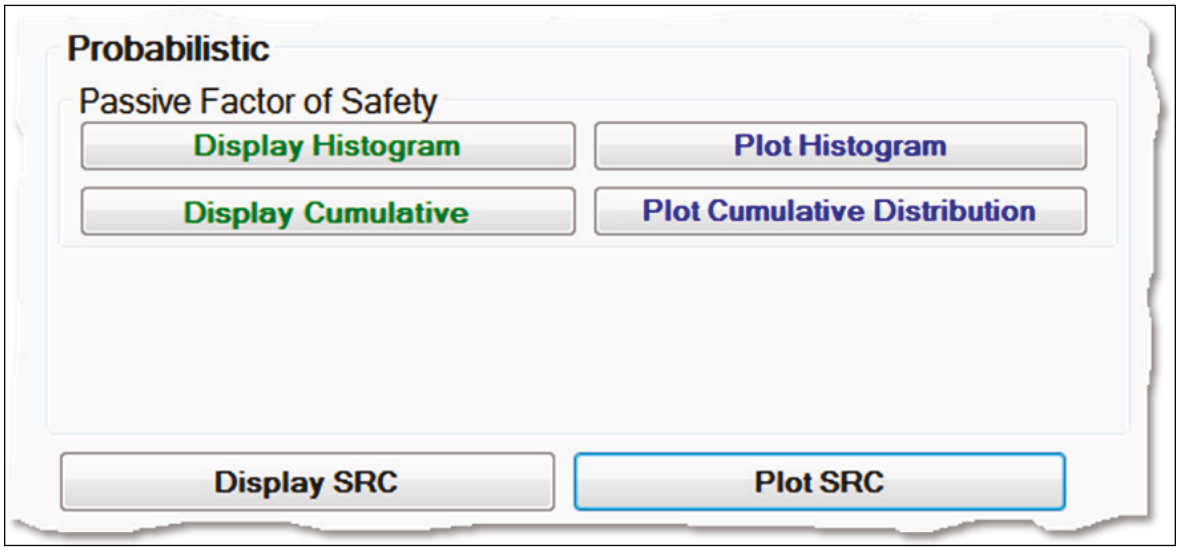


Figure 3.94. The selection of probabilistic output for an *Analysis* mode problem.



Figures 3.95 and 3.96 are a display and plot of the histogram data showing the discrete probabilities (divided into bins) covering a range of passive factors of safety for the *Analysis* mode example problem with a flood elevation of 4 ft. This is the typical means for viewing histogram data for all of the elevations where data were returned. If an elevation has no successful runs, then the buttons for viewing that data are grayed out. The passive Factor of Safety with the greatest probability of occurrence is 2.52 (bin six) with a probability of 0.25. The mean passive Factor of Safety is at 2.69 and the standard deviation is 0.76.

Figures 3.97 and 3.98 show a display and plot of the cumulative distribution data of the discrete probabilities (divided into bins) covering a range of passive factors of safety for the elevation at 4 ft. This is the typical means for viewing histogram data for all of the elevations where data were returned. If an elevation has no successful runs, then the buttons for viewing that data are grayed out. Again, the mean passive Factor of Safety is at 2.69 and the standard deviation is 0.76.

Figure 3.95. Histogram data of passive Factor of Safety probabilities for flood elevation 4 ft after execution of an *Analysis* mode.

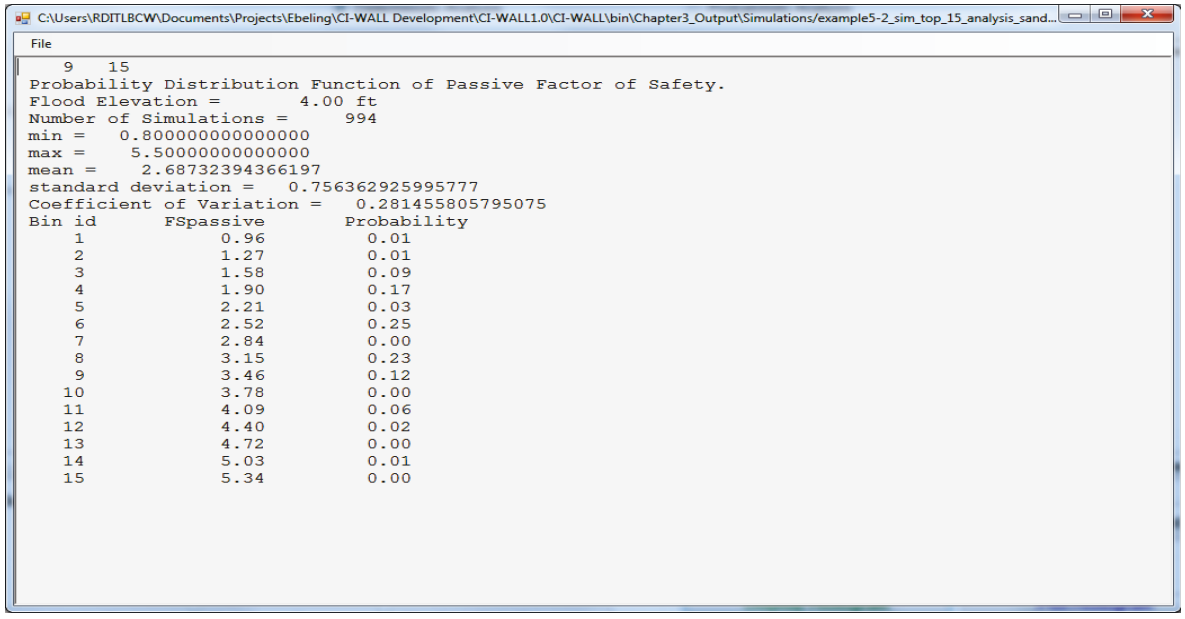


Figure 3.96. Histogram plot of passive Factor of Safety probabilities for flood elevation 4 ft after execution of an *Analysis* mode.

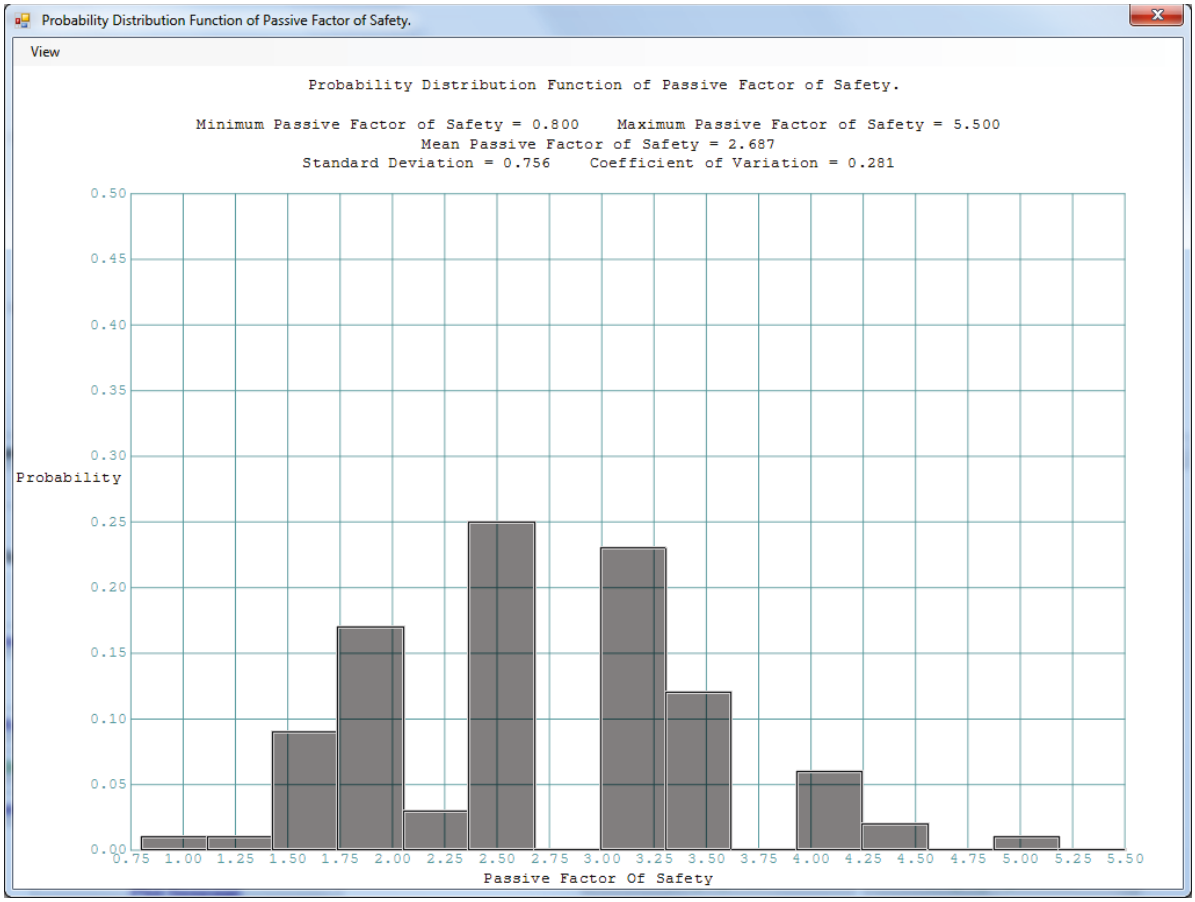


Figure 3.97. Cumulative distribution data of probabilities given a passive Factor of Safety for flood elevation 4 ft after execution of an *Analysis* mode.

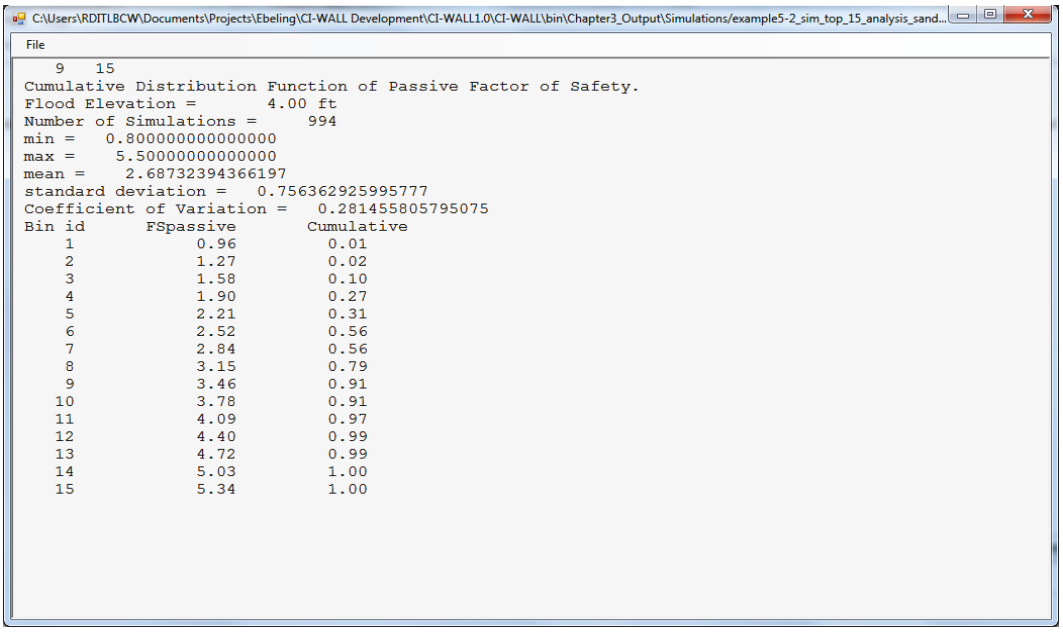
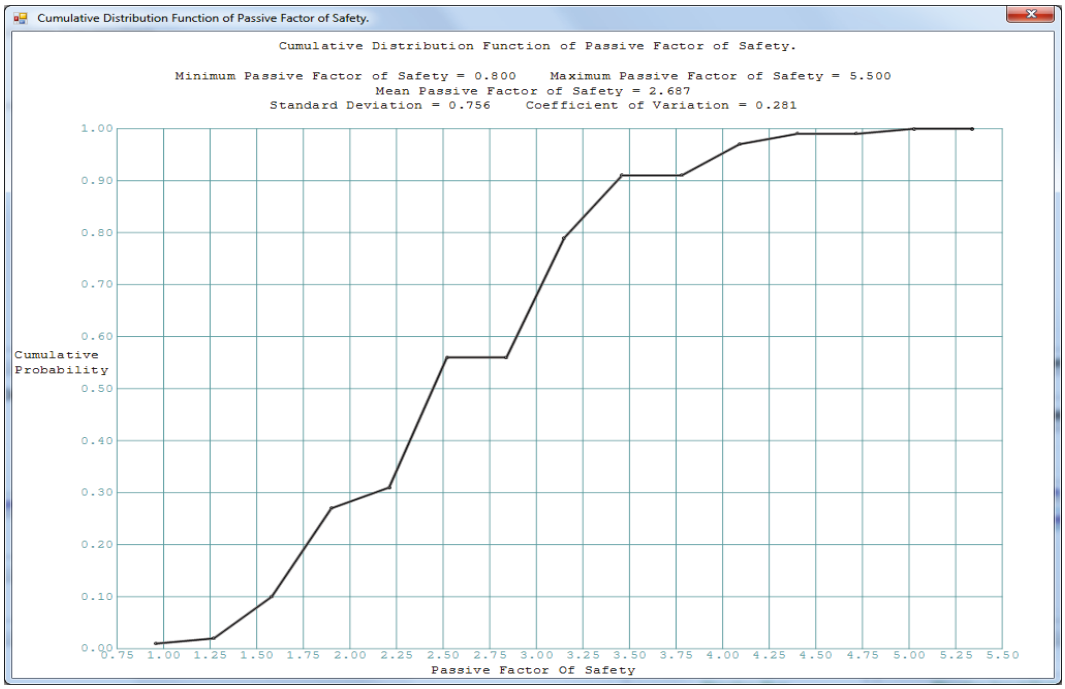


Figure 3.98. Cumulative distribution plot of probabilities given a passive Factor of Safety for flood elevation 4 ft after execution of an *Analysis* mode.



The SRC data and plot shows the probability of exceeding the rotational limit state for an I-Wall, over a series of flood elevations (entered by the user). A SRC is only created in a probabilistic *Analysis* mode, where the sheet-pile tip depth of the I-Wall is known. For the example problem, twelve flood elevations were entered, ranging from 15 to 4 ft. Figure 3.99 shows the computed SRC values, with the first column being the case number, the second column being the flood elevation, and the last column being the probability that the limits state will be exceeded. These data can be saved, printed, or the dialog exited from the menu. Figure 3.100 is a plot of the system response curve, showing the trend as the flood elevation increases. The *Plot* window for the SRC curve is similar to the *Plot* window for the cumulative distribution data, in that the user can close the dialog only with the controls at the upper right of the window.

Figure 3.99 Displayed SRC for 1,000 simulations per flood elevation with fifteen bins.

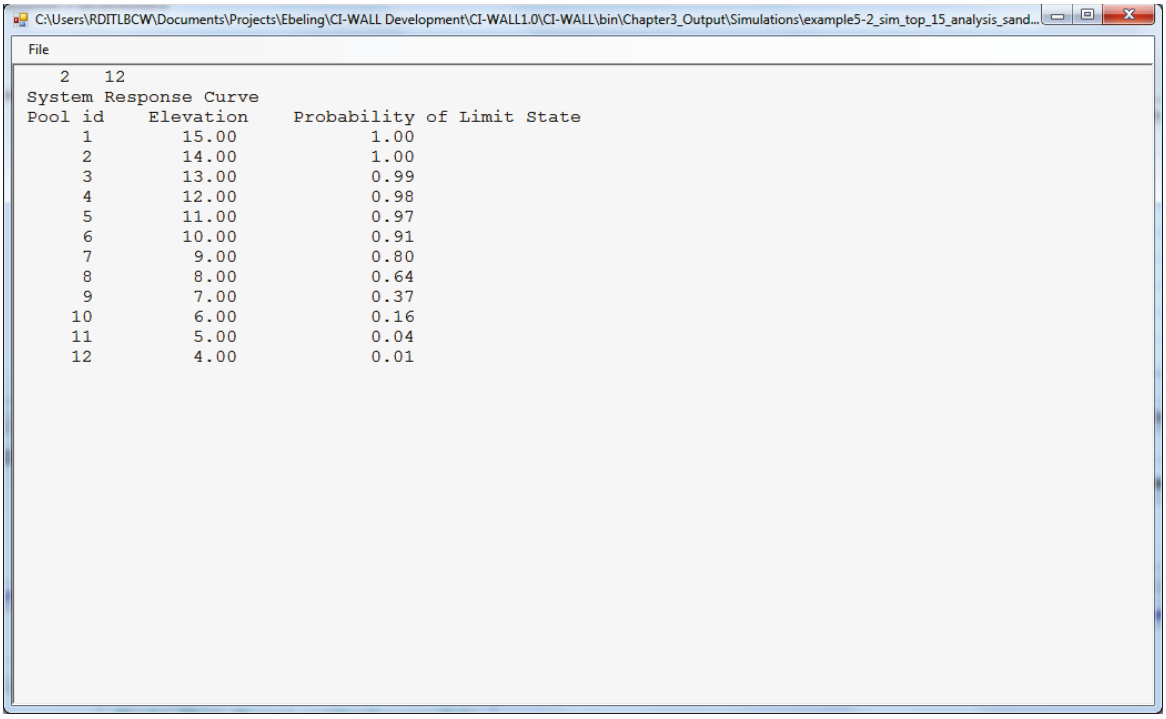
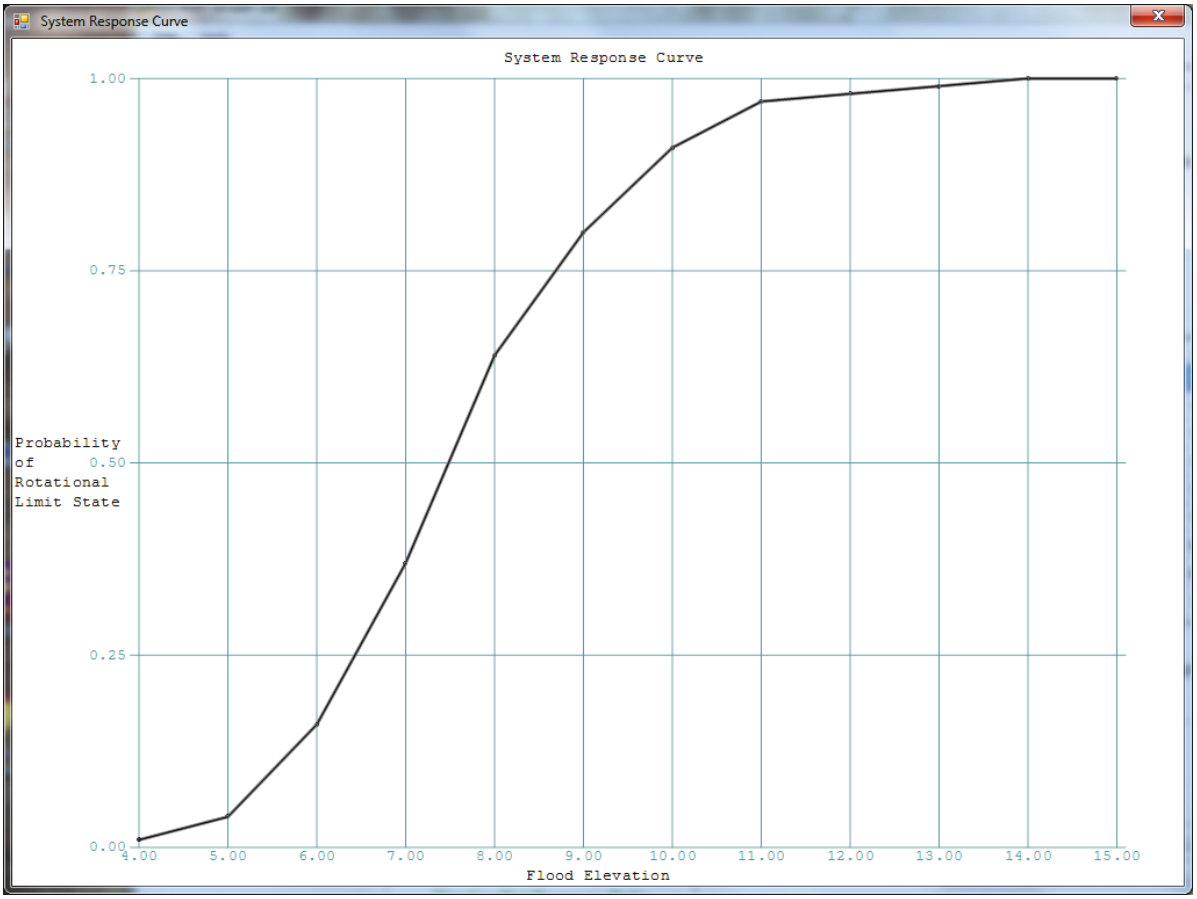


Figure 3.100. Plotted SRC for 1,000 simulations per flood elevation with fifteen bins.



4 Deterministic Example Problems

4.1 Example 4.1 sand site, effective stress strength definition with φ′ = 30, c′=0, with either hydrostatic pore water pressures or homogeneous seepage

An effective stress definition with φ′ = 30 deg and c′ = 0 is illustrated by a series of five design problems that determine the depth of embedment (d) of the sheet-pile wall embedded into a sand site. These example problems apply a Factor of Safety of 1.0 for computing active earth pressures, and a Factor of Safety of 1.5 for computing passive earth pressures beneath the soil layers. In this example, the I-Wall has an exposed height of 10 ft. The water surfaces at both sides of the I-Wall are at elevation (el), el 40 ft on the flood side and el 34 ft on the landside. The homogeneous sand layer of soil has a level ground surface on both sides of the I-Wall at 30 ft, with saturated unit weight of 122.4 pcf and an effective angle of internal friction (φ′) of 30 degrees. Figure 4.1 outlines the basic geometry and structural parameters for the sheet-pile wall, and Figure 4.2 illustrates the schematic produced by Corps_I-Wall for the same problem. The top row of text listed in Figure 4.2 documents the input values of all parameters associated with each material type. For this problem, there is only one material assigned for the sand site and recorded as "M01," the "M" signifies the material type and is followed by the ID, which starts at "01." All information concerning material types are written in black text. The representation of a layer of soil on each side of the I-Wall is characterized as a region. Regions are labeled with an "R" and followed by an ID starting from "01." For this problem two soil regions are required to represent each soil layer; Region 1 (as R01), is located on the LHS of the sheet-pile wall and Region 2 (as R02) is located on the RHS of the sheet-pile wall. Each region and its surface elevation are written in red text. Piezometric surfaces are labeled as "P" and followed by an ID starting from 01. Piezometric water surfaces are listed in the upper left-hand corner and drawn with the water symbol at its defined elevation and shown in blue. Observe that piezometric surface ID, P01, is assigned to both regions. The LHS piezometric surface elevation is assigned as the LHS surface water elevation. Similarly, the RHS piezometric surface elevation is assigned as the RHS surface water elevation. This allows for the assignment of submerged unit weights to the soil regions. This geometry will be used for the following example problems and are described in the following subsections.

Figure 4.1. Sheet-pile wall in sand site.

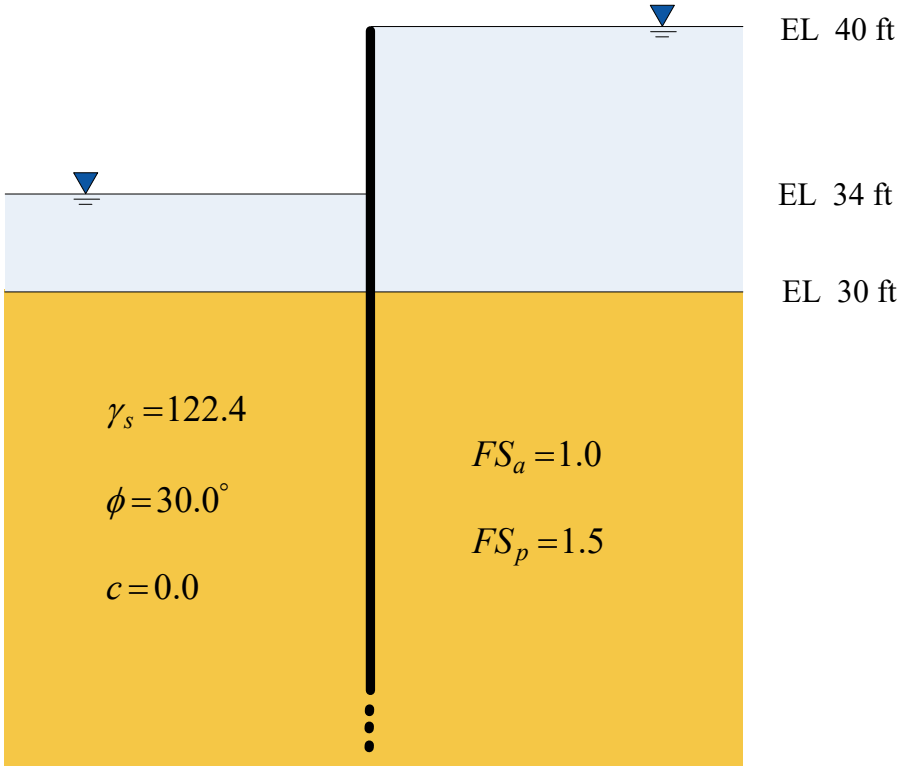
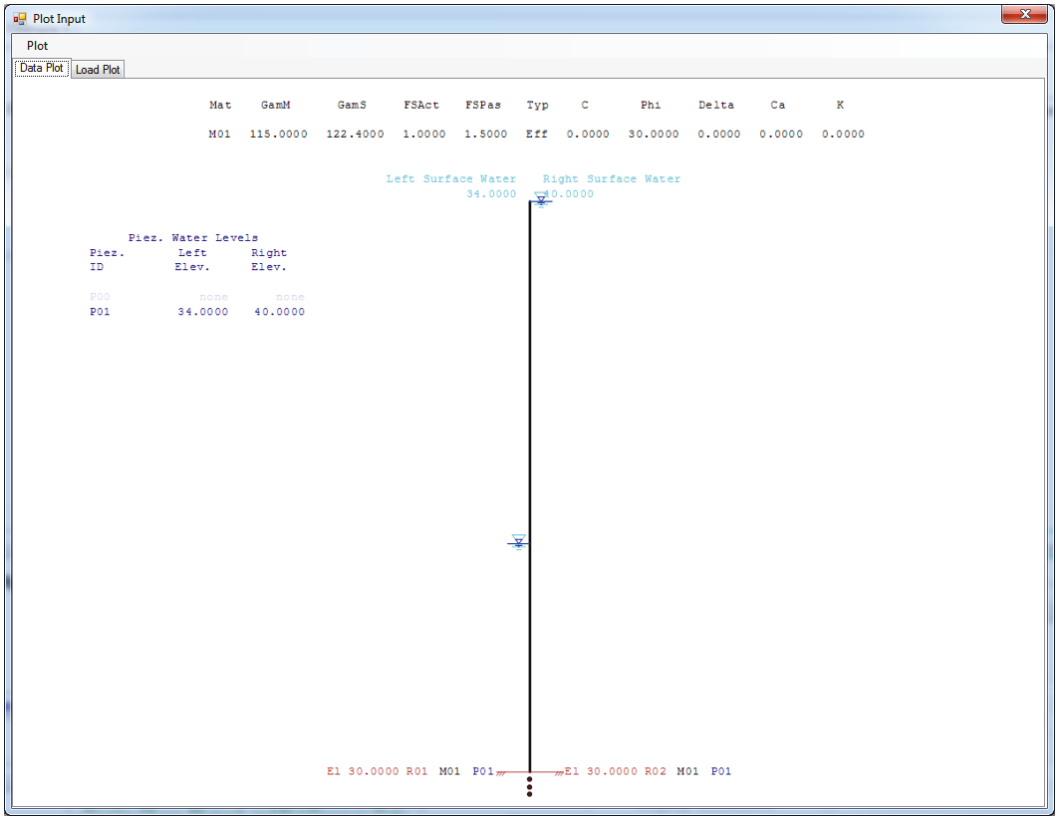


Figure 4.2. Corps_I-Wall schematic of sheet-pile wall in sand site.



4.1.1 Example 4.1.1

An effective stress definition with φ′=30 degrees and c'=0 as illustrated in Figure 4.2 is considered for the evaluation of the depth of embedment. Homogeneous soil, hydrostatic pore water pressures, effective angle of wall friction (δ′) of 0 degrees, and the Coulomb earth pressure Coefficient Method of analysis (for K_a and K_p) form the basis for this example[1]. Hydraulic fracturing is not included as an option for this analysis since c'=0.

This analysis resulted in a computed active earth pressure coefficient (K_a) of 0.3333 and a "mobilized" passive pressure coefficient (K_p) of 2.1212.[2] The distribution of active and passive earth pressures with elevation for both sides of the sheet-pile wall are illustrated in Figures 4.3a and 4.3b.[3] The hydrostatic water pressures acting on both sides of the sheet-pile wall are shown in Figure 4.4a[4] with the resultant net water pressure calculated by taking the difference between the water pressures acting on both sides of the wall (Figure 4.4a) (as shown in Figure 4.4b).[5] Observe the differential water pressure at the tip of the sheet pile (= 6 ft times 62.4 pcf), a common outcome when the piezometric surface elevations (defined as equal to the surface water elevations in this problem) for the two sides of the I-Wall differ (e.g., 34 ft on the LHS and 40 ft on the RHS), and hydrostatic water pressures are specified by the user.

From these pressures (Figures 4.3 and 4.4), the net active and net passive pressures are constructed and presented in Figure 4.5a.[6] For the applied flood loading, the I-Wall will rotate counterclockwise. The net active pressure is determined from the difference between the RHS-mobilized active earth pressure and the LHS-mobilized passive earth pressure (i.e., acting on the other side of the wall) with the addition of any net water pressures and any external horizontal net pressures and overburden pressures (if any). The net passive pressure is determined by the difference between the RHS- mobilized passive earth pressure and the LHS-mobilized active earth pressure acting on the other side of the sheet-pile

[1] For no soil-to-I-Wall interface friction (i.e., δ = 0 deg), the Coulomb solution for active and passive earth pressure coefficients corresponds to the Rankine earth pressure coefficients.

[2] A $FS_{passive}$ value equal to 1.5 is used in this example, consistent with EM 1110-2-2504 (HQUSACE 1994).

[3] The earth pressures in all four Figure 4.3 diagrams act toward the wall.

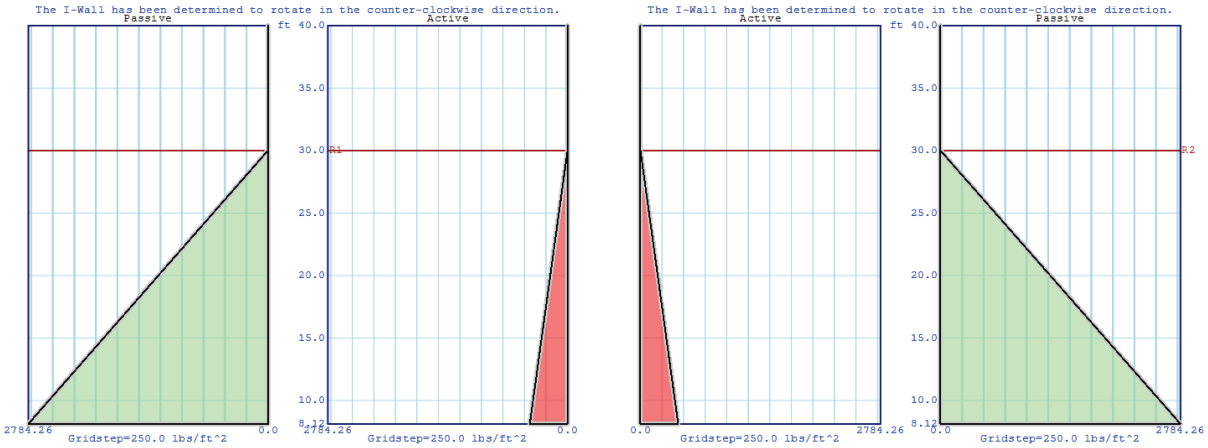
[4] The water pressures in the two Figure 4.4a diagrams act toward the wall.

[5] The net water pressure in the Figure 4.4b diagram acts toward the wall.

[6] The net earth pressures in the two Figure 4.5a diagrams act towards the wall.

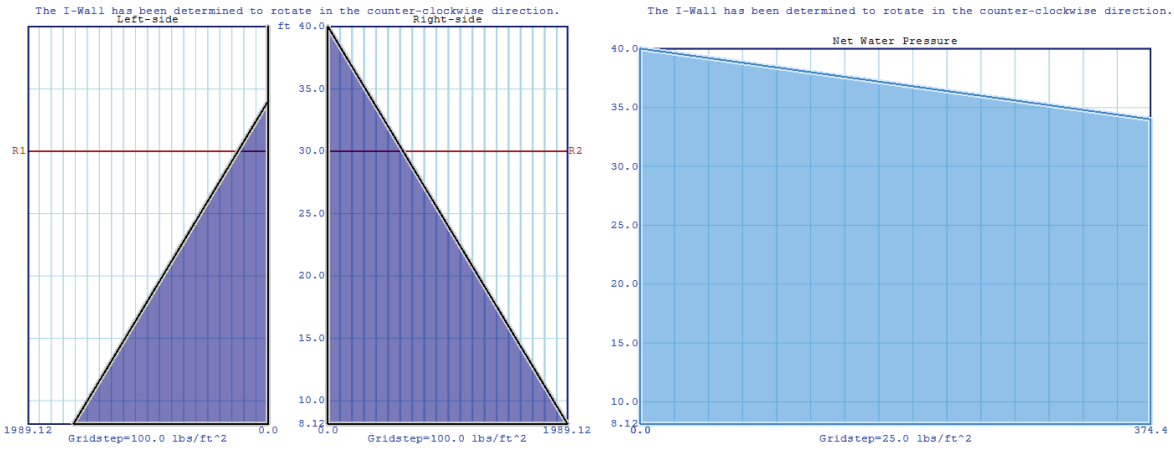
wall with the addition of any net water pressures and any external horizontal net pressures and overburden pressures (if any). The net pressure diagram of Figure 4.5b is derived from the replication of all values of the net active pressures, from the top of the wall until the elevation at the PR (el 14.48 ft), at which instant the remaining values of the net pressure diagram is assumed to be linear with elevation between (1) the net active pressure value at the elevation of the PR, and (2) the net mobilized passive pressure at the elevation of the approximated sheet-pile tip (i.e., el 8.12).[1]

Figure 4.3. Active and passive earth pressures. (a) LHS of wall. (b) RHS of wall.



(a) (b)

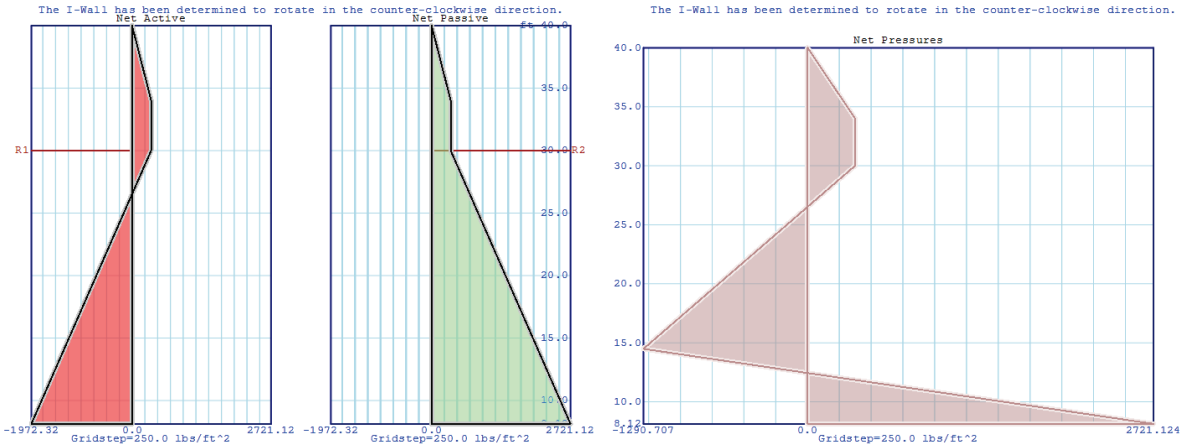
Figure 4.4. (a) Pore water pressures for the LHS and RHS of the wall. (b) Net water pressures.



(a) (b)

[1] Thus, only one mobilized net passive pressure value in Figure 4.5a is used to construct the Figure 4.5b net pressure diagram; corresponding to the sheet-pile tip elevation at el 8.12. The majority of the net pressure diagram is derived from the Figure 4.5a net active pressure diagram.

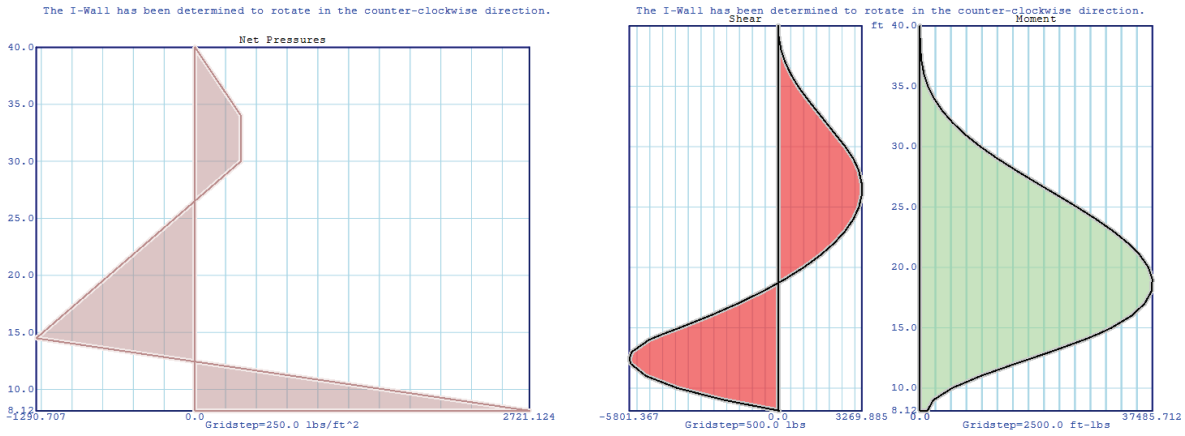
Figure 4.5. Net pressures. (a) Net active and net passive. (b) Net pressure diagram.



(a) (b)

Figure 4.5b is an illustration of how the net pressure diagram was formed.[1] The final results are illustrated in Figure 4.6 by the presentation of the net pressure diagram, Figure 4.6a (replica of Figure 4.5b), and 4.6b, the shear and moment diagrams. Figure 4.6b shows that the maximum bending moment occurs at the zero crossing of the shear diagram.

Figure 4.6. (a) Net pressure diagram. (b) Shear and moment.



(a) (b)

The various input conditions and final results for Example 4.1.1 are tabulated as check problem 1 in Table 4.1. The sheet-pile tip elevation is computed at el 8.12 ft with a calculated depth of embedment of 21.88 ft.

[1] The net pressures in the Figure 4.5b diagram act towards the wall.

Table 4.1. Examples of effective stress strength definitions (sands with c′=0).

Check Problems	Coulomb (C) or Logarithmic spiral (L)	Hydraulic Fracture Option	Seepage Gradient	δ' (deg)	K_a mob	K_p mob	$\frac{2c'}{\sqrt{K_a}\gamma_{buoy}}$	Hydraulic Fracture Depth	Elevation at Point of Rotation	Elevation at Tip of Pile
1	C	Off	HY	0	0.3333	2.1212	0.0000	NG	14.48	8.12
2	C	Off	HY	15	0.3014	2.7681	0.0000	NG	17.43	11.92
3	L	Off	HY	15	0.3014	2.7645	0.0000	NG	17.42	11.91
4	L	On	HY	15	0.3014	2.7645	0.0000	0.0000	17.42	11.91
5	L	On	0.1603	15	0.3014	2.7645	0.0000	0.0000	16.24	11.29

Note: All check problems have a single sand layer of homogeneous soil with an effective angle of internal friction (φ′) of 30 degrees. Factor of Safety is 1.0 for active earth pressures and Factor of Safety is 1.5 for passive earth pressures. All elevations and depths are reported in units of feet.

NG – Hydraulic fracturing (gap) not considered.

HY – Hydrostatic pore water pressure.

Example problem 4.1.1 was solved using the Coefficient Method of analysis, this was introduced with Corps_I-Wall Version 1.0. Table 4.2 shows a comparison of the results between the Coefficient Method and the Wedge Solution Method. The resulting elevations of the PR and the the fully embedded pile tip are nearly identical for the two methods.

Table 4.2. Comparison of earth coefficient results to Wedge Solution Method results for Example 4.1.1

Method	Point of Rotation (PR) (elevation in feet)	Pile Tip (elevation in feet)
Coefficient Method	14.48	8.12
Wedge Solution	14.50	8.10

4.1.2 Example 4.1.2

An effective stress definition with φ′ = 30 degrees and c′ = 0, as illustrated in Figure 4.2, is considered for the evaluation of the depth of embedment. Homogeneous soil, hydrostatic pore water pressures, effective angle of soil-to-I-Wall friction (δ′) of 15 deg, and the Coulomb Coefficient Method of analysis (for K_a and K_p) form the basis for this example. Hydraulic fracturing is not included as an option for this analysis. This Example 4.1.2 differs from Example 4.1.1 by a δ′ of 15 degrees.

The analysis resulted in a computed, mobilized active earth pressure coefficient (K_a) of 0.3014, and a mobilized passive pressure coefficient (K_p) of 2.7681. The active and passive earth pressures for both sides of the sheet-pile wall will be slightly higher, and with the same triangular shape as Example 4.1.1 (Figures 4.3a and 4.3b). The hydrostatic water pressures acting on both sides of the sheet-pile wall are similar to those shown in Figure 4.4a, with the resultant net water pressure calculated by taking the difference between the water pressures acting on both sides of the wall (Figure 4.4a), and similar to that shown in Figure 4.4b for the Example 4.1.1 problem.

From the calculated pressures, the net active and net passive pressures are estimated. The net pressure diagram (not shown) is similar to Figure 4.5b, and is derived from the replication of all values of the net active pressures from the top of the wall until the elevation at the PR (el 17.43 ft), at that instant the remaining values of the net pressure diagram is assumed to be linear with elevation between 1) the net active pressure value at the elevation of the PR, and 2) the net mobilized passive pressure at the

elevation of the approximated sheet-pile tip (i.e., el 11.92). For the applied flood loading, the I-Wall will rotate counterclockwise.

The various input conditions and final results for Example 4.1.2 are tabulated as check problem 2 in Table 4.1. The sheet-pile tip elevation is computed at el 11.92 ft with a calculated depth of embedment of 18.08 ft. With the addition of soil-to-I-Wall friction of 15 degrees as compared with Example 4.1.1, the approximated sheet-pile tip elevation is higher than the 8.12 ft of Example 4.1.1, this is acceptable as the mobilized passive earth pressures have increased along the sheet-pile wall and thereby, resulted in a shallower depth of embedment by nearly 3.8 ft.

Table 4.3 shows a comparison of the results between the Coefficient Method and the Wedge Solution Method for Example Problem 4.1.2. The resulting elevations of the PR, and the elevation of the fully embedded pile tip are very consistent, varying by about half a foot, for the two methods.

Table 4.3. Comparison of Earth Coefficient results to Wedge Solution Method results - Example 4.1.2.

Method	Point of Rotation (PR) (elevation in feet)	Pile Tip (elevation in feet)
Coefficient Method	17.43	11.92
Wedge Solution	17.03	11.4

4.1.3 Example 4.1.3

An effective stress definition with $\varphi' = 30$ degrees and $c' = 0$, as illustrated in Figure 4.2, is considered for the evaluation of the depth of embedment. Homogeneous soil, hydrostatic pore water pressures, effective angle of soil-to-I-Wall friction (δ') of 15 degrees, and the passive earth pressure coefficient obtained from the logarithmic spiral procedure form the basis for this example. Hydraulic fracturing is not included as an option for this analysis. Example 4.1.3 differs from Example 4.1.2 by the logarithmic spiral procedure for the calculation of mobilized passive earth pressures with $\delta' = \varphi'/2$ or 15 degrees.

The analysis resulted in a computed, mobilized active earth pressure coefficient (K_a) of 0.3014, and a mobilized passive pressure coefficient (K_p) of 2.7645. There is a slight change in K_p values as compared to example 4.1.2, this is anticipated because there is less than a 10 percent difference between the Coulomb and logarithmic spiral K_p solutions when δ' is less than or

equal to φ′/2. The active and passive earth pressures for both sides of the sheet-pile wall and all other net pressures are calculated to be similar in shape to those for Example 4.1.2.[1] The various input conditions and final results for Example 4.1.3 are tabulated as check problem 3 in Table 4.1. The sheet-pile tip elevation is computed at 11.91 ft with a calculated depth of embedment of 17.42 ft. With the change from Coulomb Coefficient Method to the logarithmic spiral method for calculating the passive earth pressures, the calculated sheet-pile tip elevation is approximately the same as that of Example 4.1.2.

For an appreciation of the logarithmic spiral K_p solution, φ′ will be assigned a larger value (i.e., δ′ > φ′/2). Table 4.4 has three check problems that tabulate the results for three wall friction angles, (i.e., δ′ = φ′/2, δ′ = 3/4 φ′, and δ′ = φ′). The first check problem in Table 4.4 is the same as check problem 3 of Table 4.1. As the wall friction angle increased from 15 to 22.5 degrees, the calculated passive earth pressure coefficient increased. With an increase in earth pressure within the Figure 1.1 passive zones, the system is more stable and the sheet-pile tip elevation is reduced, it was moved higher from elevation 11.91 to 13.05 ft. This trend is further established by the assignment of the effective angle of soil-to-I-Wall friction of 30 degrees, the same value as the effective angle of internal friction. Here, the sheet-pile tip elevation is reduced to el 13.38 ft. Increasing the effective angle of wall friction δ′ from 15 to 30 deg reduced the required depth of embedment by nearly 1.47 ft.

Table 4.4. Results from wall friction angles with K_p coefficients from logarithmic spiral procedure.

Check Problems	δ′ (deg)	K_a mob	K_p mob	$\frac{2c'}{\sqrt{K_a}\gamma_{buoy}}$	Hydraulic Fracture Depth	Elevation at Point of Rotation	Elevation at Tip of Pile
4.1.3.1	15	0.3014	2.7645	0.0000	NG	17.42	11.91
4.1.3.2	22.5	0.2963	3.0952	0.0000	NG	18.30	13.05
4.1.3.3	30	0.2972	3.2792	0.0000	NG	18.56	13.38

Note: All check problems have a single homogeneous sand layer of soil with an effective angle of internal friction (φ′) of 30 degrees. Factor of Safety is 1.0 for active earth pressures and Factor of Safety is 1.5 for passive earth pressures. Hydrostatic pore water pressures. Passive earth pressure coefficients obtained from logarithmic spiral procedure. All elevations and depths are reported in units of feet.

NG – Hydraulic fracturing (gap) not considered.

[1] For the applied flood loading, the I-Wall will rotate counterclockwise.

Table 4.5 shows a comparison of the results between the Coefficient Method and the Wedge Solution Method for the Example Problems of 4.1.3. The resulting elevations of the PR and the elevation of the fully embedded pile tip are very consistent, varying by about half a foot, for the two methods.

Table 4.5. Comparison of earth coefficient results to Wedge Solution Method results - Example Problems of 4.1.3.

Example Problem	Method	Point of Rotation (PR) (elevation in feet)	Pile Tip (elevation in feet)
4.1.3.1	Coefficient Method	17.42	11.91
	Wedge Solution	17.03	11.4
4.1.3.2	Coefficient Method	18.30	13.05
	Wedge Solution	17.97	12.60
4.1.3.3	Coefficient Method	18.56	13.38
	Wedge Solution	18.66	13.50

4.1.4 Example 4.1.4

An effective stress definition with φ′ = 30 degrees and c′ = 0 as illustrated in Figure 4.2, is considered for the evaluation of the depth of embedment. Homogeneous soil, hydrostatic pore water pressures, effective angle of soil-to-I-Wall friction (δ′) of 15 degrees, and the mobilized passive earth pressure coefficient obtained from the logarithmic spiral procedure form the basis for this example. Hydraulic fracturing is considered an option for this analysis. Example 4.1.4 differs from Example 4.1.3 with the estimation of hydraulic fracturing using the procedure discussed in Appendix B.

The analysis resulted in a computed mobilized active earth pressure coefficient (K_a) of 0.3014, and a mobilized passive earth pressure coefficient (K_p) of 2.7645. The active and passive earth pressures for both sides of the sheet-pile wall, and all other net pressures are calculated to be those from Example 4.1.3.[1] The various input conditions and final results for Example 4.1.4 are tabulated as check problem 4 in Table 4.1. The sheet-pile tip elevation is computed at el 11.91 ft with a calculated depth of embedment of 18.09 ft.

[1] For the applied flood loading, the I-Wall will rotate counterclockwise.

For this analysis, with hydrostatic pore water pressures and a cohesion value of zero, the estimated gap depth is 0.0 ft with the elevation at bottom of gap at 30 ft (i.e., at ground surface on the flood side of the I-Wall). The hydraulic fracture procedure (outlined in Appendix B) implemented in Corps_I-Wall provides the same gap depth as the standard equation (this is valid for hydrostatic water pressures only) of Table 4.1 and is given by

$$Gap = \frac{2c'}{\sqrt{K_a}\,\gamma_{buoy}} \tag{4.1}$$

Observe in Equation 4.1 that in order for the standard equation to indicate a non-zero gap depth, the soil must be assigned a value for effective cohesion, c', greater than zero.

Table 4.6 shows a comparison of the results between the Coefficient Method and the Wedge Solution Method for Example Problem 4.1.4. The resulting elevations of the PR and the elevation of the fully embedded pile tip are very consistent, varying by about half a foot, for the two methods.

Table 4.6. Comparison of Earth Coefficient results to Wedge Solution Method results - Example 4.1.2.

Method	Point of Rotation (PR) (elevation in feet)	Pile Tip (elevation in feet)
Coefficient Method	17.42	11.91
Wedge Solution	17.03	11.4

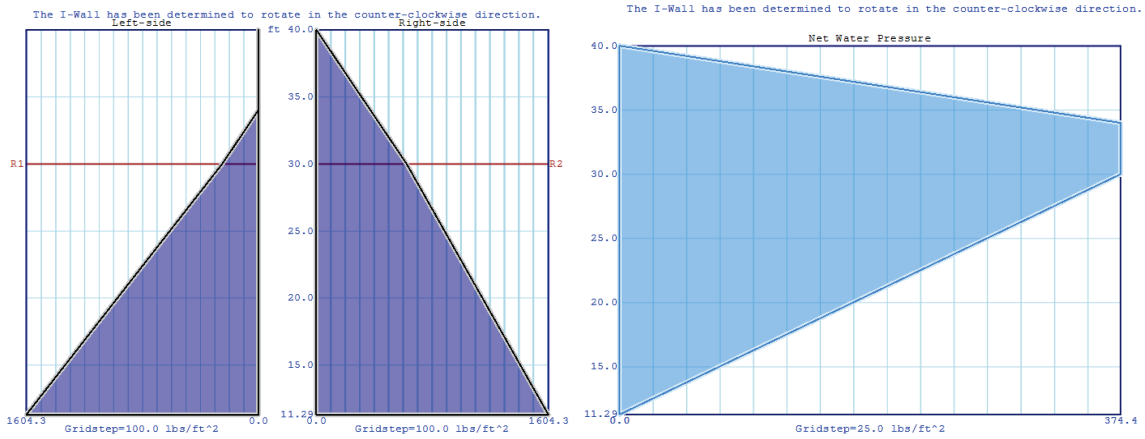
4.1.5 Example 4.1.5

An effective stress definition with φ′ = 30 degrees and c′ = 0, as illustrated in Figure 4.2, is considered for the evaluation of the depth of embedment. Homogeneous soil, homogeneous seepage by the line of seepage method (a.k.a. line of creep), effective angle of soil-to-I-Wall friction (δ′) of 15 degrees, the coefficients obtained from the logarithmic spiral procedure, and the hydraulic fracturing form the basis for this example. Example 4.1.5 differs from Example 4.1.4 because of the addition of homogenous seepage.

The analysis resulted in a computed mobilized active earth pressure coefficient (K_a) of 0.3014 and a mobilized passive pressure coefficient (K_p) of 2.7645. The hydrostatic water pressures acting on both sides of the sheet-pile wall are shown in Figure 4.7a with the resultant net water

pressure calculated by taking the difference between the water pressures acting on both sides of the wall (Figure 4.7a), shown in Figure 4.7b. Homogeneous seepage in this problem is clearly shown by the net water pressure diagram of Figure 4.7b, this differs from the net water pressure diagram of Figure 4.4b for hydrostatic pore water pressures. The net water pressure diagram of Figure 4.7b is first calculated from hydrostatic water pressures from el 40 ft to el 34 ft, resulting in the uppermost triangular distribution between these two elevations. Between el 34 ft and el 30 ft, the increase in water pressure on both sides of the wall is the same, resulting in a uniform net pressure diagram between these two elevations. At the ground surface elevation of 30 ft, which coincides with a gap depth elevation of 30 ft, homogeneous seepage calculations are initiated from RHS ground surface down the RHS to the sheet-pile tip and then up the LHS of the sheet pile, concluding at the LHS ground surface. Corps_I-Wall line of seepage (a.k.a. line of creep) computations result in a net water pressure of 0.0 psf at the sheet-pile tip elevation of 11.29 ft.[1]

Figure 4.7. Pore water pressures. (a) LHS and RHS of wall. (b) Net water pressures.



(a) (b)

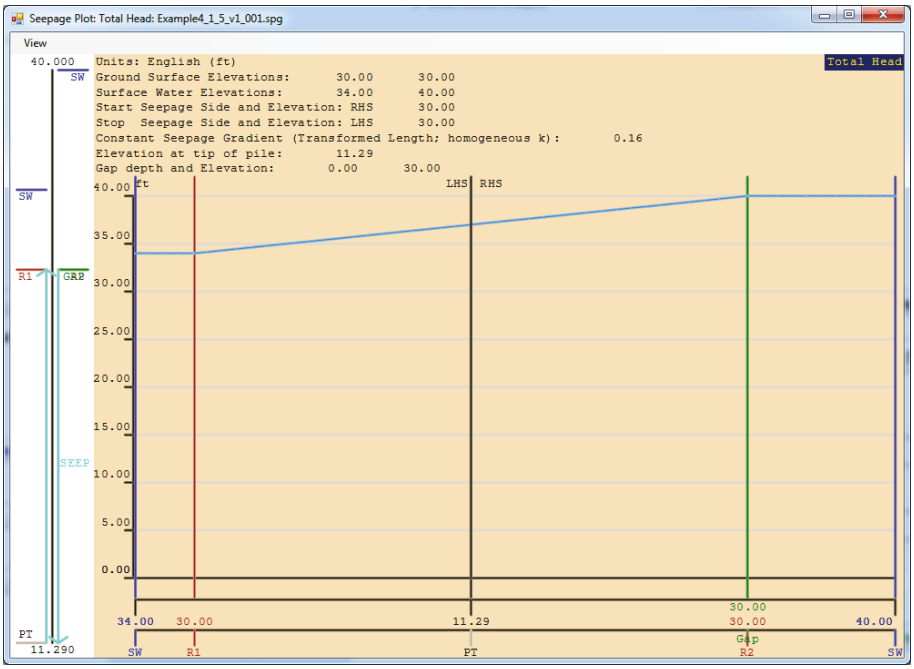
The active and passive earth pressures for both sides of the sheet-pile wall and all other net pressures are shown to have the same shape as those from Example 4.1.3. For the applied flood loading, the I-Wall will rotate counter-clockwise. The various input conditions and final results for Example 4.1.5

[1] This Figure 4.7b zero net water pressure computed at the sheet-pile tip from steady-state seepage contrasts with the 374.4 psf net water pressure value at sheet-pile tip for the hydrostatic water pressure condition shown in Figure 4.4b. Additionally, the line of seepage results in a linear variation in net water pressure from the ground surface to the sheet-pile tip in Figure 4.7b while the hydrostatic water pressure condition results in a uniform net water pressure distribution from the ground surface to the sheet-pile tip (Figure 4.4b). Higher net water pressures act on the embedded portion of sheet-pile wall when hydrostatic water pressure is specified.

are tabulated as check problem 5 in Table 4.1. The sheet-pile tip elevation is computed at el 11.29 ft, with a depth of embedment of 18.71 ft. With the addition of homogeneous seepage, the approximated sheet-pile tip elevation is deeper by 0.62 ft, more than the 11.91 ft of Example 4.1.4.

This problem required the analysis with homogeneous seepage. An input hydraulic conductivity for sand (i.e., 3.28e-5 ft/sec) was entered and the constant seepage gradient was calculated to be 0.16. Figure 4.8 provides an interpretation of the line of seepage (a.k.a. line of creep) method by a graph of the total head along the seepage path. The first graph (Figure 4.8a), shows that seepage starts at the ground surface of R2 at the RHS of the wall (i.e., flood side), continues down to the sheet-pile tip at el 11.29 ft, then continues upward towards the ground surface of R1 at the LHS (i.e., landside) of the sheet-pile wall. The second graph (Figure 4.8b) displays total head values of flow along the distance travelled. Total heads are constant from el 40.0 ft to the ground surface at el 30.0 ft (vertical red line). The slope of 0.16 starts at el 30 ft, continues past the sheet-pile tip, and stops at el 30 ft (vertical green line). Total head values are constant from el 30.0 ft to the water surface at el 34 ft on the LHS of the wall. Further details on the line of seepage method are given in Appendix C.

Figure 4.8. Line of seepage. (a) Direction of flow. (b) Total head along distance of flow.



(a) (b)

Table 4.7 shows a comparison of the results between the Coefficient Method and the Wedge Solution Method for Example Problem 4.1.5. The resulting elevations of the PR and the elevation of the fully embedded pile tip are very consistent, varying by less than a foot, for the two methods. This example problem included seepage, which is not handled by the Wedge Solution Method. It was expected that the Coefficient Method would generate deeper wall embedments because of seepage than the Wedge Solution Method without seepage. The results were still similar, with less than half a foot difference between the solution sets.

Table 4.7. Comparison of Earth Coefficient results to Wedge Solution Method results - Example 4.1.5.

Method	Point of Rotation (PR) (elevation in feet)	Pile Tip (elevation in feet)
Coefficient Method	16.24	11.29
Wedge Solution	17.03	11.4

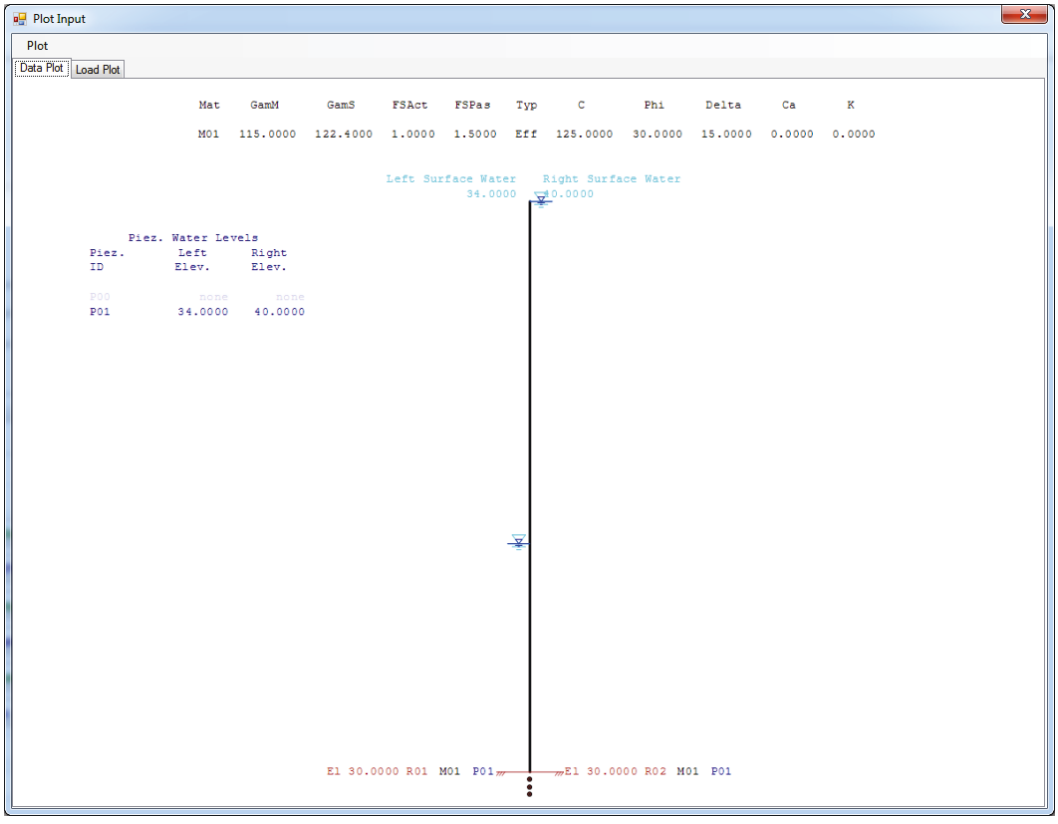
4.2 Example 4.1 sand site, effective stress strength definition with φ′ = 30 degrees and c′ = 125 psf, with either hydrostatic pore water pressures or homogeneous seepage

An effective stress strength definition with φ′ = 30 degrees and c′ = 125 psf (lightly cohesive) is illustrated by a series of three design problems. This will determine the depth of embedment (d) of the sheet-pile wall embedded into a sand site. These example problems apply a Factor of Safety of 1.0 for computing active earth pressures and a Factor of Safety of 1.5 for computing the mobilized passive earth pressures beneath the soil layers.

Figure 4.9 provides a schematic of the basic geometry and structural parameters for the sheet-pile wall. This I-Wall system has an exposed height of 10 ft. The water surfaces at both sides of the I-Wall are at 40 ft on the flood side and 34 ft on the landside. The homogeneous sand layer of soil has a level ground surface on both sides of the I-Wall at 30 ft, with saturated unit weight of 122.4 pcf, and an effective angle of internal friction of 30 degrees. The top row of listed text documents the input values of all parameters associated with each material type. For this problem, there is only one material assigned for the sand site and recorded as “M01.” The “M” signifies the material type and is followed by the ID, which starts from “01.” All information concerning material types is written in black text. The

representation of a soil structure is characterized by a region. Regions are labeled with an "R" and followed by an ID starting from "01." For this problem, two regions are assigned, Region 1 (as R01), is located on the LHS of the sheet-pile wall, and Region 2 (as R02) is located on the RHS of the sheet-pile wall. Each region and its surface elevation are written in red text. Piezometric surfaces are labeled as "P" and followed by an ID starting from 01. Piezometric water surfaces are listed in the upper left-hand corner and drawn with the water symbol at its defined elevation and shown in blue. Observe that piezometric surface ID, P01, is assigned to both regions. The LHS piezometric surface elevation is assigned as the LHS surface water elevation. Similarly, the RHS piezometric surface elevation is assigned as the RHS surface water elevation. This allows for the assignment of submerged unit weights to the soil regions. This geometry will be used in Example 4.2.1 and Example 4.2.3.

Figure 4.9. Corps_I-Wall schematic of sheet-pile wall in sand site.



The series of subsection 4.2 problems differ from the series of subsection 4.1 problems, in that, an effective cohesion value of 125 psf is assigned to the homogenous sand site in subsection 4.2 problems.

4.2.1 Example 4.2.1

An effective stress definition with c′ = 125 (lightly cohesive), as illustrated in Figure 4.9, is considered for the evaluation of the depth of embedment. Homogeneous soil, hydrostatic pore water pressures, effective angle of internal friction (φ′) of 30 degrees, effective angle of soil-to-I-Wall friction (δ′) of 15 degrees, hydraulic fracturing, and the logarithmic spiral procedure for calculating K_p form the basis for this example.

The analysis resulted in a mobilized active earth pressure coefficient (K_a) of 0.3014 and a mobilized passive pressure coefficient (K_p) of 2.7645.[1] The active and passive earth pressures for both sides of the sheet-pile wall are illustrated in Figures 4.10a and 4.10b. The hydrostatic water pressures acting on both sides of the sheet-pile wall are shown in Figure 4.11a, with the resultant net water pressure calculated by taking the difference between the water pressures acting on both sides of the wall (Figure 4.11a), as shown in Figure 4.11b.

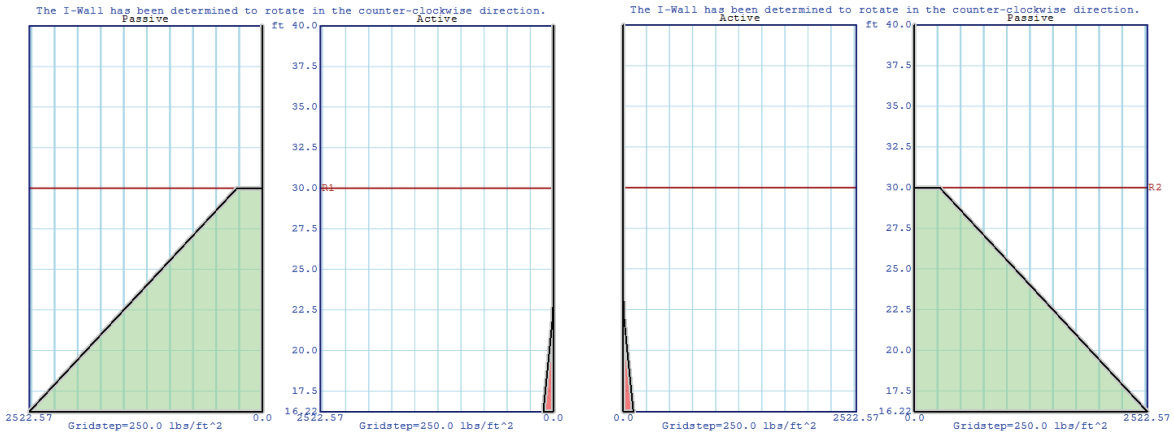
From these pressures (Figures 4.10 and 4.11), the net active and net passive pressures are constructed and presented in Figure 4.12a. For the applied flood loading, the I-Wall will rotate counterclockwise. The net active pressure is determined from the difference between the RHS-mobilized active earth pressure and the LHS-mobilized passive earth pressure (i.e., acting on the other side of the wall), with the addition of any net water pressures, any external horizontal net pressures, and overburden pressures (if any). The net passive pressure is determined by the difference between the RHS-mobilized passive earth pressure and the LHS-mobilized active earth pressure acting on the other side of the sheet-pile wall, with the addition of any net water pressures, any external horizontal net pressures, and overburden pressures (if any). The net pressure diagram of Figure 4.12b is derived from the replication of all values of the net active pressures, from the top of the wall until the elevation at the PR (el 20.92 ft), at which instant the remaining values of the net pressure diagram is assumed to be linear with elevation between 1) the net active pressure value at the elevation of the PR, and 2) the net-mobilized passive pressure at the elevation of the approximated sheet-pile tip (i.e., el 16.22).[2]

---

[1] Recall that an $FS_{passive}$ value equal to 1.5 was specified in this example.

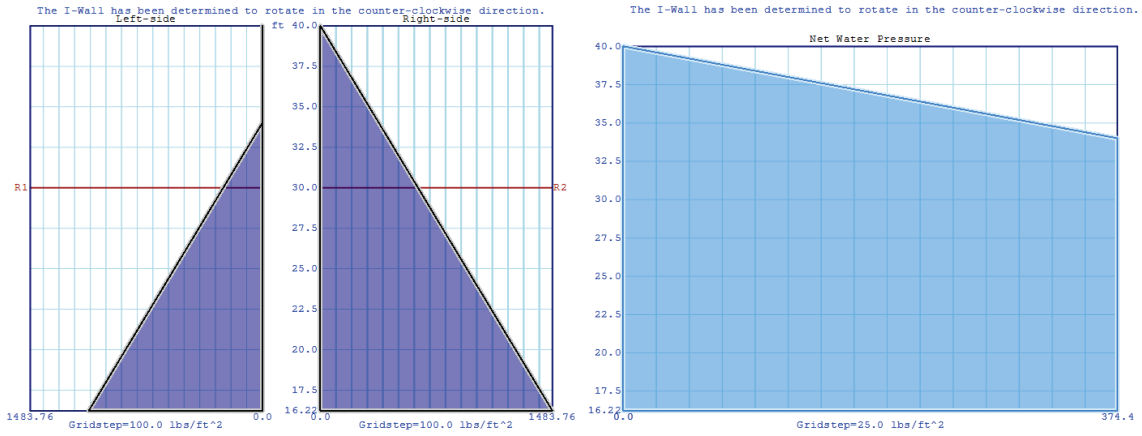
[2] Thus, only one mobilized net passive pressure value in Figure 4.12a is used to construct the Figure 4.12b net pressure diagram, corresponding to the sheet-pile tip elevation at el 16.22. The majority of the net pressure diagram is derived from the Figure 4.12a net active pressure diagram.

Figure 4.10. Active and passive earth pressures. (a) LHS of wall. (b) RHS of wall.



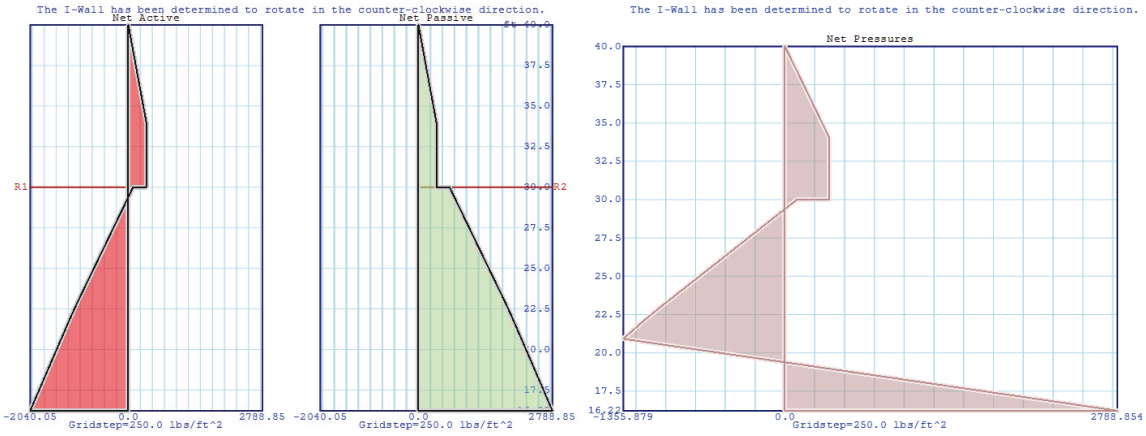
(a) (b)

Figure 4.11. Pore water pressures. (a) LHS and RHS of wall. (b) Net water pressures.



(a) (b)

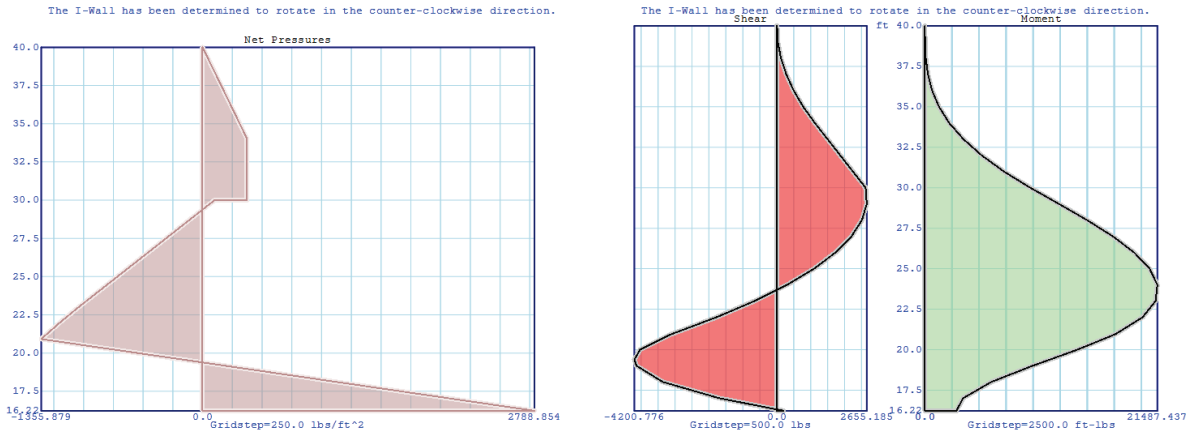
Figure 4.12. Net pressures. (a) Net active and net passive. (b) Net pressure diagram.



(a) (b)

The final results are illustrated in Figure 4.13 by the presentation of the net pressure diagram Figures 4.13a (replica of Figure 4.12b) and 4.13b, the shear and bending moment diagrams. Figure 4.13b shows that the maximum bending moment occurs at the zero crossing of the shear diagram.

Figure 4.13. (a) Net pressure diagram. (b) Shear and moment.



(a) (b)

The various input conditions and final results for Example 4.2.1 are tabulated as check problem 4.2.1 in Table 4.8. For a gap depth of approximately 7.59 ft, the sheet-pile tip elevation is computed at 16.22 ft with a calculated depth of embedment of 13.78 ft.

Table 4.8. Examples of effective stress strength definitions (sands with c′ = 125).

Check Problems	Seepage Gradient	No. Layers	c1′ (psf)	c2′ (psf)	$K_a$mob	$K_p$mob	$\frac{2c'}{\sqrt{K_a}\,\gamma_{buoy}}$	Hydraulic Fracture Depth	Elevation at Point of Rotation	Elevation at Tip of Pile
4.2.1	HY	1	125	-	0.3014	2.7645	7.5894	7.59	20.92	16.22
4.2.2	HY	2	125	0	0.3014	2.7645	7.5894	5.0000	19.45	14.76
4.2.3	0.26	1	125	-	0.3014	2.7645	7.5894	8.20	19.39	14.14

Note: All check problems have sand layers of soil with an effective angle of internal friction (φ′) of 30 degrees and effective angle of wall friction (δ′) of 15 deg. Factor of Safety is 1.0 for active earth pressures and Factor of Safety is 1.5 for passive earth pressures. Passive earth pressure coefficients obtained from logarithmic spiral procedure. HY refers to Hydraulic Fracturing. All elevations and depths are reported in units of feet.

HY – Hydrostatic pore water pressure.

Table 4.9 shows a comparison of the results between the Coefficient Method and the Wedge Solution Method for Example Problem 4.2.1. The resulting elevations of the PR and the elevation of the fully embedded pile tip are very consistent, varying by less than half a foot for the two methods.

Table 4.9. Comparison of Earth Coefficient results to Wedge Solution Method results - Example 4.2.1.

Method	Point of Rotation (PR) (elevation in feet)	Pile Tip (elevation in feet)	Gap (depth, feet)	Gap (elevation, feet)
Coefficient Method	20.92	16.22	7.59	22.41
Wedge Solution	20.8	15.9	7.22	22.78

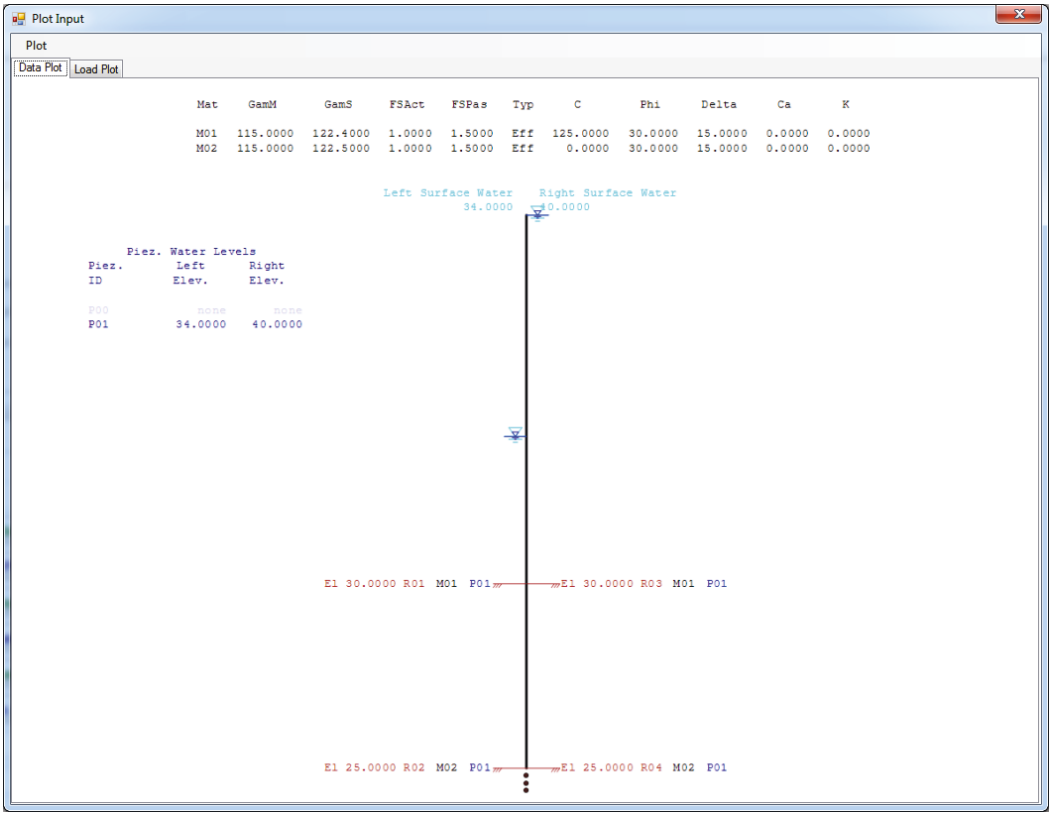
This method also features the formation of gaps in the surface soils on the opposite side of the wall that the wall is rotating away from. The Coefficient Method and Wedge Solution Method use different methods for determining Gap propagation depth as described in Appendix B. For this example, the gap depths formed are within 3/10^{ths} of a ft.

4.2.2 Example 4.2.2

A sand site using an effective stress definition with $\varphi' = 30$ degrees, as illustrated in Figure 4.14, is considered for the evaluation of the depth of embedment. A two-layer sand soil, with $c' = 125$ psf (lightly cohesive) for the upper sand layer at el 30 ft, and $c' = 0$ for the lower layer sand at el 25 ft. Hydrostatic pore water pressures, effective angle of soil-to-I-Wall friction (δ') of 15 degrees, hydraulic fracturing, and the logarithmic spiral procedure form the basis for this example. Example 4.2.2 differs from Example 4.2.1 by the introduction of a second layer of sandy soil with $c' = 0$ and all other soil parameters retaining the same values.

Figure 4.14 provides a schematic of the basic geometry and structural parameters for the sheet-pile wall. This I-Wall has an exposed height of 10 ft. The water surfaces at both sides of the I-Wall are at 40 ft on the flood side and 34 ft on the landside. There are two material types and four regions. Each sand layer has a level ground surface on both sides of the I-Wall at 30 ft and at 25 ft, respectivly, a saturated unit weight of 122.4 pcf, and an effective angle of internal friction of 30 degrees.

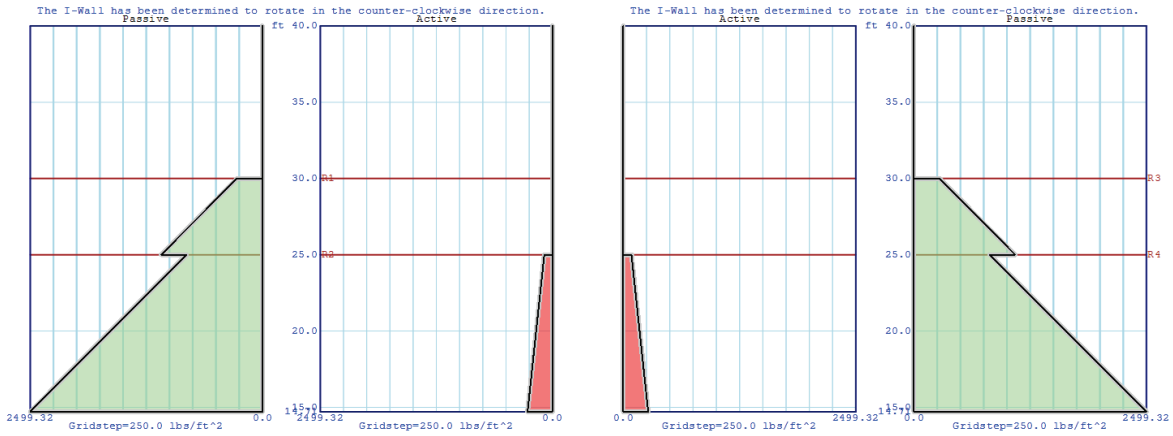
Figure 4.14. Corps_I-Wall schematic of sheet-pile wall in sand site with two layers.



The top row of text documents the input values of all parameters associated with each material type. For this problem, there is only one material assigned for the sand site and it is recorded as “M01,” the “M” signifies the material type and is followed by the ID which starts from “01.” All information concerning material types are written in black text. The representation of a soil structure is characterized by a region. Regions are labeled with an “R” and followed by an ID starting from “01.” For this problem two regions are assigned, Region 1 (as R01), is located on the LHS of the sheet-pile wall and Region 2 (as R02) is located on the RHS of the sheet-pile wall. Each region and its surface elevation are written in red text. Piezometric surfaces are labeled as “P” and followed by an ID starting from 01. Piezometric water surfaces are listed in the upper left-hand corner, drawn with the water symbol at its defined elevation, and are shown in blue. Observe that the piezometric surface ID, P01, is assigned to all four regions. The LHS piezometric surface elevation is assigned as the LHS surface water elevation. Similarly, the RHS piezometric surface elevation is assigned as the RHS surface water elevation. This allows for the assignment of submerged unit weights to the four soil regions.

The analysis resulted in a computed mobilized active earth pressure coefficient (K_a) of 0.3014, and a mobilized passive pressure coefficient (K_p) of 2.7681. The active and passive earth pressures for both sides of the sheet-pile wall are illustrated in Figures 4.15a and 4.15b for this two soil layer problem. Note the change in earth pressures at el 25 ft, which is the interface of Region 1 and Region 2 (labeled R2). The hydrostatic water pressures acting on both sides of the sheet-pile wall are the same as the water pressures of Example 4.2.1, and are shown in Figure 4.11a, with the resultant net water pressure calculated by taking the difference between the water pressures acting on both sides of the wall (Figure 4.11a) and as shown in Figure 4.11b.

Figure 4.15. Active and passive earth pressures. (a) LHS of wall. (b) RHS of wall.



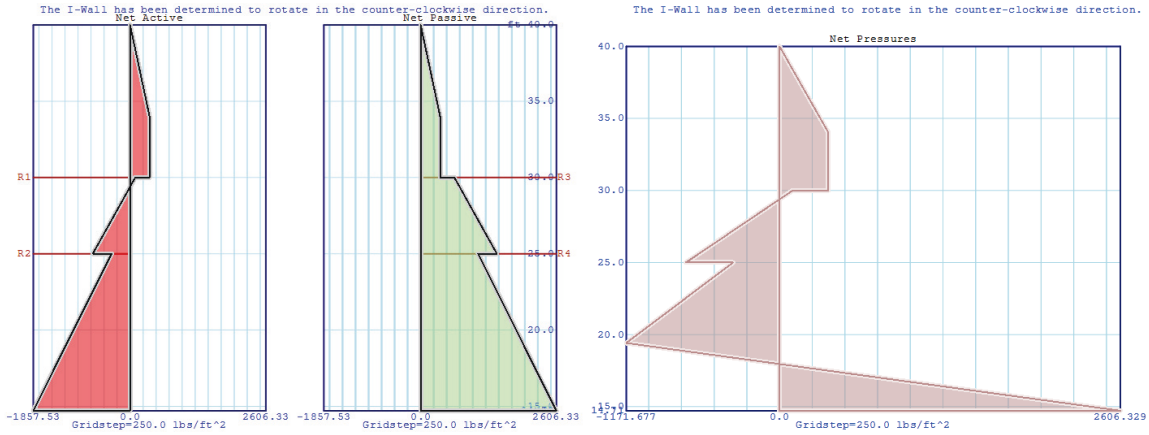
(a) (b)

From the calculated pressures, the net active and net passive pressures are estimated. For the applied flood loading, the I-Wall will rotate counter-clockwise. The net pressure diagram of Figure 4.16b is derived from the replication of all values of the net active pressures, from the top of the wall until the values of the net pressure diagram is assumed to be linear with elevation between 1) the net active pressure value at the elevation of the PR, and 2) the net mobilized passive pressure at the elevation of the approximated sheet-pile tip (i.e., el 14.76).[1] The final results are illustrated in Figure 4.17 by the presentation of the net pressure diagram Figures 4.17a (replica of Figure 4.16b) and 4.17b, the shear and bending moment diagrams. Figure 4.17b shows that the maximum bending moment occurs at the zero crossing of the shear diagram.

[1] Thus, only one mobilized net passive pressure value in Figure 4.16a is used to construct the Figure 4.16b net pressure diagram, corresponding to the sheet-pile tip elevation at el 14.76. The majority of the net pressure diagram is derived from the Figure 4.16a net active pressure diagram.

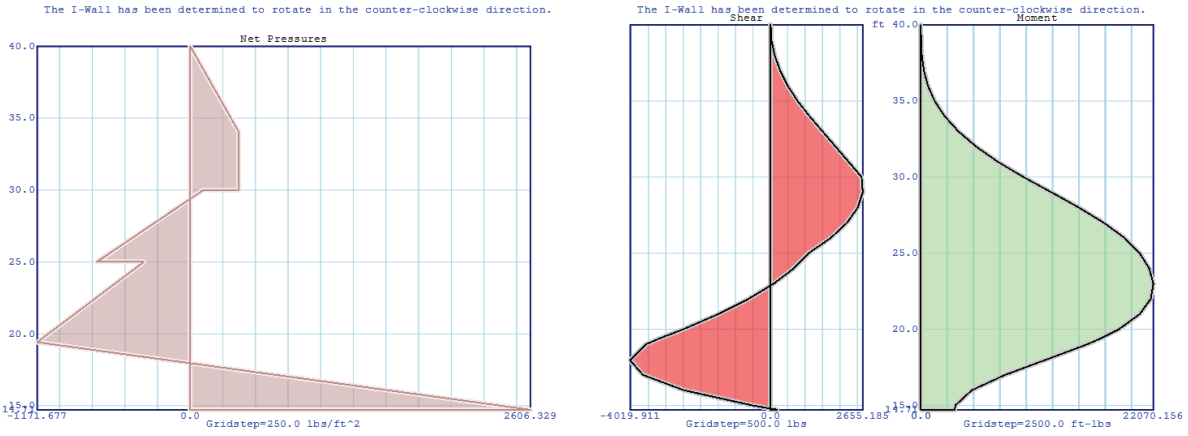
The various input conditions and final results for Example 4.2.2 are tabulated as check problem 4.2.2 in Table 4.8. The sheet-pile tip elevation is computed at el 14.76 ft with a calculated depth of embedment of 15.24 ft. With the addition of second sand layer with c′ = 0 at el 25 ft as compared with Example 4.2.1, the approximated sheet-pile tip elevation is calculated higher than the el 16.22 ft of Example 4.2.1. This is reasonable as the change in effective cohesion of c′ = 0 at el 25 ft "arrests" (i.e., stops) the gap, at which the (positive) active RHS earth pressures will start and increase with decreasing elevation along the sheet-pile wall until the PR is reached (at el 19.45 ft). Because (active) earth pressures acting on the wall occur at a higher (RHS) elevation, the sheet-pile tip will be calculated at a higher elevation and the I-Wall will have a shallower depth of embedment.

Figure 4.16. Net pressures. (a) Net active and net passive. (b) Net pressure diagram.



(a) (b)

Figure 4.17. (a) Net pressure diagram. (b) Shear and moment.



(a) (b)

Table 4.10 shows a comparison of the results between the Coefficient Method and the Wedge Solution Method for Example Problem 4.2.2. The resulting elevations of the PR and the elevation of the fully embedded pile tip are very consistent, varying by less than half a foot, for the two methods.

In this example, gapping was arrested at the boundary between a clay region with cohesion, and the next layer with a cohesionless sand region. This is why the gap calculation yielded the same results.

Table 4.10. Comparison of Earth Coefficient results to Wedge Solution Method results - Example 4.2.2.

Method	Point of Rotation (PR) (elevation in feet)	Pile Tip (elevation in feet)	Gap (depth, feet)	Gap (elevation, feet)
Coefficient Method	19.45	14.76	5.00	25.00
Wedge Solution	19.25	14.40	5.00	25.00

4.2.3 Example 4.2.3

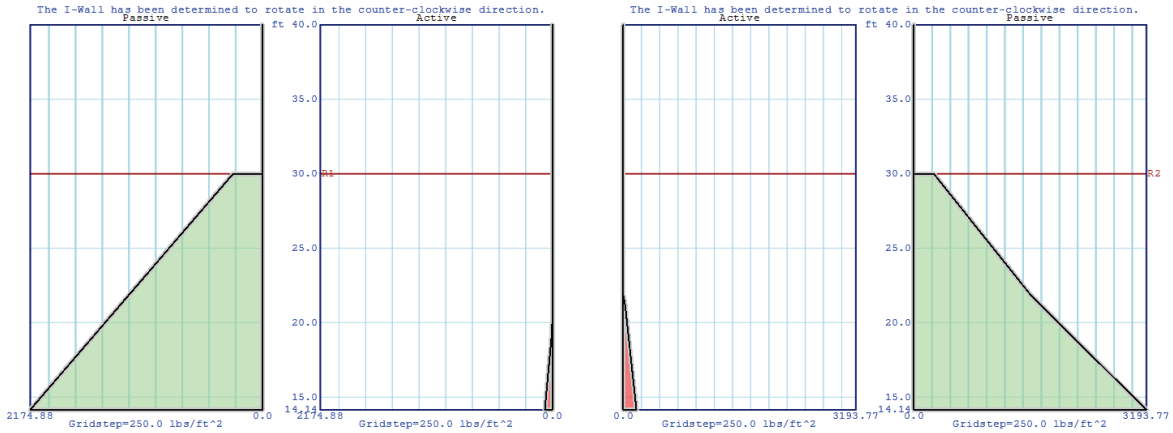
A sand site using an effective stress definition with $\varphi' = 30$ degrees and $c' = 125$ psf (lightly cohesive), as illustrated in Figure 4.9, is considered for the evaluation of the depth of embedment. Homogeneous soil, homogeneous seepage by the line of seepage method, effective angle of soil-to-I-Wall friction (δ') of 15 degrees, and the passive earth pressure coefficient obtained from the logarithmic spiral procedure and hydraulic fracturing, form the basis for this example. Example 4.2.3 differs from Example 4.2.1 with the addition of homogenous seepage (versus hydrostatic pore water pressures).

The analysis resulted in a computed mobilized active earth pressure coefficient (K_a) of 0.3014, and a mobilized passive pressure coefficient (K_p) of 2.7645. The active and passive earth pressures for both sides of the sheet-pile wall are illustrated in Figure 4.18. Note the earth pressures at the gap elevation of 21.80 ft (i.e., a gap depth of 8.20 ft).

The hydrostatic water pressures acting on both sides of the sheet-pile wall are shown in Figure 4.19a, with the resultant net water pressure calculated by taking the difference between the water pressures acting on both sides of the wall (Figure 4.19a), as shown in Figure 4.19b. Homogeneous seepage in this problem is clearly shown by the net water pressure diagram of Figure 4.19b, this differs from the net water pressure diagram of

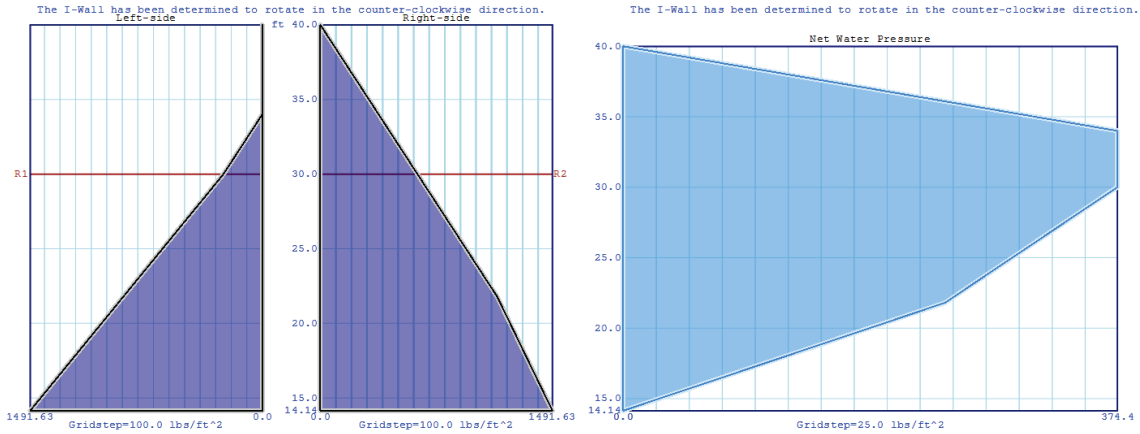
Figure 4.11b for hydrostatic pore water pressures. The net water pressure diagram of Figure 4.19b is first calculated by evaluating hydrostatic water pressures from el 40 ft to el 30 ft. A gap is initiated at the ground surface elevation (i.e., 30 ft). Corps_I-Wall computed a gap depth equal to 8.20 ft, corresponding to a gap tip elevation of el 21.80 ft. Figure 4.19a shows the RHS water pressures to be hydrostatic from el 40 ft, down to the gap tip el of 21.80 ft. The net water pressures will decrease linearly under this hydrostatic condition until the gap is arrested at el 21.80 ft. Homogeneous seepage calculations are then initiated on the RHS, these steady-state seepage calculations will continue down the I-Wall where the net water pressure will decrease to zero at the sheet-pile tip elevation of el 14.14 ft, then upwards on the LHS face of the sheet-pile wall until the LHS ground surface is met at el 30 ft.

Figure 4.18. Active and passive earth pressures. (a) LHS of wall, (b) RHS of wall.



(a) (b)

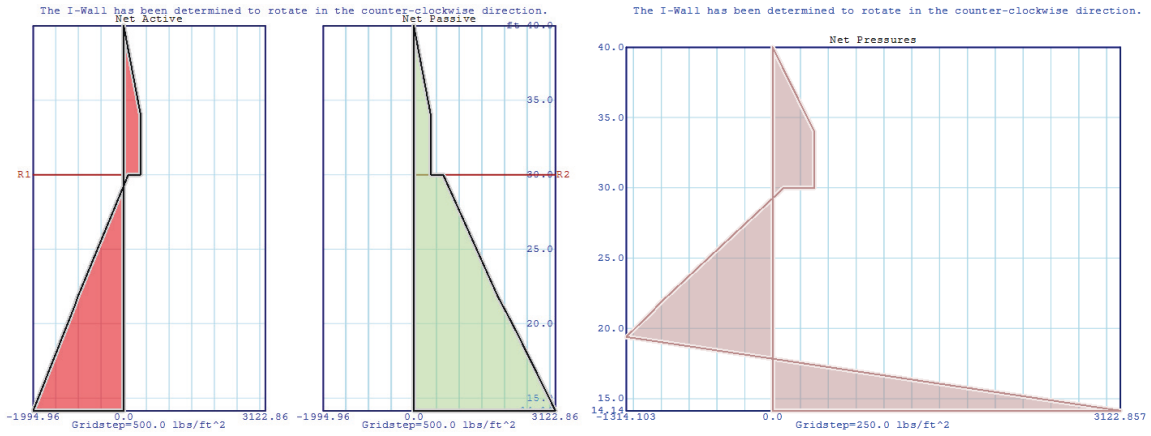
Figure 4.19. Pore water pressures. (a) LHS and RHS of wall. (b) Net water pressures.



(a) (b)

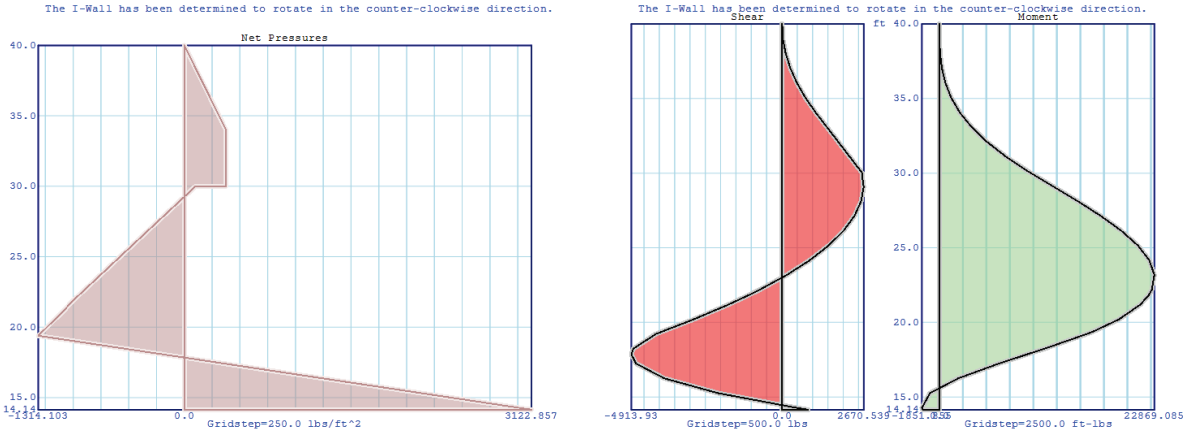
The active and passive earth pressures for both sides of the sheet-pile wall and all other net pressures are shown to have the same shape as those from Example 4.1.3.[1] The resulting net active and net passive earth pressures, and the net pressure diagram, is shown in Figure 4.20. Figure 4.21 shows the resulting distribution shear and moment internal to the sheet-pile wall. The various input conditions and final results for Example 4.2.3 are tabulated as check problem 4.2.3 in Table 4.3. The sheet-pile tip elevation is computed at el 14.14 ft with a depth of embedment of 15.86 ft. With the addition of homogeneous seepage, the approximated sheet-pile tip elevation is shallower by 2.08 ft than the el 16.22 ft of Example 4.2.1.

Figure 4.20. Net pressures. (a) Net active and net passive. (b) Net pressure diagram.



(a) (b)

Figure 4.21. (a) Net pressure diagram. (b) Shear and moment.

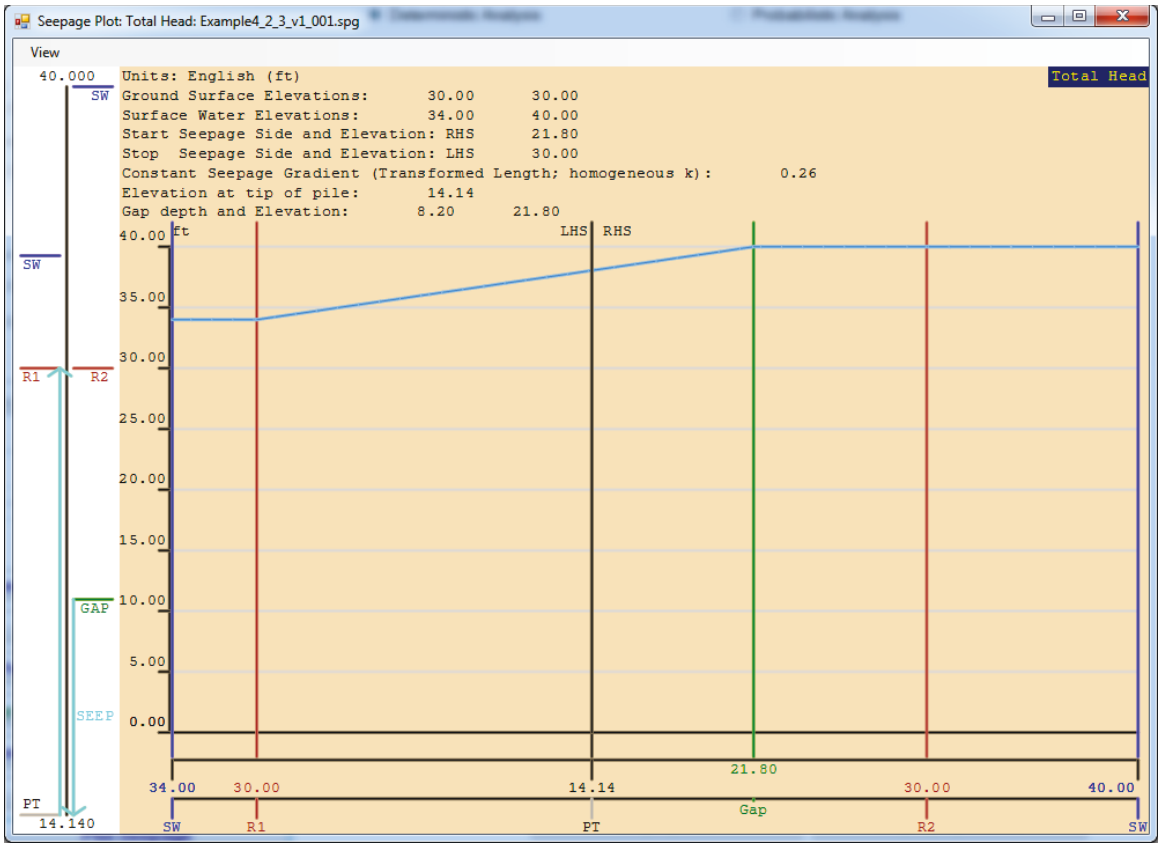


(a) (b)

[1] For the applied flood loading, the I-Wall will rotate counterclockwise.

Due to seepage and the presence of lightly cohesive soil regions, this problem required the analysis with homogeneous seepage and with hydraulic fracturing. An input hydraulic conductivity for sand (i.e., 3.28e-5 ft/sec) was entered and the constant seepage gradient was calculated to be 0.2760. Figure 4.22 provides an interpretation of the line of seepage method by a graph of the total head along the seepage path. The first graph, or Figure 4.22a, shows that seepage starts the gap elevation of 21.80 ft of R2 at the RHS of the wall (i.e., flood side), continues down to the sheet-pile tip at el 14.14 ft, then continues upward towards the ground surface of R1 at the LHS (i.e., landside) of the sheet-pile wall. The second graph or Figure 4.22b displays total head values of flow along the distance travelled.

Figure 4.22. Line of seepage. (a) Direction of flow. (b) Total head along distance of flow.



(a) (b)

Total heads are constant from el 40.0 ft to the gap elevation at 21.80 ft (vertical red line at R2). The slope of 0.2760 starts at the gap elevation of 21.74 ft on the LHS, continues past the sheet-pile tip, and stops at el 30 ft (vertical green line) on the RHS. Total head values are constant from el 30.0 ft (R1) to the water surface at el 34 ft on the LHS of the wall.

Table 4.11 shows a comparison of the results between the Coefficient Method and the Wedge Solution Method for Example Problem 4.2.3. The resulting elevations of the PR and the elevation of the fully embedded pile tip are very consistent, varying by about one and one-half feet, for the two methods. This example problem uses seepage (Coefficient Method only) and gapping.

Table 4.11. Comparison of Earth Coefficient results to Wedge Solution Method results - Example 4.2.3.

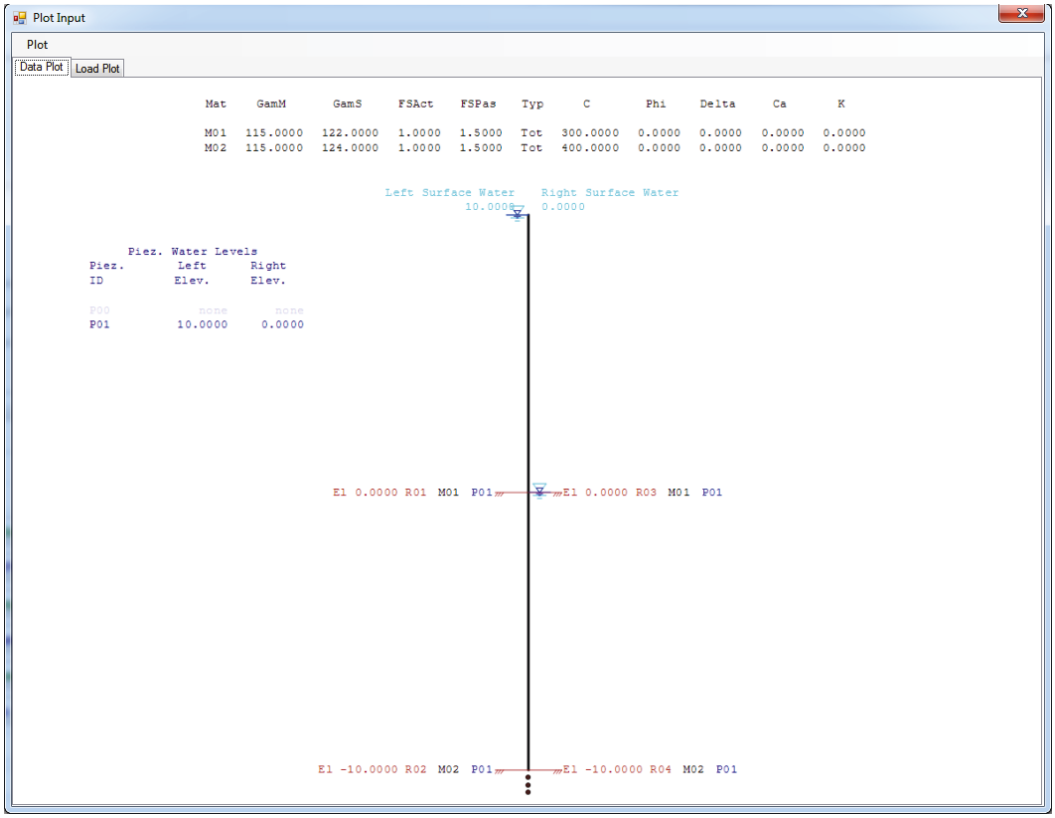
Method	Point of Rotation (PR) (elevation in feet)	Pile Tip (elevation in feet)	Gap (depth, feet)	Gap (elevation, feet)
Coefficient Method	19.39	14.14	8.20	21.80
Wedge Solution	20.80	15.90	7.22	22.78

4.3 Example 4.3 clay site, total stress strength definition with $\phi = 0$

A total stress definition with the angle of internal friction of (φ) of 0 degrees and two material layers, where the upper clay layer differs with the undrained shear strength (c) of 300 psf, and the lower clay layer with c = 400 psf, is illustrated by this design problem to determine the depth of embedment. In this example problem, a Factor of Safety of 1.0 is assigned for computing active earth pressures and a Factor of Safety of 1.5 is assigned for computing passive earth pressures within the two clay soil layers. This I-Wall system has an exposed height of 10 ft. The water surfaces on both sides of the I-Wall are at 10 ft on the flood side and 0 ft on the landside. In this example, the flood side corresponds to the LHS of the I-Wall. In this scenario, the I-Wall will rotate clockwise during flood loading. The clay layers have a level ground surface on both sides of the I-Wall, at el 0 ft with a saturated unit weight of 122 pcf, and at el 10 ft, with a saturated unit weight of 124 pcf.

Figure 4.23 outlines the basic geometry and structural parameters for the sheet-pile wall. The top row of text documents the input values of all parameters associated with each material type. For this problem, two materials are assigned and listed as M01 and M02, the "M" signifies the material type and is followed by the ID, which starts from "01." All information concerning material types are written in black text. The representation of a portion of a layer of soil on each side of the I-Wall is characterized as a region. Two soil regions are required to represent each soil layer.

Figure 4.23. Corps_I-Wall schematic of sheet-pile wall in clay site.



Regions are labeled with an “R” and followed by an ID starting from “01.” For this problem four regions are assigned, Region 1 and Region 2 (as R01 and R02), are located on the LHS of the sheet-pile wall, and Region 3 and Region 4 (as R03 and R04) are located on the RHS of the sheet-pile wall. Each region and its surface elevation are written in red text. Surface water on either side of the sheet-pile wall are drawn with the water symbol at its defined elevation and labeled as “Left Water Surface” and “Right Water Surface” at the top of the wall in light blue text. Piezometric surfaces are labeled as “P” and followed by an ID starting from 01. Piezometric water surfaces are listed in the upper left-hand corner and drawn with the water symbol at its defined elevation and shown in blue. Observe that piezometric surface ID, P01, is assigned to all four regions. The LHS piezometric surface elevation is assigned as the LHS surface water elevation. Similarly, the RHS piezometric surface elevation is assigned as the RHS surface water elevation. This allows for the assignment of submerged unit weights to the four soil regions.

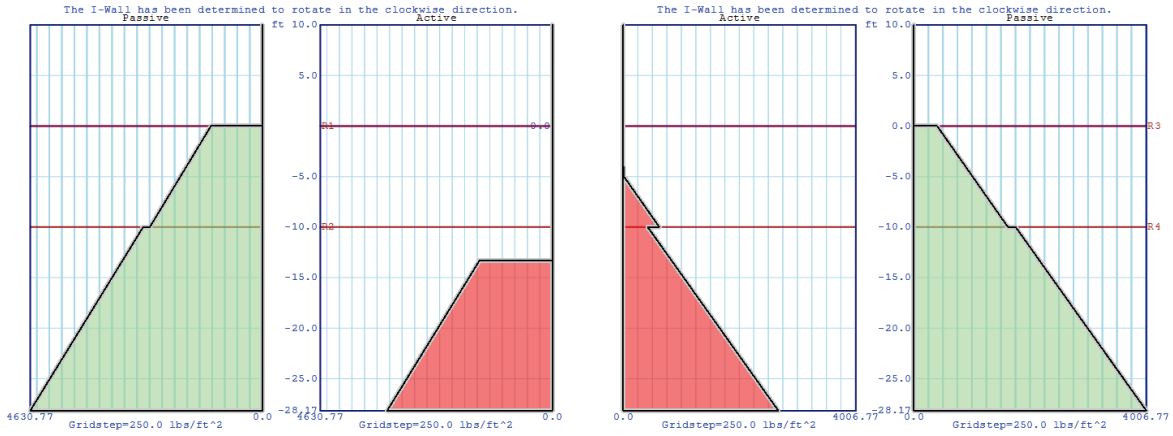
A clay site using a total stress definition with φ = 0 as illustrated in Figure 4.23 is considered for the "design" computation of the depth of embedment. Hydrostatic water pressures, the Coulomb Coefficient Method of analysis, and hydraulic fracturing form the basis for this example.[1]

This φ = 0 analysis resulted in a computed mobilized active earth pressure coefficient (K_a) of 1.0 and a mobilized passive pressure coefficient (K_p) of 1.0.[2] The active and passive earth pressures for both sides of the sheet-pile wall are illustrated in Figure 4.24. The hydraulic fracturing procedure discussed in Appendix B estimates a gap depth of 13.31 ft. Active earth pressures only develop at the gap depth or where the fracturing terminates, this is shown by the (LHS) active earth pressure diagram of Figure 4.24a. Note the change in earth pressures at el -10 ft, at the interface of Region 1 and Region 2 of the passive earth pressure of Figure 4.24a, and also at the interface of Region 3 and Region 4 of Figure 4.24b. Please refer to Chapter 2 for a detailed description of multilayered soils. The hydrostatic water pressures acting on both sides of the sheet-pile wall are shown in Figure 4.25a, with the resultant net water pressure calculated by taking the difference between the water pressures acting on both sides of the wall (Figure 4.25a), as shown in Figure 4.25b. In a total stress analysis, only overburden water pressure is included in the analysis (i.e., there is no pore water pressures calculated within the soil below the gap on the LHS and below the ground surface on the RHS). Also note that boundary water pressures acting on the flood wall for this total stress clay site increase with the propagation of the fracture down to the gap depth.

[1] For no soil-to-I-Wall interface friction (i.e., δ = 0 deg), the Coulomb solution for active and passive earth pressure coefficients corresponds to the Rankine earth pressure coefficients.

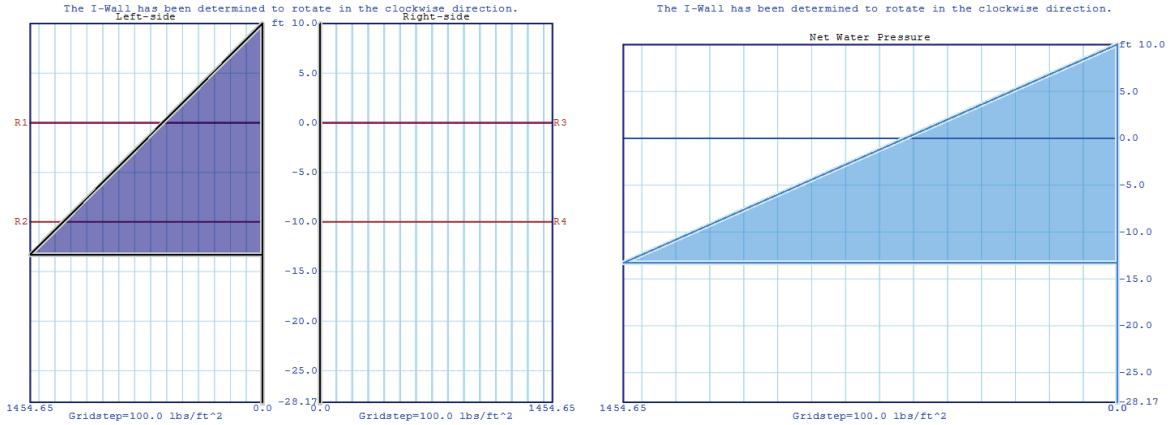
[2] For a total stress definition, φ = 0 deg, the active and passive earth pressure coefficients will equal to unity ($K_a = K_p = 1.0$).

Figure 4.24. Active and passive earth pressures for undrained shear strength. (a) LHS of wall. (b) RHS of wall.



(a) (b)

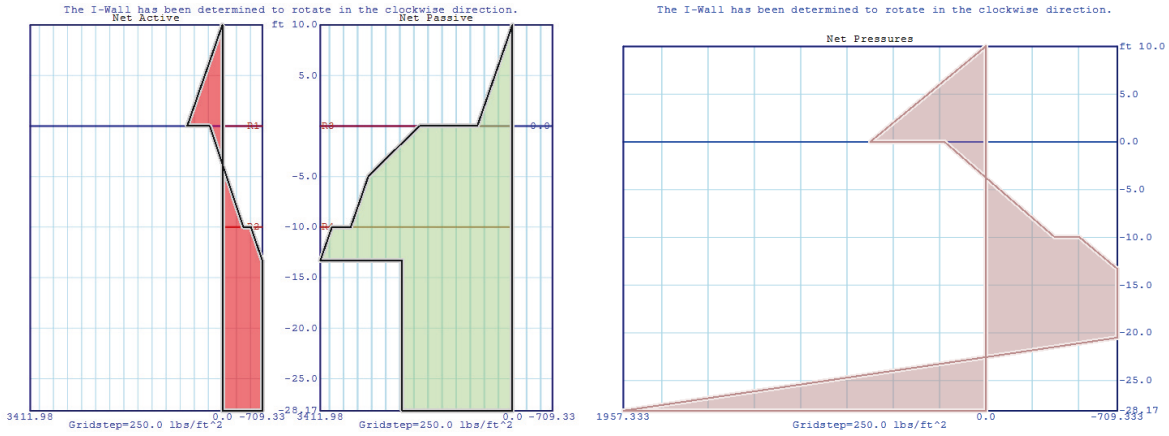
Figure 4.25. Pore water pressures. (a) LHS and RHS of wall. (b) Net water pressures.



(a) (b)

From the calculated pressures of Figures 4.24 and 4.25, the net active and net passive pressures are constructed and presented in Figure 4.26a. For the prescribed LHS flood loading, the I-Wall will rotate in a clockwise direction. The net active pressure is determined from the difference between the LHS-mobilized active earth pressure and the RHS-mobilized passive earth pressure (i.e., acting on the other side of the wall), with the addition of the net water pressures, and any external horizontal net pressures and overburden pressures (if any). The net passive pressure is determined by the difference between the LHS-mobilized passive earth pressure and the RHS-mobilized active earth pressure acting on the other side of the sheet-pile wall, with the addition of any net water pressures and any external horizontal net pressures and overburden pressures (if any). The calculated net active and net passive pressures above the ground surface el 0 (and above R01 and R03) of Figure 4.26 are solely derived from the net water pressures of Figure 4.25b.

Figure 4.26. Net pressures. (a) Net active and net passive. (b) Net pressure diagram.



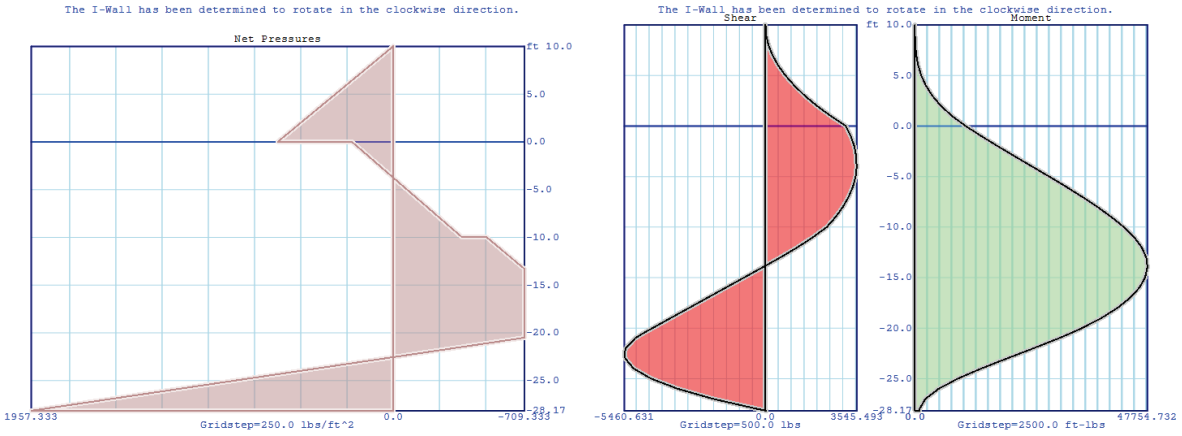
(a) (b)

The net pressure diagram of Figure 4.26b is derived from the replication of all values of the net active pressures, from the top of the wall until the elevation at the PR (at el -20.52 ft), at this instant the remaining values of the net pressure diagram is assumed to be linear with elevation between 1) the net active pressure value at the elevation of the PR, and 2) the net mobilized passive pressure at the elevation of the approximated sheet-pile tip (i.e., el -28.17).[1] Figure 4.26b is an illustration of how the net pressure diagram was formed. Because the I-Wall has been determined to rotate in a clockwise direction, the net pressure diagram of Figure 4.26b shows that the upper zone of net active pressures are plotting on the LHS, and the lower zone are plotting on the RHS. The net passive pressures are plotted on the LHS of the sheet-pile wall.[2] The final results are illustrated in Figure 4.27 by the presentation of the net pressure diagram 4.27a (replica of Figure 4.26b) and 4.27b, the shear and moment diagrams. Figure 4.27b shows that the maximum bending moment occurs at the zero crossing of the shear diagram. The sheet-pile tip elevation is computed at el -28.17 ft with a calculated depth of embedment of approximately 28.17 ft.

[1] Thus, only one mobilized net passive pressure value in Figure 4.26a is used to construct the Figure 4.26b net pressure diagram, corresponding to the sheet-pile tip elevation at el -28.17 ft. The majority of the net pressure diagram is derived from the Figure 4.26a net active pressure diagram.

[2] The net earth pressures in the two Figure 4.26a diagrams and the Figure 4.26b net pressures act towards the wall.

Figure 4.27. (a) Net pressure diagram. (b) Shear and moment.



(a) (b)

Table 4.12 shows a comparison of the results between the Coefficient Method and the Wedge Solution Method for Example Problem 4.3. The resulting elevations of the PR and the elevation of the fully embedded pile tip are very consistent, varying by about half a foot, for the two methods. This example problem uses seepage (Coefficient Method only) and gapping. A more full comparison of the Coefficient Method and the Wedge Method will be presented later in this chapter.

Table 4.12. Comparison of Earth Coefficient results to Wedge Solution Method results - Example 4.3.

Method	Point of Rotation (PR) (elevation in feet)	Pile Tip (elevation in feet)	Gap (depth, feet)	Gap (elevation, feet)
Coefficient Method	-20.52	-28.17	13.31	-13.31
Wedge Solution	-20.80	-28.60	12.99	-12.99

4.4 Example 4.4 mixed total and effective stress based shear strength definitions in layered soils site

Mixed layered soils of total stress and effective stress definitions where clay layers differ with the undrained shear strength (c) between 400 and 475 psf, and cohesionless soil comprise sand layers with varying effective angles of internal friction (φ′) of 30 and 32 degrees. Ten soil layers are presented for this design problem to determine the depth of embedment. A Factor of Safety of 1.0 is assigned for computing active earth pressures and a Factor of Safety of 1.5 is assigned for computing passive earth pressures within the soil layers. The ground surface of the I-Wall is at 0 ft on the flood side and at 15 ft on the landside. Surface water on the flood side is at 10 ft. Piezometric surfaces are at el 7 ft and el 10 ft on the

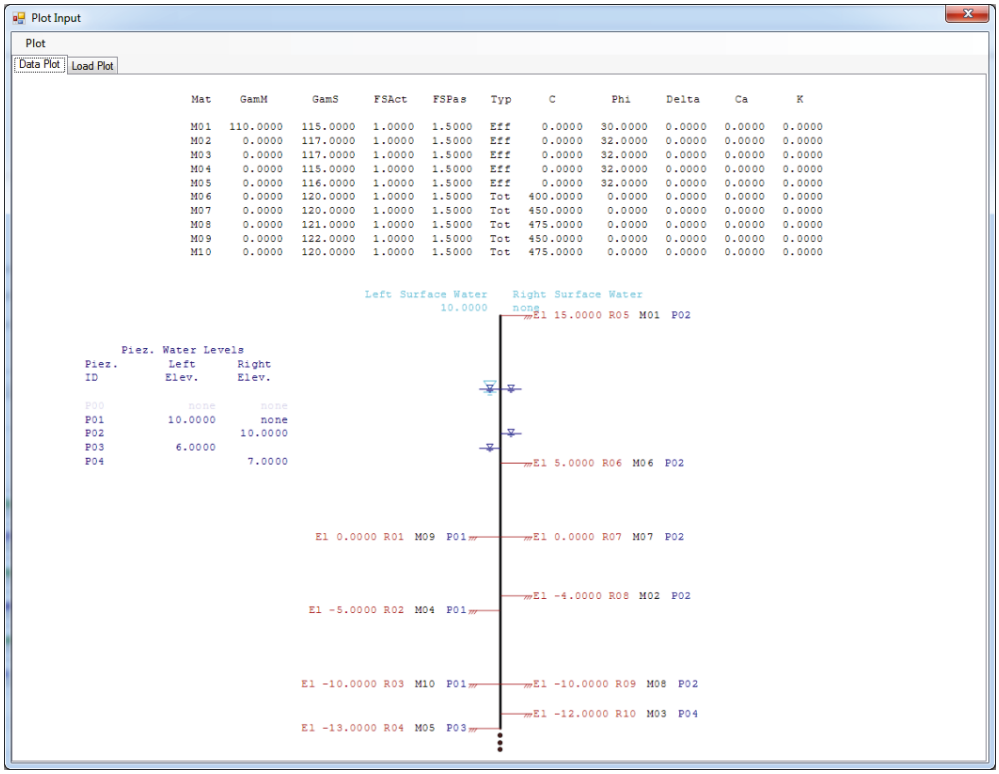
landside, and at el 6 ft on the flood side of the I-Wall. In this problem, the flood side corresponds to the LHS of the I-Wall and the I-Wall will rotate counterclockwise. Saturated unit weights range from 115 pcf of 122 pcf.

Figure 4.28 outlines the basic geometry and structural parameters for the sheet-pile I-Wall. The top row of text documents the input values of all parameters associated with each material type. For this problem, 10 materials are assigned and listed as M01 through M10, the "M" signifies the material type and is followed by the ID, which starts from "01." All information concerning material types are written in black text. The representation of a portion of a layer of soil on each side of the I-Wall is characterized as a region. A soil region represents a soil layer. Regions are labeled with an "R" and followed by an ID starting from "01." The flood side consists of four regions, Region 1 through Region 4 (as R01 to R04), and the landside is assigned six regions, Region 5 through Region 10 (as R05 to R10). Each region, and its top surface elevation, are written in red text. Piezometric surface information is listed at the left side of Figure 4.28 (shown in blue) and are labeled as "P" followed by an ID. Their respective locations are represented by water symbols at user-defined elevations along the wall. P01 is associated with surface water on both sides of the sheet-pile wall. It is drawn with the water symbol located at the defined elevation. Surface water elevations are also listed at the top of the I-Wall in light blue text and labeled as "Left Water Surface" and "Right Water Surface." Piezometric surfaces, P02 and higher, refer to piezometric surfaces other than surface water. Observe that piezometric surface ID, P01, is associated with regions R01 thru R03, these soil regions have water levels that relate to the surface water at el 10 ft on the LHS. Also, piezometric surface ID P02 at el 10 ft, is associated with regions R05 thru R08 on the RHS.

Clay sites using a total stress definition with $\varphi = 0$, and sand sites using an effective stress definition with $c' = 0$, are illustrated in Figure 4.28 and are considered for the "design" computation of the depth of embedment. Hydrostatic water pressures and the Coulomb Coefficient Method of analysis, form the basis for this example[1]. Please refer to Chapter 2 for a detailed description of multilayered soils.

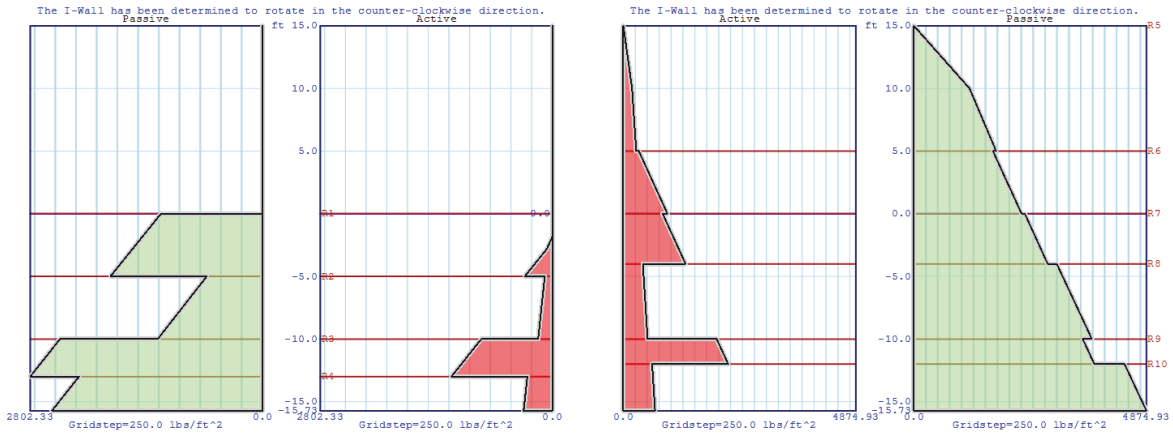
[1] For no soil-to-I-Wall interface friction (i.e., $\delta = 0$ deg), the Coulomb solution for active and passive earth pressure coefficients corresponds to the Rankine earth pressure coefficients.

Figure 4.28. Corps_I-Wall schematic of sheet-pile wall in clay site.



The active and passive earth pressures for both sides of the sheet-pile wall are illustrated in Figure 4.29. Note the change in earth pressures at the region interfaces at el -5, el -10 and el -13 ft of Figure 4.29a, illustrating active and passive earth pressures on the LHS, as well as the change in earth pressures at the region interfaces at el 5, el 0, el -4, el -10 and el -12 ft as shown in Figure 4.29b.

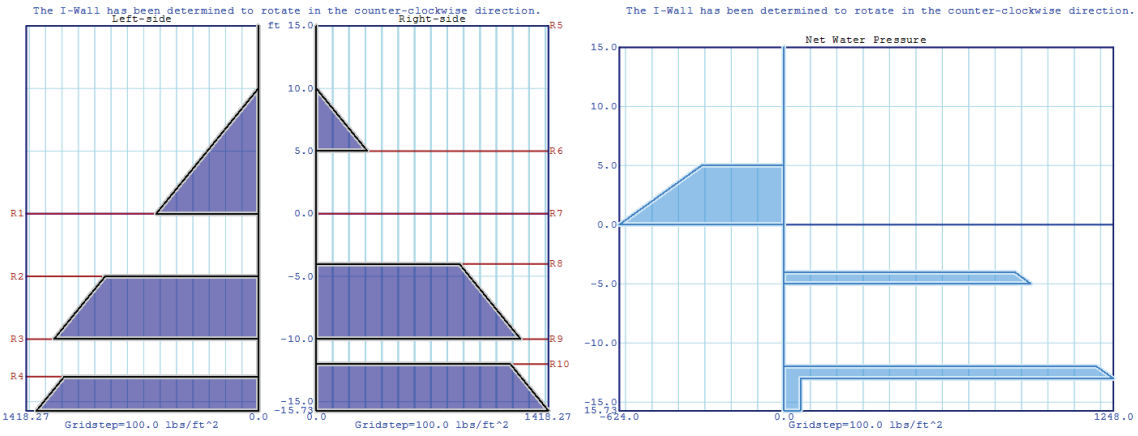
Figure 4.29. Active and passive earth pressures. (a) LHS of wall. (b) RHS of wall.



(a) (b)

The hydrostatic water pressures acting on both sides of the sheet-pile wall are shown in Figure 4.30a, with the resultant net water pressure calculated by taking the difference between the water pressures acting on both sides of the wall (Figure 4.30a), as shown in Figure 4.30b.

Figure 4.30. Pore water pressures. (a) LHS and RHS of wall. (b) Net water pressures.



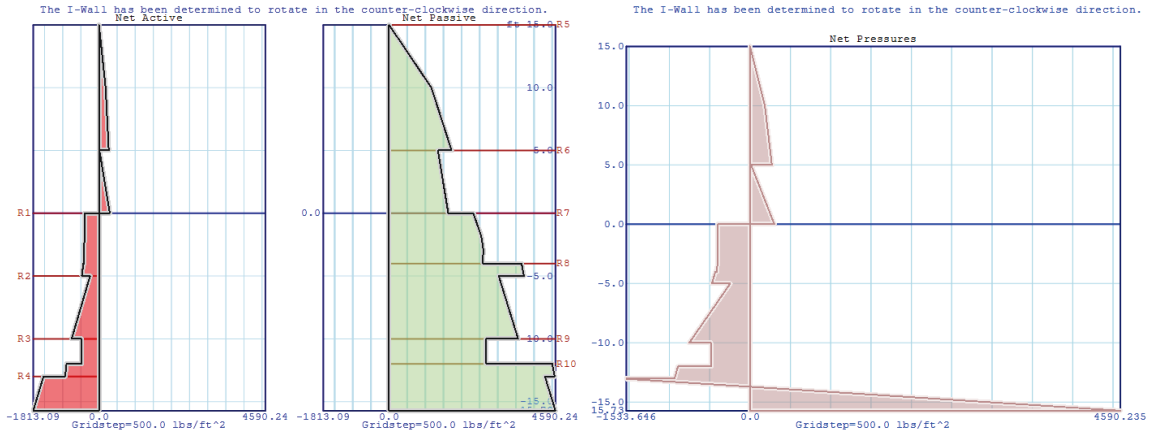
(a) (b)

From the calculated pressures of Figures 4.29 and 4.30, the net active and net passive pressures are constructed and presented in Figure 4.31a. For the prescribed LHS flood loading, the I-Wall will rotate in a counterclockwise direction. The net active pressure is determined from the difference between the LHS-mobilized active earth pressure and the RHS-mobilized passive earth pressure (i.e., acting on the other side of the wall), with the addition of the net water pressures and any external horizontal net pressures and overburden net pressures (if any). The net passive pressure is determined by the difference between the LHS-mobilized passive earth pressure and the RHS-mobilized active earth pressure acting on the other side of the sheet-pile wall, with the addition of any net water pressures and any external horizontal net pressures and overburden net pressures (if any). The net pressure diagram of Figure 4.31b is derived from the replication of all values of the net active pressures, from the top of the wall until the elevation at the PR (at el -13.04 ft), at which instant the remaining values of the net pressure diagram are assumed to be linear with elevation between 1) the net active pressure value at the elevation of the PR, and 2) the net mobilized passive pressure at the elevation of the approximated sheet-pile tip (i.e., el -15.73).[1] Figure 4.31b is an illustration

[1] Only one mobilized net passive pressure value in Figure 4.31a is used to construct the Figure 4.31b net pressure diagram corresponding to the sheet-pile tip elevation at el -15.73 ft. The majority of the net pressure diagram is derived from the Figure 4.31a net active pressure diagram.

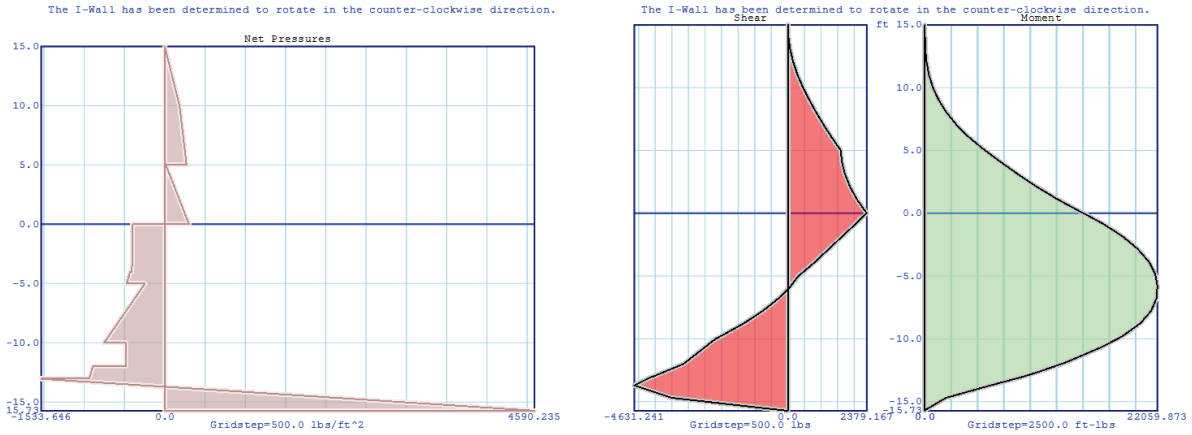
of how the net pressure diagram was formed. Because the I-Wall has been determined to rotate in a counterclockwise direction, the net pressure diagram of Figure 4.31b shows that the upper zone of net active pressures is plotted on the RHS and the lower zone is plotted on the LHS. The net passive pressures are plotted on the RHS of the sheet-pile wall. The final results are illustrated in Figure 4.32 by the presentation of the net pressure diagram Figures 4.32a (replica of Figure 4.31b) and 4.32b, the shear and moment diagrams. Figure 4.32b shows that the maximum bending moment occurs at the zero crossing of the shear diagram.

Figure 4.31. Net pressures. (a) Net active and net passive. (b) Net pressure diagram.



(a) (b)

Figure 4.32. (a) Net pressure diagram. (b) Shear and moment.



(a) (b)

The various input conditions for the ten layers of soil and final results for Example 4.4 are tabulated in Table 4.13.

Table 4.13. Multilayered soils with effective stress strength definitions (sands with c′ = 0) and total stress strength definitions (clays with φ = 0).

Region ID	Material Layer ID	Soil Type	Piezometric Surface ID	φ' (deg)	c (psf)	γ_moist (pcf)	γ_sat (pcf)	K_a*mob*	K_p*mob*	Elevation at Point of Rotation	Elevation at Tip of Pile
1	9	Clay	1	0	450	0	122	1.0000	1.0000	-13.04	-15.73
2	4	Sand	1	32	0	0	115	0.3073	2.2496		
3	10	Clay	1	0	475	0	120	1.0000	1.0000		
4	5	Sand	3	32	0	0	116	0.3073	2.2496		
5	1	Sand	2	30	0	110	115	0.3333	2.1212		
6	6	Clay	2	0	400	0	120	1.0000	1.0000		
7	7	Clay	2	0	450	0	120	1.0000	1.0000		
8	2	Sand	2	32	0	0	117	0.3073	2.2496		
9	8	Clay	2	0	475	0	121	1.0000	1.0000		
10	3	Sand	4	32	0	0	117	0.3073	2.2496		

The angle of wall friction (δ) and the adhesion (Ca) for all soil layers are zero. The Coulomb earth pressure Coefficient Method is being used to compute the earth pressures acting on the faces of the sheet-pile wall and hydrostatic pore water pressures are being used in the effective stress calculations. The design Factor of Safety is 1.0 for active earth pressures, and for passive earth pressures the design Factor of Safety is 1.5. Elevations and depths are reported in units of feet.

The sheet-pile tip elevation is computed at el -15.73 ft with a calculated depth of embedment of approximately 15.73 ft.

Table 4.14 shows a comparison of the results between the Coefficient Method and the Wedge Solution Method for Example Problem 4.4. The resulting elevations of the PR and the elevation of the fully embedded pile tip are very consistent, varying by less than a foot, for the two methods.

Table 4.14. Comparison of Earth Coefficient results to Wedge Solution Method results - Example 4.4.

Method	Point of Rotation (PR) (elevation in feet)	Pile Tip (elevation in feet)
Coefficient Method	-13.04	-15.73
Wedge Solution	-12.58	-14.90

4.5 Coastal site evaluation, designing for wave loads

For coastal sites, I-Wall designs must take into account the effect of storm surges and the action of waves against the I-Walls. The design of the I-Wall should proceed in steps to assure that the I-Wall can remain stable with normal loads and with storm surge loads. If unsatisfactory performance results due to the loading of the I-Wall, it may be necessary to remediate the I-Wall design with the addition of a stabilizing berm on the landside of the I-Wall to counter the detrimental effects of storm surge action. If the I-Wall design is enhanced by the addition of a berm, analysis of the new system under normal and surge loads will be performed.

For the four design examples discussed in this subsection, the I-Wall is assumed to be constructed with PZ38 sections of steel having a yield stress of

$$\sigma_{Yield} = 39 \frac{kips}{in.^2} \tag{4.1}$$

By EM-1110-2-2504 (HQUSACE 1994), the allowable bending stress is

$$\sigma_{Allowable} = 0.5 \times \sigma_{Yield} = 0.5 \times 39 \frac{kips}{in.^2} = 19.5 \frac{kips}{in.^2} \tag{4.2}$$

The allowable bending moment ($M_{Allowable}$) is computed as

$$M_{Allowable} = S \times \sigma_{Allowable} \text{ per foot run of wall} \tag{4.3}$$

Where S = Section modulus per foot run of wall. Given a PZ38 section with S = 46.8 in.^{3} per foot run of wall

$$M_{Allowable} = 46.8\ in.^3 \times\ 19.5 \frac{kips}{in.^2} =\ 912.6\ kip - in. \div 12 \frac{in.}{ft} = 76.1\ kip - ft \quad (4.4)$$

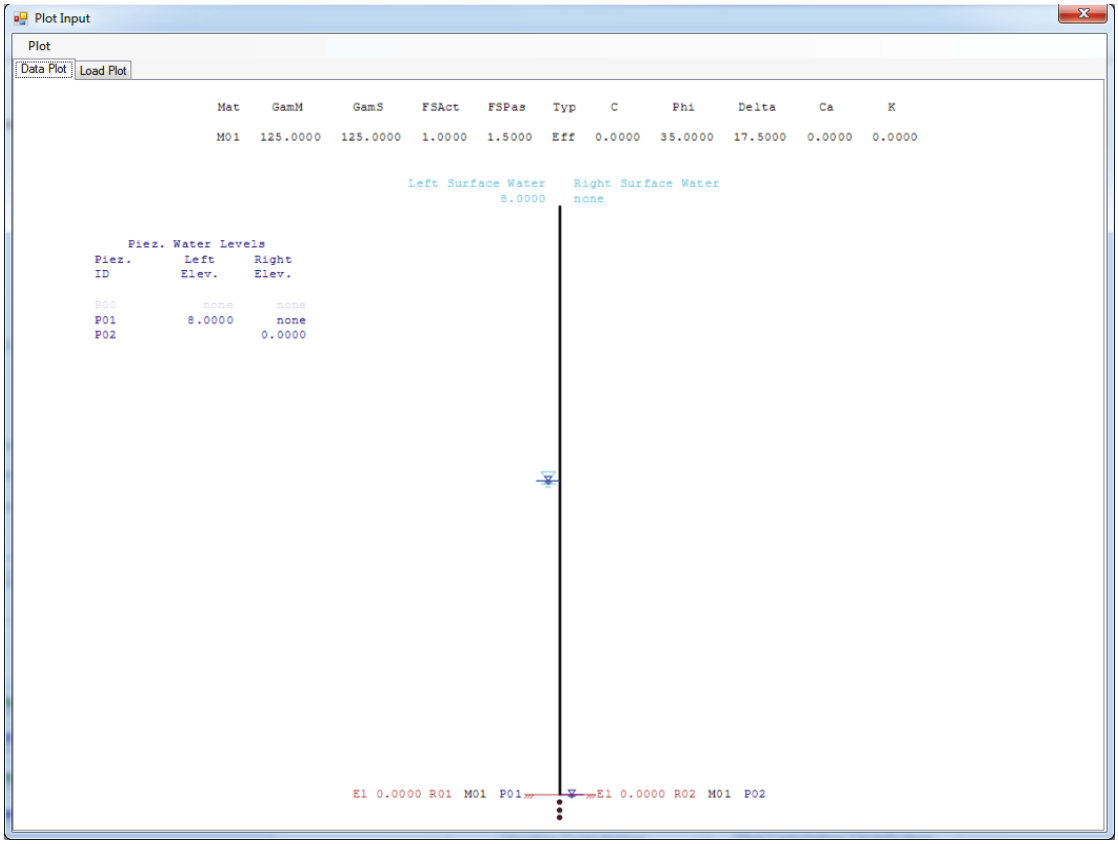
Therefore, a demand bending moment is required to be less than 76.1 kip-ft.

4.5.1 Example 4.5.1: Coastal site, effective stress strength definition with φ ′ = 35°

This first design problem for a coastal I-Wall is for the determination of the depth of embedment for an I-Wall with an exposed height of 15 ft above the ground surface on the flood side in dense sand. The ground surface is defined to have an elevation of 0.0 ft. The dense sand has an effective stress definition with no cohesion, an effective angle of internal friction of (φ′) of 35 degrees, a soil-to-sheet-pile effective interface friction angle (δ′) of 17.5 degrees (= φ′/2), and a hydraulic conductivity (K') of 0.0000328 ft/second in a single material layer definition. In this design example problem, a Factor of Safety of 1.0 is assigned for computing active earth pressures and a Factor of Safety of 1.5 is assigned for computing passive earth pressures within the soil layer for designing the I-Wall. The water surfaces on both sides of the I-Wall are at 8.0 ft on the flood side and 0.0 ft on the landside. For this example, the flood side corresponds to the LHS of the I-Wall. In this analysis, it is assumed that the I-Wall will rotate clockwise (i.e., away from the floodwater) during design loading. The sand layers have a level ground surface on both sides of the I-Wall at elevation 0.0 ft and assigned unsaturated (not used) and saturated unit weights of 125 pcf. Because the effective cohesion (c′) is 0.0 psf, there will be no gap formation, but the hydraulic fracture option is enabled because it will be used with future runs. Homogeneous seepage is specified in the design calculations.

Figure 4.33 outlines the basic geometry and structural parameters for the sheet-pile wall. A design computation run is performed to determine the embedment depth that will allow this wall to be stable for the required Factor of Safety applied to the passive earth pressures of the sand foundation (i.e., $FS_{Passive}$ = 1.50).

Figure 4.33. Corps_I-Wall schematic of sheet-pile wall in sand site.



The resulting depth of embedment is shown in Figure 4.34. The I-Wall becomes stable when the pile tip is embedded to a depth of 15.79 ft for a soil surface defined at an elevation of 0 ft. The point about which the wall will rotate is at a depth of 12.06 ft below the ground surface.

From the calculated pressures of Figures 4.35 and 4.36, the net active and net passive pressures are constructed and presented in Figure 4.37a. For the prescribed LHS flood loading, the I-Wall will rotate in a clockwise direction. The net active pressure is determined from the difference between the LHS-mobilized active earth pressure and the RHS-mobilized passive earth pressure (i.e., acting on the other side of the wall), with the addition of the net water pressures and any external horizontal net pressures and overburden pressures (if any). The net passive pressure is determined by the difference between the LHS-mobilized passive earth pressure and the RHS-mobilized active earth pressure acting on the other side of the sheet-pile wall, with the addition of any net water pressures and any external horizontal net pressures and overburden pressures (if any). Both the calculated net active and net passive pressures above the ground surface el 0.0 (and above Figure 4.33 R01 and R02) of Figure 4.37a are solely derived from the net water pressures of Figure 4.36b.

Figure 4.34. Corps_I-Wall run file for the specified input.

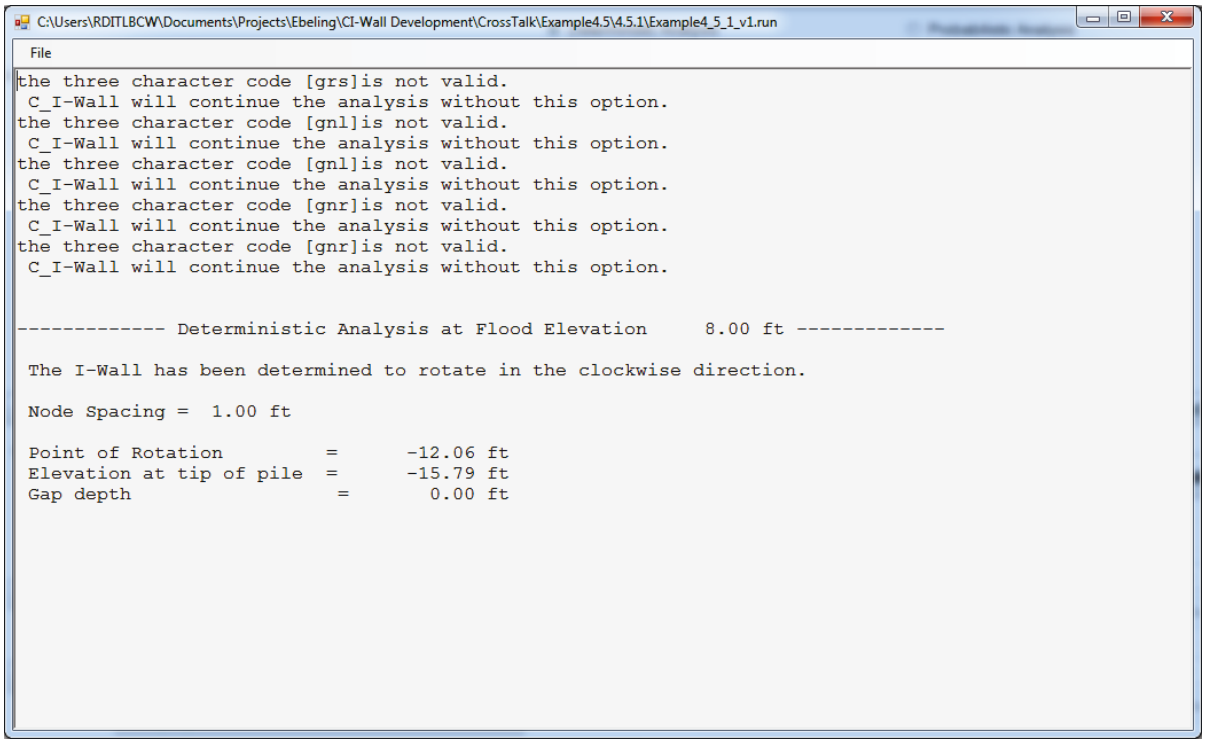
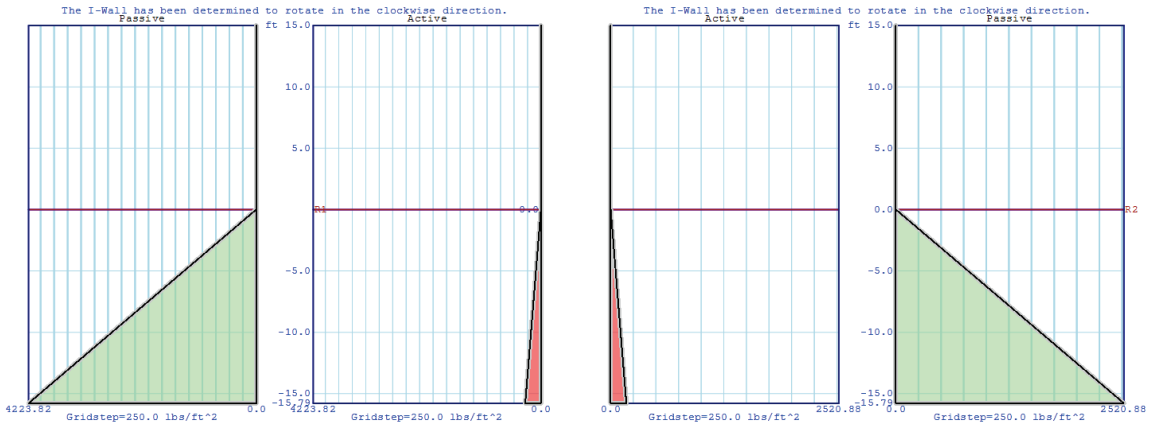
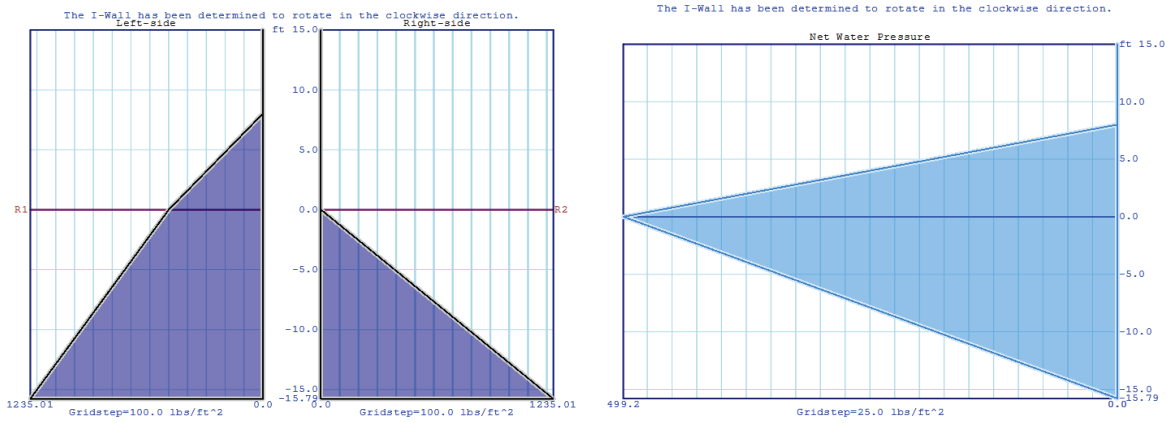


Figure 4.35. Corps_I-Wall run file for the specified input.



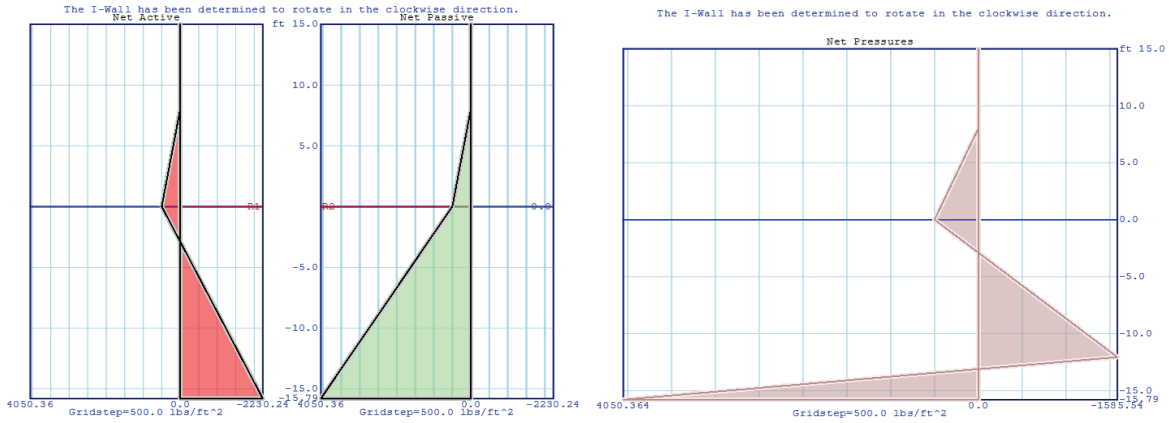
(a) (b)

Figure 4.36. Pore water pressures. (a) Left- and right- hand side of wall. (b) Net water pressures.



(a) (b)

Figure 4.37. Net pressures. (a) Net active and net passive. (b) Net pressure diagram.



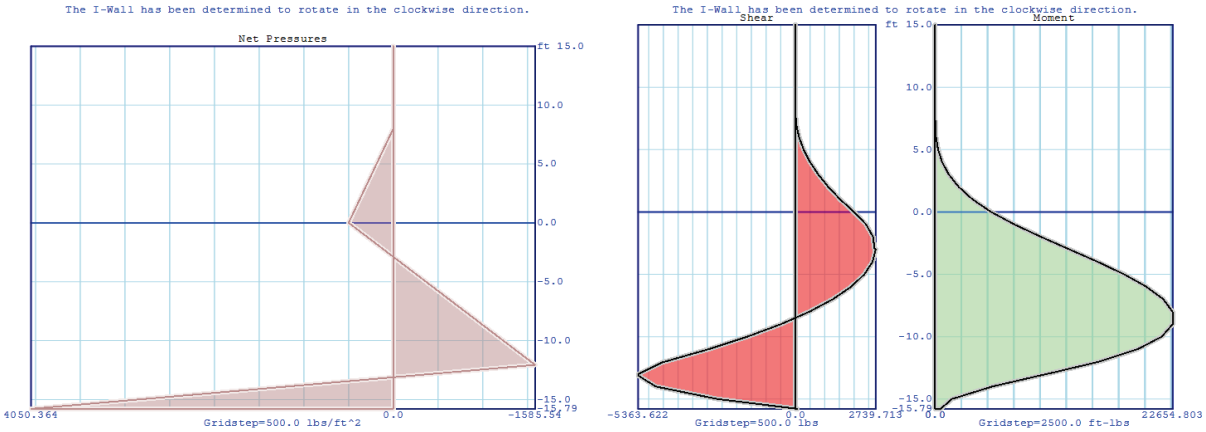
(a) (b)

The net pressure diagram of Figure 4.37b is derived from the replication of all values of the net active pressures, from the top of the wall until the elevation at the PR (at el -12.06 ft), at which instant the remaining values of the net pressure diagram is assumed to be linear with elevation between 1) the net active pressure value at the elevation of the PR, and 2) the net-mobilized passive pressure at the elevation of the approximated sheet-pile tip (i.e., el -15.79).[1] Figure 4.37b is an illustration of how the net pressure diagram was formed. Because the I-Wall has been determined to rotate in a clockwise direction, the net pressure diagram of Figure 4.37b shows that the net active pressures plot on the LHS in the upper zone and on the RHS in the lower zone. The net passive pressures plot on the LHS of the sheet-pile wall. The final results are illustrated in Figure 4.38 by the presentation

[1] Thus, only one mobilized net passive pressure value in Figure 4.37a is used to construct Figure 4.37b net pressure diagram; corresponding to the sheet-pile tip elevation at el -15.79 ft. The majority of the net pressure diagram is derived from Figure 4.37a net active pressure diagram.

of the net pressure diagram Figure 4.38a (replica of Figure 4.37b), and Figure 4.38b, the shear and moment diagrams. Figure 4.38b shows that the maximum bending moment occurs at the zero crossing of the shear diagram. This maximum bending moment is 22.6 kip-ft. This moment calculation is below the allowable bending moment of 76.1 kip-ft, so the wall will withstand the pressures that it is under. The sheet-pile tip elevation is computed at el -15.79 ft with a calculated depth of embedment of approximately 15.79 ft.

Figure 4.38. (a) Net pressure diagram, (b) Shear and moment.



(a) (b)

A diagram of the drop in total head is given in Figure 4.39. To the left is a diagram of the wall showing the surface water, soil region surfaces, gap definition, wall depth, and the direction of seepage. The drop in total heads due to seepage is given in the right side plot. This plot follows the line of seepage along the wall from one side to the other on the horizontal axis, and displays the head values on the vertical axis. The head loss occurs as water seeps from el 0.0, down the LHS foundation sands to the sheet-pile tip, and then up the RHS foundation sands to the ground surface (at el 0.0). This is represented by the blue line. Because this site possesses a homogeneous value of hydraulic conductivity (i.e., a K′ value of 0.0000328 ft/sec specified for the single material definition applied to the LHS and RHS dense sand regions), the head loss with distance shown in Figure 4.39 is linear along the line of seepage, as anticipated.

Table 4.15 shows a comparison of the results between the Coefficient Method and the Wedge Solution Method for Example Problem 4.5.1. The resulting elevations of the PR and the elevation of the fully embedded pile tip are very consistent, varying by about a foot, for the two methods. This example problem uses seepage.

Figure 4.39. Drop in total heads due to seepage diagram.

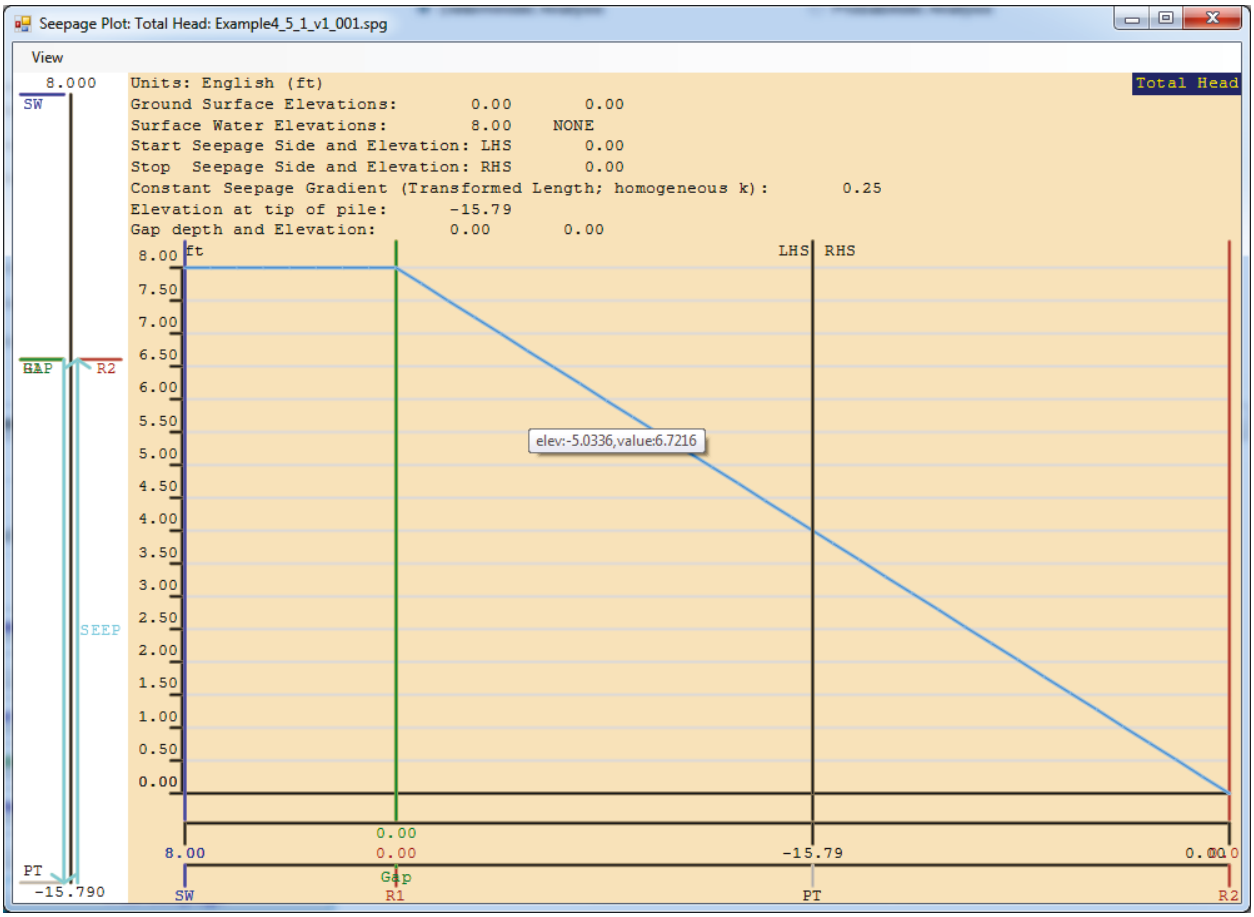


Table 4.15. Comparison of Earth Coefficient results to Wedge Solution Method results - Example 4.5.1.

Method	Point of Rotation (PR) (elevation in feet)	Pile Tip (elevation in feet)
Coefficient Method	-12.06	-15.79
Wedge Solution	-11.00	-15.2

4.5.2 Example 4.5.2 Coastal site with surge loading

The second design problem for a coastal I-Wall is determining the depth of embedment for an I-Wall with a 15 ft exposed height, embedded in dense sand (at elevation 0.0 ft), and subjected to a surge loading. The dense sand has an effective stress definition with no cohesion, an effective angle of internal friction of (φ′) of 35 degrees, a soil-to-sheet-pile effective interface friction angle (δ′) of 17.5 deg (= φ′/2), and a hydraulic conductivity (K′) of 0.0000328 ft/sec in a single material layer definition. In this design example problem, a Factor of Safety of 1.0 is assigned for computing active

earth pressures and a Factor of Safety of 1.5 is assigned for computing passive earth pressures within the soil layer. This I-Wall system has an exposed height of 15 ft. The sand layers have a level ground surface on both sides of the I-Wall at el 0.0 ft, and assigned unsaturated (not used) and saturated unit weights of 125 pcf. Because the effective cohesion (c′) is 0.0 psf, there will be no gap formation, but the hydraulic fracture option is enabled because it will be used with future runs. Homogeneous seepage is specified in the design calculations.

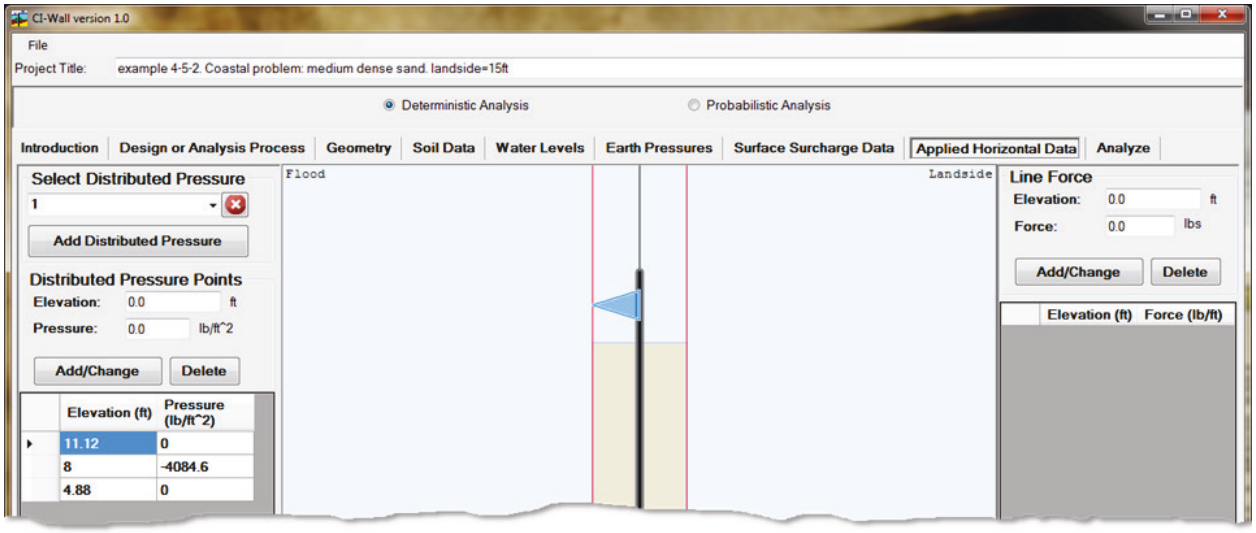
The water surface on the LHS of the I-Wall is determined by the possible surge wave size calculation in Appendix F, using the Minikin breaking wave method for determining forces. The Minikin method is diagrammed in Figure F.2. In essence, a pseudostatic pressure distribution is applied to the wall composed of the dynamic component of the breaking wave and the hydrostatic pressure component acting on the wall. The hydrostatic pressures acting on the LHS of the wall are equivalent to the pressure as if the swell height was the actual water level acting on the wall. The dynamic pressures are caused by the effects of the forward motion of the water in the wave as it collides with the wall.

The Minikin method is used to compute the peak dynamic pressure and wave height based on the average still-water level and the period of the wave. The dynamic pressure component is modeled as a triangular distributed pressure that begins with a pressure of 0.0 at half the height of the wave above the still-water level, reaches the maximum pressure at the still-water level, and returns to a pressure of 0.0 at the elevation of the still-water level minus one-half the height of the wave.

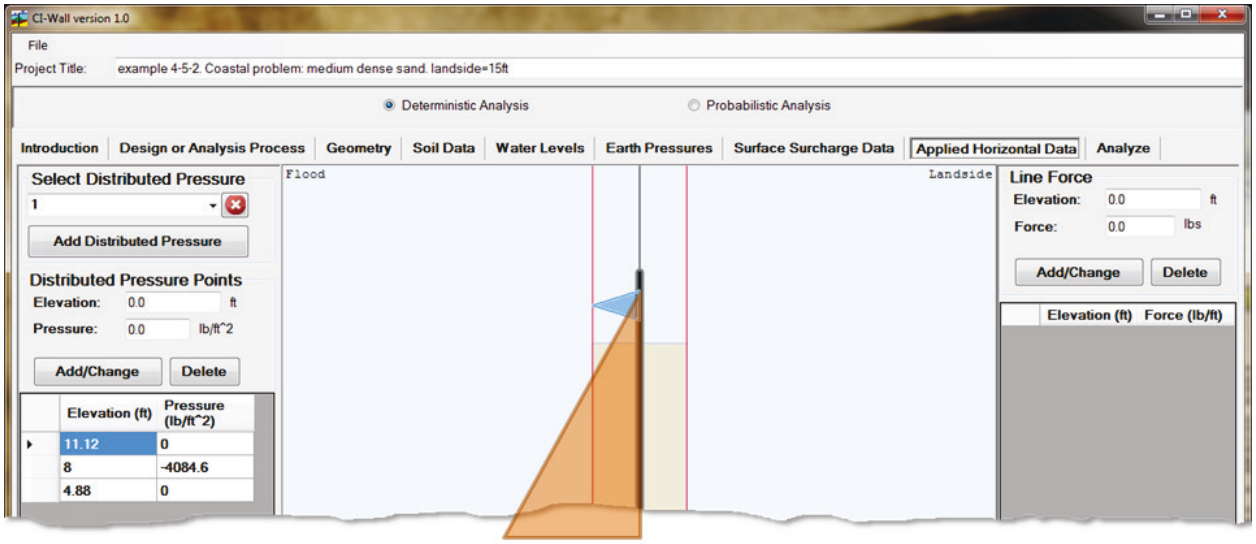
For Corps_I-Wall, the hydrostatic component is modeled by setting the water surface as half the height of the wave above the still-water level as it breaks against the wall. This elevation is then used to calculate pressures.

These pressures are shown in Figure 4.40. Figure 4.40a shows the dynamic wave as a horizontal pressure distribution entered into Corps_I-Wall. Figure 4.40b adds a representation of hydrostatic pressures when the water surface elevation is increased to the still-water level plus half the height of the breaking wave (in brown).

Figure 4.40. The components of Minikin wave pressure diagram.



(a) Corps_I-Wall input for the Minikin dynamic pressure component.



(b) The dynamic pressure component input with a representation of the hydrostatic pressure component (altered based on the still-water level and wave height).

Because the swell height is the elevation of the still-water level, added to half of the breaking wave height (~6.24 from Equation F.2 and Table F.3), the water level on the flood side is set equal to the swell height of 8 ft +3.12 ft = 11.12 ft and at 0 ft on the landside. The additional horizontal pressure due to the motion of the wave is accounted for by having a triangular horizontal load that goes from 0.0 lb/ft^2 at 11.12 ft to a maximum pressure of 4,084.6 lb/ft^2 (computed using equation F.4) at 8 ft, and reducing to 0.0 lb/ft^2 at 4.88 ft (8 ft - 3.12 ft). For this example, the flood

side corresponds to the LHS of the I-Wall. In this analysis, it is assumed that the I-Wall will rotate clockwise during flood loading.

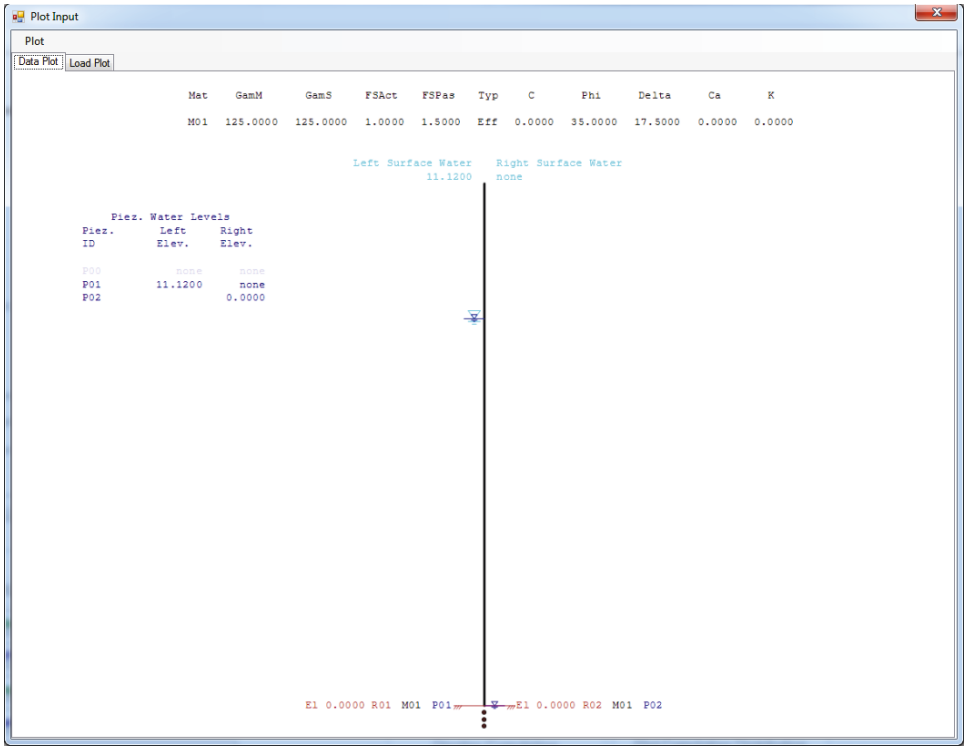
Figure 4.41 outlines the basic geometry and structural parameters for the sheet-pile wall. A design computation analysis is performed to determine an adequate depth of embedment for stability of the sheet-pile wall.

The resulting depth of embedment is shown in Figure 4.42. Because of the higher water levels and the additional wave loading (applied as a horizontal surcharge load), the I-Wall becomes stable when the pile tip is embedded to el -36.37 ft, with the soil surface defined at an elevation of 0.0 ft. The point about which the wall will rotate is at el -25.41 ft below the ground surface.

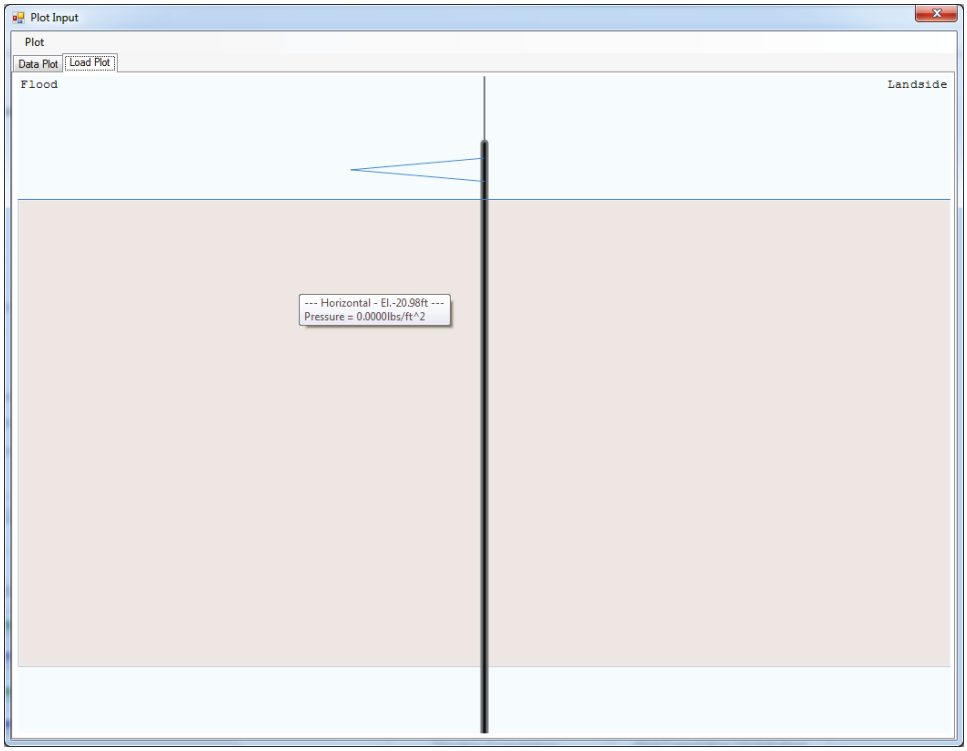
This calculation shows that the sheet-pile wall tip is embedded more than twice as deep as its exposed height. This situation also has the PR at a depth lower than the exposed height.

From the calculated pressures of Figures 4.43 and 4.44, both the net active and net passive pressures are constructed and presented in Figure 4.45a. For the prescribed LHS flood loading, the I-Wall will rotate in a clockwise direction. The net active pressure is determined from the difference between the LHS-mobilized active earth pressure and the RHS-mobilized passive earth pressure (i.e., acting on the other side of the wall), with the addition of the net water pressures and any external horizontal net pressures and overburden pressures (if any). The net passive pressure is determined by the difference between the LHS-mobilized passive earth pressure and the RHS-mobilized active earth pressure acting on the other side of the sheet-pile wall, with the addition of any net water pressures and any external horizontal net pressures and overburden pressures (if any). Both the calculated net active and net passive pressures above the ground surface el 0.0 (and above R01 and R02) of Figure 4.45 are solely derived from the net water pressures of Figure 4.44b.

Figure 4.41. Corps_I-Wall. (a) Schematic of sheet-pile wall in sand site. (b) Wave load applied to flood side (LHS) of sheet-pile wall.



(a)



(b)

Figure 4.42. Corps_I-Wall run file for the specified input.

C:\Users\RDITLBCW\Documents\Projects\Ebeling\CI-Wall Development\CrossTalk\Example4.5\4.5.2\Example4_5_2_v1.run

File

```
the three character code [grs]is not valid.
 C_I-Wall will continue the analysis without this option.
the three character code [gnl]is not valid.
 C_I-Wall will continue the analysis without this option.
the three character code [gnl]is not valid.
 C_I-Wall will continue the analysis without this option.
the three character code [gnr]is not valid.
 C_I-Wall will continue the analysis without this option.
the three character code [gnr]is not valid.
 C_I-Wall will continue the analysis without this option.

Horizontal Distributed Load
 1) EL =    11.12, Pressure =         0.00
 1) EL =     8.00, Pressure =     -4084.60
 1) EL =     4.88, Pressure =         0.00

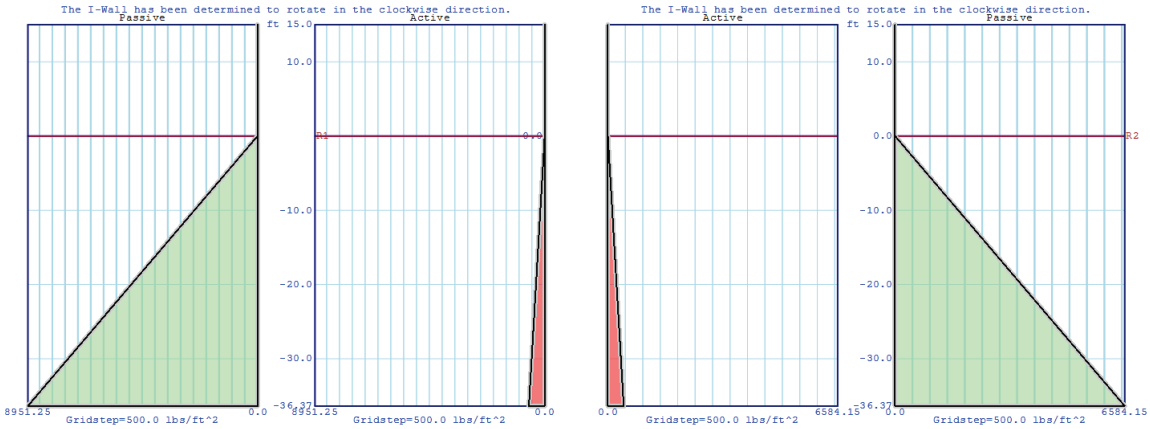

------------- Deterministic Analysis at Flood Elevation    11.12 ft -------------

 The I-Wall has been determined to rotate in the clockwise direction.

 Node Spacing =  1.00 ft
 Node Spacing =  0.99 ft
 Node Spacing =  0.98 ft
 Node Spacing =  0.97 ft

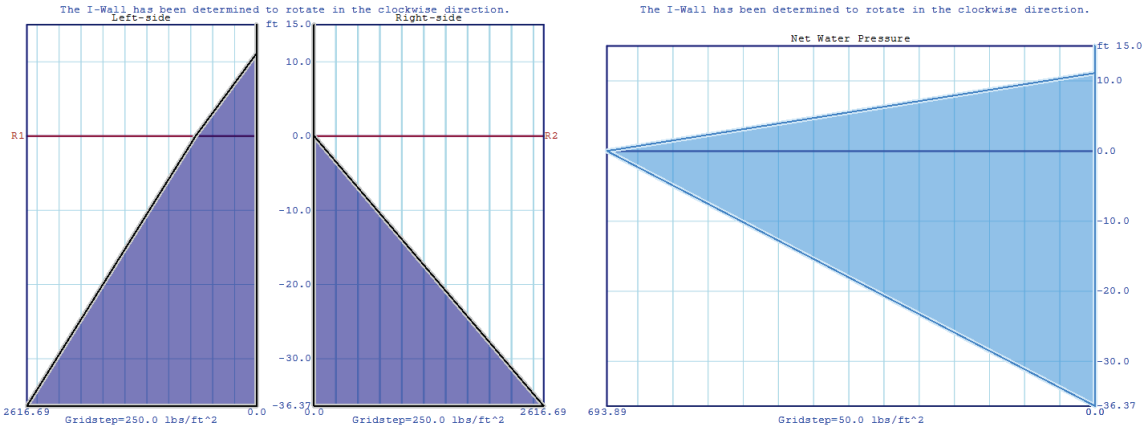
 Point of Rotation         =      -25.41 ft
 Elevation at tip of pile  =      -36.37 ft
 Gap depth                 =        0.00 ft
```

Figure 4.43. Active and passive earth pressures for drained shear strength. (a) LHS of wall. (b) RHS of wall.



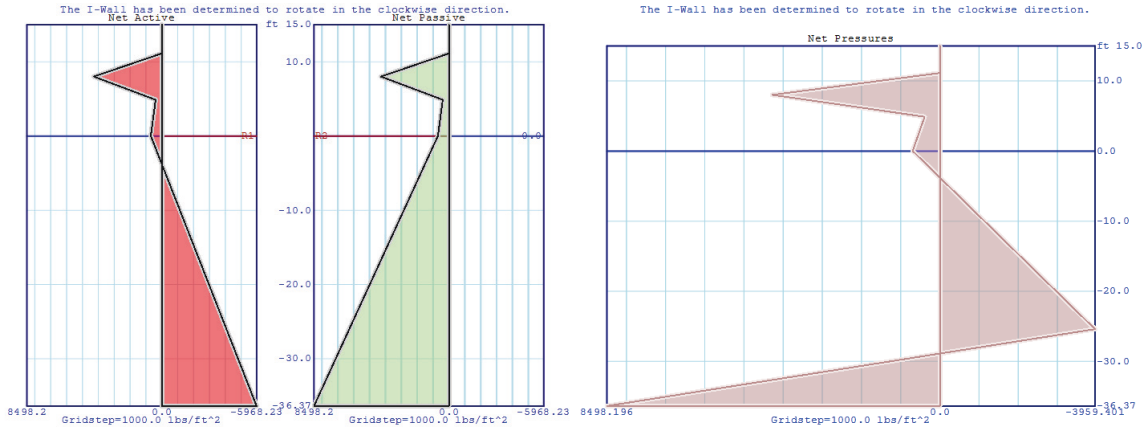
(a) (b)

Figure 4.44. Pore water pressures. (a) LHS and RHS of wall. (b) Net water pressures.



(a) (b)

Figure 4.45. Net pressures. (a) Net active and net passive. (b) Net pressure diagram.



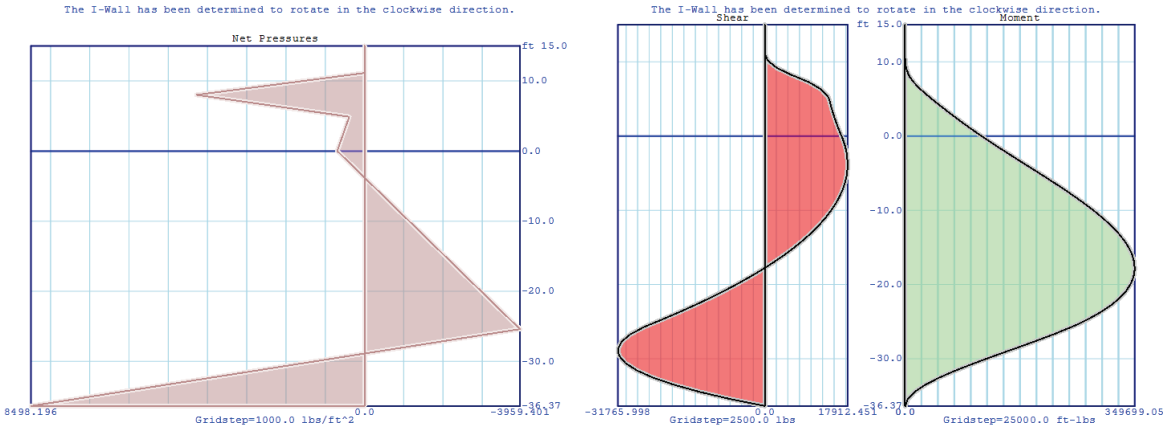
(a) (b)

The net pressure diagram of Figure 4.45b is derived from the replication of all values of the net active pressures, from the top of the wall until the elevation at the PR (at el -25.41 ft), at which instant the remaining values of the net pressure diagram are assumed to be linear with elevation between 1) the net active pressure value at the elevation of the PR, and 2) the net mobilized passive pressure at the elevation of the approximated sheet-pile tip (i.e., el -36.37).[1] Figure 4.45b is an illustration of how the net pressure diagram was formed. Because the I-Wall has been determined to rotate in a clockwise direction, the net pressure diagram of Figure 4.45b shows the net active pressures plotting on the LHS in the upper zone and on the RHS in the lower zone. The net passive pressures plot on the LHS of

[1] Thus, only one mobilized net passive pressure value in Figure 4.45a is used to construct the Figure 4.45b net pressure diagram, corresponding to the sheet-pile tip elevation at el -36.37 ft. The majority of the net pressure diagram is derived from the Figure 4.45a net active pressure diagram.

the sheet-pile wall. The final results are illustrated in Figure 4.46 by the presentation of the net pressure diagram Figures 4.46a (replica of Figure 4.45b) and 4.46b, the shear and moment diagrams.

Figure 4.46. (a) Net pressure diagram. (b) Shear and moment.



(a) (b)

Figure 4.46b shows that the maximum bending moment occurs at the zero crossing of the shear diagram. The maximum moment here is much higher than the previous example, with a value of 349.6 kip-ft. This value is much higher than the allowable bending moment of 76.1 kip-ft, therefore, the wall will yield under the specified wave and pressure loads. The sheet-pile tip elevation is computed at el -36.37 ft with a calculated depth of embedment of approximately 36.37 ft, which is more than twice the exposed height of 15 ft.

A diagram of drop in total head, with seepage around the sheet-pile wall, is given in Figure 4.47. To the left is a diagram of the wall showing the surface water, soil region surfaces, gap definition, wall depth, and the direction of seepage. The drop in total heads due to steady-state seepage is given in the right side plot. This plot follows the line of seepage along the wall, from one side to the other on the horizontal axis, and displays the head values on the vertical axis. The head loss occurs as water seeps from el 0.0, down the LHS foundation sands to the sheet-pile tip, and then up the RHS foundation sands to the ground surface (at el 0.0), this is shown in the blue line. Because this site possesses a homogeneous value of hydraulic conductivity, the Figure 4.47 head loss with distance is linear along the line of seepage.

Figure 4.47. Drop in total heads due to seepage diagram.

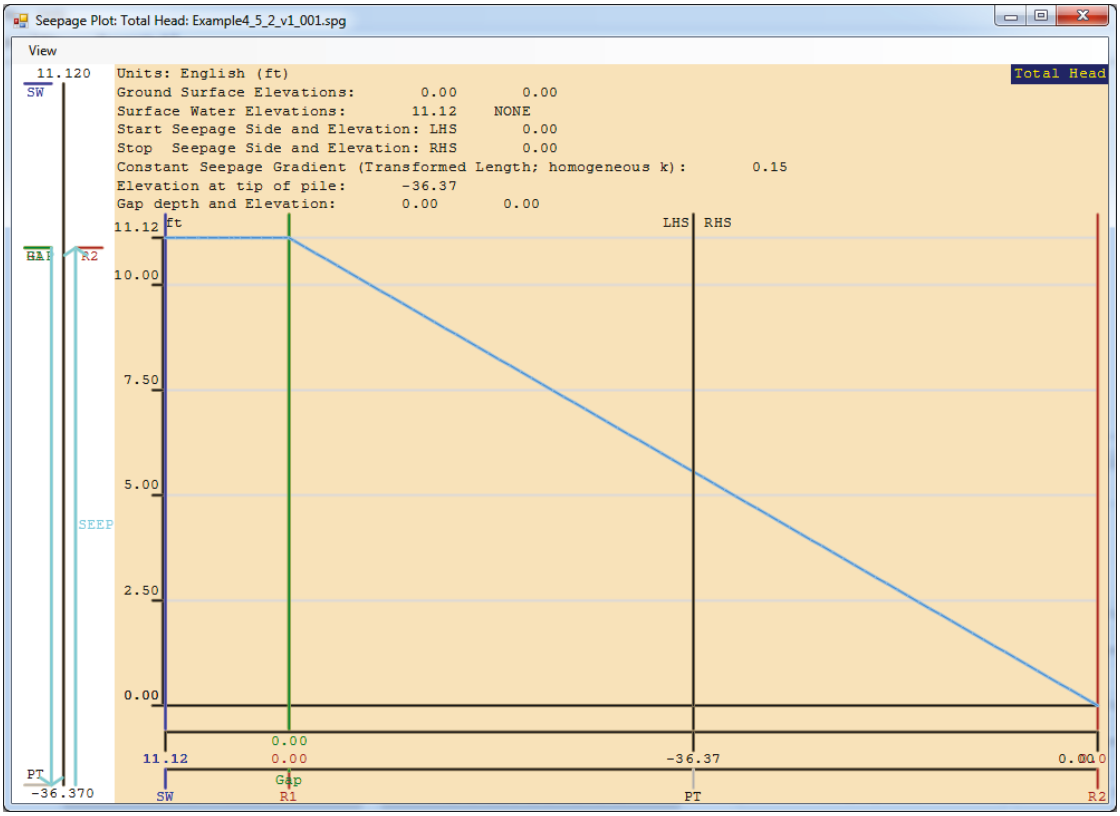


Table 4.16 shows a comparison of the results between the Coefficient Method and the Wedge Solution Method for Example Problem 4.5.2. The resulting elevations of the PR and the elevation of the fully embedded pile tip are very consistent, varying by under half a foot, for the two methods. This example problem uses seepage for the Coefficient Method of analysis only.

Table 4.16. Comparison of Earth Coefficient results to Wedge Solution Method results - Example 4.5.2.

Method	Point of Rotation (PR) (elevation in feet)	Pile Tip (elevation in feet)
Coefficient Method	-25.41	-36.37
Wedge Solution	-24.25	-36.3

4.5.3 Example 4.5.3 Coastal site including backfill

The third design problem for a coastal I-Wall is determining the depth of embedment for a 15 ft-high I-Wall in dense sand (at elevation 0.0 ft), with a berm constructed above the 0 ft ground surface on the RHS of the I-Wall. The placement of a berm is being investigated to counter the effect

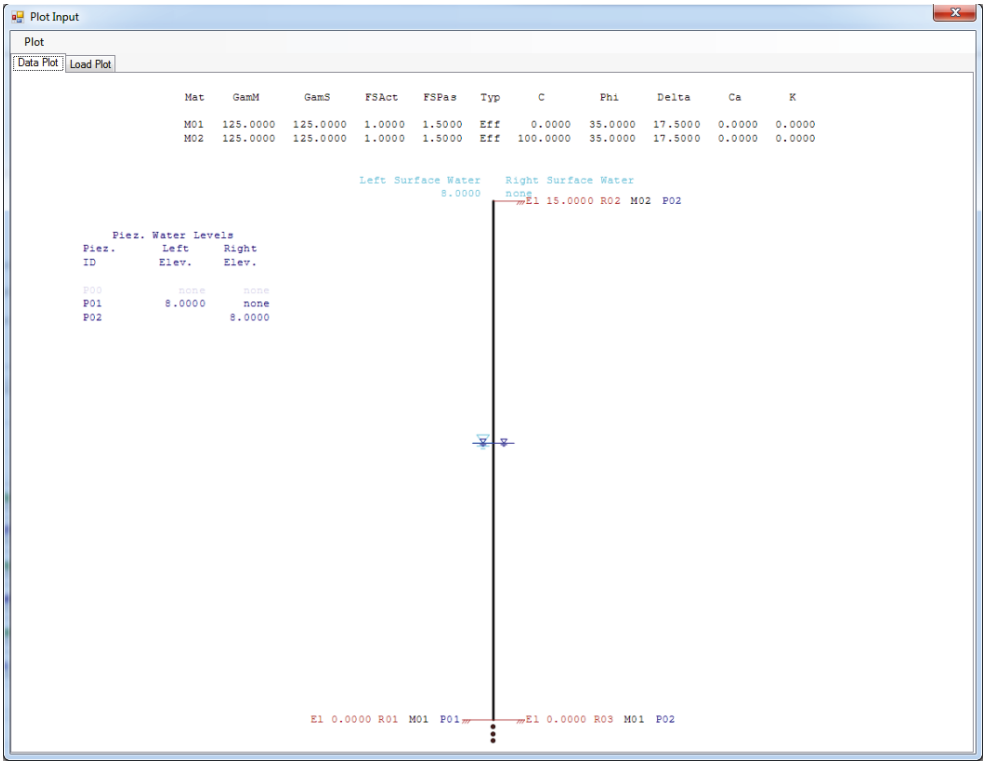
of the wave loading that was first introduced in the previous example. The calculations made in this example do not yet include the wave loading. The performances of the I-Wall and berm are being investigated first. The dense sand has an effective stress definition with no cohesion, an effective angle of internal friction of (φ′) of 35 degrees, a soil-to-sheet-pile effective interface friction angle (δ′) of 17.5 degrees (= φ′/2), and a hydraulic conductivity (K′) of 0.0000328 in all sand layers. The berm material consists of compacted dense sand with φ′ of 35 degrees, and an effective cohesion (c′) value of 100.0 lb/ft^2.

In this example problem, a Factor of Safety of 1.0 is assigned for computing the mobilized active earth pressures and a Factor of Safety of 1.5 is assigned for computing the mobilized passive earth pressures within the soil layers. This I-Wall system has an exposed height of 15 ft on the flood side. The water surfaces on both sides of the I-Wall are at 8 ft (flood side and landside). For this example, the flood side corresponds to the LHS of the I-Wall. In this analysis, it is assumed that the I-Wall will rotate counterclockwise due to the berm loading. The sand layers have an unsaturated and saturated unit weight of 125 pcf. With a berm effective cohesion (c′) of 100.0 psf, a gap can form, so hydraulic fracturing is enabled. Homogeneous seepage is allowed although seepage would not occur with coincident water levels.

Figure 4.48 outlines the basic geometry and structural parameters for the sheet-pile wall. As can be seen in Figure 4.48b, there are no external pressures (i.e., wave load) exerting on the RHS of the sheet-pile wall. A design computation run is performed to determine the embedment depth that will allow this wall to be stable for the required Factor of Safety applied to the passive earth pressures of the sand foundation (i.e., $FS_{Passive} = 1.50$).

The resulting depth of embedment is shown in Figure 4.49. The I-Wall becomes stable when the sheet-pile tip is embedded to el -11.51 ft, because the soil surface is defined at an elevation of 0.0 ft. This is a much lower required depth of embedment when compared with the results from Example 4.5.1 at el -15.79 ft, because the wall is supported on the landside by the berm, and by the surface water on the flood side. The point about which the wall will rotate is at el -9.75 ft below the ground surface.

Figure 4.48. Sheet-pile wall with berm on landside (RHS). (a) Schematic of sheet-pile wall in sand site. (b) Plot of external loads.

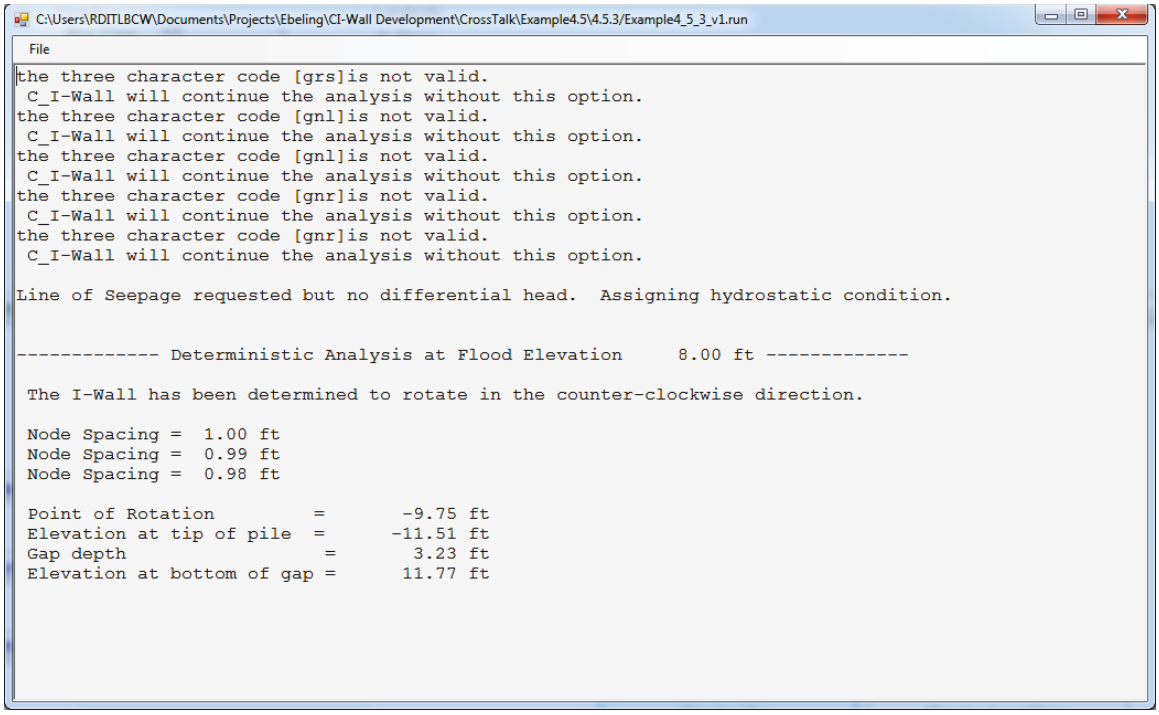


(a)



(b)

Figure 4.49. Corps_I-Wall run file for the specified input.

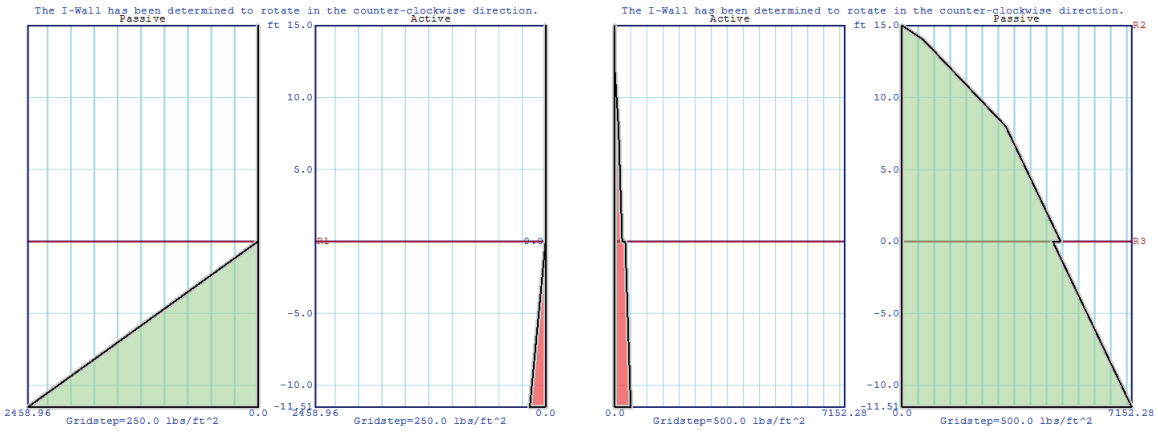


From the calculated pressures of Figures 4.50 and 4.51, both the net active and net passive pressures are constructed and presented in Figure 4.52a for the prescribed earth (berm) loading, and the I-Wall will rotate in a counter clockwise direction. The net active pressure is determined from the difference between the RHS-mobilized active earth pressure and the LHS-mobilized passive earth pressure (i.e., acting on the other side of the wall), with the addition of the net water pressures (zero in this case), and any external horizontal net pressures and overburden pressures (if any). The net passive pressure is determined by the difference between the RHS-mobilized passive earth pressure and the LHS-mobilized active earth pressure acting on the other side of the sheet-pile wall, with the addition of any net water pressures, any external horizontal net pressures, and overburden pressures (if any). Both the calculated net active and net passive pressures above the ground surface el 0.0 (and above R01 and R02) of Figure 4.52 are solely derived from the net active soil pressures of Figure 4.52a.

The net pressure diagram of Figure 4.52b is derived from the replication of all values of the net active pressures, from the top of the wall until the elevation at the PR (at el -9.75 ft), at which instant the remaining values of the net pressure diagram are assumed to be linear with elevation between 1) the net active pressure value at the elevation of the PR, and 2) the net

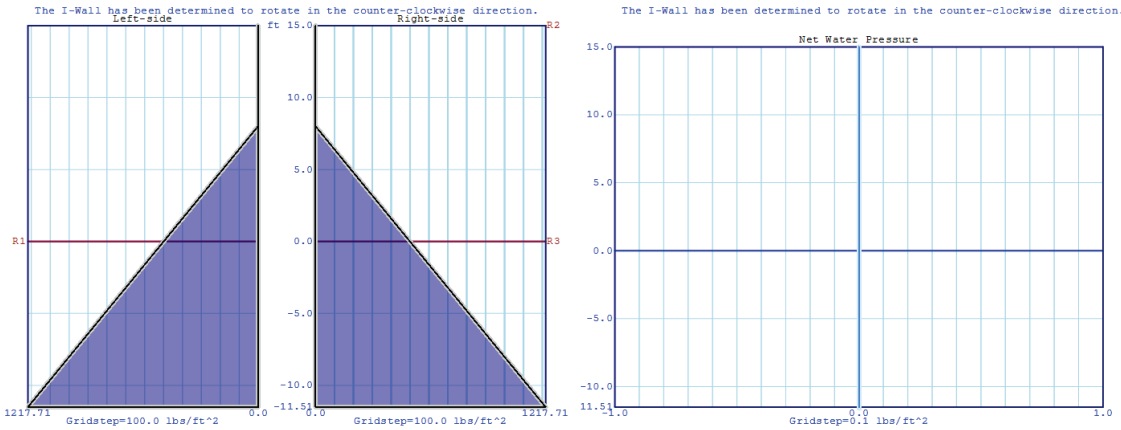
mobilized passive pressure at the elevation of the approximated sheet-pile tip (i.e., el -11.51).[1] Figure 4.52b is an illustration of how the net pressure diagram was formed. Because the I-Wall has been determined to rotate in a clockwise direction, the net pressure diagram of Figure 4.52b shows that in the upper zone the net active pressures plot on the RHS, and on the LHS in the lower zone. The net passive pressures plot on the RHS of the sheet-pile wall. The final results are illustrated in Figure 4.53 by the presentation of the net pressure diagram Figures 4.53a (replica of Figure 4.52b) and 4.53b, the shear and moment diagrams.

Figure 4.50. Active and passive earth pressures for drained shear strength. (a) LHS of wall. (b) RHS of wall.



(a) (b)

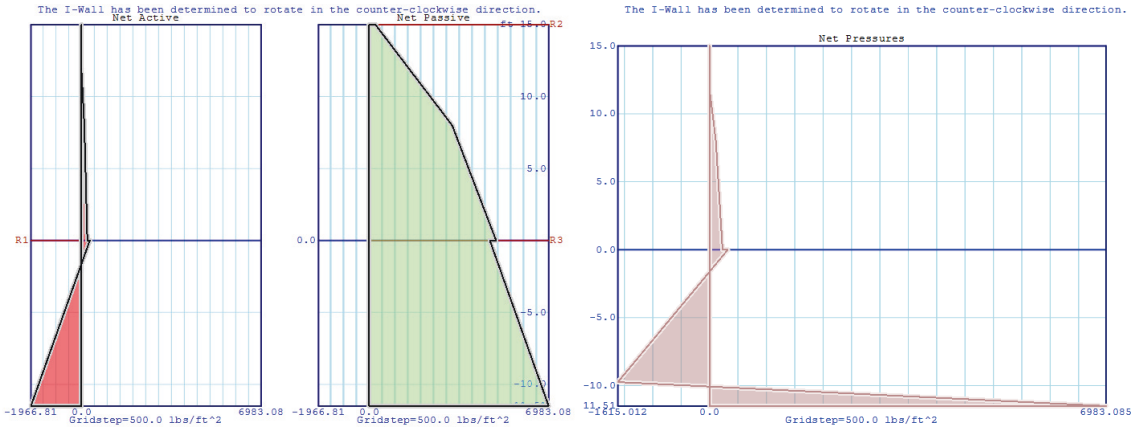
Figure 4.51. Pore water pressures. (a) LHS and RHS of wall. (b) Net water pressures.



(a) (b)

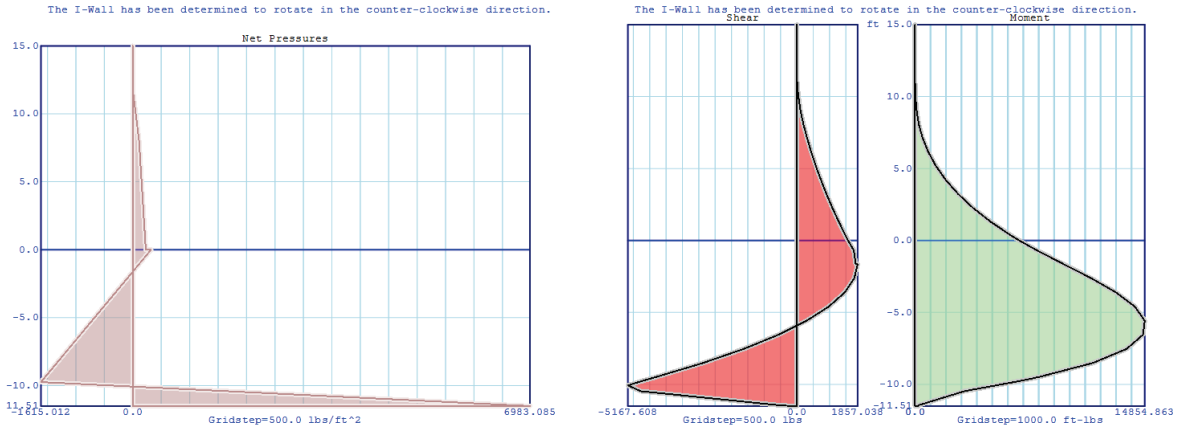
[1] One mobilized net passive pressure value in Figure 4.52a is used to construct the Figure 4.53a net pressure diagram, corresponding to the sheet-pile tip elevation at el -11.51 ft. The majority of the net pressure diagram is derived from the Figure 4.52a net active pressure diagram.

Figure 4.52. Net pressures. (a) Net active and net passive. (b) Net pressure diagram.



(a) (b)

Figure 4.53. (a) Net pressure diagram. (b) Shear and moment.



(a) (b)

Figure 4.53b shows that the maximum bending moment occurs at the zero crossing of the shear diagram. The maximum moment has a value of 14.8 kip-ft, which is much less than the allowable bending moment of 76.1 kip-ft. The sheet-pile tip elevation is computed at el -11.51 ft with a calculated depth of embedment of approximately 11.51 ft.

Because the water elevations are the same for the flood side and landside of the wall, the net water pressures, and therefore seepage, are 0.0. Seepage calculations are automatically stopped in Corps_I-Wall when this condition occurs and the problem is run with hydrostatic conditions.

Table 4.17 shows a comparison of the results between the Coefficient Method and the Wedge Solution Method for Example Problem 4.5.3. The resulting elevations of the PR and the elevation of the fully embedded pile tip are nearly identical for the two methods.

Table 4.17. Comparison of Earth Coefficient results to Wedge Solution Method results - Example 4.5.3.

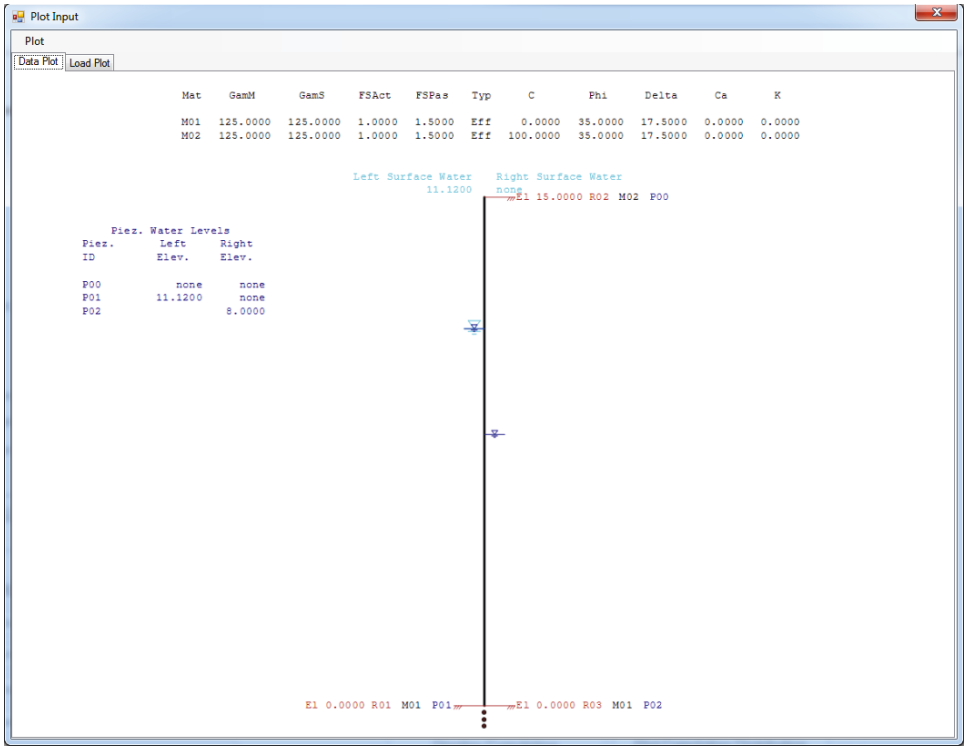
Method	Point of Rotation (PR) (elevation in feet)	Pile Tip (elevation in feet)	Gap (depth, feet)	Gap (elevation, feet)
Coefficient Method	-9.75	-11.51	3.23	11.77
Wedge Solution	-9.75	11.50	3.07	11.93

4.5.4 Example 4.5.4 coastal site including backfill with surge loading

The fourth design problem for a coastal I-Wall is determining the depth of embedment for an I-Wall with a 15 ft height that is exposed to surge loading. The I-Wall is founded in dense sand (at elevation 0.0 ft) (Figure 4.54) and has a retaining berm on the RHS of the I-Wall. The intent of the berm is to counter the detrimental effects of wave loading. The dense sand at 0.0 elevation and below has an effective stress definition with no effective cohesion, an effective angle of internal friction of (φ') of 35 degrees, a soil-to-sheet-pile effective interface friction angle (δ') of 17.5 degrees (= $\varphi'/2$), and a hydraulic conductivity (K′) of 0.0000328 ft/sec in all sand layers. In this example problem, a Factor of Safety of 1.0 is assigned for computing active earth pressures and a Factor of Safety of 1.5 is assigned for computing passive earth pressures within the soil layer. The sand layers are unsaturated (not used in the analysis) and saturated unit weights of 125 pcf. The compacted dense sand that forms the berm on the landside of the I-Wall has an effective cohesion (c′) of 100.0 psf, so hydraulic fracture option is enabled. Homogeneous seepage is also allowed.

The flood side corresponds to the LHS of the I-Wall. The water surface on the LHS of the I-Wall is determined by the possible surge wave size calculation in Appendix F, and detailed in Example 4.5.2 using the Minikin formulation for breaking waves. Because the swell height is the elevation of the average still-water level added to half of the breaking wave height (~6.24 ft from Equation F.2 and Table F.3), the water level on the flood side is set equal to the swell height of 8 ft +3.12 ft = 11.12 ft on the flood side and 0 ft landside. The additional horizontal pressure due to the motion of the wave is accounted for by having a triangular horizontal pressure distribution that ranges from 0.0 lb/ft^2 at 11.12 ft to a maximum pressure of 4,084.6 lb/ft^2 (computed using equation F.4) at 8 ft to 0.0 lb/ft^2 at 4.88 ft (8 ft - 3.12 ft). In this analysis, it is assumed that the I-Wall will rotate clockwise during flood and surge loading. However, this is not guaranteed and, as will be discussed, the wall was found to show no rotation.

Figure 4.54. Sheet-pile wall with berm on landside (RHS). (a) Schematic of sheet-pile wall in sand site. (b) Wave load applied to flood side (LHS) of sheet-pile wall.



(a)



(b)

Figures 4.55 and 4.56 show the results from the run specified, given seepage for an assumed clockwise I-Wall rotation. For this example, the RHS-mobilized passive earth pressure forces balance the LHS net water and dynamic forces, meaning that the I-Wall does not have to resist any of the applied forces through a transfer of loading into the foundation via bending of the sheet-pile. The I-Wall is simply a separator between the RHS soil berm and the LHS water loading. In this situation, the computed Factor of Safety for the structure becomes higher than the required value of 1.5 for the passive earth pressure region, and there is no means to compute a sheet-pile tip elevation because the I-Wall is held in place by the water pressure on one side, and the earth loading provided by the berm on the other side. In practical terms, it is sufficient to build the wall to the depth for normal water levels (Example 4.5.3) because the wall is superfluous when wave loading is applied. The sheet-pile wall does serve the purpose to prevent soil erosion due to wave action applied to the earthen berm.

Figure 4.55. Corps_I-Wall run file for the specified input (with seepage enabled).

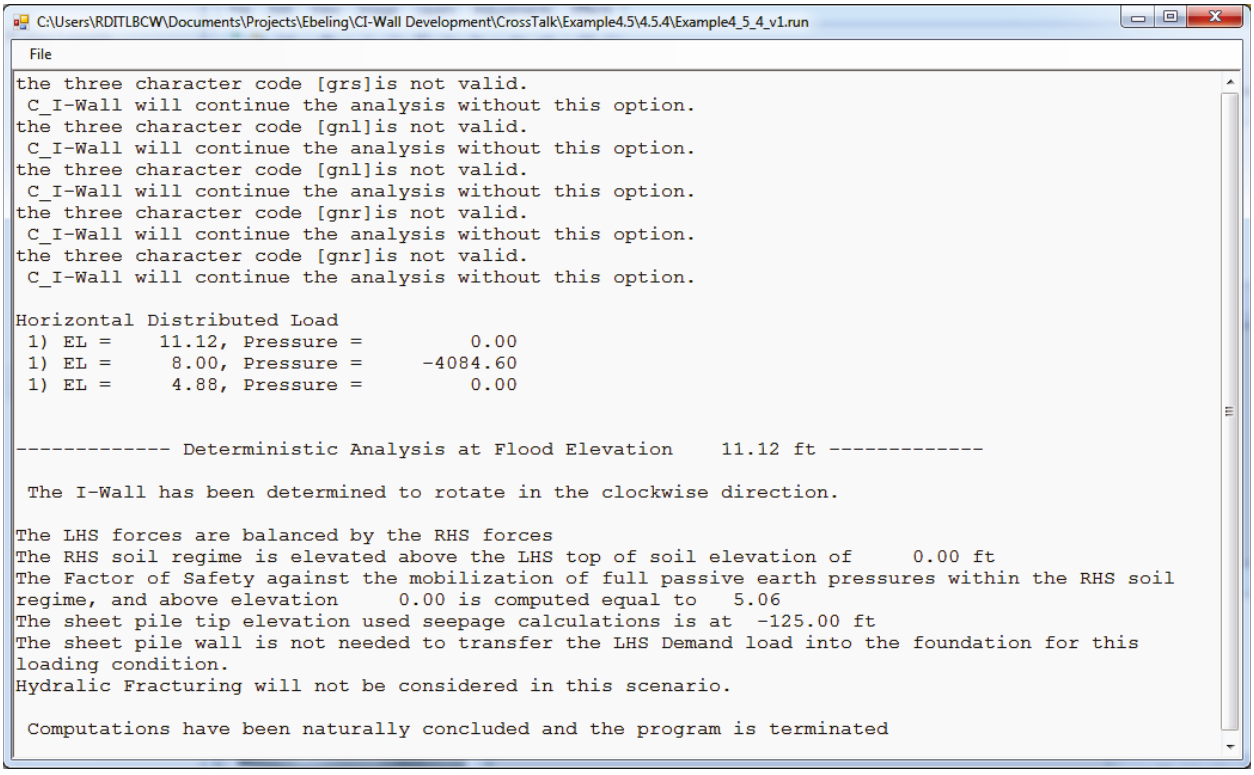


Figure 4.56. Corps_I-Wall run file for the specified input (without seepage).

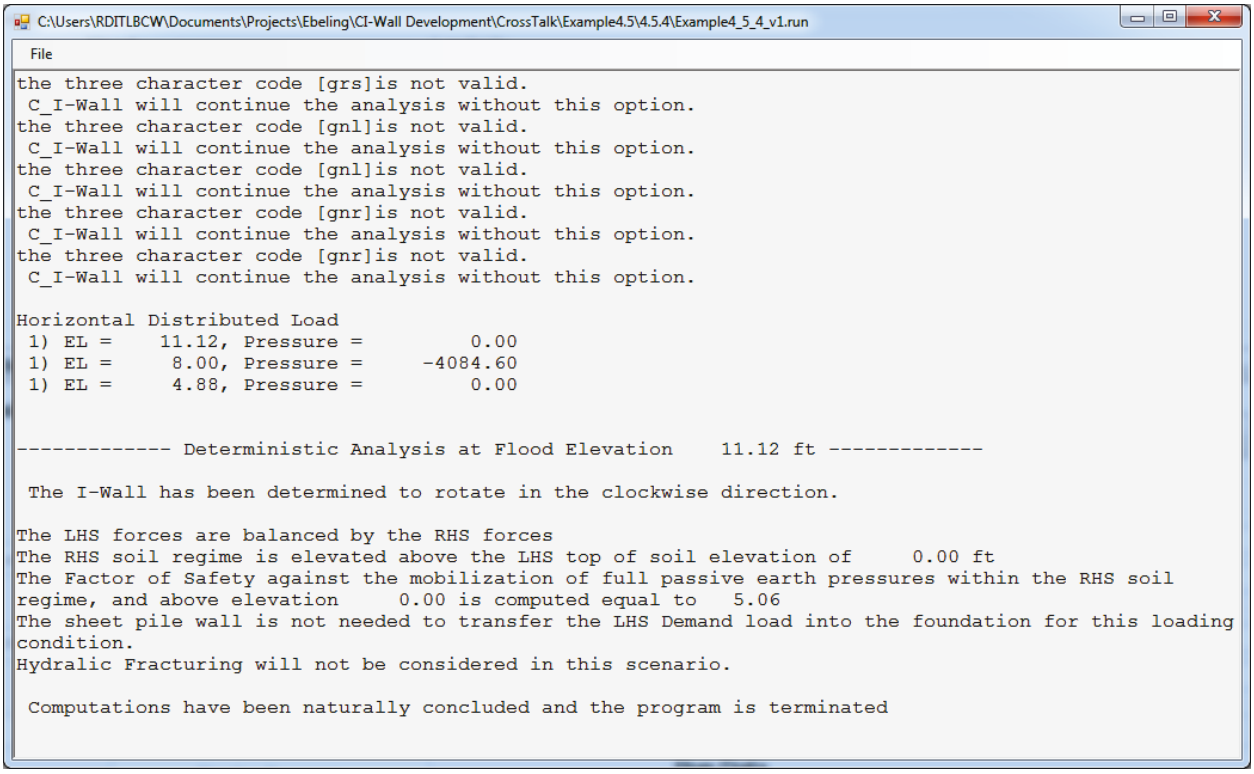


Table 4.18 shows a comparison of the results between the Coefficient Method and the Wedge Solution Method for Example Problem 4.5.4. The resulting elevations of the PR and the elevation of the fully embedded pile tip are not needed because the wall is stable for both solutions.

Table 4.18. Comparison of Earth Coefficient results to Wedge Solution Method results - Example 4.5.3.

Method	Point of Rotation (PR) (elevation in feet)	Pile Tip (elevation in feet)	Gap (depth, feet)	Gap (elevation, feet)
Coefficient Method	N/A (wall is stable)	N/A (wall is stable)	N/A (wall is stable)	N/A (wall is stable)
Wedge Solution	N/A (wall is stable	N/A (wall is stable	N/A (wall is stable	N/A (wall is stable

4.5.5 Comparison and interpretation of backfill with surge loading

Figure 4.57 shows the loads that are acting on the I-Wall of Example 4.5.4, which is expected to rotate clockwise about a point at, or below the datum elevation. This model is for pseudostatic wave pressures acting on the I-Wall. Hand calculations can be performed to confirm the calculations made by Corps_I-Wall that determine the Factor of Safety for the I-Wall.

In order for the I-Wall to be unengaged, the net moment acting on the wall must be 0.0 ft-lb with a Factor of Safety greater than 1.5.

Two hydrostatic water pressures act on the wall, the pressure due to the landside piezometric water level at elevation 8 ft above the datum, and the flood side water level determined by applying the Minikin method as an elevation of 11.12 ft. The pressures from both sides are given in Table 4.19. These hydrostatic pressures are added to form the net hydrostatic water pressures, as detailed in Table 4.20.

The dynamic water pressures resulting from the moving water in the wave colliding with the I-Wall is calculated by the Minikin method. These values are shown in Table 4.21.

Figure 4.57. Representation (not to scale) of both the water and earth pressures acting on the I-Wall in Example 4.5.4.

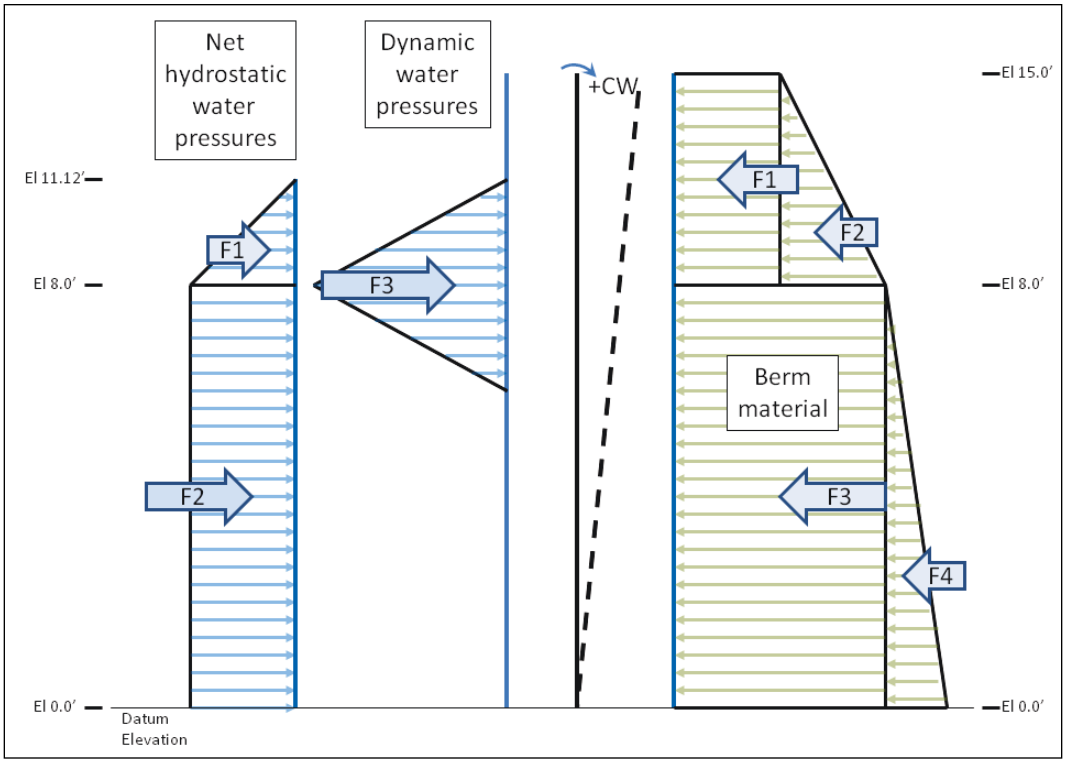


Table 4.19. Hydrostatic pressures with elevations from the site.

Hydrostatic Water Pressures			
Left-Hand Side (LHS)		Right-Hand Side (RHS)	
Elevation (ft)	Pressure (psf)	Elevation (ft)	Pressure (psf)
11.12	0.00		
8.0	194.69	8.0	0
0.0	693.89	0.0	499.2

Table 4.20. Combining the LHS and RHS hydrostatic pressures to get the net pressure.

Net Hydrostatic Water Pressure (Applied as water pressure on the LHS side)		
Elevation (ft)	Depth (ft)	Pressure (psf)
11.12	0.0	0.00
8.0	3.12	194.69
0.0	11.12	194.69

Table 4.21. Dynamic water pressures with elevations calculated with the Minikin method.

Dynamic Water Pressures (Applied as water pressure on the LHS)		
Elevation (ft)	Depth (ft)	Pressure (psf)
11.12	0.0	0.00
8.0	3.12	4,084.60
4.88	6.24	0.00

Figure 4.57 gives a representation (not to scale) of these pressures acting on the LHS of an I-Wall. These pressures can be represented as a set of resultant forces (F1, F2, and F3) acting at locations shown along the wall for determining the moment at the datum of the wall with elevation 0.0 for this example. The resulting forces and resultant moments are given in Table 4.22.

Table 4.22. Forces and moments calculated from water pressure distributions at the datum elevation.

	Force (lb)	Moment Arm (ft)	Moment (ft-lb)
F1	303.71	9.04	2,745.57
F2	1,557.50	4.0	6,230.02
F3	12,743.95	8.0	101,951.60
Sum_f	14,605.16	Sum_m	110,927.19

Assuming a clockwise rotation, the RHS berm material properties must be taken into account to determine the mobilized passive earth pressures, the resulting forces, and moments acting as "passive" resistance to the water pressures on the LHS of the wall. In this example problem, a Factor of Safety of 1.0 is assigned for computing active earth pressures, and a Factor of Safety of 1.5 is assigned for computing passive earth pressures within the soil layer. This I-Wall system has an exposed height of 15 ft on the flood side. In this analysis, it is assumed that the I-Wall will rotate clockwise due to the wave loads. The sand layers have an effective angle of internal friction of (φ') of 35 degrees, a soil-to-sheet-pile effective interface friction angle (δ') of 17.5 degrees (= $\varphi'/2$), a hydraulic conductivity (K') of 0.0000328 ft/sec, ground surface slope (β) of 0.0 degrees, and unsaturated and saturated unit weights of 125 pcf. With a berm effective cohesion (c') of 100.0 psf, a gap can be formed, so hydraulic fracturing is enabled.

The resisting moment provided by the earth retaining structural berm can meet or exceed the driving moment caused by flood water pressures on the wall. If this occurs, the wall serves only to provide erosion protection for the berm, and does not need to provide moment or force resistance.

In order to determine the resisting moment provided by the earth retaining structural berm, the Factor of Safety (passive) is applied to the berm's material properties. The LHS driving moment of the flood water pressures, and the RHS resisting moment provided by the berm are computed.

If the resisting moment, which is acting in the opposite direction as the driving moment is less than the driving moment, then the I-Wall must also add its resistance (through a transfer of loading into the foundation soils) to counteract the driving moment of the water loading. If the resisting moment is greater than the driving moment, then the Factor of Safety (passive) can be raised iteratively, resulting in different computed values for the mobilized berm material properties until the resisting moment is virtually equivalent to the driving moment.

The Factor of Safety is applied to the material properties in the following ways to determine the actual mobilized passive earth pressure properties:

$$c'_{mobilized} = \frac{c'}{FS_{passive}} \tag{4.5}$$

$$\tan \varphi'_{mobilized} = \frac{\tan \varphi'}{FS_{passive}} \tag{4.6}$$

$$\tan \delta'_{mobilized} = \frac{\tan \delta'}{FS_{passive}} \quad (4.7)$$

From Coulomb's equation, the passive earth pressure coefficient is

$$K_p = \frac{\cos^2(\varphi'_{mobilized})}{\cos(\delta'_{mobilized})\left[1-\sqrt{\frac{\sin(\varphi'_{mobilized}+\delta'_{mobilized})\sin(\varphi'_{mobilized})}{\cos(\delta'_{mobilized})}}\right]} \quad (4.8)$$

For a Factor of Safety (passive) of 1.5, the mobilized material values are

$$c'_{mobilized} = 66.67\ psf$$

$$\varphi'_{mobilized} = 25.02\ deg$$

$$\delta'_{mobilized} = 11.87\ deg$$

The RHS earth pressures can be computed based on Coulomb's equation, as shown in Table 4.23.

Table 4.23. Determining earth pressures on the RHS of the wall with Factor of Safety 1.5.

RHS Earth Pressures				$K_p * \sigma_{v'} + 2c'_{mobilized}\sqrt{K_p}$	$\sigma_{p_{mob}} * \cos \delta'_{mobilized}$
Elevation (ft)	Depth (ft)	$\sigma_{v'}$ (psf)	$K_p * \sigma_{v'}$ (psf)	$\sigma_{p_{mob}}$ (psf)	$horz_{\sigma_{p_{mob}}}$ (psf)
15	0	0.0	0.00	248.94	243.62
8	7	875.0	3,050.16	3,299.10	3,228.54
0	15	1,375.8	4,795.89	5,044.83	4,936.94

These pressures are trapezoidal, as shown in the RHS pressures in Figure 4.57. Each pressure trapezoid can be divided into rectangular and right triangular distribution, resulting in easier calculations for the equivalent acting force and its moment arm to the datum. For the Factor of Safety (passive) of 1.5, the resulting forces and moment are shown in Table 4.24.

Table 4.24. Forces and moments acting on the RHS of the wall with Factor of Safety 1.5.

	Force (lb)	Lever arm (ft)	Moment (ft-lb)
F1	1,705.32	11.50	19,611.15
F2	10,447.24	10.33	107,954.83
F3	25,828.34	4.00	103,313.37
F4	6,833.60	2.67	18,222.95
Sum_f	44,814.51	Sum_m	249,102.30

For the Factor of Safety (passive) of 1.5, the total moment at the datum (i.e., el 0.0) is much higher due to cumulative effects of the earth pressure distribution on the RHS of the retaining structure (249,102.30 ft-lb) than the total driving moment due to water pressures (110,927.19 ft-lb). In this case, the Factor of Safety (passive) can be iterated to find the case at which the moments are virtually equivalent.

When the Factor of Safety (passive) is set equal to 3.7581, the moments on both sides of the wall are virtually equivalent at 110,900 ft-lb. The results are shown in Tables 4.25 and 4.26, and are consistent with the Corps_I-Wall computations.

Table 4.25. Determining earth pressures on the RHS of the wall with Factor of Safety 3.7581.

RHS Earth Pressures				$K_p * \sigma_{v'} + 2c'_{mobilized}\sqrt{K_p}$	$\sigma_{p_{mob}} * \cos \delta'_{mobilized}$
Elevation (ft)	Depth (ft)	$\sigma_{v'}$ (psf)	$K_p * \sigma_{v'}$ (psf)	$\sigma_{p_{mob}}$ (psf)	$horz_{\sigma_{p_{mob}}}$ (psf)
15	0	0.0	0.00	67.24	243.62
8	7	875.0	1,396.92	1,464.17	3,228.54
0	15	1,375.8	2,196.44	5,044.83	2,263.69

Table 4.26. Forces and moments acting on the RHS of the wall with Factor of Safety 3.7581.

	Force (lb)	Lever arm (ft)	Moment (ft-lb)
F1	469.05	11.50	5,394.07
F2	4,872.12	10.33	50,345.23
F3	11,672.33	4.00	46,689.31
F4	3,186.88	2.67	8,498.35
Sum_f	20,200.38	Sum_m	110,926.97

For a Factor of Safety (passive) of 3.7581, the mobilized material values are:

$$c'_{mobilized} = 26.67\ psf$$

$$\varphi'_{mobilized} = 10.58\ deg$$

$$\delta'_{mobilized} = 4.81\ deg$$

In summary, the 15 ft-high soil berm resists the applied wave loading force. The sheet-pile wall is not needed to transfer the applied loading into the foundation through bending action. The sole purpose of the presence of the I-Wall in this case would be to protect the berm soil from erosion due to wave action.

The earth pressure relationships implemented in Corps_I-Wall, Version 1.0, are for level ground conditions. The lateral extent needed at the top of the RHS berm is approximated using the planar Rankine passive earth pressure's slide plane relationship of

$$\alpha_{mobilized} = 45° - \frac{\varphi'_{mobilized}}{2} \tag{4.9}$$

For a Factor of Safety (passive) of 3.7581, this angle would be computed as

$$\alpha_{mobilized} = 45° - \frac{10.58°}{2} = 39.71 \tag{4.10}$$

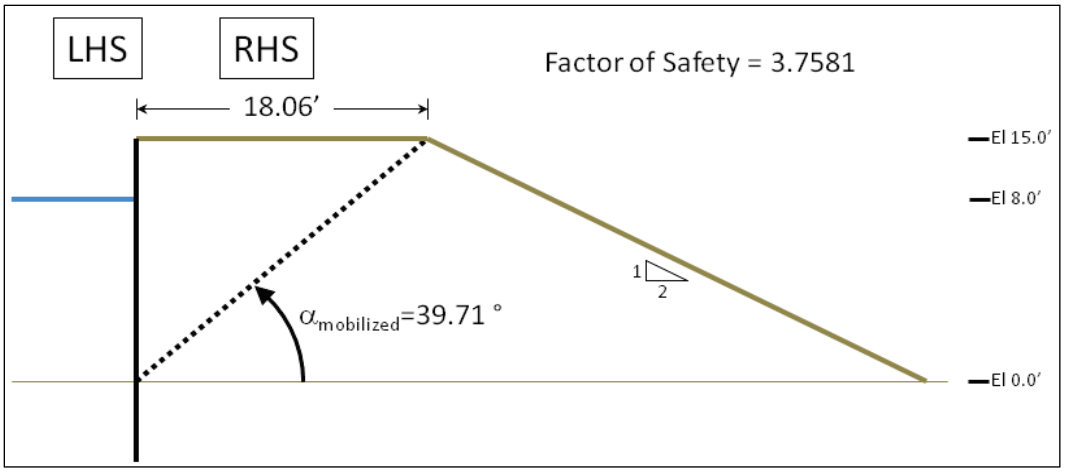
The lateral extent for the top of a berm with an elevation of 15 ft would be

$$extent = \frac{15\ ft}{\tan 39.71°} = 18.06\ ft \tag{4.11}$$

And, with a rise over run for the advancing slope of 1 to 2, the berm would extend another 30 ft, as shown in Figure 4.58.

The next stage of the analysis would be an investigation to reduce the required height of the berm because a $FS_{Passive}$ equal to 3.76 is larger than what is normally required. Reducing the height of berm may require the I-Wall to be engaged, and some of the applied loading may be transferred into the foundation through bending action of the sheet-piling.

Figure 4.58. Results of lateral berm extent calculations for a 15-ft-high berm and a Factor of Safety (passive) within the berm of 3.7581.



4.6 Example 4.6 comparison to Corps_I-Wall results contained within other technical publications (Das 2007; Bowles 1968; Pace et al. 2012)

This section discusses Corps_I-Wall results when compared with design problems from Das (2007), Bowles (1968), and Pace et al. (2012) for the determination of the depth of embedment. An effective stress definition of granular soils, a total stress definition with undrained shear strength, S_u, for clays, and a mixture of sand above saturated clays constitute the various design problems analyzed. The Das (2007) example problems of Sections 4.6.1 and 4.6.2 include granular soils and sandy soils over saturated clay. Bowles (1968) has similar examples in Sections 4.6.3 and 4.6.4. Bowles (1968), Section 4.6.5, examines a total stress definition of clays and the evaluation of gap depth from hydraulic fracturing.

4.6.1 Example 4.6.1 sheet-pile wall penetrating sand (Das 2007)

To determine the depth of embedment of sheet-pile walls in granular soil, Figure 4.59 is examined. This example problem (Das 2007) represents the case of homogeneous sandy soil below the dredge line on the flood side (LHS), and retained above the dredge line on the landside (RHS) of the sheet-pile wall. The dense sand has an effective stress definition with no cohesion and an effective angle of internal friction (φ′) of 40 degrees. The sand layers are assigned a moist unit weight of 120 pcf and a saturated unit weight of 129.4 pcf. Hydrostatic water pressures are at el 20 ft on both sides of the sheet-pile wall. For the Das (2007) calculation steps in a CI-wall *Design* mode, the specified Factors of Safety on both the active and

passive pressures are assigned 1.0.[1] An effective angle of wall to soil interface friction (δ′) of 0 degrees and the Coulomb Coefficient Method of analysis (for K_a and K_p) form the basis for this example[2]. Hydraulic fracturing is not included as an option for this analysis. The Corps_I-Wall representation of this problem is presented by the schematic of Figure 4.60. This figure outlines and describes the geometry and structural parameters for the sheet-pile wall.

This analysis resulted in a computed mobilized active earth pressure coefficient (K_a) of 0.2174 and a mobilized passive pressure coefficient (K_p) of 4.5989. Figure 4.61 displays the results obtained from this analysis with the sheet-pile tip elevation computed at el -21.64 ft for a calculated depth of embedment of 21.64 ft. The final results for this Example 4.6.1 has been recorded as check problem 1 in Table 4.27.

The distribution of active and passive earth pressures for both sides of the sheet-pile wall are illustrated in Figures 4.62a and 4.62b. The hydrostatic water pressures acting on both sides of the sheet-pile wall are shown in Figure 4.63a, with the resultant net water pressure calculated by taking the difference between the water pressures acting on both sides of the wall. In the case when the piezometric surface elevation is equal to the surface water elevation, no resultant net water pressure will be calculated (as shown in Figure 4.63b).

[1] Assigning a value for $FS_{Passive}$ of 1.0 is not consistent with Corps design criteria.

[2] For no soil-to-I-Wall interface friction (i.e., δ = 0 deg), the Coulomb solution for both active and passive earth pressure coefficients corresponds to the Rankine earth pressure coefficients.

Figure 4.59. Sheet-pile wall penetrating sand.

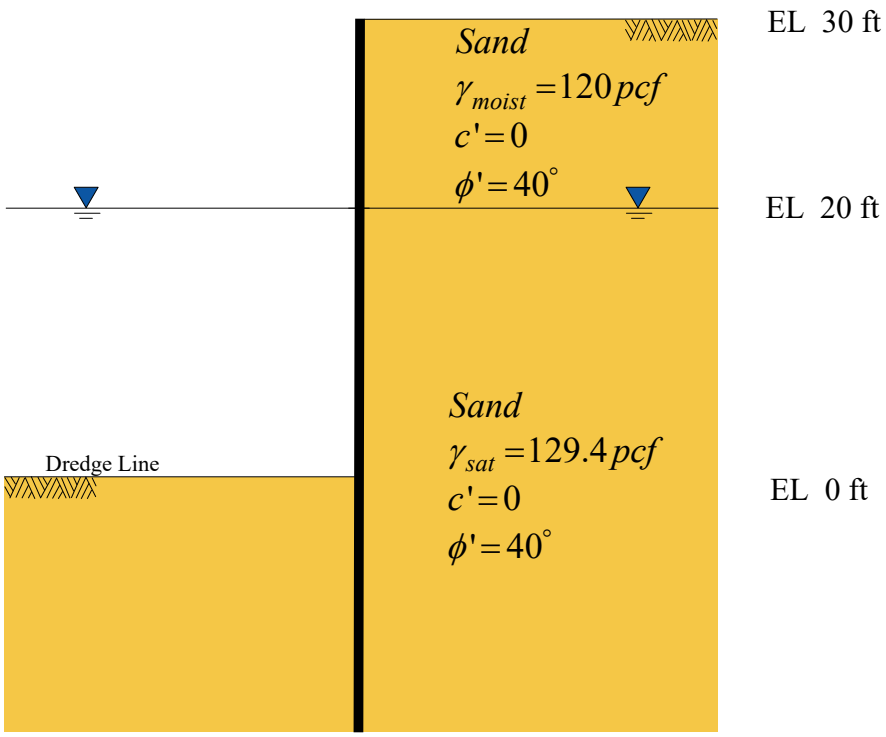


Figure 4.60. Corps_I-Wall schematic of sheet-pile wall in sand site.

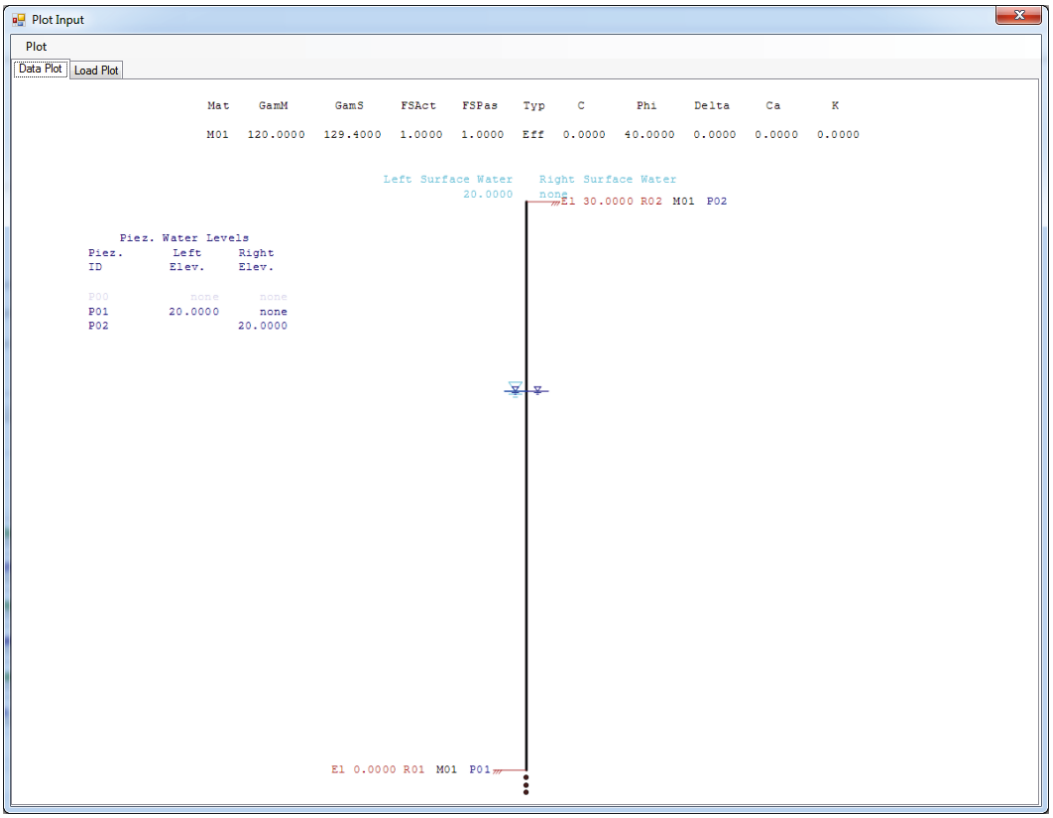


Figure 4.61. Corps_I-Wall output information.

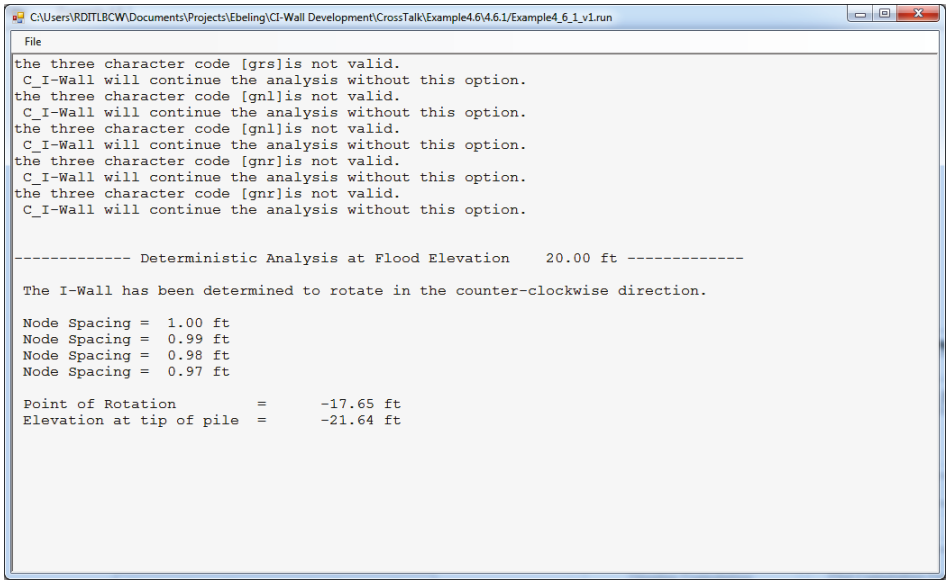
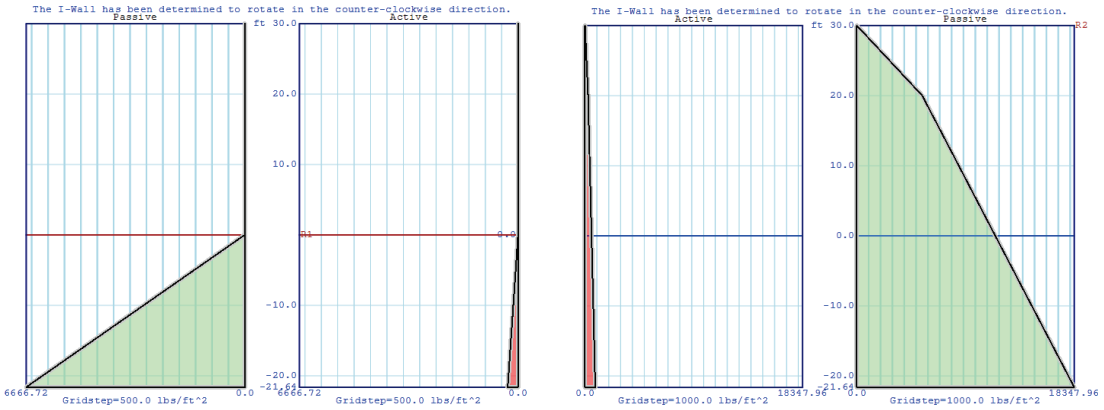
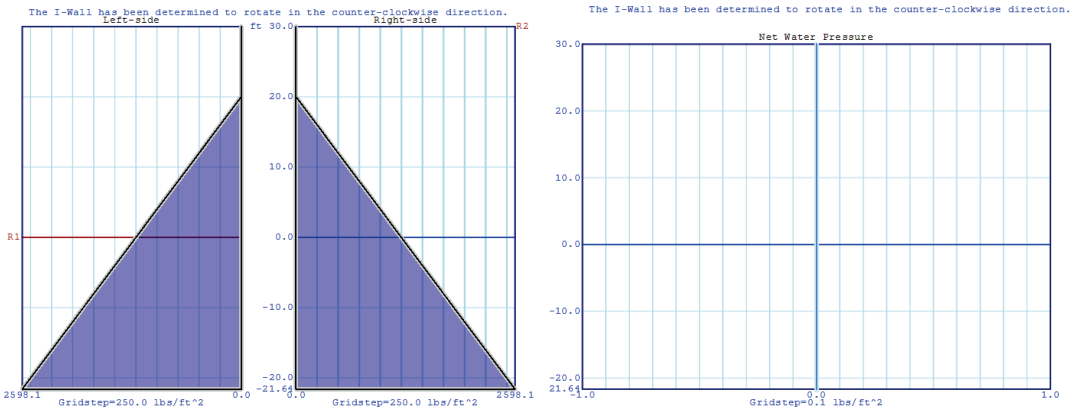


Figure 4.62. Active and passive earth pressures for drained shear strength. (a) LHS. (b) RHS.



(a) (b)

Figure 4.63. Hydrostatic water pressures. (a) LHS and RHS of wall. (b) Net water pressures.



(a) (b)

Table 4.27. Comparisons of I-Wall results contained within Das (2007).

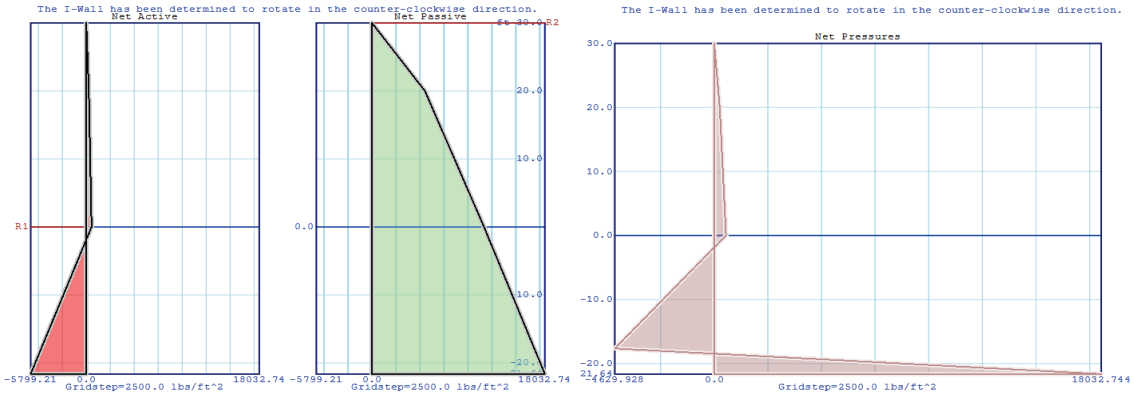
Check Problem	Das (2007) Principles of Foundation	Layer No.	Layer Soil Type	γ Moist	γ Sat	φ′ (deg)	c′ (psf) or (kN/m²)	Point of Rotation				Sheet-pile tip		Unit
								EL		z		EL		
				(pcf) or (kN/m³)				Reference	Corps_I-Wall	Reference	Corps_I-Wall	Reference	Corps_I-Wall	
1	9-1	1	Sand	120	129.4	40	0	-17.81	-17.65	4.07	3.99	-21.88	-21.64	ft
2	9-2	1	Sand	15.9	19.33	32	0	-0.96	-0.87	1.17	1.27	-2.13	-2.14	m
		2	Clay	15.9	19.33	0	47							

Reference is Das (2007) principles of foundation for check problems 1 and 2. Corps_I-Wall has an active Factor of Safety of 1.0 and a passive Factor of Safety of 1.0. Check problem 1 is in English units and check problem 2 is in metric.

From these pressures (Figures 4.62 and 4.63), both the net active and net passive pressures are constructed and presented in Figure 4.64a. For the applied flood loading, the I-Wall will rotate counterclockwise. The net active pressure is determined from the difference between the RHS-mobilized active earth pressure, and the LHS-mobilized passive earth pressure (i.e., acting on the other side of the wall), with the addition of any net water pressures and any external horizontal net pressures and overburden pressures (if any). The net passive pressure is determined by the difference between the RHS-mobilized passive earth pressure and the LHS-mobilized active earth pressure acting on the other side of the sheet-pile wall, with the addition of any net water pressures and any external horizontal net pressures and overburden pressures (if any).

The net pressure diagram of Figure 4.64b is derived from the replication of all values of the net active pressures, from the top of the wall until the elevation at the PR (el -17.65 ft), at which instant the remaining values of the net pressure diagram are assumed to be linear with elevation between 1) the net active pressure value at the elevation of the PR, and 2) the net mobilized passive pressure at the elevation of the approximated sheet-pile tip (i.e., el -21.64).[1] Figure 4.64b is an illustration of how the net pressure diagram was formed. The final results are illustrated in Figure 4.65 by the presentation of the net pressure diagram Figures 4.65a (replica of Figure 4.64b) and 4.65b, shear and moment diagrams. Figure 4.65b shows that the maximum bending moment occurs at the zero crossing of the shear diagram.

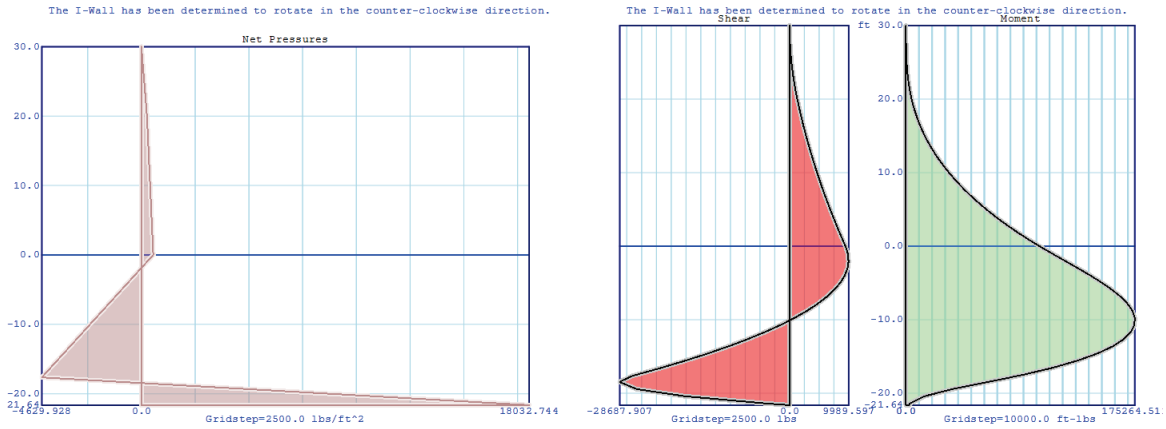
Figure 4.64. (a) Net pressure diagram. (b) Shear and moment diagram.



(a) (b)

[1] Thus, only one mobilized net passive pressure value in Figure 4.64a is used to construct the Figure 4.64b net pressure diagram, corresponding to the sheet-pile tip elevation at el -21.64. The majority of the net pressure diagram is derived from the Figure 4.64a net active pressure diagram.

Figure 4.65. (a) Net pressure diagram. (b) Shear and moment diagram.



(a) (b)

Table 4.28 shows a comparison of the results between the Coefficient Method and the Wedge Solution Method for Example Problem 4.6.1. The resulting elevations of the PR and the elevation of the fully embedded pile tip are very consistent, varying by less than half a foot, for the two methods.

Table 4.28. Comparison of Earth Coefficient results to Wedge Solution Method results - Example 4.6.1.

Method	Point of Rotation (PR) (elevation in feet)	Pile Tip (elevation in feet)
Coefficient Method	-17.65	-21.64
Wedge Solution	-17.52	-21.5

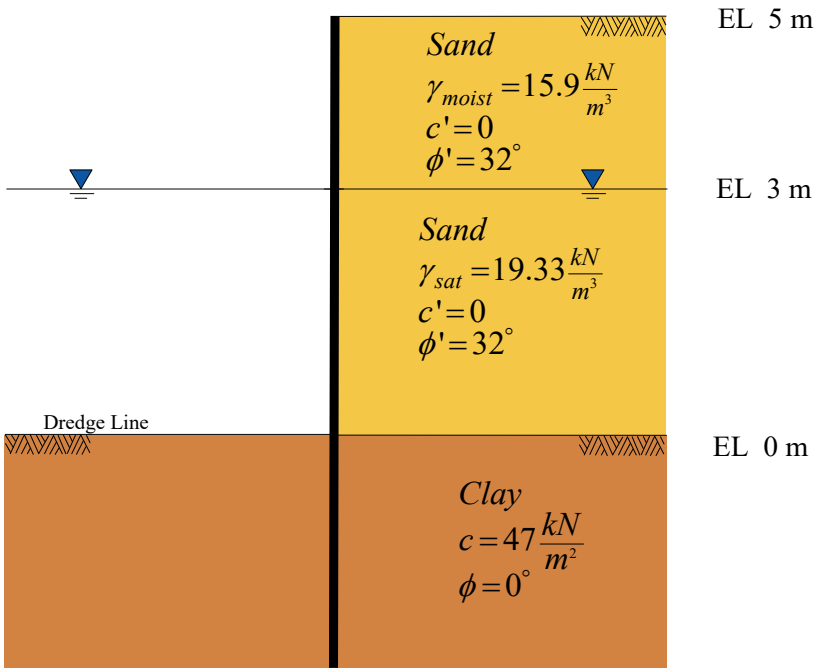
4.6.2 Example 4.6.2 sheet-pile wall penetrating saturated clay (Das 2007)

To determine the depth of embedment of a sheet-pile wall in two-layered soil, Figure 4.66 is examined. This example problem from Das (2007) represents the case of saturated clay soil below the dredge line on both sides of the sheet-pile wall, with retained sandy soil above the dredge line on the landside (RHS) of the sheet-pile wall. The sand has an effective stress definition with no cohesion and an effective angle of internal friction (φ') of 32 degrees. The sand is assigned a moist unit weight of 15.9 kN/m^3 and a saturated unit weight of 19.33 kN/m^3. The clay soil layer has a total stress definition with $\varphi = 0$, and cohesion (c) of 47 kN/m^2. Hydrostatic water pressures are at el 3 m on both sides of the sheet-pile wall. For this design, the required factors of safety on both the active and passive pressures are assigned 1.0.[1] An effective angle of wall to soil interface friction (δ') of

[1] Assigning a value for $FS_{Passive}$ of 1.0 is not consistent with Corps' design criteria.

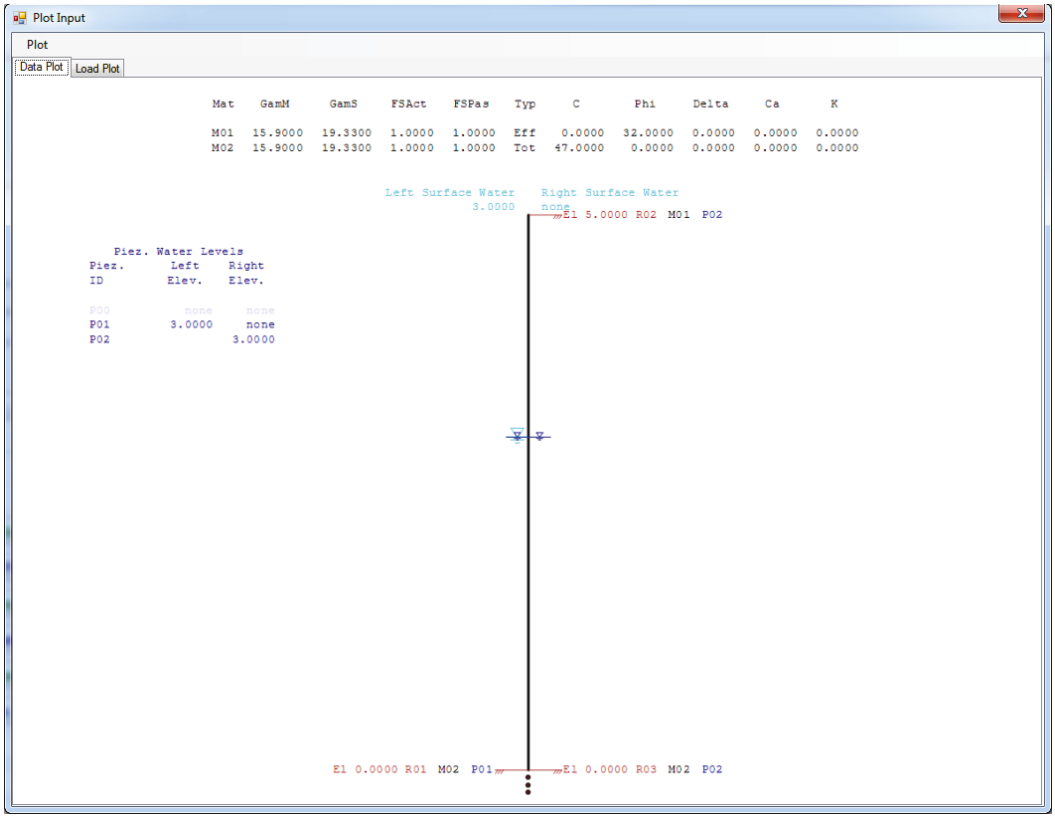
0 degrees and the Coulomb Coefficient Method of analysis (for K_a and K_p) form the basis for this example[1]. Hydraulic fracturing is not included as an option for this analysis. The Corps_I-Wall representation of this problem is presented by the schematic of Figure 4.67. This figure outlines and describes the geometry and structural parameters for the sheet-pile wall.

Figure 4.66. Sheet-pile wall penetrating saturated clay.



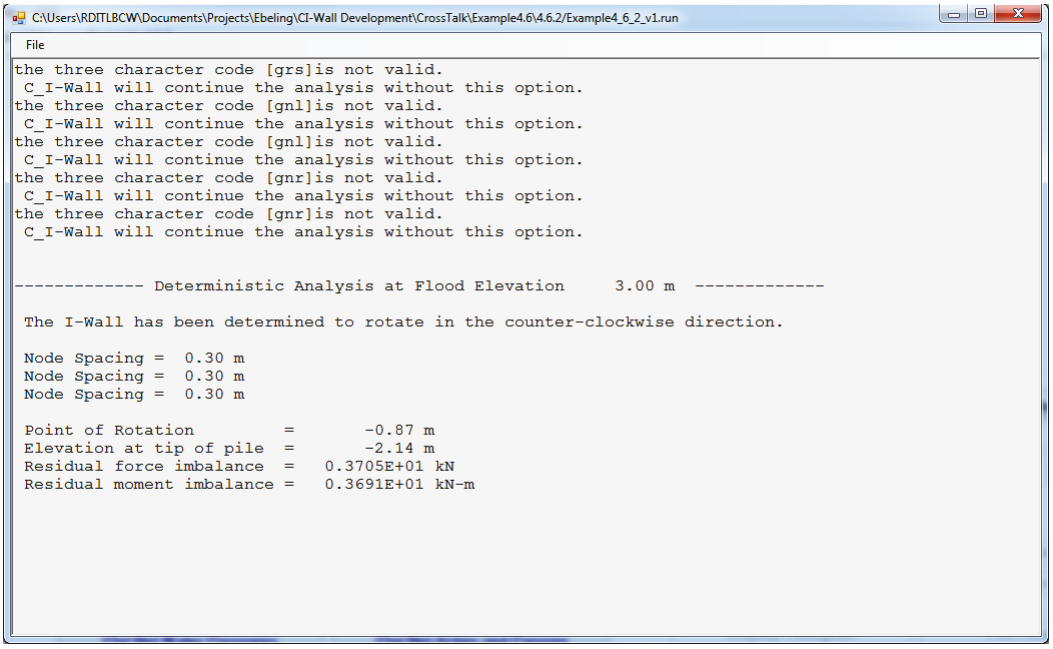
[1] For no soil-to-I-Wall interface friction (i.e., δ = 0 deg), the Coulomb solution for active and passive earth pressure coefficients corresponds to the Rankine earth pressure coefficients.

Figure 4.67. Corps_I-Wall schematic of sheet-pile wall in sand and saturated clay site.



This analysis resulted in a computed mobilized active earth pressure coefficient (K_a) of 0.30726 and a mobilized passive pressure coefficient (K_p) of 3.25459 for the sandy soil on the retained side above the dredge line. For the clay layers (with φ = 0) below the dredge line, K_a and K_p obtained values of 1.0. Figure 4.68 displays the results obtained from this analysis with the sheet-pile tip elevation computed at el -2.14 m, for a calculated depth of embedment of 2.14 m. The final results for this Example 4.6.2 have been recorded as check problem 2 (Table 4.27).

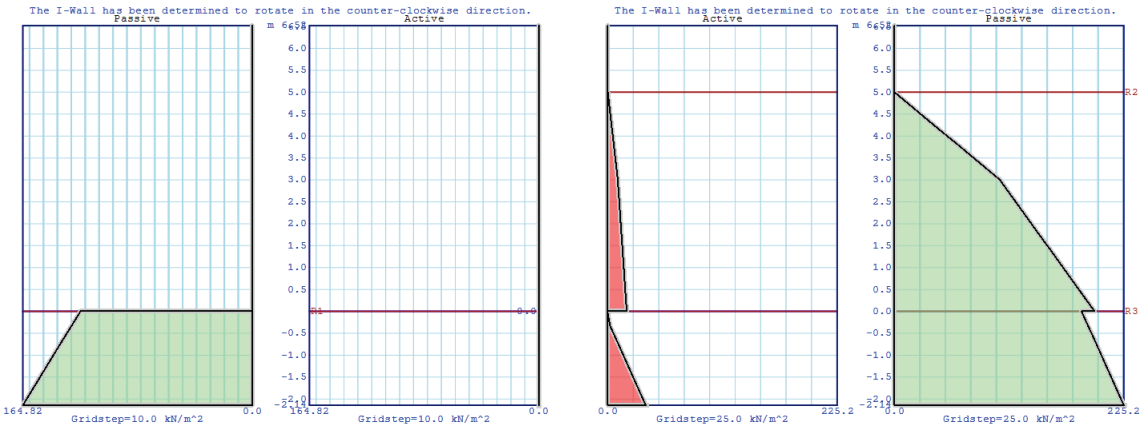
Figure 4.68. Corps_I-Wall output information.



The distribution of both active and passive earth pressures for both sides of the sheet-pile wall are illustrated in Figures 4.69a and 4.69b. The hydrostatic water pressures acting on both sides of the sheet-pile wall are shown in Figure 4.70a with the resultant net water pressure calculated by taking the difference between the water pressures acting on both sides of the wall. In the case when the piezometric surface elevation is equal to the surface water elevation, no resultant net water pressure will be calculated (Figure 4.70b).

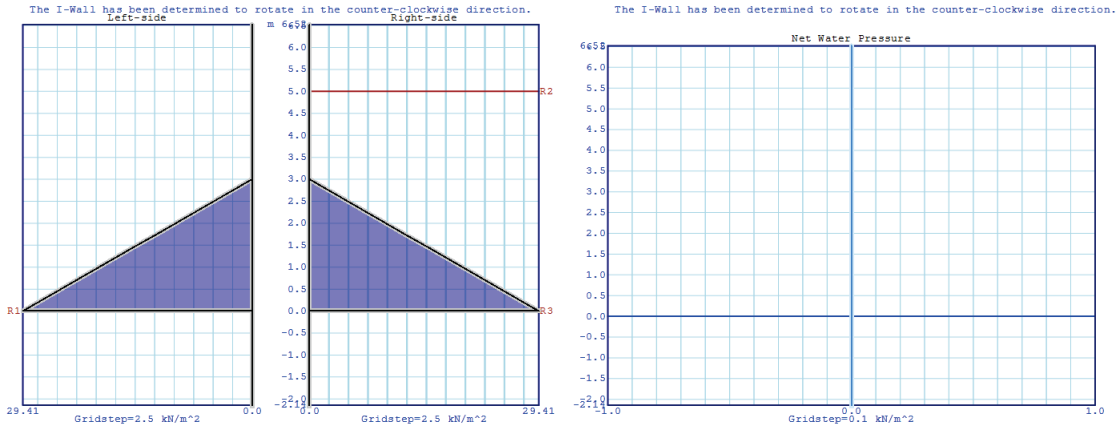
From these pressures (Figures 4.69 and 4.70), the net active and net passive pressures are constructed and presented in Figure 4.69a. For the applied flood loading, the I-Wall will rotate counterclockwise. The net active pressure is determined from the difference between the RHS-mobilized active earth pressure and the LHS-mobilized passive earth pressure (i.e., acting on the other side of the wall), with the addition of any net water pressures and any external horizontal net pressures and overburden pressures (if any). The net passive pressure is determined by the difference between the RHS-mobilized passive earth pressure and the LHS-mobilized active earth pressure acting on the other side of the sheet-pile wall with the addition of any net water pressures and any external horizontal net pressures and overburden pressures (if any).

Figure 4.69. Active and passive earth pressures. (a) LHS. (b) RHS.



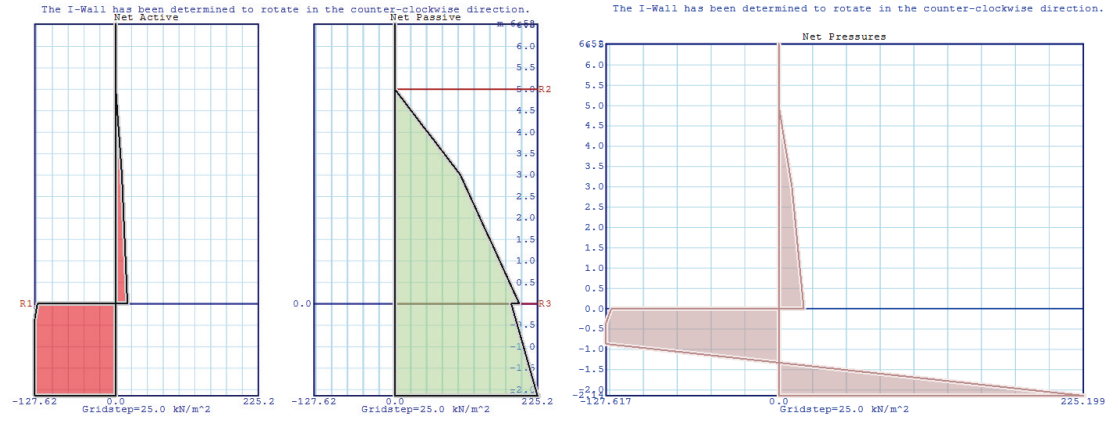
(a) (b)

Figure 4.70. Hydrostatic water pressures. (a) LHS and RHS of wall. (b) Net water pressures.



(a) (b)

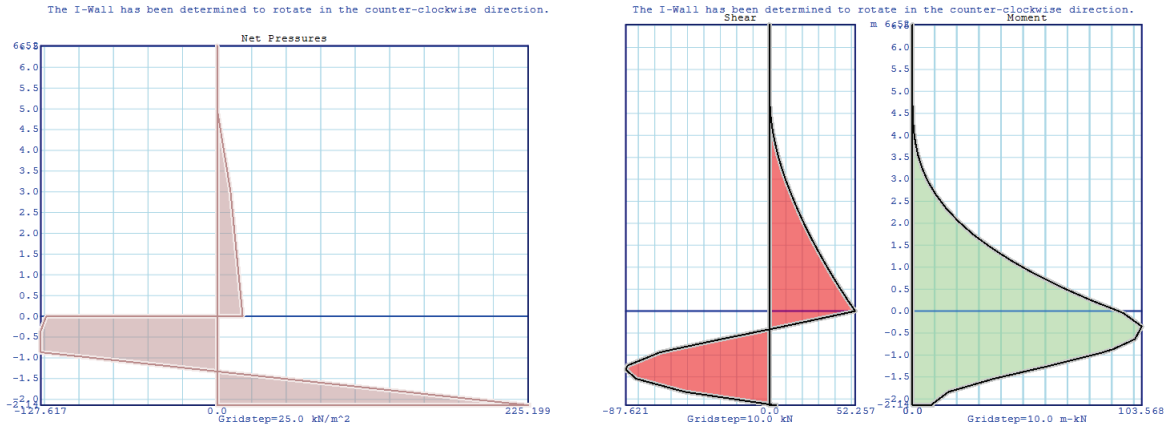
Figure 4.71. Net pressures. (a) Net active and net passive pressures. (b) Net pressure diagram.



(a) (b)

The net pressure diagram of Figure 4.71b is derived from the replication of all values of the net active pressures, from the top of the wall until the elevation at the PR (el -0.87 m), at which instant the remaining values of the net pressure diagram is assumed to be linear with elevation between 1) the net active pressure value at the elevation of the PR, and 2) the net mobilized passive pressure at the elevation of the approximated sheet-pile tip (i.e., el -2.14 m).[1] Figure 4.71b is an illustration of how the net pressure diagram was formed. The final results are illustrated in Figure 4.72 by the presentation of the net pressure diagram Figures 4.72a (replica of Figure 4.69b) and 4.72b, the shear and moment diagrams. Figure 4.72b shows that the maximum bending moment occurs at the zero crossing of the shear diagram.

Figure 4.72. (a) Net pressure diagram. (b) Shear and moment diagram.



(a) (b)

The Corps_I-Wall computed results for PR and sheet-pile tip agree with those from Das (2007) for the two sheet-pile walls analyzed.

Table 4.29 shows a comparison of the results between the Coefficient Method and the Wedge Solution Method for Example Problem 4.6.2. The resulting elevations of the PR, and the elevation of the fully embedded pile tip are very consistent for the two methods.

[1] Thus, only one mobilized net passive pressure value in Figure 4.71a is used to construct the Figure 4.71b net pressure diagram; corresponding to the sheet-pile tip elevation at el -2.14 m. The majority of the net pressure diagram is derived from the Figure 4.71a net active pressure diagram.

Table 4.29. Comparison of Earth Coefficient results to Wedge Solution Method results - Example 4.6.2.

Method	Point of Rotation (PR) (elevation in feet)	Pile Tip (elevation in feet)
Coefficient Method	-0.87	-2.14
Wedge Solution	-0.97	-2.2

4.6.3 Sheet-pile wall penetrating sand (Bowles 1968)

To determine the depth of embedment of sheet-pile walls in granular soil, two problems, Examples 4.6.3 and 4.6.4, are examined. This pair of Bowles (1968) example calculations represents the case of homogeneous sandy soil that has an effective stress definition with no cohesion and an effective angle of internal friction (φ′) of 30 degrees. These two problems differ with the assignment of the Factor of Safety for passive earth pressures of 1.0 (Section 4.6.3.1)[1] and of 1.633 (Section 4.6.3.2). Table 4.30 shows the material properties for the problems.

4.6.3.1 Example 4.6.3 sheet-pile wall penetrating sand (Bowles 1968)

To determine the depth of embedment of sheet-pile walls in granular soil, Figure 4.73 summaries an example problem of a cantilever sheet-pile wall retaining moist and saturated sand. The Corps-Wall idealization of this problem is shown in Figure 4.74. This example problem (Bowles 1968) represents the case of homogeneous sandy soil below the dredge line on the flood side (LHS) and retained above the dredge line on the landside (RHS) of the sheet-pile wall. The sand has an effective stress definition with no cohesion and an effective angle of internal friction (φ′) of 30 degrees. The sand layers are assigned a moist unit weight of 110 pcf and a saturated unit weight of 122.4 pcf. Hydrostatic water pressures are at el 10 ft on both sides of the sheet-pile wall. For this design, the required Factors of Safety on both the active and passive pressures are assigned 1.0. An effective angle of wall to soil interface friction (δ′) of 0 degrees and the Coulomb Coefficient Method of analysis (for K_a and K_p) form the basis for this example.[2] Hydraulic fracturing is not included as an option for this analysis. The Corps_I-Wall representation of this problem is presented by the schematic of Figure 4.61. This figure outlines and describes the geometry and structural parameters for the sheet-pile wall.

[1] Assigning a value for $FS_{Passive}$ of 1.0 is not consistent with Corps' design criteria.

[2] For no soil-to-I-Wall interface friction (i.e., δ = 0 deg), the Coulomb solution for both active and passive earth pressure coefficients corresponds to the Rankine earth pressure coefficients.

Table 4.30. Comparisons of I-Wall results contained within Bowles (1968).

Check Problem	Bowles (1968) Foundation Analysis and Design	Layer No.	Layer Soil Type	Corps_I-Wall Factors of Safety		φ′ (deg)	c′ (psf)	Point of Rotation				Sheet-Pile Tip	
								EL		z		EL	
				Active	Passive			Reference	Corps_I-Wall	Reference	Corps_I-Wall	Reference	Corps_I-Wall
1	8-1a	1	Sand	1	1	30	0	-20.64	-20.68	4.96	4.97	-25.60	-25.65
2	8-1b	1	Sand	1	1.633	30	0	-27.65	-27.58	6.85	6.86	-34.50	-34.44
3	8-2a	1	Sand	1	1	30	0	-4.83	-4.61	4.98	5.43	-9.81	-10.04
		2	Clay	1	1	0	1200						
4	8-2b	1	Sand	1	1	30	0	-10.05	-10.16	5.05	5.09	-15.10	-15.25
		2	Clay	1.5	1.5	0	1200						

Reference is Bowles (1968). Foundation Analysis and Design for check problems 1 – 4. The moist unit weight of soil (γ_{moist}) is 100 pcf and the saturated unit weight of soil (γ_{sat}) is 122.4 pcf. All check problems are in English units.

Figure 4.73. Sheet-pile wall penetrating sand.

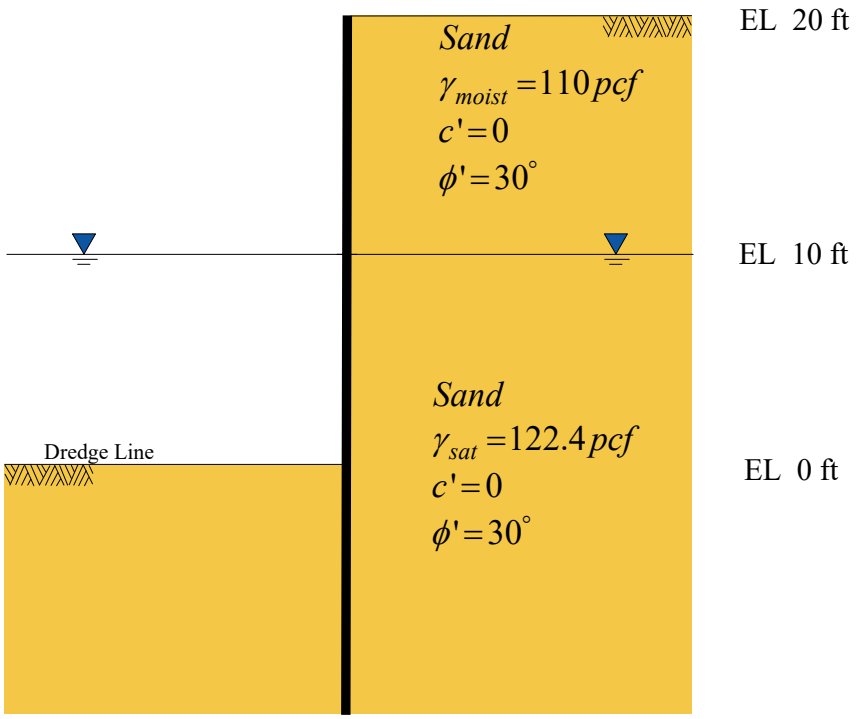
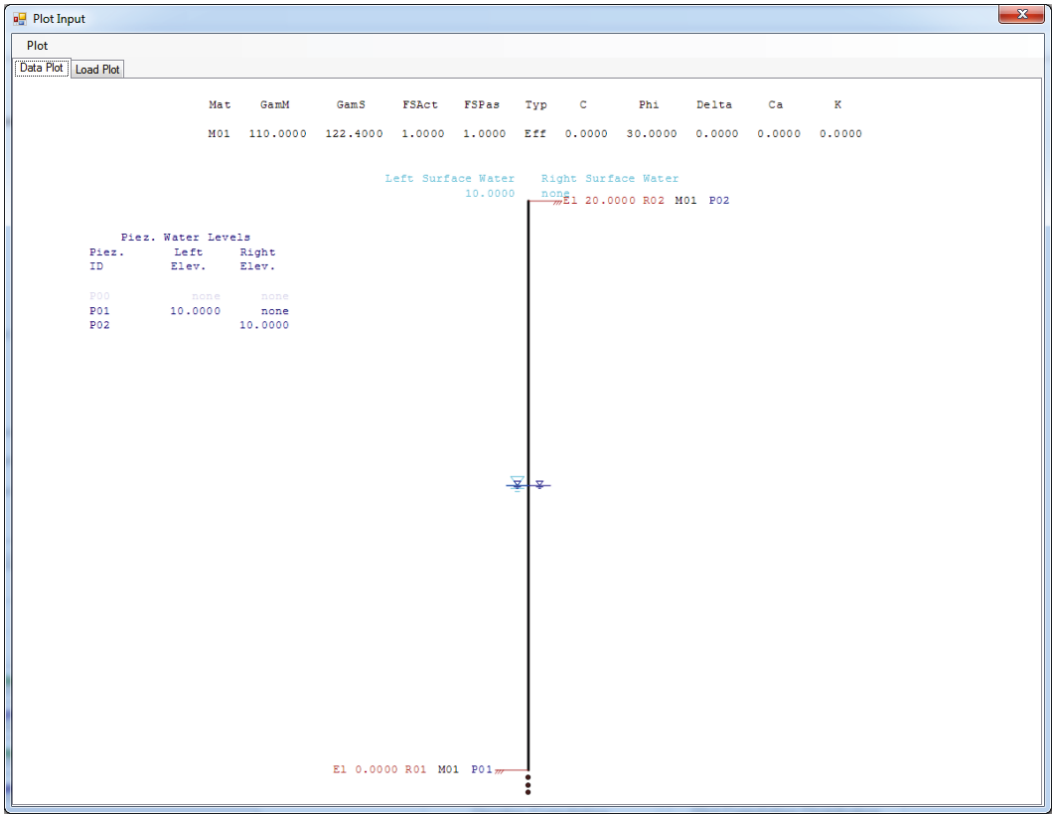
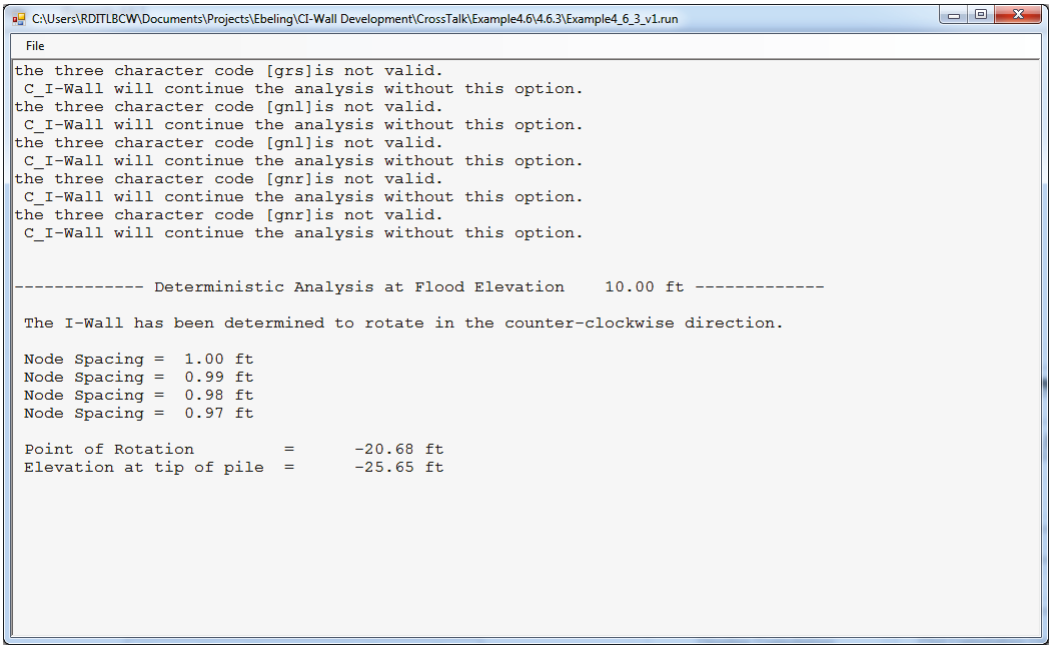


Figure 4.74. Corps_I-Wall schematic of sheet-pile wall in sand site.



This analysis resulted in a computed mobilized active earth pressure coefficient (K_a) of 0.3333 and a mobilized passive pressure coefficient (K_p) of 3.0. Figure 4.75 displays the results obtained from this analysis with the sheet-pile tip elevation computed at el -25.65 ft for a calculated depth of embedment of 25.65 ft. The final results for this Example 4.6.3 have been recorded as check problem 1 in Table 4.30.

Figure 4.75. Corps_I-Wall output information.

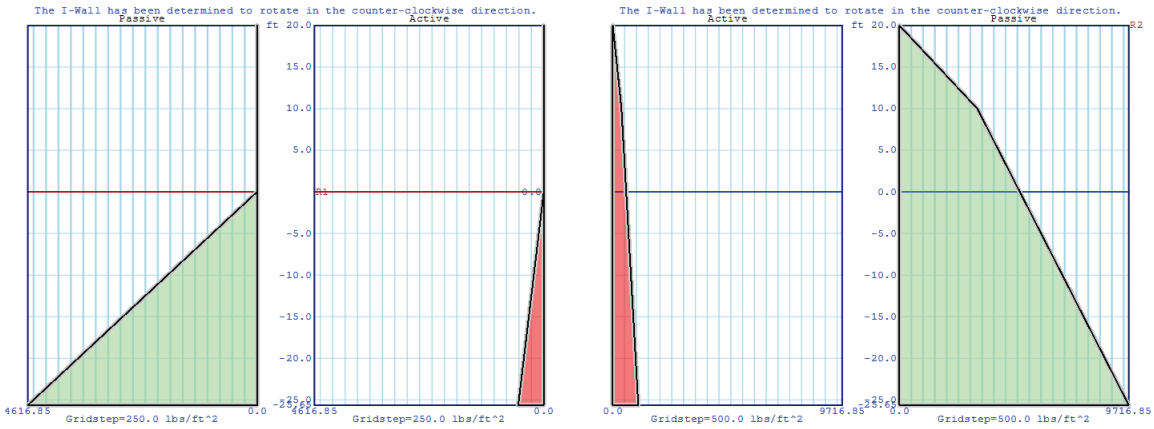


The distribution of both active and passive earth pressures for both sides of the sheet-pile wall are illustrated in Figures 4.76a and 4.76b. The hydrostatic water pressures acting on both sides of the sheet-pile wall are shown in Figure 4.77a, with the resultant net water pressure calculated by taking the difference between the water pressures acting on both sides of the wall. In the case when the piezometric surface elevation is equal to the surface water elevation, no resultant net water pressure will be calculated as shown in Figure 4.77b.

From these pressures (Figures 4.76 and 4.77), both the net active and net passive pressures are constructed and presented in Figure 4.78a. For the applied flood loading, the I-Wall will rotate counterclockwise. The net active pressure is determined from the difference between the RHS-mobilized active earth pressure, and the LHS-mobilized passive earth pressure (i.e., acting on the other side of the wall), with the addition of any net water pressures, any external horizontal net pressures, and

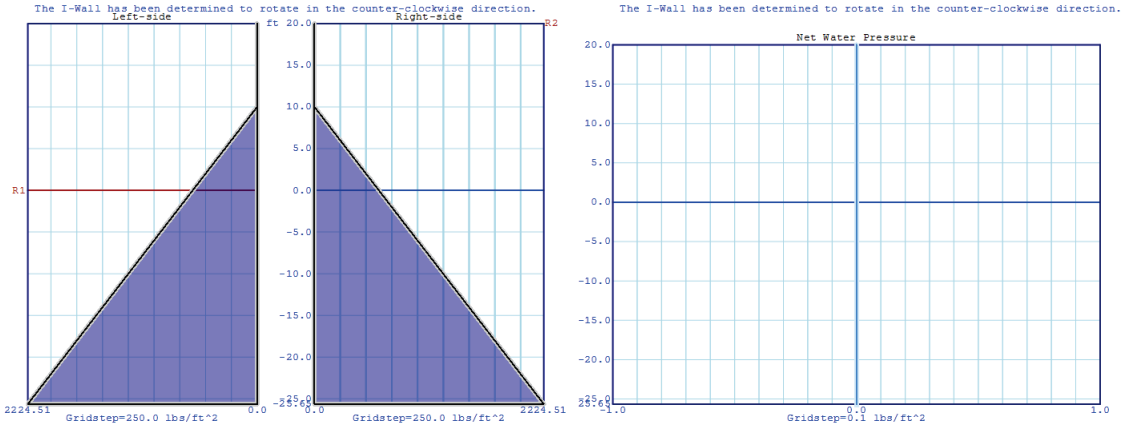
overburden pressures (if any). The net passive pressure is determined by the difference between the RHS-mobilized passive earth pressure and the LHS-mobilized active earth pressure acting on the other side of the sheet-pile wall, with the addition of any net water pressures, any external horizontal net pressures, and overburden pressures (if any).

Figure 4.76. Active and passive earth pressures for drained shear strength. (a) LHS. (b) RHS.



(a) (b)

Figure 4.77. Hydrostatic water pressures. (a) LHS and RHS of wall. (b) Net water pressures.

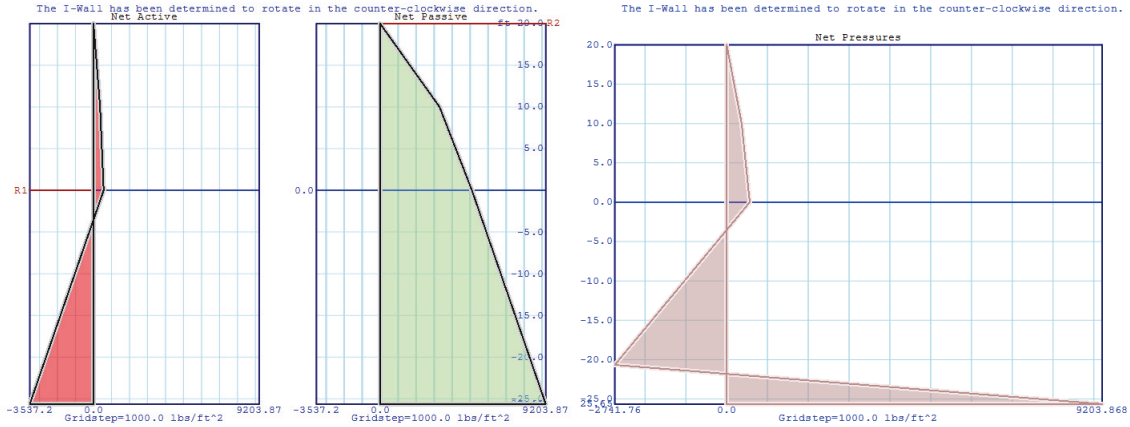


(a) (b)

The net pressure diagram of Figure 4.78b is derived from the replication of all values of the net active pressures, from the top of the wall until the elevation at the PR (el -20.68 ft). At this instant, the remaining values of the net pressure diagram is assumed to be linear with elevation between 1) the net active pressure value at the elevation of the PR, and 2) the net mobilized passive pressure at the elevation of the approximated sheet-pile

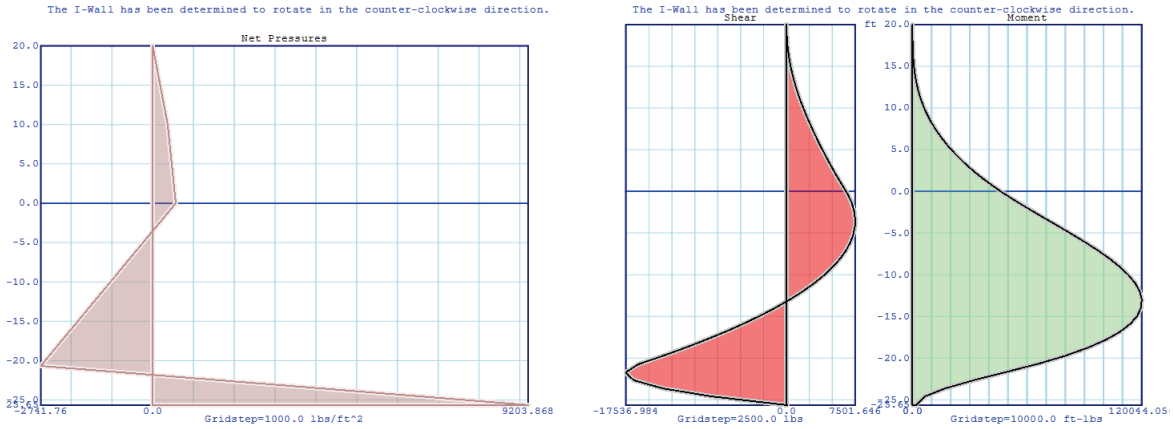
tip (i.e., el -25.65).[1] Figure 4.78b is an illustration of how the net pressure diagram was formed. The final results are illustrated in Figure 4.79 by the presentation of the net pressure diagram Figure 4.79a (replica of Figure 4.78b) and 4.79b, the shear and moment diagrams. Figure 4.79b shows that the maximum bending moment occurs at the zero crossing of the shear diagram.

Figure 4.78. Net pressures. (a) Net active and net passive pressures. (b) Net pressure diagram.



(a) (b)

Figure 4.79. (a) Net pressure diagram. (b) Shear and moment diagram.



(a) (b)

[1] Thus, only one mobilized net passive pressure value in Figure 4.78a is used to construct the Figure 4.79a net pressure diagram; corresponding to the sheet-pile tip elevation at el -25.72. The majority of the net pressure diagram is derived from the Figure 4.78a net active pressure diagram.

Table 4.31 shows a comparison of the results between the Coefficient Method and the Wedge Solution Method for Example Problem 4.6.3. The resulting elevations of the PR and the elevation of the fully embedded pile tip are very consistent for the two methods.

Table 4.31. Comparison of Earth Coefficient results to Wedge Solution Method results - Example 4.6.3.

Method	Point of Rotation (PR) (elevation in feet)	Pile Tip (elevation in feet)
Coefficient Method	-20.68	-25.65
Wedge Solution	-20.64	-25.60

4.6.3.2 Example 4.6.4 sheet-pile wall penetrating sand (Bowles 1968)

This example problem uses the same sheet-pile conditions as problem 4.6.3, but requires the Factor of Safety for passive earth pressures of 1.5 for determining the depth of embedment of sheet-pile walls in granular soil. The Corps_I-Wall adaptation to Bowles (1968) calculations required the passive Factor of Safety to be set to 1.6333 because Bowles applied the Factor of Safety to φ′ (i.e., $\varphi'_{mob} = 30/1.5$) rather than as $\tan(\varphi'_{mob}) = \tan(\varphi')/1.5$.

This analysis resulted in a computed mobilized active earth pressure coefficient (K_a) of 0.3333 and a mobilized passive pressure coefficient (K_p) of 1.9999. Figure 4.80 displays the results obtained from this analysis with the sheet-pile tip elevation computed at el -34.44 ft for a calculated depth of embedment of 34.44 ft. The final results for this Example 4.6.4 has been recorded as check problem 2 in Table 4.30.

Table 4.32 shows a comparison of the results between the Coefficient Method and the Wedge Solution Method for Example Problem 4.6.4. The resulting elevations of the PR and the elevation of the fully embedded pile tip are very consistent for the two methods.

Figure 4.80. Corps_I-Wall output information.

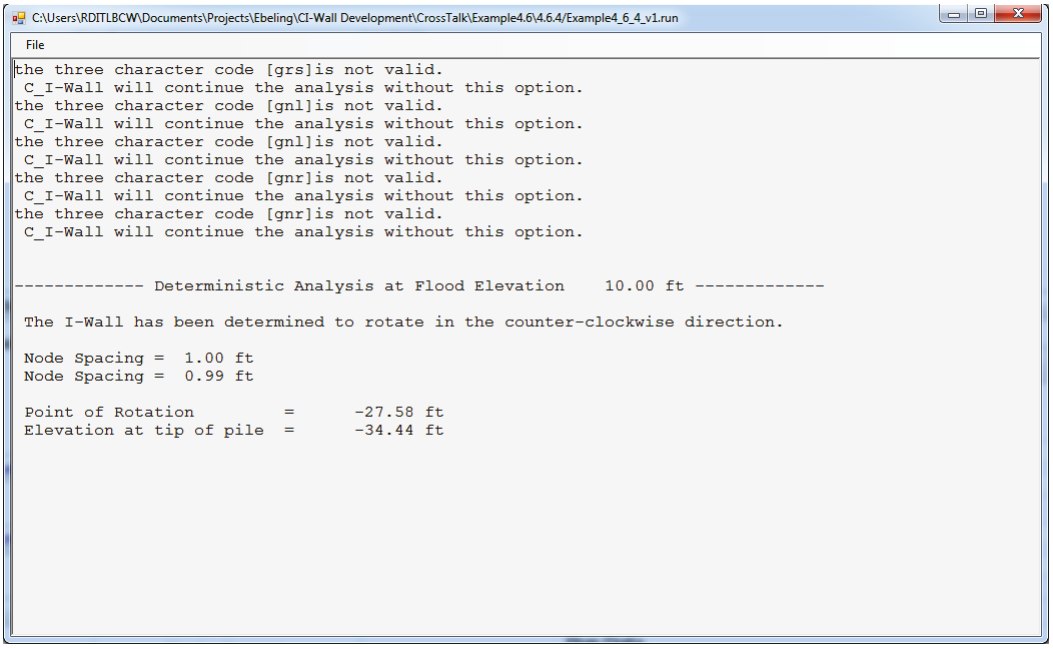


Table 4.32. Comparison of Earth Coefficient results to Wedge Solution Method results - Example 4.6.4.

Method	Point of Rotation (PR) (elevation in feet)	Pile Tip (elevation in feet)
Coefficient Method	-27.58	-34.44
Wedge Solution	-27.52	-34.4

4.6.4 Sheet-pile wall penetrating saturated clay (Bowles 1968)

To determine the depth of embedment of sheet-pile walls of retained sand and saturated clay, the following two example problems (Bowles 1968), 4.6.5 and 4.6.6, are examined. These two problems differ with the assignment of the Factor of Safety for both active and passive earth pressures of 1.0 (Section 4.6.4.1) and of 1.5 (Section 4.6.4.2). Table 4.30 shows the material properties for the problems.

4.6.4.1 Example 4.6.5 sheet-pile wall penetrating saturated clay (Bowles 1968)

To determine the depth of embedment of a sheet-pile wall in two-layered soil, Figure 4.81 is examined. This example problem (Bowles 1968) represents the case of saturated clay soil below the dredge line on both sides of the sheet-pile wall, with retained sandy soil above the dredge line on the landside (RHS) of the sheet-pile wall. The sand layer has an

effective stress definition with no cohesion, and an effective angle of internal friction (φ′) of 30 degrees. The sand is assigned a moist unit weight of 110 pcf, and a saturated unit weight of 122.4 pcf. The clay soil layer has a total stress definition with φ = 0 and cohesion (c) of 1,200 psf. Hydrostatic water pressures are at el 10 ft on both sides of the sheet-pile wall. For this design, the required factors of safety on the active and passive pressures are assigned 1.0. An effective angle of wall to soil interface friction (δ′) of 0 degrees and the Coulomb Coefficient Method of analysis (for K_a and K_p) form the basis for this example[1]. Hydraulic fracturing is not included as an option for this analysis. The Corps_I-Wall representation of this problem is presented by the schematic of Figure 4.82. This figure outlines and describes the geometry and structural parameters for the sheet-pile wall.

This analysis resulted in a computed mobilized active earth pressure coefficient (K_a) of 0.3333 and a mobilized passive pressure coefficient (K_p) of 3.0 for the sandy soil on the retained side above the dredge line. For the clay layers (with φ = 0) below the dredge line, K_a and K_p obtained values of 1.0. Figure 4.83 displays the results obtained from this analysis with the sheet-pile tip elevation computed at el -10.04 ft for a calculated depth of embedment of 10.04 ft. The final results for this Example 4.6.5 have been recorded as check problem 3 in Table 4.30.

The distribution of both active and passive earth pressures for both sides of the sheet-pile wall is illustrated in Figures 4.84a and 4.84b. The hydrostatic water pressures acting on both sides of the sheet-pile wall are shown in Figure 4.85a, with the resultant net water pressure calculated by taking the difference between the water pressures acting on both sides of The wall. In the case when the piezometric surface elevation is equal to the surface water elevation, no resultant net water pressure will be calculated (as shown in Figure 4.85b).

[1] For no soil-to-I-Wall interface friction (i.e., δ = 0 deg), the Coulomb solution for both active and passive earth pressure coefficients corresponds to the Rankine earth pressure coefficients.

Figure 4.81. Sheet-pile wall penetrating saturated clay.

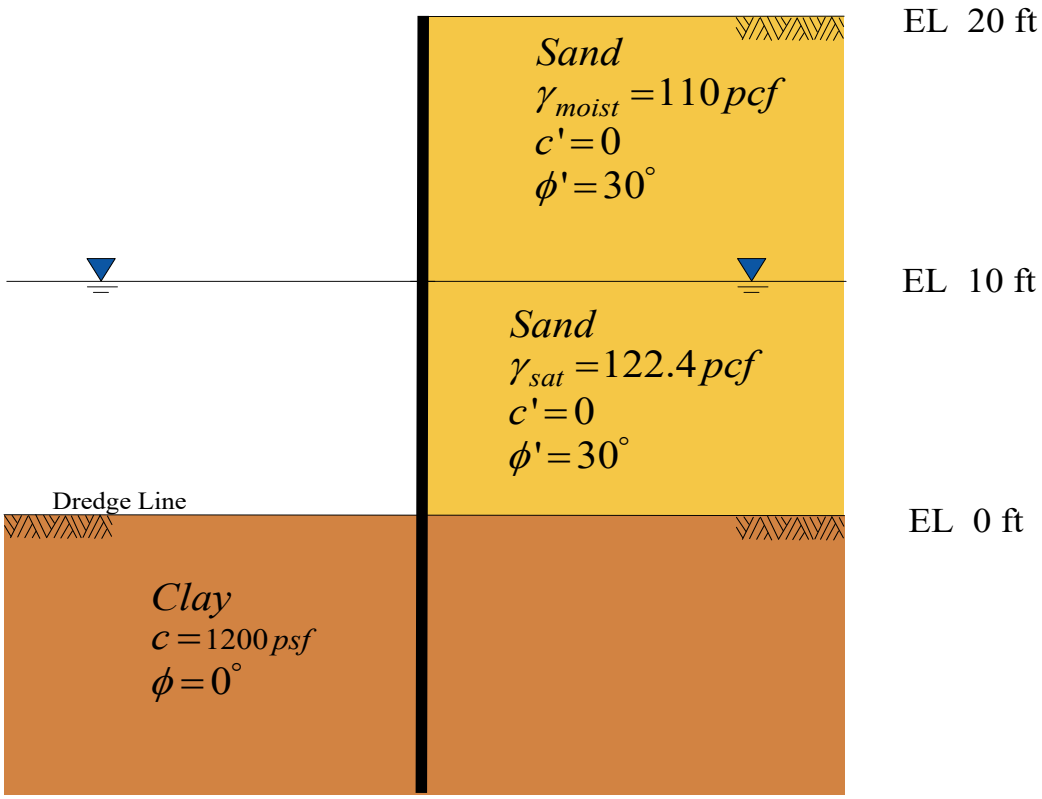


Figure 4.82. Corps_I-Wall schematic of sheet-pile wall in sand and saturated clay site.

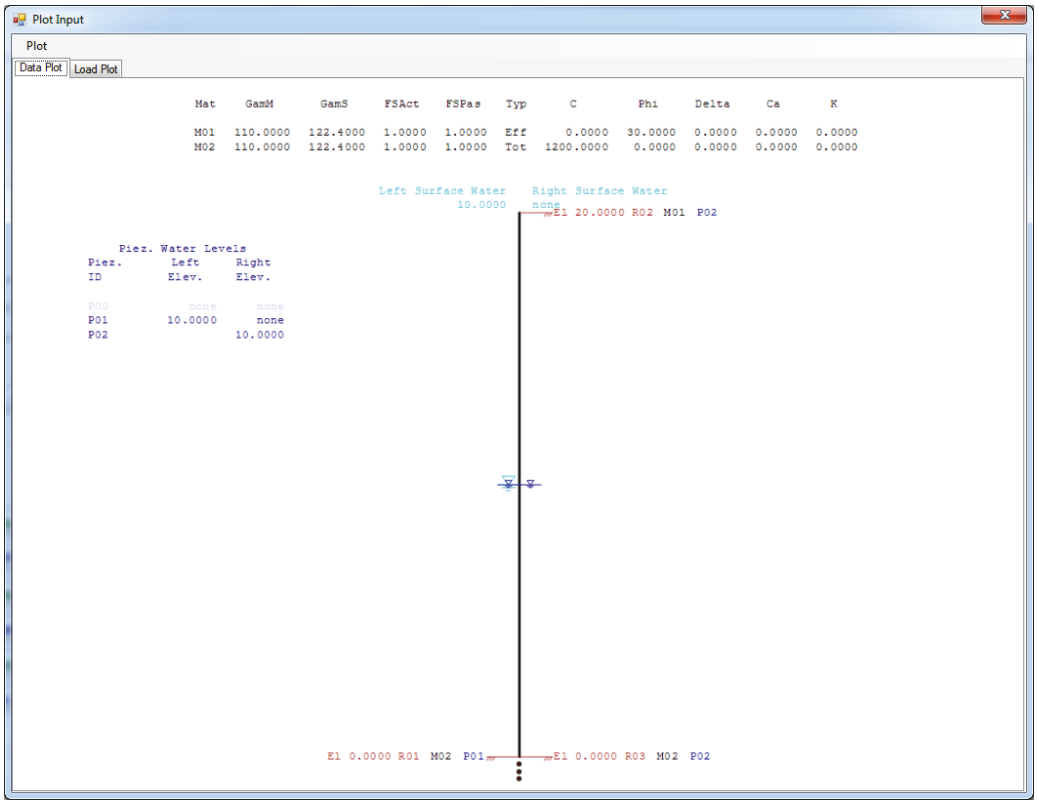


Figure 4.83. Corps_I-Wall output information.

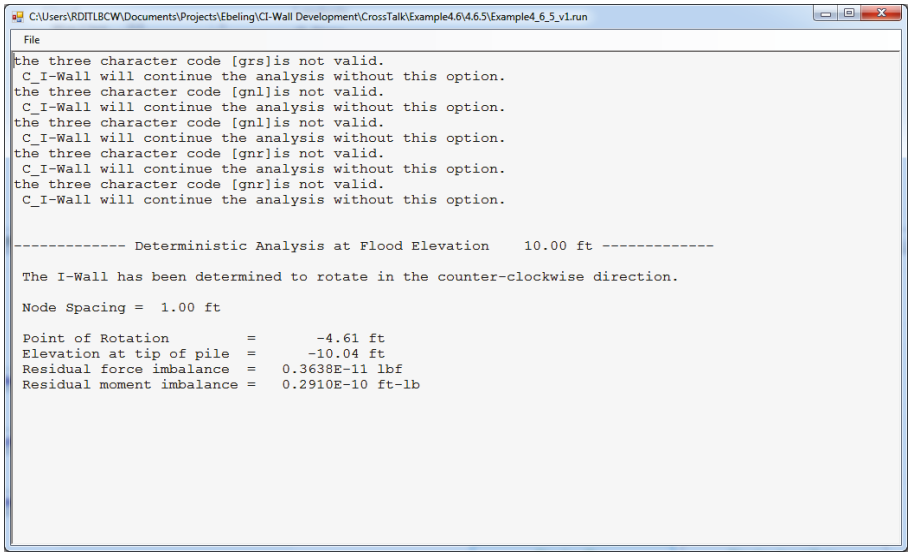
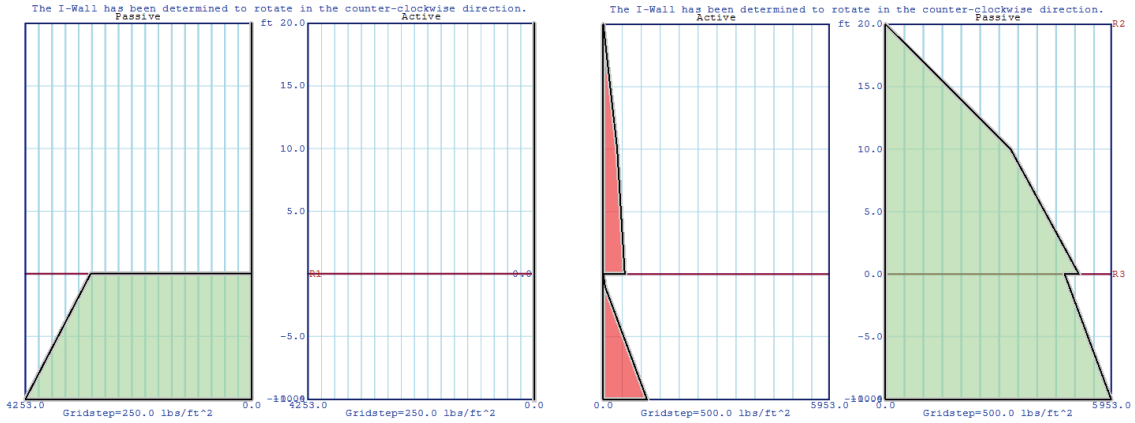
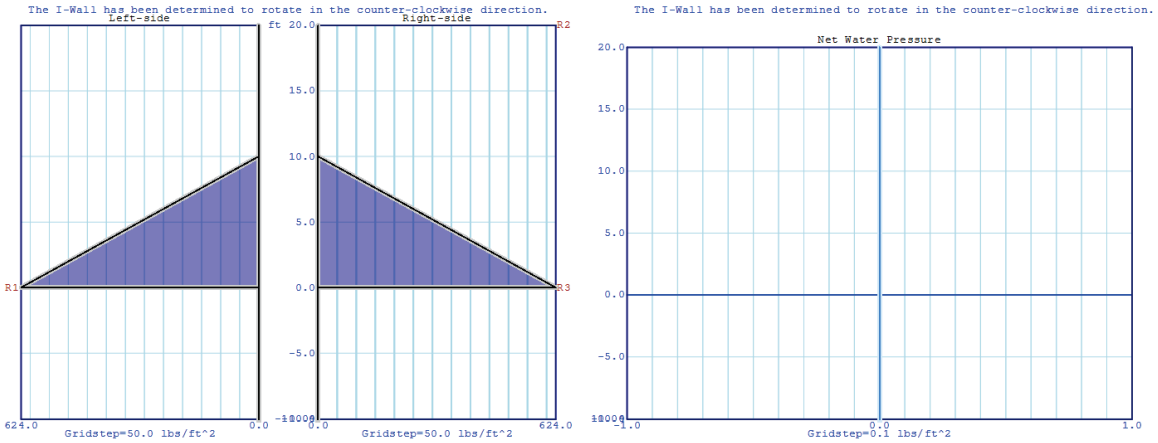


Figure 4.84. Active and passive earth pressures. (a) LHS. (b) RHS.



(a) (b)

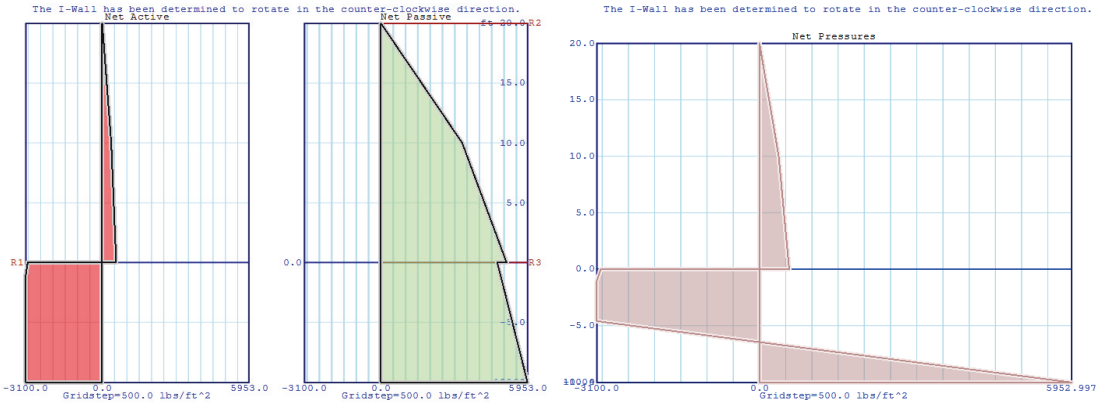
Figure 4.85. Hydrostatic water pressures. (a) LHS and RHS of wall. (b) Net water pressures.



(a) (b)

From these pressures (Figures 4.84 and 4.85), the net active and net passive pressures are constructed and presented in Figure 4.86a. For the applied earth loading, the I-Wall will rotate counterclockwise. The net active pressure is determined from the difference between the RHS-mobilized active earth pressure and the LHS-mobilized passive earth pressure (i.e., acting on the other side of the wall), with the addition of any net water pressures (none in this case), any external horizontal net pressures, and overburden pressures (if any). The net passive pressure is determined by the difference between the RHS-mobilized passive earth pressure and the LHS-mobilized active earth pressure acting on the other side of the sheet-pile wall, with the addition of any net water pressures and any external horizontal net pressures and overburden pressures (if any).

Figure 4.86. Net pressures. (a) Net active and net passive pressures. (b) Net pressure diagram.



(a) (b)

The net pressure diagram of Figure 4.86b is derived from the replication of all values of the net active pressures, from the top of the wall until the elevation at the PR (el -4.61 ft). At this instant, the remaining values of the net pressure diagram is assumed to be linear with elevation between 1) the net active pressure value at the elevation of the PR, and 2) the net mobilized passive pressure at the elevation of the approximated sheet-pile tip (i.e., el -10.04 ft).[1] Figure 4.86b is an illustration of how the net pressure diagram was formed. The final results are illustrated in Figure 4.87 by the presentation of the net pressure diagram Figures 4.87a (replica of Figure 4.86b) and 4.87b, the shear and moment diagrams. Figure 4.87b shows that the maximum bending moment occurs at the zero crossing of the shear diagram.

[1] Only one mobilized net passive pressure value in Figure 4.86a is used to construct the Figure 4.86b net pressure diagram, corresponding to the sheet-pile tip elevation at el -10.04 ft. The majority of the net pressure diagram is derived from the Figure 4.86a net active pressure diagram.

Figure 4.87. (a) Net pressure diagram. (b) Shear and moment diagram.



(a) (b)

Table 4.33 shows a comparison of the results between the Coefficient Method and the Wedge Solution Method for Example Problem 4.6.5. The resulting elevations of the PR and the elevation of the fully embedded pile tip are very consistent for the two methods.

Table 4.33. Comparison of Earth Coefficient results to Wedge Solution Method results - Example 4.6.5.

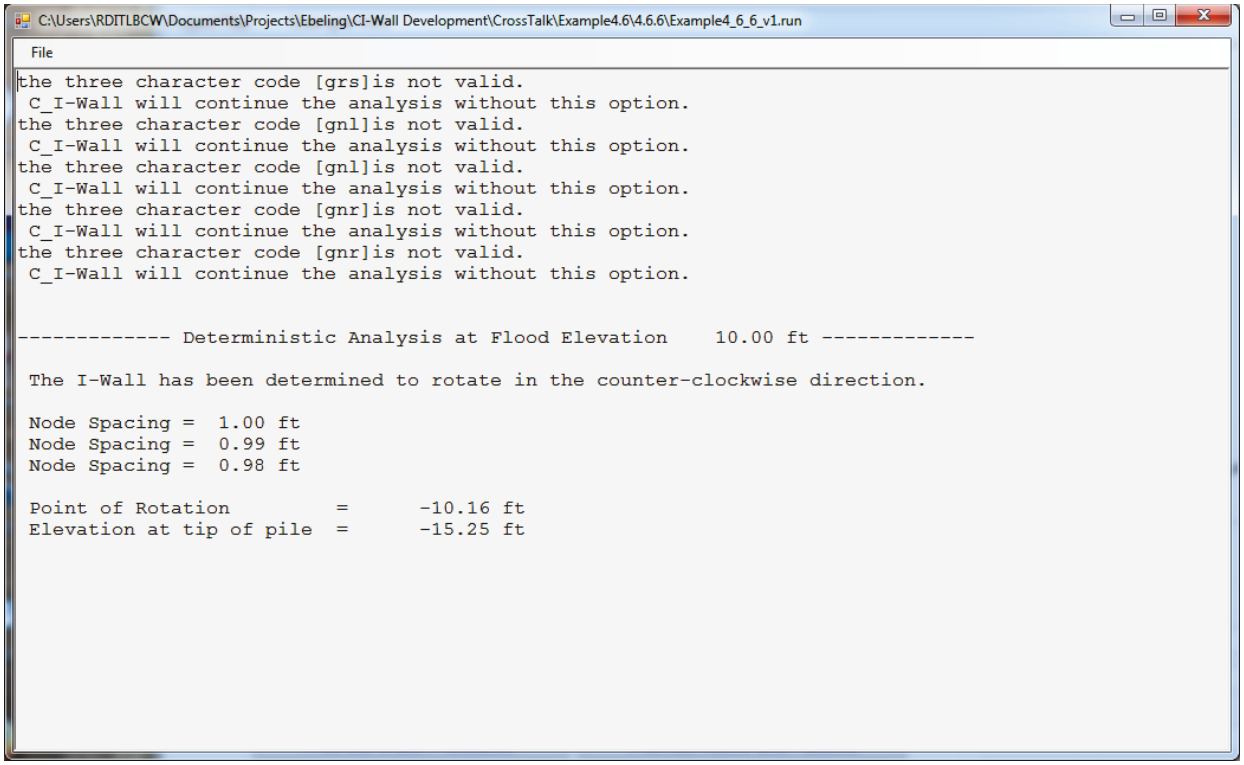
Method	Point of Rotation (PR) (elevation in feet)	Pile Tip (elevation in feet)
Coefficient Method	-4.61	-10.04
Wedge Solution	-4.83	-10.20

4.6.4.2 Example 4.6.6 sheet-pile wall penetrating saturated clay (Bowles 1968)

This example problem uses the same sheet-pile conditions as problem 4.6.5, but uses the Factor of Safety of 1.5 instead of 1.0 for both the active earth pressure and passive earth pressure for determining the depth of embedment of sheet-pile walls in granular soil.

This analysis resulted in a computed mobilized active earth pressure coefficient (K_a) of 0.3333 and a mobilized passive pressure coefficient (K_p) of 3.0. Figure 4.88 displays the results obtained from this analysis with the sheet-pile tip elevation computed at el -15.25 ft for a calculated depth of embedment of 15.25 ft. This depth of embedment required an increase of approximately 5.21 ft when the Factor of Safety was increased from 1.0 to 1.5.

Figure 4.88. Corps_I-Wall output information.



The final results for this Example 4.6.6 has been recorded as check problem 4 in Table 4.30.

The Corps_I-Wall computed results for PR and sheet-pile tip agree with those from Bowles for the four sheet-pile walls analyzed.

Table 4.34 shows a comparison of the results between the Coefficient Method and the Wedge Solution Method for Example Problem 4.6.6. The resulting elevations of the PR and the elevation of the fully embedded pile tip are very consistent for the two methods.

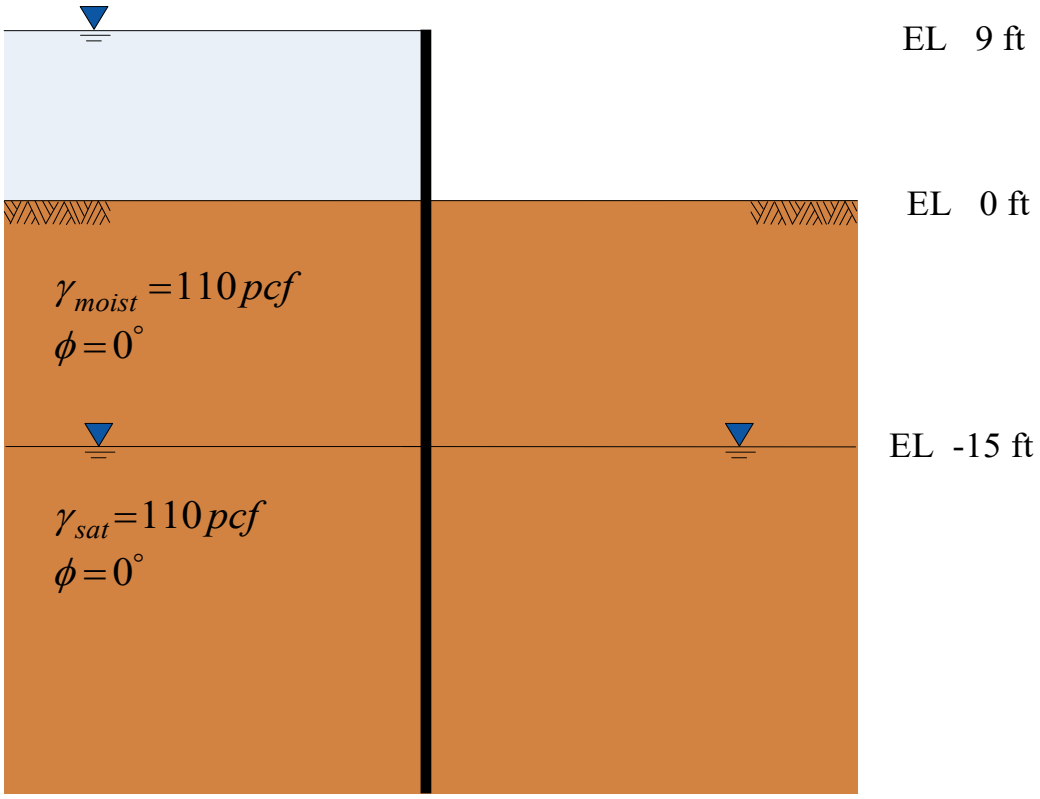
Table 4.34. Comparison of Earth Coefficient results to Wedge Solution Method results - Example 4.6.6.

Method	Point of Rotation (PR) (elevation in feet)	Pile Tip (elevation in feet)
Coefficient Method	-10.16	-15.25
Wedge Solution	-10.08	-15.10

4.6.5 Example 4.6.7 sheet-pile wall penetrating clay (Pace et al. 2012)

To determine the depth of embedment of sheet-pile walls in clay soil, Figure 4.89 is examined. This example problem, taken from Pace et al. (2012), represents a total stress method of analysis where pore pressures are not calculated within the soil. The cohesive soil ($\varphi = 0$ and $\delta = 0$) has undrained shear strength (S_u) and adhesion (C_a) parameters. The clay layers are assigned a moist unit weight of 110 pcf and a saturated unit weight of 110 pcf. Flood side surface water is at 9 ft. Hydrostatic water pressures are at el -15 ft on both sides of the sheet-pile wall. For this design, the required Factor of Safety for active earth pressures is 1.0 and the Factor of Safety for passive earth pressures is assigned 1.5. The Coulomb Coefficient Method of analysis (for K_a and K_p) as well as hydraulic fracturing forms the basis for this analysis[1].

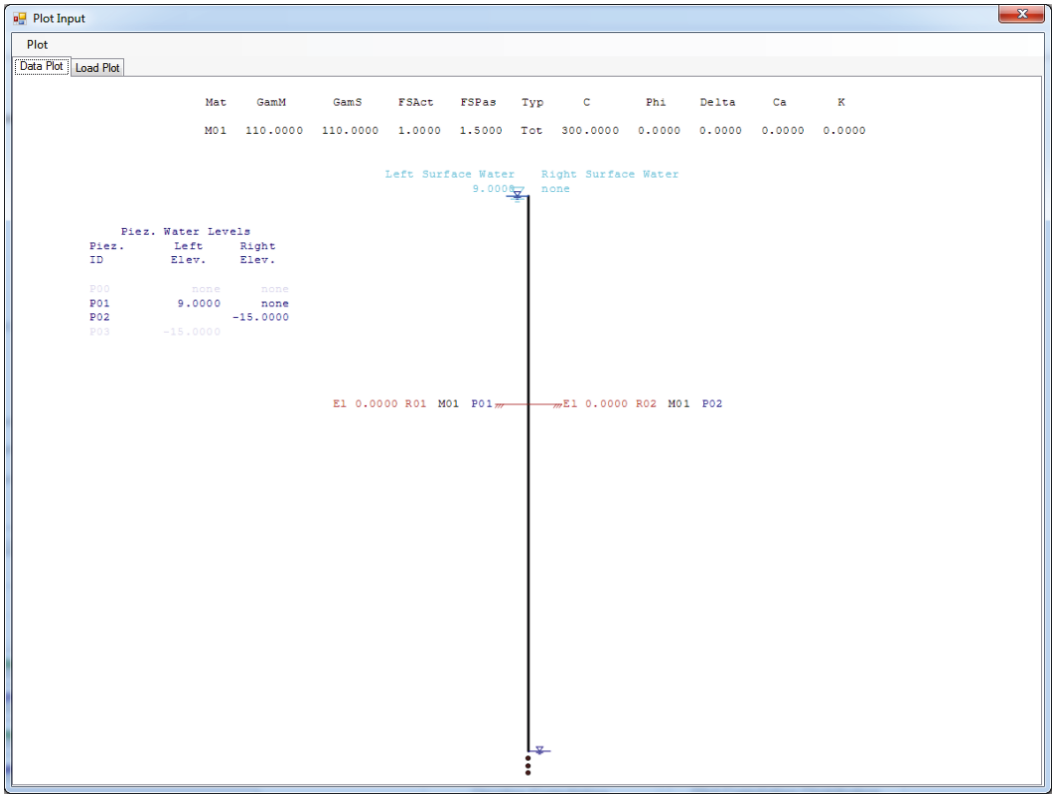
Figure 4.89. Sheet-pile wall penetrating clay.



[1] For no soil-to-I-Wall interface friction (i.e., $\delta = 0$ deg), the Coulomb solution for both active and passive earth pressure coefficients corresponds to the Rankine earth pressure coefficients.

The Corps_I-Wall representation of this problem with S_u = 300 psf and C_a = 0 psf is presented by the schematic of Figure 4.90. This figure outlines and describes the geometry and structural parameters for the sheet-pile wall.

Figure 4.90. Corps_I-Wall schematic of sheet-pile wall in clay site.



For clay soil (with φ = 0), this analysis resulted in computed mobilized earth pressure coefficients K_a and K_p of 1.0. Figure 4.91 displays the results obtained from this analysis with the sheet-pile tip elevation computed at el -29.74 ft for a calculated depth of embedment of 29.74 ft. The depth of gap is computed to be 12.61 ft. The final results for Example 4.6.7 have been recorded as check problem 2 in Table 4.30.

The distribution of active and passive earth pressures for both sides of the sheet-pile wall is illustrated in Figures 4.92a and 4.92b. The hydrostatic water pressures acting on both sides of the sheet-pile wall are shown in Figure 4.93a, with the resultant net water pressure calculated by taking the difference between the water pressures acting on both sides of the wall. Note that the active earth pressure in Figure 4.92a only develops at the gap depth of 12.61 ft, and hydrostatic water pressure is applied within the gap below the ground surface as shown in Figure 4.93a, and at the resultant net water pressure of Figure 4.93b.

Figure 4.91. Corps_I-Wall output information.

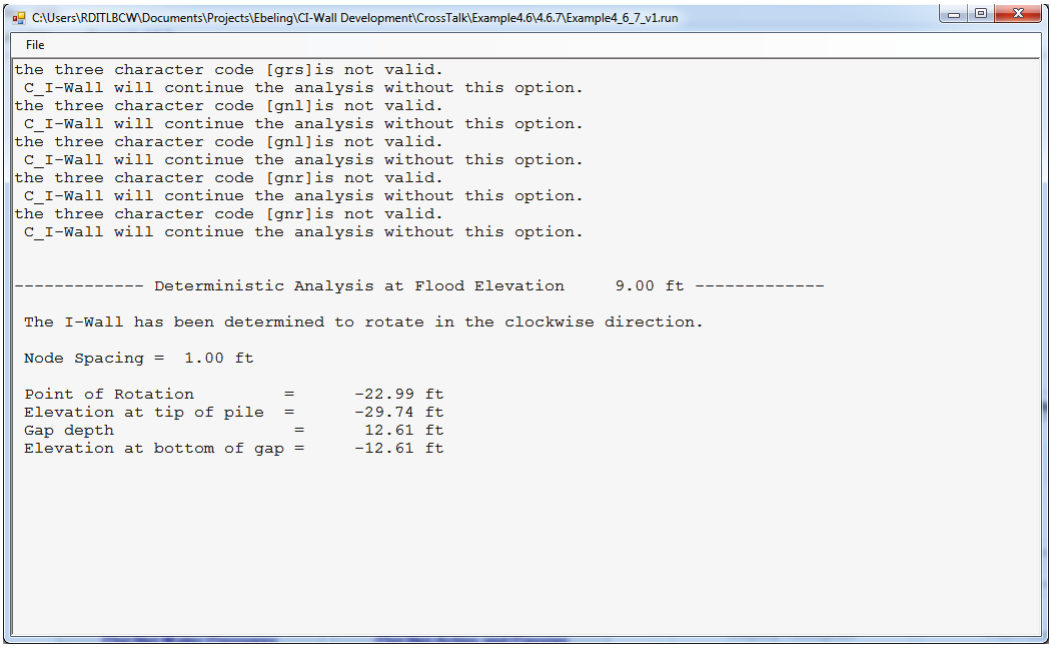
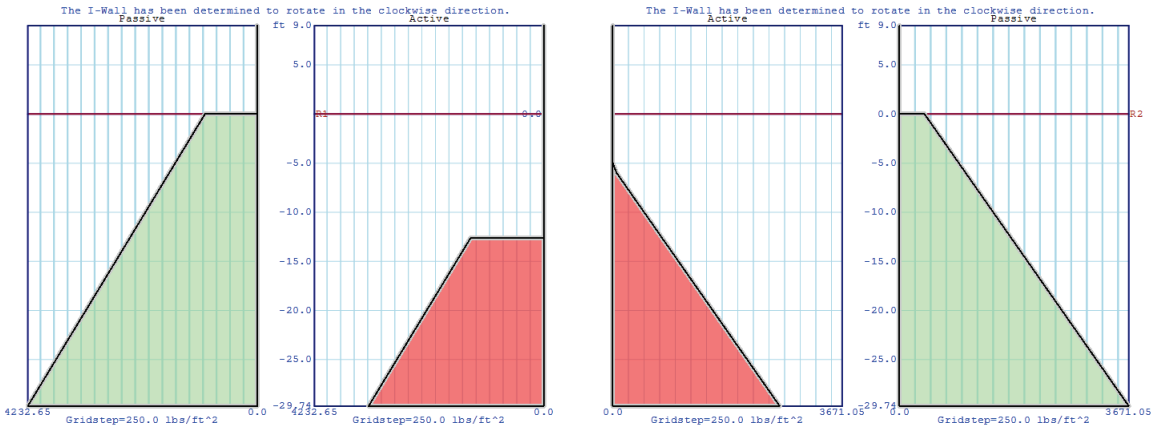
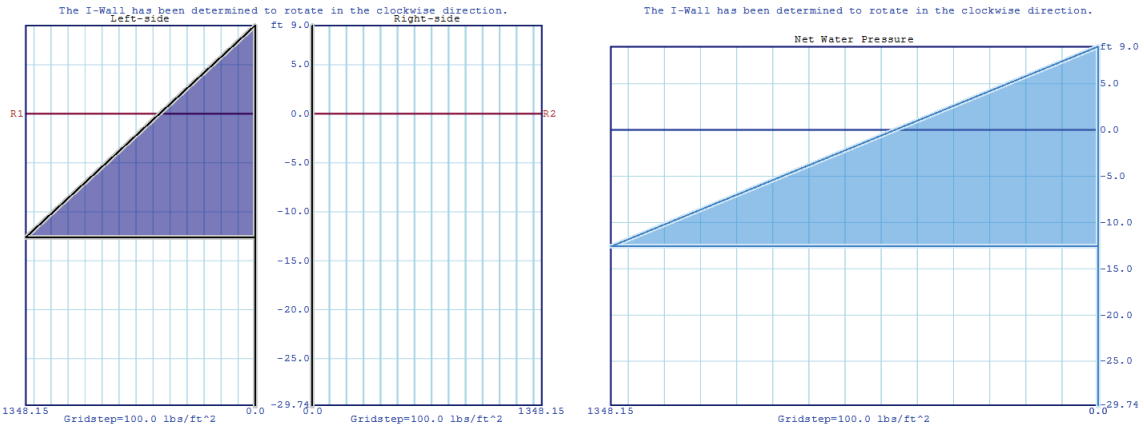


Figure 4.92. Active and passive earth pressures. (a) LHS. (b) RHS.



(a) (b)

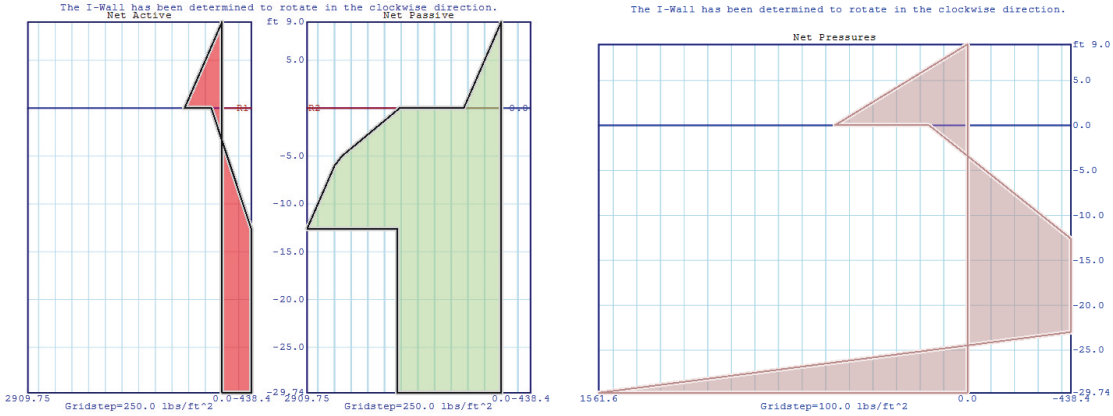
Figure 4.93. Hydrostatic water pressures. (a) LHS and RHS of wall.(b) Net water pressures.



(a) (b)

From these pressures (Figures 4.92 and 4.93), the net active and net passive pressures are constructed and presented in Figure 4.94a. For the applied flood loading, the I-Wall will rotate counterclockwise. The net active pressure is determined from the difference between the RHS-mobilized active earth pressure, and the LHS-mobilized passive earth pressure (i.e., acting on the other side of the wall), with the addition of any net water pressures, any external horizontal net pressures, and overburden pressures (if any). The net passive pressure is determined by the difference between the RHS-mobilized passive earth pressure, and the LHS-mobilized active earth pressure acting on the other side of the sheet-pile wall, with the addition of any net water pressures, any external horizontal net pressures, and overburden pressures (if any).

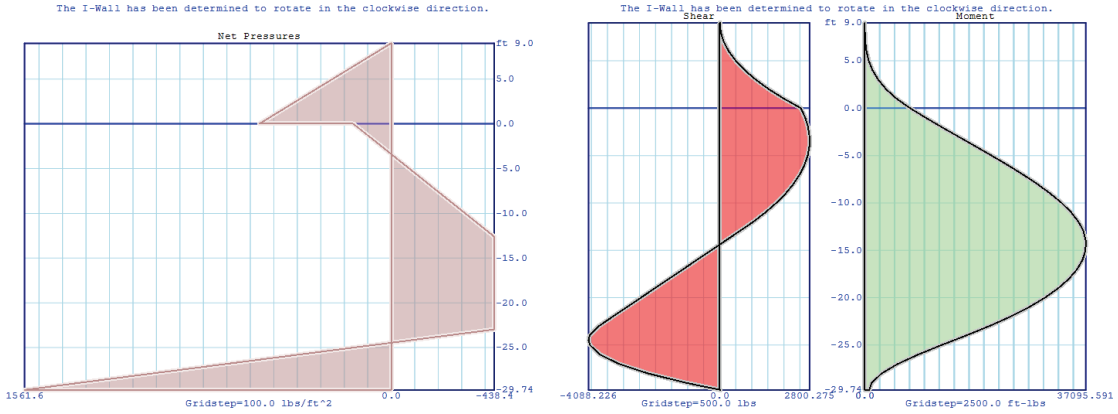
Figure 4.94. Net pressures (a) Net active and net passive pressures. (b) Net pressure diagram.



(a) (b)

The net pressure diagram of Figure 4.94b is derived from the replication of all values of the net active pressures, from the top of the wall until the elevation at the PR (el -22.99 ft). At this instant the remaining values of the net pressure diagram are assumed to be linear with elevation between 1) the net active pressure value at the elevation of the PR, and 2) the net mobilized passive pressure at the elevation of the approximated sheet-pile tip (i.e., el -29.74 ft).[1] Figure 4.94b is an illustration of how the net pressure diagram was formed. The final results are illustrated in Figure 4.95 by the presentation of the net pressure diagram, Figure 4.95a (replica of Figure 4.94b) and Figure 4.95b, the shear and moment diagrams. Figure 4.95b shows that the maximum bending moment occurs at the zero crossing of the shear diagram.

Figure 4.95. (a) Net pressure diagram. (b) Shear and moment diagram.



(a) (b)

Corps_I-Wall designs were further performed for different material properties of S_u and C_a. All the various example problems and final results have been recorded as check problems 1 through 5 in Table 4.35.

Check problem 2 was previously evaluated as Example 4.6.7 with depth of embedment of the sheet-pile wall equal to 29.74 ft, and a gap depth of 12.61 ft. Both analyses had similar results. Check problem 4 was also evaluated with similar results for the two analyses. As shown on Table 4.35, reference results using Computer Program for Design and Analysis of Sheet-pile Walls by Classical Methods (CWALSHT) software (Dawkins, 1991) were not available for check problems 1, 3, and 5.

[1] Thus, only one mobilized net passive pressure value in Figure 4.94a is used to construct Figure 4.94b net pressure diagram; corresponding to the sheet-pile tip elevation at el -29.74 ft. The majority of the net pressure diagram is derived from Figure 4.94a net active pressure diagram.

Table 4.35. Comparisons of I-Wall results contained within Pace (2012).

Check Problem	S_u (psf)	C_a (psf)	Point of Rotation (PR) EL (ft)		Gap Depth (ft)		Depth of Embedment (ft)	
			Reference	Corps_I-Wall	Reference	Corps_I-Wall	Reference	Corps_I-Wall
1	200	0	-	-75.99	8.4	8.4	No solution	82.75
2	300	0	-	-22.99	12.6	12.61	29.85	29.75
3	300	240	-	-15.70	16.91	15.70	No solution	21.15
4	300	15	-	-22.13	12.92	12.92	28.98	28.85
5	400	0	-	-15.77	16.8	15.77	No solution	21.26

Reference is Pace et al. (2012) Complete Soil-Structure Interaction (SSI) Analyses of I-Walls embedded in level ground during flood loading, Table 4.3. Corps_I-Wall has an active Factor of Safety of 1.0 and a passive Factor of Safety of 1.5. γ_{moist} and γ_{sat} are the moist and saturated unit weights of the soil, respectively, with both given the same value of 110 pcf. γ' is equal to the buoyant unit weight of the soil. Point of rotation elevations were not recorded for CWALSHT results. All problems are in English units.

Corps_I-Wall produced results for these problems with the sheet-pile wall rotating in a clockwise direction. For check problem 3, Corps_I-Wall produced a 15.70 ft gap depth that is less than the CWALSHT computed value of 16.91 ft. This gap depth at 15.70 ft was set to the PR elevation of el -15.70 ft. This situation will occur in a Corps_I-Wall analysis when the gap depth progresses to the PR (see Appendix B for more details). Below the PR, higher than active earth pressures will develop, this type of response has been seen to arrest the gap in Corps_I-Wall analyses and in complete SSI analyses (Pace et al. 2012). Corps_I-Wall hydraulic fracture calculations for check problem 5 also produced a gap depth that was less than calculated because the gap depth extended below the PR.

Check problem 2 showed a depth of embedment of 29.74 ft, with S_u = 300 psf, and an adhesion of C_a = 0. For check problem 1 (S_u = 200 psf), the wall depth increased to 82.75 ft, and for check problem 5 (S_u = 400 psf), the wall depth decreased to 21.26 ft. The undrained shear strength affects the depth of sheet-pile embedment. Inclusion of a small amount of adhesion of C_a = 15 psf resulted in a reduction in the calculated depth of embedment, from 29.74 ft (check problem 2) to 28.85 ft (check problem 4). Check problem 3 incorporates a larger amount of adhesion (C_a = 0.8 * c = 240 psf), which results in a deeper gap depth as compared with the no adhesion condition of check problem 2, 15.70 ft versus 12.61 ft. A change in the specified C_a value from 0 to 240 psf results in a calculated Corps-I-Wall depth of embedment of 21.15 ft versus 29.74 ft, a 8.59-ft shallower sheet-pile tip.

The suite of five analyses summarized in Table 4.35 verifies Corps_I_Wall software and demonstrate the robustness of its engineering solution process.

Table 4.36 shows a comparison of the results between the Coefficient Method and the Wedge Solution Method for the Example Problems of 4.6.7. The resulting elevations of the PR and the elevation of the fully embedded pile tip are very consistent, varying by approximately two and one-half feet or less, for the two methods.

Table 4.36. Comparison of Earth Coefficient results to Wedge Solution Method results - Example problems of 4.6.7.

Problem Number	Method	Point of Rotation (PR) (elevation in feet)	Pile Tip (elevation in feet)	Gap (depth, feet)	Gap (elevation, feet)
4.6.7.1	Coefficient Method	-75.99	-82.75	8.40	-8.40
	Wedge Solution	-77.50	-84.3	8.40	-8.40
4.6.7.2	Coefficient Method	-22.99	-29.74	12.61	-12.61
	Wedge Solution	-23.45	-30.40	12.61	-12.61
4.6.7.3	Coefficient Method	-15.70	-21.15	15.70	-15.70
	Wedge Solution	-16.95	-23.5	12.61	-12.61
4.6.7.4	Coefficient Method	-22.13	-28.85	12.92	-12.92
	Wedge Solution	-22.70	-29.50	12.61	-12.61
4.6.7.5	Coefficient Method	-15.77	-21.26	15.77	-15.77
	Wedge Solution	-16.65	-22.8	16.81	-16.81

4.7 Example 4.7 *analysis* mode of operation for a clay site, an extension of Example 4.3

A total stress definition with the angle of internal friction of (φ) of 0 degrees and two material layers, where the upper clay layer possesses an undrained shear strength (c) of 300 psf and the lower clay layer has c = 400 psf. This I-Wall system has an exposed height of 10 ft. The water surfaces on both sides of the I-Wall are at 10 ft on the flood side and 0 ft on the landside. The flood side corresponds to the LHS of the I-Wall. In this scenario, the I-Wall will rotate clockwise during flood loading. The clay layers have a level ground surface on both sides of the I-Wall at el 0.0 ft with saturated unit weight of 122 pcf, and at el -10 ft with saturated unit weight of 124 pcf. A user-specified sheet-pile tip elevation of el -28.17 ft has been assigned for this analysis of the design problem of Example 4.3.

Figure 4.96 outlines the basic geometry and structural parameters for the sheet-pile wall. The top row of text documents the input values of all parameters associated with each material type. For this problem, two materials are assigned and listed as M01 and M02, the "M" signifies the material type and is followed by the ID, which starts from "01." All information concerning material types are written in black text. The representation of a portion of a layer of soil on each side of the I-Wall is characterized as a region. Two soil regions are required to represent each soil layer. Regions are labeled with an "R" and followed by an ID starting from "01." For this problem four regions are assigned, Region 1 and Region 2 (as R01 and R02), they are located on the LHS of the sheet-pile wall. Region 3 and Region 4 (as R03 and R04) are located on the RHS of the sheet-pile wall. Each region and its surface elevation are written in red text. Surface water on either side of the sheet-pile wall are drawn with the water symbol at its defined elevation and labeled as "Left Water Surface" and "Right Water Surface" at the top of the wall in light blue text. Piezometric surfaces are labeled as "P" and followed by an ID starting from 01. Piezometric water surfaces are listed in the upper left-hand corner, drawn with the water symbol at its defined elevation, and shown in blue. Observe that piezometric surface ID, P01, is assigned to all four regions. The LHS piezometric surface elevation is assigned as the LHS surface water elevation. Similarly, the RHS piezometric surface elevation is assigned as the RHS surface water elevation. This allows for the assignment of submerged unit weights to the four soil regions.

A clay site using a total stress definition with φ = 0 as illustrated in Figure 4.96, is considered for the "Analysis" process where the passive Factor of Safety is successively adjusted until the calculated sheet-pile tip is approximately equal to the user-specified input within a set tolerance. Hydrostatic water pressures, as well as the Coulomb Coefficient Method of analysis and hydraulic fracturing, are specified in this example.

This φ = 0 analysis resulted in a computed mobilized active earth pressure coefficient (K_a) of 1.0 and a mobilized passive pressure coefficient (K_p) of 1.0. Both the active and passive earth pressures for both sides of the sheet-pile wall are illustrated in Figure 4.97. The hydraulic fracturing procedure discussed in Appendix B estimates a gap depth of 13.31 ft. Active earth pressures only develop at the gap depth, or where the fracturing terminates, this is shown by the LHS active earth pressure diagram of Figure 4.97a. Note the change in earth pressures at el -10 ft, at the interface of Regions 1 and 2 of the passive earth pressure of Figure 4.97a, and also at the interface

of Regions 3 and 4 of Figure 4.97b. Please refer to Chapter 2 for a detailed description of multilayered soils. The hydrostatic water pressures acting on both sides of the sheet-pile wall are shown in Figure 4.98a.

Figure 4.96. Corps_I-Wall schematic of sheet-pile wall in clay site.

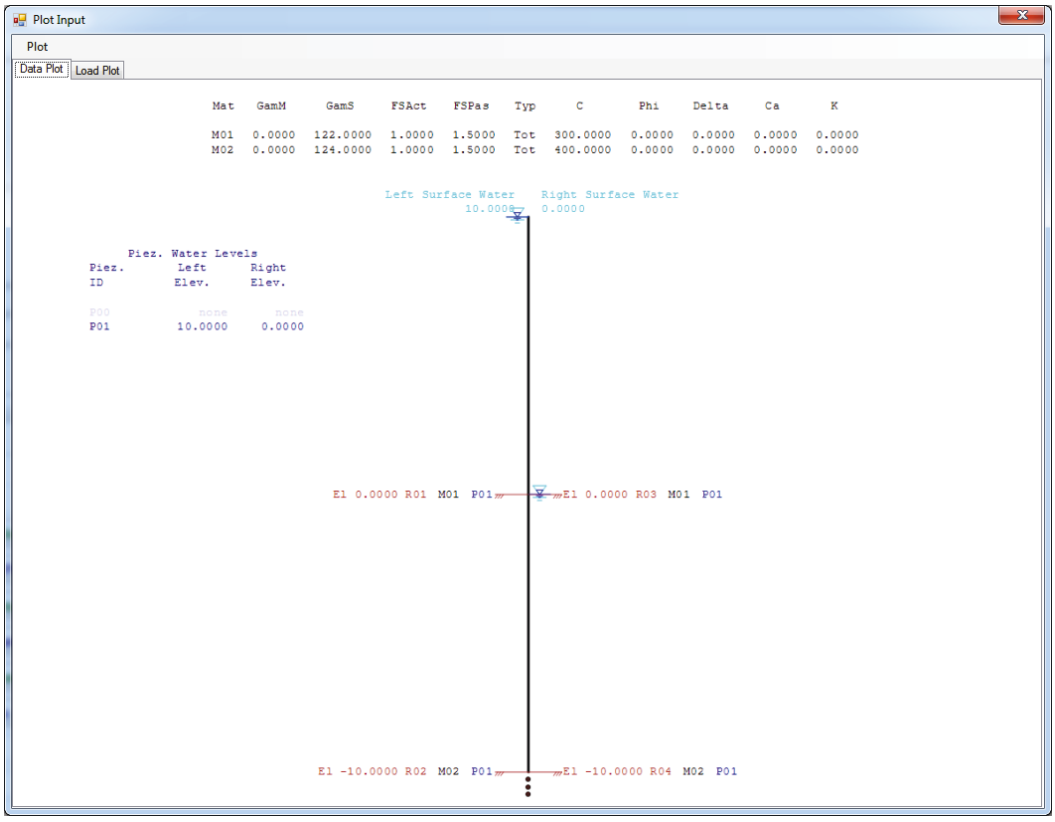
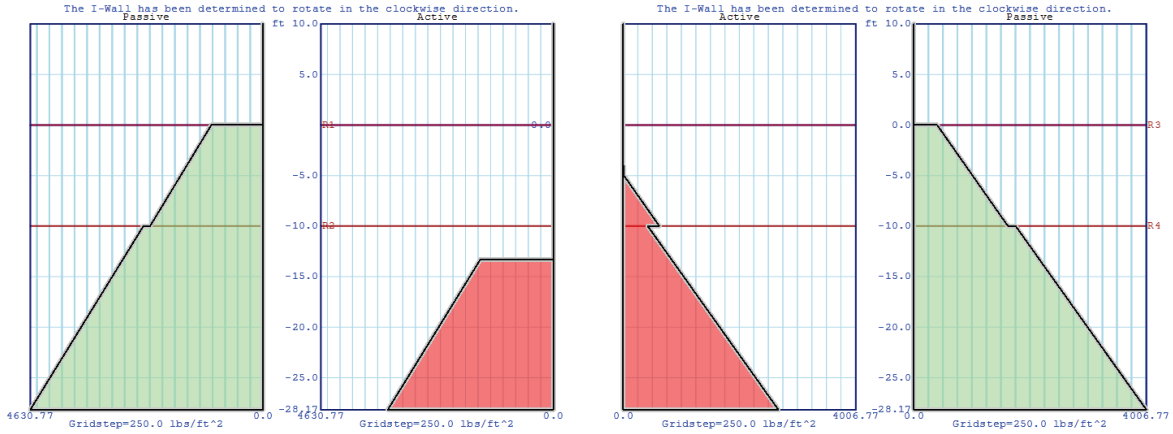
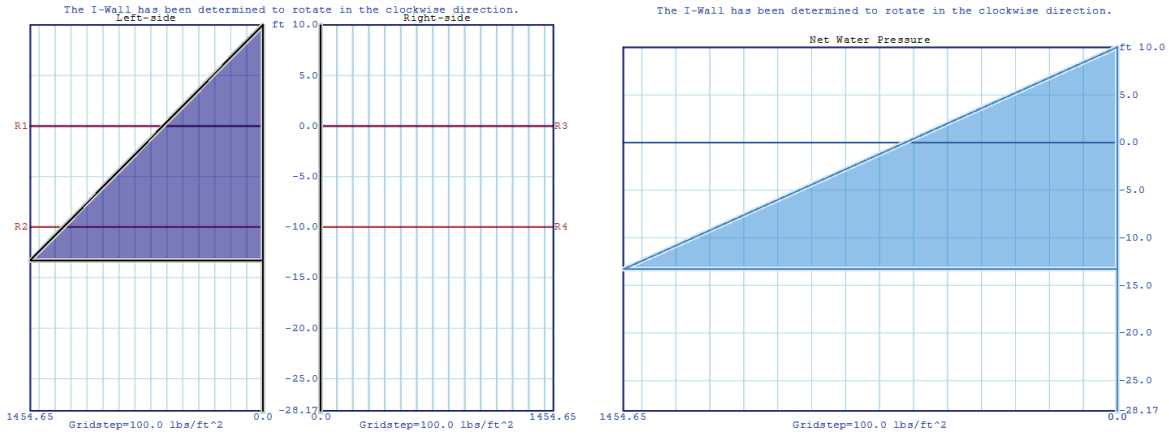


Figure 4.97. Active and passive earth pressures for undrained shear strength. (a) LHS of wall, (b) RHS of wall.



(a) (b)

Figure 4.98. Pore water pressures. (a) LHS and RHS of wall. (b) Net water pressures.

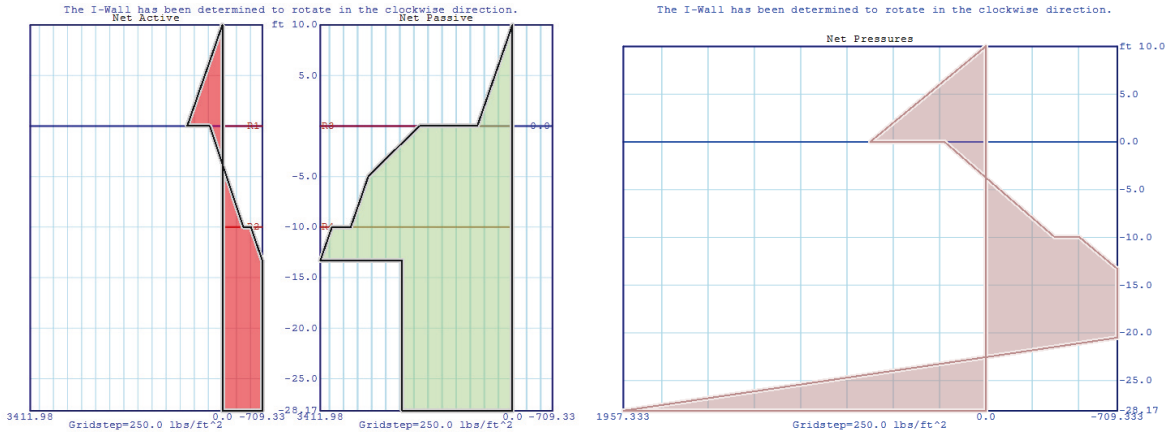


(a) (b)

The resultant net water pressure, calculated by taking the difference between the water pressures acting on both sides of the wall (Figure 4.98a), is shown in Figure 4.98b. In a total stress analysis, only overburden water pressure is included in the analysis (i.e., there is no pore water pressure calculated within the soil below the gap on the LHS and below the ground surface on the RHS). Also note, that boundary water pressures acting on the flood wall for this total stress clay site increase with the propagation of the fracture down to the gap depth.

From the calculated pressures of Figures 4.97 and 4.98, the net active and net passive pressures are constructed and presented in Figure 4.99a. For the prescribed LHS flood loading, the I-Wall will rotate in a clockwise direction. The net active pressure is determined from the difference between the LHS-mobilized active earth pressure and the RHS-mobilized passive earth pressure (i.e., acting on the other side of the wall), with the addition of the net water pressures, any external horizontal net pressures, and overburden pressures (if any). The net passive pressure is determined by the difference between the LHS-mobilized passive earth pressure, and the RHS-mobilized active earth pressure acting on the other side of the sheet-pile wall, with the addition of any net water pressures, any external horizontal net pressures, and overburden pressures (if any). The calculated net active and net passive pressures above the ground surface el 0.0 (and above R01 and R03) of Figure 4.99 are solely derived from the net water pressures of Figure 4.98b.

Figure 4.99. Net pressures. (a) Net active and net passive. (b) Net pressure diagram.

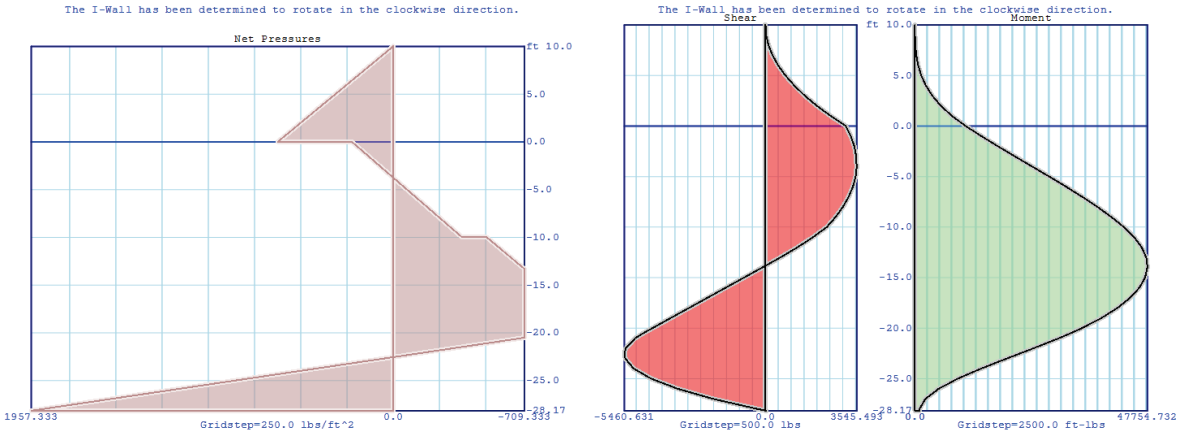


(a) (b)

The net pressure diagram of Figure 4.99b is derived from the replication of all values of the net active pressures, from the top of the wall until the elevation at the PR (at el -20.52 ft). At this instant the remaining values of the net pressure diagram are assumed to be linear with elevation between 1) the net active pressure value at the elevation of the PR, and 2) the net mobilized passive pressure at the elevation of the approximated sheet-pile tip (i.e., el -28.17).[1] Figure 4.99b is an illustration of how the net pressure diagram was formed. Because the I-Wall has been determined to rotate in a clockwise direction, the net pressure diagram of Figure 4.99b shows that the upper zone of net active pressures plot on the LHS and the lower zone plot on the RHS. The net passive pressures plot on the LHS of the sheet-pile wall. The final results are illustrated in Figure 4.100 by the presentation of the net pressure diagram, Figures 4.100a (replica of Figure 4.99b), and 4.100b, the shear and moment diagrams. Figure 4.100b shows that the maximum bending moment occurs at the zero crossing of the shear diagram.

[1] Only one mobilized net passive pressure value in Figure 4.99a is used to construct the Figure 4.99b net pressure diagram; corresponding to the sheet-pile tip elevation at el -28.17 ft. The majority of the net pressure diagram is derived from the Figure 4.99a net active pressure diagram.

Figure 4.100. (a) Net pressure diagram. (b) Shear and moment.



(a) (b)

The sheet-pile tip elevation is computed to be at -28.17 ft, this is equivalent to the value specified as input. For this analysis, the results produced a passive Factor of Safety of 1.5, this corresponds to the same passive Factor of Safety for this problem executed as the Example 4.3 design problem.

Table 4.37 shows a comparison of the results between the Coefficient Method and the Wedge Solution Method for Example Problem 4.7. The resulting elevations of the PR, and the elevation of the fully embedded pile tip are very consistent, varying by half a foot for the two methods. Gapping is also included.

Table 4.37. Comparison of Earth Coefficient results to Wedge Solution Method results - Example 4.7.

Method	Point of Rotation (PR) (elevation in feet)	Pile Tip (elevation in feet)	Gap (depth, feet)	Gap (elevation, feet)
Coefficient Method	-20.52	-28.17	13.31	-13.31
Wedge Solution	-20.90	-28.60	12.99	-12.99

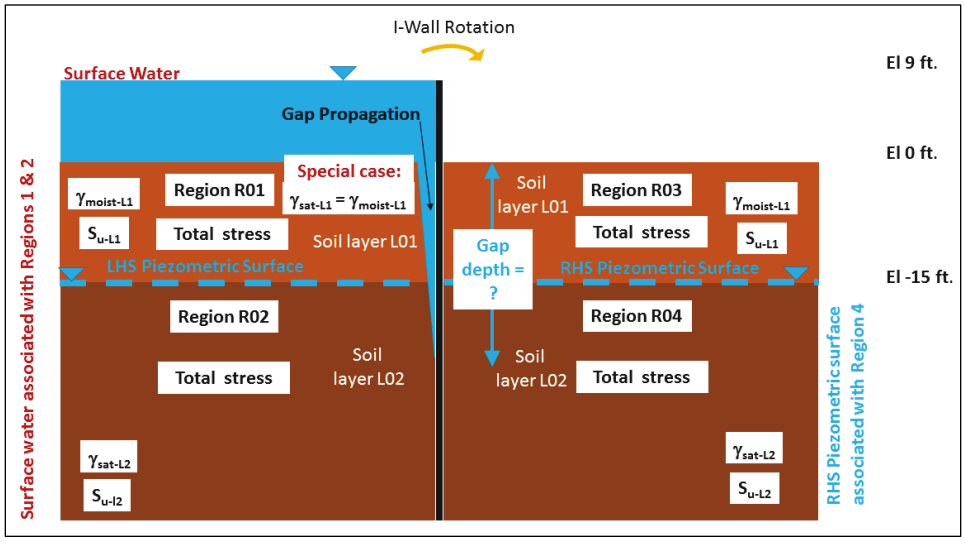
4.8 Model setup tips for calculating a depth of hydraulic fracturing

Corps_I-Wall has the capability to assess the depth that a zone of separation (i.e., a gap) forms along the flood side of the soil to sheet pile I-Wall interface during flood loading. The devised gap initiation, and gap propagation engineering methodology, implemented within the software (CI-Wall) makes use of a hydraulic fracturing criterion (as discussed in Appendix B). The following two prerequisites for gap development are included by CI-Wall: 1) The soil that may potentially develop a gap must

be assigned a nonzero value for its cohesive strength (either total or effective stress shear strength parameters), and 2) On the side of the I-Wall with flood loads, the surface flood water (elevation, designated as el) must be associated with all soil regions that may develop a gap within or through the region. Additionally, gap propagation proceeds from the ground surface down on the flood side of the I-Wall as the I-Wall rotates away from the flood pool loading side. Note that if during the course of the hydraulic fracturing analysis, the gap propagation algorithm detects that the gap is about to enter into a zero cohesion soil region, then gap propagation will terminate at the top of the cohesionless region.

Model setup tips for a gap initiation and gap propagation can be explained using an example sheet-pile wall penetrating clay problem similar to Example 4.6.7, (as discussed in subsection 4.6.5 on pages 217–223 of ERDC/ITL TR-16-3). This example's unique feature is a partially saturated (i.e., moist) clay top layer (versus a saturated layer) in a total stress site response analysis to a LHS, that is flood loaded. The model setup would follow the updated Figure 4.89, now Figure 4.101.

Figure 4.101. Sheet-pile wall penetrating clay with two soil layers.



For this expanded version, the site consists of two layers of homogenous clay. Each soil layer, designated L01 and L02, possesses values of moist unit weight, saturated unit weight and constant undrained shear strength, S_u. The total angle of internal friction, ϕ, is equal to zero. Table 4.38 summarizes this soil material information for each of the layers.

Table 4.38. Geotechnical properties for the two soil layers contained in Example 4.6.7.

Soil layer no.	Total or effective stress analysis	Moist Unit weight, γ_{moist} (pcf)	Saturated Unit weight, γ_{sat} (pcf)	Cohesion, c (psf)	Angle of internal friction, ϕ (degrees)
L01	Total	$\gamma_{moist\text{-}L1}$	$\gamma_{sat\text{-}L1}$	$S_{u\text{-}L1}$	0.0
L02	Total	$\gamma_{moist\text{-}L2}$	$\gamma_{sat\text{-}L2}$	$S_{u\text{-}L2}$	0.0

A total stress analysis is being specified in the CI-Wall material properties input for this problem because a soil shear strength definition is given in terms of S_u values. The top of moist clay layer L01 is at ground surface el 0.0 ft. The upper region of this clay layer is partially saturated while below a piezometric surface of el -15.0, the second clay layer L02 is saturated.

Insight: In a total stress analysis, without gapping, using CI-Wall, the only purpose a piezometric surface specification serves is to distinguish between the assignments of moist or saturated unit weights within that soil region. A piezometric surface is associated with this region. Specifically, for the soil within the region located above the piezometric surface (that is assigned to that region), a moist unit weight is assigned by the software while a saturated unit weight is assigned to the soil below the piezometric surface el for use in overburden computations. With CI-Wall, an alternative modeling procedure for piezometric boundaries is to divide a total stress soil layer into two regions at the el of the piezometric surface. In this case, no piezometric surface is associated with the upper region where a moist unit will be used by the software. But the piezometric surface must be associated with the lower region so that the saturated unit weight is assigned to this lower soil region for the overburden computations.

When conducting a gap initiation and propagation analysis using CI-Wall, the surface water must be associated with the potential gapping regions of the cohesive soil(s). This also means that the saturated unit weight input data will be used exclusively for total overburden computations. Thus, unsaturated soil layers (above the piezometric surface) that may experience gapping need to have their actual moist unit weight input for the modeled saturated unit weight. Again, the alternative modeling procedure of dividing this total stress layer into two regions at the el of the piezometric surface should be considered.

Four regions: The two soil layers are subdivided into four regions as shown in the Figure 4.89 CI-Wall model. This results in two soil layer regions on each side of the wall. Three material properties are specified for this model and are listed in Table 4.39. Table 4.40 associates the material numbers with the appropriate Figure 4.101 region numbers.

Table 4.39. Material property information for the four-region model of Example 4.6.7.

Material no.	Total or effective stress analysis	Moist Unit weight, γ_{moist} (pcf)	Saturated Unit weight, γ_{sat} (pcf)	Cohesion, c (psf)	Angle of internal friction, ϕ (degrees)
M01	Total	$\gamma_{moist-L1}$	set equal to $\gamma_{moist-L1}$	S_{u-L1}	0
M02	Total	$\gamma_{moist-L2}$	γ_{sat-L2}	S_{u-L2}	0
M03	Total	$\gamma_{moist-L1}$	γ_{sat-L1}	S_{u-L1}	0

Table 4.40. Material property assignments to the four-region model of Example 4.6.7.

Region no.	Material no.
R01	M01
R02	M02
R03	Mo3
R04	M02

***Surface water at el 9 ft*:** A flood el of 9 ft is specified on the LHS of the I-Wall in this total stress analysis. Since c (S_u for total stress analysis) is nonzero, the CI-Wall hydraulic fracturing criteria will be engaged to calculate the depth of gapping on the LHS of the I-Wall. Prior to CI-Wall analysis, it is not known if the gap propagates partially into region R01 or fully through region R01 and into region R02. In order to allow the CI-Wall hydraulic fracturing criteria to compute the depth of gapping on the LHS of the soil-to-sheet pile interface, it is necessary to associate the LHS surface water (at el 9.0 ft) with both region R01 and region R02 (refer to Figure 4.101) in the CI-Wall model input. Because this is a total stress analysis, associating these two regions with the surface water means that overburden computations are made using the saturated unit weight inputs.

LHS piezometric surface at el -15 ft: Since there is a possibility in this total stress analysis that the gap may propagate through region R01 and into region R02, the LHS piezometric surface is not associated with

region R02. This allows for the surface water to be associated with region R02 for gap propagation considerations. Recall that since the surface water is associated with region R02, a saturated unit weight is used in CI-Wall overburden computations for this region (versus using the moist unit weight input).

RHS piezometric surface at el -15 ft: The RHS piezometric surface at el -15.0 ft is specified at the top of soil region R04. Since the RHS piezometric surface is associated with region R04, a saturated unit weight is used in CI-Wall overburden computations for this region (versus using a moist unit weight).

Soil unit weights: Because of the presence of the upper moist (i.e., non-saturated) region R01 clay layer that is immediately below the flood surface water, three different material types are specified for the model. The lower clay regions, R02 and R04, are assigned a saturated unit weight and soil region, R03 is assigned a moist unit weight in total stress, overburden computations. This is consistent with conventional geotechnical criteria. For soil region R01, a moist unit weight value is assigned to the saturated unit weight input in CI-Wall. A special material number M01 shows this special input data in Table 2. This data input is required because, in a total stress soil region for which the LHS surface water is associated with, the CI-Wall hydraulic fracturing algorithm makes exclusive use of the saturated unit weight input value in its total stress, overburden calculations.

4.9 Comparison of Coefficient Method results with Wedge Method results

The following figures are based on two analyses of the Example Problem 4.3. The results have already been discussed in subsection 4.3. These figures show the qualitative difference between the Coefficient Method for the design of an I-wall and the Wedge Method. Figure 4.102 reviews the input parameters for Example 4.3.

Figure 4.102. Input geometry, material properties, and water levels used for Coefficient and Wedge Analysis of Example 4.3.

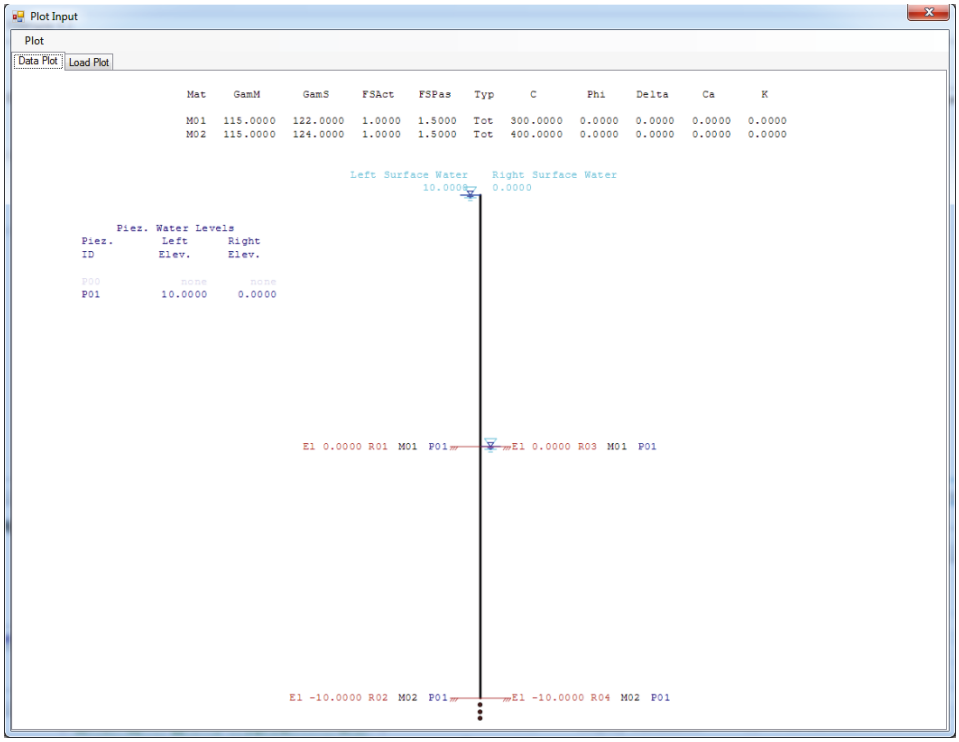
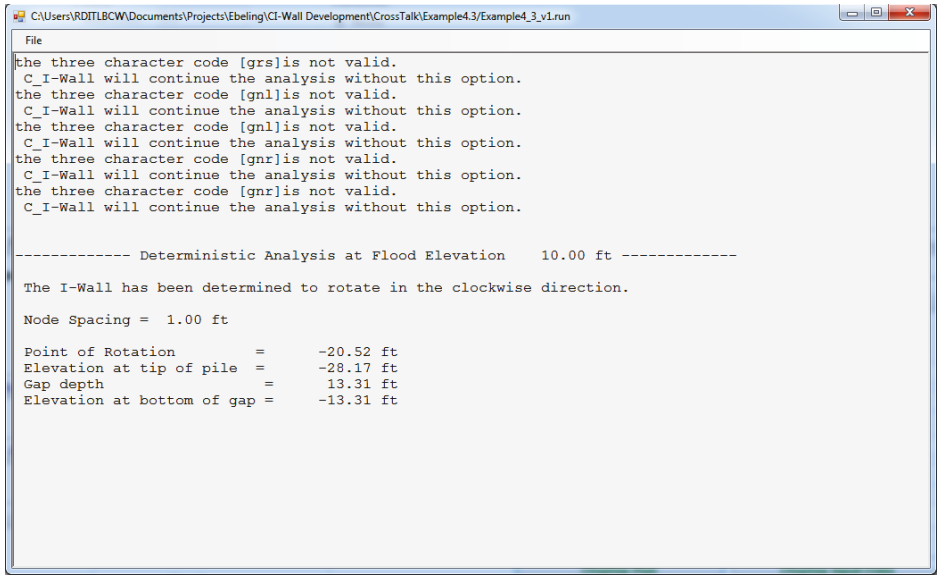


Figure 4.103 a and b show the resulting outputs for the Coefficient Method and the Wedge Method, respectively. The results show minor differences. The PR for the two methods varies by 0.28 feet. The pile tip elevation for the two methods varies by 0.43 feet. Finally, the gap depth varies by 0.323 feet. All of these values differ by less than 0.5 feet.

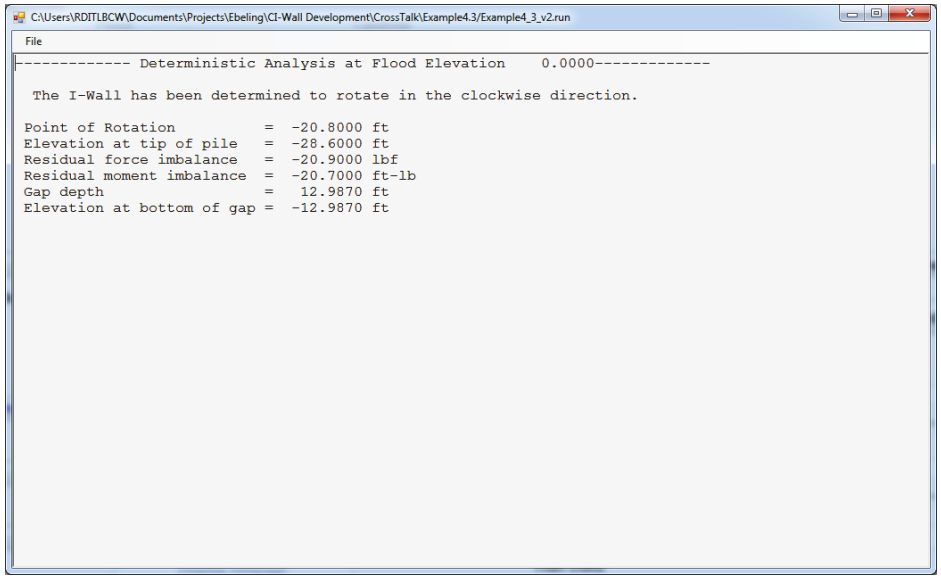
One would expect the gap depth to vary, because the solution method used by the Coefficient Method performs tests at points along the wall as the depth increases, and the Wedge Method estimates the gap depth by solving equation B.7 for each material region and progressing to the deepest depth for the final calculation.

The results for the PR and pile tip elevation need a little more explanation as the following figures show. But before a discussion of earth pressures, a comparison of the water pressures between the two methods needs to be discussed.

Figure 4.103 Results from analyzing the Example 4.3 input using the (a) Coefficient and (b) Wedge Method.



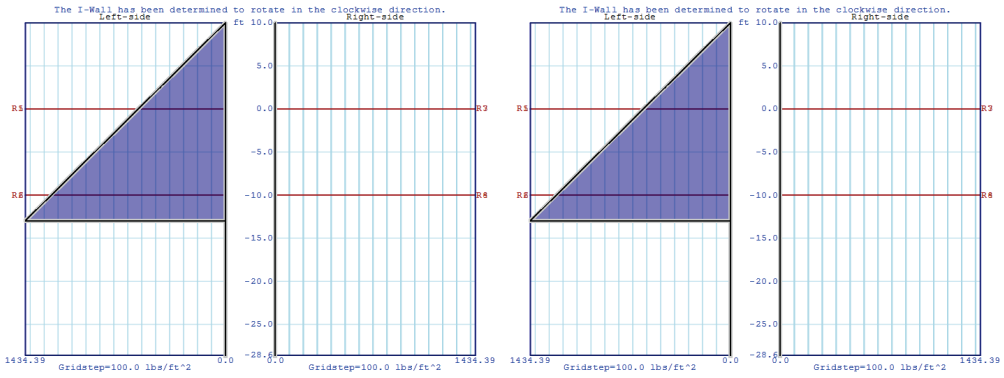
(a)



(b)

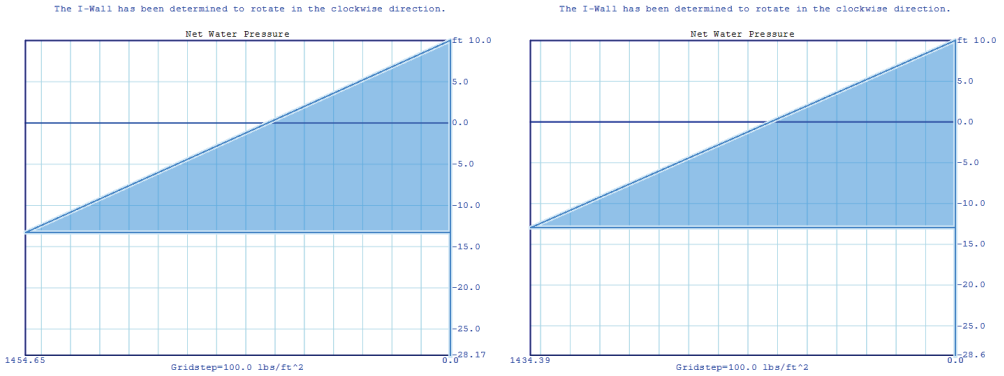
Figure 4.104 and Figure 4.105 show the resulting water pressures calculated by the Coefficient and Wedge Methods of analysis. These pressures are acting against the wall directly and are calculated in a similar manner for both methods. The only difference between the two plots is the final depth of the water pressure acting against the wall and the resultant higher pressure at that depth because of the very small difference in gap depth.

Figure 4.104 Resulting left and right hand side water pressures for the (a) Coefficient and (b) Wedge Methods.



(a) (b)

Figure 4.105 Resulting net water pressures for the (a) Coefficient and (b) Wedge Methods.



(a) (b)

Figure 4.106 and Figure 4.107 reveal the major difference when comparing the results of the Coefficient Method of analysis to the Wedge Method of analysis. While the curves are similar, as expected with coincident input data, the curves are revealing at the boundaries of regions. Because the Coefficient Method works directly with pressures, this is possible because of the restriction that only horizontal soil regions may be used, the curves for pressures can show discontinuities at region boundary elevations.

Because the Wedge Method works from the forces acting between earth wedges as they approach the wall along a slip plane, the pressures have to be derived from the forces of the wedge and their subwedges. Therefore, the curves may change steeply at the interface regions, however, they cannot go completely horizontal. The sample points for forces at these region boundaries are placed close on either side of the boundary region at the wall to minimize the effects on the derived curve.

Figure 4.106 Resulting LHS active and passive soil pressures for the (a) Coefficient and (b) Wedge Methods.

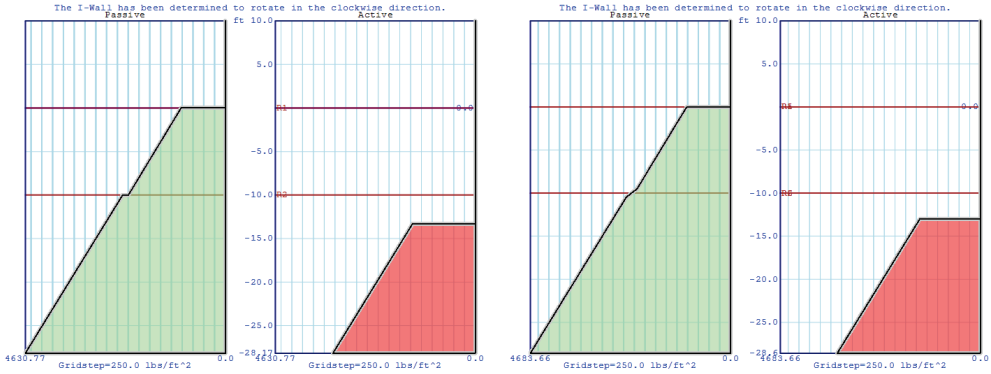


Figure 4.107 Resulting right hand side active and passive soil pressures for the (a) Coefficient and (b) Wedge Methods.

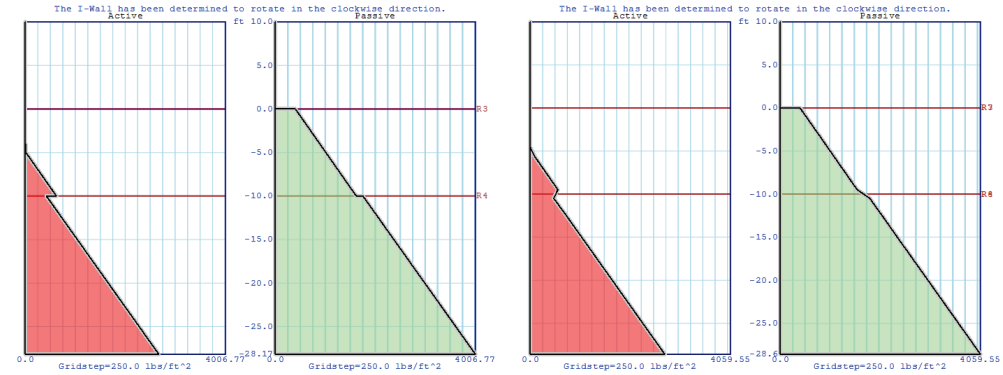


Figure 4.108 through Figure 4.110 show the results of using the derived pressure curves with the water pressures and user-defined horizontal pressures to determine the net active and passive pressure curves, the net pressure curve of the balanced I-Wall structural feature, and the shear and moment diagrams along the length of the wall to the pile tip for the balanced I-wall structural feature.

Figure 4.108 Resulting net active and passive pressures given the direction of rotation for the (a) Coefficient and (b) Wedge Methods.

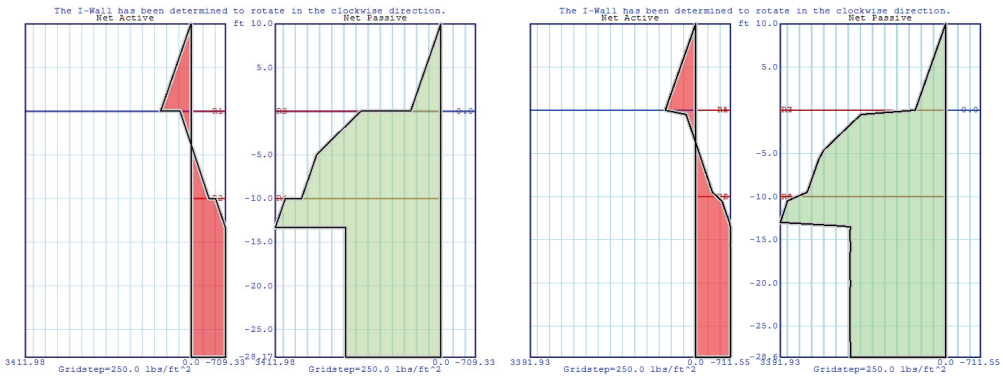


Figure 4.109 Resulting net pressures given wall tip depth and PR resulting in balanced forces and moments for the (a) Coefficient and (b) Wedge Methods.

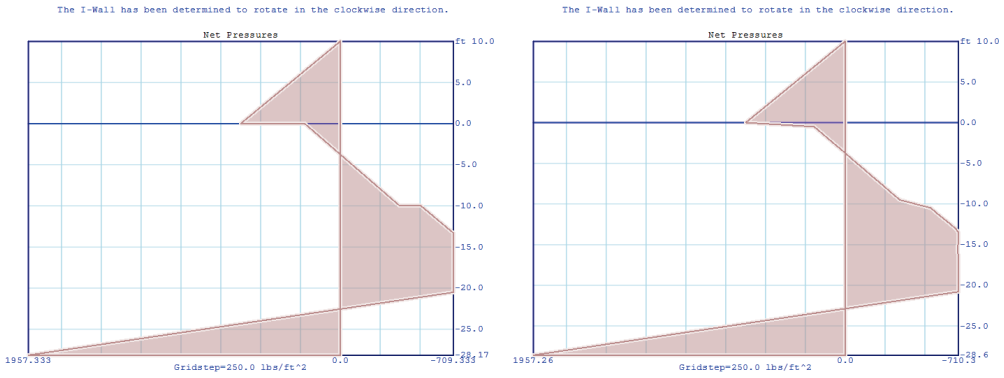
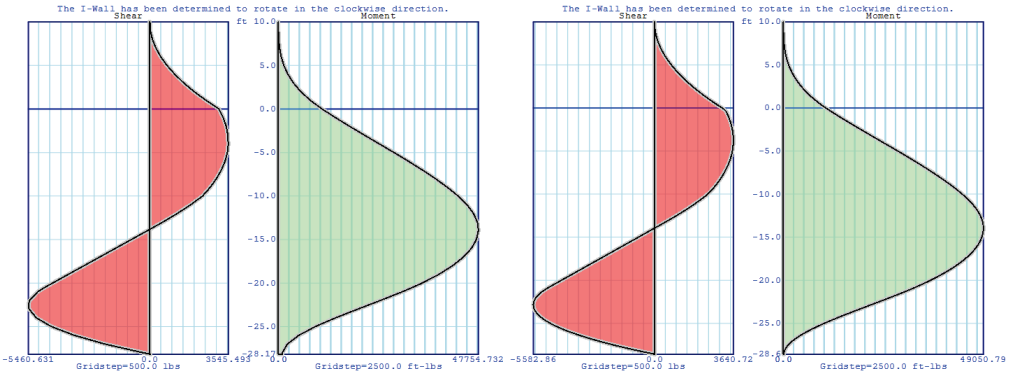


Figure 4.110 Shear and moment diagrams for the pressures acting along the designed I-wall.



4.10 A nonlevel ground example showing the fexibility of Wedge Method results

The Wedge Method of Analysis was introduced in Version 2.0 to calculate non-level soil surfaces and piezometric water levels. This section contains an example that illustrates the difference that non-level soil surfaces can make.

Figure 4.111 and Figure 4.112 show the input geometry and properties for the model using three soil materials. The example problem is based on a levee founded I-Wall situated at the center of a levee with a 30 ft crown. The elevation of the crown at the centerline of the I-Wall is 0 ft, and the elevation at the two edges of the crown, 15 ft away from the I-Wall, drops to el -2 ft. From the crown, the levee fill has a slope of 1V:2H for a drop of 13 ft in elevation. At this levee's lateral extents, the elevation is -15 ft at a distance 67 ft from the I-Wall. The levee fill has been placed on a clayey sand foundation. The foundation material underwent settlement as a result of the placement of the levee fill. The base of level elevation is -19 ft.

The clayey sand and silty sand foundation soil depositions are approximated as level, at -15 ft and -40 ft, respectively.

The LHS surface water flood elevation is specified as 10 ft in this problem. No surface water is assumed on the RHS Landside.

The first material (M01) is a clayey sand levee fill. This is used to build up the area and reduce the potential for landside flooding. This material makes up the uppermost region. For simplicity in this example, the material has been assigned a moist and saturated unit weight of 115 pcf. The material's effective cohesion (c') is 50 psf and the effective angle of internal friction (ϕ') is 28 degrees. The water levels for determining saturation of the soil regions are defined by the surface water, these have an elevation of 10 ft on the flood side and no water surface elevation on the landside.

The second material (M02) is clayey sand which forms the bed of the LHS flood channel and soil surface on the landside, respectively, away from the levee. This material makes up the two middle soil regions. For simplicity in this example, the material has been assigned a moist and saturated unit weight of 121 pcf. The material's effective cohesion (c') is 75 psf and the effective angle of internal friction (ϕ') is 27 degrees. The water levels for determining saturation of these soil regions are defined by a level piezometric surface with an elevation of 0 ft on the flood and landsides.

The last material (M03), is silty sand which forms the supporting base below the clayey sand soil layer. This material makes up the bottom regions from elevation -40ft and lower. For simplicity in this example, the material has been assigned a moist and saturated unit weight of 120 pcf. The material's effective cohesion (c') is 20 psf and effective angle of internal friction (ϕ') is 30 degrees. The water levels for determining saturation of these soil regions are defined by a level piezometric surface with an elevation of 0 ft on the flood and landsides.

The geometry of these regions is where the Wedge Method input differs from the Coefficient Method input. Figure 4.113 shows the "reduced model equivalent" computational geometry that is important to the Coefficient Method model, because the Coefficient Method assumes level soil strata for the soils contacting the wall, as identified in Figure 4.111. Figure 4.112 shows the actual, non-level geometry of the soils around the I-Wall, this can only be solved using the Wedge Method.

Figure 4.111 Material properties and water levels for the Wedge Method model.

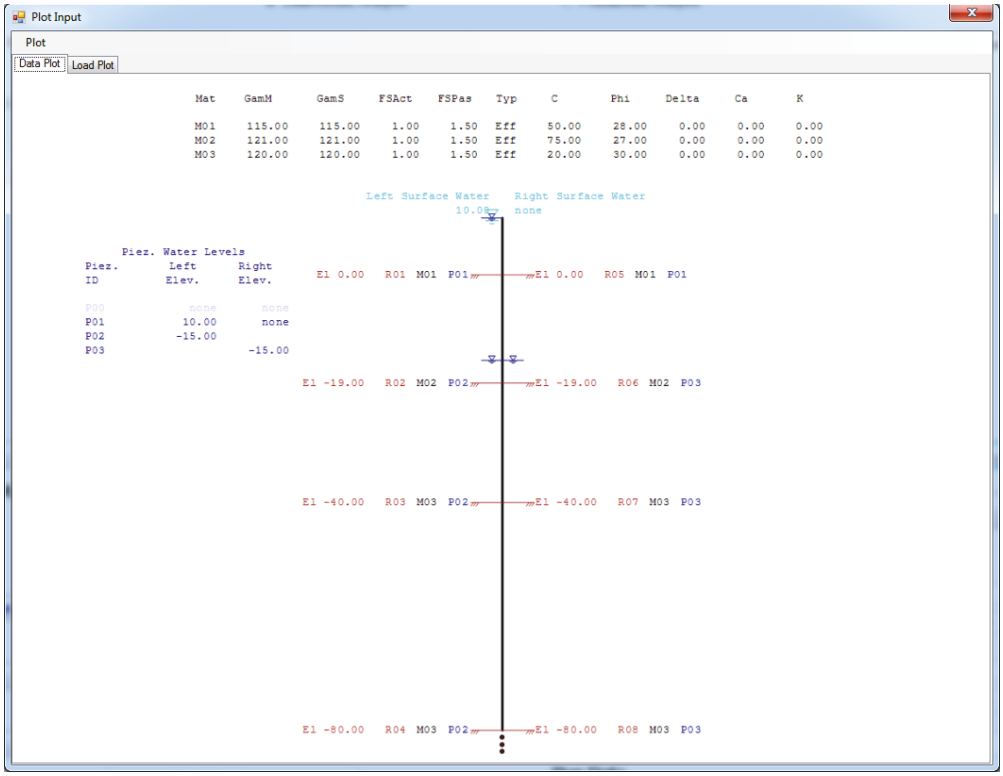


Figure 4.112 Non-level soil geometry for the Wedge Method model.

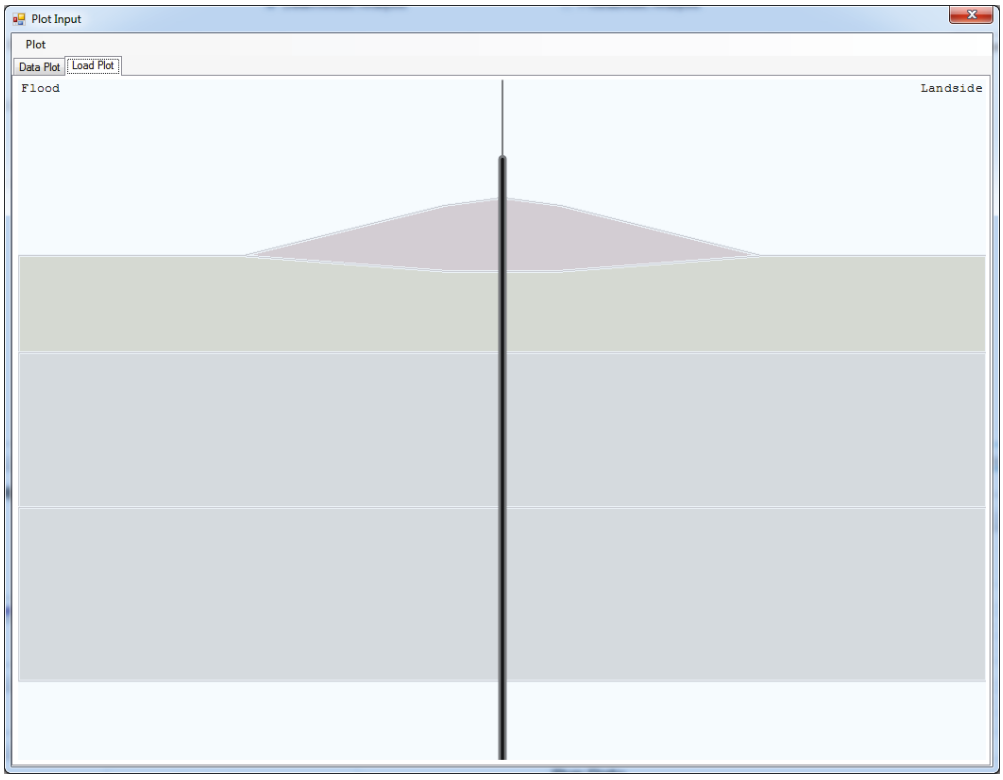
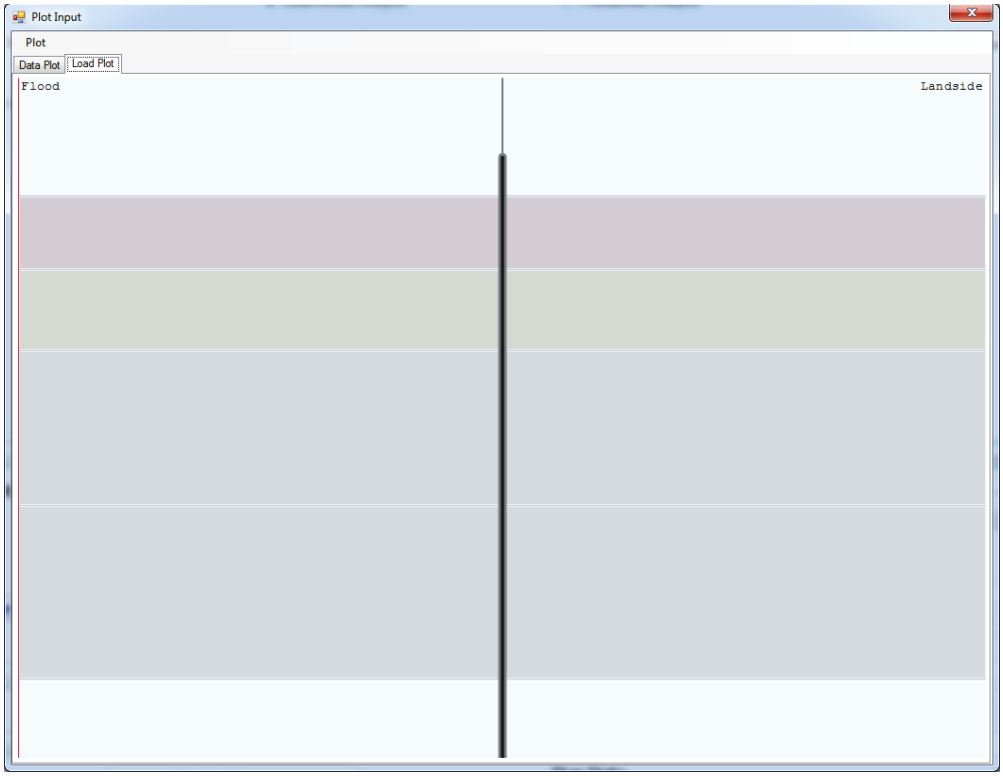


Figure 4.113 Effective soil geometry for the Coefficient Method model.

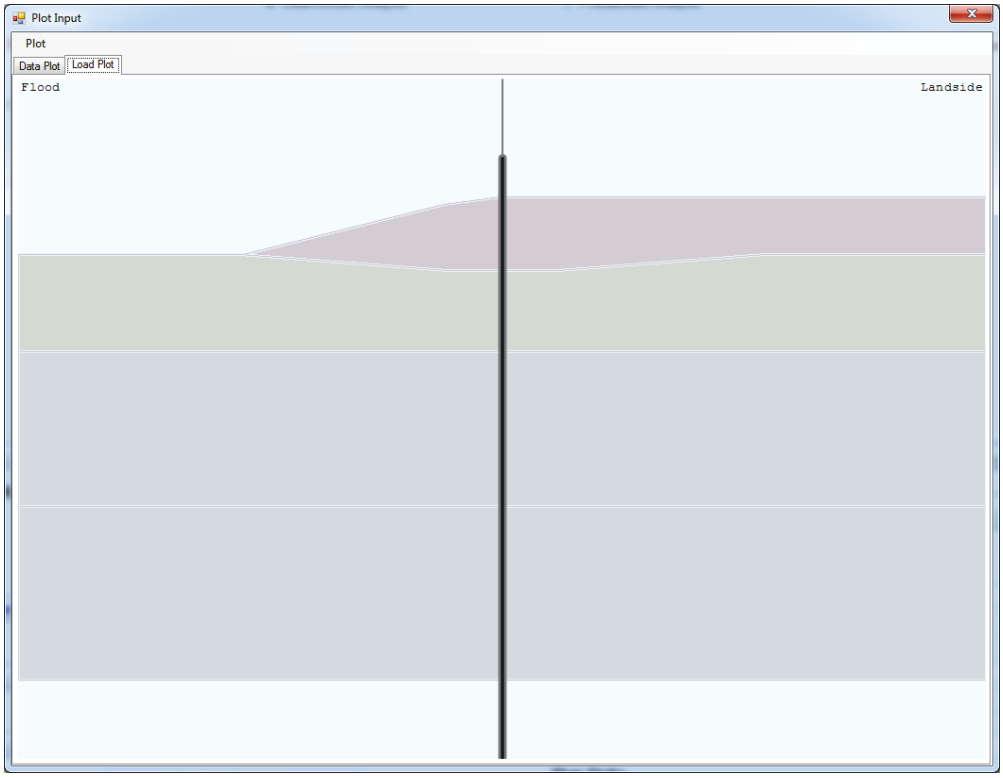


The results of running the non-level soil geometry with the Wedge Method for a el 10 ft LHS flood surface water gives a clockwise wall rotation, a wall tip elevation of -27.6 ft, a rotation point elevation of -23.55 ft, and a gap elevation to -3.164 ft (on the LHS). Running the same problem with the Coefficient Method, with the reduced model equivalent of an all horizontal soil strata of Figure 4.113, gives a clockwise wall rotation, a wall tip elevation of -19.61 ft, a rotation point of -14.94 ft, and a gap elevation to -3.16 ft. There is a considerable difference between the results computed by the two methods, a difference of nearly 8 ft for the wall tip, and a difference of nearly 9 ft for the rotation point. The Coefficient Method gave deeper resulting depths.

The authors hypothesized that the difference between the two computed results is explained by the reduction of soil providing passive resistance to the RHS of the levee structure. Because the material 1 (M01) layer dropped off rather than continuing to the (lateral) extents of the model, much material was not there to provide the RHS passive resistance to the LHS flood loading condition. To test this hypothesis, the authors adjusted the model to include a horizontal levee fill material layer to the RHS extents of the model on the landside (as shown in Figure 4.114). Notice that this

example has the same reduced model equivalent RHS soil geometry profile as for the RHS of the Figure 4.113 Coefficient Method initial problem. Running this hypothesis problem should provide a nearly similar passive response as the Coefficient Method problem.

Figure 4.114 Changed soil geometry for hypothesis Wedge Solution Method model.



The hypothesis Wedge Method resulted in a clockwise rotation for a LHS flood elevation of 10 ft, a wall tip elevation of -19.7 ft, a rotation point elevation of -14.7 ft, and a LHS gap elevation to -3.164 ft. These computed results are very similar to the Coefficient Method results. The wall tip elevation between the methods varied by about 0.1 ft with the Wedge Method being deeper, and the rotation point elevation varied by nearly 0.25 ft with the Wedge Method being shallower. The similarity of these results validates the authors' hypothesis which provides validity to the original Wedge Method solution.

5 Probability Analysis and Example Problems

5.1 Fragility curve (i.e., SRC)

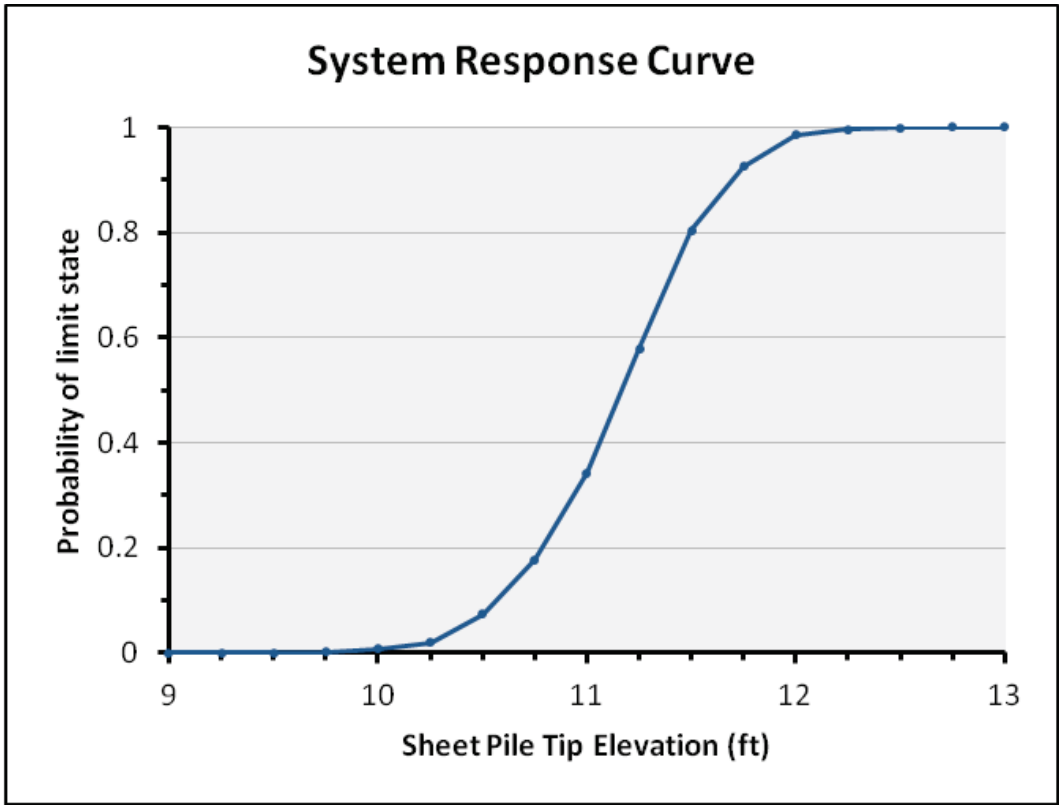
Within the USACE, the term SRC (i.e., System Response Curve) is now being used to describe what has been commonly referred to in the technical literature as the fragility curve. This term is also used for the hydrologic fragility assessment of rock-founded concrete gravity dams. This report uses the new USACE terminology. Tekie and Ellingwood (2002) discuss the development of fragility curves used in a hydrologic fragility assessment for gravity dams. The procedure for constructing an SRC for an I-Wall with a rotational limit state is analogous.

In safety or risk assessment of sheet-pile I-Walls, limit states or probability of failure serve as a measure of system performance. The SRC is used to predict the probably of failure, given the hydraulic hazard. Consider the example of a sheet-pile I-Wall in which the rotational limit state (i.e., $FS_{rotate} \leq 1.0$) is the limit state resulting in failure of the I-Wall. Introducing the names for the variables used in this report into Equation 5.1 of Tekie and Ellingwood (2002), the probability of failure, $P_{failure}$, is given by the expression

$$P_{failure} = \sum_{H_{Flood}} [P(FS_{rotate} \leq 1.0 \mid Flood = H_{Flood}) \cdot P(Flood = H_{Flood})] \quad (5.1)$$

in which *Flood* is a vector of random variables describing the intensity of demand (e.g., flood elevation) and other factors to include: $P(Flood = H_{Flood})$ is the hazard, which considers river floods that overtop the I-Wall or from a coastal surge and is expressed in terms of annual probability, and $P(FS_{slide} \leq 1.0 \mid Flood = H_{Flood})$ is the conditional probability of I-Wall rotational structural failure, given that $Flood = H_{Flood}$, as obtained for the Figure 5.1 SRC developed using the engineering procedure and corresponding PC-based software discussed in this report. Expressing the limit state probability, as in Equation 5.1, allows the overall risk to be deconstructed into its significant contributors.

Figure 5.1. SRC for rotational limit state.



In Chapter 6 of Tekie and Ellingwood (2002), they observed that a fully coupled probabilistic safety assessment combines the probabilistic/ statistical definitions of hazard (i.e., demand) and SRC (i.e., capacity) and leads to a point or interval estimate of failure state probability for the limit state associated with structure failure, depending on how the epistemic uncertainties are incorporated in the analysis. The hazard is described by the complementary cumulative distribution function (CCDF) and the SRC is defined by the cumulative distribution function (CDF). Tekie and Ellingwood (2002) observed that the probability of failure can be expressed as the convolution of the hazard function and the SRC in their Equation 6.1, an integral form of Equation 5.1. Additionally, modeling (epistemic) uncertainties propagated through the analysis of the hazard and fragility will give rise to a distribution for the probability of failure, $P_{failure}$, as depicted in Figure 6.1 in Tekie and Ellingwood (2002). Therefore, if the mean hazard and mean SRC are used, they observed that the convolution integral (their Equation 6.1) yields a point estimate for the limit state probability. Citing previous research published by Tekie and Ellingwood (2002) they conclude that this point estimate does not necessarily yield the mean of $P_{failure}$, as the uncertainties are not propagated in the same way but this estimate is usually close to the mean of $P_{failure}$.

5.2 Random variables for each soil layer (φ, c, δ, Ca) and correlation between variables

The shear strength parameters of soil are derived from the Mohr-Coulomb relationship between cohesion (c) and the angle of internal friction (φ). These two variables, including the soil adhesion (Ca) and the angle of soil-wall interface friction (δ), have been determined to behave inherently random and are, therefore, considered as uncertain variables in this report. These variables are represented by their mean (μ) and standard deviation (σ) and representative coefficient of variation (COV), along with their correlation (ρ) relationship.

Correlation measures the relationship between two variables. Two variables are positively correlated when one variable increases as the other increases, or one variable decreases as the other decreases. They are inversely correlated, as one variable increases, the other decreases or conversely when one variable decreases, the other increases. The value for the correlation ρ between two variables ranges from -1.0 to 1.0. A ρ value set equal to 0 implies that the variables have no correlation, but it does not mean that they are independent from each other. However, independent variables possess zero correlation. Considering Mohr-Coulomb shear strength parameters {c, φ}, a strong correlation is represented by values ranging from (±0.7 to ±0.99), moderately correlated values range from (±0.7 to ±0.3), and values closer to 0.0 represent weak correlations. These correlation strength definitions have been used only as guidelines for this report.

When non-zero correlations are specified between two random variables, a rank correlation method is used by the software to determine the correlation between the two variables, this results in a rank correlation matrix. For n-variables, a symmetric n-by-n correlation matrix will be applied. Correlation between variables should be specified for every pair of random variables. When more than two random variables are defined, and one variable is correlated to two or more variables, there could be the possibility of the introduction of an adjusted rank correlation matrix. This adjusted correlation matrix will contain correlation coefficients that have been modified from the original matrix for numerical stability.

Table 5.1 represents the correlation relationship in some examples contained within this report between c and φ as being inversely correlated, between c and Ca as positively correlated, and between φ and δ as also

positively correlated. Correlations can also be assigned among pairs of variables from different soil layers. It is anticipated that actual project data will be used to establish the statistics for each of the variables and the correlation between variables. From these statistical properties, each variable can be characterized by either a normal, log-normal, or uniform probability distribution function, and the variables generated for the number of simulations requested will vary between 0 and $\mu + 3\sigma$. The lower limit of a value of zero is specified in the distribution so as to eliminate the possibility of negative values being generated for c, φ, δ, or Ca variables during Latin hypercube simulations. These variables can also be represented with distributions that allow user defined limits. The bounded normal, bounded log-normal, and triangular functions require lower and upper bounds in addition to the aforementioned statistical parameters of μ, σ, and COV.

Table 5.1. Correlations used among variables in some example problems.

	Cohesion	Angle of Internal Friction	Soil-to-Sheet-pile Wall Interface Friction Angle	Adhesion
	(c)	(φ)	(δ)	(Ca)
Correlation between two variables	x			x
		x	x	
	-x	-x		

Note: x signifies that the variables are positively correlated, and -x signifies the variables are inversely correlated

Total stress (c, φ, δ, or Ca) or effective stress (c′, φ′, δ′, or Ca′) based shear strength parameters may be used in the analyses.

As discussed in Cherubini (2000), for drained tests, Harr (1987) indicates correlation between effective cohesion c′ and friction angle φ′. In particular, the results of Wolff (1985) (correlation coefficient $\rho = -0.47$), Yucemen et al. (1973) ($-0.24 \leq \rho \geq -0.49$), and Lumb (1970) ($-0.37 \leq \rho \geq -0.70$) are cited. Cherubini (1997) found a value of $\rho = -0.61$ for drained triaxial tests on Blue Matera clays.

According to Cherubini (2000), Table 5.2 shows the range of most frequent values of COV for some geotechnical soil properties (Becker 1996; Cherubini 1997).

Table 5.2. Ranges of the most frequent values of COVs.

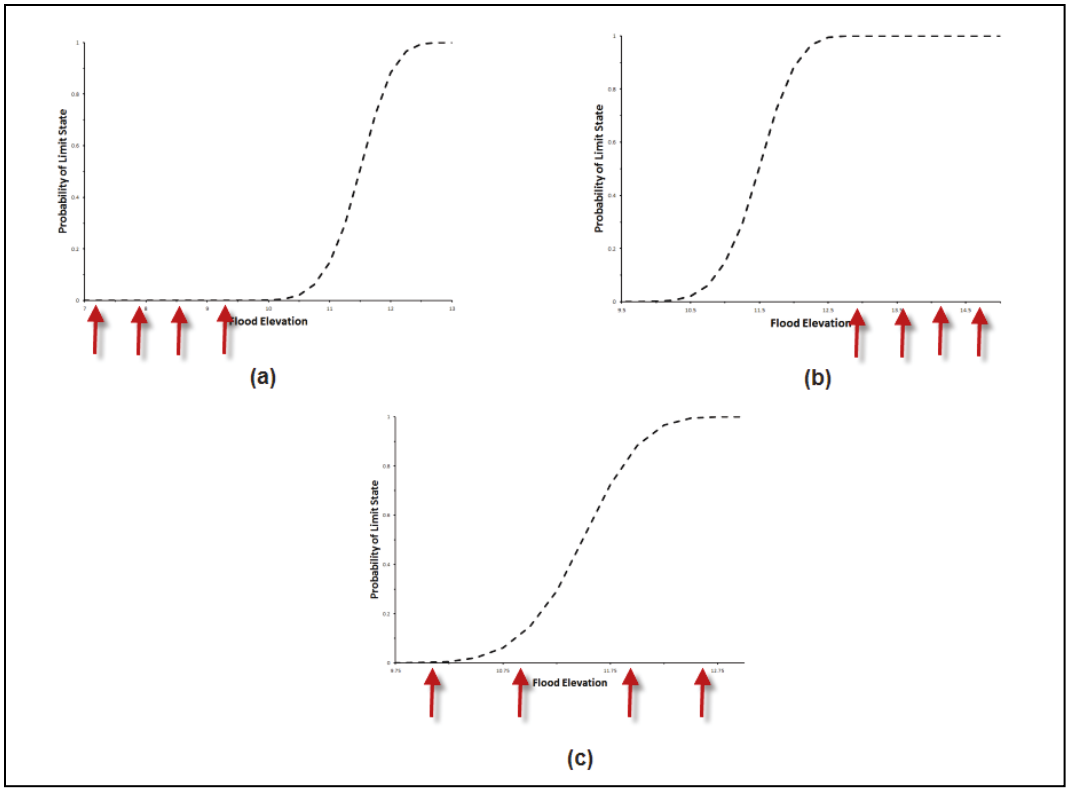
Unit Weight	Range (%) 3 - 10
Effective friction angle φ'	
Clay	10 - 50
Silt	5 - 25
Sand	5 - 15
Effective cohesion c'	10 - 70

5.3 Finding the SRC for an analysis of an existing I-Wall

The analysis of an I-Wall considers the estimation of the passive Factor of Safety of an existing wall. A probabilistic assessment for the passive Factor of Safety of less than, or equal to 1 for a predetermined number of simulations and specified flood elevation is used to define a point on the SRC. It is recommended to initially experiment with 100 simulations. After completion of analyzing the 100 simulations at the various flood elevations, the SRC should be found.

An important feature on locating the SRC is to establish flood elevations that will cover the region that contains the curve, as shown in Figure 5.2c. If flood elevations are defined too low at the I-Wall, the result would cause an underestimation of the SRC and completely miss the curve (as shown in Figure 5.2a). This similar result could occur for an overestimation of higher flood elevations that are close to or above the top of the wall (as shown in Figure 5.2b). Vertical red arrows of Figure 5.2 indicate flood elevations. When the SRC requires only a few flood elevations to define its shape (e.g., narrow at 1 ft increments), it might be necessary to decrease flood elevations by 0.5 ft or 0.25 ft increments, this increases the number of flood elevations to better visualize the entire region.

Figure 5.2. System response curve. (a) Underestimated flood elevations for SRC. (b) Overestimated flood elevations for SRC. (c) Located region of SRC curve.



5.4 Accuracy and timing

Accuracy and timing influence the number of simulations required for a probabilistic analysis that results in the construction of a cumulative distribution function or SRC. Initially, from numerous observations of simulating either a new design of a sheet-pile wall or the analysis of an existing I-Wall (Sections 5.5–5.7), the number of simulations applied was established to be around 1,000 while retaining the most accuracy. However, in some of these cases the resulting execution times were excessively lengthy and considered inadequate. Further investigation provided insight necessary to decrease execution times. It has been determined that the most time-consuming executions resulted from the probabilistic analysis of an existing I-Wall containing effective stress-based earth pressure calculations with seepage. The following scenarios were examined for the improvement of execution times for the above conditions:

1. A consistent relationship between the number of simulations and the execution time. When the number of simulations was decreased, the execution time decreased. Therefore, many simulations studied would produce the best acceptable accuracy while minimizing the execution time.
2. The sheet-pile base elevation. The designated sheet-pile base elevation is initially set at -125 ft. All estimated pressures and resultant forces are calculated from the top of the wall down to the sheet-pile tip elevation by an iterative solution that approximates the depth of embedment. It was decided that decreasing the initial sheet-pile base elevation (about one half and depending on soil classifications) would lower execution times by reducing the number of computations along the shorter wall.
3. Change the minimum node spacing. The computational procedure, as discussed in Appendix A, determines pressures and forces estimated from nodal points along the wall. If numerical convergence is not achieved with the initial nodal point spacing (set to 1 ft), the node spacing will be decreased by the node spacing interval, and this process is repeated until the minimum node spacing is reached and the program stops. Decreasing the minimum node spacing (to 0.8 or 0.9) most often allows the program to stop computations when $FS_{passive}$ is well below 1.0.

The following sections describe results and show the minimum number of simulations selected for each example problem. Section 5.6 describes the design of an I-Wall with effective stress-base shear strength parameters, seepage, and hydraulic fracturing. Section 5.7 describes the analysis of an I-Wall with total stress-based shear strength parameters, hydrostatic water pressures, and hydraulic fracturing. Section 5.10 also describes the analysis of an I-Wall, but with effective stress based shear strength parameters, seepage, and hydraulic fracturing. These two analysis sections each develop an SRC.

5.5 Differences between the Coefficient Method and the Wedge Solution Method for computing earth pressures for probabilistic simulation

With the introduction of Version 2.0 of Corps_I-Wall, there are now two methods for computing earth pressures, the Coefficient Method, which was introduced in Version 1.0, and the Wedge Solution Method. These two methods both search for the appropriate depth of embedment for the I-Wall given a factor of safety in Design Mode.

The Coefficient Method runs considerably faster than the Wedge Method because it is more fully constrained, being only concerned with the pressures that occur at the wall, and assuming that all region surfaces are horizontal. The Wedge Solution Method is complicated by a search for the appropriate slip plane, this involves continual meshing of subwedges that each contain computed pressures. This procedure must be followed for each design.

For an Analysis Mode simulations, these timings are compounded by the fact that several designs must be computed to converge on the appropriate Factor of Safety that leads to a specified analysis wall depth. Using the Coefficient Method, this procedure was used for all of the simulation runs so that a full histogram of factors of safety for passive earth pressures ($FS_{passive}$) could be collected, and the SRC could be calculated by counting the number of $FS_{passive}$ runs that were less than or equal to 1.0 at each flood elevation. The probability of limit state (structural weakness) for the analysis wall tip depth for a given flood elevation would be the number of $FS_{passive}$s that were less than, or equal to 1.0 divided by the total number of simulation runs.

Using the Wedge Solution Method, the cost of doing a full analysis for the specified wall tip depth will be exhorbitant. Each analysis run requires five to fifteen plus design runs to determine the $FS_{passive}$ for the simulation variables. A different method was devised that would allow for the determination of limit state without an explicit computation of $FS_{passive}$ via the Design mode. The limit state calculation only depends on whether the $FS_{passive}$ for a simulation run exceeds a value of 1.0. In this case, a single design run would need to be given an $FS_{passive}$ of 1.0 and the design wall tip depth computed. If the specified wall tip depth was shallower, or equal to the computed design wall tip depth, then the $FS_{passive}$ for the specified wall tip depth would have to be less than, or equal to 1.0, even though the exact value is not known. Conversely, if the specified wall tip depth was deeper than the computed design wall tip depth, then the $FS_{passive}$ for the specified wall tip depth would have to be greater than 1.0. Using this method, it is possible to calculate a SRC without having a histogram of $FS_{passive}$ values, this greatly reduced simulation run-times. For this reason, running analysis simulation runs with the Wedge Solution Method will not return a histogram of $FS_{passive}$ values. However, this deficiency is inconsequential to the construction of the desired SRC curve.

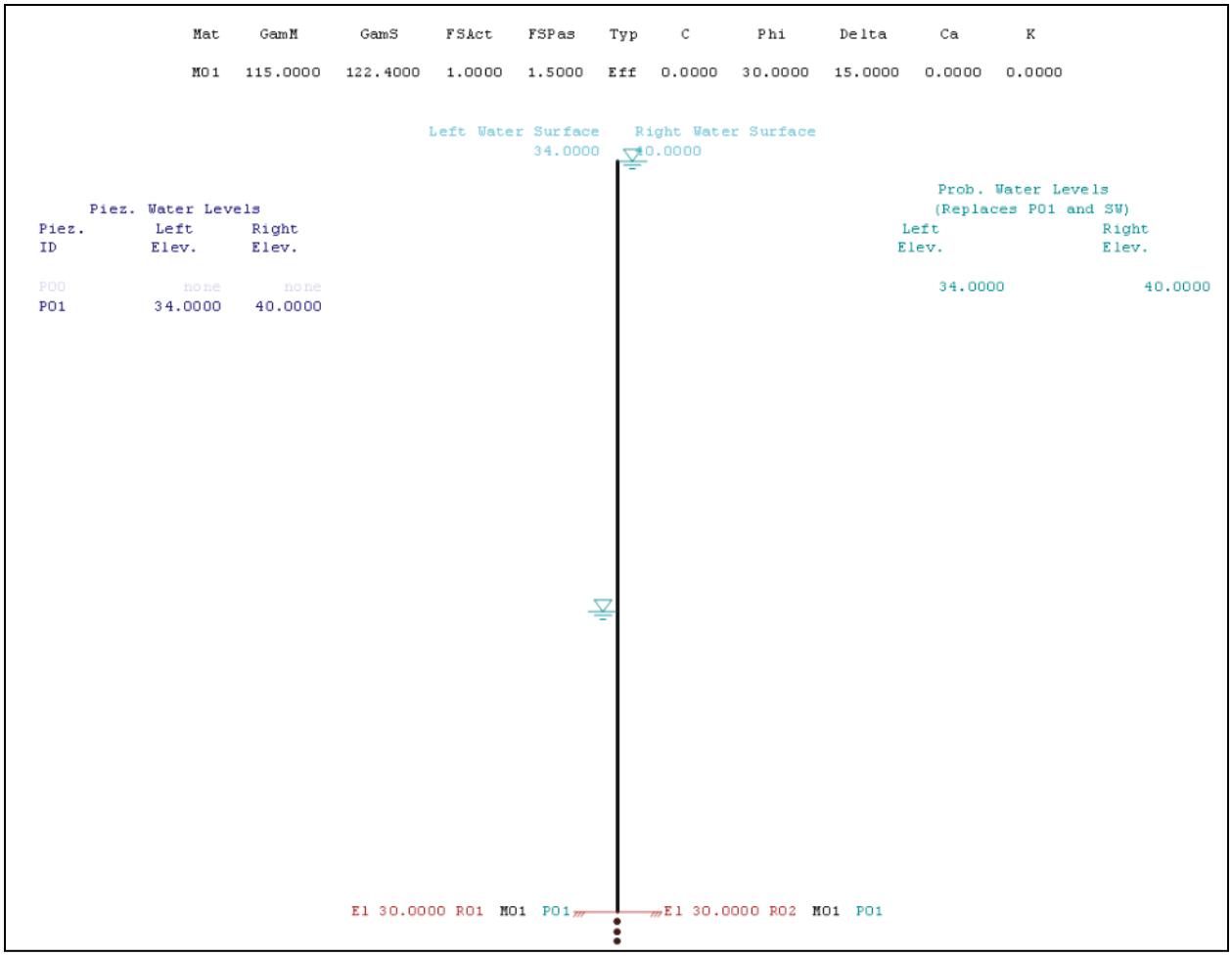
A procedure for approximating the probability of limit state, which would also approximate $FS_{passive}$ values, was devised using a Taylor Series approximation. This proposed procedure would require partial derivatives for each variable. The partial derivatives would require three analysis runs for each variable. Since each analysis run would require five to fifteen design runs for convergence, it was determined that this method would take as much time, if not more, to estimate the values of $FS_{passive}$ and the probability of limit state to construct the SRC as the simplified method outlined above, and the quality of the results would depend on user assumptions of the probable output histogram shape. For this reason, the Taylor Series approximation based procedure of analysis was not added to Corps_I-Wall Version 2.0.

5.6 Example 5.1 sand site with hydraulic fracturing criteria and seepage, an extension of design problem 4.1.5

An effective stress definition of an I-Wall founded in sand with c′ = 0 is illustrated by a design problem in order to determine the depth of embedment (d) of the sheet-pile wall. This example problem applies an active Factor of Safety of 1.0 for computing active earth pressures, and a passive safety factor of 1.5 for computing passive earth pressures of all soil layers. This I-Wall system has an exposed height of 10 ft. Water surfaces at both sides of the I-Wall are at 40 ft on the flood side or RHS, and 34 ft on the landside or LHS. The homogeneous soil layer of sand has a level ground surface on both sides of the I-Wall at 30 ft with a saturated unit weight of 122.4 pcf, the effective angle of internal friction of 30 degrees, and the effective angle of soil-to-sheet-pile wall interface friction of 15 degrees. This analysis also considers homogeneous seepage. Figure 5.3 outlines the basic geometry and structural parameters for the sheet-pile wall.

The top row of text listed in Figure 5.3 documents the input values of all parameters associated with each material type. For this problem, there is only one material assigned for the sand site and recorded as “M01,” the “M” signifies the material type and is followed by the ID, which starts from “01.” All information concerning material types are written in black text. The representation of a soil structure is characterized by a region. Regions are labeled with an “R” and followed by an ID starting from “01.” For this problem two regions are assigned, Region 1 (as R01) is located on the LHS of the sheet-pile wall, and Region 2 (as R02) is located on the RHS of the sheet-pile wall. Each region and its surface elevation are written in red text.

Figure 5.3. Corps_I-Wall schematic of sheet-pile wall in sand site.

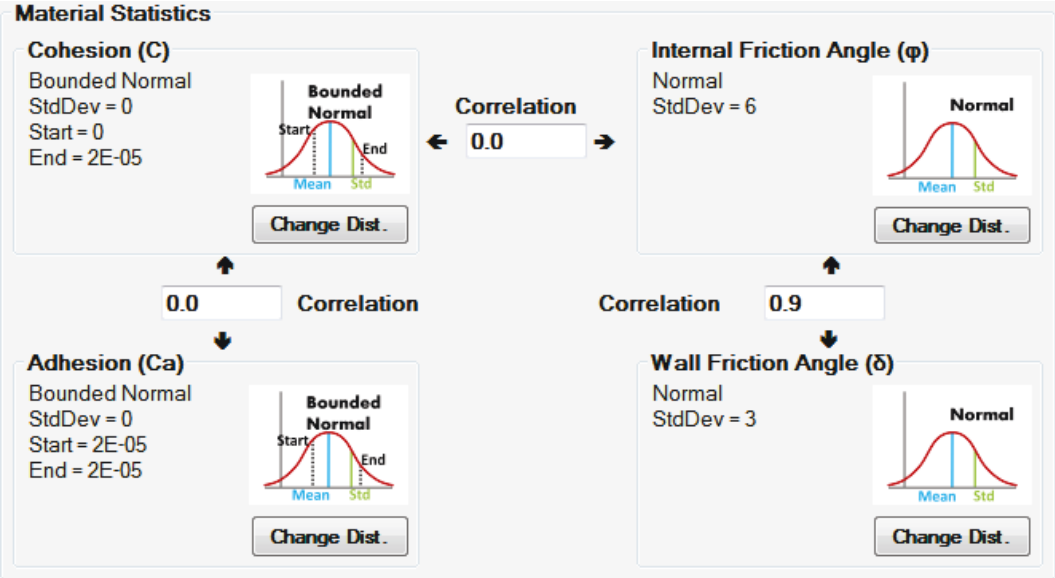


Water elevations are listed in the upper left-hand corner and shown in dark blue. Water levels are labeled at the soil interface of any specified region with an initial character "P" and followed by an ID. Label "P00" is one that signifies that there is no water associated with a soil layer or region, and the soil is partially saturated. If all soil regions are fully saturated, "P00" will be grayed out (as shown in Figure 5.3). Surface water on either side of the sheet-pile wall is represented by water symbols at its defined elevation along the sheet-pile wall and labeled as "P01." If there is no surface water associated with any soil region, "P01" will be grayed out.

For the probabilistic analysis considered in this section, the mean of the effective angle of internal friction and the mean of the effective angle of wall-soil interface friction were defined previously as 30 degrees and 15 degrees respectively. The standard deviation, COV, the correlation coefficient, and probability distribution function provided for these two variables are shown in Figure 5.4. Note that the two variables are strongly

correlated, with a correlation coefficient of 0.9. Only one flood elevation will be considered for the probabilistic analysis of the design depth of embedment. Upon completion, a histogram detailing the frequency of sheet-pile tip elevations together with its cumulative distribution at each flood level are reported.

Figure 5.4. Statistical parameters of sandy soil.



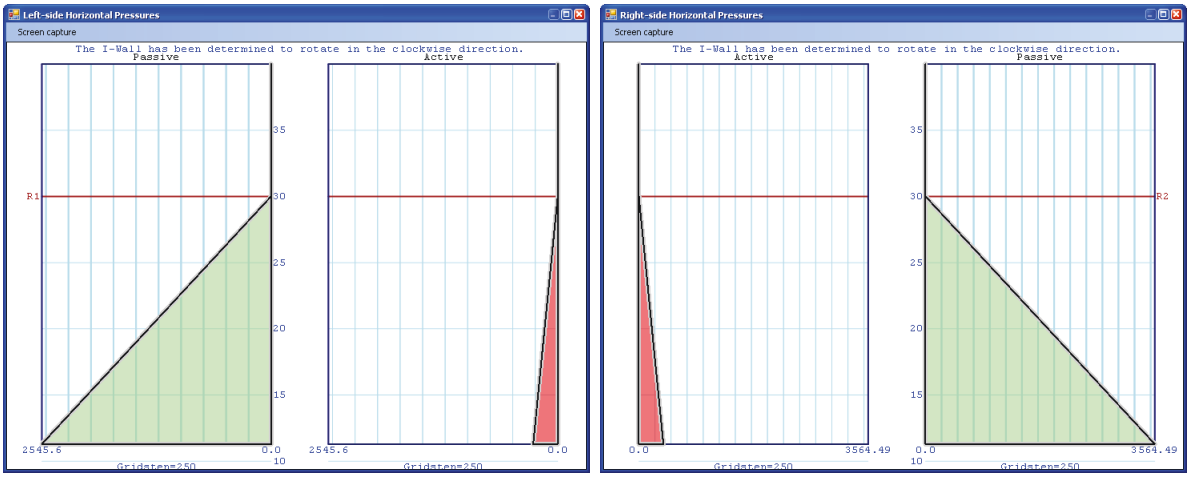
5.6.1 Evaluation of results from the deterministic solution with flood elevation pairs of 40 ft and 34 ft

An effective stress definition with φ′ = 30 degrees, δ′ = 15 degrees, and c′ = 0 as illustrated in Figure 5.4 is considered for the evaluation of the depth of embedment. Homogeneous soil, homogeneous seepage by the line of seepage method, and the passive earth pressure coefficient obtained from the logarithmic spiral procedure, form the basis for this example.

At the flood elevation of 40 ft, a deterministic analysis is first evaluated to estimate the design depth of embedment and various output parameters. This analysis resulted in a mobilized active earth pressure coefficient (K_a) of 0.3014 and a mobilized passive pressure coefficient (K_p) of 2.7645.[1] The distribution of active and mobilized passive earth pressures for both sides of the sheet-pile wall is illustrated in Figures 5.5a and 5.5b.

[1] Recall that an $FS_{passive}$ value equal to 1.5 was specified in this example, consistent with EM 1110-2-2504 (HQUSACE 1994).

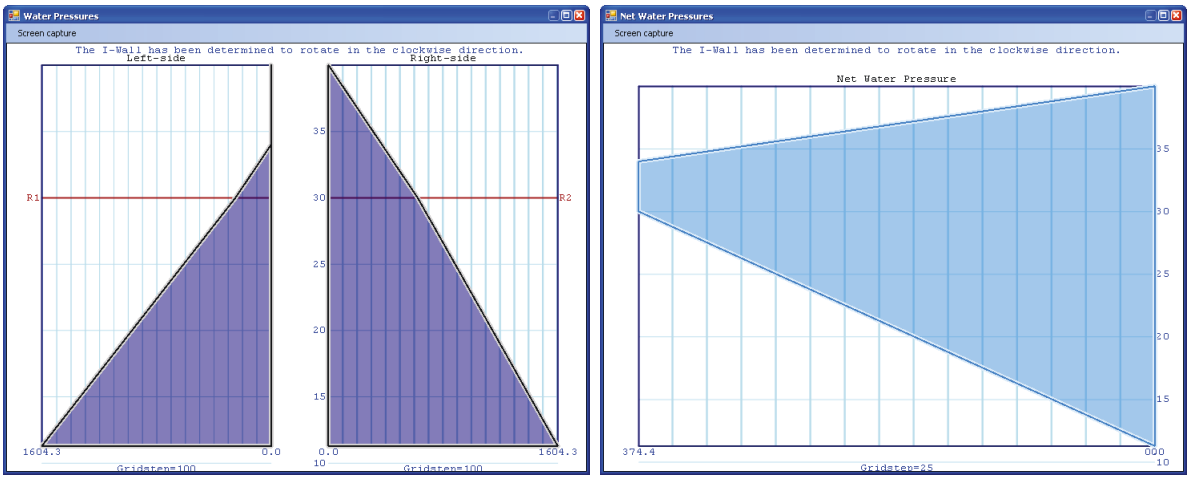
Figure 5.5. Active and passive earth pressures. (a) LHS of wall, (b) RHS of wall.



(a) (b)

The resulting water pressures acting on both sides of the sheet-pile wall are shown in Figure 5.6a. The resultant net water pressure calculated by taking the difference between sum of the water pressures (Figure 5.6a) and seepage on both sides of the wall is shown in Figure 5.6b.

Figure 5.6. Pore water pressures. (a) LHS and RHS of wall, (b) net water pressures.



(a) (b)

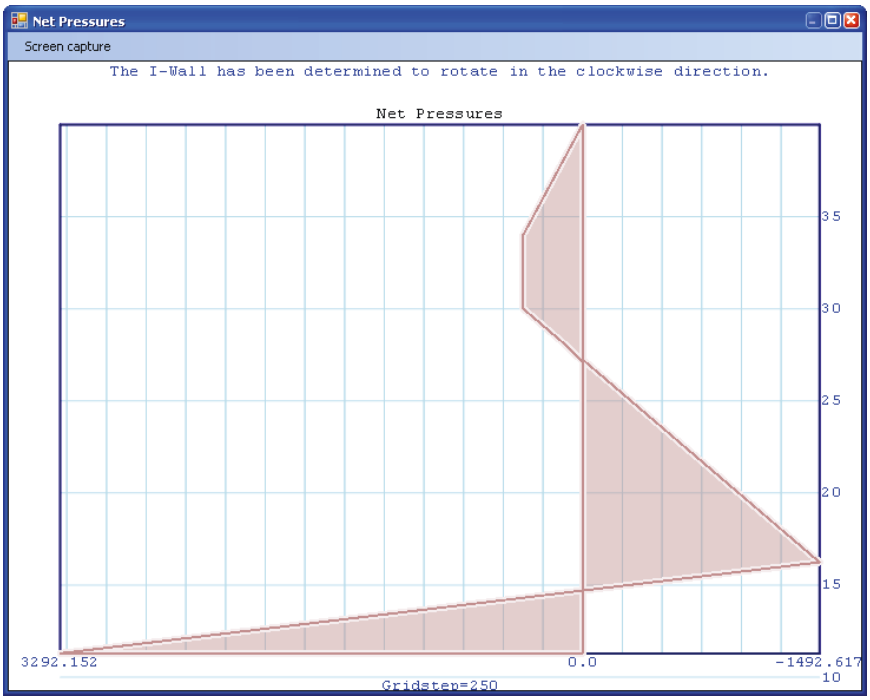
Homogeneous seepage occurring in this problem is clearly shown by the net water pressure diagram of Figure 5.6b. The net water pressure diagram of Figure 5.6b is first calculated from the RHS hydrostatic water pressures from el 40 ft to el 34 ft, resulting in the uppermost triangular distribution. Between el 34 ft and el 30 ft, the increase in water pressure on both sides of the wall is the same, resulting in a uniform net pressure diagram between these two elevations. At the ground surface elevation of

30 ft, which coincides with a gap depth elevation of 30 ft (i.e., a zero gap depth because c′ is equal to zero), homogeneous seepage calculations are initiated from the RHS ground surface (on the high head side), down the RHS to the sheet-pile tip, and then up the LHS of the sheet pile, concluding at the LHS ground surface. Corps_I-Wall line of seepage computations result in a net water pressure of 0.0 psf at the sheet-pile tip elevation of 11.29 ft.

From these pressures (Figures 5.5 and 5.6), both the net active and net passive pressures are constructed and presented in Figure 5.7a. For the applied flood loading, the I-Wall will rotate counterclockwise. The net active pressure is determined from the difference between the RHS-mobilized active earth pressure and the LHS-mobilized passive earth pressure (i.e., acting on the other side of the wall), with the addition of any net water pressures, and any external horizontal net pressures and overburden pressures (if any). The net passive pressure is determined by the difference between the RHS-mobilized passive earth pressure and the LHS-mobilized active earth pressure acting on the other side of the sheet-pile wall, with the addition of any net water pressures, and any external horizontal net pressures and overburden pressures (if any). The net pressure diagram of Figure 5.7b is derived from the replication of all values of the net active pressures, from the top of the wall until the elevation at the PR (el 16.24 ft), at this instant the remaining values of the net pressure diagram is assumed to be linear with elevation between 1) the net active pressure value at the elevation of the PR, and 2) the net mobilized passive pressure at the elevation of the approximated sheet-pile tip (i.e., el 11.29).[1] Figure 5.7b is an illustration of how the net pressure diagram was formed. The final results are illustrated in Figure 5.8 by the presentation of the net pressure diagram, Figures 5.8a (replica of Figure 5.7b), and 5.8b the shear and moment diagrams. Figure 5.8b shows that the maximum bending moment occurs at the zero crossing of the shear diagram. The sheet-pile tip elevation of the deterministic analysis is computed at 11.29 ft with a depth of embedment of 18.71 ft.

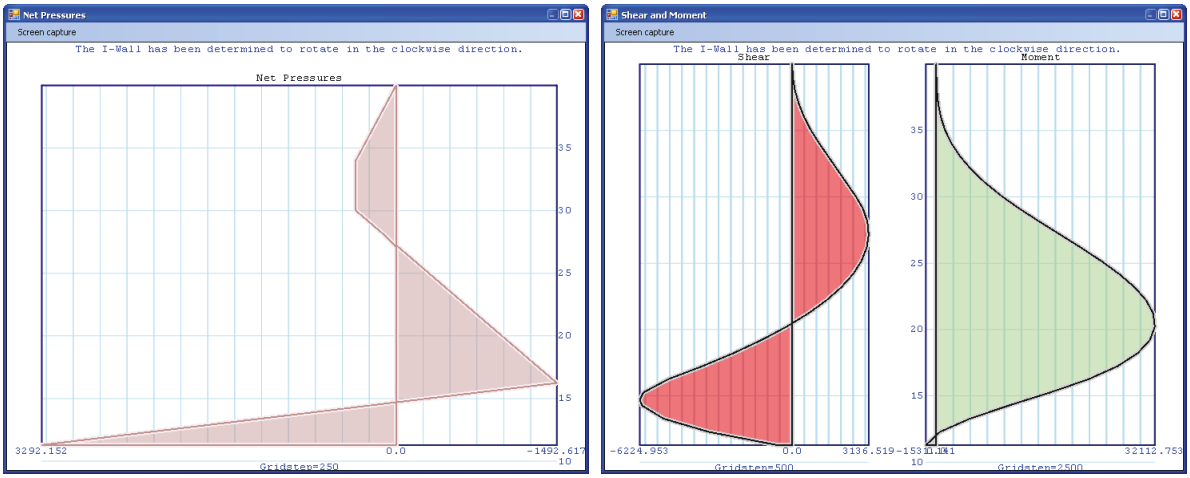
[1] Only one mobilized net passive pressure value in Figure 5.7a is used to construct the Figure 5.7b net pressure diagram, corresponding to the sheet-pile tip elevation at el 11.29. The majority of the net pressure diagram is derived from the Figure 5.7a net active pressure diagram.

Figure 5.7. Net pressures. (a) Net active and net passive. (b) Net pressure diagram.



(a) (b)

Figure 5.8. (a) Net pressure diagram. (b) Shear and moment.



(a) (b)

This problem required using homogeneous seepage in the analysis. An input hydraulic conductivity for sand (i.e., 3.28e-5 ft/sec) was entered and the constant seepage gradient was calculated to be 0.1603. Figure 5.9 provides an interpretation of the line of seepage method by a graph of the total head along the seepage path. The LHS graph, or Figure 5.9a, shows a schematic of seepage, this starts at the ground surface of R2 at the RHS of

the wall (i.e., flood side), continues down to the sheet-pile tip at 11.29 ft, then continues upward toward the ground surface of R1 at the LHS (i.e., landside) of the sheet-pile wall. The second graph (Figure 5.9b) displays total head values of flow along the distance travelled. Head loss occurs as water seeps from el 40.0 ft at the RHS to the ground surface at 30.0 ft (vertical green line). The seepage slope (also referred to as the seepage gradient) of 0.16 starts at el 30 ft, continues past the sheet-pile tip of 11.29 ft (vertical black line), and terminates at the LHS ground surface at el 30 ft (vertical red line), where it merges with the surface water at el 34 ft on the LHS of the wall. Further details on the line of seepage method are given in Appendix C.

Figure 5.9. Line of seepage. (a) Direction of flow. (b) Head loss along distance of flow.



(a) (b)

5.6.2 Evaluation of results for 1,000 simulations with seepage

This section discusses the computed results of the probabilistic version of the Example 5.1 design problem for 1,000 simulations. Only one flood level is tested and set at 40 ft. Section 5.4.1 discussed the results for the deterministic solution part of this problem. For the probabilistic analysis, the COV was set at 20 percent of the mean for both variables (φ' and δ'),

with a correlation coefficient of 0.9 between the two variables. This characterized the variables as having a strong correlation with some dispersion. The normal distribution was selected and bounded between 0 and $\mu + 3\sigma$, this is the default when bounds are not specified. Results from sheet-pile wall design, with 1,000 simulations for the estimation of the sheet-pile tip, led to a histogram of frequency at intervals of equally spaced sheet-pile tip elevations.

For the 1,000 simulation output recorded in the run file of Figure 5.10, designs for the calculated sheet-pile tip elevations ranged from -11 ft to 19 ft. The mean sheet-pile tip elevation was 10.81 ft with the standard deviation being 3.61 ft. Figure 5.11a shows the histogram, Figure 5.11b shows the relative cumulative distribution function for this analysis. From Figure 5.11, the histogram shows the largest fractional frequency of sheet-pile tip elevation at 12 ft, this is deeper than the 11.29 ft for the deterministic analysis that results from the applied dispersion of this analysis.

The 1,000 designs were also evaluated for depth of embedment parameter. Additionally, statistical parameters were calculated and produced in Figure 5.12. The mean of the depth of embedment was 19.20 ft, with the standard deviation of 3.61 ft, and COV of approximately 0.18. Values ranged from a minimum of 12 ft to a maximum of 40 ft. Figure 5.12a shows the histogram and its related cumulative distribution function, the depth of embedment variable is shown in Figure 5.12b. From Figure 5.12, the histogram shows the largest fractional frequency of 0.27 at the depth of embedment of 18 ft.

Figure 5.10. Output runtime file.

```
Gap depth                  =       0.00 ft

-------- Probabilistic Analysis at Flood Elevation    40.00 ft --------

The number of successful designs = 1000 out of 1000 simulations at flood elevation of      40.00ft
```

Figure 5.11. Design probabilistic analysis of sheet-pile tip with 1,000 simulations. (a) Histogram. (b) Cumulative distribution function.

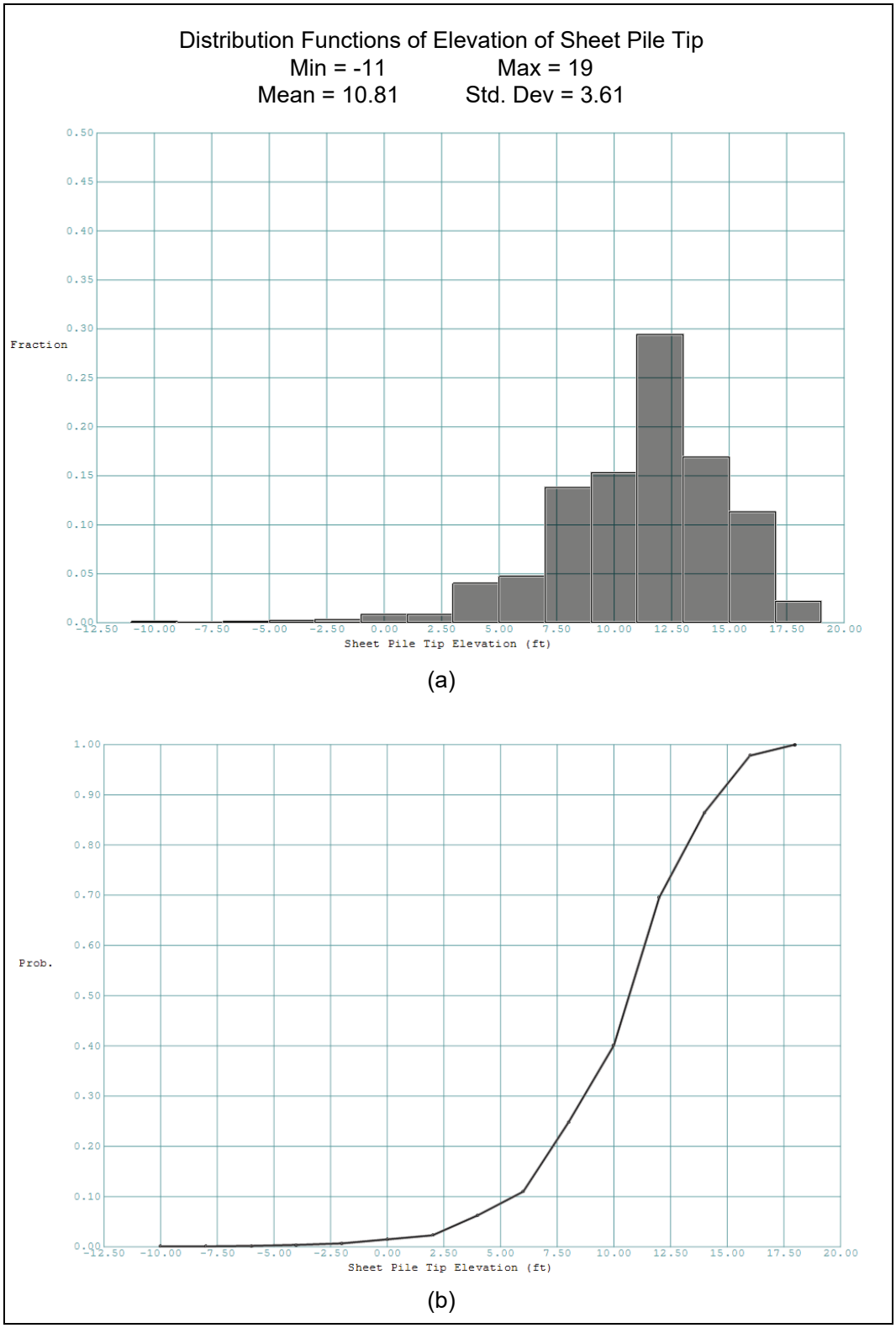
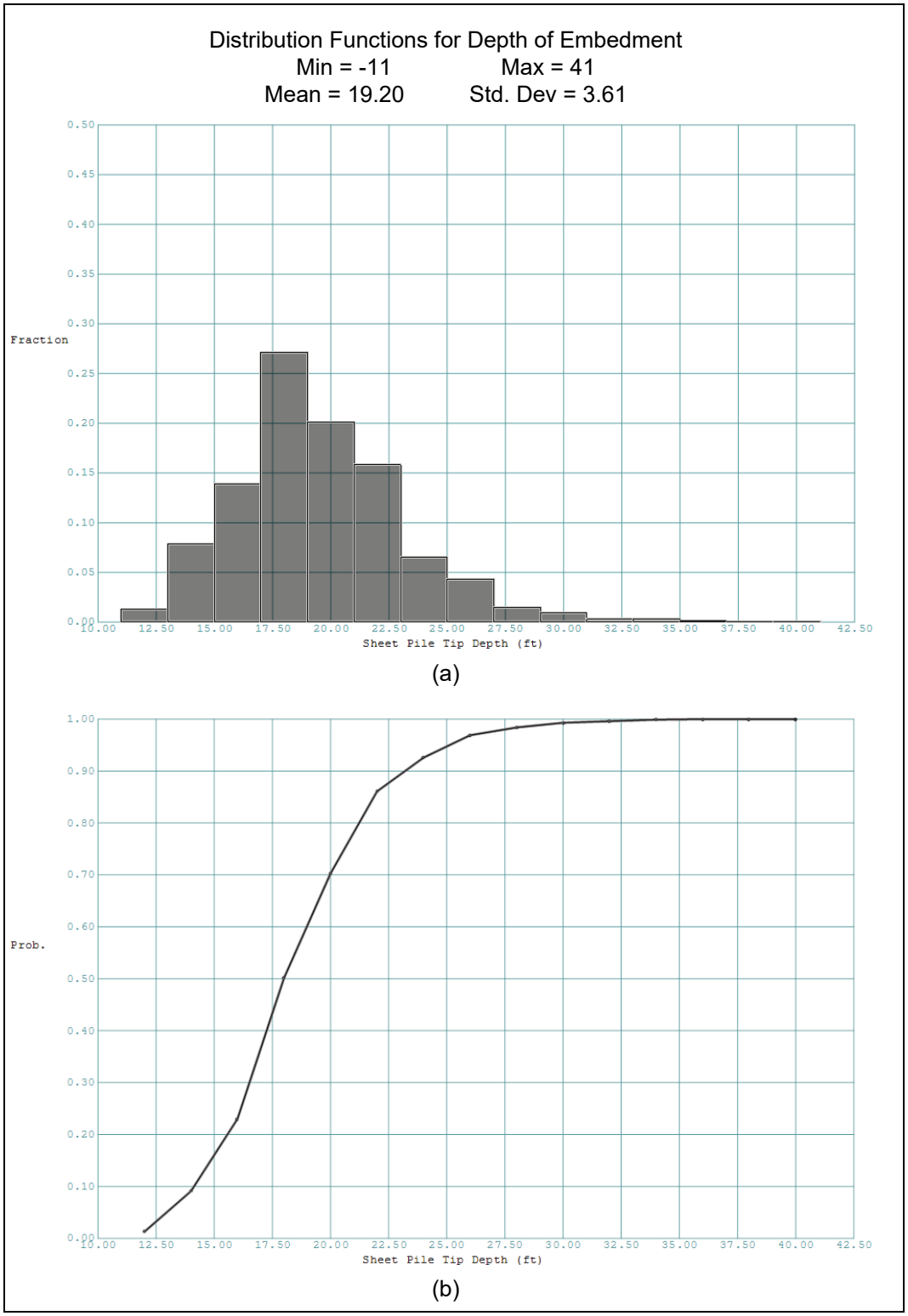


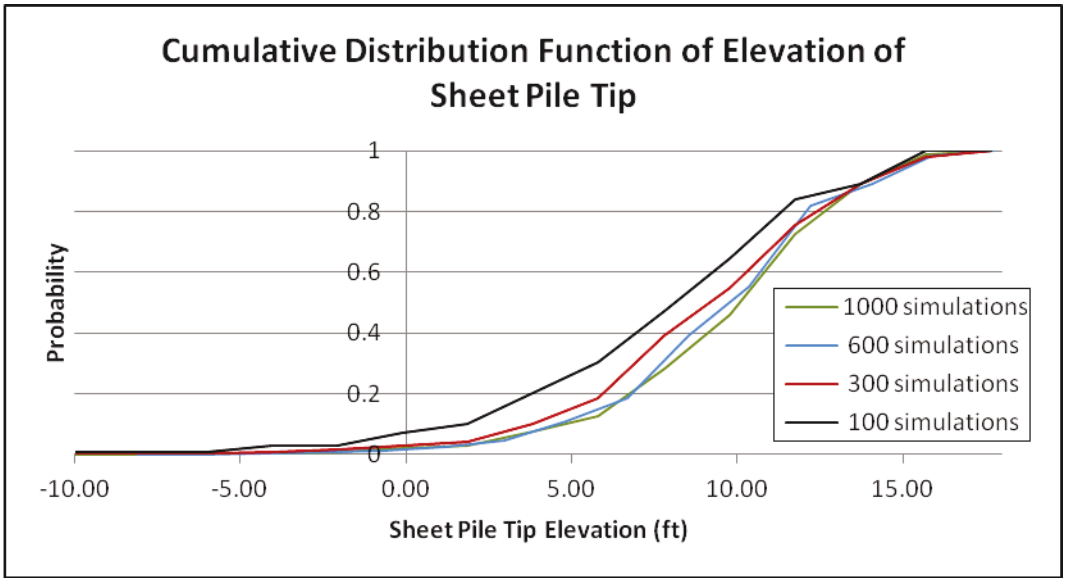
Figure 5.12. Design probabilistic analysis of depth of embedment with 1,000 simulations. (a) Histogram. (b) Cumulative distribution function.



5.6.3 Comparisons of results for 100, 300, 600, and 1,000 simulations

This subsection discusses the results of Example 5.1 for 100, 300, 600 and 1,000 simulations. As discussed in the previous Section 5.5.2, the probabilistic design of a sheet-pile wall resulted in histograms and probability distribution functions for 1,000 simulations. Further simulations of 100, 300, 600, and 1,000 were conducted with results shown in Figure 5.13. Sheet-pile tip elevations ranged from -8 ft to 17 ft for all four simulations.

Figure 5.13. Cumulative distribution function for sheet-pile tip elevation for 100, 300, 600, and 1,000 simulations.



Observe in Figure 5.13 the near perfect agreement in cumulative distribution function curves for the 1,000 and 600 simulation results. This suggests convergence is achieved for 600 or more simulations in this design problem. A comparison of the curve for the 300 simulation analysis, to the 600, and 1,000 simulation curves indicates that 300 simulations will provide adequate results for this design.

Execution times were also recorded for various simulations. These timings, and the normalized values as recorded with the timing for 300 simulations, are tabulated in Table 5.3. Data from the table show that there is a near linear relationship between timing and number of simulations.

Table 5.3. Execution times for 100, 300, 600, and 1,000 simulations.

Number of Simulations	Execution Time (hh:mm)	Normalized
100	0:01	0.5
300	0:02	1
600	0:05	0.1
1,000	0:09	0.18

5.6.4 Comparing the Coefficient Method solution to the Wedge Solution Method solution for Example 5.1

Example 5.1 was also solved using the Wedge Solution Method (only available in Corps_I-Wall Version 2.0) so that a comparison could be made between the simulation run times and results. Because the Wedge Solution Method does not accommodate for seepage analysis, and handles gap inititiation and propogation differently than the Coefficient Method, the comparison will not be exact. It will however reveal the differences between the two methods.

The input values are identical to the Example 5.1 (based on Example 4.1.5) inputs for the Coefficient Method with a few exceptions. The inputs are recounted here with the changes.

Figures 5.14–5.19 show the input parameters in GUI format for Example Problem 5.1. Figures 5.14 and 5.15 set up the geometry as was found in Figure 4.1 for the example problem.

Figure 5.16 sets up the homogeneous soil material with statistical parameters. The mean values for the material are the unit weights, with γ_{Moist} = 60 lb/ft^3, and $\gamma_{Saturated}$ = 122.4 lb/ft^3. The material Factors of Safety are 1.0 and 1.5 for active and passive, respectively. Effective stress is used for the material with mean values of C’ = 0.0 lb/ft^2, φ’ = 30 degrees, δ’ = 15 degrees, Ca’ = 0.0lb/ft^2, and K’ = 0.0 ft/sec. For simulations, two of these values are allowed to vary, φ’ and δ’. These two variables (φ’ and δ’) will have simulation values chosen from a normal (Guassian) distribution with standard deviations of six and three, respectively. Additionally, the values are correlated with a high correlation coefficient, ρ, value of 0.9.

Figure 5.14. Establishing design mode parameters for Example 5.1 in Corps_I-Wall Version 2.0.

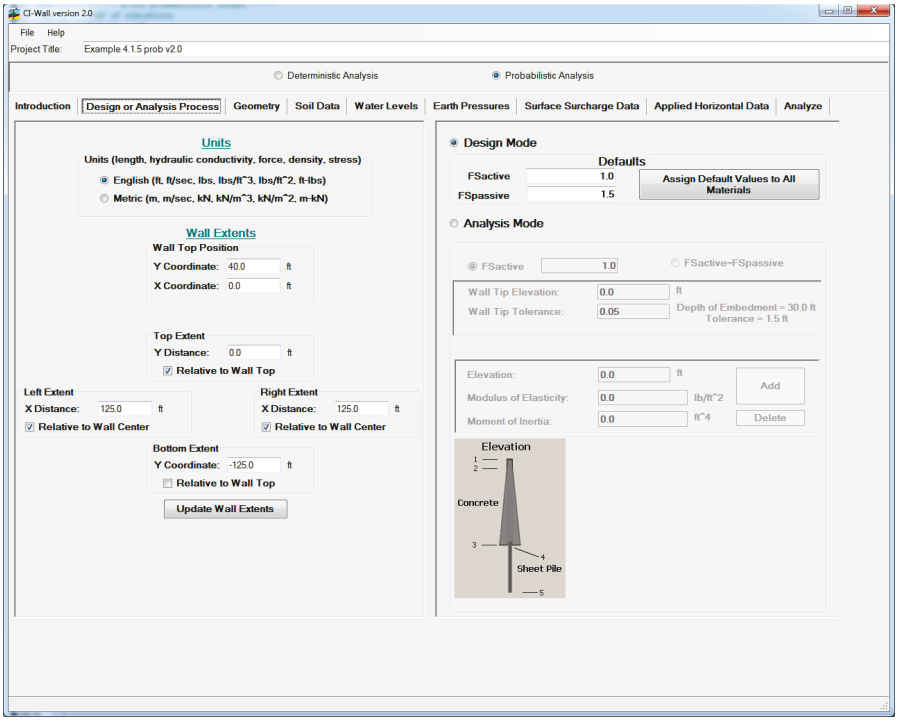


Figure 5.15. Establishing geometry for Example 5.1 in Corps_I-Wall Version 2.0.

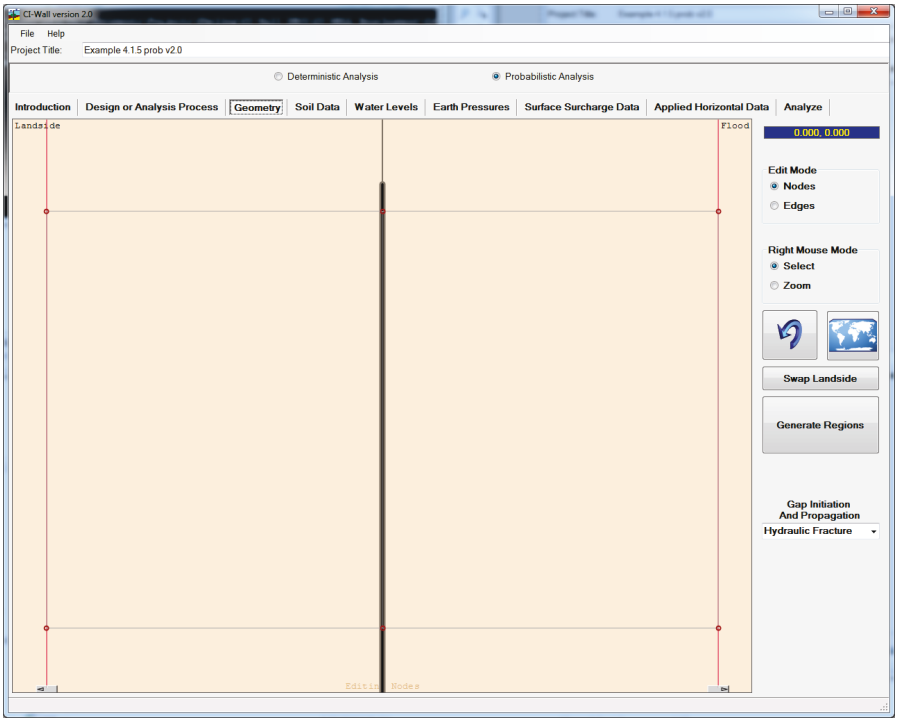


Figure 5.16. Establishing soil property parameters for Example 5.1 in Corps_I-Wall Version 2.0.

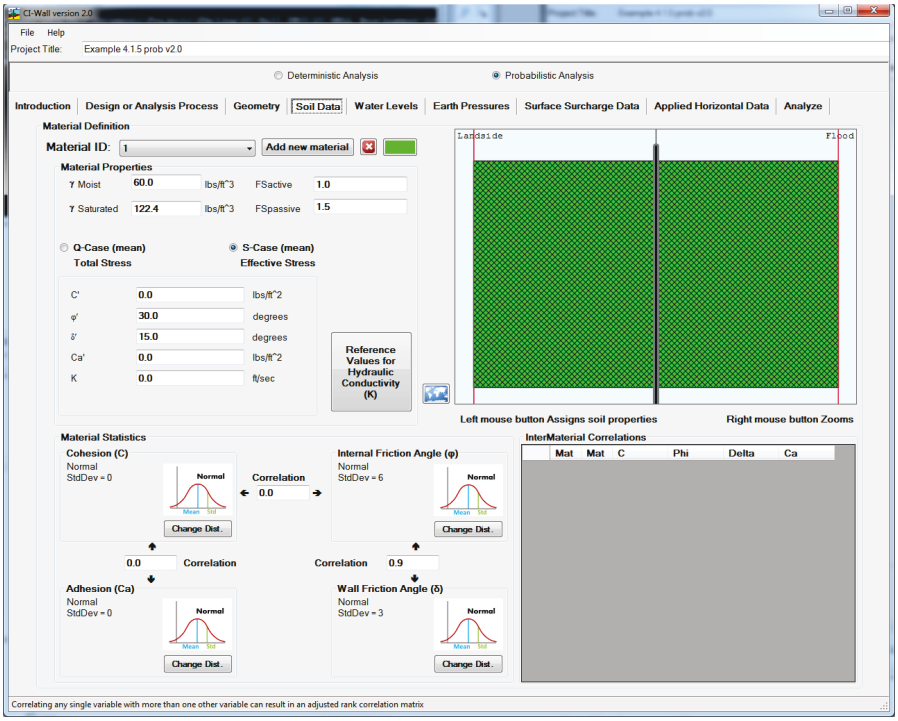


Figure 5.17. Establishing water and seepage parameters for Example 5.1 in Corps_I-Wall Version 2.0.

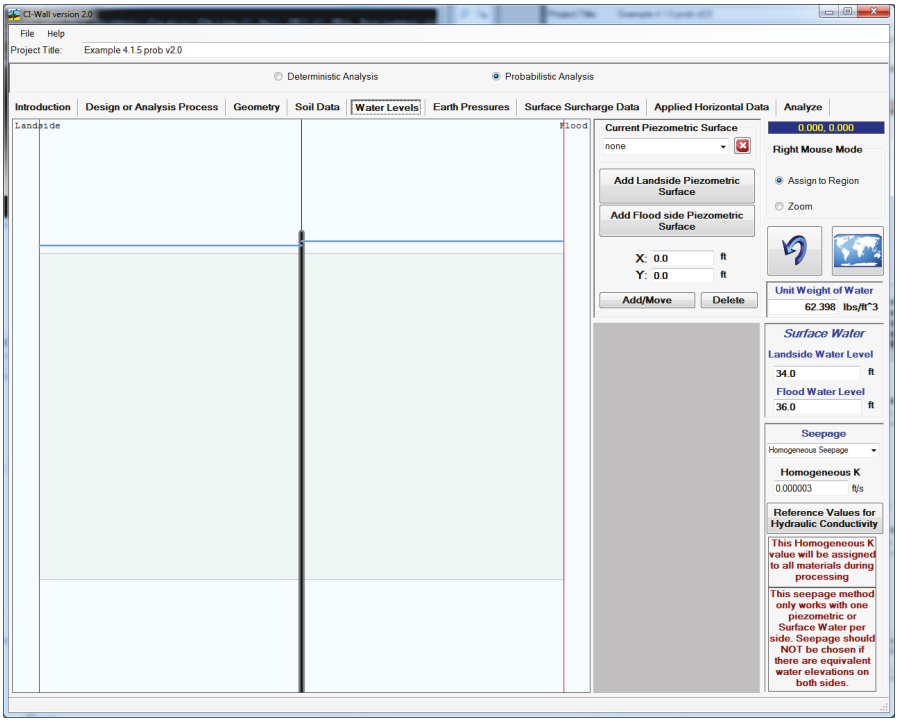


Figure 5.18. Establishing the Earth Pressure Solution Method for Example 5.1 in Corps_I-Wall Version 2.0.

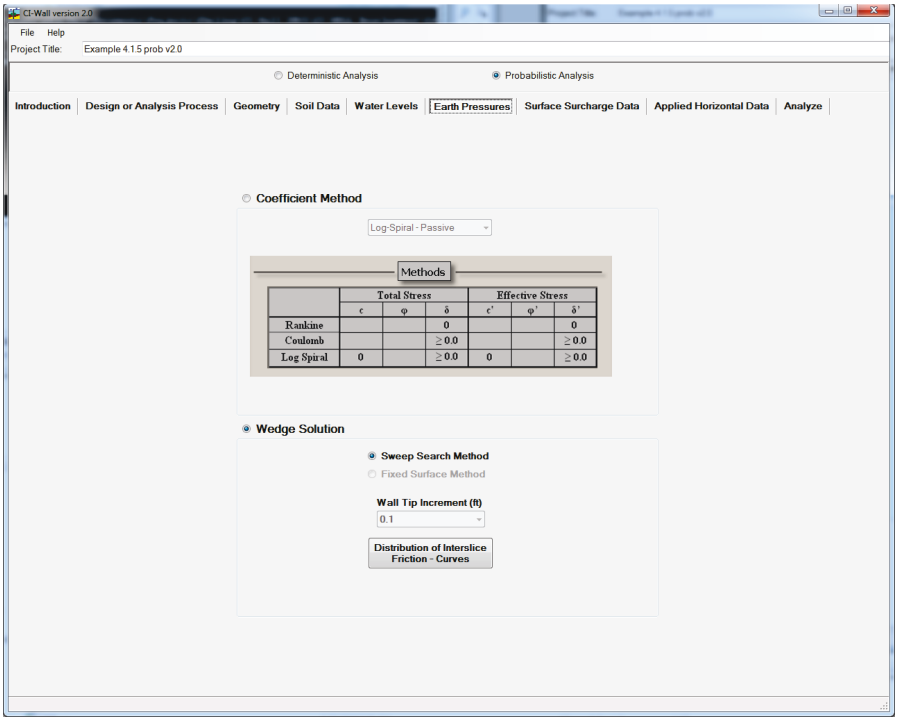
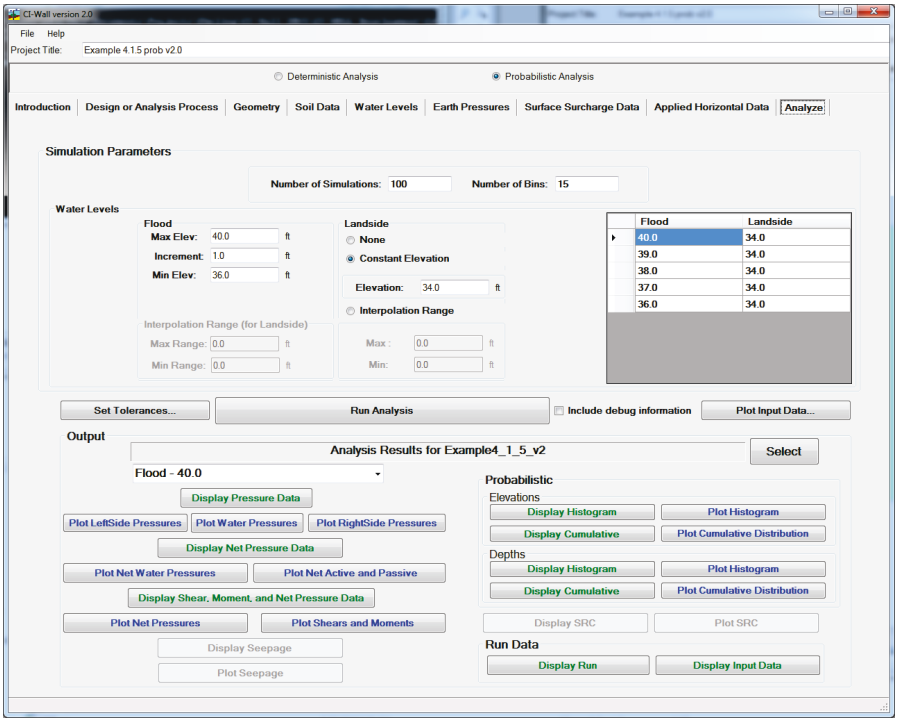


Figure 5.19. Establishing simulation parameters for Example 5.1 in Corps_I-Wall Version 2.0.



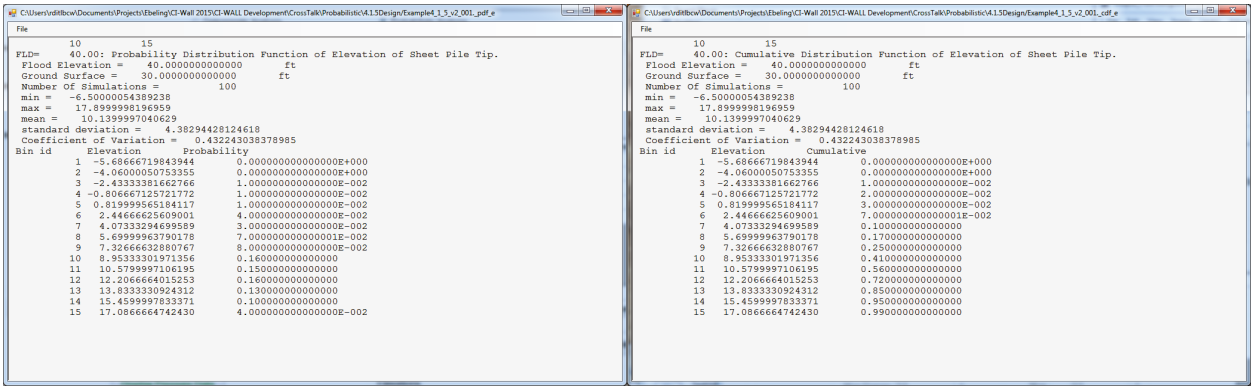
In Figure 5.17, deterministic water levels are established for the example problem. These water levels are over-ridden by the simulation water levels given in the Analyze Tab. Notice that homogeneous seepage was turned on for the Coefficient Method solution, so that the results will not exactly match the Wedge Solution Method.

Figure 5.18 shows how the input was selected for the Wedge Solution Method. However, it also shows that when the Coefficient Method was used, the Log-Spiral passive solution was used.

Figure 5.19 shows the simulation parameters that were used for both methods. There were 100 simulation runs performed with each combination of water levels, and the resulting output values were collected in a histogram using 15 bins, with each bin being as wide as the range between the minimum and maximum simulation output value divided by the number of bins.

Figure 5.20 shows the results of binning wall tip elevations for 100 simulation design runs from Example 5.1 using the Wedge Model. Each bin has a wall tip elevation, its probability of occurrence in Figure 5.20(a), and the cumulative probability (e.g., the cumulative probability of bin 5 is the summation of bins 1 through 5) in Figure 5.20(b).

Figure 5.20. Binned distributions of the dependent output parameter (wall tip elevation) in Example 5.1 with flood height 40.0 ft.



(a)

```
C:\Users\rditlbcw\Documents\Projects\Ebeling\CI-Wall 2015\CI-WALL Development\CrossTalk\Probabilistic\4.1.5Design\Example4_1_5_v2_001_pdf_e
File
         10          15
FLD=     40.00: Probability Distribution Function of Elevation of Sheet Pile Tip.
 Flood Elevation =    40.0000000000000       ft
 Ground Surface =    30.0000000000000       ft
 Number Of Simulations =          100
 min =   -6.50000054389238
 max =    17.8999998196959
 mean =    10.1399997040629
 standard deviation =    4.38294428124618
 Coefficient of Variation =   0.432243038378985
Bin id      Elevation       Probability
         1  -5.68666719843944       0.000000000000000E+000
         2  -4.06000050753355       0.000000000000000E+000
         3  -2.43333381662766       1.000000000000000E-002
         4  -0.806667125721772      1.000000000000000E-002
         5   0.819999565184117      1.000000000000000E-002
         6    2.44666625609001      4.000000000000000E-002
         7    4.07333294699589      3.000000000000000E-002
         8    5.69999963790178      7.000000000000001E-002
         9    7.32666632880767      8.000000000000000E-002
        10    8.95333301971356      0.160000000000000
        11    10.5799997106195      0.150000000000000
        12    12.2066664015253      0.160000000000000
        13    13.8333330924312      0.130000000000000
        14    15.4599997833371      0.100000000000000
        15    17.0866664742430      4.000000000000000E-002
```

(a)

```
C:\Users\rditlbcw\Documents\Projects\Ebeling\CI-Wall 2015\CI-WALL Development\CrossTalk\Probabilistic\4.1.5Design\Example4_1_5_v2_001_cdf_e
File
         10          15
FLD=     40.00: Cumulative Distribution Function of Elevation of Sheet Pile Tip.
 Flood Elevation =    40.0000000000000       ft
 Ground Surface =    30.0000000000000       ft
 Number Of Simulations =          100
 min =   -6.50000054389238
 max =    17.8999998196959
 mean =    10.1399997040629
 standard deviation =    4.38294428124618
 Coefficient of Variation =   0.432243038378985
Bin id      Elevation       Cumulative
         1  -5.68666719843944       0.000000000000000E+000
         2  -4.06000050753355       0.000000000000000E+000
         3  -2.43333381662766       1.000000000000000E-002
         4  -0.806667125721772      2.000000000000000E-002
         5   0.819999565184117      3.000000000000000E-002
         6    2.44666625609001      7.000000000000001E-002
         7    4.07333294699589      0.100000000000000
         8    5.69999963790178      0.170000000000000
         9    7.32666632880767      0.250000000000000
        10    8.95333301971356      0.410000000000000
        11    10.5799997106195      0.560000000000000
        12    12.2066664015253      0.720000000000000
        13    13.8333330924312      0.850000000000000
        14    15.4599997833371      0.950000000000000
        15    17.0866664742430      0.990000000000000
```

(b)

Figure 5.21 shows plots of the histograms revealing the probability density functions (on the left), and cumulative density functions (on the right), for each flood elevation. Also included is information about the statistical values (mean, minimum, maximum, standard deviation, and coefficient of variation) of the dependent output parameter (wall tip elevation), as generated using the Wedge Solution earth pressures procedure.

Figure 5.21. Binned distributions (plotted) of the dependent output parameter (wall tip elevation) in Example 5.1 with flood heights ranging from 40.0 to 36.0 ft using the Wedge Solution Method. (continued)

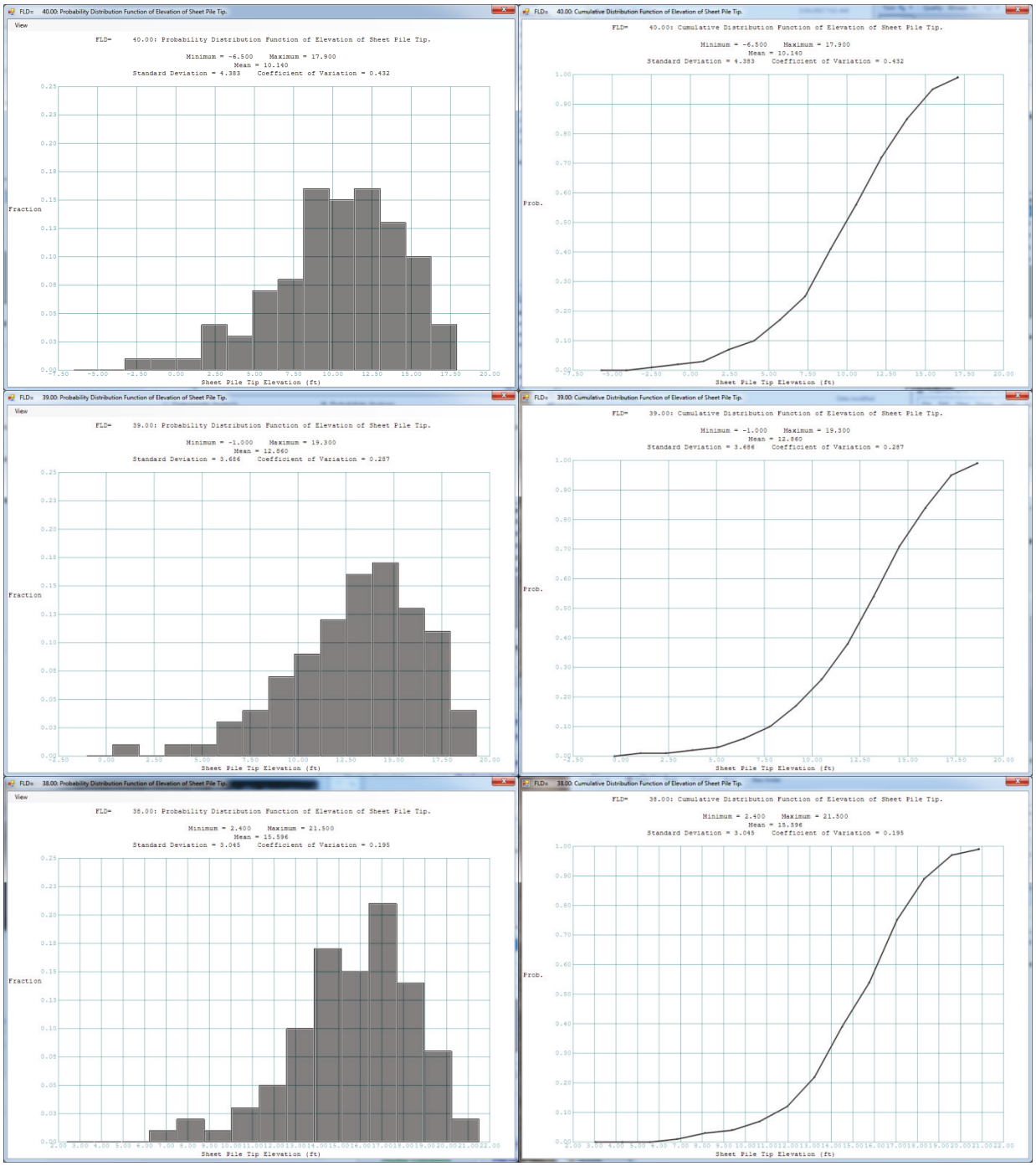


Figure 5.21. Concluded

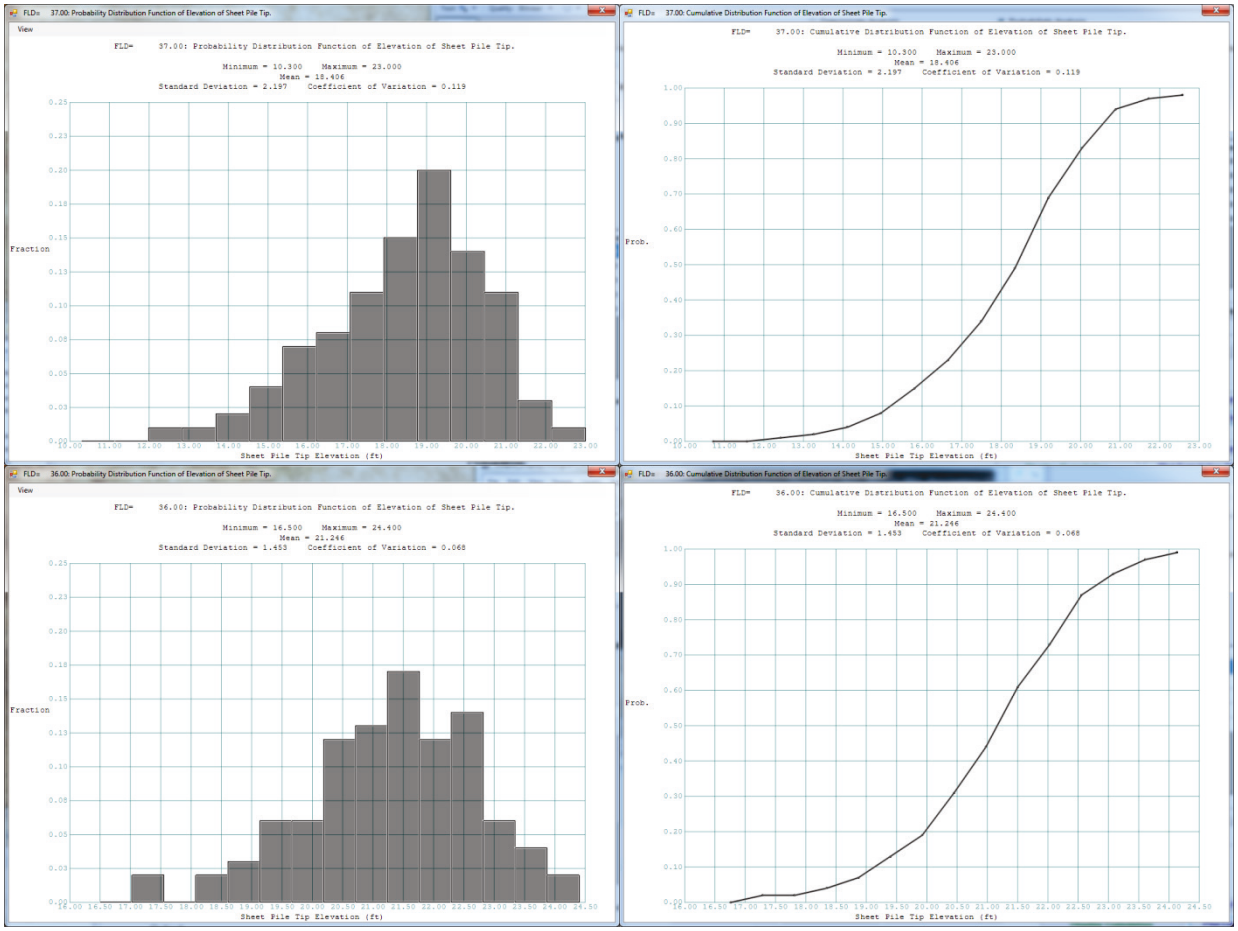


Figure 5.22 shows a probability density function for the dependent output variable when the Coefficient Method is chosen. This probability function is for the 40 ft flood.

Table 5.4 gives a comparison of results between the two methods. It must be restated that the Coefficient Method results were performed with seepage, the Wedge Solution Method did not take seepage into account. For both earth pressure methods of analysis, the mean pile tip elevation is inversely related to the flood side water elevation, this is to be expected because of the additional differential water pressure affecting how deep the wall must be embedded. For the Coefficient Method, the resulting pile tip elevations were, on average, nearly a foot higher than the Wedge Solution pile tip elevations, yielding shallower wall embedments. This is likely attributable to the effects of seepage.

Figure 5.22. Binned distributions (plotted) of the dependent output parameter (wall tip elevation) in Example 5.1 with flood height 40.0 ft using the Coefficient Method.

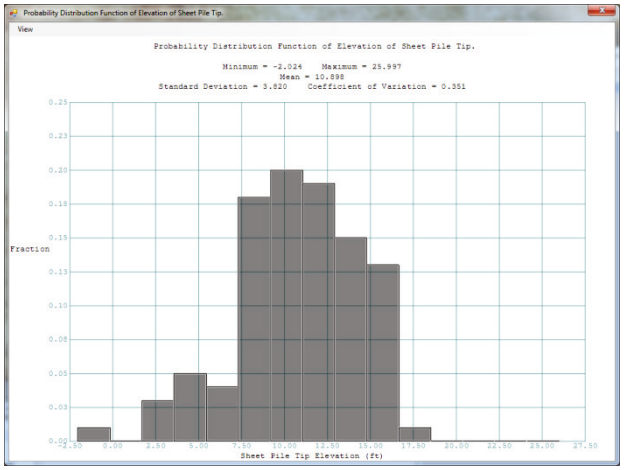


Table 5.4. Results of Example 5.1 using the Coefficient Method and the Wedge Solution Method.

Flood Elevation (ft)	Coefficient Method (including seepage analysis)					Wedge Solution Method (without seepage analysis)				
	Minimum Pile Tip Elevation (ft)	Maximum Pile Tip Elevation (ft)	Mean Pile Tip Elevation (ft)	Standard Deviation	Coefficient of Variation	Minimum Pile Tip Elevation (ft)	Maximum Pile Tip Elevation (ft)	Mean Pile Tip Elevation (ft)	Standard Deviation	Coefficient of Variation
40.0	-2.024	25.997	10.898	3.82	0.351	-6.5	17.9	10.140	4.383	0.432
39.0	-0.351	26.998	13.401	3.382	0.252	-1.0	19.3	12.860	3.686	0.287
38.0	6.983	26.998	16.266	3.429	0.211	2.4	21.5	15.596	3.045	0.195
37.0	12.259	22.347	18.556	1.973	0.106	10.3	23.0	18.406	2.197	0.119
36.0	16.990	27.998	23.831	3.898	0.164	16.5	24.4	21.246	1.453	0.068

There is also a difference between the Coefficient Method and the Wedge Solution standard deviations. This may be attributable to the small number of simulations chosen and to input variances introduced into making the wedges for the Wedge Solution Method.

The largest difference in the two methods was the amount of time required to obtain a solution with 100 simulations. On the same computer with the Design Mode Example 5.1, the Coefficient Method took seconds to process 100 simulation runs while the Wedge Solution Method took (on average) nearly six minutes to process 100 simulations. While accounting for more diverse soil conditions, the Wedge Solution calculations are more complicated and take more time.

Simulation runs were also performed on the Design Mode Example 5.1 problem to determine the effect of running more simulations. The results of running 1,000 simulations with a flood elevation are presented in Figure 5.23 and Table 5.5. Table 5.5 shows that while the range of results (from minimum to maximum) changes from 100 to 1,000 simulation runs, the resulting mean and standard deviations are similar.

Figure 5.23. Wedge Solution Method results for Example 5.1 with a flood height 40.0 ft and 1,000 simulations.

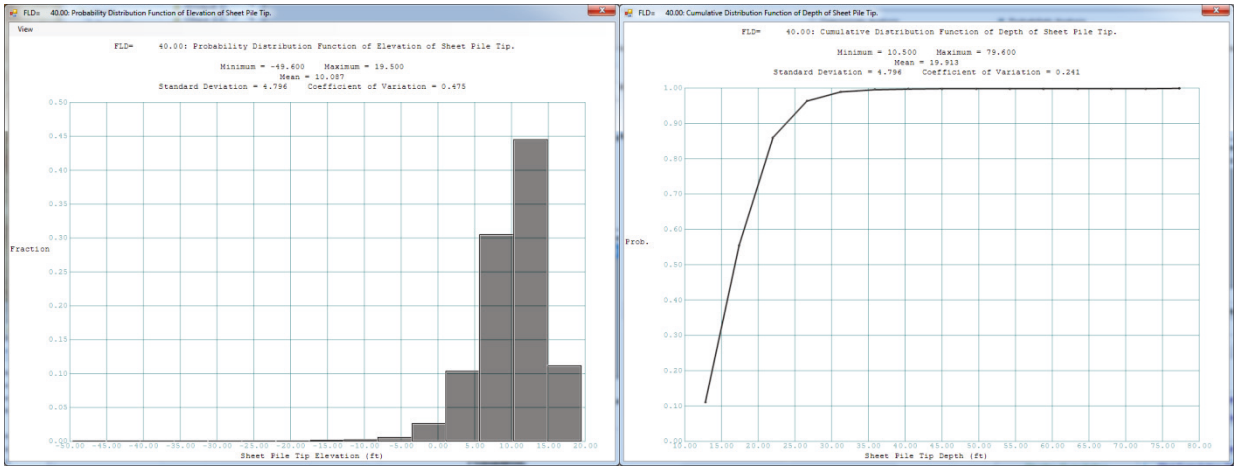


Table 5.5. Results of Example 5.1 with a flood elevation of 40 ft using 1,000 and 100 simulation runs with the Wedge Solution Method.

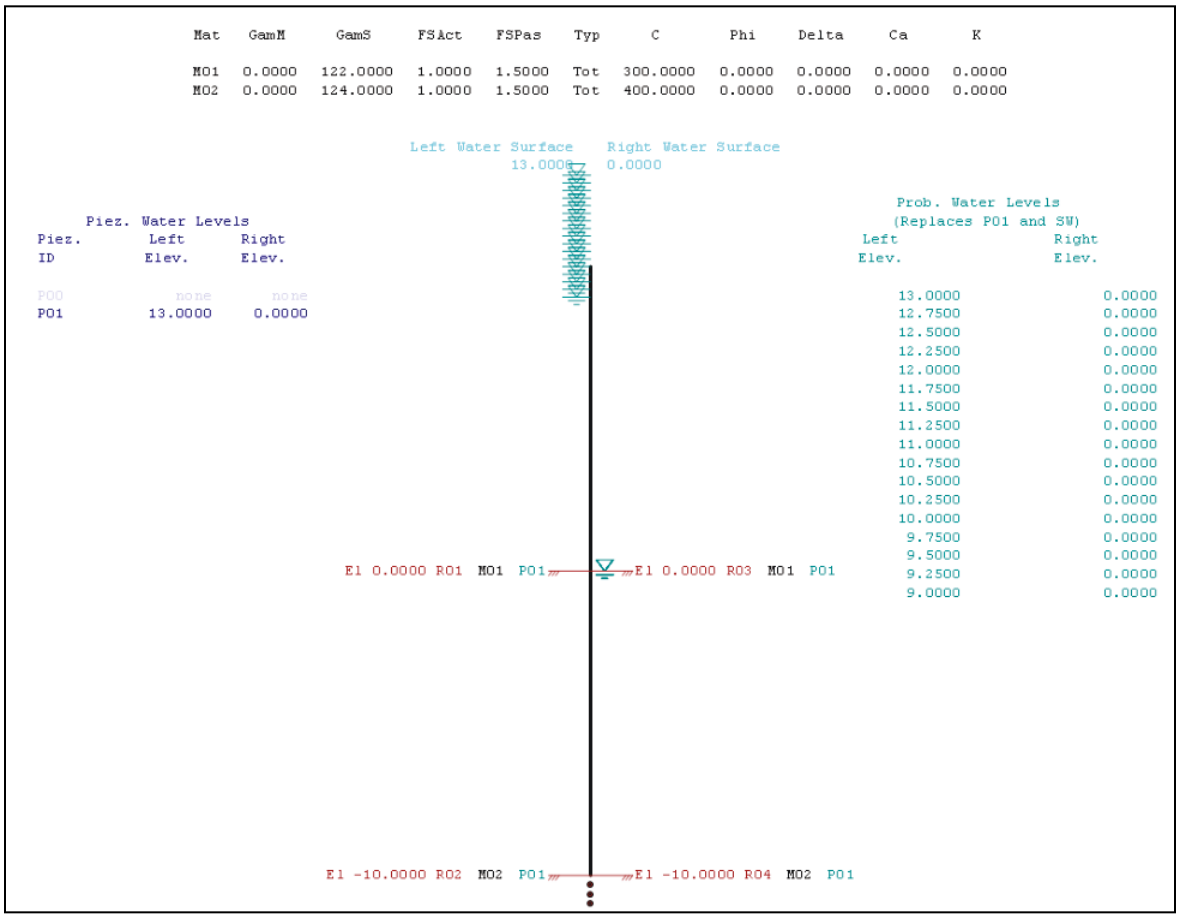
Number of Simulations	Flood Elevation (ft)	Wedge Solution Method (without seepage analysis)				
		Minimum Pile Tip Elevation (ft)	Maximum Pile Tip Elevation (ft)	Mean Pile Tip Elevation (ft)	Standard Deviation	Coefficient of Variation
1,000	40.0	-49.5	19.5	10.87	4.796	0.475
100	40.0	-6.5	17.9	10.140	4.383	0.432

5.7 Example 5.2 SRC (clay site with hydraulic fracturing, an extension of Example 4.7)

A total stress definition with φ = 0 and an undrained shear strength (*Su*) is illustrated using a series of total stress analysis problems in order to calculate a uniform passive Factor of Safety (FS_p) of an existing sheet-pile wall in *Analysis* mode. A global active Factor of Safety of 1.0 for computing active earth pressures is applied to all soil layers. This I-Wall system has an exposed height of 10 ft. The four regions consist of two soil, or material layers, with level ground interfaces on both sides of the I-Wall at 0 ft and -10 ft. The saturated unit weight of 122 pcf, and cohesion of 300 psf,

for the upper soil layer, and a saturated unit weight of 124 pcf, and cohesion of 400 psf, for the lower soil layer have been assigned. The water surfaces at both sides of the I-Wall are at 13 ft on the flood side (LHS) and at 0 ft on the landside. Figure 5.24 outlines the geometry and soil parameters of the sheet-pile wall. This analysis procedure was specified given a predesigned wall tip el -28.2679 ft. This sheet-pile tip elevation was established in the Example 4.7 deterministic analysis of Chapter 4.

Figure 5.24. Schematic of sheet-pile wall in clay site for various water levels.



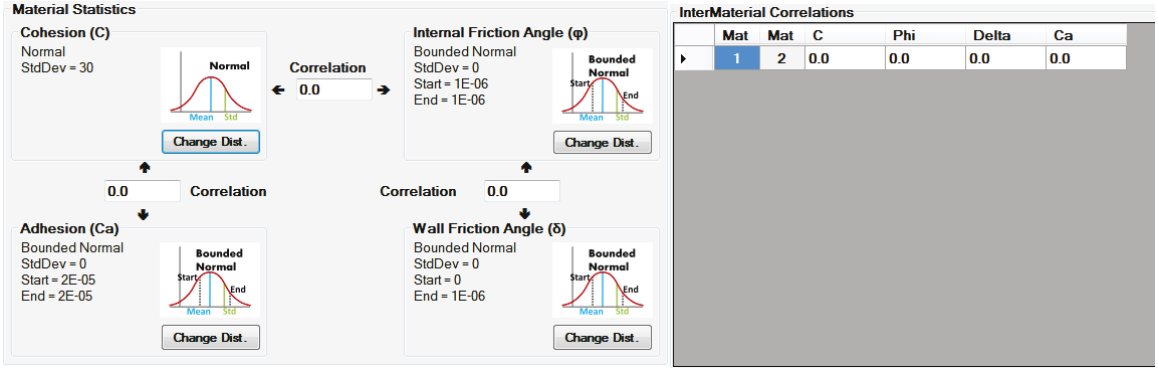
The top row of text listed in Figure 5.24 documents the input values of all parameters associated with each material type. For this problem, there are two materials assigned for the clay site, they are recorded as M01 and M02, the "M" signifies the material type and is followed by the ID which starts from "01." All information concerning material types are written in black text. The representation of a soil structure is characterized by a region. Regions are labeled with an "R" and are followed by an ID starting from "01." For this problem four regions are assigned, Region 1 and Region 2 (as R01 and R02) are located on the LHS of the sheet-pile wall, Region 3 and

Region 4 (as R03 and R04) are located on the RHS of the sheet-pile wall. Each region and its surface elevation are written in red text.

Hydrostatic water elevations are listed in the upper left-hand corner and are shown in dark blue. Water levels are labeled at the soil interface of any specified region with an initial character "P" and followed by an ID Label. The label "P00" is one that signifies that there is no water associated with a soil layer or region and the soil is partially saturated. If all soil regions are fully saturated, "P00" will be grayed out (as shown in Figure 5.24). Surface water on either side of the sheet-pile wall is represented by water symbols at its defined elevation along the sheet-pile wall and labeled as "P01." If there is no surface water associated with any soil region, "P01" will be grayed out.

For the probabilistic analysis, the mean of the cohesion is listed in the table of Figure 5.25 for the materials designated as M01 and M02. A standard deviation of 300 psf, a COV of 0.1, and bounded normal probability distribution function are specified for the material M01 cohesion (as shown in Figure 5.25). A standard deviation of 400 psf, a COV of 0.1, and bounded normal probability distribution function are specified for the material M02 cohesion. The cohesions of the two layers are considered independent variables, so there is zero correlation specified between them.

Figure 5.25. Statistical parameters for the clayey soil of material M01.



This problem was analyzed for flood elevations ranging from 9 ft to 13 ft with a constant landside water elevation of 0 ft. These flood elevations were tested initially with 1 ft increments totaling five water levels, and later at 0.25 ft increments for a total of seventeen water levels. Four different tests were conducted by varying the number of simulations of 100, 300, 1,000, and 2,000 simulations for all seventeen water levels.

5.8 Comparisons of results for 100, 300, 1,000, and 2,000 simulations

This subsection discusses the analyzed results of Example 5.2 for 100, 300, 1,000, and 2,000 simulations using the Coefficient Method for earth pressures. Flood levels were set at 0.25 ft increments, with a maximum flood elevation at 13 ft, and a minimum flood elevation at 9 ft. A total of seventeen pairs of flood levels are considered for each of the flood level simulation groups. At the RHS of the I-Wall, a constant water elevation at 0 ft is assigned.

This analysis resulted with a SRC of an I-Wall rotational limit state for 100, 300, 1,000, and 2,000 simulations and seventeen flood levels. Table 5.6 lists the probabilities for the rotational limit state for each of the simulation groups tabulated at all seventeen flood elevations.

Table 5.6. Probabilities of a rotational limit state for 100, 300, 1,000, and 2,000 number of simulations.

	Number of Simulations			
Flood Elevation (ft)	100	300	1,000	2.000
13.00	1.00	1.00	1.00	1.00
12.75	1.00	1.00	1.00	1.00
12.50	0.97	1.00	0.99	1.00
12.25	0.92	0.96	0.97	0.97
12.00	0.88	0.86	0.86	0.88
11.75	0.72	0.68	0.69	0.73
11.50	0.44	0.45	0.46	0.51
11.25	0.32	0.28	0.28	0.29
11.00	0.16	0.12	0.14	0.15
10.75	0.05	0.06	0.06	0.06
10.50	0.02	0.02	0.02	0.02
10.25	0.00	0.01	0.00	0.01
10.00	0.01	0.00	0.00	0.00
9.75	0.00	0.00	0.00	0.00
9.50	0.00	0.00	0.00	0.00
9.25	0.00	0.00	0.00	0.00
9.00	0.00	0.00	0.00	0.00

Figure 5.26 plots SRC using the results from the Table 5.6 and the 1,000 simulation analysis (blue curve). Each point on the Figure 5.26 SRC gives the probability of the rotational limit state of the I-Wall using 1,000 simulations at each flood level to define each point. The probability for a rotational limit state is shown with a value of 0.0 at the 10 ft flood elevation, and reaching a maximum value of 1.0 at 12.75 ft. The curves in Figure 5.26 show a difference between the different flood levels chosen for 1,000 simulations. The 1 ft increments in flood elevations (green line), from 9 ft to 13 ft of Figure 5.26, only provided five data points, and therefore, could not fully describe the SRC. A much finer flood level increment of 0.25 ft was used for the 1,000 simulations, and a more refined SRC was produced and represented by the blue curve.

Figure 5.26. SRC for 1,000 simulations at 0.25 ft and 1 ft flood increments.

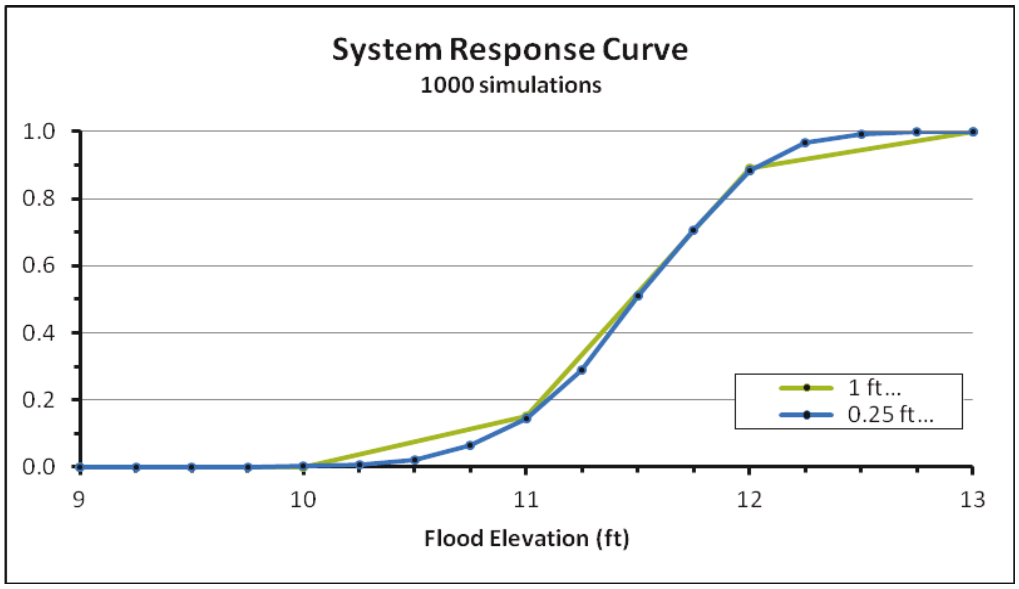
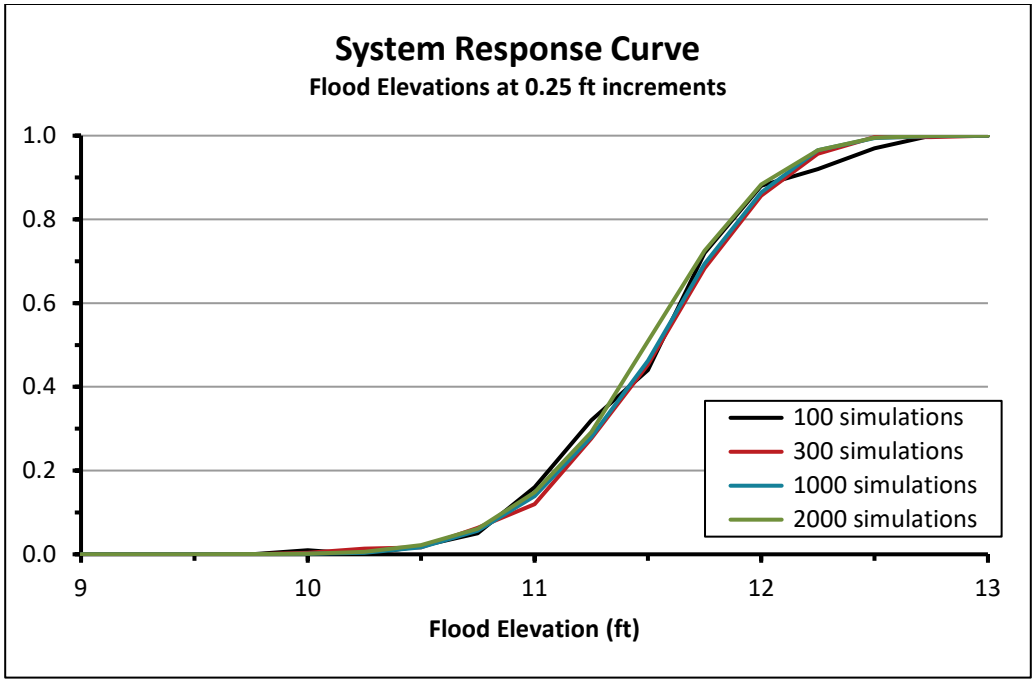


Figure 5.27 presents all four Table 5.6 SRC curves representing the 100, 300, 1,000, and 2,000 simulations for seventeen flood levels. A close inspection of this figure, and the data contained in Table 5.6, show that the response curve from the 2,000 simulations are close to the results for the response curves of 1,000 and 300 simulations. Comparison between the Table 5.6 data for the 300 and 2,000 simulation results at flood el 11.50 ft, and at el 11.75 ft demonstrates a difference between the probability for rotational limit state values for both the 300 and 2,000 simulation results of 0.45 and 0.51, and 0.68, and 0.73, respectively. The fact that the 2,000 simulation results are in agreement with the 300 simulation results, demonstrate that 300 simulations are ideal for the calculation of the SRC with close accuracy and much better execution times as compared to the 1,000 simulations.

Figure 5.27. SRC for 100, 300, 1,000, and 2,000 simulations at 0.25 ft increments.



Execution times were recorded for the various simulations. These timings and the normalized values with the timing for 300 simulations are tabulated in Table 5.7. Data from the table show that there is a linear relationship between the timings and number of simulations.

Table 5.7. Execution times for 100, 300, 1,000, and 2,000 number of simulations.

Number of Simulations	Execution Time (hh:mm)	Normalized
100	0:17	0.34
300	0:50	1.00
1,000	2:46	3.32
2000	5:24	6.48

5.9 Comparisons of results Coefficient Method and Wedge Solution Method with 100 simulations

Using Example 5.2, a comparison was made between the SRC for the Coefficient Method and the Wedge Solution earth pressure methods. Because seepage is not used, this should be an apples-to-apples comparison between the methods. One hundred simulations were performed for each flood elevation, from 13 to 9 ft at 0.25 ft intervals, with only variance in the cohesion of the two soil materials. Each simulation run was said to have

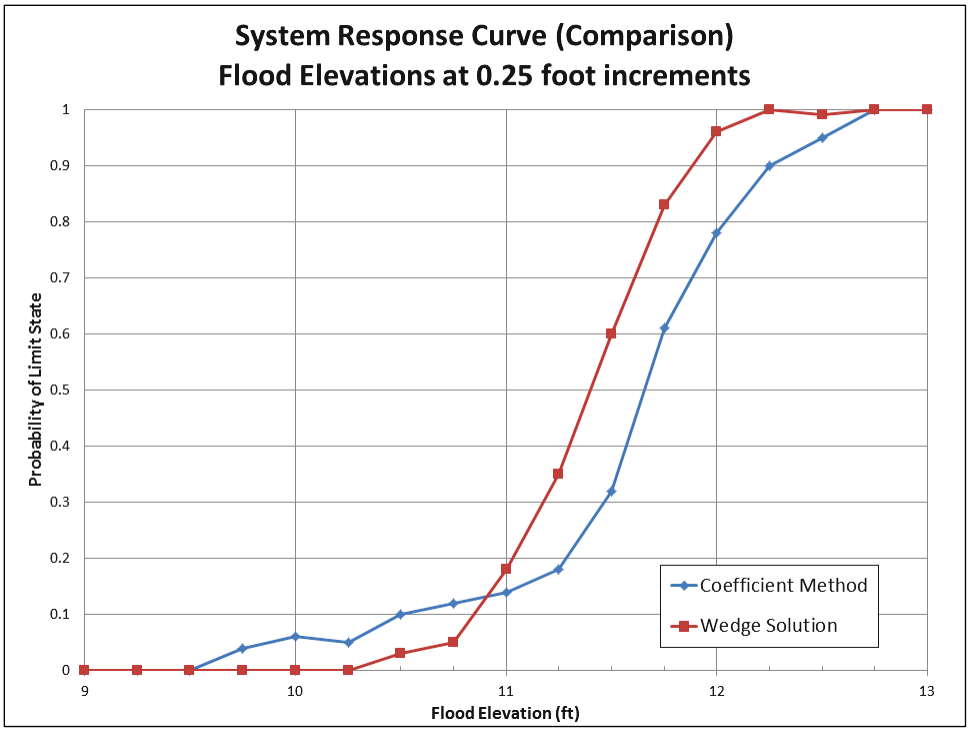
reached the limit state (and gone into failure) when the Factor of Safety is less than, or equal to 1.0. From these simulations, the probability of limit state is calculated as the ratio of the number of runs with a Factor of Safety less than, or equal to 1.0, divided by the total number of runs. Table 5.8 and Figure 5.28 show the results of the comparison runs and the resulting SRC.

The resultant SRC for the Coefficient Method and and the Wedge Solution Method had a 0.0 probability of limit state from flood elevation 9.0 ft to 9.5 ft. Likewise, both SRCs had a 1.0 probability of limit state from flood elevation of 12.75 ft to 13.0 ft. The Coefficient Method of computing earth pressure provides an SRC with a larger range of flood elevations, and with a changing probability of limit state. Both SRCs seem to have the same slope at the steepest change of limit state probabilities, though the Wedge Solution Method reaches this rate of change with a flood elevation approximately 0.25 ft lower than the Coefficient Method, resulting in more conservative values.

Table 5.8. Comparison of probability of limit state between the Coefficient Method and the Wedge Solution Method.

Flood Elevation (ft)	Coefficient Solution Probability of Limit State	Wedge Solution Probability of Limit State
13	1	1
12.75	1	1
12.5	0.95	0.99
12.25	0.9	1
12	0.78	0.96
11.75	0.61	0.83
11.5	0.32	0.6
11.25	0.18	0.35
11	0.14	0.18
10.75	0.12	0.05
10.5	0.1	0.03
10.25	0.05	0.00
10	0.06	0.00
9.75	0.04	0.00
9.5	0	0.00
9.25	0	0.00
9	0	0.00

Figure 5.28. SRC for Design, Coefficient Method vs Wedge Solution Method.



A full parametric study needs to be performed to find the cause of the difference between the curves, but one possibility may be the effect of interslice friction curves used by the Wedge Solution Method, especially with regard to the limit state probability separation of 0.25 ft between the SRCs. Also, differences could be caused by the changes in selection of depth increments used to determine wall pressures between the two methods.

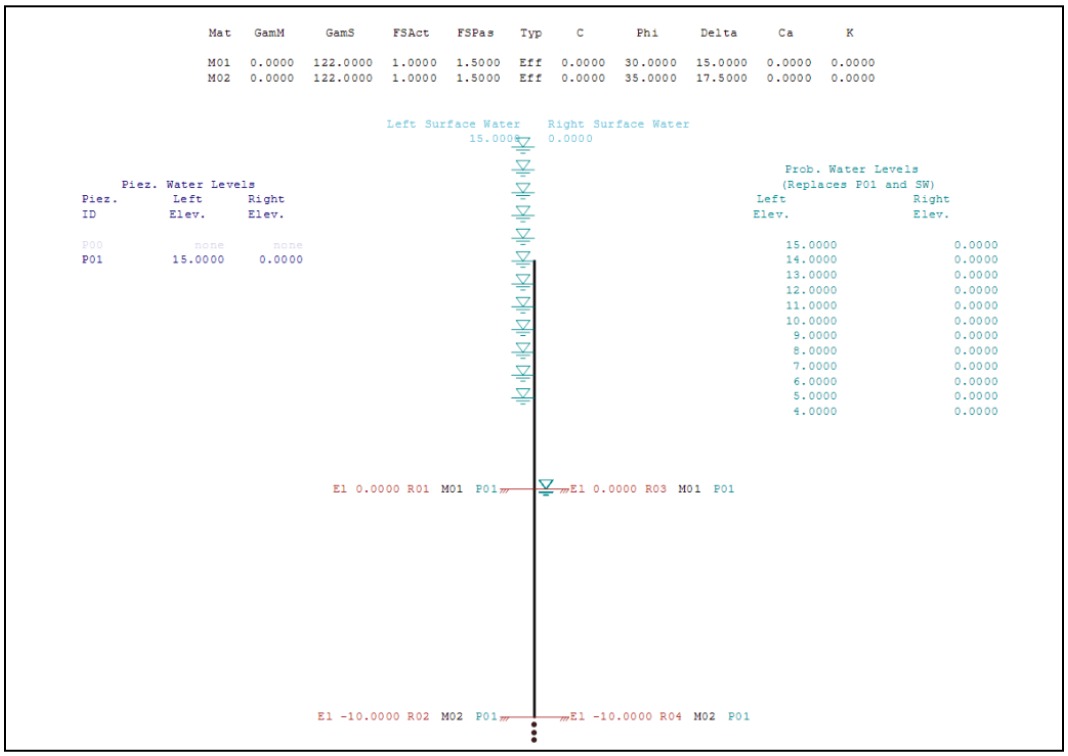
The amount of time to run each method was also recorded. The Coefficient Method took twelve minutes to run the complete simulation run. The Wedge Solution Method, for the same complete simulation run, took eleven hours and eight minutes to complete. Again, the primary reason for performing the Wedge Solution Method is for non-level soil regions that cannot be adequately modeled with the Coefficient Method.

5.10 Example 5.3 SRC for a two-layer sand site with hydraulic fracturing criteria and seepage

An effective stress definition of an I-Wall founded in a two-layer sand site (i.e., two regions on either side of I-Wall) with $c' = 0$ is illustrated using a series of effective stress-based analyses in order to calculate a uniform passive Factor of Safety (*FSp*) of an existing sheet-pile wall in an *Analysis* mode. A global active Factor of Safety of 1.0 for computing active earth

pressures is applied to all soil layers. This I-Wall system has an exposed height of 10 ft. The four regions consist of two soil or material layers with level ground interfaces on both sides of the I-Wall at 0 ft and -10 ft. All soil layers are assigned a saturated unit weight of 122.0 pcf. The upper soil layers have an effective angle of internal friction of 30 degrees and the effective angle of soil-to-sheet-pile wall interface friction of 15 degrees. The lower soil layers have been assigned an effective angle of internal friction of 35 degrees and the effective angle of soil-to-sheet-pile wall interface friction of 17.5 degrees. Surface water on both sides of the I-Wall are at el 15 ft on the flood side (LHS) and at el 0 ft on the landside (RHS). This analysis also considers homogeneous seepage. Figure 5.29 outlines the geometry and soil parameters for the sheet-pile wall. For the analysis of an existing sheet-pile wall, the sheet-pile tip el was predesigned for -13 ft.

Figure 5.29. Schematic of sheet-pile wall in sandy site for twelve flood levels.



The top row of text listed in Figure 5.29 documents the input values of all parameters associated with each material type. For this problem, there are two materials assigned for the clay site and recorded as M01 and M02, the "M" signifies the material type and is followed by the ID, which starts from "01." All information concerning material types are written in black text. The representation of a soil structure is characterized by a region. Regions are labeled with an "R" and followed by an ID starting from "01." For this

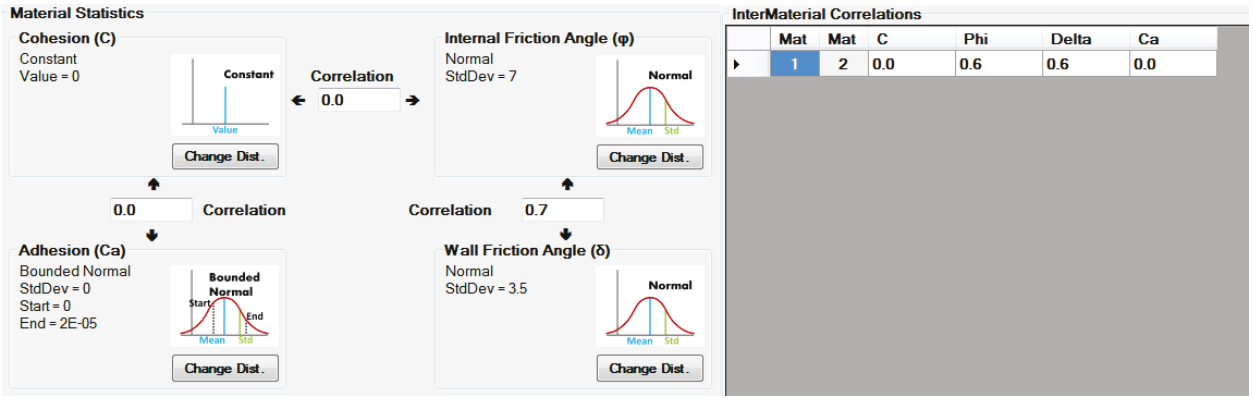
problem the following four regions are assigned: Region 1 and Region 2 (as R01 and R02), are located on the LHS of the sheet-pile wall, and Region 3 and Region 4 (as R03 and R04), are located on the RHS of the sheet-pile wall. Each region and its surface elevation are written in red text.

Water elevations are listed in the upper left-hand corner and shown in dark blue. Water levels are labeled at the soil interface of any specified region with an initial character "P" and are followed by an ID. Label "P00" is one that signifies that there is no water associated with a soil layer or region and the soil is partially saturated. If all soil regions are fully saturated, "P00" will be grayed out (Figure 5.29). Surface water on either side of the sheet-pile wall is represented by water symbols at its defined elevation and labeled as "P01." If there is no surface water associated with any soil region, "P01" will be grayed out.

For the probabilistic analysis considered in this section, the mean effective angle of internal friction (φ'), and the mean effective angle of wall-soil interface friction (δ'), were defined previously as 30 degrees and 15 degrees for material M01, and 35 degrees and 17.5 degrees for material M02, respectively. These are listed in the table of Figure 5.29. A standard deviation of 6 degrees, a COV of 0.2, and normal probability distribution function is specified for the effective angle of internal friction (as shown in Figure 5.30). A standard deviation of 3 degrees, a COV of 0.2, and normal probability distribution function is specified for the effective angle of wall-soil interface friction. Note that these two variables are strongly correlated with a correlation coefficient of 0.7, and the intermaterial correlations of φ' and δ'. Therefore, materials M01 and M02 have been assigned values of 0.6 (as shown in Figure 5.30). Section 5.2 discusses random variables and the correlation between them.

This example was analyzed for flood elevations ranging from 4 ft to 15 ft on the RHS, and with a constant landside water elevation of 0 ft on the LHS of the I-Wall. These flood elevations were tested with 1 ft increments for a total of twelve water levels. Four different tests were conducted. The number of simulations were 100, 300, 500, and 1,000 for all twelve water levels.

Figure 5.30. Statistical parameters for the sandy soils.



5.11 Comparisons of results for 100, 300, 500, and 1,000 simulations

This subsection discusses the analyzed results of Example 5.2 for 100, 300, 500, and 1,000 simulations using the Coefficient Method for earth pressures. Flood levels on the LHS are set at 1 ft increments with maximum flood elevation at 15 ft, and a minimum flood elevation at 4 ft. A total of twelve pairs of flood levels are considered for each of the flood level simulation groups. At the RHS of the I-Wall, a constant water elevation at 0 ft is assigned.

This analysis resulted with a SRC of an I-Wall rotational limit state with 100, 300, 500, and 1,000 simulations and twelve flood levels. Table 5.9 lists the probabilities for the rotational limit state for each of the simulations tabulated at all twelve flood elevations.

Figure 5.31 plots the four SRCs (Table 5.9). Each point on the gray SRC gives the probability of rotational limit state of the I-Wall, using 1,000 simulations to define each point (Figure 5.31). The probability for a rotational limit state is shown with values approximately 0 at 4 ft flood elevation, and reaching a maximum value of 1.0 at 14 ft. The black, red, and blue SRC curves correspond to 100, 300, and 500, simulations, respectively, of twelve flood levels (Figure 5.31). A close inspection of this figure, and the data contained in Table 5.9, show that responses from all simulations are close to the results for the 1,000 simulations. Table 5.9 numerically shows minimal changes, however, Figure 5.31 shows the response of the 100 simulations does not provide a smooth curve, which implies more than 100 simulations are needed.

Figure 5.31. SRC for 100, 300, 500, and 1,000 simulations.

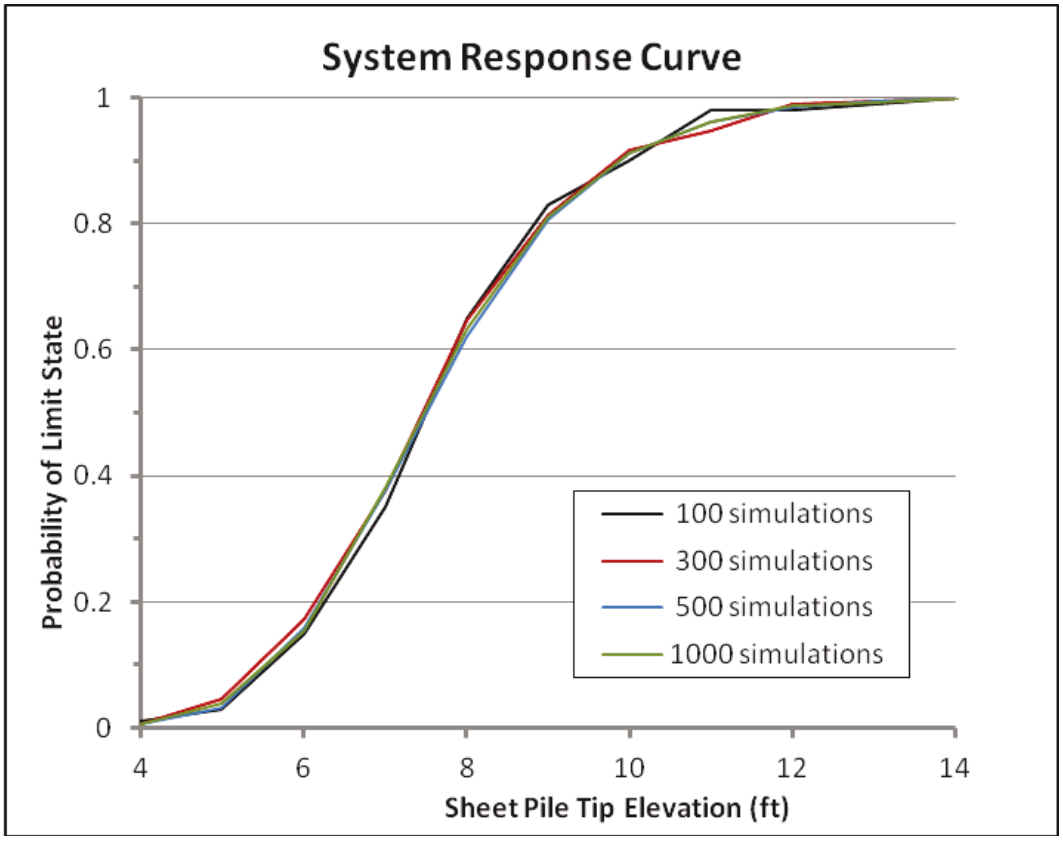


Table 5.9. Probabilities of a rotational stability for 100, 300, 500, and 1,000 simulations.

	Number of Simulations			
Flood Elevation (ft)	1,000	500	300	100
15	1.00	1.00	1.00	1.00
14	1.00	1.00	1.00	1.00
13	0.99	0.99	0.99	0.99
12	0.99	0.98	0.99	0.98
11	0.96	0.96	0.95	0.98
10	0.91	0.91	0.92	0.90
9	0.81	0.81	0.81	0.83
8	0.63	0.62	0.65	0.65
7	0.38	0.38	0.38	0.35
6	0.15	0.16	0.17	0.15
5	0.04	0.03	0.05	0.03
4	0.01	0.01	0.01	0.01

Recognizing that this is the most computational intensive problem, (the evaluation of a probabilistic, analysis of rotational stability of the I-Wall, effective stress-based earth pressure calculations, and seepage), the determination of the number of simulations essential to produce the best acceptable accuracy is a necessity while minimizing run time for the evaluation of the SRC. From this reasoning, the 300-simulation SRC curve was determined to provide good accuracy and a smoother SRC.

Execution times have been recorded for the various simulations. These timings, and the normalized values with the timing for 300 simulations, are tabulated in Table 5.10. Data from the table show that there is a near linear relationship between execution times and number of simulations.

Table 5.10. Execution times for 100, 300, 500, and 1,000 simulations.

Number of Simulations	Execution Time (hh:mm)	Normalized
100	1:41	0.34
300	5:01	1.00
500	8:28	1.69
1,000	15:52	3.16

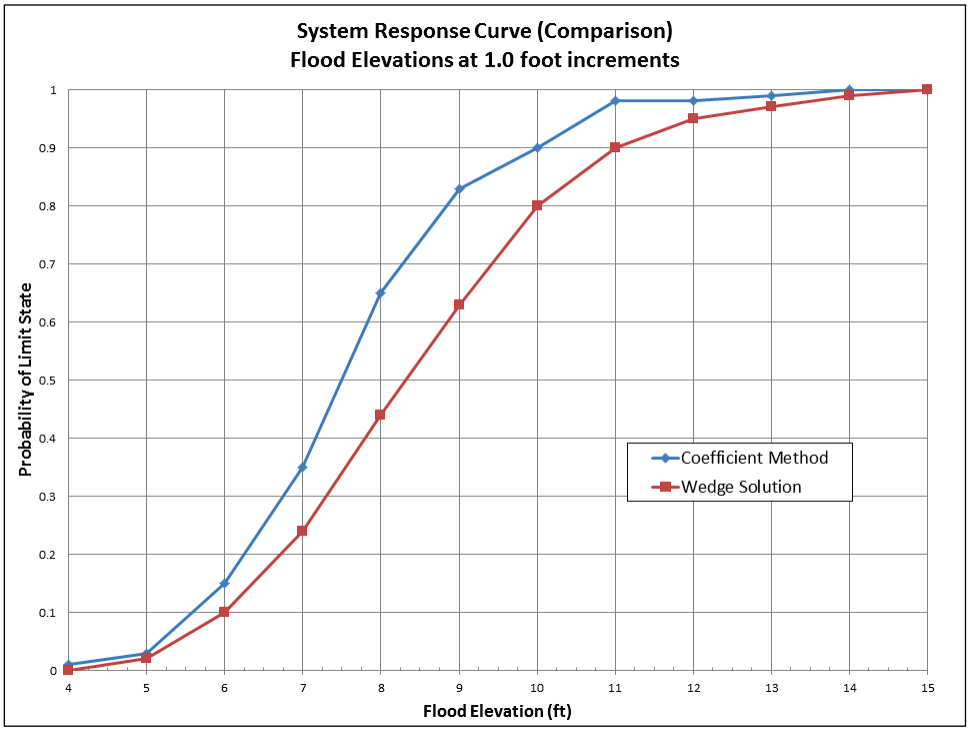
5.12 Comparisons of analysis results for the Coefficient Method and the Wedge Solution Method with 100 simulations

Using Example 5.3, a comparison was made between the SRC for the Coefficient and the Wedge Solution earth pressure methods for analysis mode calculations. Because seepage is not used, this should be an apples-to-apples comparison between the methods. One hundred simulations were performed for each flood elevation, from 15 to 4 ft at 1.0 ft intervals, with only variance in the cohesion of the two soil materials. Each simulation run is said to have reached the limit state (and gone into failure) when the Factor of Safety is less than or equal to 1.0. From these simulations, the probability of limit state is calculated as the ratio of the number of runs with Factor of Safety less than or equal to 1.0 divided by the total number of runs. Table 5.11 and Figure 5.32 show the results of the comparison runs and the resulting SRCs.

Table 5.11. Comparison of probability of limit state between Coefficient Method and Wedge Solution Method.

Flood Elevation (ft)	Coefficient Solution Probability of Limit State	Wedge Solution Probability of Limit State
15	1.00	1.00
14	1.00	0.99
13	0.99	0.97
12	0.98	0.95
11	0.98	0.90
10	0.90	0.80
9	0.83	0.63
8	0.65	0.44
7	0.35	0.24
6	0.15	0.10
5	0.03	0.02
4	0.01	0.00

Figure 5.32. SRC for Analysis: Coefficient Method vs Wedge Solution Method.



The resultant SRCs for the Coefficient Method and and the Wedge Solution Method had a very low probability of limit state (less than 10% probability) from flood elevation 4.0 ft to 5.0 ft. Likewise, both SRCs had a very high probability of limit state (greater than 10% probability) from flood elevation of 12.0 ft to 15.0 ft. The Coefficient Method of computing earth pressures gives a SRC with a faster increase in the probability of limit state with change in flood elevation, while the Wedge Solution Method has a smoother transition. The smoother transition may come from the averaging of soil transitions with the corresponding soil wedges that were created with with all of the simulations as the soil material was changed. Both SRCs have the same sigmoid-type curve of cumulative limit state probabilities, though the Wedge Solution Method seems to have a smoother rate of change with a flood elevation, resulting in more conservative probabilities.

A full parametric study would need to be performed to find the cause of the difference between the curves, but one possibility may be the effect of interslice friction curves, especially with regard to the limit state probability separation of 1.0 ft between the SRCs. There may also be differences caused by the different possible increments used to determine wall pressures between the two methods.

The amount of time for each method was also recorded. The Coefficient Method took eight minutes to run the complete simulation. The Wedge Solution Method, for the same complete simulation run, took 24 hours and 56 minutes. Again, the primary reason for performing the Wedge Solution Method is for non-level soil regions that cannot be adequately modeled with the Coefficient Method.

5.13 Comparisons of the Wedge Solution Method with 100 and 50 simulations

Clearly, the run times for the Wedge Solution Method are much longer than the Coefficient Method. Simple methods to estimate these run times, like the Taylor Series Method, will not provide any relief. With these obstacles to efficiency, it becomes necessary to try to reduce the number of runs that are required to get a fairly accurate SRC. Table 5.12 and Figure 5.33 show a comparison reducing the number of simulations from 100 to 50 for the Example 5.3 problem. The number of simulations was initially set to 100 to match the corresponding Coefficient Method number of simulations that would give sufficient results. The resulting curves given by the Wedge Solution Method for the two full runs, with 100 and 50 simulations, are very similar, with variations of 3% at most at for any given flood elevation.

Table 5.12. Comparison of probability of limit state for the Wedge Solution Method with 100 and 50 simulations.

Flood Elevation (ft)	Wedge Solution Method Probability of Limit State – 100 simulations	Wedge Solution Method Probability of Limit State – 50 simulations
15	1.00	1.00
14	0.99	1.00
13	0.97	1.00
12	0.95	0.92
11	0.90	0.90
10	0.80	0.82
9	0.63	0.60
8	0.44	0.44
7	0.24	0.26
6	0.15	0.08
5	0.03	0.02
4	0.01	0.00

Figure 5.33. SRC for Analysis: Coefficient Method vs Wedge Solution Method.

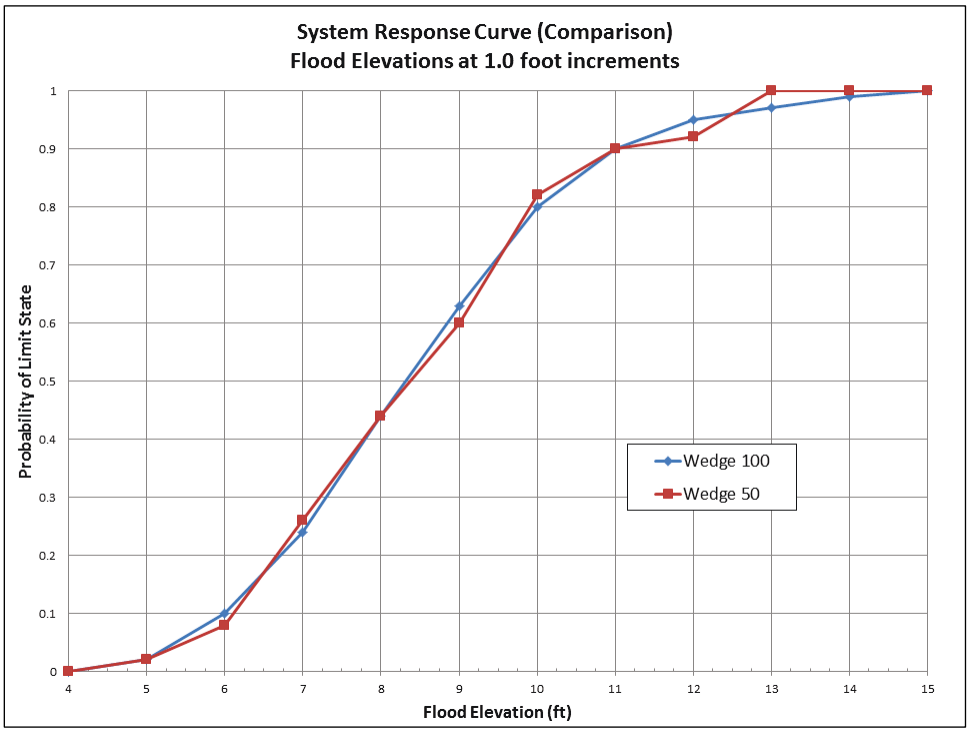


Table 5.13 shows the run times for the two sets of simulations. As expected, halving the number of simulation runs nearly halved the amount of time to make the full run. Because a 50 run simulation gives a percentile resolution of 2%, it is not recommended that runs be performed with a smaller number of simulations.

Table 5.13. Run times for Example 5.3 Wedge Solution Method with 100 and 50 simulations.

Number of Simulations	Time (hr:min)
50	13:33
100	24:56

6 Summary, Conclusions, and Recommendations

6.1 Summary

This report summarizes two engineering methods, and the implementation of these methods, in the software Corps_I-Wall Version 2.0 used for the design of new I-Walls, or the analysis of existing I-Walls in floodplains (i.e., I-Walls embedded in level ground), or in riverbanks and levees (i.e., I-Walls embedded in non-level ground, with non-level soil layers, and/or non-level piezometric surfaces) during flood loading. Earth pressures are computed using either the Coefficient Method or Wedge Solution Method of analysis.

Other Corps_I-Wall software capabilities for engineering analysis include the following: total stress and/or effective stress earth pressure calculations, Rankine, Coulomb, or logarithmic spiral-based earth pressure coefficients for the Coefficient Method of analysis, hydrostatic pore water pressure computed from surface water(s) and/or piezometric surface(s) within each of the layered soil regions, pore water pressures computed from line of seepage, steady-state seepage in soil regions with different hydraulic conductivities (for the Coefficient Method of analysis only), gap initiation and propagation using hydraulic fracturing criterion, and boundary pressures (e.g., for wave loading of coastal structures) and/or surface surcharge.

Probabilistic analysis is a primary component of Corps_I-Wall for new and existing I-Wall analysis. The probabilistic analysis capabilities for the design of new I-Walls results in a statistical characterization of sheet-pile tip embedment. The probabilistic analysis capabilities for analyzing existing I-Walls include the construction of a SRC (fragility curve), this gives the probability of rotational instability as a function of flood elevation. The Coefficient Method of analysis provides a vehicle for efficient probabilistic solutions. Probabilistic solutions are also available for the Wedge Solution Method of analysis, however, these will take more time to perform due to the complicated solution method.

Examples are provided to highlight each of these capabilities. Select examples from geotechnical literature and an ERDC TR were used to validate the basic engineering methodologies as they were implemented in

the software. A user's manual for using the GUI and executing CI-Wall is also included.

6.2 Conclusions

The I-Wall Analysis research and development effort summarized in this report provides the USACE Districts with essential tools in analyzing and evaluating I-Wall performance in riverine, fluvial, and coastal environments. The validated engineering methodologies and GUI implemented in the software provide ease of use for the modeling and evaluation of these soil-structure interactions. Advanced techniques are included to address hydraulic fracturing, seepage, etc. With the implementation of the Wedge Solution Method of analysis, non-horizontal soil surfaces and water levels can be modeled to allow for a greater variety of structural environments.

6.2 Recommedations

The extension of Corps_I-Wall Version 1.0 to Version 2.0 adds the Wedge Solution Method of analysis option for computing earth pressure forces to the Version 1.0 Coefficient Method. The Wedge Solution Method of analysis allows for consideration of a non-horizontal ground surface, non-horizontal soil layers, and non-horizontal piezometric surfaces. These enhancements greatly expand the versatility and usage of Corps_I-Wall software to the analysis of many more USACE flood mitigation problems.

The following two Corps_I-Wall software features have been requested by District engineers:

1. Expand the Wedge Solution Method of analysis to account for thin, weak soil layers in the earth force analyses. This is of particular importance to levee structures.
2. Expand the software to perform a simplified I-Wall deformation analysis, comparable to that provided by CWALSHT.

To date, the request for the addition of these features, submitted by District engineers as Statements of Needs to the Flood and Coastal Storm Damage Reduction Program, have not been funded.

References

Abramson, Lee W., Thomas L. Lee, Sunil Sharma, and Glenn M. Boyce. 1996. *Slope Stability and Stabilization Methods*. New York, NY: John Wiley and Sons, Inc.

Bardet, Jean-Pierre. 1997. *Experimental Soil Mechanics*. Upper Saddle River, NJ: Prentice Hall.

Becker, D. E. 1996. Eighteenth Canadian geotechnical colloquium: Limit states design for foundations. Part II. Development for the National Building Code of Canada. *Canadian Geotechnical Journal* 33(6):984–1007. https://doi.org/10.1139/t96-125.

Bowles, Joseph E. 1968. *Foundation Analysis and Design*. New York: McGraw-Hill Book Company.

Bullock, G., C. Obhrai, G. Wolters, G. Müller, H. Peregrine, and H. Bredmose. 2004. Characteristics and design implications of breaking wave impacts. In *Proceedings of the 29th International Conference National Civil Engineering Laboratory, Lisbon, Portugal*. https://doi.org/10.1142/9789812701916_0320.

Caquot, A., and J. Kerisel. 1948. Tables for the calculation of passive pressure, active pressure and bearing capacity of foundations. *Gauthier-Villars, Paris*.

Cedergren, H. R. 1977. *Seepage, drainage and flownets*. 2nd edition. New York: John Wiley and Sons.

Cherubini, C. 2000. Reliability evaluation of shallow foundation bearing capacity on c', ϕ' soils. *Canadian Geotechnical Journal* 37(1): 264–269. https://doi.org/10.1139/t99-096.

Cherubini, C. 1997. Data and considerations on the variability of geotechnical properties of soils. In *Proceedings of the International Conference on Safety and Reliability (ESREL) 1997, Lisbon, Portugal* 2:1583–1591.

Chen, W. F., and X. L. Liu. 1990. Limit analysis in soil mechanics. *Developments in geotechnical engineering 52*. New York: Elsevier Science Publishers.

Chugh, A. K. 1986. Variable interslice force inclination in slope stability analysis. *Soils and Foundations* 26(1):115–121.

Clough, G. W., and J. M. Duncan. 1991. Earth pressures. In *Foundation engineering handbook*. 2nd edition: 223–235. Ed: Hsai-Yang Fang and van Nostrand. New York: Reinhold.

Das, B. M. 2007. *Principles of Foundation Engineering*. 6th edition. Canada Ltd.:Nelson/Thomson.

Dawkins, W. P. 1991. *Users Guide: Computer Program for Design and Analysis of Sheet-Pile Walls by Classical Methods (CWALSHT) Including Rowe's Moment Reduction*. Instruction Report ITL-91-1. Vicksburg, MS: U.S. Army Engineer Waterways Experiment Station.

Department of the Navy. 1982. *Foundations and Earth Structures. Design Manual, DM 7.2*. Alexandria, VA: Naval Facilities Engineering Command.

Duncan, M. J., and Stephen G. Wright. 2005. *Soil Strength and Slope Stability*. Hoboken, NJ: John Wiley and Sons, Inc.

Duncan, M. J., Stephen G. Wright, and Thomas L. Brandon. 2014. *Soil Strength and Slope Stability*. Second edition. Hoboken, NJ: John Wiley and Sons, Inc.

Ebeling, Robert M., Moira T. Fong, and Barry C. White. 2016. *Analysis of a Floodplain I-Wall Embedded in Horizontally Stratified Soil Layers During Flood Events Using Corps_I-Wall Software Version 1.0*. ERDC/ITL TR-16-3. Vicksburg, MS: U.S. Army Engineer Research and Development Center.

Ebeling, Robert M., and E. E. Morrison. 1992. *The Seismic Design of Waterfront Retaining Structures*. WES Technical Report ITL-92-11. Vicksburg, MS: U.S. Army Engineer Waterways Experiment Station.

Goda, Y. 1974. New wave pressure formulae for composite breakwater. In *Proceedings of the 14th Conference on Coastal Engineering, Copenhagen, Denmark*.

Harr, M. E. 1987. *Reliability-based design in civil engineering*. New York: McGraw-Hill Book Company.

Headquarters, U.S. Army Corps of Engineers.1989. *Retaining and Flood Walls*. EM 1110-2-2502. Washington, DC: Headquarters, U.S. Army Corps of Engineers.

Headquarters, U.S. Army Corps of Engineers. 1990. *Retaining and Flood Walls*. ETL 1110-2-322. Washington, DC: Headquarters, U.S. Army Corps of Engineers.

Headquarters, U.S. Army Corps of Engineers. 1994. *Design of Sheet-Pile Walls*. EM 1110-2-2504. Washington, DC: Headquarters, U.S. Army Corps of Engineers.

Headquarters, U.S. Army Corps of Engineers. 2002. *Coastal Engineering Manual*. EM 1110-2-1100, Part VI. Washington DC: Headquarters, U.S. Army Corps of Engineers.

Headquarters, U.S. Army Corps of Engineers. 2011a. *Engineering and Design of I_Walls*. Engineering Circular 1110-2-6066. Washington, DC: Headquarters, U.S. Army Corps of Engineers.

Headquarters, U.S. Army Corps of Engineers. 2011b. *Evaluation of I-Walls*. ETL 1110-2-575. Washington, DC: Headquarters, U.S. Army Corps of Engineers.

Independent Panel to Review Cause of Teton Dam Failure.1976. *Report to U.S. Department of the Interior and the state of Idaho on failure of Teton Dam*. Washington, DC: Superintendent of Documents, U.S. Government Printing Office.

Interagency Performance Evaluation Task Force. 2007. *The Performance-Levees and Floodwall*. Performance Evaluation of the New Orleans and Southeast Louisiana Hurricane Protection System. Final Report of the Interagency Performance Evaluation Task Force. Vol V. Washington, DC: Interagency Performance Evaluation Task Force. https://ipet.wes.army.mil/

Jumikis, A. R. 1984. *Soil Mechanics*. Malabar, FL.: Robert E. Krieger Publishing Company, Inc.

Kerisel, J., and E. Absi. 1990. *Active and Passive Earth Pressure Tables*. 3rd edition. A.A. Balkema/Rotterdam/Brookfield.

Lumb, P. 1970. Safety factors and the probability distribution of soil strength. *Canadian Geotechnical Journal* 7(3):225–242.

Nobari, E. S., K. L. Lee, and J. M. Duncan. 1973. *Hydraulic Fracturing in Zoned Earth and Rockfill Dams*. Waterways Experiment Station Contract Report S-73-2. Vicksburg, MS: U.S. Army Engineer Waterways Experiment Station.

Pace, M. C., K. Abraham, and Robert M. Ebeling. 2012. *Complete Soil-Structure Interaction (SSI) Analyses of I-walls Embedded in Level Ground During Flood Loading*. ERDC/ITL TR-12-4. Vicksburg, MS: U.S. Army Engineer Research and Development Center.

Sherard, J. L. 1973. Embankment dam cracking. *Embankment Dam Engineering-the Casagrande Volume*. New York: John Wiley and Sons.

Sherard, J. L. 1986. Hydraulic fracturing in embankment dams. *ASCE Journal of Geotechnical Engineering* 112(10):905–927.

Sokolovskii, V. V. 1965. *Static of Granular Media*. New York: Pergamon Press.

Spangler, M. G., and R. L. Handy. 1973. *Soil engineering*. 3rd edition. New York: Educational Publishers.

Spencer, E. 1973. Thrust line criterion in embankment stability analysis. *Geotechnique* 17(23):11–26.

Tekie, P. B., and B. R. Ellingwood. 2002. *Fragility Analysis of Concrete Gravity Dams*. ERDC/ITL TR-02-6. Vicksburg, MS: U.S. Army Engineer Research and Development Center.

Terzaghi, K. 1943. *Theoretical Soil Mechanics*. New York: John Wiley and Sons.

Terzaghi, K., and Ralph B.Peck. 1948. *Soil Mechanics in Engineering Practice*. New York: John Wiley and Sons.

Terzaghi, K., Ralph B. Peck, and G. Mesri. 1996. *Soil Mechanics in Engineering Practice*. 3rd edition. New York: Wiley-Interscience.

U.S. Army Engineer Waterways Experiment Station. 1984. *Shore Protection Manual*. 4th ed., 2 Vol. Washington DC: U.S. Government Printing Office.

Weggel, J. R. 1972. Maximum breaker height for design. *Journal of the Waterways, Harbors and Coastal Engineering Division* 98(WW4):529–548.

Widjaja, H., J. M. Duncan, and H. B.Seed. 1984. *Scale and Time Effects in Hydraulic Fracturing*. Miscellaneous Paper GL-84-10. Vicksburg, MS: U.S. Army Engineer Waterways Experiment Station.

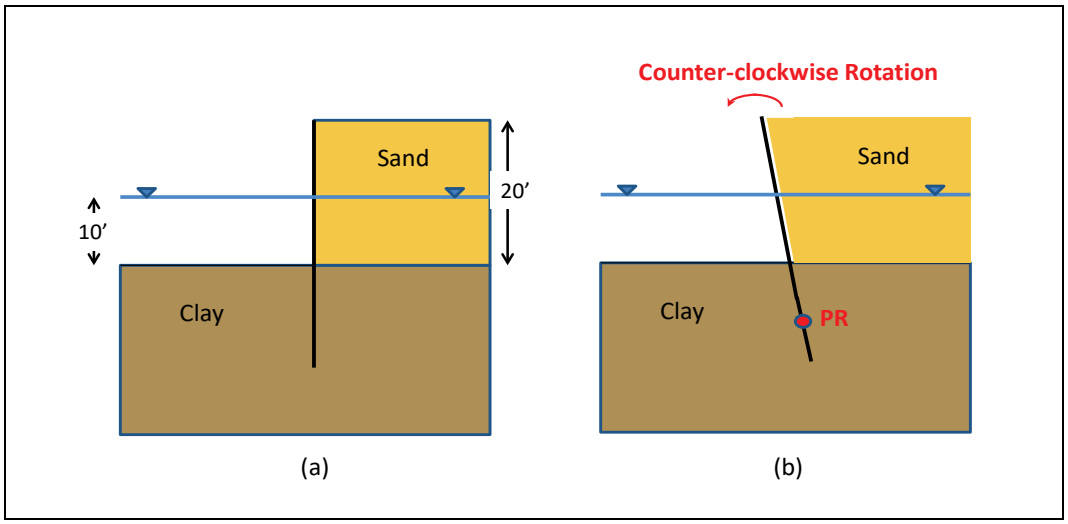
Wolff, T. H. 1985. Analysis and design of embankment dam slopes: A probabilistic approach. Ph.D. diss., Purdue University, Lafayette, Ind.

Yucemen, M. S., W. H. Tang, and A. H. S. Ang. 1973. *A probabilistic study of safety and design of earth slopes*. Civil Engineering Studies, Structural Research Series 402, University of Illinois, Urbana.

Appendix A: Iterative Solution to Compute the Design Depth Using a Force and a Moment Imbalance Based Computational Procedure

The design of an I-Wall/sheet-pile wall to resist flood loading requires the determination of 1) its depth of embedment and 2) its point of rotation (PR). Appendix A highlights key aspects of the numerical procedure implemented in Corps_I-Wall by means of an application to the design shown in Figure A1.[1]

Figure A1. Cantilever retaining wall. (a) Two layered soil site. (b) Counterclockwise rotation of the cantilever sheet-pile wall about its PR.



This design problem was first presented in Bowles (1968) and referred to as Example 8-2b. A closed-form solution was used by Bowles (1968) to determine its depth of embedment and PR. A comparison will be made between Corps_I-Wall numerical procedure results using the Coefficient Method of analysis and those from the Bowles (1968) solution.

The Figure A1 design problem consists of a cantilever sheet-pile wall retaining sand that overlays a clay layer. The clay possesses undrained shear strength, S_u, equal to 1,200 psf. The cantilever wall retains a 20 ft high sand layer with an effective angle of internal friction, φ', equal to 30 degrees, and an effective interface friction, δ', between the sheet-pile wall and the

[1] The design mode method of analysis is specified in this Corps_I-Wall analysis.

retained sand equal to zero degrees. A pool of water exists on the LHS of the cantilever wall to a height of 10 ft above the top of the clay layer. A hydrostatic water table exists mid-height within the retained sand layer. Moist and saturated unit weights assigned in this problem are 110 pcf and 122.4 pcf, respectively. The unit weight of water is 62.4 pcf. User-specified values of Factors of Safety are applied to the soil shear strengths when calculating both the active and passive earth pressures acting on the portion of the I-Wall/sheet-pile wall embedded within the soil foundation. Table A1 lists the Factors of Safety assigned to the layers of sand and clay.

Table A1. Factors of Safety assigned to the sand and clay layers.

Soil Material	FS_{active}	$FS_{passive}$
Sand	1.0	1.5
Clay	1.5[1]	1.5

[1] This user assigned FS_{active} value of 1.5 in the clay is not consistent with Corps' design criteria. This value is required so that the Corps_I-Wall results match the problem analyzed by Bowles (1968).

Two equations are required to solve for the two unknowns (i.e., depth of embedment and PR). At the precise value for depth of embedment, and for the precise PR elevation, the summation of horizontal forces and summation of moments acting on vertical I-Wall/sheet-pile wall are in static equilibrium

$$\sum F_h = 0 \tag{A1}$$

$$\sum M = 0 \tag{A2}$$

When imprecise values for depth of embedment and PR are assumed, the summation of horizontal forces and/or moments is nonzero.

A region-based (soil layer) geometry definition is implemented within Corps_I-Wall. This feature easily accommodates a multilayereded soil site. However, an iterative solution scheme is now required to perform these two sets of calculations (i.e., summation of externally applied forces and moments of Equations A1 and A2).

Points along the center line of the vertical I-Wall/sheet-pile wall are discretized at approximately every foot[1] into nodal points and then connected sequentially by a series of vertical I-Wall/sheet-pile wall line elements when using the Coefficient Method of Analysis. The following are each converted into equivalent nodal point forces using the one-third/one-sixth relationship discussed in Chapter 2: 1) net water pressures, 2) net soil pressure distributions acting normal to the vertical I-Wall/sheet-pile wall line model, 3) the net external horizontal forces (or pressures), and 4) horizontal forces due to external overburden pressures acting on an elevation behind the sheet-pile wall. These computations are performed for each trial depth of embedment and for each trial PR value.

The iterative solution developed for Corps_I-Wall is a numerical method for determining the 1) depth of embedment, and 2) PR values corresponding to static equilibrium (i.e., satisfying Equations A1 and A2). The solution procedure starts with the assignment of a shallow trial depth of embedment and a shallow trial PR value. For this first trial depth of embedment and first shallow trial PR, the summations of horizontal forces and the summation of moments are computed along the sheet-pile wall. A large force and moment imbalance are usually achieved. For the second computation, the (first) trial depth of embedment is maintained while the trial PR point is moved down a foot, the net forces are reformulated (because the PR value has changed), and the summation of horizontal forces and the summation of moments are computed along the sheet-pile wall. The PR point is then moved down another foot if there is a force and moment imbalance. The process is repeated until the trial PR is lowered and there is a change in sign for the force and moment imbalance. When the trial PR has moved 1 ft above the tip of the sheet pile and there is still no change in sign, then the trial depth of embedment is increased by 1 ft and the entire computational process is repeated, starting over with a shallow trial PR value.

The trial PR value and trial depth of embedment are considered to be converged in the calculations when both Equations A1 and A2 are satisfied or have small, non-zero values.

The following subsections further discuss details regarding the numerical procedures being used when applied to the Figure A1 cantilever wall

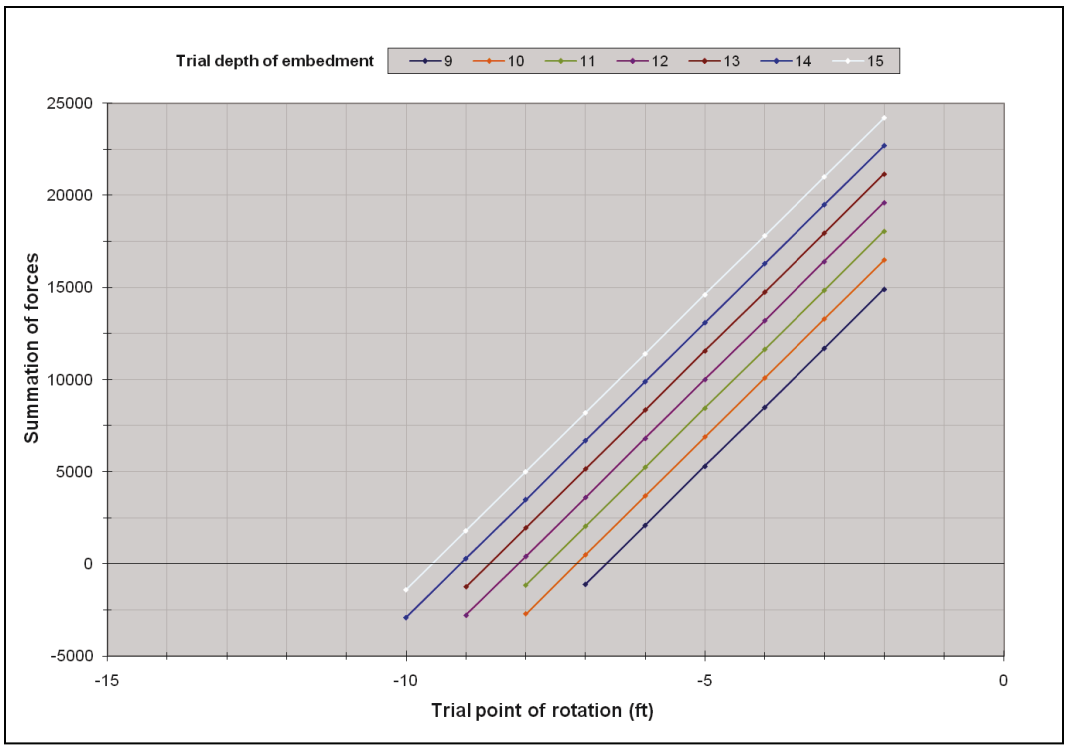
[1] The nodal point discretization is more sparse when the Wedge Solution Method of analysis is used.

problem. Although the summation of forces and summation of moment computations are done concurrently within Corps_I-Wall, the results from the summation of horizontal force calculations are discussed first. This is followed by a discussion of moment imbalance for these same pair of variables. Further details on arriving at the resulting design depth of embedment are discussed last.

A.1 Summation of horizontal forces

A trial depth of embedment is first established as 9 ft. Next the elevation for the first, shallow, trial value for PR is assigned as -2 ft. The total horizontal force at each nodal point elevation (at approximately 1 ft increments), acting normal to the sheet-pile wall, is accumulated down to the trial depth of embedment of 9 ft. This results in an imbalance of nearly 15,000 lb per foot run of wall. The trial value for PR is next lowered by 1 ft to -3 ft. The imbalance in horizontal forces reduces to approximately 12,000 lb per foot run of wall. This resultant summation of horizontal forces is now compared to the value of the previous resultant summation of horizontal forces for the previous trial depth of embedment. If there is a sign change, this means that the summation of horizontal forces has reached a value that is close to zero and this iteration has converged. The dark blue line of data in Figure A2 shows that there was no sign change (in force imbalance) until the trial PR value was lowered to -7 ft (2 ft above the trial sheet-pile tip depth). When this change in sign is achieved, the incremental increase in trial PR values is terminated for the trial depth of embedment (that has been held constant).

Figure A2. Schematic of summation of horizontal forces versus trial points of rotation.



This process of varying trial PR values is repeated for the next trial depth of embedment, 10 ft. The results are added to Figure A2 (orange line of data).

Trial depths of embedment equal to 11, 12, 13, 14, and 15 ft are also examined with these results added to Figure A2. A total of seven trial depths of embedment were investigated. Table A2 lists the elevations that straddle the zero summation of horizontal force crossings for the trial PR values for each trial depth of embedment. Each label in this table signifies the trial depth of embedment (in feet).

Table A2. PR elevations bounding the zero crossings for summation of forces.

Label	Current Elevation (ft)	Previous Elevation (ft)
9	-7	-6
10	-8	-7
11	-8	-7
12	-9	-8
13	-9	-8
14	-10	-9
15	-10	-9

A.2 Summation of moments

For the trial depth of embedment and the trial PR value, the summation of moment computation is made immediately following the summation of forces computation discussed in the previous A.1 section. The summation of moments is calculated as the product of the total horizontal force at each nodal point elevation (at approximately 1 ft increments) on the sheet-pile wall and the lever arm, about the trial PR, and accumulated down to the trial depth elevation. During this stage of analyses, after the moment imbalance has been made for two consecutive trial PR values, the resultant summation of moments is compared to the value of the previous PR's resultant summation of moments. If there is a sign change, this signifies that the summation of moments has reached a value that is close to zero and that this iteration has converged. Figure A3 shows the results of the same seven iterations of Figure A2 for trial depths of 9–15 ft at 1 ft increments. Each trial PR curve in Figure A3 starts at elevation -2 ft and proceeds down to 1 ft above its trial depth of embedment. This figure shows that all of the seven curves have crossed the summation of moments (imbalance) line. These PR values that bound the crossover PR value for each of the seven trial depths of embedment (from 9–15 ft) have been tabulated and are listed in Table A3. Each label in this table signifies the trial depth of embedment (in feet).

Figure A3. Schematic of summation of moments versus trial points of rotation.

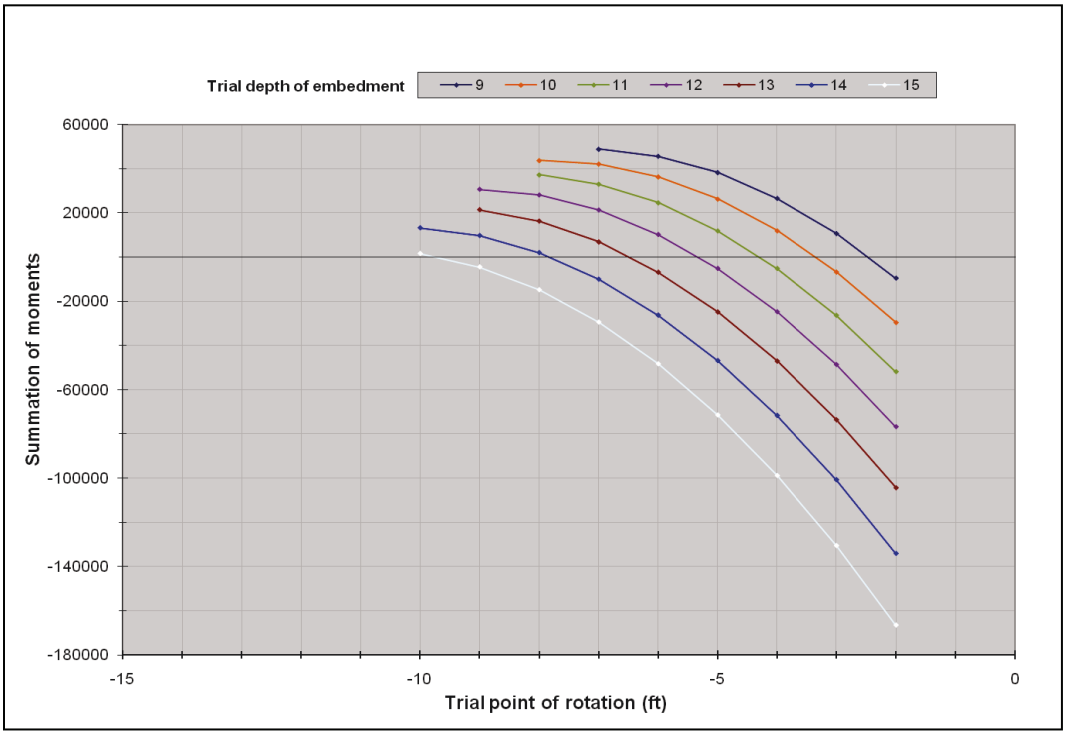


Table A3. PR elevations bounding the zero crossings for summation of moments.

Label	Current Elevation	Previous Elevation
9	-3	-2
10	-4	-3
11	-5	-4
12	-6	-5
13	-7	-6
14	-8	-7
15	-10	-9

A.3 Resulting design depth of embedment

The resulting design depth of embedment is arrived at when 1) the summation of forces converge at a trial PR value, and 2) the summation of moments also converge at the same trial PR value for the same iteration. Corps_I-Wall achieves this in the following two stages: 1) an approximation is made for the trial depth of embedment and for a pair of trial PR values in the first stage of analysis, and 2) the next stage of analysis uses the Stage 1 data as initial conditions to a Newton-Raphson procedure that performs a refined search within close proximity of this resulting Stage 1 set of data.

A Stage 1 evaluation consists of the following: For force equilibrium, as shown in Table A2, for a trial depth of embedment equal to 15 ft (i.e., label 15 in Table A2), or the light blue curve in Figure A2, the PR convergence occurs between els -9 ft (1805 lbf) and -10 ft (-13.95 lbf). For moment equilibrium, for a trial depth of embedment equal to 15 ft (i.e., label 15 in Table A3) or the light blue curve in Figure A3, the PR convergence occurs between els of -9 ft (-4543.89 ft-lb) and -10 ft (1527.78 ft-lb). This signifies that both Equations A1 and A2 have been satisfied for the design depth of approximately 15 ft and a PR between 9 ft and 10 ft.

Note: If the two conditions of Equations A1 and A2 are not met for the same trial depth of embedment, the iterative procedure will restart at the top of the sheet-pile wall and the initial node spacing of 1 ft increments used to determine elevations for computations on the sheet-pile wall will be changed by the node spacing increment factor or 0.01-ft increments. Therefore, the nodal point spacing will decrease from 1.0 to 0.99 and static equilibrium will be tested from Stage 1 evaluations. This process continues

until static equilibrium is satisfied or the minimum node spacing of 0.7 is reached.

A Stage 2 evaluation consists of the following: Once the resulting Stage 1 set of data is defined (coming close to satisfying static equilibrium), the trial depth of embedment and trial PR are presented as initial values to a Newton-Raphson procedure (contained within Corps_I-Wall), this will then numerically approximate the resultant depth of embedment and PR values by iteratively solving the expressions of Equations A1 and A2. The computed PR is equal to -9.5391 ft and the computed elevation at tip of pile is equal to -14.9472 ft.

Bowles (1968) solved a closed-form equation for the depth of embedment and obtained a value of 15.1 ft. The Corps_I-Wall numerical solution agrees with Bowles.

Appendix B: Gap Initiation and Propagation Criteria and Formulation

When the user selects (Figure 3.31) the (earth pressure) Coefficient Method of analysis, hydraulic fracturing criteria is applied to determine if a gap develops and if it propagates down the soil-to-sheet-pile/I-Wall interface.[1] In this procedure of analysis, the horizontal earth pressure[2] (i.e., a value of total horizontal stress) at the ground surface soil-to-sheet-pile/I-Wall interface on the flood side of the wall, is compared to the hydrostatic water pressure developing at the top of the ground surface due to the presence of the (specified) flood pool elevation. If the hydrostatic water pressure of the flood pool (i.e., the demand) exceeds the total horizontal stress (i.e., the capacity) at the ground surface, a gap will initiate at the ground surface along the soil-to-sheet-pile/I-Wall interface.[3] After hydraulic fracturing commences (at the ground surface), the next or lower element of soil interface at the soil-to-sheet-pile/I-Wall interface[4] is then checked for hydraulic fracturing. Its total horizontal stress is compared to a hydrostatic water pressure for the same flood pool elevation that initiated/propagated a gap above the top of this current soil interface element in question. If the hydrostatic water pressure of the flood pool exceeds the total horizontal stress at this soil interface element, a gap will propagate through this element and down to the next soil interface element along the soil-to-sheet-pile/I-Wall interface. This check for gap propagation proceeds until a depth is reached for which the total horizontal stress at the soil-to-sheet-pile/I-Wall interface (i.e., capacity) exceeds the hydrostatic water pressure

[1] This hydraulic fracturing type of analysis was first adapted to I-Wall finite element modeling in 2005 by Dr. Ebeling when analyzing gap initiation/propagation responses of New Orleans I-Walls during hurricane Katrina (Volume V of IPET 2007), from the procedure used to estimate the potential for "crack" formation in earthen dams (e.g., Nobari et al. 1973; Widjaja et al. 1984; Sherard 1973, 1986; and the Independent Panel to Review Cause of Teton Dam Failure 1976) and in particular, in a clay core.

[2] In many instances the total horizontal earth pressure is based on the horizontal component of the "mobilized active" earth pressure at the ground surface. However, under circumstances involving a shallow PR for the sheet-pile/I-Wall, the horizontal component of the "mobilized passive" earth pressure (refer to passive Zone IV in Figure 1.1) to the ground surface may be used. The required relationships are given later in Appendix B.

[3] Zero tensile strength capability is assumed along this soil-to-sheet-pile/I-Wall interface.

[4] For the Coefficient Method of analysis, Corps_I-Wall checks for gap propagation using trial gap depths progressing in 1 ft increments along the soil-to-sheet-pile/I-Wall interface. Should convergence not be achieved, the gap prorogation process starts over using a 0.01 ft increment. It is anticipated that this numerical procedure and size of the soil interface elements will be refined in subsequent versions.

of the flood pool (i.e., demand) at this same elevation, and thus, the gap is arrested by the horizontal total stresses contained within that soil element.

When the user selects (Figure 3.31) the Wedge Solution Method as the procedure to be used to compute the earth forces and corresponding earth pressures acting on the vertical faces of the sheet-pile wall, the depth of gapping is approximated by means of a single calculation. This simplified method of analysis is less rigorous than the hydraulic fracturing criteria used by the Coefficient Method of analysis. However, studies using the example problems discussed in this report demonstrate this simplified depth of gapping analysis is slightly conservative when compared to the results from the Coefficient Method of analysis.

The formulation used in Corps_I-Wall assumes the sheet-pile/I-Wall rotates as a rigid body about some point along the embedded portion of the I-Wall. This point falls somewhere between the ground surface and the tip of the sheet-pile and is designated as the PR. The value for PR is an unknown variable for both the *Design* mode as well as for the *Analysis* mode in Corps_I-Wall.

The first two sections, B.1 and B.2, describe the gap formulation and propagation criteria used by the Coefficient Method of analysis when the PR is below the trial soil-to-sheet-pile/I-Wall soil interface element. Sections B.3 and B.4 describe the formulation used by the Coefficient Method of analysis when the PR is at or above the trial soil-to-sheet-pile/I-Wall interface gap depth. Sections B.5 and B.6 describe the simplified procedure used to calculate the depth of gapping when using the Wedge Solution Method of analysis in a saturated or a moist soil, respectively. Section B.7 discusses the procedure used to determine gap depth propagation in layered soils, where gap depths may exceed the bottom depth of the layer, when using the Wedge Solution Method of analysis.

For the Coefficient Method of analysis, a gap is developed and/or determined to propagate by a total stress gap criteria, such that

$$\text{Gap Propagation Criteria:} \quad \text{Demand} > \text{Capacity} \tag{B1}$$

$$\text{Demand:} \quad \gamma_w * Depth_w \tag{B2}$$

$$\text{Capacity:} \quad \sigma_h \tag{B3}$$

where

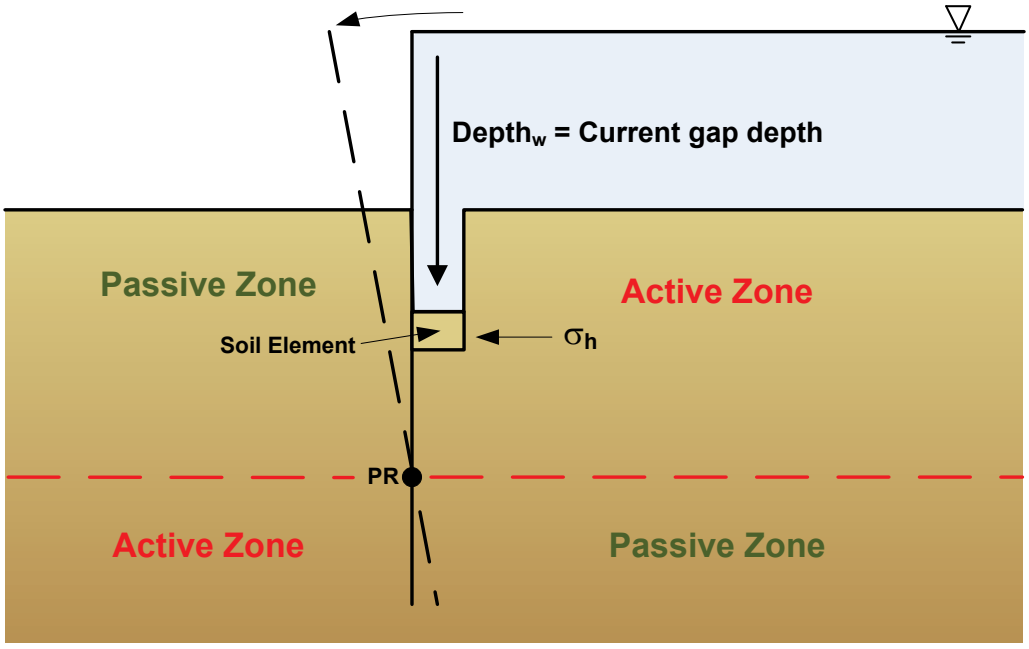
γ_w = unit weight of water
$Depth_w$ = depth of water to the center of the trial soil-to-sheet-pile/I-Wall soil interface element
σ_h = mobilized total stress for defining the horizontal earth pressure at the center of the trial soil-to-sheet-pile/I-Wall soil interface element gap depth

Note: Mobilized parameters are stated throughout this appendix and are assigned (via soil material properties) to each soil layer on either side of the I-Wall. The user-defined values for the active Factor of Safety and for the passive Factor of Safety define the level of mobilization, as discussed in Chapter 2.

B.1 Total stress gap criteria – Coefficient Method of analysis

Total stress gap criteria are based on the assumptions that 1) the wall rotates (away) from the flood side and, 2) the PR is below the current gap depth. Figure B1 provides the schematic for the total stress gap criteria for this counterclockwise I-Wall rotation situation.

Figure B1. Schematic of gap propagation for a soil element above the PR with a mobilized total horizontal earth pressure definition.



In soils, the analytical solution for the active earth pressure equation is given as

$$\sigma_a = \sigma_v K_a - 2c_a\sqrt{K_a} \tag{B4}$$

where σ_a, is the mobilized active earth pressure, σ_v, is the overburden pressure, c_a, the mobilized active cohesion(total stress), and K_a, the mobilized active earth pressure coefficient, this can be calculated using one of the earth pressure relationships given in Chapter 2. The mobilized horizontal active stress or horizontal component of the mobilized active earth pressure is expressed as

$$\sigma_h = \sigma_a \cos(\delta_a) \tag{B5}$$

with δ_a defined as the mobilized active wall friction angle (total stress). From the two assumptions and Equations B1 through B3, the gap initiation and propagation criteria are

$$\gamma_w * Depth_w > \sigma_h \tag{B6}$$

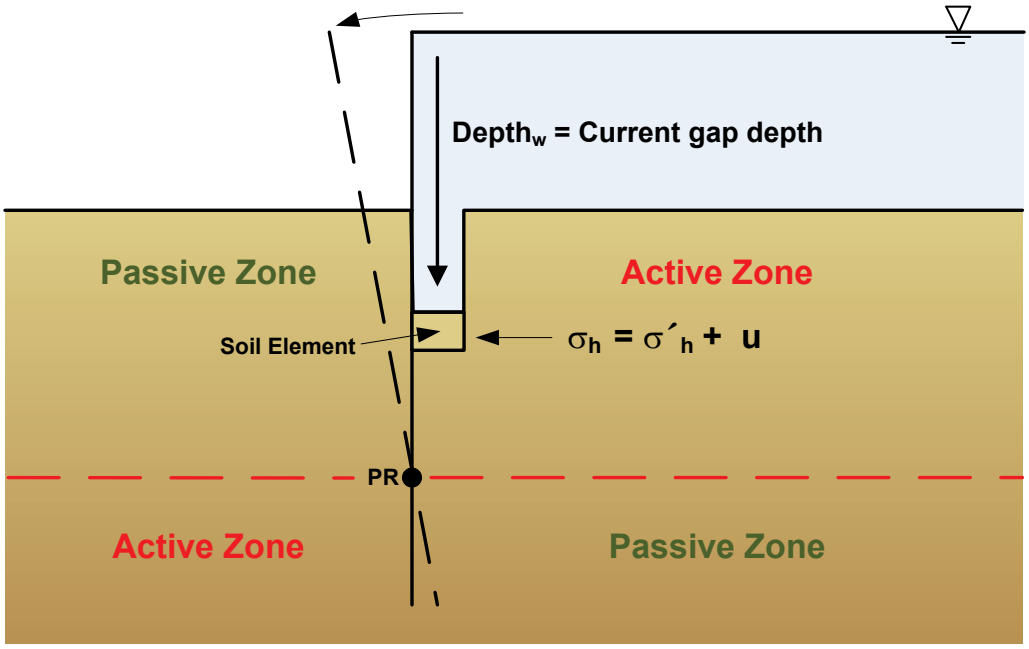
This can be expanded using Equations B4 and B5 to obtain the total stress gap initiation and propagation criteria of

$$\gamma_w * Depth_w > \left[\sigma_v K_a - 2c_a\sqrt{K_a}\right]\cos(\delta_a) \tag{B7}$$

B.2 Total stress gap criteria but using effective stress and pore water pressure to define total stress – Coefficient Method method of analysis

Total stress gap criteria is based on the assumptions that 1) the wall rotates (away) from the flood side and, 2) the PR is below the current gap depth. Figure B2 provides the schematic for the total stress gap criteria but using effective stress and pore water pressure to define total stress for this counterclockwise I-Wall rotation situation.

Figure B2. Schematic of gap propagation for a soil element above the PR with a mobilized effective horizontal earth pressure definition.



In soils, the analytical solution for gap propagation criteria is based on total stress, given previously as

$$\gamma_w * Depth_w > \sigma_h \quad \text{(bis B6)}$$

The mobilized total stress, σ_h, and the overburden pressure, σ_v, may both be rewritten for an effective stress analysis, respectively as

$$\sigma_h = \sigma'_h + u \quad \text{(B8)}$$

$$\sigma_v = \sigma'_v + u \quad \text{(B9)}$$

where σ'_h is the effective mobilized horizontal stress, and u, the pore water pressure in soil. The mobilized effective horizontal stress is given as

$$\sigma'_h = \sigma'_a \cos(\delta'_a) \quad \text{(B10)}$$

with σ'_a as the effective mobilized active earth pressure, δ'_a, the effective mobilized active wall friction angle. The effective mobilized active earth pressure equation can be defined as follows

$$\sigma'_a = \sigma'_v K_a - 2c'_a\sqrt{K_a} \quad \text{(B11)}$$

with c'_a defined as the effective mobilized active cohesion. Equations B10 and B11 can be substituted into Equations B6 and B8 to produce the following equation

$$\gamma_w * Depth_w > \sigma'_a \cos(\delta'_a) + u \quad \text{(B12)}$$

that can be further expanded with Equations B9 and B11 as

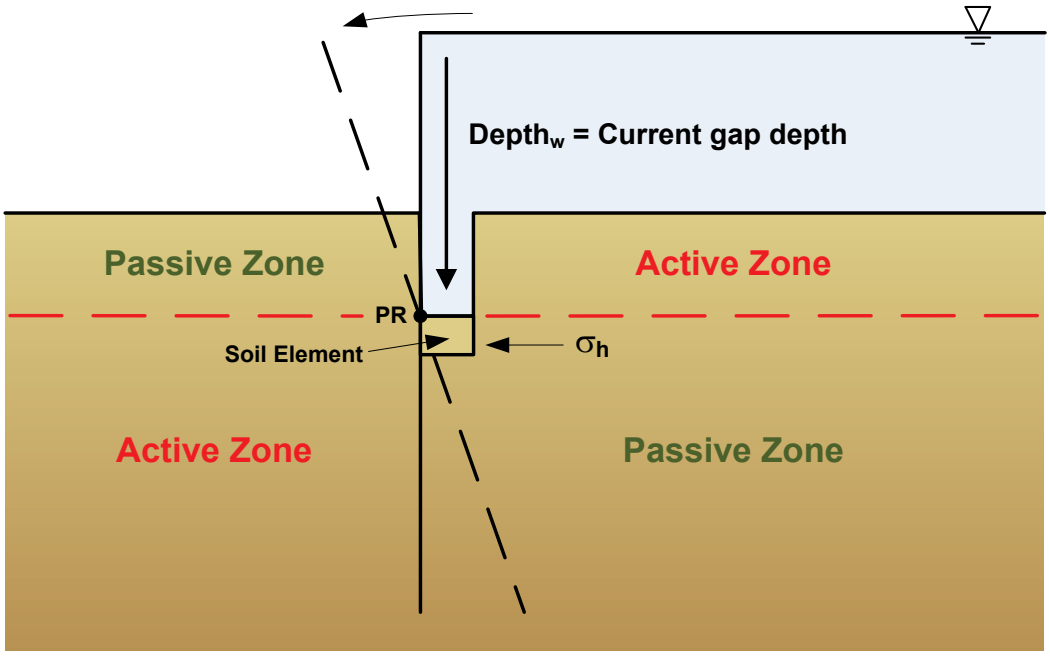
$$\gamma_w * Depth_w > \left[(\sigma_v - u)K_a - 2c'_a\sqrt{K_a}\right]\cos(\delta'_a) + u \quad \text{(B13)}$$

This equation expresses the total stress gap initiation and propagation criteria with a mobilized effective horizontal earth pressure definition.

B.3 Total stress gap criteria with shallow PR – Coefficient Method of analysis

The total stress gap criteria in this section is based on the assumptions that 1) the wall rotates (away) from the flood side, and 2) the PR is at (or above) the current gap depth. Figure B3 illustrates this condition for this counterclockwise I-Wall rotation situation.

Figure B3. Schematic of gap propagation for a soil element located at the PR with a mobilized total horizontal earth pressure definition.



For the soil element just below the PR and on the flood side of the wall, the horizontal stress, located in the passive zone of Figure B3, is expressed as the mobilized passive earth pressure equation and given as

$$\sigma_h = \sigma_p \cos(\delta_p) \tag{B14}$$

with σ_p, the mobilized passive earth pressure, and δ_p, the mobilized passive wall friction angle. The mobilized passive earth pressure can be expressed as

$$\sigma_p = \sigma_v K_p + 2c_p\sqrt{K_p} \tag{B15}$$

where c_p, the mobilized passive cohesion, and K_p, the mobilized lateral passive earth pressure, which can be calculated using the earth pressure relationships given in Chapter 2. From Equations B1 through B3, there is

$$\gamma_w * Depth_w > \sigma_h \tag{bis B6}$$

that can be further expanded using Equations B14 and B15 for the total stress gap criteria with a shallow PR

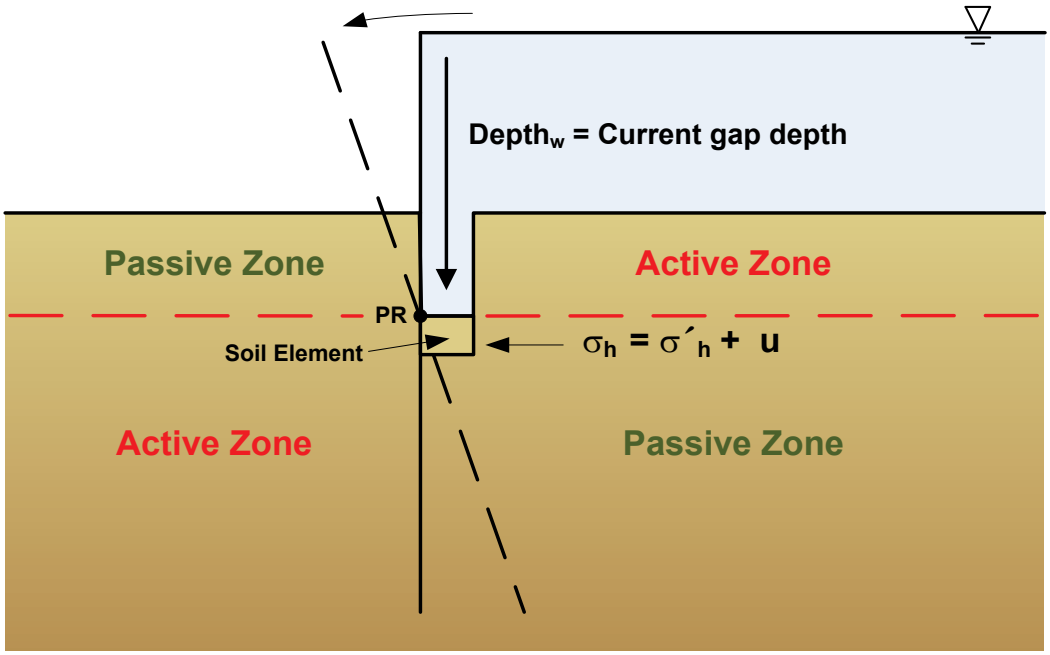
$$\gamma_w * Depth_w > \left[\sigma_v K_p + 2c_p\sqrt{K_p}\right]\cos(\delta_p) \tag{B16}$$

This equation expresses the total stress gap initiation and propagation criteria.

B.4 Total stress gap criteria but using effective stress and pore water pressure to define total stress and with shallow PR – Coefficient Method of analysys

The total stress gap criteria in this section is based on the assumptions that 1) the wall rotates (away) from the flood side, and 2) the PR is at (or above) the current gap depth. Figure B4 provides the schematic for the total stress gap criteria but using effective stress and pore water pressure to define total stress for this counterclockwise I-Wall rotation situation.

Figure B4. Schematic of gap propagation for a soil element located above the PR with a mobilized effective horizontal earth pressure definition.



For the soil element just below the PR and on the flood side of the wall, the horizontal stress, located in the passive zone of Figure B4, is expressed as the mobilized passive earth pressure equation and given as

$$\sigma'_h = \sigma'_p \cos(\cos \delta'_p) \tag{B17}$$

with σ'_p is the effective mobilized passive earth pressure, δ'_p, the effective mobilized passive wall friction angle. The effective mobilized passive earth pressure equation can be defined as follows

$$\sigma'_p = \sigma'_v K_p + 2c'_p\sqrt{K_p} \tag{B18}$$

with c'_p defined as the effective mobilized passive cohesion. Equations B17 and B18 can be substituted into Equations B1 and B8 to produce the following equation

$$\gamma_w * Depth_w > \sigma'_p \cos(\delta'_p) + u \tag{B19}$$

that can be further expanded with Equations B9 and B18 as

$$\gamma_w * Depth_w > \left[(\sigma_v - u)K_p + 2c'_p\sqrt{K_p}\right]\cos(\delta'_p) + u \tag{B20}$$

This equation expresses the total stress gap initiation and propagation criteria with a mobilized effective horizontal earth pressure definition.

B.5 Depth of gapping in saturated soil –Wedge Solution Method of analysis

B.5.1 Total stress soil layer

For a soil region that is saturated because it is below a piezometric surface or an associated water surface and specified with a total stress criteria, the depth of gapping, d_{GAP}, is approximated as

$$d_{GAP} = \frac{2*c_a*\sqrt{K_a}}{\gamma_{buy}*K_a} \tag{B21}$$

with the buoyant unit weight given by

$$\gamma_{buy} = \gamma_{sat} - \gamma_w \tag{B22}$$

Equation B21 is derived (not shown) from Equation B7.

B.5.2 Effective stress soil layer

For a soil region that is saturated because it is below a piezometric surface or an associated water surface and specified with an effective stress criteria, the depth of gapping is approximated as

$$d_{GAP} = \frac{2*c'_a*\sqrt{K_a}}{\gamma_{buy}*K_a} \tag{B23}$$

Equation B23 is derived (not shown) from Equation B13.

B.6 Depth of gapping in moist soil –Wedge Solution Method of analysis

B.6.1 Total stress soil layer

For a soil region that is moist because it does not have an associated piezometric surface or exists above its associated piezometric surface and is specified with a total stress criteria, the depth of gapping is approximated as

$$d_{GAP} = \frac{2*c_a*\sqrt{K_a}}{\gamma_{moist}*K_a} \quad \text{(B24)}$$

Equation B24 is derived (not shown) from Equation 2.5 with the mobilized active stress set equal to zero and the total vertical stress equal to $\gamma_{moist}*d_{GAP}$.

B.6.2 Effective stress soil layer

For a soil region that is moist because it does not have an associated piezometric surface, or exists above its associated piezometric surface and is specified with an effective stress criteria, the depth of gapping is approximated as

$$d_{GAP} = \frac{2*c'_a*\sqrt{K_a}}{\gamma_{moist}*K_a} \quad \text{(B25)}$$

Equation B25 is derived (not shown) from Equation 2.19 with the mobilized active stress set equal to zero and the effective vertical stress equal to $\gamma_{moist}*d_{GAP}$.

B.7 Gap propagation in layered soils – Wedge Solution Method of analysis

In Corps_I-Wall, gapping can occur and propagate when the upper layers of the soil are cohesive (i.e., c>0 or c'>0). It is assumed that gapping starts at the ground surface and proceeds downward into the soil.

The analysis of a layered soil regime starts with the calculation of d_{GAP} for the top-most soil region using the Equation B21, B23, B24 or B25 that is appropriate for this soil material (i.e., saturated or moist soil; total or effective stress). If the value for d_{GAP} is calculated to be less than the thickness of the soil region, then the gap is arrested within this top-most soil region at that depth. The gapping analysis stops because d_{GAP} does not extend down into the next soil region.

If d_{GAP} extends down into the second soil region and the second soil region is not cohesive, then the gap is arrested at the bottom of the top-most soil region. If the second soil region is cohesive, another d_{GAP} calculation is made using the appropriate Equation B21, B23, B24 or B25 for the second soil region, immediately below the top-most soil region. The assigned depth of gapping into this second soil region is equal to the calculated d_{GAP}

value minus the thickness of the top soil region. If the new region gap depth is less than the second region thickness, then the gap is arrested at that depth.

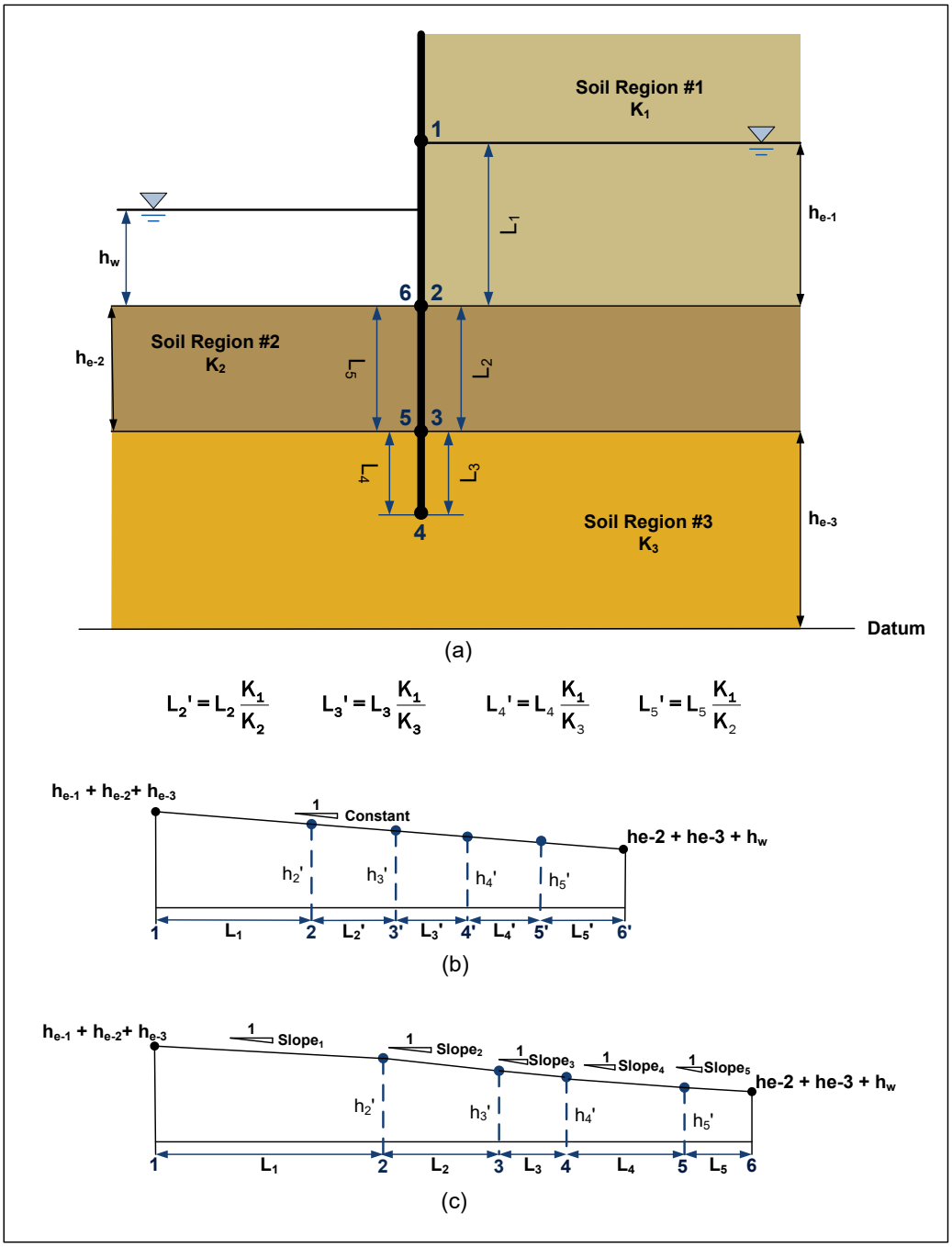
If d_{GAP} extends down into the next soil region and the next soil region is not cohesive, then the gap is arrested at the bottom of the previous soil region. If this is not the case, then the depth of gapping is computed in a manner similar to the previous paragraph. The depth of gap for this region is computed using the appropriate equation (i.e., Equation B21, B23, B24 or B25) and subtracting all of the thicknesses of the regions above. These calculations continue until the gap is arrested within a region or at a region boundary.

Appendix C: Line of Seepage Formulation

This appendix discusses the line of seepage (a.k.a. line of creep) associated with the one-dimensional (1-D) seepage analysis where the seepage gradient and length of seepage are to be determined first. This line of seepage analysis option is only solved when used with the Coefficient Method of analysis. The results from this simplified method of analysis are then used for determining water pressures acting within the soil adjacent to the vertical sheet-pile wall and acting normal to both flood side and landside embedded faces of this sheet-pile wall. Water will travel from high (total) head to low (total) head, dictating the direction of flow within the soil regions. Consequently, the side with the highest (total) head dictates that the direction of flow is downward along that side of the sheet-pile wall. A vertical streamline, or flow line, is assumed within the soil and adjacent to the sheet-pile wall. Water flows within the soil, downward and parallel to the face of the vertical sheet-pile wall, to the sheet-pile tip. At the sheet-pile tip, the vertical flow of water reverses direction (by 180 degrees) and travels up through the soil along the opposite face of the sheet-pile wall.

The transformation procedure for the line of seepage method is for 1-D flow along a singular path, consisting of 1-D flow paths connected in series from one soil region into the next soil region. These paths are aligned along the two faces of the vertical sheet-pile wall. These flow paths contained within the soil regions, may possess different values for the saturated hydraulic conductivity of the soil. For example, Figure C1 contains three unique soil regions. Each flow line contained within each soil region has a unique value for its saturated hydraulic conductivity, K. The hydraulic conductivity of soil Regions 2 and 3 (K_2 and K_3) are greater than the hydraulic conductivity of the soil contained within soil Region 1 (K_1). Consequently, a transformation is required in order to first construct a 1-D flow regime down one face of the sheet-pile wall, and up the opposite face of the sheet-pile wall, in order to represent a 1-D flow regime of constant hydraulic conductivity of value K_1.

Figure C1. I-Wall. (a) Potential slip plane within soil regions with different saturated hydraulic conductivities (K) (lengths not to scale). (b) Constant slope in total head with distance along the transformed length of line of seepage. (c) Variation of slope in total head with distance along the three soil regions of the line of seepage.



The transformed horizontal axis is first constructed (Figure C1b) using the four transformed lengths L_2', L_3', L_4', and L_5' by means of the equations given in Figure C1. Note that starting with the second 1-D flow path (of transformed length L_2'), there is a transformed position denoting the end of

the 1-D flow path 2, designated as point 3'. With K_2 being greater than K_1, the length of the transformed segment L_2' is less than the physical distance from points 2 to 3 (i.e., the height of soil Region 2), L_2. Similarly, for 1-D flow Path 3 of transformed length L_3', its starting and ending transformed points are 3' and 4', respectively. With K_3 being greater than K_1, the length of the transformed segment L_3' is less than the physical distance from points 3 to 4, L_3. Because the transformed 1-D line of flow model now possesses a constant hydraulic conductivity of value K_1, the variation in head along the transformed section is linear (see Figure 12-1 in Spangler and Handy [1973]). There exists a linear variation in total head from point 1 to point 6' as denoted in Figure C1b for this transformed 1-D line of flow. The gradient is defined as equal to the change in total head (from point 1 to point 6'), divided by the total length of the transformed 1-D line of flow (= $L_1 + L_2' + L_3' + L_4' + L_5'$). Also at points 2 and 3' of Figure C1b, the value for total head is obtained and is designated as h_2' and h_3', respectively, computed by taking advantage of the key feature of the Figure C1b, this shows that the hydraulic gradient is a known constant. The total head values h_2' and h_3' are easily obtained from a linear relationship in total head with distance between Figure C1b points 1 and 6'.

Figure C1c shows the original axis for the problem using the actual dimensions (labeled L_1, L_2, L_3, L_4, and L_5) for the entire length of the 1-D streamline contained within the three soil regions and along the front and back vertical faces of the embedded sheet-pile wall. The values for total head are mapped from points 1, 2, 3', 4', 5' and 6' from Figure C1b, to points 1, 2, 3, 4, 5 and 6 in Figure C1c. Observe that the transformed Figure C1b is required to compute the head values h_2', h_3', h_4', and h_5' at the transformed position points of 2, 3', 4', 5' respectively. Figure C1c shows these computed heads of h_2', h_3', h_4', h_5' are mapped back to their actual position points 2, 3, 4, and 5, respectively.

Further observe in Figure C1c that the slope of total head with distance along each of the five 1-D flow line segments is no longer a single constant, as is the case for the transformed horizontal axis plot of the Figure C1b streamline segments. Here, the hydraulic gradient is constant along the segment of the 1-D flow line contained within each of the five Figure C1b soil regions. Recall that each 1-D flow line possesses a different value for saturated hydraulic conductivity, resulting in a different hydraulic gradient for each of the five Figure C1c streamline segments.

Values of water pressures at points 1, 2, 3, 4, 5, and 6 of Figure C1c are calculated using Bernoulli's equation by determining the total head at each point. For point 1, the total head value is established by the boundary condition stipulated at point 1 in Figure C1, with a value of $h_{e\text{-}1}+h_{e\text{-}2}+h_{e\text{-}3}$.[1]. Additionally, according to Bernoulli's equation the total head (h_1) at this point can be expressed as

$$h_1 = hp_1 + hv_1 + he_1 \tag{C1}$$

where hp_1 is the pressure head, hv_1 is the velocity head, and he_1 is the elevation head at point 1. Because groundwater seeps and flows slowly for finer materials than open-pored, coarse gravels, the velocity head is considered negligible. Total head is frequently calculated as the sum of the pressure head and elevation head, and the pressure head is the difference between the total head and the elevation head.

$$hp_1 = h_1 - he_1 \tag{C2}$$

Once the pressure head at point 1 is determined, it can be multiplied by the unit weight of water to determine the pore water pressure (u_1)

$$u_1 = hp_1 * \gamma_w \tag{C3}$$

Equations C2 and C3 are used to compute the pressure head for points along the line of seepage and the pore water pressure at that point based on the pressure head. Figure C1c provides the total head value for all points along the line of seepage.

[1] A similar boundary condition exists at point 6 as stipulated in Figure C1; the total head h_6 is equal to $h_w+h_{e\text{-}2}+h_{e\text{-}3}$.

Appendix D: Description of Corps_I-Wall Information Interchange (ASCII) Input Data File (*project*.in)

The prefix of the input filename, *project,* is a user-defined base filename that may include a drive letter, a path and name of a project.

The exclamation mark '!' at the first column signifies the start of a comment (maximum number of characters is 256 per comment line).

A blank line is acceptable.

Descriptive code words are in bold and are three characters in length. They are followed by their relevant parameters. All are separated by spaces.

Some of these codes are optional and do not need to be specified. The mandatory codes for an analysis are **nnd, nrg, mod, mth, wal, gmw, mat, nod, wat, reg, ndr, inc, tol.** Codes **nnd**, **nrg** should be placed at the beginning of the file. Code words preceded by "*"denote multiple entries possible for the same code word.

nrg	*lrg, rrg*	Number of regions at each side of wall
	lrg	Number of regions at the left side of wall
	rrg	Number of regions at the right side of wall
nnd	*nnodes*	Number of nodes
***nod**	*node_id,*	X-, Y-coordinates of nodes defining regions *X, Y*
	node_id	id of node
	X	X-coordinate of node
	Y	Y-coordinate of node

mod	*mode, unit*	Modes of operation and unit system
	mode	=1, *Design* mode =2,*Analysis* mode
	unit	=1, English unit =2,metric
mth	*method, method_type*	Method for the determination of earth pressure distributions
	method	=1, coefficient method =2,wedge solution

	method_type	if (method=1)
		Coefficient methods for determining earth pressures
		=1, Rankine
		=2,Coulomb
		=3,logarithmic spiral – passive
		
		if (method=2)
		Wedge solution for determining earth pressures
		=1, Sweep search method
		=2,Fixed search method

wal	*x-pos, wall_top*	Position at top of I-Wall
	x-pos	X-coordinate of I-Wall. (=0 at center)
	wall_top	Elevation at the top of the I-Wall

wlt	*wall_tip,* tol_d,	Wall tip elevation, tolerance, and maximum number of iterations for an analysis (mode = 2)
	wall_tip	Elevation at the base of the I-Wall for an analysis
	tol_d	tolerance for estimating the passive factor of safety. decimal fraction of the depth of embedment (default = 0.05)
***wls**	*wall_id,* *wall_ele,* *modulus_elasticity,* *moment_inertia*	Number of sections delineating the I-Wall. The first value given for "wall_ele" is the elevation at the top of the Wall
	wall_id	Section of I-Wall
	wall_ele	Elevation at the top of the I-Wall section
	modulus_elasticity	Modulus of elasticity (psi -- kPascals) of the I-Wall section
	moment_inertia	Moment of inertia (in.^{4} – cm^4) of the I-Wall section
gmw	*gamma_w*	Unit weight of water
dbg		Debug output file
sim	*num_sims,* *num_bins*, *num_pools*	Simulation variables for a probabilistic analysis.

num_sims Number of simulations (> 3000)

num_bins Number of bins for a histogram (> 3)

num_pools Number of pools in order to establish a
SRC with passive factors of safety <= 1.0
(*Analysis* mode only)

***fld** *swl, swr* Surface water elevations and sometimes used for piezometric elevations. The number of "fld" entries should match the num_pools (see sim section for probabilistic analysis). For a deterministic analysis, there will only be one entry.

swl surface water elevation on the left side of wall

swr surface water elevation on the right side of wall

***pmv** *sim_vars* Probabilistic material variables

sim_vars The four variables evaluated are C, φ, δ, Ca, respectively are provided for each material. Please see Appendix C for detailed description. Each of the four variables will have a value of 0 or 1. (ex. 1 1 0 0)
= 1, probabilistic
= 0, deterministic

***mat** *material_id, gamma_moist, gamma_saturated, FS_active, FS_passive, C,* φ, δ, β, C_a*, K, stress* Material properties

	material_id	Material number
	gamma_moist	Moist unit weight of soil
	gamma_saturated	Saturated unit weight of soil
	FS_active	Active Factor of Safety associated with this material
	FS_passive	Passive Factor of Safety associated with this material
	C	cohesion
	φ	internal friction angle (deg)
	δ	wall friction angle (deg)
	β	surface angle to the horizontal (deg)
	C_a	wall/soil adhesion
	K	Saturated hydraulic conductivity (ft/sec in English units or m/sec in metric units)
	stress	Method to define strength parameters =1 Q-Case (total stress) =2 S-Case (effective stress)
***wat**	*water_id,* *w_nodes,* *w_id(1:n_nodes)*	piezometric surface or surface water
	water_id	water ID
	w_nodes	the number of nodes identifying the water surface for this region

	w_id*(1:n_nodes)*	all the nodes associated with this piezometric surface or water surface These nodes are listed from the X-coordinate nearest the I-Wall to the X-coordinate farthest away from the I-Wall (1 to w_nodes). The coordinates for the w_id's can be found in the "**nod**" section.
***reg**	*region_id, side, water_type, water_id, material_id*	Region located on either side of wall
	region_id	global region number
	side	=1 left side of wall =2 right side of wall
	water_type	Piezometric water surface associated with this region (for pore water pressure calculations only[1]) =0, No water[2] =1, Surface water[3] =2, Piezometric surface[4]

[1] For each nodal elevation the pore water pressure, *u*, acting at that node is computed as $u = \gamma_w$*(piezometric elevation – nodal elevation).

[2] For water_type=0, the pore water pressure $u = 0.0$.

[3] The piezometric elevation for water_type = 1 is obtained from the ***fld*** data line. In a probabilistic analysis this piezometric elevation may be made to vary over a series of elevation values by specifying multiple fld data lines.

[4] The piezometric elevation for water_type = 2 is obtained from the ***wat*** data lines for elevation of the node corresponding to the water_id index designated for the region in question. In a probabilistic analysis this piezometric elevation does not vary.

	water_id	Water ID associated with this region =0, No water source >0, Water surface or piezometric surface
	material_id	Material number associated with this region
***rgn**	*region_id,* *n_nodes,* *n_id(1:n_nodes)*	nodes defining the region
	region_id	global region number
	n_nodes	the number of nodes defining this region
	n_id*(1:n_nodes)*	all nodes defining this region. The coordinates for the node_id's can be found in the "**nod**" section. These nodes are listed in the counter-clockwise direction (1 to n_nodes) from the X-coordinate nearest to the I-Wall.
gap	*gap_type*	Gap initiation and propagion
	gap_type	=1 Hydraulic fracture
spg	*spg_type,*	Seepage effects. Current version allows only one water source on each side of wall
	spg_type	=3, line of seepage (Homogeneous or heterogeneous soils)[1]

[1] Pore water pressures are computed within the soil regime using the line of seepage method (Appendix C) to first compute total heads at each node along the I-Wall/sheet-pile wall, combined with the application of Bernoulli's equation to compute the pressure head h_p. Bernoulli's equation states that the total head H is equal to the elevation head, h_e, plus the pressure head, h_p, i.e., $H = h_e + h_p$. The nodal elevation provides for the value for h_e. Using the computed value for h_p, the pore water pressure u is equal to $\gamma_w * h_p$.

***hll**	*horz_line_load_el, horz_line_load*	Horizontal line load. Positive load acts to the left of the wall
	horz_line_load_el	elevation of the i^{th} horz_line_load
	horz_line_load	horizontal load of the i^{th} line load normal to the wall (plf)
***hdl**	*horz_dist_nodes, horz_dist_load_el, horz_dist_load*	Horizontal distributed load. Positive load acts to the left of the wall
	horz_dist_nodes	number of nodes comprising the i^{th} horizontal
	horz_dist_load_el	distribution elevation of the j^{th} node of the i^{th} horizontal distribution
	horz_dist_load	the magnitude of the j^{th} node of the i^{th} horizontal distribution (psf)
***vll**	*vert_line_load_side, vert_line_load_x, vert_line_load_mag*	Surface surcharge vertical line loads applied to the ground surface. Positive loads act vertically downward
	vert_line_load_side	location of the i^{th} vertical line load = 1, Left side of wall = 2, Right side of wall
	vert_line_load_x	x-position of the i^{th} vertical line load
	vert_line_load_mag	positive magnitude of the i^{th} vertical line load (plf)

***vul**	*vert_uniform_load_side,* *vert_ uniform_load_mag*	Vertical distributed uniform load. Only one or none on each side of wall.
	vert_uniform_load_side	location of the vertical uniform load = 1, Left side of wall = 2, Right side of wall
	vert_uniform_load_mag	positive magnitude of the uniform load (psf)
***vsl**	*vert_strip_side,* *vert_strip_x1,* *vert_strip_x2,* *vert_strip_mag*	Surface surcharge vertical distributed strip loads applied to the ground surface. Positive loads act vertically downward.
	vert_strip_side	location of the i^{th} vertical strip load = 1, Left side of wall = 2, Right side of wall
	vert_strip_x1	x-position ar the start of the i^{th} strip load
	vert_strip_x2	x-position at the end of the i^{th} vertical strip load
	vert_strip_mag	magnitude of the i^{th} uniform strip load. (psf)
***vrl**	*vert_ramp_side,* *vert_ramp_x1,* *vert_ramp_x2,* *vert_ramp_mag*	vertical distributed ramp loads. Only one or none on each side of wall.

	vert_ramp_side	location of the vertical ramp load = 1, Left side of wall = 2, Right side of wall
	vert_ramp_x1	x-position at the start of the ramp
	vert_ramp_x2	x-position at the end of the ramp. (this point is the start of uniform loading).
	vert_ramp_mag	positive magnitude at uniform loading. (psf)
***vtl**	*vert_tri_side,* *vert_tri_x1,* *vert_tri_x2,* *vert_tri_x3,* *vert_tri_mag*	vertical distributed triangular loads. Positive loads act vertically downward.
	vert_tri_side	location of the i^{th} vertical triangular load = 1, Left side of wall = 2, Right side of wall
	vert_tri_x1	x-position at the start of the i^{th} triangular load.
	vert_tri_x2	x-position at the peak of the i^{th} triangular load.
	vert_tri_x3	x-position at the end of the i^{th} vertical triangular load.
	vert_tri_mag	magnitude of the i^{th} vertical triangular load. (psf)
***vdl**	*vert_trap_side,* *vert_trap_x1,* *vert_trap_mag1,* *vert_trap_x2,* *vert_trap_mag2*	vertical trapezoidal loads

	vert_trap_side	location of the ith vertical trapezoidal load = 1, Left side of wall = 2, Right side of wall
	vert_trap_x1	x-position at the start of the ith trapezoid
	vert_trap_mag1	magnitude at the start of the ith trapezoidal distribution (psf)
	vert_trap_x2	x-position at the end of the ith trapezoidal distribution
	vert_trap_mag2	magnitude at the end of the ith trapezoidal distribution (psf)
inc	*init_node_spacing, node_inc, min_node_spacing*	length defining the distance separating each I-Wall node initial node spacing (default = 1 ft; 0.30480 m)
	init_node_spacing	
	node_inc	node spacing increment. Decimal fraction of the initial node spacing (default = 0.01)
	min_node_spacing	minimum node spacing. Decimal fraction of the initial node spacing (default = 0.7)
tol	*tol_m*	For the case when there is ample resistance within a soil berm on the landside to withstand load, the tolerance used for the sum of moment calculations (default = 10 ft-lb; 13.55818 N-m)
itr	*max_iter*	maximum number of iterations executed for an analysis (= 100)
grs	*num_surf_left,*	number of surface nodes (LHS)

	num_surf_right	number of surface nodes (RHS)
gnl	*surf_x, surf_y*	surface node positions (LHS from 1 to num_surf_left)
gnr	*surf_x, surf_y*	surface node positions (RHS from 1 to num_surf_right)
pdm	*num_ip*	number of interslice friction points (passive)
pdx	*ip(num_ip)*	list of x positions for passive interslice friction curve (all on one line)
pdy	*ip(num_ip)*	list of y positions for passive interslice friction curve (all on one line)
adm	*num_ip*	number of interslice friction points (active)
adx	*ip(num_ip)*	list of x positions for active interslice friction curve (all on one line)
ady	*ip(num_ip)*	list of y positions for active interslice friction curve (all on one line)

*note: the interslice friction curves are a normalized ordinate and abscissa curves. See Appendix H.

Appendix E: Description of Corps_I-Wall ASCII Output Data Files

The *prefix* of all the output filenames is a user-defined base filename that may include a drive letter, a path, and name of a project. A three-digit numeric field preceding the dot of a filename identifies the flood level for this particular analysis. The following sections discuss the various output files, with the prefix appended before each output filename.

E.1 prefix_001.out

The first line of the file lists information regarding the LHS of the I-Wall. The first value of this line is the number of text lines that follow. The second value represents the number of data lines following the text lines. The rest of the line lists the flood elevation.

As part of the data, the value of the first data character is defined. Values in this file are tabulated with the wall elevation, the water pressure, the soil vertical stress, the mobilized active stress, the mobilized passive stress, the mobilized horizontal active stress, and mobilized horizontal passive stress. Data are recorded at every nodal point elevation of the I-Wall.

Following the data lines, the next line starts the same set of data for the RHS of the I-Wall. Figure A1 is an example code of the first several lines of this file.

Table E1. Example code of the first several lines of the prefix_001.out file.

```
   11   62   Flood Level at    10.00 ft
-----------------------------------Left side of wall-----------------------------------
Soil Pressures
T => Total Stress
E => Effective Stress
W => Surface Water Pressure
A => Air
:
:             |           |    soil    |    sigma       sigma | sigma_horz  sigma_horz
:  Elevation  |     u     | sigma_vert |   active     passive |     active     passive
:             |           |            |     mob        mob   |        mob         mob
-------------------------------------------------------------------------------------
A       20.00         -          0.00        0.00        0.00        0.00        0.00
A       19.03         -          0.00        0.00        0.00        0.00        0.00
A       18.06         -          0.00        0.00        0.00        0.00        0.00
A       17.09         -          0.00        0.00        0.00        0.00        0.00
A       16.12         -          0.00        0.00        0.00        0.00        0.00
```

E.2 *prefix*_net_pressures_001.out

The first line lists relevant information of this file. The first value of this line is the number of text lines that follow. The second value represents the number of data lines following the text lines. The rest of the line lists the flood elevation.

Data values in this file record the node ID, the wall elevation, the net water pressure, the net active earth pressure, and the net passive earth pressure. The net water pressure is the difference between the water pressure of the side that the wall will rotate from, and the other side water pressure. The net active pressure is calculated by taking the difference between the horizontal active stress and the horizontal passive stress, and adding the net water pressure, net horizontal, and net vertical external pressures. Table E2 is an example of the first seven lines of this file.

Table E2. Example of the first seven lines of the *prefix*_net_pressures_001.out file.

1 220 Flood Level at 14.00 ft

node	wall_ele	net_u	net_a	net_p
1	20.00	0.00	0.00	0.00
2	19.76	0.00	8.62	56.83
3	19.52	0.00	17.24	113.66
4	19.28	0.00	25.86	170.49
5	19.04	0.00	34.48	227.33

E.3 prefix_internal_shear_moment_001.out

The first line lists relevant information of this file. The first value of this line is the number of text lines that follow. The second value represents the number of data lines following the text lines. The rest of the line lists the flood elevation.

Data values in this file record the wall elevation, the shear force, the bending moment, and the overall net pressure. Net is defined as the sum of horizontal pressures acting on both sides of the I-Wall. Table E3 is an example of the first six lines of this file.

Table E3. Example of the first six lines of the prefix_internal_shear_moment_001.out file.

1 63 Flood Level at 10.00 ft

Elevation	Shear	Moment	Net Pressure
20.000000	5.749944	0.000000	0.000000
19.030000	17.249833	5.577446	35.566667
18.060000	68.999333	44.619569	71.133333
17.090000	155.248500	150.591045	106.700000
16.120000	275.997333	356.956551	142.266667

E.4 *prefix*.run

This file displays runtime information such as the direction that the wall will rotate. The node spacing, the sum of forces, and sum of moment calculations at each estimated PR, and depth of embedment. The final calculated PR and elevation at tip of pile is recorded at the end of this file. Table E4 is an example of the first several lines of this file.

Figure E4. The first several lines of thi *prefix*.run file.

```
------------- Deterministic Analysis at Flood Elevation    10.00 ft ---------

 The I-Wall has been determined to rotate in the counter-clockwise direction.

 Node Spacing =  1.00 ft
  -7.000   -9.000  sumf=   10050.00  12183.33 summ=   98400.02  94133.37
  -8.000   -9.000  sumf=   12183.33   9866.67 summ=   94133.37 106316.70
  -9.000   -9.000  sumf=    9866.67   7550.01 summ=  106316.70 115411.15
  -8.000  -10.000  sumf=   14416.66  12000.00 summ=   86777.83 102000.04
```

E.5 *prefix*.inp

This file is an echo to the input file as described in Appendix D: Description of Corps_I-Wall ASCII Input Data File (*project*.in).

E.6 *prefix* _001._pdf

This file displays statistical information of the probability density function for the depth of embedment variable. The first line gives information on the number of proceeding text lines with the second value representing the number of data lines following the text lines. Data values for the histogram representing the probability density function are the ID, the midpoint of each bin, and the frequencies occurring at this bin. Recall that the number of bins is a user input. Table E6 is a sample of this file.

Figure E6. Sample of the *prefix* _001._pdf.

```
   8   12
Probability Density Function of Depth of Embedment.
Flood Elevation =      18.00 ft
Number of Simulations =      10
min =   -41.7101719057096
max =   -25.2038679248267
mean =   -33.1620072582522
standard deviation =    5.14074812117626
Coefficient of Variation =  -0.155019208612501
          1  -41.0224092398395       0.000000000000000E+000
          2  -39.6468839080993       0.125000000000000
          3  -38.2713585763590       0.000000000000000E+000
          4  -36.8958332446188       0.125000000000000
          5  -35.5203079128786       0.125000000000000
          6  -34.1447825811383       0.125000000000000
          7  -32.7692572493981       0.125000000000000
          8  -31.3937319176578       0.125000000000000
          9  -30.0182065859176       0.000000000000000E+000
         10  -28.6426812541773       0.125000000000000
         11  -27.2671559224371       0.125000000000000
```

E.7 *prefix*_001._cdf

This file displays statistical information of the CDF for the depth of embedment variable. The first line gives information on the number of proceeding text lines with the second value representing the number of data lines following the text lines. Data values representing this CDF are the ID, the midpoint of each bin, and the probability that the variable will have a value less than, or equal to the midpoint of the bin. Recall that the number of bins is a user input. Table E7 is a sample of this file.

Figure E7. Sample of the *prefix*_001._cdf file.

```
   8   12
Cumulative Distribution Function of Depth of Embedment.
Flood Elevation =      18.00 ft
Number of Simulations =      10
min =   -41.7101719057096
max =   -25.2038679248267
mean =   -33.1620072582522
standard deviation =    5.14074812117626
Coefficient of Variation =  -0.155019208612501
          1  -41.0224092398395       0.000000000000000E+000
          2  -39.6468839080993       0.125000000000000
          3  -38.2713585763590       0.125000000000000
          4  -36.8958332446188       0.250000000000000
          5  -35.5203079128786       0.375000000000000
          6  -34.1447825811383       0.500000000000000
          7  -32.7692572493981       0.625000000000000
          8  -31.3937319176578       0.750000000000000
          9  -30.0182065859176       0.750000000000000
         10  -28.6426812541773       0.875000000000000
         11  -27.2671559224371        1.00000000000000
         12  -25.8916305906969        1.00000000000000
```

E.8 *prefix*.src

This file displays the SRC for an *Analysis* mode study. For each pool, the probability of a sliding limit state is given. The first line of the file gives information on the number of proceeding text lines with the second value representing the number of data lines following the text lines. Data values representing this SRC are the ID, the pool elevation, and the probability of the sliding limit state. Table E8 is a sample of this file.

Figure E8. Sample of the *prefix*.src file.

```
1               12
System Response Curve
1               18.0            0.6
2               17.0            0.584
3               16.0            0.503
4               15.0            0.411
5               14.0            0.347
6               13.0            0.127
```

Appendix F: Calculation of Coastal Surge Pressures Acting on an I-Wall for a Breaking Wave

This appendix summarizes material adapted from a Memorandum for Record created in August 2008 by Dr. Kevin Abraham and Dr. Robert Ebeling of ERDC for support of the development of Engineering Circular 1110-2-6066 *Engineering and Design of I-Walls* (April 2011)(HQUSACE 2011a).

F.1 Background

The purpose of this example was to investigate the feasibility of using an I-Wall type retaining wall and levee system to provide protection against flood and wave loading in a coastal environment using simplified limit equilibrium procedures. Typical coastal structural systems consist of seawalls, anchored bulkheads, and revetments (*Shore protection manual* 1984). These systems are generally more robust and stiffer systems than a more flexible I-Wall section.[1]

First, a literature review was performed in an attempt to develop a database of projects that used I-walls for flood protection in a coastal environment. Regrettably, this literature review did not find a published example of an I-Wall and levee system in a coastal environment that provided flood and wave protection. However, a generic I-Wall system was developed based on general design guidance in Engineering Manuals 1110-2-2502 and 1110-2-2504, Retaining and flood walls, and design of sheet-pile walls, respectively. This example outlines the process of using simplified limit equilibrium procedures and simplified methods of computing wave load to perform an initial design for an I-Wall in a coastal environment. The simplified Minikin method (for computing breaking wave loads on vertical walls) was used in the analysis/design of this I-Wall system. If a new I-Wall is being investigated, then it is recommended that the design of this I-Wall be performed using an incremental approach. First, obtain an initial I-Wall design that satisfies the USACE criteria without any applied wave loading. Second, a series of analyses is performed in an effort to obtain an I-Wall initial design with an applied wave loading that would satisfy the USACE design criteria (given in EM

[1] The moment resistance of a sheet-pile wall can be enhanced with the addition of a landside soil berm that acts to counter the effects of surge loading during wave action sea side of the wall.

1110-2-2504 (HQUSACE [1994]). Last, a parametric study may need to be performed in an effort to modify the elevation of the ground surface on the landside of the wall. This ground surface is needed in an I-Wall design that satisfies the USACE criteria and soil profile consistent with a typical buttress levee when the I-Wall is subjected to significant surge loading during wave action.

F.2 Initial I-Wall design without wave loading

Typical cantilevered I-wall systems have an exposed height above the dredge level of 15 ft or less, so a profile with an exposed height of 15 ft was selected. The soil for this example is a medium dense sand with a unit weight ($\gamma_{moist} = \gamma_{sat}$ = 135 pcf), shear strength parameters of $\varphi' = 35$ degrees, and $c' = 0$. Coastal protection structures, such as seawall and anchored bulkheads, could have soil surface elevations on the landside at or near the top of the wall. Additionally, these structures are often designed with a stick-up height (exposed height of the wall above the design wave) of a minimum of 2 ft. With respect to wave heights, Hurricane Katrina generated surges 5 ft to 7 ft above what was assumed in the I-Wall design (IPET report Vol. 1) at some locations on the eastern side of New Orleans. Figure F1 shows a general profile that was used as a basis for the 2008 preliminary designs. Note that the 2008 initial design calculations did not include a complete breaking wave loading applied pressure definition as per the simplified Minikin method.

In 2008, the only sheet-pile wall analysis/design software available to the Corps was CWALSHT. After numerous attempts, Dr. Abraham and Dr. Ebeling determined that CWALSHT was not able to accommodate the modeling of breaking wave loading using the simplified Minikin method. Consequently, a series of preliminary cantilever design calculations were performed in 2008 using CWALSHT to compute depths of penetration (d) for an overly simplified, incomplete, and unconservative representation of wave load-induced pressures applied sea side of the sheet-pile wall in order to gain insight into the range in required depth(s) of sheet-pile wall penetration. The design calculations complied with USACE design criteria of applying a Factor of Safety 1.0 to the shear strength of the soil used to compute active soil pressures, and applying a Factor of Safety of 1.5 to the shear strength of the soil used to the compute passive soil pressures below the dredge level. Table F1 shows results of computed depths of penetration (d) for varied soil surface elevations on the landside without wave loads being applied and an average SWL of elevation 8 ft. These results were

used in subsequent analysis to determine if otherwise reasonable cantilever designs (including the wave load) were feasible.

Figure F1. Profile used in the initial I-Wall design calculations, including a soil buttress on the landside using an overly simplified and incomplete representation of wave load-induced, pseudo-static pressures.

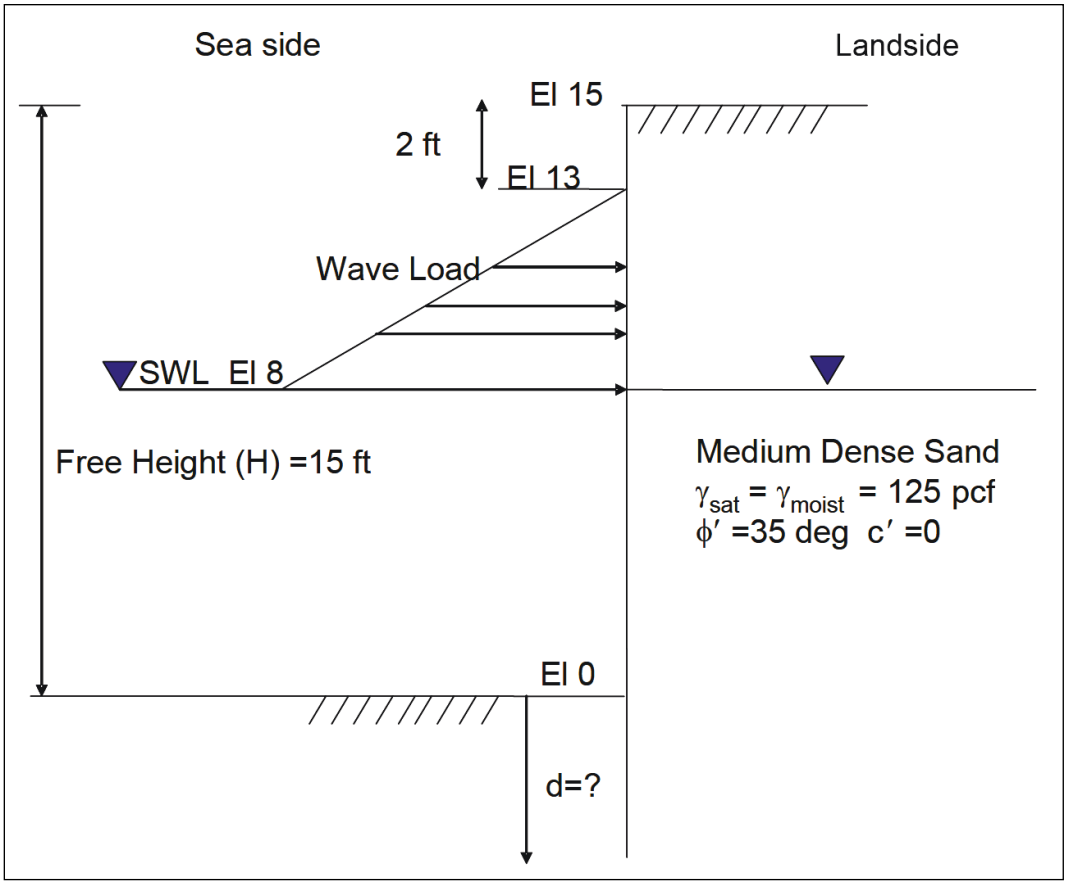


Table F1. Summary of 2008 preliminary I-Wall analysis results for varied heights of soil surface on the landside for an overly simplified and incomplete representation of wave load-induced pressures.

Protected Side Surface EL (ft)	Free Height (*H*) (ft)	Design Depth of Penetration (*d*) (ft)
0	15	NA
5	15	5
9	15	10
12	15	15
15	15	20

The following subsection outlines the calculations associated with the simplified Minikin method for computing breaking wave loads on vertical walls.

F.3 I-Wall design including wave loading

The following two general groups of procedures for computing wave impact loads on vertical walls in a coastal environment exist: the method used by Goda for nonbreaking waves (*Coastal engineering manual* 2002), and the Minikin method for breaking waves (*Shore protection manual* 1984 and Dr. Steven Hughes' presentation, *Wave Forces on Vertical Wall*, at the 20th Annual National Conference on Beach Preservation Technology).[1] In Dr. Hughes' presentation, the following two comments were made that pertain to the discussion in this report: 1) The Minikin method was not included in the *Coastal Engineering Manual* because some experts think it gives excessively high forces, and 2) Bullock et al. (2004) found that Minikin estimates of p_{max} (maximum pressure) matched full-scale tests results. The Minikin method of computing breaking wave impact loads on vertical walls was used in this example.

The simplified procedure used to estimate the effects of wave loading in a sheet-pile wall design is as follows:

Step 1. Compute p_m by the Minikin method.

The maximum pressure (p_m) is assumed to act on the elevation corresponding to the SWL and is given by Equation F1. (Refer to Figure 1). In this example the SWL is at el 8 ft.

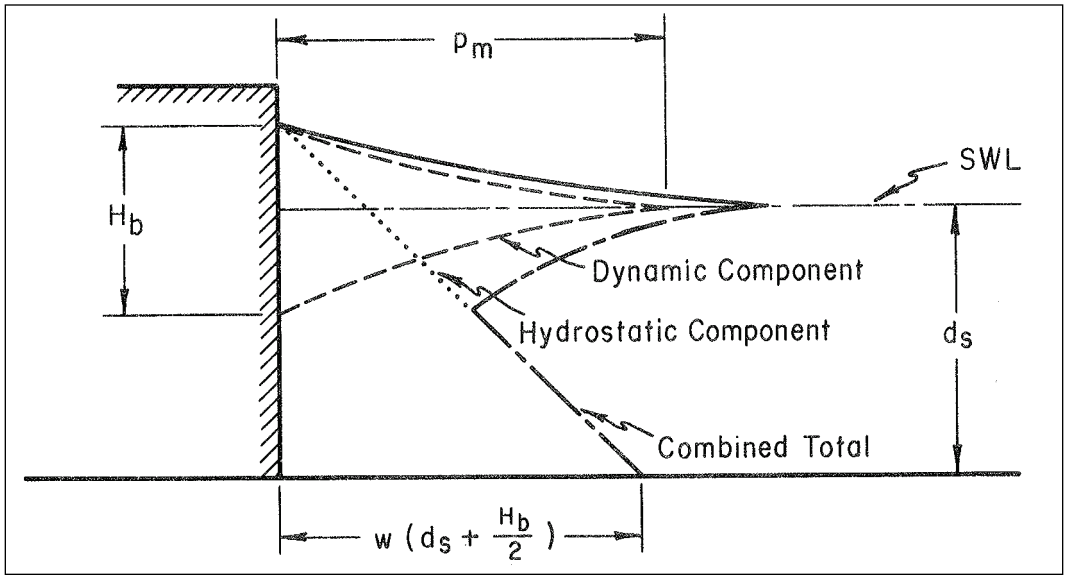
$$p_m = 101w \frac{H_b}{L_b} \frac{d_s}{D} (D + d_s) \quad \text{(F1)}$$

where w is the specific weight of water, H_b is the breaking wave height, L_D is the local wavelength of water of depth D, and d_s is depth to the toe of the wall. The distribution of the dynamic breaking wave pressure is shown in Figure F2. As shown in Figure F2, the pressure distribution consists of the

[1] A 1988 Coastal Engineering Technical Note on *Breaking wave forces on walls* (CETN-III-38, 3/88) observed that "as the Minikin method is based on the shock pressure caused by breaking waves, the resulting forces and structure designs analyzed by using this procedure are generally considered to be conservative. It also stated that a less conservative method recommended by Goda (1974) is an alternative procedure for breaking wave force determination. The rationale of using the Goda method for design analysis is that the duration of the impulsive breaking wave is relatively brief, on the order of tenth or hundredth of a second, and the effect of this force on the stability of massive concrete wall structures may be rather insignificant."

following three components: 1) hydrostatic, 2) dynamic, and 3) a combined total. Note that Equation F1 only computes the dynamic component of the pressure diagram.

Figure F2. Minikin breaking wave pressure diagram (after Figure 7-99; *Shore protection manual* 1984).



a. Compute the breaking wave height (H_b)

Assume d_s = 8 ft (depth to dredge level) (Refer to Figure F1) and wave period

T = 10 sec. Note: This wave period corresponds to typical maximum value (*Shore protection manual* 1984). The near shore slope value *m* assumed to be zero.

Next compute the relative depth at structure using Equation F2.

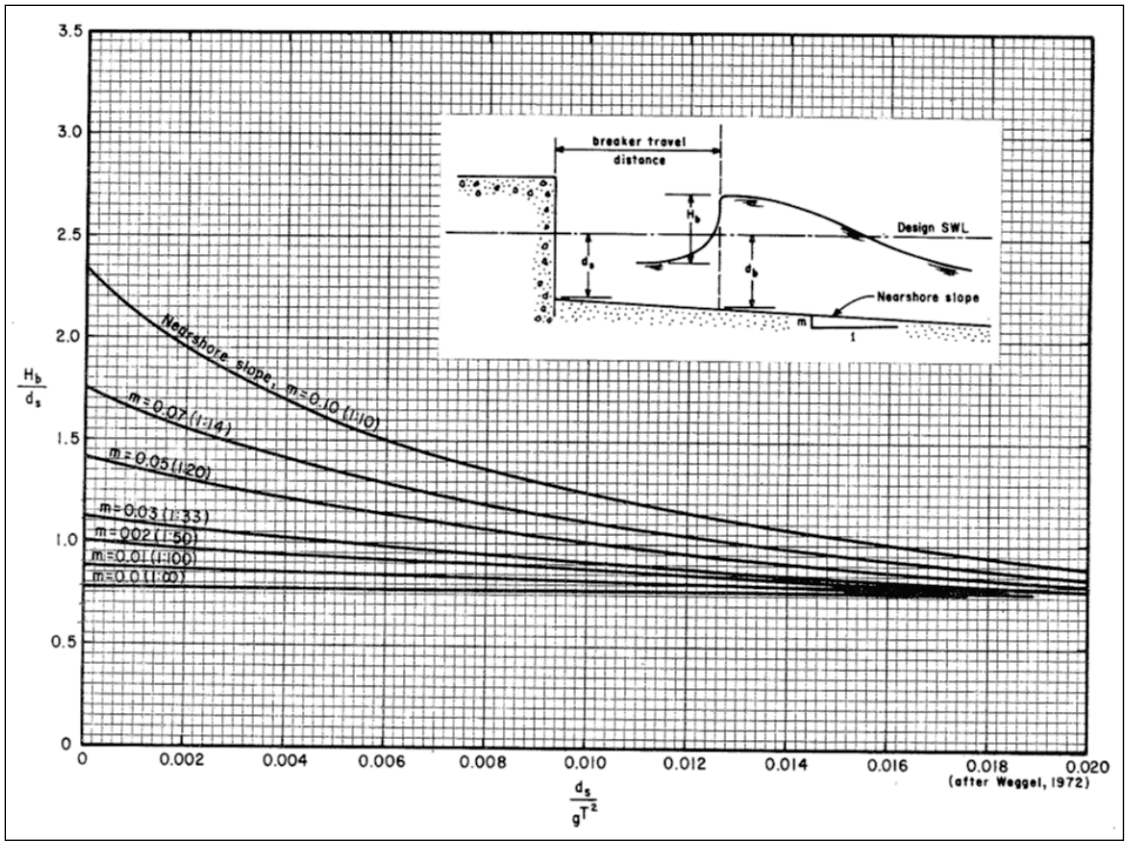
$$\frac{d_s}{gT^2} = \frac{8\,ft}{32.2\frac{ft}{sec}10^2} = 0.0025 \quad \text{(F2)}$$

Using this value and Figure F3 with m = 0 gives

$$\frac{H_b}{d_s} \approx 0.78$$

$$H_b \approx 6.24\,ft$$

Figure F3. Dimensionless design breaker height versus relative depth at the wall (after Figure 7-4 *Shore Protection Manual* 1984 and Weggel 1972).



b. Compute local wavelength in water depth (D)

First, compute the wavelength in deep water (L_o) for (T = 10 sec) using Equation F3

$$L_o = \frac{gT^2}{2\pi} = \frac{32*10^2}{2\pi} = 512.48\ ft \quad \text{(F3)}$$

Then

$\frac{d}{L_o} = \frac{8}{512.48} = 0.0156$; where $d = d_s$

Using Table C1, Appendix C of the *Shore protection manual* (1984) and the computed value of $\frac{d}{L_o}$ gives $\frac{d}{L} \approx 0.050684$ where L is wavelength at depth d

$$L_d = \frac{8\ ft}{0.050648} \approx 158\ ft$$

c. Compute the water depth, D, one wavelength seaward of the vertical wall using Equation F4

$$D = d_s + L_d m; \text{ since m = 0} \tag{F4}$$

$D = d_s = 8$ ft

Therefore: $\frac{D}{L_o} = \frac{d}{L_o}$ and $L_d = L_D$

$$p_m = 101 w \frac{H_b}{L_D} \frac{d_s}{D} (D + d_s)$$

$$p_m = 101 * 64 \frac{lb}{ft^3} \frac{6.24\ ft}{158\ ft} \frac{8\ ft}{8\ ft} (8\ ft + 8\ ft)$$

$$p_m \approx 4{,}084.6 \frac{lb}{ft^2}$$

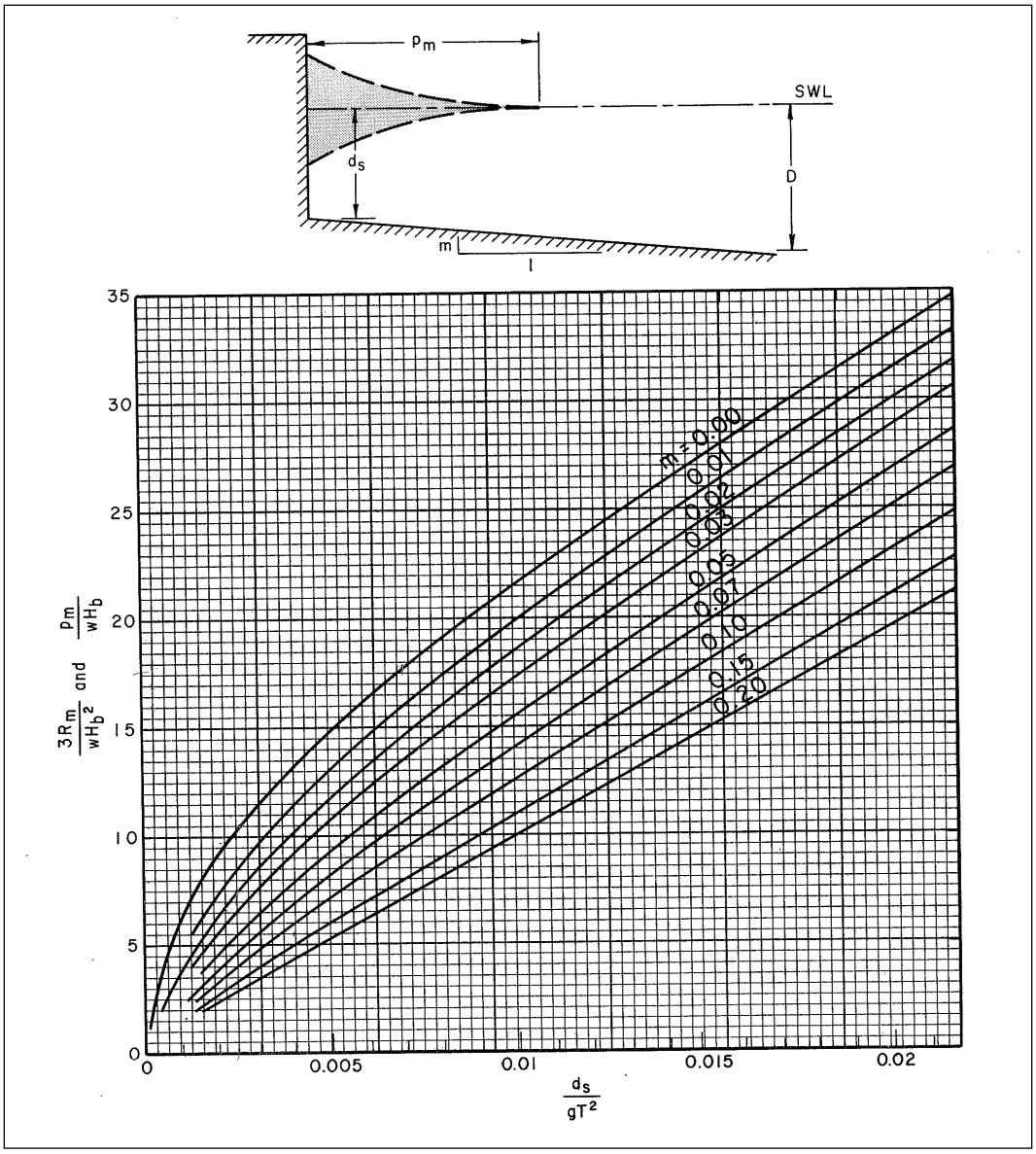
Using Figure F4, the curve for $m = 0$ and Equation F2, an approximate value for p_m can be computed

$$\frac{d_s}{gT^2} = \frac{8\ ft}{32.2 \frac{ft^2}{sec} 10^2} = 0.0025$$

The ratio of $\frac{p_m}{wH_b} \approx 10.2$ w is the specific weight of water, H_b is the breaking wave height, $p_m = 10.2 * 64 \frac{lb}{ft^3} * 6.24$ ft $\approx 4{,}073.5 \frac{lb}{ft^2}$ $p_m \approx 4{,}073.5 \frac{lb}{ft^2}$; is approximately equal to p_m computed using Equation F1 $\left(4{,}084.6 \frac{lb}{ft^2}\right)$.

Recall this computed wave load pressure distribution acting over breaking wave height H_b, designated "Dynamic Component" in Figure F2 with a maximum magnitude p_m is then incorporated in an initial sheet-pile wall design calculation as an applied horizontal distributed load on the wall. Note that in the sheet-pile wall analysis, the elevation of the SWL specified on the coastal side of the sheet-pile wall increases from SWL to the elevation of this surge wave (depicted in Figure F1). Again, this simplified pressure load approximates the dynamic wave effects on the I-Wall. In 2008, calculations were attempted using the Figure 1 overly simplified approximation for a surge wave loading using CWALSHT. These attempts were deemed unsuccessful. This experience contributed to requests being made by district engineers for the development of new I-Wall analysis software that is capable of analyzing coastal sheet-pile walls using the simplified Minikin method for computing breaking wave loads on vertical walls.

Figure F4. Dimensionless Minikin wave pressure and force (after Figure 7-100; *Shore protection manual* 1984).



Appendix G: Formulation for the Wedge Method of Analysis of Passive and Active Earth Pressure Forces Acting on the Sheet-Pile Wall

Appendix G summarizes the Wedge Solution Method engineering formulation implemented in Corps_I-Wall. This formulation provides an alternative analysis option to the Coefficient Method for computation of active and passive earth forces acting on the sheet-pile wall. These forces are used to derive the corresponding pressure distributions with depth along the wall. The *method of slices* (Duncan et al. 2014; Abramson et al. 1996) is the specified procedure used to determine the active and passive earth forces acting on the sheet-pile wall, with each slice corresponding to the earthen wedges in the analysis. Once the distribution of active and passive forces with depth are determined, these two force distributions are numerically differentiated in order to obtain distributions of active and passive earth pressures with depth along the wall.

Recall that the Coefficient Method of analysis in Corps_I-Wall assumes that soil regions and piezometric surfaces that touch the wall extend horizontally from the wall, and therefore, the solution only handles horizontal soil regions and piezometric surfaces. The advantage of using the Wedge Solution Method over the Coefficient Method of analysis is that non-level ground surfaces and soil region interface geometry are easily accounted for. The analysis allows for non-level soil regions because the forces are described using directed vectors for each soil wedge. Additionally, non-level piezometric surface(s) may also be specified in the Wedge Solution Method of analysis.

G.1 Procedure of analysis for the Wedge Solution Method of analysis

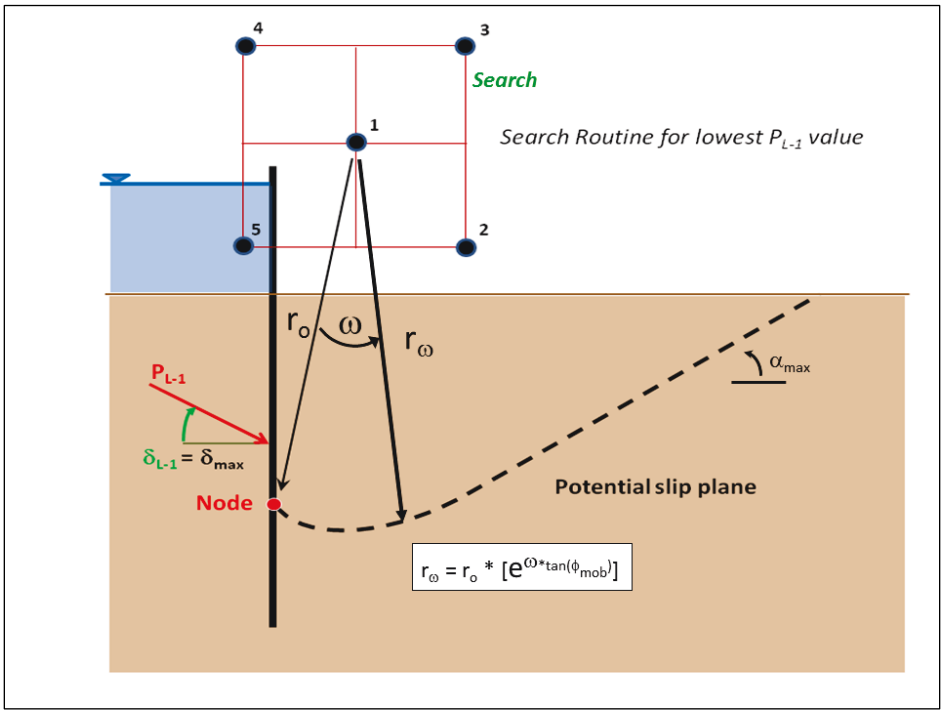
The procedure of analysis used by the Wedge Solution Method to determine the passive earth force distribution with depth and corresponding earth pressures is as follows:

1. With the user specified Factor of Safety for passive force calculations and the user specified material soil properties as input, calculate the mobilized Mohr-Coulomb shear strength total stress parameters of c_{mob}, ϕ_{mob}, δ_{mob}

and $c_{A\text{-}mob}$ or effective stress parameters of c'_{mob}, ϕ'_{mob}, δ'_{mob} and $c'_{A\text{-}mob}$ for each soil region. The equations used are given in Chapter 2.

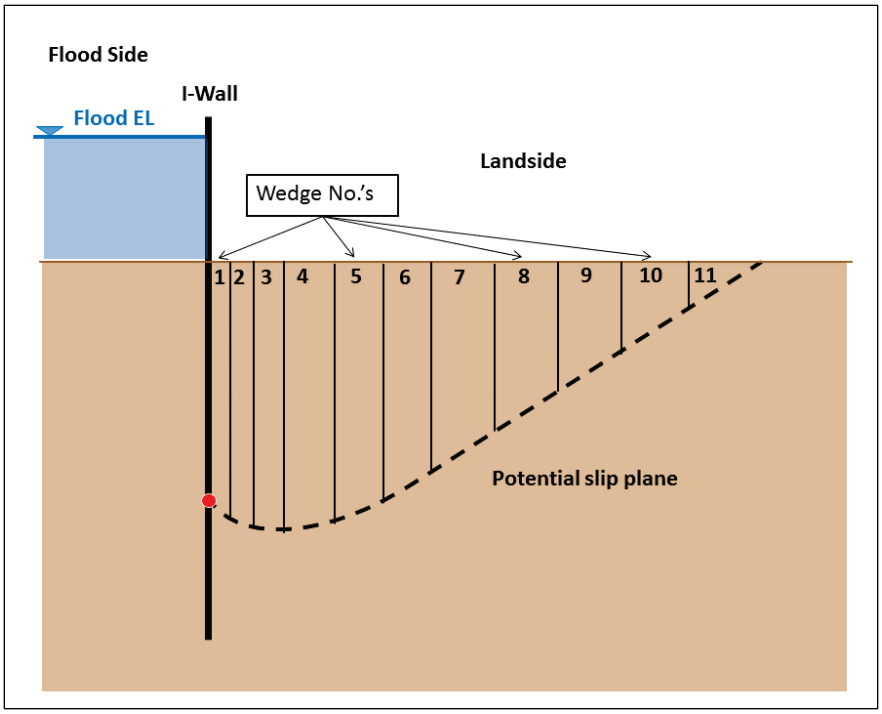
2. Assign the deepest trial depth of sheet-pile wall embedment to be considered. The default value is set to 125 ft.
3. Define nodes with depth along the (trial) embedded portion of the wall. The top-most node is typically one foot below the ground surface. The last node is at the deepest trial tip depth of the sheet pile. Additionaly, intermediate nodes are added using a Soil Region Based, Nodal Division Method.
4. Starting with the top-most node, define a trial slip plane emanating from this node on the wall. For passive earth force computations, a logarithmic spiral shaped (also referred to as log-spiral) potential slip plane is used. An idealization of its shape is depicted in Figure G.1. The equation for a logarithmic spiral is also included in Figure G1. Note that the log-spiral emanates from a central point that is designated point number 1 for the log-spiral shown in this figure. Note that the log-spiral controls the shape of the slip plane until a bounding slip angle, α_{max} is reached. At that point, slip plane follows α_{max}.

Figure G.1. A potential log-spiral slip plane originating at a node on the wall and the definition of the search box consisting of five log-spiral centers being investigated.



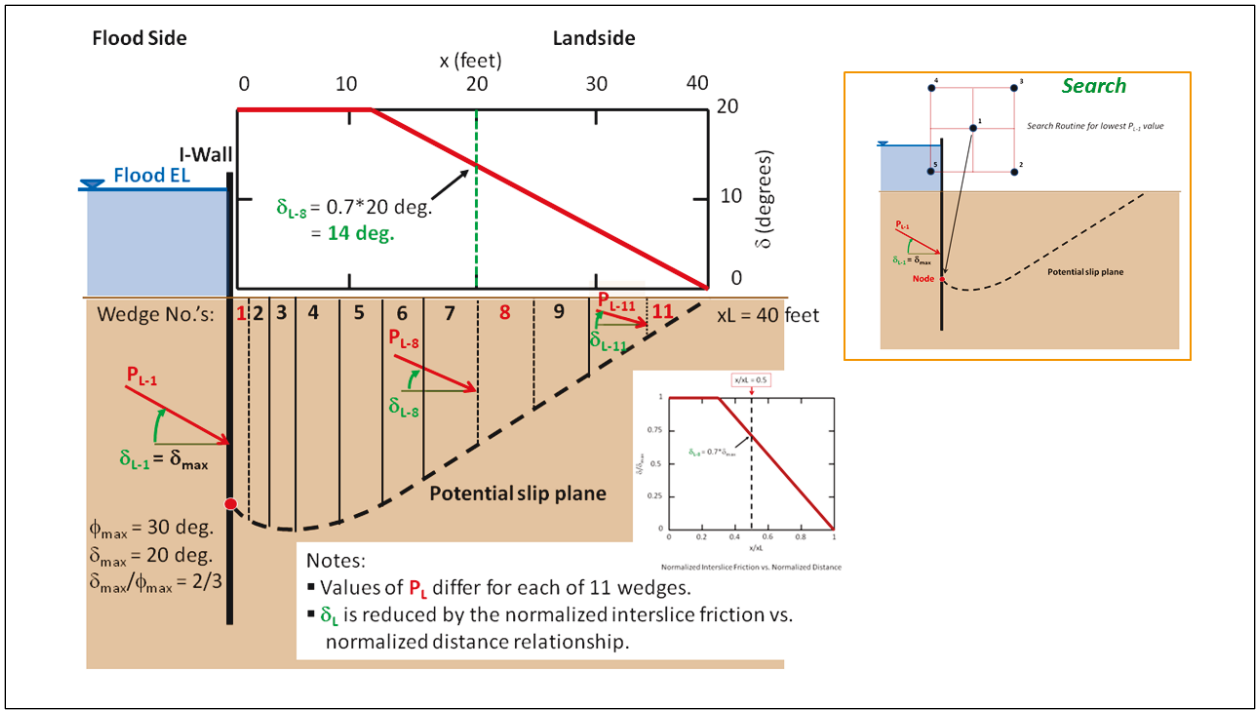
5. The geometry of the soil mass contained within the trial slip plane is divided into soil wedges. Figure G.2 idealization depicts a soil mass defined by Figure G.1 trial slip plane, and is divided into eleven soil wedges. Each of the wedges can be of a different width. This procedure of analysis is referred to as the *method of slices*.

Figure G.2. The definition of the soil mass contained within the potential log-spiral slip plane and its idealization as 11 soil wedges.



6. Solve for Figure G.3, passive soil force $P_{L\text{-}1}$ applied to the wall by soil wedge 1 using the *generalized limit equilibrium method of analysis*. Subscript L-1 designates the force is acting on the LHS of this soil wedge 1. This method of analysis starts by solving for the value of $P_{L\text{-}11}$, acting on the LHS of Figure G.3's soil wedge 11. For each wedge, the forces acting on the left side of the wedge (for this example) is equal and opposite to the forces acting on right hand side, plus the internal forces (e.g. weight). For the furthest right wedge (wedge 11 in the example), the forces acting on the right side of the wedge are 0.0. Then the solution progresses through a series of ten wedge equations in which the unknown force value is the LHS force value $P_{L\text{-}i}$ of each wedge i is calculated. The new right hand side force for the next wedge is equal and opposite to the current wedge's LHS resisting force. The last calculated force is $P_{L\text{-}1}$, acting on the LHS of soil wedge number 1. This force corresponds to the passive soil force acting on the wall, P_P.

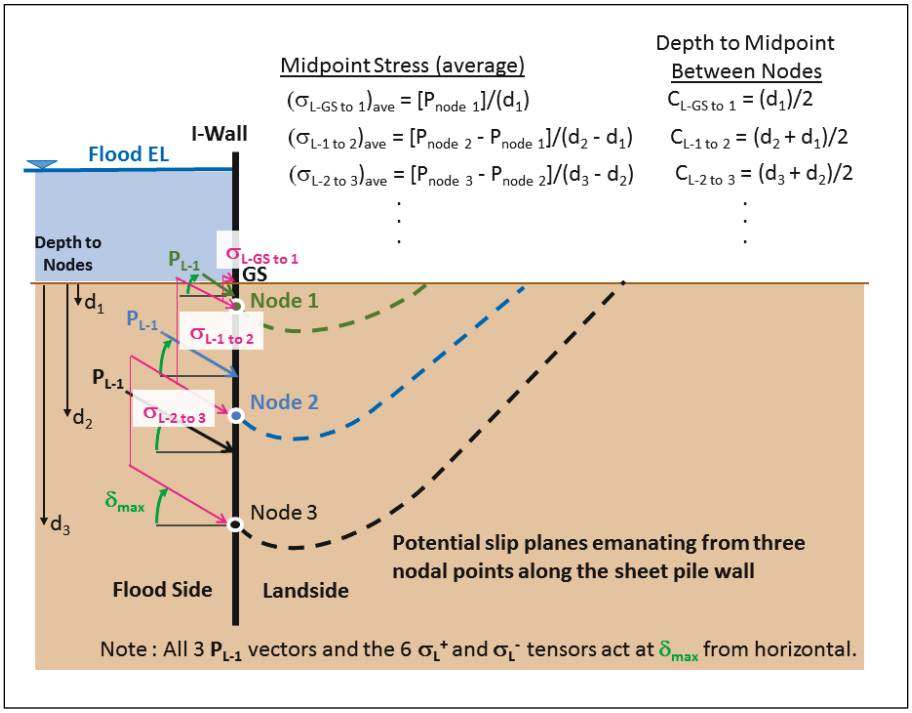
Figure G.3 Identification of the LHS wedge forces acting on soil wedges 1, 8, and 11. The angle orientation of each of the eleven LHS forces P_L with distance from the wall, and the search box routine consisting of five log-spiral centers.



7. For a log-spiral shaped trial slip plane anchored to this same top-most wall node, repeat steps four through six for a new log-spiral with center point 2 shown in Figure G.1. This results in a new (Figure G.3) passive soil force $P_{L\text{-}1}$ corresponding to this new trial slip plane with a center at point 2. Repeat these same four steps (three thourgh six) for three other (i.e., new) log-spirals with center points designated as points 3, 4 and 5 (Figure G.1). Now all five center points have a corresponding $P_{L\text{-}1}$ value (Figure G.2).
8. Adjust the center point search box location by relocating the center of the search box to the center point corresponding to the lowest computed $P_{L\text{-}1}$ value among the five center points (Figure G.3). Reconfigure the coordinates of the four search box corner points and repeat steps four through seven.
9. Steps four through eight is repeated until point 1 in the center of the four point search box of log-spiral centers possesses the lowest $P_{L\text{-}1}$ value. During the later stages of this analysis, the center of the log-spiral search box dimensions are reduced so as to ensure that the lowest $P_{L\text{-}1}$ value has been found. At this stage, the log-spiral trial slip plane analysis is concluded for the top-most node and the lowest $P_{L\text{-}1}$ value is assigned to its passive soil force.
10. Move the intercept node at the wall to the next node down and repeat steps four through nine.

11. The end result is an array of passive earth force values, one for each node down the wall.
12. Numerically differentiate the distribution of passive earth force values for the nodes at which these resultant forces were computed, and then construct the corresponding passive earth pressure distribution at mid-node elevations as depicted in Figure G.4.
13. Repeat steps three through twelve for the other side of the wall.

Figure G.4. The definition of three mid-point average earth pressure values from three earth force values collected at three wall nodes (idealization).



The thirteen steps outlined above for developing the passive force distribution along both sides of the wall are nearly the same as those used for computing the active earth force distribution with depth. Three changes are made to the details described above for developing an active earth force distribution: 1) The potential slip surface is assumed planar in an active force analysis. This assumption contrasts with the use (i.e., assumption) of a log-spiral slip plane in a passive earth force analysis. This active earth force analysis is also made using the *method of slices*. 2) For each wall node in an active earth force analysis, the planer potential slip surface possessing the highest $P_{L\text{-}1}$ value (at the wall) is the focus of the search. This contrasts with the passive earth force analysis in which lowest $P_{L\text{-}1}$ value is the focus of the search. 3) At each wall node, a sweep search of potential planar slip surfaces is made to determine the maximum $P_{L\text{-}1}$ value of all the slip planes

investigated. This sweep search starts with a potential slip plane oriented at 80 degrees from horizontal, and then sweeps down in one degree increments to investigate other potential slip planes. The last plane investigated is oriented at one degree from horizontal.

G.2 Method of slices

The *method of slices* is used to compute the passive thrust force acting on the wall. It is designated as earth force $P_{L\text{-}1}$ acting on the LHS of soil wedge 1 in Figure G.3. The *method of slices* has its roots in slope stability. It was selected for use in the calculation of the passive force in Corps_I-Wall because it has the ability to accommodate a varying ground surface, varying soil region elevations, thicknesses and region extents, and a varying piezometric surface elevation with extent.

G.2.1 Passive soil wedge

For passive earth force computations, a log-spiral shaped potential slip plane is used (Figure G.1) and the soil mass contained within the log-spiral is divided up into soil wedges (Figure G.2). The base of each of these eleven Figure G.2 wedges is assumed planar for a piecewise linear representation of the log-spiral slip plane. Figure G.5 shows the forces acting on an individual passive soil wedge that is not at the wall. Note the planar base representation from points B to D of the soil wedge in this figure.

The list of symbols used in this and subsequent individual wedge diagrams are given in the last section of this appendix, along with their symbol definitions.

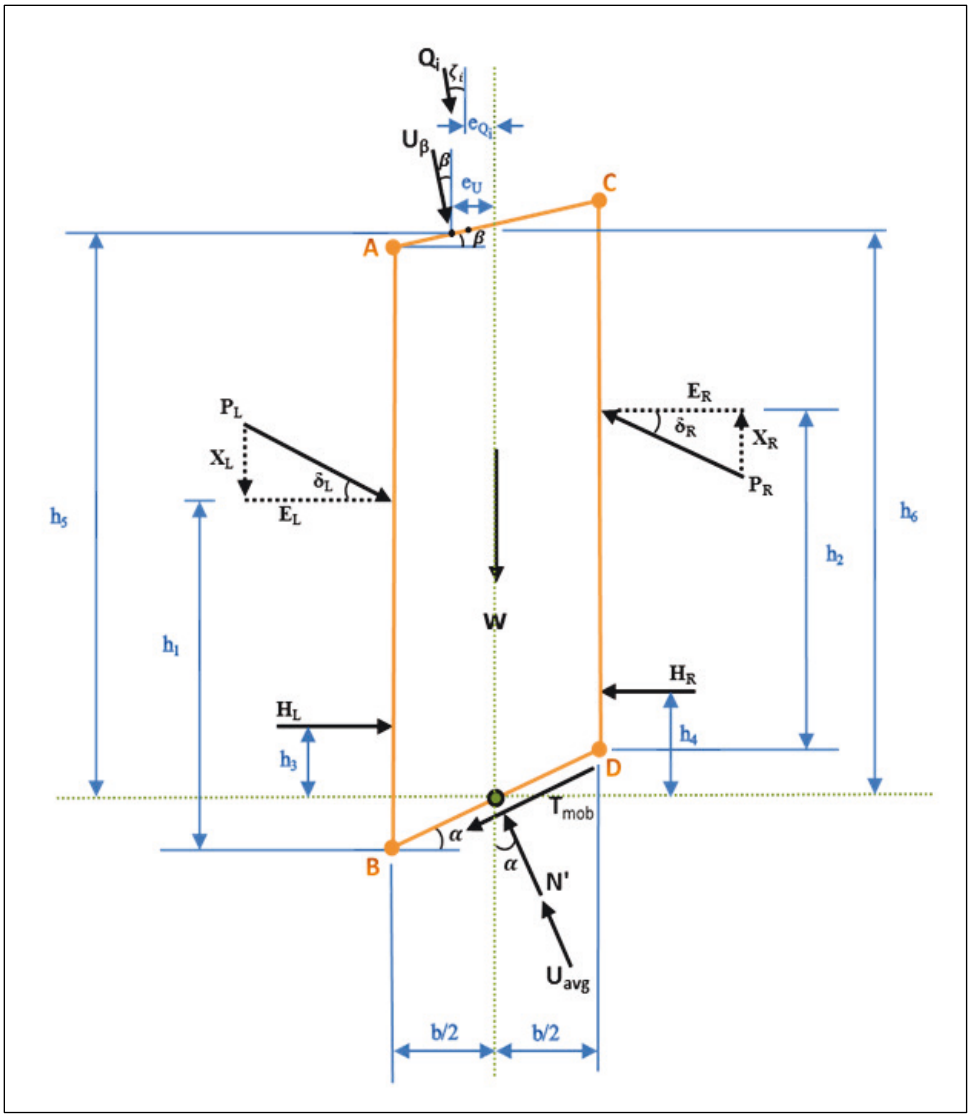
In a passive soil state, the Figure G.3 wall is plowing into the soil wedge. Consequently, for each passive soil wedge the shear force required for equilibrium T along the base of the wedge acts in the direction shown in Figure G.5 to counter this soil wedge movement. Note that T is set equal to and designated by the mobilized shear force T_{mob} in this Figure. For an effective stress analysis, T_{mob} is given by

$$T_{mob} = c'_{mob-Passive} * \frac{b}{\cos(\alpha)} + N' * \tan(\phi'_{mob-Passive}) \quad \text{(G.1)}$$

And for total stress, T_{mob} is

$$T_{mob} = c_{mob-Passive} * \frac{b}{\cos(\alpha)} + N * \tan(\phi_{mob-Passive}) \quad \text{(G.2)}$$

Figure G.5. Forces acting on a typical individual passive soil wedge.



G.2.2 Active soil wedge

For the active earth force computations a planar potential slip plane is used. The soil mass is divided up into soil wedges in a similar fashion as used for the passive soil wedge. Figure G.6 shows the forces acting on an individual active soil wedge not at the wall.

Figure G.6 Forces acting on a typical individual active soil wedge.

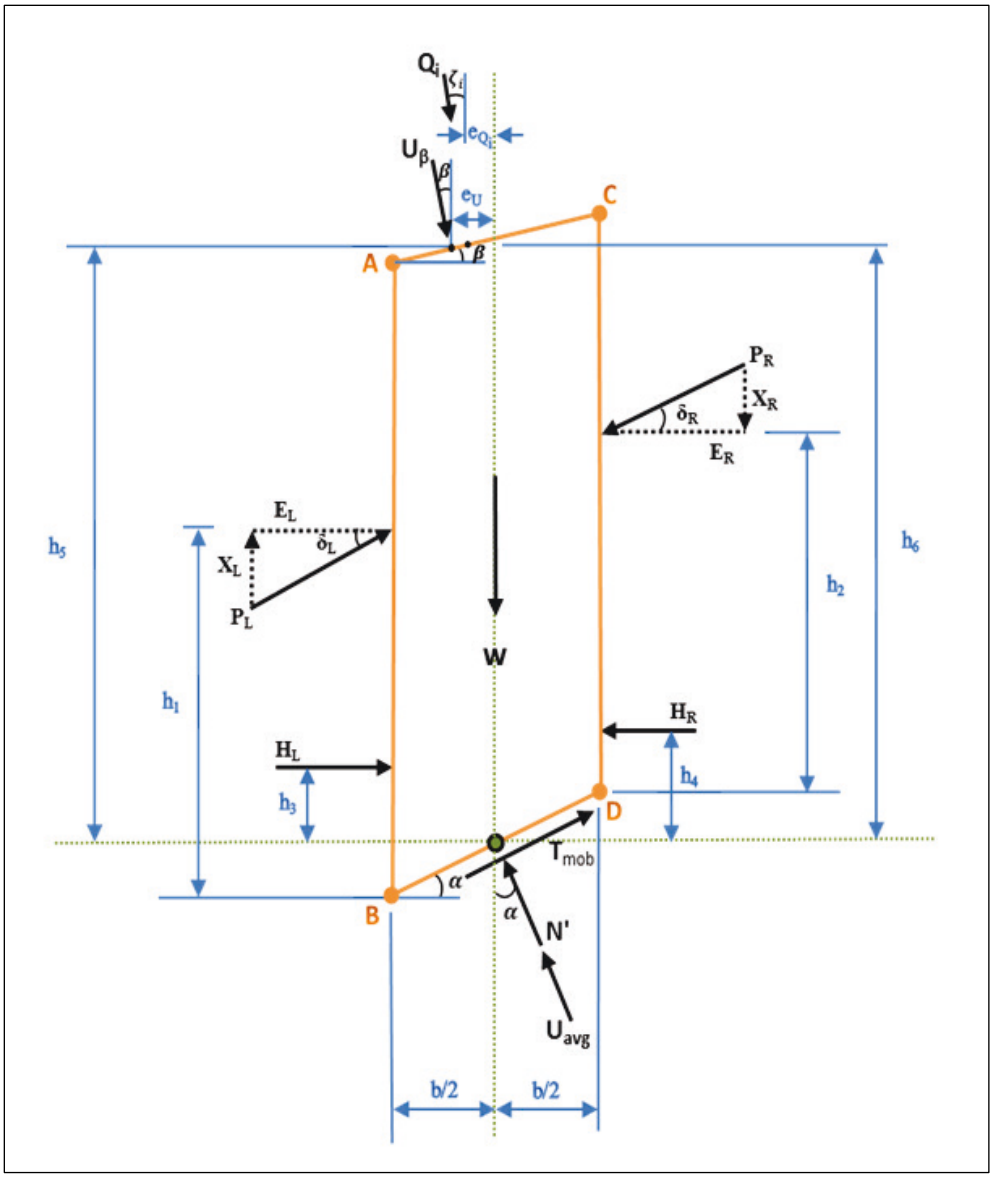


Figure G.6 contrasts with Figure G.5 in the direction of the shear force acting along the base of the wedge, in an active soil state, the wall is moving away from the soil wedge. Consequently, for each active soil wedge the shear force required for equilibrium T along the base of the wedge acts in the direction shown in Figure G.6. Again, T is set equal to and designated by the mobilized shear force T_{mob} in this figure. For an effective stress analysis, T_{mob} is given by

$$T_{mob} = c'_{mob-Active} * \frac{b}{\cos(\alpha)} + N' * \tan(\phi'_{mob-Active}) \qquad \text{(G.3)}$$

And for total stress, T_{mob} is

$$T_{mob} = c_{mob-Active} * \frac{b}{\cos(\alpha)} + N * \tan(\phi_{mob-Active}) \quad \text{(G.4)}$$

G.2.3 Pore water pressures and their resultant forces

In an effective stress analysis using the soil wedge formulation, pore water pressures are computed along the base and sides of the soil wedge. The procedure used follows the Duncan and Wright (2005), and Duncan et al. (2014) recommendation to account for the slope of a piezometric surface when computing the pore water pressure at a point in the ground. Figure G.7 provides this relationship, expressed in terms of pressure head at point B, hp_B, for the piezometric surface PS_2 with an inclination angle of θ_L at the left interslice position. Note that PS_2 possesses an inclination angle of θ_R at the right interslice position. In Corps_I-Wall, θ_L need not be equal to θ_R.

The pore water pressure at point B, u_B, is given by

$$u_B = \gamma_w * hp_B \quad \text{(G.5)}$$

The ordinary method of slices requires the specification of boundary forces applied to each soil wedge. For pore water pressures, this requires the computation of resultant forces for each of the boundary pore water press distributions applied to a soil wedge. Figure G.8 shows various pore water pressure distributions (in black) and their corresponding resultant forces (in red) for this multilayered soil wedge.

Figure G.7 Pressure head from inclined piezometric surface, PS_2 acting at point B on the left interslice of a multilayered soil wedge.

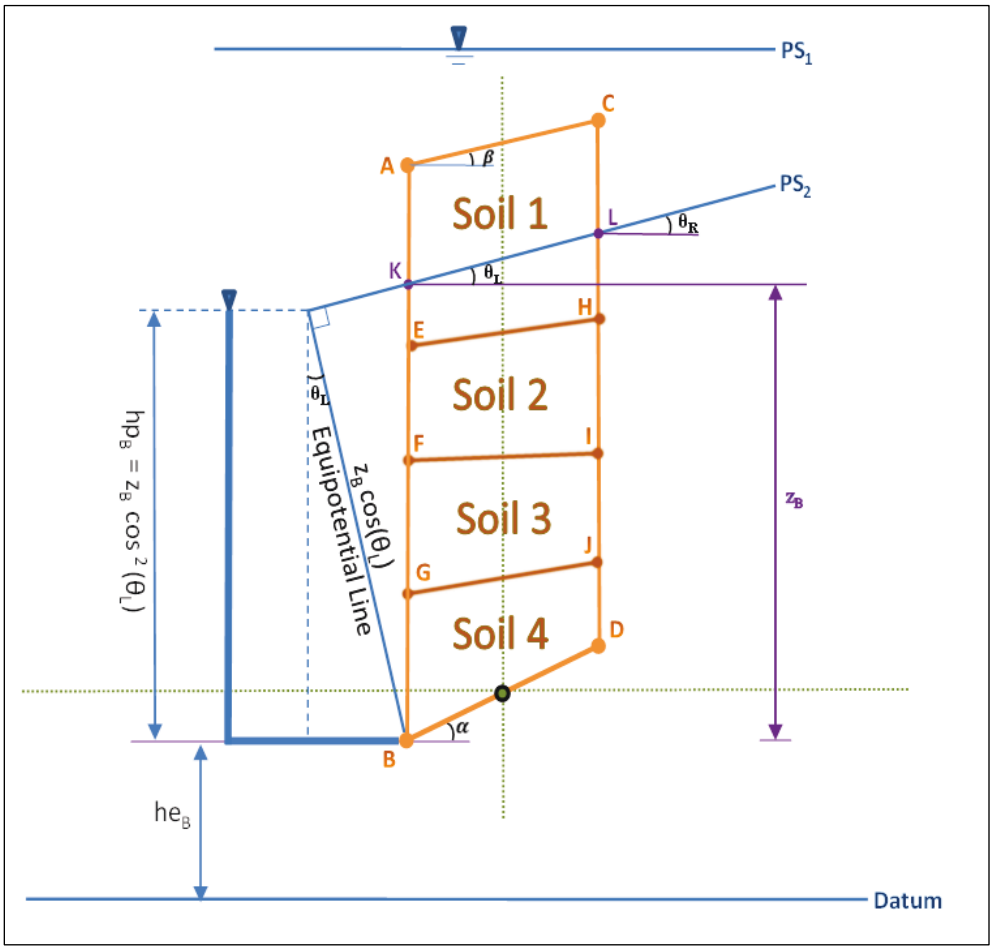
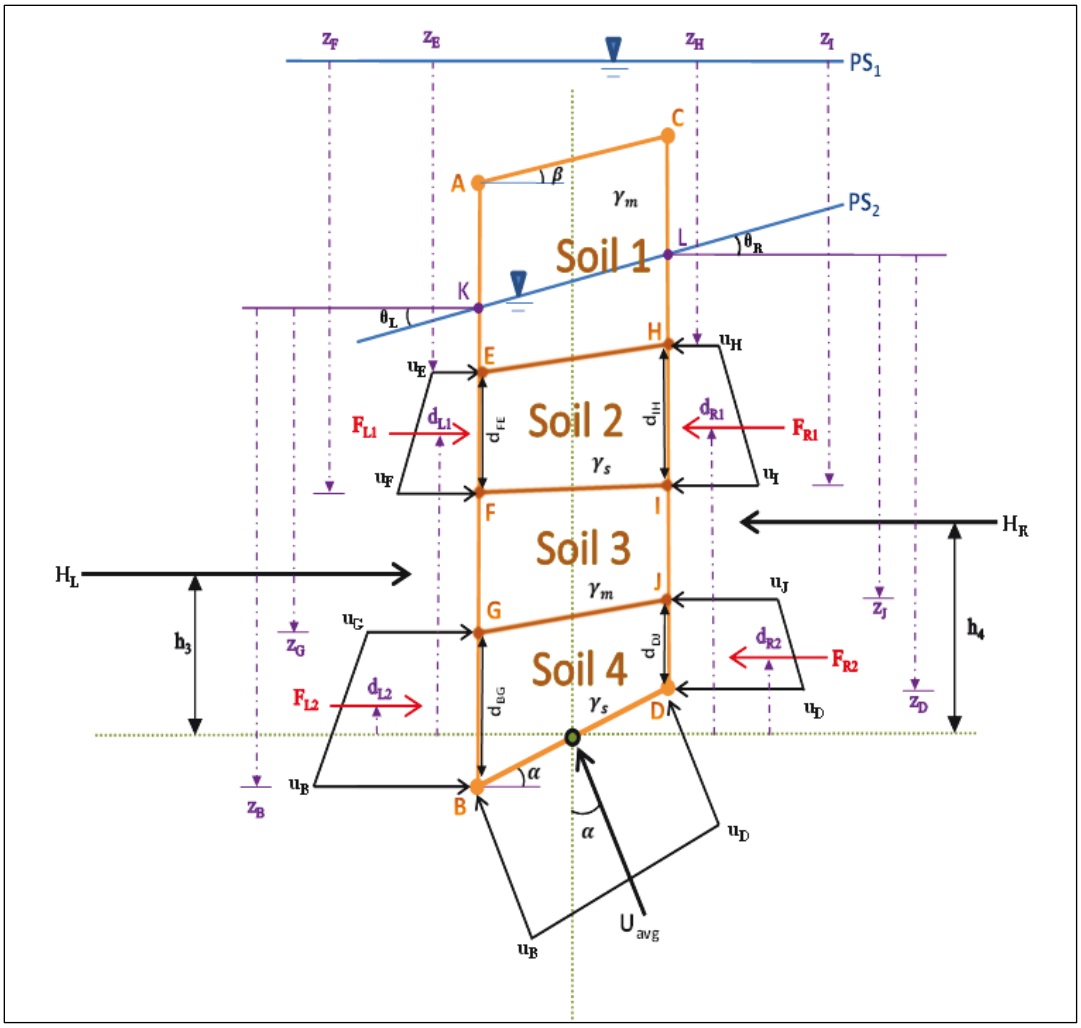


Figure G.8 Pore water pressure distributions and resultant water forces acting along the left and right interslices of a multilayered soil wedge and wedge base.



Some of the key equations used in the Corps_I-Wall individual wedge computations are as follows:

From Bernoulli's equation, the total head h_B at point B is

$$h_B = hp_B + he_B \tag{G.6}$$

The pore fluid velocity is assumed negligible and the velocity head is therefore ignored.

The pressure head hp_B at point B

$$hp_B = z_B * cos^2(\theta_L) \tag{G.7}$$

Water forces at point B and G on the left interslice are

$$F_B = \left(\frac{u_B}{6} + \frac{u_G}{3}\right) d_{BG} \tag{G.8}$$

$$F_{L_G} = \left(\frac{u_G}{3} + \frac{u_B}{6}\right) d_{BG} \tag{G.9}$$

These two forces are equivalent to the water pressure distribution acting from B to G.

Resultant force from water forces at the left interslice are

$$H_L = \sum F_{L_i} \tag{G.10}$$

Distance from at the left interslice resultant force H_L to midpoint of soil wedge base is

$$h_3 = \frac{\sum \left(F_{L_i} d_{L_i} \right)}{H_L} \tag{G.11}$$

With a change in subscripts to terms in Equations G.6 through G.11, the heads, pore water pressures, and interslice forces on the right-hand side of the Figure G.8 soil wedge are computed.

The resultant water force U_{avg} acting normal to the base of the soil wedge is

$$U_{avg} = \bar{u} * \frac{b}{cos(\alpha)} \tag{G.12}$$

where $\bar{u}$ is the average pore water pressure at the wedge base (=[u_B + u_D]/2).

The weight of the wedge is

$$W = \sum \left(\gamma_i \, b_i \, h_i \right) \tag{G.13}$$

where

i = 1 through 4
γ = unit weight of soil (moist or saturated)
b = width of wedge
h = height of wedge (at wedge centerline)

G.3 Generalized limit equilibrium method

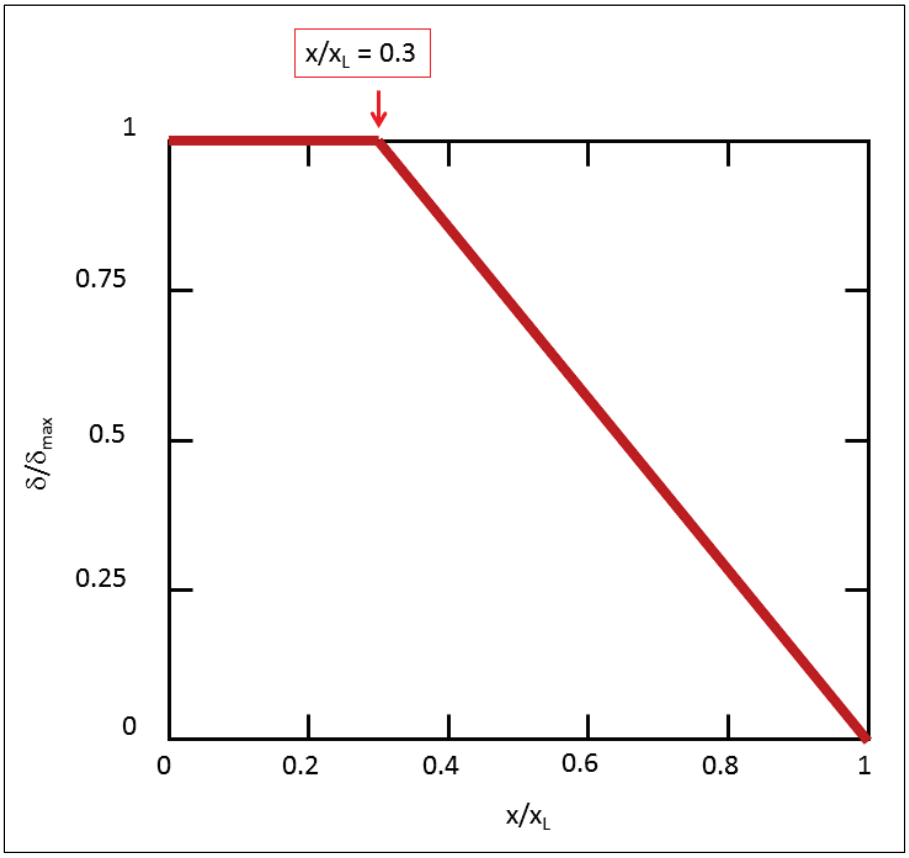
The *generalized limit equilibrium method* formulation is used in Corps_I-Wall to solve for the passive and active soil forces acting on the wall. The roots of this procedure of analysis lay in slope stability. The *generalized limit equilibrium method* is an extension of Spencer's (1973) procedure, this has been generalized by Chugh (1986). Section 6.9.4 in Abramson et al. (1996) provides a summary of the wedge equations. They provided a check to the derivations made independently by the authors of this report. The following subsections summarize the details of the analysis.

G.3.1 Normalized interslice friction vs. normalized lateral distance from the wall

The *generalized limit equilibrium method* has the advantage of allowing the assignment of a variable interslice friction force angles δ_L and δ_R along the faces of each of the soil wedges with distance from the wall. This is a significant advantage when applied to I-Wall problems. The accuracy of the computations have been found in this research and development effort to be affected by the distribution of interslice friction values with position of a particular soil wedge in the sequence of soil wedges comprising the soil mass.

The general framework of specifying the distribution of interslice friction angle in Corps_I-Wall is the use of a normalized interslice friction distribution function versus normalized distance. A hypothetical interslice angle of friction distribution with distance from the wall is shown in Figure G.3. The ordinate is the interslice friction δ at a lateral point away from the wall of distance x, divided by the interslice friction value at the wall, designated δ_{max}. The log-spiral intersects the ground surface at a lateral distance of x_L away from the wall. Consequently, the lateral distance x to any interslice position is normalized by the value of x_L in this procedure. An example relationship is shown in Figure G.9.

Figure G.9 Normalized interslice friction δ/δ_{max} distribution versus normalized distance (x/x_L) from the wall.



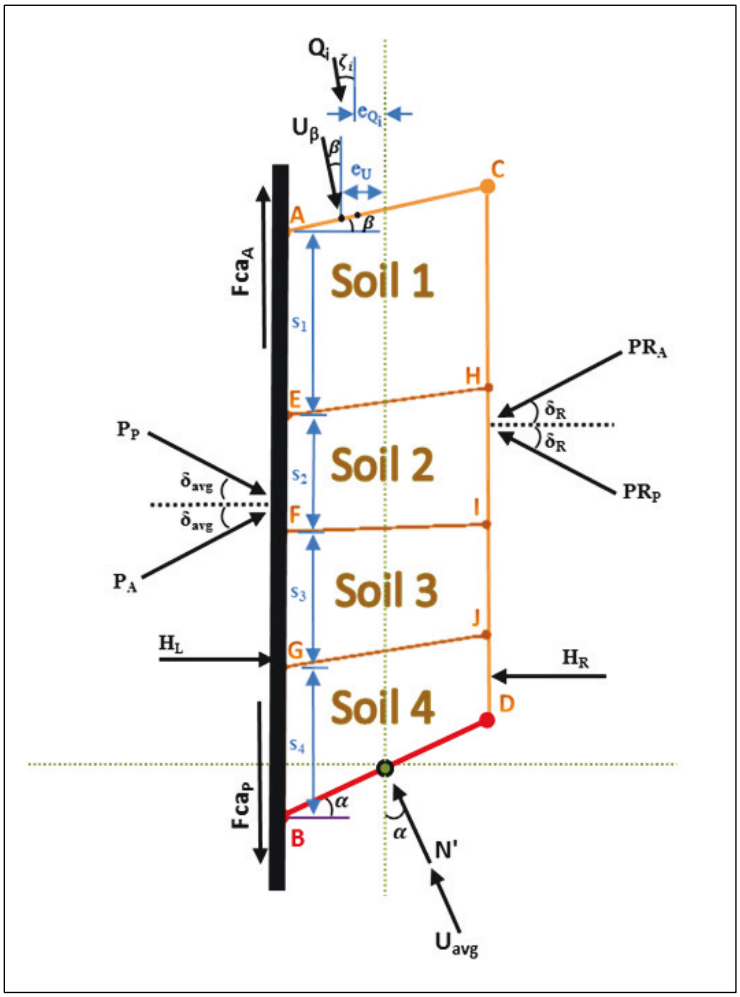
According to Figure G.9, the interslice friction force at any soil wedge interslice up to a distance of 0.3 times x_L will be assigned an interslice friction angle of δ_{max}, where δ_{max} is the interslice friction at the wall. For interslices located beyond a distance of 0.3 times x_L, the value of δ will be less than δ_{max}, by the linearly decreasing relationship with normalized distance given in Figure G.9. The interslice friction at the wall δ_{max} is set equal to the mobilized interface shear friction as discussed in Chapter 2.

An extensive series of parametric studies were conducted as part of this research effort to determine an appropriate distribution for normalized interslice friction distribution versus normalized distance from the wall. The results from this study are summarized in Appendix H. Chapter 3 presents the recommended distribution as a user default when discussing this GUI input selection.

G.3.2 The *generalized limit equilibrium method* relationships for P_L for the soil wedge 1 interslice face at the wall

Figure G.10 shows the forces acting on wedge 1, including the wall-to soil interslice adhesion force. Note that although both active and passive resultant forces are shown in in Figure G.10, they do not act concurrently on the same soil wedge.

Figure G.10 Forces acting on the multilayed soil wedge 1 adjacent to the wall.



Passive: The passive wedge interslice forces include the LHS passive soil wedge force $\boldsymbol{P_P}$, the adhesion force $\boldsymbol{F_{CaP}}$, and the RHS passive soil wedge force $\boldsymbol{PR_P}$. All other weight and boundary water forces are the same as first introduced using the generalized passive soil wedge of Figure G.5.

Active: Similarly, the Figure G.10 active wedge interslice forces would include the LHS active soil wedge force $\boldsymbol{P_A}$, the adhesion force $\boldsymbol{F_{CaA}}$ and

the RHS passive soil wedge force $\boldsymbol{PR_A}$. All other weight and boundary water forces are the same as first introduced using the generalized active soil wedge of Figure G.6.

For a soil wedge containing layered soils, average soil properties are used in the ordinary method of slices soil wedge formulation. The average wall to soil interslice friction angle is

$$\delta_{avg} = \frac{\sum(\delta'_{mob_i}\ s_i)}{\sum s_i} \tag{G.14}$$

with

i = 1 to 4
δ'_{mob_i} = mobilized wall to soil friction
s_i = height of soil layer

Similarly, the average wall to soil adhesion force is

$$Fca = \sum\left(ca'_{mob_i}\ s_i\right) \tag{G.15}$$

with

i = 1 to 4
ca'_{mob_i} = effective mobilized adhesion

For the passive soil wedge 1 formulation, the LHS passive force at the wall is given by

$$P_P = \frac{\left\{\begin{array}{c} PR_P\left[cos(\delta_R+\alpha)-sin(\delta_R+\alpha)\tan\phi'_{mob}\right] \\ +\left[c'_{mob}\ b\sec\alpha + \mathrm{W}\sin\alpha + \left(W\cos\alpha - U_{avg}\right)\tan\phi'_{mob}\right] \\ -\left(H_L - H_R\right)\left[\cos\alpha - \sin\alpha\ \tan\phi'_{mob}\right] \\ +U_\beta\left[\cos(\beta-\alpha)\ \tan\phi'_{mob} - \sin(\beta-\alpha)\right] \\ +Q\left[\cos(\zeta-\alpha)\ \tan\phi'_{mob} - \sin(\zeta-\alpha)\right] \\ +Fca_P\left[\cos(\alpha)\ \tan\phi'_{mob} + \sin(\alpha)\right] \end{array}\right\}}{cos(\delta_{avg}+\alpha)-sin(\delta_{avg}+\alpha)\tan\phi'_{mob}} \tag{G.16}$$

with

$$h_1 = \frac{\left\{\begin{array}{c} PR_P\ \cos(\delta_R)\left[h_2 + \frac{b}{2}[\tan(\delta_R) + \tan\alpha]\right] \\ -\ U_\beta \cos\beta(h_5 \tan\beta - e_U) \\ -\ Q\cos\zeta(h_6 \tan\zeta - e_Q) \\ -\ (H_L h_3 - H_R h_4) \\ +\ \frac{b}{2} Fca_P \end{array}\right\}}{P_P \cos(\delta_{avg})} + \frac{b}{2}\left[\tan(\delta_{avg}) + \tan\alpha\right] \quad \text{(G.17)}$$

and

$$N' = \begin{bmatrix} P_P \sin(\delta_{avg} + \alpha) - PR_P \sin(\delta_R + \alpha) \\ +\ H_L \sin\alpha - H_R \sin\alpha + W\cos\alpha\ - U_{avg} \\ +U_\beta \cos(\beta - \alpha) + Q\cos(\zeta - \alpha) + Fca_P \cos\alpha \end{bmatrix} \quad \text{(G.18)}$$

Similarly, for the active soil wedge 1 formulation, the LHS active force at the wall is given by

$$P_A = \frac{\left\{\begin{array}{c} PR_A[cos(\delta_R - \alpha) - sin(\delta_R - \alpha)\tan\phi'_{mob}] \\ -\ [c'_{mob}\ b\sec\alpha - W\sin\alpha + (W\cos\alpha - U_{avg})\ \tan\phi'_{mob}] \\ -\ (H_L - H_R)\left[\cos\alpha + \sin\alpha\ \tan\phi'_{mob}\right] \\ -\ U_\beta[\cos(\beta - \alpha)\ \tan\phi'_{mob} + \sin(\beta - \alpha)] \\ -\ Q[\cos(\zeta - \alpha)\ \tan\phi'_{mob} + \sin(\zeta - \alpha)] \\ +\ Fca_A\left[\cos(\alpha)\ \tan\phi'_{mob} - \sin(\alpha)\right] \end{array}\right\}}{cos(\delta_{avg} - \alpha) - sin(\delta_{avg} - \alpha)\tan\phi'_{mob}} \quad \text{(G.19)}$$

with

$$h_1 = \frac{\left\{\begin{array}{c} PR_A\ \cos(\delta_R)\left[h_2 - \frac{b}{2}[\tan(\delta_R) - \tan\alpha]\right] \\ -\ U_\beta \cos\beta(h_5 \tan\beta - e_U) \\ -\ Q\cos\zeta(h_6 \tan\zeta - e_Q) \\ -\ (H_L h_3 - H_R h_4) \\ -\ \frac{b}{2} Fca_A \end{array}\right\}}{P_A\ \cos(\delta_{avg})} - \frac{b}{2}\left[\tan(\delta_{avg}) - \tan\alpha\right] \quad \text{(G.20)}$$

and

$$N' = \begin{bmatrix} PR_A \sin(\delta_R - \alpha) - P_A \sin(\delta_{avg} - \alpha) \\ -\ H_L \sin\alpha + H_R \sin\alpha + W\cos\alpha - U_{avg} \\ +U_\beta \cos(\beta - \alpha) + Q\cos(\zeta - \alpha) -\ Fca_A\ \cos\alpha \end{bmatrix} \quad \text{(G.21)}$$

G.3.3 The *generalized limit equilibrium method* relationships for P_L for each soil wedge interslice face of soil wedges 2, 3, etc.

Passive: Figure G.5 shows the forces acting on passive wedge *i*, where *i* is greater than one. The passive wedge interslice forces include the LHS passive soil wedge force P_L, is given by

$$P_L = \frac{\left\{\begin{array}{c} P_R\left[cos(\delta_R+\alpha)-sin(\delta_R+\alpha)\tan\phi'_{mob}\right] \\ +\left[c'_{mob}\, b\sec\alpha + \mathrm{W}\sin\alpha + \left(W\cos\alpha - U_{avg}\right)\tan\phi'_{mob}\right] \\ -\left(H_L - H_R\right)\left[\cos\alpha - \sin\alpha\ \tan\phi'_{mob}\right] \\ +U_\beta\left[\cos(\beta-\alpha)\ \tan\phi'_{mob} - \sin(\beta-\alpha)\right] \\ +Q\left[\cos(\zeta-\alpha)\ \tan\phi'_{mob} - \sin(\zeta-\alpha)\right] \end{array}\right\}}{cos(\delta_L+\alpha)-sin(\delta_L+\alpha)\tan\phi'_{mob}} \qquad \text{(G.22)}$$

with

$$\mathrm{h}_1 = \frac{\left\{\begin{array}{c} P_R\ \cos(\delta_R)\left[h_2 + \frac{b}{2}\left[\tan(\delta_R)+\tan\alpha\right]\right] \\ -U_\beta\cos\beta\left(h_5\tan\beta - e_U\right) \\ -Q\cos\zeta\left(h_6\tan\zeta - e_Q\right) \\ -\left(H_L h_3 - H_R h_4\right) \end{array}\right\}}{P_L\cos(\delta_L)} + \frac{b}{2}\left[\tan(\delta_L)+\tan\alpha\right] \qquad \text{(G.23)}$$

and

$$\mathrm{N}' = \begin{bmatrix} \mathrm{P_L}\sin(\delta_\mathrm{L}+\alpha) - \mathrm{P_R}\sin(\delta_\mathrm{R}+\alpha) \\ +\mathrm{H_L}\sin\alpha - \mathrm{H_R}\sin\alpha + W\cos\alpha \\ +\mathrm{U}_\beta\cos(\beta-\alpha) + \mathrm{Q}\cos(\zeta-\alpha) - \mathrm{U_{avg}} \end{bmatrix} \qquad \text{(G.24)}$$

Recall that the LHS and RHS interslice force angle of frictions are varied with position among the soil wedges according to a relationship like that shown in Figure G.9.

Active: Figure G.6 shows the forces acting on active wedge *i*, where *i* is greater than one. The active wedge interslice forces include the LHS active soil wedge force $\mathrm{P_L}$, and is given by

$$P_L = \frac{\left\{\begin{array}{c} P_R\left[cos(\delta_R-\alpha)-sin(\delta_R-\alpha)\tan\phi'_{mob}\right] \\ -\left[c'_{mob}\, b\sec\alpha - \mathrm{W}\sin\alpha + \left(W\cos\alpha - U_{avg}\right)\tan\phi'_{mob}\right] \\ -\left(H_L - H_R\right)\left[\cos\alpha + \sin\alpha\ \tan\phi'_{mob}\right] \\ -U_\beta\left[\cos(\beta-\alpha)\ \tan\phi'_{mob} + \sin(\beta-\alpha)\right] \\ -Q\left[\cos(\zeta-\alpha)\ \tan\phi'_{mob} + \sin(\zeta-\alpha)\right] \end{array}\right\}}{cos(\delta_L-\alpha)-sin(\delta_L-\alpha)\tan\phi'_{mob}} \qquad \text{(G.25)}$$

with

$$h_1 = \frac{\left\{\begin{array}{c} P_R \cos(\delta_R)\left[h_2 - \frac{b}{2}[\tan(\delta_R) - \tan\alpha]\right] \\ - U_\beta \cos\beta(h_5 \tan\beta - e_U) \\ - Q\cos\zeta(h_6 \tan\zeta - e_Q) \\ - (H_L h_3 - H_R h_4) \end{array}\right\}}{P_L \cos(\delta_L)} - \frac{b}{2}\left[\tan(\delta_L) - \tan\alpha\right] \quad \text{(G.26)}$$

and

$$N' = \begin{bmatrix} P_R \sin(\delta_R - \alpha) - P_L \sin(\delta_L - \alpha) \\ - H_L \sin\alpha + H_R \sin\alpha + W\cos\alpha \\ +U_\beta \cos(\beta - \alpha) + Q\cos(\zeta - \alpha) - U_{avg} \end{bmatrix} \quad \text{(G.27)}$$

Again, the LHS and RHS interslice forces angle of friction are varied with position among the soil wedges according to a relationship similar to that shown in Figure G.9.

G.3.4 Solution of the *generalized limit equilibrium method* relationships for P_L for each LHS soil wedge interslice face for soil wedges 2 through 11

The equations given in the preceding sections in the form of recursive relationships for the variable interslice force inclination are used to compute the Figure G.10 passive resultant force P_P (or the active resultant force P_A) acting on the wall for the Figure G.3 problem with eleven wedges. The solution always starts with the farthest wedge from the wall (e.g., wedge eleven in Figure G.2), calculating the value of $P_{L\text{-}11}$ (Figure G.3). The value of $P_{R\text{-}11}$ is set equal to zero in this triangular shaped, last soil wedge. The next step is to apply $P_{L\text{-}11}$ as a known value, equal to $P_{R\text{-}10}$, on the right interslice face of soil wedge ten and solve for the LHS interface value of $P_{L\text{-}10}$. This sequential solution process proceeds back through each wedge and to soil wedge one for which the last calculation is made for the value of $P_{L\text{-}1}$ (=P_P) acting on the wall (Figure G.3). In an active force computation, the calculated $P_{L\text{-}1}$ force acting on soil wedge one is equal to P_A.

G.3.5 Numerically differentiate the distributions of passive P_P and active P_A wedge force solutions with depth to obtain the soil pressure distributions

Numerically differentiate the distribution of passive earth force values for the nodes at which these resultant forces were computed according to the equations given in Figure G.4, and then construct the corresponding passive earth pressure distribution at mid-node elevations. The Figure G.4 depiction illustrates this construction process using three idealized nodes.

G.4 The Corps_I-Wall Version 2.0 wedge sub-division procedure

This section provides a numerical definition of the slip plane which defines the soil mass. The slip plane is used to guide the wedge subdivision procedure which divides the soil mass above the slip plane. Each subwedge divided soil mass can then be examined with the equations of Subsections G.3.2 and G.3.3.

G.4.1 Slip planes

A slip plane describes the area of soil that contributes to forces acting on the wall. This area is comprised of all the soil above the slip plane to the ground surface.

G.4.1.1 Active slip planes

The active slip plane is described linearly. The linear slip plane adequately describes the slip surface for the sliding soil wedge moving toward the I-wall. In this case, for the elevation point on the wall where the active soil contribution of force is measured, a line with constant slope from that point to the surface defines the plane. This procedure works the same for uneven and sloped soil surfaces as it does for horizontal soil surfaces. Corps_I-Wall Version 2.0 allows for slip planes with small angles from the horizontal by extending the material regions at the furthest horizontal extent. These outside boundary regions keep the same elevations and material properties, but are extended for a long distance from the wall.

G.4.1.2 Passive slip planes

The passive slip plane is described with a log-spiral curve (Figure G.1). Geotechnical studies have shown that when the value of wall to soil interface friction is greater than one-half the angle of soil friction (Table 1.1),

a log-spiral spiral based slip surface definition provides a better estimate for the passive earth force than a (Coulomb) solution based on the assumption of a planar slip surface (Section 2.3.5; subsection 3.3.4.1 in Ebeling and Morrison 1992). Due to interslice friction effects, the affected soil will sometimes progress to a deeper depth than the wall and then will slope back to the surface.

The log-spiral curve is described by the equation in Figure G.1. This equation requires three inputs, the "center" point of the spiral, the radius at the wall, and a growth rate parameter.

Since the log-spiral curve can develop severe slopes that the soil properties will not allow (because it is not a one-to-one mathematical function), it is necessary to provide slope constraints to the slip plane based on log-spiral curves. An advancing front log-spiral solution method that starts with a node at the wall is used Corps_I-Wall Version 2.0.

For a specified step-size X distance, the log-spiral Y elevation is calculated. If the resulting line from the previous point to the new, log-spiral point does not intersect the ground surface or exceed the downslope or upslope angle as described in Section G.6, the log-spiral point is added to the slip-plane piecewise linear curve (PLC), and the radius for the log-spiral is replaced with the distance from the log-spiral "center" point to the new log-spiral point.

If the line from the previous point to the new, log-spiral point intersects the ground surface, then the point of intercept between the new line and the ground surface is calculated. This point is added to the PLC and the advancing front algorithm is concluded.

If the resulting line from the previous point to the new, log-spiral point exceeds the downslope angle (Section G.6), then the next point is computed at the same x distance using the constraining slope angle, and that downslope computed point is added to the PLC. The radius of the log-spiral is then set to the distance from the "center" point to the newly created point.

If the resulting line from the previous point to the new, log-spiral point exceeds the upslope angle (Section G.6), then the next point is computed by finding the intercept of the ray extending from the previous point at the

upslope angle with the ground surface. This point is then added to the slip-plane PLC and the advancing front algorithm is concluded.

G.4.2 Dividing the slip plane soils into wedges and sub-wedges

Once a slip plane has been determined, the area determined by the slip plane has to be broken up into vertical wedges and the material region sub-wedges that make up each vertical wedge. The same procedure is performed for either active (linear) or passive (log-spiral) slip planes.

The algorithm requires the following three initial parameters that are determined by the software: the maximum wedge width for downslope (W_{DMax}), the maximum wedge width for upslope (W_{UMax}), and a minimum wedge width (W_{min}). These values are determined by using the distance from the wall to the slip plane intercept with the ground surface in the software. First, the W_{min} establishing a minimal value as a relationship between the slip plane angle (α) approaching the ground surface, and the distance from the wall to the ground surface intercept or a tolerance value, whichever is less.

W_{DMax} is determined using a fraction of the distance to the deepest part of the slip plane from the wall or W_{min}, whichever is greater. W_{UMax} is determined using a fraction of the distance of the slip plane ground surface intercept from the wall or W_{min}, whichever is greater.

Downslope and upslope are determined by the minimum elevation point of the slip-plane PLC. The downslope region exists between the wall and the minimum elevation point of the slip-plane PLC. Since the downslope part of the curve has more wall interaction (using delta curves), W_{DMax} is smaller than W_{UMax}. The upslope region exists between the minimum elevation point of the slip-plane PLC and the ground surface. Since active slip-planes start with the minimum elevation point of the slip-plane PLC at the wall, the active slip-planes do not have a downslope region. The purpose of all three parameters will be described later.

The first step in dividing the area into wedges is to form a priority list of X-location boundary conditions within the slip plane. The first two boundary locations entered are the X locations of the start and end point of the slip plane. All other boundary locations will be between those two primary locations. The next most important locations are X locations for every region point above the slip plane. The next most important locations are,

for regions that use a piezometric surface, the piezometric surface locations that exist INSIDE that region and intersections between that piezometric surface and the region boundaries. Of course, only the piezometric *X* locations for points above the slip plane are put in the list.

Once all these *X* locations have been entered in the list, the lowest priority points are added. These points are for distances between *X* locations that exceed W_{DMax} or W_{UMax}. If either of the *X* locations in the list exists on the downslope portion of the slip-plane PLC and exceed W_{DMax}, the number of points between those locations is determined by

$$Np = ceil\left(\frac{X[i]-X[i-1]}{W_{DMax}}\right) \tag{G.28}$$

The actual *X* interval between the new points is given by

$$Xd = \frac{X[i]-X[i-1]}{Np} \tag{G.29}$$

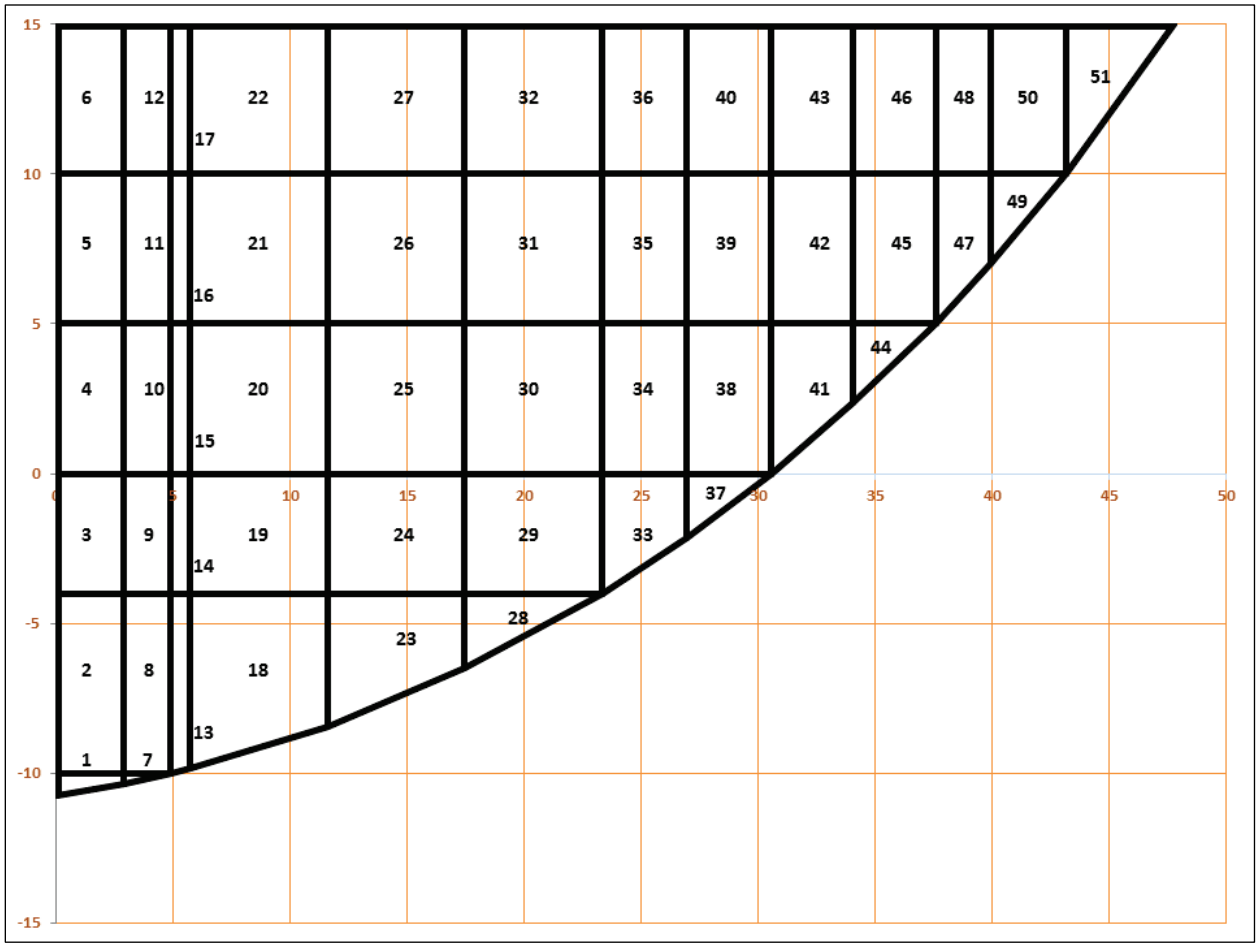
Points are added to the priority list at this interval starting at *X[i-1]* and proceeding to *X[i]* linearly.

Once all of these points have been entered, the resulting locations must be culled, as some of the location distances may be less than W_{min}. Proceeding from the wall (in a positive direction for slip planes on the right hand side of the wall and negative direction for the LHS), each location distance to the next location is tested to see if it meets the W_{min} constraint. If the distance is less than W_{min}, then one of the locations is removed. If one of the locations has a lower priority than the other, then that location is removed, else the location closest to the wall is removed.

When the *X*-location priority list is completed, wedges are determined. The wedges are numbered proceeding from the wall. A wedge is defined by four points (in counter-clockwise order). The first point is given by *X[i]* and the *Y*-location on the slip-plane PLC for *X[i]*. The second point is given by *X[i+1]* and the *Y*-location on the slip-plane PLC for *X[i+1]*. The third point is given by *X[i+1]* and the *Y*- location on the ground surface PLC for *X[i+1]*. The fourth point is given by *X[i]* and the *Y*-location on the ground surface PLC for *X[i]*.

Each wedge is further divided into sub-wedges in the same vertical column (Figure G.11). The subwedges are determined by finding the intersecting lines of the regions that cross the vertical column, within a tolerance and bounded by the ground and slip-plane surfaces. If a piezometric region intercepts its region, then that piezometric line intercepts with the vertical column to divide the wedge further. One last split occurs for active regions depending on the depth of gapping. Once all the subwedge geometries are defined, the centroid of the subwedge is used to assign a region ID to the subwedge and whether the region is saturated or not.

Figure G.11 Sub-Wedge definition used for Example 4.4 in Chapter 4.



G.5 The soil region based, nodal division method

The soil region-based, nodal division method is used to define points where earth forces determined by the Wedge Solution Method will be collected along the wall, therefore, accurate pressures can be derived acting along the wall. The selection of force collection points has to be performed in a way to measure the rate of change (in force) caused by the

earth as it acts against the wall, with lesser effect the further the soil is away from the wall. The results of this nodal division method should be found to adequately characterize the distribution of passive earth force with depth.

Because the forces are given by the Wedge Solution Method, the first point for force computation is at the soil top minus the unit depth (feet or meters). This first depth allows enough soil that the method of slices of the Wedge Solution Method can determine the force acting on the wall for that section. After this node has been created, the primary locations where forces show the most change along the wall are at the boundary locations between soil regions that are touching the wall. Each of these boundary locations are added as nodes for force determination. For regions that touch the wall, and have a piezometric surface that touches the wall between the top and bottom of where the region meets the wall, a node is added at the point where the piezometric surface touches the wall. The deepest node is placed at the tip of the wall.

All of these nodes will collect forces acting at the region and piezometric interfaces with the wall, however, they are not enough to catch the sometimes sudden changes caused by the change of soil properties above and below the region and piezometric boundaries. In order to gather this data, nodes are also added within the node ranges already selected.

When more points are gathered between the already selected nodes, the trends of the material effect on forces can be more accurately modeled. To model immediate changes between regions, two step sizes are specified by the Corps_I-Wall software. The first step size (Estep1) is 0.25 unit depth. This size allows for seeing the fine change at the border between regions at the wall. The second step size (Estep2) is 0.75 unit depth. This value allows for the settling of the rate of change of the material along the wall, because the creation of the wedges may lead to small errors in calculation.

These step sizes (Estep1 and Estep2) are used with the existing nodes to determine how nodes are added to subdivide the existing boundaries. For each pair of nodes that exist, starting at the top-most node, and the one immediately below, and incrementing until the bottom-most node ends the pair, nodes are added to subdivide the range based on the distance between the pair of nodes.

If the distance between the nodal pair is less than Estep1*2.0, then two nodes are added that trisect the range between the nodal pair. This guarantees the enough nodes to catch the material effects in the region touching the wall, though the nodes are less than Estep1 distance apart.

Otherwise, if the distance between the nodal pair is less than Estep2*2.0, then the nodal pair range is broken into four parts using three additional nodes. The first node is placed at top node depth minus Estep1 for gathering the material effect on force of the region touching the wall. A bisecting node is placed centered between the nodal pair top node and bottom node to collect the effects of the regions acting away from the wall. The last node is placed at the bottom node depth plus Estep1 to capture the final material effect within the region touching the wall before the next region begins.

The case where the distance between the nodal pair exceeds both Estep1*2.0, and Estep2*2.0 is the most accurate, having six subdivisions using five additional nodes. The first additional node is placed at the top-most node depth + Estep1 for the same reasons cited above. The second additional node is placed at the top-most node depth + Estep2 to account for numerical errors caused by the creation of wedges in the Wedge Solution Method. A central node is added to capture the effect of regions away from the wall. The fourth additional node is placed at the bottom-most node depth - Estep2 for much the same reason as the second node for this set. The fifth additional node is placed at the bottom-most node depth - Estep1 for the same reasons cited for the last node of the previous condition.

The soil region-based, nodal division method provides a way to gather forces that can be derived to generate a piecewise linear pressure curve acting along the wall, preserving the primary effect of soil regions that touch the wall, while still gathering the distilled effect of the regions that exist away from the wall and the slopes of all the soil regions.

G.6 Geometry restriction applied to passive soil wedges

Duncan et al. (2014) points out in Section 14.4 that problems can develop at the far end of the passive soil wedge for steep slip planes. This results when the resultant force along the base of any soil wedge is very close to the orientation of the interslice resultant force. In this case, the resultant force on the base of the wedge and the interslice force can become either very large or negative. This results in an indeterminate solution for P_A.

Corps_I-Wall deals with this limitation by restricting the steepness of the passive soil wedge.

There are two zones of concern, the first is with soil wedges close to the wall, and the second is for soil wedges that are furthest from the wall.

Near the wall, and relative to the elevation of the wall node, the first few soil wedges can be digging deeper into the soil mass. There is a concern about the steepness of the slip plane in this downward sloping region. Consequently, and through analysis of the resulting Corps_I-Wall wedge solution results, the slip plane is restricted to

$$\alpha_{max} < 85° - [\phi_{mob} + \delta_{mob}] \tag{G.30}$$

where α_{max} is reported as a positive value.

The second region of concern is identified in Figure G.2. The angle of the potential slip plane within this region that is located furthest from the wall is restricted to less than

$$\alpha_{max} < 45° - \frac{\phi_{mob}}{2} \tag{G.31}$$

The Corps_I-Wall Wedge Method uses the greater result from the equations G.30 and G.31 for the upward slope of the slip plane.

G.7 Appendix G List of symbols

N' = Effective Normal Force at base
Q = Surface Surcharge Force acting on top of slice
W = Weight of slice
U_{avg} = Water Force from average pore water pressure at midpoint at base
X_L = Shear Force at left side of slice
P_L = Interslice Force at left side of slice
E_L = Normal Interslice Force at left side of slice
δ_L = angle of interslice friction at left side of slice
h_1 = height from point B to E_L
h_3 = height from midpoint of base to H_L
h_5 = height from midpoint of base to top of slice where surface water forces act at an angle from the vertical
u = pore water pressure at a point on slice
U_β = Surface water force acting on top of slice
z = height from water pressure to point on slice
H_L = resultant force exerted by pore water at left side of slice interface
e_U = eccentricity of surface water force
θ_L = angle of PS on the left side of slice from the horizontal
γ_m= Moist unit weight of soil
Soil 1 = total stress layer with both γ_m
Soil 3 = total stress layer with γ_m
F_L = resultant force exerted by pore water pressures at nodes u at the left side of slice interface
d_L = height from midpoint slice base to force F_L at the left side of slice interface
PR_P = Passive interslice Force at right side of slice
P_P = Passive Force at I-Wall
Fca_P = Passive Adhesion Force at Wall to soil interface
s_1 = height from point E to point A
s_3 = height from point G to point H
ϕ'_{mob} = mobilized effective angle of internal friction along the wedge base
δ_{avg} = average wall friction angle
T_{mob} = Mobilized shear resistance at base
h = height (at midpoint) of slice
α = angle of base of slice from horizontal
b = width of slice
β = angle of top of slice from horizontal
X_R = Shear Force at right side of slice
P_R = Interslice Force at right side of slice
E_R = Normal Interslice Force at right side of slice
δ_R = angle of interslice friction at right side of slice
h_2 = height from point D to E_R
h_4 = height from midpoint of base to H_R
h_6 = height from midpoint of base to top of slice where surface surcharge forces act at an angle from the vertical
PS = Piezometric surfaces
ζ = angle of surface surcharge force from vertical at top of slice
H_R = resultant force exerted by pore water at right side of slice interface
e_Q = eccentricity of surface surcharge force
θ_R = angle of PS on the right side of slice from the horizontal
γ_s = saturated unit weight of soil
Soil 2 = effective stress layer with γ_s
Soil 4 = effective stress layer with γ_s
F_R = resultant force exerted by pore water pressures at nodes u at the right side of slice interface
d_R = height from midpoint slice base to force F_R at the right side of slice interface
PR_A = Active interslice Force at right side of slice
P_A = Active Force at I-Wall
Fca_A = Active Adhesion Force at Wall to soil interface
s_2 = height from point F to point E
s_4 = height from point B to point G
c'_{mob} = mobilized effective cohesion along the wedge base

*Factor of Safety is assumed to be the same at all points of the sliding plane

Appendix H: Benchmark Wedge Solution Method Analyses and Their Accuracy

In the Wedge Solution Method of analysis, the interslice friction acting on the left and right face of each of the individual Figure G.5 soil wedges comprising the soil mass must be specified. In a Corps_I-Wall Wedge Solution Method of analysis, the soil mass is typically defined by more than ten soil wedges (Figure G.4). The value for interslice friction δ' can be assigned any value between zero and ϕ' for each interslice. This appendix provides insight into an appropriate distribution of δ' values with distance among the soil wedges that results in an accurate passive earth force value computed at the wall by Corps_I-Wall. The investigation was carried out for a wide range of retained soil friction (ϕ') values.

Results from a series of Corps_I-Wall Wedge Solution Method analyses, and the computed passive earth force for a 20 ft. high granular fill are tabulated in this appendix. The computed values are also compared against what is considered a standard solution for this same passive earth pressure problem by the geotechnical profession. The standard solution uses the earth pressure Coefficient Method of analysis (presented in subsection 2.3.5) and specifically, the earth pressure coefficient given in Equation 2.39. Values for $K_{Passive}$, and the reduction factor R that are used in the standard solution, are tabulated in Tables 2.2 and 2.3. The percent difference between the standard solution results and the Wedge Solution Method computed results are also reported in the tables of results.

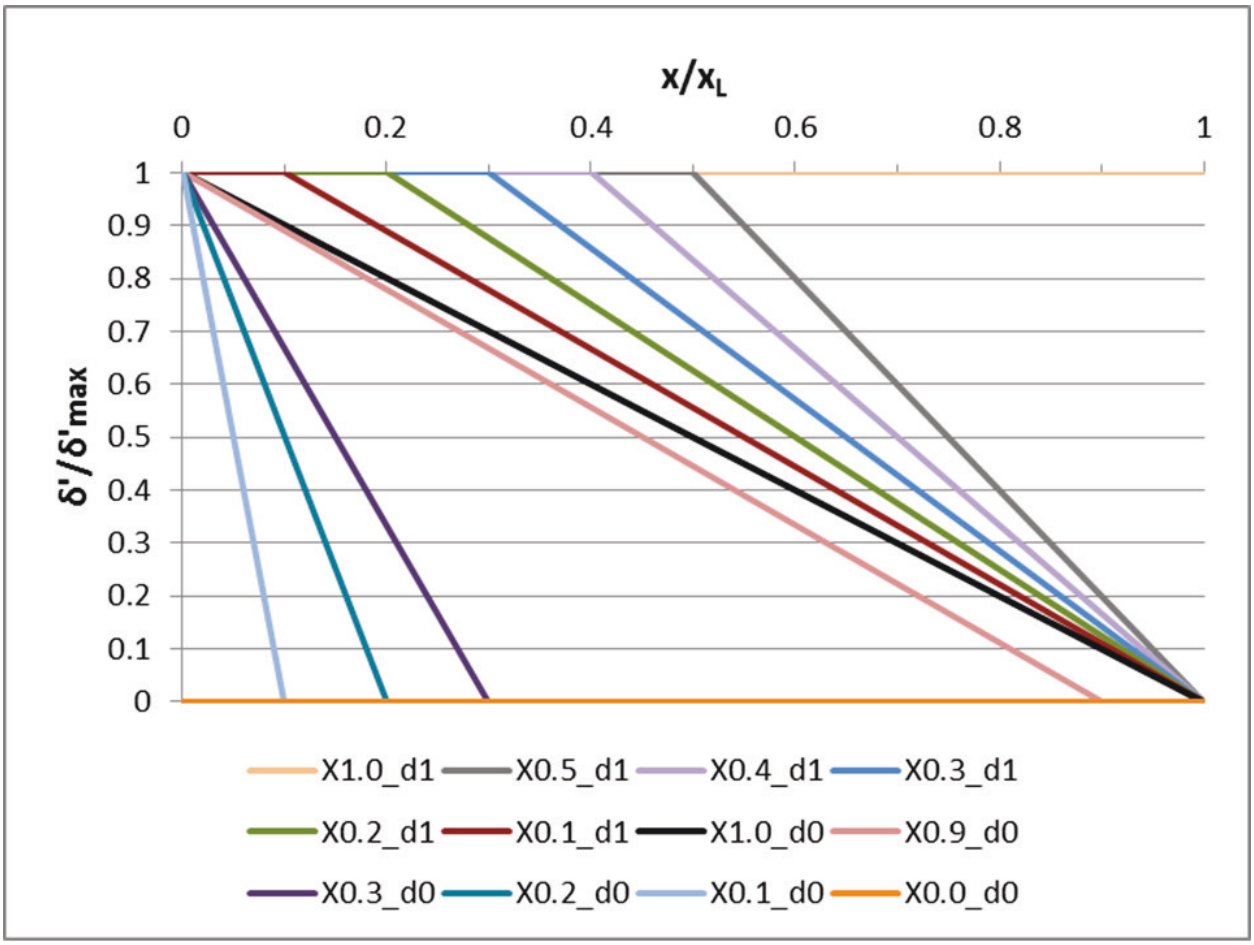
Six sets of analyses were made for the moist, cohesionless granular retained soil with ϕ' ranging from 20 to 45 degrees in five degree increments. For each set of analyses, the maximum interface friction value (at the wall) was varied from a value of δ' = 0 degrees to a value of $\delta' = \phi'$, in ten ($0.1*\phi'$) degree increments.

Note that a Factor of Safety equal to one is assigned in the calculations made in this appendix. This results in $\phi'_{mob} = \phi'$ by Equation 2.34.

Normalized interslice friction variation with distance from the wall Figure H.1 shows the various distributions of normalized interslice friction distribution that were used in the six sets of Wedge Solution

Method analyses. The objective of the investigation was to find which of the distributions result in a computed passive earth force value at the wall that comes closest to the standard passive force value over the wide range in values of ϕ', and wall friction δ', at the wall that were investigated. In this figure, x is the distance to each interslice and x_L is the lateral extent of the soil wedge, as measured from the wall. The Figure H.1 normalized plot is a convenient plot that scales to the interslice friction at the wall, and scales to the specific geometry of every logarithmically defined Figure G.4 potential soil wedge being investigated in the Corps_I-Wall analyses.

Figure H.1 Distributions describing the variation in interslice friction δ' normalized by the wall fiction δ'_{max} versus normalized distance along the passive soil wedges.



To transform the selected normalized interslice friction distribution to the logarithmic spiral defined slip plane being analyzed, the following transformation procedure is followed:

1. A trial slip plane is constructed by the Corps_I-Wall software, as discussed in Appendix G.

2. The lateral extent of the soil wedge as measured from the wall to where slip plane intersects the ground surface is determined (x_L).
3. The value for δ'_{max} is obtained from the user specified material property information for the retained soil. It is the value of interslice friction at the wall.
4. At each interslice distance x, the value of (x/x_L) is determined.
5. At each interslice normalized distance of (x/x_L), the value for (δ'/δ'_{max}) is obtained from the selected Figure H.1 distribution.
6. At each interslice distance x and corresponding normalized distance of (x/x_L), the interslice friction value, δ', is determined by Equation H.1.

For each interslice, δ' is obtained from the Figure H.1 normalized distribution using the relationship

$$\delta' = \left(\frac{\delta\prime}{\delta\prime_{max}}\right) * \delta'_{max} \quad \text{(H.1)}$$

H.1 Passive earth force values for a 20 ft high cohesionless sand with ϕ‘ = 20 degrees

The results of the Corps_I-Wall Wedge Solution Method analyses and error computations for all of the Figure H.1 normalized interslice friction distributions are summarized in Figures H.2 and H.3, respectively, for ϕ' equal to 20 degrees. The Figure H.3 horizontal axis is the value for interface friction at the wall, divided by the friction value of the retained soil. The data shows that the normalized interslice friction distribution designated as X0.3_d0 provides for the minimum passive force error over the widest range in δ' (at the wall) and ϕ' values of all the Figure H.1 distributions that were investigated. For this normalized distribution, the value of (δ'/δ'_{max}) is equal to 1.0 at (x/x_L) equal to zero. The distribution decreases linearly with distance to a value for (δ'/δ'_{max}) equal to zero at (x/x_L) equal to 0.3. The value of (δ'/δ'_{max}) is maintained at a value of zero from (x/x_L) equal to 0.3 to a value of 1.0.

Figure H.2 Values of passive earth force by the Wedge Solution Method, standard solution, and the corresponding errors (in percent), for ϕ' equal to 20 degrees.

| | | |

H.2 Passive earth force values for a 20 ft. high cohesionless sand with ϕ' = 25 degrees

The results of the Corps_I-Wall Wedge Method analyses and error computations for all of the Figure H.1 normalized interslice friction distributions are summarized in Figures H.4 and H.5, respectively, for ϕ' equal to 25 degrees. The data shows that the normalized interslice friction distribution designated as X0.3_d0 provides for the minimum passive force error over the widest range in δ' and ϕ' values of all the Figure H.1 distributions that were investigated.

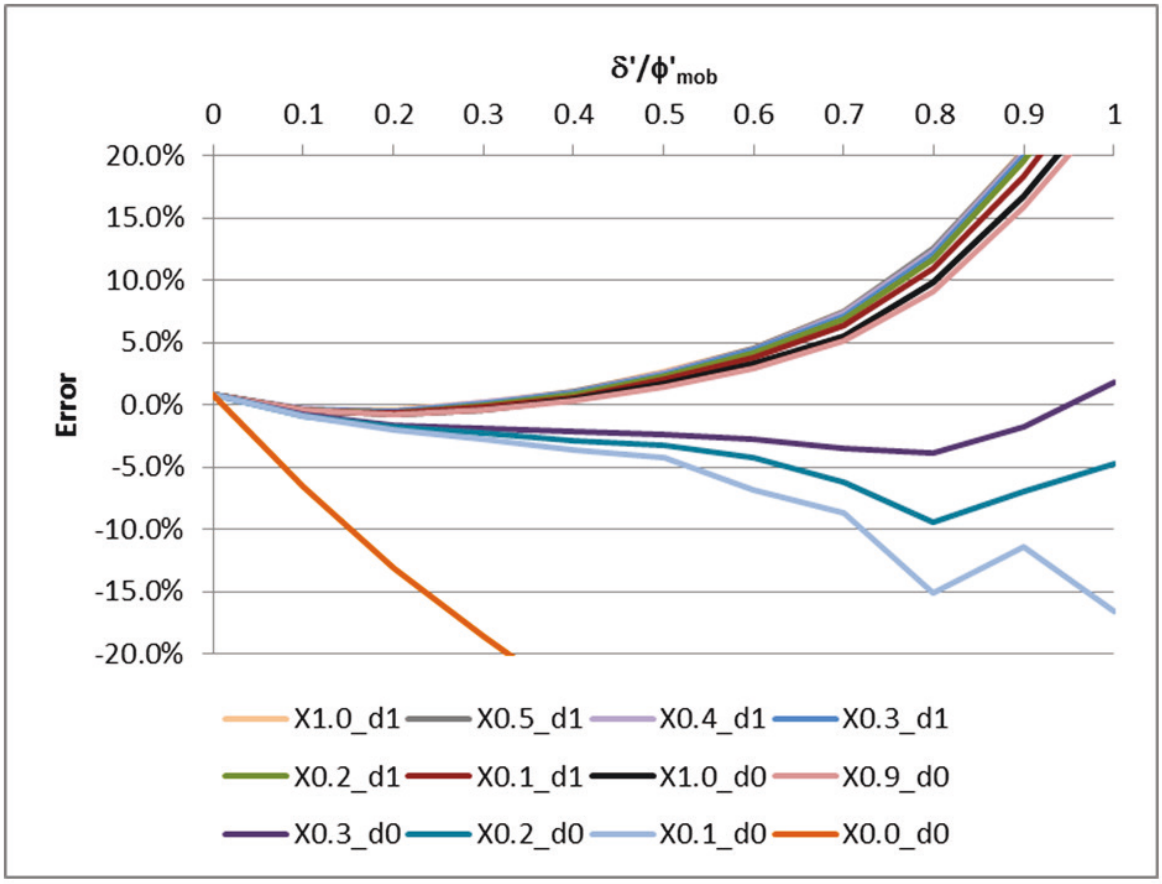
Figure H.4 Values of passive earth force using the Wedge Solution Method, and the standard solution and corresponding errors (in percent), for ϕ' equal to 25 degrees.

ϕ'_{mob}	25														
γ_{moist}	122				Passive Force (Pp)										
depth	10				Rankine	Corps I-Wall curves									
$K_{passive}$	4.29			δ'/ϕ'_{mob}	0	0.1	0.2	0.3	0.4	0.5	0.6	0.7	0.8	0.9	1
curves	axis	pt1	pt2	pt3	15029.87	16224.78	17428.6	18606	19862.3	21144.6	22505.3	23866.1	24965.2	25645.6	26169
X1.0_δ1	x/xL	0	0.5	1	15147.76	16158.66	17349.1	18633	20083.3	21702.5	23533.5	25638.9	28059.3	30879.4	34199.5
	δ/δmax	1	1	1	0.8%	-0.4%	-0.5%	0.1%	1.1%	2.6%	4.6%	7.4%	12.4%	20.4%	30.7%
X0.5_δ1	x/xL	0	0.5	1	15147.76	16153.12	17337.2	18627	20068.5	21683.4	23524.1	25652.5	28080.6	30858.6	34205.6
	δ/δmax	1	1	0	0.8%	-0.4%	-0.5%	0.1%	1.0%	2.5%	4.5%	7.5%	12.5%	20.3%	30.7%
X0.4_δ1	x/xL	0	0.4	1	15147.76	16167.05	17338.1	18632	20053.7	21675.2	23501.5	25613.2	28027.6	30831.8	34115.7
	δ/δmax	1	1	0	0.8%	-0.4%	-0.5%	0.1%	1.0%	2.5%	4.4%	7.3%	12.3%	20.2%	30.4%
X0.3_δ1	x/xL	0	0.3	1	15147.76	16151.35	17325.6	18613	20047.7	21650.1	23481.4	25567.5	27965.3	30753.1	34020.9
	δ/δmax	1	1	0	0.8%	-0.5%	-0.6%	0.0%	0.9%	2.4%	4.3%	7.1%	12.0%	19.9%	30.0%
X0.2_δ1	x/xL	0	0.2	1	15147.76	16153.45	17311	18599	20018.3	21620.7	23440.7	25504.8	27870.2	30652.5	33812.6
	δ/δmax	1	1	0	0.8%	-0.4%	-0.7%	0.0%	0.8%	2.3%	4.2%	6.9%	11.6%	19.5%	29.2%
X0.1_δ1	x/xL	0	0.1	1	15147.76	16145.18	17302.4	18570	19982.8	21572.5	23357.6	25381.6	27692.4	30349.1	33442.8
	δ/δmax	1	1	0	0.8%	-0.5%	-0.7%	-0.2%	0.6%	2.0%	3.8%	6.3%	10.9%	18.3%	27.8%
X1.0_δ0	x/xL	0	0.5	1	15147.76	16159.21	17291.5	18537	19941	21494.4	23234.8	25189.5	27404.7	29931.8	32833.1
	δ/δmax	1	0.5	0	0.8%	-0.4%	-0.8%	-0.4%	0.4%	1.7%	3.2%	5.5%	9.8%	16.7%	25.5%
X0.9_δ0	x/xL	0	0.9	1	15147.76	16153.17	17279.7	18521	19917	21456	23169.2	25077.9	27244.9	29705.4	32527.9
	δ/δmax	1	0	0	0.8%	-0.4%	-0.9%	-0.5%	0.3%	1.5%	2.9%	5.1%	9.1%	15.8%	24.3%
X0.3_δ0	x/xL	0	0.3	1	15147.76	16101.25	17146.6	18255	19426.3	20647.5	21889.7	23020	23995.1	25184.6	26632
	δ/δmax	1	0	0	0.8%	-0.8%	-1.6%	-1.9%	-2.2%	-2.4%	-2.7%	-3.5%	-3.9%	-1.8%	1.8%
X0.2_δ0	x/xL	0	0.2	1	15147.76	16084.95	17115.3	18175	19287.2	20443	21549.4	22377.5	22620.2	23865.3	24935.2
	δ/δmax	1	0	0	0.8%	-0.9%	-1.8%	-2.3%	-2.9%	-3.3%	-4.2%	-6.2%	-9.4%	-6.9%	-4.7%
X0.1_δ0	x/xL	0	0.1	1	15147.76	16067.33	17069.7	18092	19149.4	20249.5	20953.2	21777.9	21192.2	22711	21827.4
	δ/δmax	1	0	0	0.8%	-1.0%	-2.1%	-2.8%	-3.6%	-4.2%	-6.9%	-8.7%	-15.1%	-11.4%	-16.6%
X0.0_δ0	x/xL	0	0.5	1	15147.76	15147.76	15147.8	15148	15147.8	15147.8	15147.8	15147.8	15147.8	15147.8	15147.8
	δ/δmax	0	0	0	0.8%	-6.6%	-13.1%	-18.6%	-23.7%	-28.4%	-32.7%	-36.5%	-39.3%	-40.9%	-42.1%

	reduction factor	
δ'_{max}	δ'/ϕ'_{mob}	$R(\delta',\phi')$
25	1	1
22.5	0.9	0.980
20	0.8	0.954
17.5	0.7	0.912
15	0.6	0.86
12.5	0.5	0.808
10	0.4	0.759
7.5	0.3	0.711
5	0.2	0.666
2.5	0.1	0.62
0	0	0.574

ϕ	Kp (δ/ϕ=1)
0	1
5	1.28
10	1.64
15	2.19
20	3.01
25	4.29
30	6.42
35	10.2
40	17.5
45	33.5
50	74.3
51	90
52	110
53	130
54	160
55	204
60	782

Figure H.5 Difference in percent between values of passive earth force using the Wedge Solution Method, including standard solution as a function of δ' at the wall, for ϕ' equal to 25 degrees.



H.3 Passive earth force values for a 20 ft high cohesionless sand with ϕ'=30 degrees

The results of the Corps_I-Wall Wedge Solution Method analyses and error computations for all of the Figure H.1 normalized interslice friction distributions are summarized in Figures H.6 and H.7, respectively, for ϕ' equal to 30 degrees. The data shows that the normalized interslice friction distribution designated as X0.3_d0 provides for the minimum passive force error over the widest range in δ' and ϕ' values of all the Figure H.1 distributions that were investigated.

Figure H.6 Values of passive earth force using the Wedge Solution Method including standard solution and corresponding errors (in percent), for ϕ' equal to 30 degrees.

| | | |

H.4 Passive earth force values for a 20 ft high cohesionless sand with ϕ'=35 degrees

The results of the Corps_I-Wall Wedge Solution Method analyses and error computations for all of the Figure H.1 normalized interslice friction distributions are summarized in Figures H.8 and H.9, respectively, for ϕ' equal to 35 degrees. The data shows that the normalized interslice friction distribution designated as X0.3_d0 provides for the minimum passive force error over the widest range in δ' and ϕ' values of all the Figure H.1 distributions that were investigated.

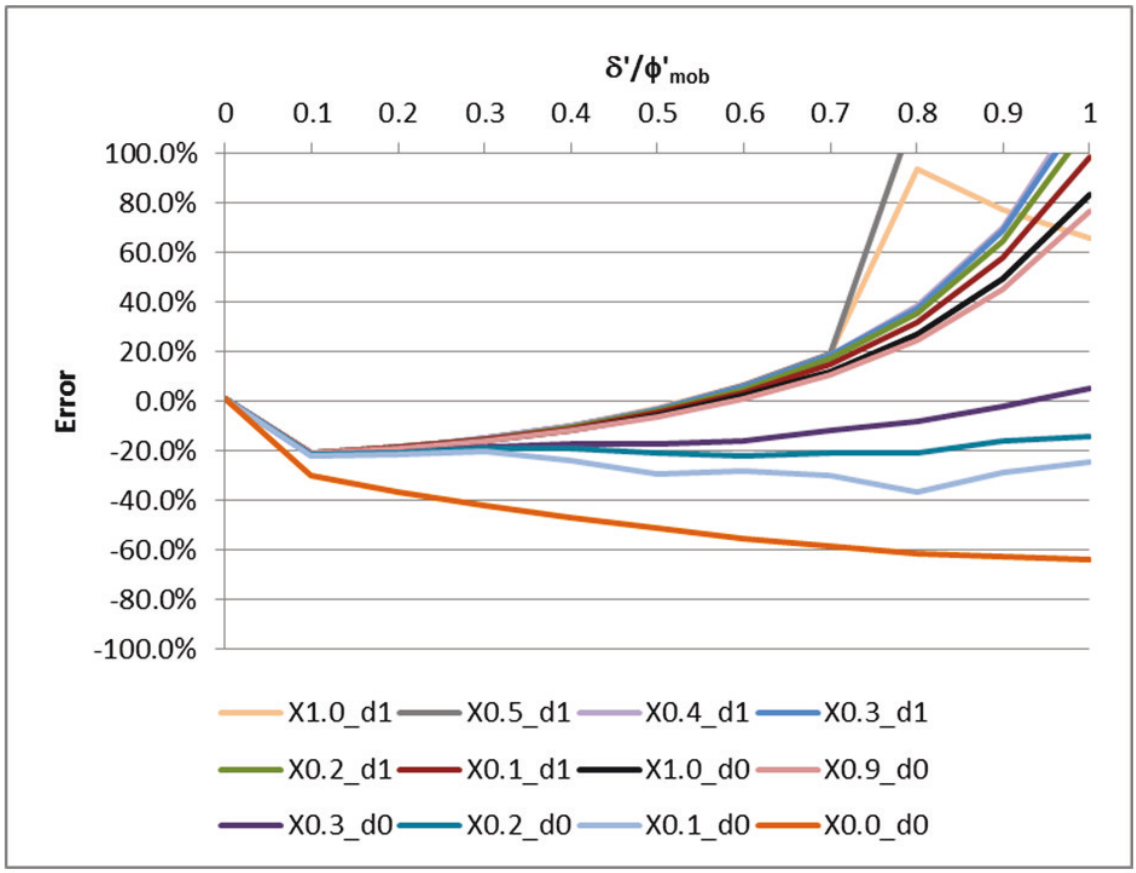
Figure H.8 Values of passive earth force using the Wedge Solution Method, including standard solution and corresponding errors (in percent), for ϕ' equal to 35 degrees.

ϕ'_{mob}	35														
γ_{mat}	122				Passive Force (Pp)										
depth	10				Rankine	Corps I-Wall curves									
$K_{Passive}$	10.2			δ'/ϕ'_{mob}	0	0.1	0.2	0.3	0.4	0.5	0.6	0.7	0.8	0.9	1
curves	axis	pt1	pt2	pt3	22510.05	32354.4	35714.3	39012	42682.9	46416.1	50460.4	54629.2	58300.1	60975.6	62220
X1.0_δ1	x/xL	0	0.5	1	22682.67	25609.42	29035.8	33191	38459.1	45073.4	53654.2	65252.4	112758	108078	102994
	δ/δmax	1	1	1	0.8%	-20.8%	-18.7%	-14.9%	-9.9%	-2.9%	6.3%	19.4%	93.4%	77.2%	65.5%
X0.5_δ1	x/xL	0	0.5	1	22682.67	25584.46	28991.1	33163	38361.1	44988	53628	65204.5	127703	137302	140823
	δ/δmax	1	1	0	0.8%	-20.9%	-18.8%	-15.0%	-10.1%	-3.1%	6.3%	19.4%	119.0%	125.2%	126.3%
X0.4_δ1	x/xL	0	0.4	1	22682.67	25567.85	29048.3	33171	38397	44941.2	53571	64913.6	80796.1	103812	139167
	δ/δmax	1	1	0	0.8%	-21.0%	-18.7%	-15.0%	-10.0%	-3.2%	6.2%	18.8%	38.6%	70.3%	123.7%
X0.3_δ1	x/xL	0	0.3	1	22682.67	25570	29269.8	33112	38288.3	44832.1	53315	64637	80246.1	102846	136954
	δ/δmax	1	1	0	0.8%	-21.0%	-18.0%	-15.1%	-10.3%	-3.4%	5.7%	18.3%	37.6%	68.7%	120.1%
X0.2_δ1	x/xL	0	0.2	1	22682.67	25705.83	29164.8	33053	38235.2	44644.2	52949.9	63956.2	78996.2	100387	131842
	δ/δmax	1	1	0	0.8%	-20.5%	-18.3%	-15.3%	-10.4%	-3.8%	4.9%	17.1%	35.5%	64.6%	111.9%
X0.1_δ1	x/xL	0	0.1	1	22682.67	25663.44	29057.6	32999	38023.2	44265	52338	62809.2	76837.2	96151.5	123343
	δ/δmax	1	1	0	0.8%	-20.7%	-18.6%	-15.4%	-10.9%	-4.6%	3.7%	15.0%	31.8%	57.7%	98.2%
X1.0_δ0	x/xL	0	0.5	1	22682.67	25502.81	28946	32904	37720.3	43845.2	51446.1	61235.8	73951.4	90973	114014
	δ/δmax	1	0.5	0	0.8%	-21.2%	-19.0%	-15.7%	-11.6%	-5.5%	2.0%	12.1%	26.8%	49.2%	83.2%
X0.9_δ0	x/xL	0	0.9	1	22682.67	25587.01	28886	32804	37583.2	43553.5	50956.8	60387.6	72544	88598.4	109950
	δ/δmax	1	0	0	0.8%	-20.9%	-19.1%	-15.9%	-11.9%	-6.2%	1.0%	10.5%	24.4%	45.3%	76.7%
X0.3_δ0	x/xL	0	0.3	1	22682.67	25427.34	28325.3	31798	35318.6	38513.3	42546.2	48318.9	53451.7	59604.1	65400.1
	δ/δmax	1	0	0	0.8%	-21.4%	-20.7%	-18.5%	-17.3%	-17.0%	-15.7%	-11.6%	-8.3%	-2.2%	5.1%
X0.2_δ0	x/xL	0	0.2	1	22682.67	25370.52	28191.9	31589	34612.2	36820.1	39472.4	43248.5	46342.2	51192.2	53508
	δ/δmax	1	0	0	0.8%	-21.6%	-21.1%	-19.0%	-18.9%	-20.7%	-21.8%	-20.8%	-20.5%	-16.0%	-14.0%
X0.1_δ0	x/xL	0	0.1	1	22682.67	25311.69	28053.8	31114	32419.5	32730.7	36393.8	38487.1	36980	43426.1	47138.8
	δ/δmax	1	0	0	0.8%	-21.8%	-21.4%	-20.2%	-24.0%	-29.5%	-27.9%	-29.5%	-36.6%	-28.8%	-24.2%
X0.0_δ0	x/xL	0	0.5	1	22682.67	22682.67	22682.7	22683	22682.7	22682.7	22682.7	22682.7	22682.7	22682.7	22682.7
	δ/δmax	0	0	0	0.8%	-29.9%	-36.5%	-41.9%	-46.9%	-51.1%	-55.0%	-58.5%	-61.1%	-62.8%	-63.5%

	reduction factor	
δ'_{max}	δ'/ϕ'_{mob}	$R(\delta',\phi')$
35	1	1
31.5	0.9	0.98
28	0.8	0.937
24.5	0.7	0.878
21	0.6	0.811
17.5	0.5	0.746
14	0.4	0.686
10.5	0.3	0.627
7	0.2	0.574
3.5	0.1	0.52
0	0	0

ϕ	Kp (δ/ϕ=1)
0	1
5	1.28
10	1.64
15	2.19
20	3.01
25	4.29
30	6.42
35	10.2
40	17.5
45	33.5
50	74.3
51	90
52	110
53	130
54	160
55	204
60	782

Figure H.9 Difference in percent between values of passive earth force using the Wedge Solution Method, including the standard solution as a function of δ' at the wall, for ϕ' equal to 35 degrees.



H.5 Passive earth force values for a 20 ft high cohesionless sand with ϕ'=40 degrees

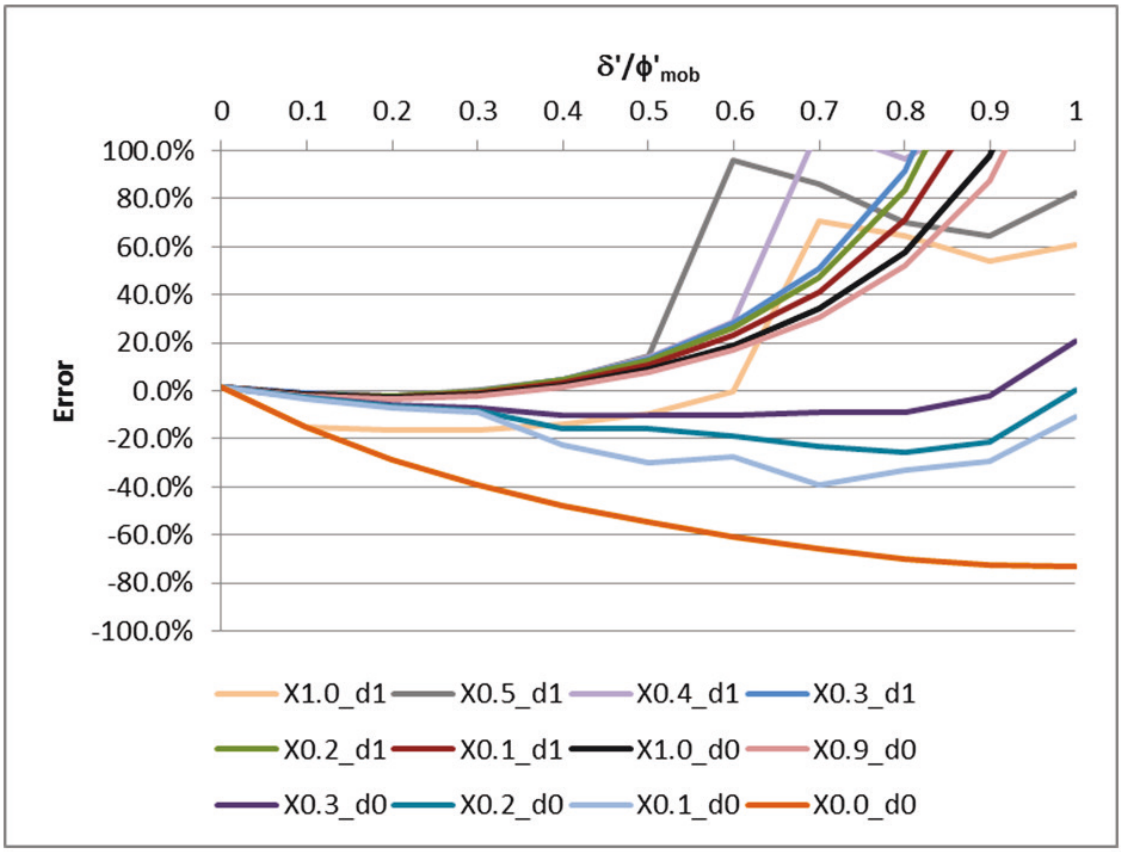
The results of the Corps_I-Wall Wedge Solution Method analyses and error computations for all of the Figure H.1 normalized interslice friction distributions are summarized in Figures H.10 and H.11, respectively, for ϕ' equal to 40 degrees. The data shows that the normalized interslice friction distribution designated as X0.3_d0 provides for the minimum passive force error over the widest range in δ' and ϕ' values of all the Figure H.1 distributions that were investigated when wall friction δ' is less than 0.9*ϕ'. Above this value, the data shows that the normalized interslice friction distribution designated as X0.2_d0 provides for the minimum passive force error.

Figure H.10 Values of passive earth force using the Wedge Solution Method, including the standard solution and corresponding errors (in percent), for ϕ' equal to 40 degrees.

ϕ'_{mob}	40														
γ_{mat}	122				Passive Force (Pp)										
depth	10				Rankine	Corps I-Wall curves									
$K_{Passive}$	17.5			δ/ϕ'_{mob}	0	0.1	0.2	0.3	0.4	0.5	0.6	0.7	0.8	0.9	1
curves	axis	pt1	pt2	pt3	28053.35	33733	40031.3	46863	54656	63196	72803.5	83585.3	94580.5	104615	106750
X1.0_δ1	x/xL	0	0.5	1	28552.09	28552.09	33511.3	39151	46929.6	57281.1	72395.9	142765	155418	161038	171796
	δ/δmax	1	1	1	1.8%	-15.4%	-16.3%	-16.5%	-14.1%	-9.4%	-0.6%	70.8%	64.3%	53.9%	60.9%
X0.5_δ1	x/xL	0	0.5	1	28552.09	33511.3	39151.3	46930	57281.1	72395.9	142765	155418	161038	171796	194707
	δ/δmax	1	1	0	1.8%	-0.7%	-2.2%	0.1%	4.8%	14.6%	96.1%	85.9%	70.3%	64.2%	82.4%
X0.4_δ1	x/xL	0	0.4	1	28552.09	33460.78	39073.3	46827	57361.2	72178.3	93848.6	175318	185728	228561	681558
	δ/δmax	1	1	0	1.8%	-0.8%	-2.4%	-0.1%	4.9%	14.2%	28.9%	109.7%	96.4%	118.5%	538.5%
X0.3_δ1	x/xL	0	0.3	1	28552.09	33389.44	39010.7	46770	57175.8	71718.1	93130.6	126070	181368	284816	513976
	δ/δmax	1	1	0	1.8%	-1.0%	-2.5%	-0.2%	4.6%	13.5%	27.9%	50.8%	91.8%	172.3%	381.5%
X0.2_δ1	x/xL	0	0.2	1	28552.09	33314.04	39086.8	46739	57179.2	71054.8	91753.4	122866	173611	264094	413504
	δ/δmax	1	1	0	1.8%	-1.2%	-2.4%	-0.3%	4.6%	12.4%	26.0%	47.0%	83.6%	152.4%	287.4%
X0.1_δ1	x/xL	0	0.1	1	28552.09	33238.24	38985.6	46555	56466.3	70048.6	89549.7	118058	162227	235648	346833
	δ/δmax	1	1	0	1.8%	-1.5%	-2.6%	-0.7%	3.3%	10.8%	23.0%	41.2%	71.5%	125.3%	224.9%
X1.0_δ0	x/xL	0	0.5	1	28552.09	33159.8	38855.1	46218	55750	68805.1	86551.1	112032	149416	206766	299208
	δ/δmax	1	0.5	0	1.8%	-1.7%	-2.9%	-1.4%	2.0%	8.9%	18.9%	34.0%	58.0%	97.6%	180.3%
X0.9_δ0	x/xL	0	0.9	1	28552.09	33114.74	38745.8	45995	55373.7	68037.5	85259.3	109296	143989	195872	276710
	δ/δmax	1	0	0	1.8%	-1.8%	-3.2%	-1.9%	1.3%	7.7%	17.1%	30.8%	52.2%	87.2%	159.2%
X0.3_δ0	x/xL	0	0.3	1	28552.09	32909.75	37694.8	43622	49248.8	56816.3	65566.5	76082.2	86178.8	102226	128812
	δ/δmax	1	0	0	1.8%	-2.4%	-5.8%	-6.9%	-9.9%	-10.1%	-9.9%	-9.0%	-8.9%	-2.3%	20.7%
X0.2_δ0	x/xL	0	0.2	1	28552.09	32787.85	37410	43111	46079.5	53100.5	59209.9	64041.9	70259.5	82222.8	106934
	δ/δmax	1	0	0	1.8%	-2.8%	-6.5%	-8.0%	-15.7%	-16.0%	-18.7%	-23.4%	-25.7%	-21.4%	0.2%
X0.1_δ0	x/xL	0	0.1	1	28552.09	32665.29	37127.5	42634	42432	44400.2	52666.2	51044.5	63428.2	74288.9	95030.5
	δ/δmax	1	0	0	1.8%	-3.2%	-7.3%	-9.0%	-22.4%	-29.7%	-27.7%	-38.9%	-32.9%	-29.0%	-11.0%
X0.0_δ0	x/xL	0	0.5	1	28552.09	28552.09	28552.1	28552	28552.1	28552.1	28552.1	28552.1	28552.1	28552.1	28552.1
	δ/δmax	0	0	0	1.8%	-15.4%	-28.7%	-39.1%	-47.8%	-54.8%	-60.8%	-65.8%	-69.8%	-72.7%	-73.3%

	reduction factor		ϕ	Kp (δ/ϕ=1)
δ'_{max}	δ'/ϕ'_{mob}	R(δ',ϕ')	0	1
40	1	1	5	1.28
36	0.9	0.980	10	1.64
32	0.8	0.886	15	2.19
28	0.7	0.783	20	3.01
24	0.6	0.682	25	4.29
20	0.5	0.592	30	6.42
16	0.4	0.512	35	10.2
12	0.3	0.439	40	17.5
8	0.2	0.375	45	33.5
4	0.1	0.316	50	74.3
0	0	0.282	51	90
			52	110
			53	130
			54	160
			55	204
			60	782

Figure H.11 Difference in percent between values of passive earth force using the Wedge Solution Method, including the standard solution as a function of δ' at the wall, for ϕ' equal to 40 degrees.



H.6 Passive earth force values for a 20 ft high cohesionless sand with ϕ'=45 degrees

The results of the Corps_I-Wall Wedge Solution Method analyses and error computations for all of the Figure H.1 normalized interslice friction distributions are summarized in Figures H.12 and H.13, respectively, for ϕ' equal to 45 degrees. The data shows that the normalized interslice friction distribution designated as X0.3_d0 provides for the minimum passive force error over the widest range in δ' and ϕ' values of all the Figure H.1 distributions when wall friction δ' is less than 0.8*ϕ'. Above this value, the data shows that the normalized interslice friction distribution designated as X0.1_d0 provides for the minimum passive force error.

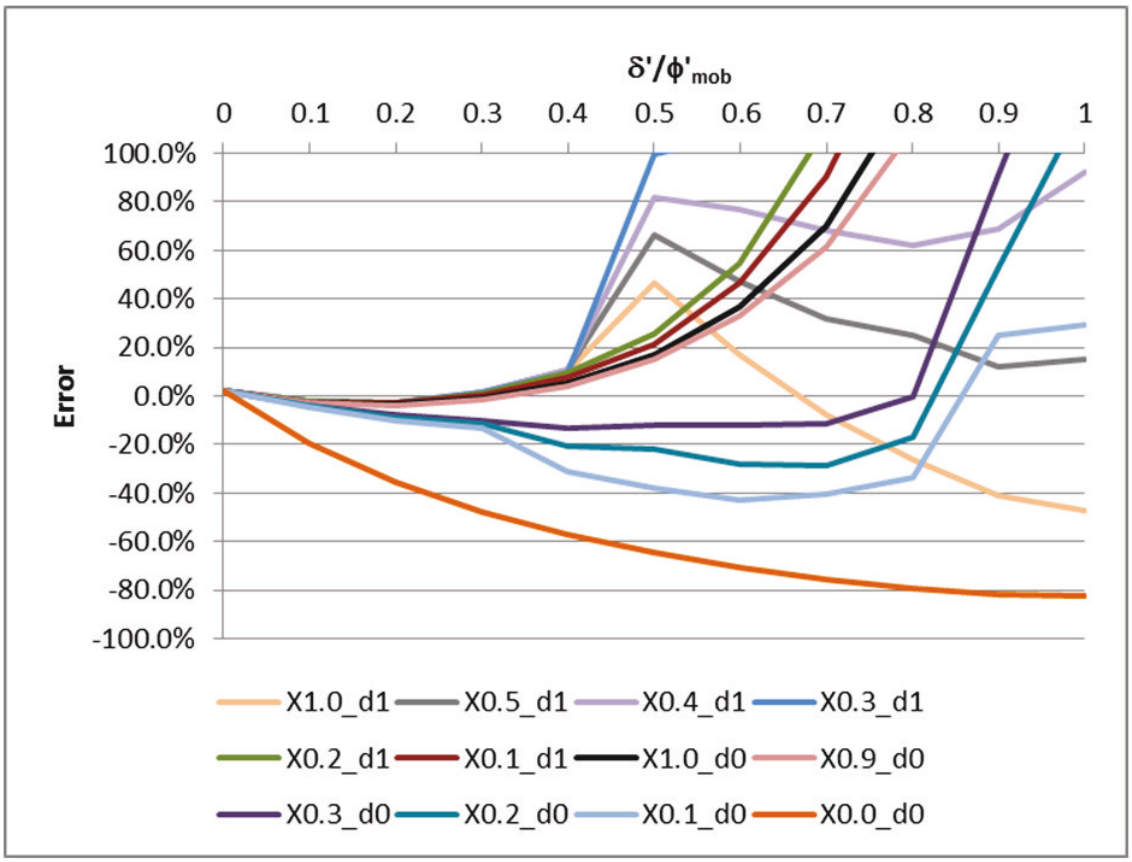
Figure H.12 Values of passive earth force using the Wedge Solution Method, including the standard solution and corresponding errors (in percent), for ϕ' equal to 40 degrees.

ϕ'_{mob}	45														
γ_{mat}	122				Passive Force (Pp)										
depth	10				Rankine	Corps I-Wall curves									
$K_{Passive}$	33.5			δ/ϕ'_{mob}	0	0.1	0.2	0.3	0.4	0.5	0.6	0.7	0.8	0.9	1
curves	axis	pt1	pt2	pt3	35553.41	45161.35	56400.6	69275	84600.9	102175	122610	146723	173289	200059	204350
X1.0_δ1	x/xL	0	0.5	1	36355.26	43982.52	54824.2	70079	93484.9	149878	143295	135828	127523	118433	108612
	δ/δmax	1	1	1	2.3%	-2.6%	-2.8%	1.2%	10.5%	46.7%	16.9%	-7.4%	-26.4%	-40.8%	-46.9%
X0.5_δ1	x/xL	0	0.5	1	36355.26	44126.29	54661.8	70282	93615.1	170097	180717	193640	216314	224826	234881
	δ/δmax	1	1	0	2.3%	-2.3%	-3.1%	1.5%	10.7%	66.5%	47.4%	32.0%	24.8%	12.4%	14.9%
X0.4_δ1	x/xL	0	0.4	1	36355.26	44130.91	54799.4	70195	93769.1	185877	216716	246815	280407	337607	393325
	δ/δmax	1	1	0	2.3%	-2.3%	-2.8%	1.3%	10.8%	81.9%	76.8%	68.2%	61.8%	68.8%	92.5%
X0.3_δ1	x/xL	0	0.3	1	36355.26	44119.04	54816.2	70172	92938.9	204032	254581	332360	657512	1135146	582428
	δ/δmax	1	1	0	2.3%	-2.3%	-2.8%	1.3%	9.9%	99.7%	107.6%	126.5%	279.4%	467.4%	185.0%
X0.2_δ1	x/xL	0	0.2	1	36355.26	44098.1	55006.4	69909	92477.1	128203	189658	309620	535562	1014341	2338510
	δ/δmax	1	1	0	2.3%	-2.4%	-2.5%	0.9%	9.3%	25.5%	54.7%	111.0%	209.1%	407.0%	1044.4%
X0.1_δ1	x/xL	0	0.1	1	36355.26	43967.18	54736.7	69342	90983.6	124050	179673	279491	453589	919818	1867118
	δ/δmax	1	1	0	2.3%	-2.6%	-3.0%	0.1%	7.5%	21.4%	46.5%	90.5%	161.8%	359.8%	813.7%
X1.0_δ0	x/xL	0	0.5	1	36355.26	43919.2	54420.3	68486	88941	119442	168014	249346	393931	852337	1554735
	δ/δmax	1	0.5	0	2.3%	-2.8%	-3.5%	-1.1%	5.1%	16.9%	37.0%	69.9%	127.3%	326.0%	660.8%
X0.9_δ0	x/xL	0	0.9	1	36355.26	43948.51	54018.7	68105	87873.2	117612	163196	236949	364471	789125	1350446
	δ/δmax	1	0	0	2.3%	-2.7%	-4.2%	-1.7%	3.9%	15.1%	33.1%	61.5%	110.3%	294.4%	560.8%
X0.3_δ0	x/xL	0	0.3	1	36355.26	43405.78	51971.1	62454	73414.5	89680.8	108193	129592	173104	381970	573504
	δ/δmax	1	0	0	2.3%	-3.9%	-7.9%	-9.8%	-13.2%	-12.2%	-11.8%	-11.7%	-0.1%	90.9%	180.6%
X0.2_δ0	x/xL	0	0.2	1	36355.26	43330.04	51390.9	61303	67211.7	79947.6	88046.1	104350	143893	305433	452645
	δ/δmax	1	0	0	2.3%	-4.1%	-8.9%	-11.5%	-20.6%	-21.8%	-28.2%	-28.9%	-17.0%	52.7%	121.5%
X0.1_δ0	x/xL	0	0.1	1	36355.26	43106.07	50838.5	60305	58324.9	63225.6	70323.7	87175.1	115166	250521	264708
	δ/δmax	1	0	0	2.3%	-4.6%	-9.9%	-12.9%	-31.1%	-38.1%	-42.6%	-40.6%	-33.5%	25.2%	29.5%
X0.0_δ0	x/xL	0	0.5	1	36355.26	36355.26	36355.3	36355	36355.3	36355.3	36355.3	36355.3	36355.3	36355.3	36355.3
	δ/δmax	0	0	0	2.3%	-19.5%	-35.5%	-47.5%	-57.0%	-64.4%	-70.3%	-75.2%	-79.0%	-81.8%	-82.2%

	reduction factor	
δ_{max}	δ/ϕ'_{mob}	R(δ,ϕ)
45	1	1
40.5	0.9	0.979
36	0.8	0.848
31.5	0.7	0.718
27	0.6	0.6
22.5	0.5	0.5
18	0.4	0.414
13.5	0.3	0.339
9	0.2	0.276
4.5	0.1	0.221
0	0	0.174

ϕ	Kp (δ/ϕ=1)
0	1
5	1.28
10	1.64
15	2.19
20	3.01
25	4.29
30	6.42
35	10.2
40	17.5
45	33.5
50	74.3
51	90
52	110
53	130
54	160
55	204
60	782

Figure H.13 Difference in percent between values of passive earth force using the Wedge Solution Method, Incluting the standard solution as a function of δ' at the wall, for ϕ' equal to 45 degrees.



H.7 Conclusion

Passive force: Based on the result of the error analysis study summarized in this appendix, Corps_I-Wall Wedge Solution Method analyses, the normalized interslice friction distribution designated as X0.3_d0 provides for the minimum passive force error over the widest range in δ' and ϕ' values of all the Figure H.1 distributions that were investigated. For this normalized distribution, the value of (δ'/δ'_{max}) is equal to 1.0 at (x/x_L) equal to zero. The distribution decreases linearly with distance to a value for (δ'/δ'_{max}) equal to zero at (x/x_L) equal to 0.3. The value of (δ'/δ'_{max}) is maintained at a value of zero from (x/x_L) equal to 0.3 to a value of 1.0. This distribution was therefore selected as the default distribution in the Corps_I-Wall software for use by the Wedge Solution Method for passive force computations. For high ϕ' values (e.g., ϕ' on the order of 40 to 45 degrees) and with wall friction δ' at or above 0.8*ϕ' to 0.9*ϕ', the user may consider specifying the X02_d0 or X0.1_d0 distribution in the Corps_I-Wall analysis.

Active force: A similar type of study (not shown) to the passive study discussed in this appendix was also conducted using the Corps_I-Wall Wedge Solution Method of analysis, but for the active earth force. The result of these studies are summarized in an error plot presented in Chapter 3 (Figure 3.37). It was concluded that the normalized interslice friction distribution designated as X0.1_d0 in Figure H.1 provides for the minimum active force error over the widest range in δ' and ϕ' values of all the Figure H.1 distributions that were investigated. For this normalized distribution, the value of (δ'/δ'_{max}) is equal to 1.0 at (x/x_L) equal to zero. The distribution decreases linearly with distance to a value for (δ'/δ'_{max}) equal to zero at (x/x_L) equal to 0.1. The value of (δ'/δ'_{max}) is maintained at a value of zero from (x/x_L) equal to 0.1 to a value of 1.0. This distribution was therefore selected as the default distribution in the Corps_I-Wall software for use by the Wedge Solution Method for active force computations.

REPORT DOCUMENTATION PAGE

Form Approved
OMB No. 0704-0188

Public reporting burden for this collection of information is estimated to average 1 hour per response, including the time for reviewing instructions, searching existing data sources, gathering and maintaining the data needed, and completing and reviewing this collection of information. Send comments regarding this burden estimate or any other aspect of this collection of information, including suggestions for reducing this burden to Department of Defense, Washington Headquarters Services, Directorate for Information Operations and Reports (0704-0188), 1215 Jefferson Davis Highway, Suite 1204, Arlington, VA 22202-4302. Respondents should be aware that notwithstanding any other provision of law, no person shall be subject to any penalty for failing to comply with a collection of information if it does not display a currently valid OMB control number. **PLEASE DO NOT RETURN YOUR FORM TO THE ABOVE ADDRESS.**

1. REPORT DATE *(DD-MM-YYYY)*
December 2018

2. REPORT TYPE
Final report

3. DATES COVERED *(From - To)*

4. TITLE AND SUBTITLE

Analysis of a River Bank, Levee, or Floodplain I-Wall Embedded in Stratified Soil Layers During Flood Events Using Corps I-Wall (CI-Wall) Version 2.0

5a. CONTRACT NUMBER

5b. GRANT NUMBER

5c. PROGRAM ELEMENT NUMBER

6. AUTHOR(S)

Robert M. Ebeling, Barry C. White, and Moira T. Fong

5d. PROJECT NUMBER

5e. TASK NUMBER

5f. WORK UNIT NUMBER
CL618F

7. PERFORMING ORGANIZATION NAME(S) AND ADDRESS(ES)

U.S. Army Engineer Research and Development Center
Information Technology Laboratory
3909 Halls Ferry Road
Vicksburg, MS 39180-6199

8. PERFORMING ORGANIZATION REPORT NUMBER

ERDC/ITL TR-18-2

9. SPONSORING / MONITORING AGENCY NAME(S) AND ADDRESS(ES)

Headquarters, U.S. Army Corps of Engineers
441 G Street NW
Washington, DC 20314-1000

10. SPONSOR/MONITOR'S ACRONYM(S)

11. SPONSOR/MONITOR'S REPORT NUMBER(S)

12. DISTRIBUTION / AVAILABILITY STATEMENT
Approved for public release; distribution is unlimited.

13. SUPPLEMENTARY NOTES

14. ABSTRACT

The purpose of the I-Wall Analysis Research and Development (R&D) effort is to provide the U.S. Army Corps of Engineers (USACE) districts with essential tools in analyzing and evaluating I-Wall performance in riverine, fluvial, and coastal environments. This report summarizes an engineering method and its implementation in the software Corps_I-Wall Version 2.0. The executable program is referred to as CI-Wall. This version of Corps_I-Wall is used for the design of new I-Walls or the analysis of existing I-Walls in floodplains (i.e., I-Walls embedded in level ground). The analysis includes riverbanks and levees (i.e., I-Walls embedded in non-level ground, with non-level soil layers and non-level piezometric surfaces) during flood loading.

Other Corps_I-Wall software capabilities for engineering analysis include total stress and/or effective stress earth pressure calculations by either 1) the Coefficient Method of analysis, or by 2) the Wedge Solution Method of analysis. The program accounts for gap initiation and propagation using hydraulic fracturing criteria in its analysis. It also allows for pseudo-static modeling of wave loading of coastal structures. Probabilistic analysis is a primary component of Corps_I-Wall for new and existing I-Wall analysis.

Examples are provided to highlight each of these capabilities and a user's manual for using the Graphical User Interface (GUI) for CI-Wall is included.

15. SUBJECT TERMS (see reverse)

Flood walls--Analysis
Levees—Analysis
Hydraulic structures—Analysis
Computer programs
Flood control
Floodplains
Soil-structure interaction

16. SECURITY CLASSIFICATION OF:			**17. LIMITATION OF ABSTRACT**	**18. NUMBER OF PAGES**	**19a. NAME OF RESPONSIBLE PERSON**
a. REPORT	**b. ABSTRACT**	**c. THIS PAGE**			**19b. TELEPHONE NUMBER** *(include area code)*
UNCLASSIFIED	UNCLASSIFIED	UNCLASSIFIED	SAR	426	

15. SUBJECT TERMS (concluded)

I-Wall
Floodwall
Corps I-Wall
CI-Wall
Hydraulic fracturing
System response curve
Fragility analysis
Flood and Coastal Storm Damage Reduction Program
Infrastructure resiliency and reliability